



---

**FINAL REPORT**

**Seismic Hazards Assessment  
for  
WNP-3, Satsop, Washington  
Contract No. C-20453**

Submitted to

**WASHINGTON PUBLIC POWER SUPPLY SYSTEM  
3000 George Washington Way  
Richland, Washington 99352-0968**

---

**Geomatrix Consultants**

8803040009 880229  
PDR ADOCK 05000508  
A DCD



---

**FINAL REPORT**

**Seismic Hazards Assessment  
for  
WNP-3, Satsop, Washington  
Contract No. C-20453**

Submitted to

**WASHINGTON PUBLIC POWER SUPPLY SYSTEM  
3000 George Washington Way  
Richland, Washington 99352-0968**

---

**Geomatrix Consultants**

One Market Plaza  
Spear Street Tower, Suite 71  
San Francisco, CA 94105  
(415) 957-9557



February 29, 1988  
Project 1133A

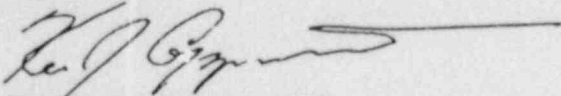
D.W. Coleman  
Washington Public Power Supply System  
WNP-3 Site  
Workman Creek Road  
Warehouse #1  
Elma, Washington 98541

Subject: Final Report  
Seismic Hazards Assessment for  
WNP-3, Satsop, Washington  
Contract No. C-20453

Dear Mr. Coleman:

Enclosed please find five (5) copies of the subject final report incorporating all of your comments. If you have any questions, please do not hesitate to call.

Sincerely,



Kevin J. Coppersmith  
Project Manager

dla

Enclosures

SATSOP SEISMIC HAZARD ANALYSIS  
TABLE OF CONTENTS

	<u>Page</u>
1.0 INTRODUCTION	1-1
2.0 APPROACH	2-1
2.1 <u>Probabilistic Hazard Model</u>	2-1
2.1.1 <u>Formulation</u>	2-1
2.1.2 <u>Basic Components of Seismic Hazard Model</u>	2-2
2.2 <u>Use of Expert Opinion</u>	2-7
2.2.1 <u>Panel Selection</u>	2-8
2.2.2 <u>Expert Interview Process</u>	2-10
2.3 <u>Aggregation of Expert Opinion</u>	2-14
3.0 SATSOP SEISMIC HAZARD MODEL	3-1
3.1 <u>Subduction Zone Hazard Model</u>	3-1
3.1.1 <u>Seismic Source Model</u>	3-1
3.1.2 <u>Ground Motion Attenuation Model</u>	3-7
3.2 <u>Shallow Crustal Hazard Model</u>	3-8
4.0 ANALYSIS RESULTS	4-1
4.1 <u>Hazard Computation</u>	4-1
4.2 <u>Exceedance Frequency for Peak Ground Acceleration</u>	4-2
4.2.1 <u>Total Hazard</u>	4-2
4.2.2 <u>Subduction Zone Sources</u>	4-2
4.2.3 <u>Shallow Crustal Sources</u>	4-6
4.3 <u>Exceedance Frequency for Spectral Acceleration</u>	4-7

## REFERENCES

- APPENDIX A - DOCUMENTATION OF EXPERT INTERVIEWS  
APPENDIX B - CHARACTERIZATION OF SHALLOW CRUSTAL SEISMIC SOURCES  
APPENDIX C - CATALOG EVALUATION AND RECURRENCE RATES  
APPENDIX D - ATTENUATION RELATIONSHIPS FOR SUBDUCTION ZONE SOURCES

TABLE OF CONTENTS (cont'd)

LIST OF TABLES

Table 2-1. Methodology for Conducting Satsop Seismic Hazard Analysis

Table 3-1. Summary of Expert Interviews

LIST OF FIGURES

Figure 1-1. Site Location Map

Figure 2-1. Subduction Zone Hazard Model

Figure 3-1. Subduction Zone Hazard Model

Figure 3-2. Aggregate distributions of 14 experts for ocean slab geometry

Figure 3-3. Aggregate distribution for probability of activity

Figure 3-4. Aggregate distributions for location of rupture

Figure 3-5. Plate boundaries and regional seismicity

Figure 3-6. Aggregate distributions for maximum magnitude

Figure 3-7. Aggregate distribution of 6 experts for return period of large interface earthquakes based on paleoseismic data

Figure 3-8. Aggregate distributions for moment rate parameters

Figure 3-9. Magnitude frequency distributions used in the hazard analysis

Figure 3-10. Complete subduction zone sources hazard model

Figure 3-11. Shallow crustal sources hazard model

Figure 4-1. Percentile hazard curves for peak horizontal acceleration showing contributions of shallow crustal and subduction zone sources to total hazard.

Figure 4-2. Contributions to total hazard shown in terms of magnitude, distance, and source contributions.

Figure 4-3. Comparison of median hazard curves of individual experts.

Figure 4-4. 15<sup>th</sup>, 50<sup>th</sup>, and 85<sup>th</sup> percentile hazard curves for individual experts.

## TABLE OF CONTENTS (cont'd)

LIST OF FIGURES  
(continued)

- Figure 4-5. 15<sup>th</sup>, 50<sup>th</sup>, and 85<sup>th</sup> percentile curves for interface (solid curves) and intraslab (dashed curves) sources for individual experts.
- Figure 4-6. Comparison of experts' median hazard curves with aggregate hazard.
- Figure 4-7. Comparison of aggregation procedures for total hazard from subduction zone sources.
- Figure 4-8. Contribution of expert-to-expert uncertainty to total uncertainty.
- Figure 4-9. Contribution of uncertainty in subduction zone attenuation relationships to total uncertainty.
- Figure 4-10. Contributions of uncertainty in subducting plate geometry to total uncertainty. Shown are the 15<sup>th</sup> and 85<sup>th</sup> percentiles considering all uncertainties (solid lines) and the 15<sup>th</sup> and 85<sup>th</sup> percentiles considering only uncertainty in plate geometry (dashed line).
- Figure 4-11. Contributions of uncertainty in source activity to total uncertainty. Shown are the 15<sup>th</sup> and 85<sup>th</sup> percentiles considering all uncertainties (solid lines) and the 15<sup>th</sup> and 85<sup>th</sup> percentiles considering only uncertainty in source activity (dashed line).
- Figure 4-12. Contributions of uncertainty in source segmentation to total uncertainty. Shown are the 15<sup>th</sup> and 85<sup>th</sup> percentiles considering all uncertainties (solid lines) and the 15<sup>th</sup> and 85<sup>th</sup> percentiles considering only uncertainty in source segmentation (dashed line).
- Figure 4-13. Contributions of uncertainty in maximum extent of rupture to total uncertainty. Shown are the 15<sup>th</sup> and 85<sup>th</sup> percentiles considering all uncertainties (solid lines) and the 15<sup>th</sup> and 85<sup>th</sup> percentiles considering only uncertainty in maximum extent of rupture.
- Figure 4-14. Contributions of uncertainty in maximum magnitude to total uncertainty. Shown are the 15<sup>th</sup> and 85<sup>th</sup> percentiles considering all uncertainties (solid lines) and the 15<sup>th</sup> and 85<sup>th</sup> percentiles considering only uncertainty in maximum magnitude (dashed line).

TABLE OF CONTENTS (cont'd)

LIST OF FIGURES  
(continued)

- Figure 4-15. Contributions of uncertainty in recurrence method (moment rate vs paleoseismicity) to total uncertainty. Shown are the 15<sup>th</sup> and 85<sup>th</sup> percentiles considering all uncertainties (solid lines) and the 15<sup>th</sup> and 85<sup>th</sup> percentiles considering only uncertainty in recurrence method (moment rate vs paleoseismicity) (dashed line).
- Figure 4-16. Contributions of uncertainty in convergence rate/paleoseismic rate to total uncertainty. Shown are the 15<sup>th</sup> and 85<sup>th</sup> percentiles considering all uncertainties (solid lines) and the 15<sup>th</sup> and 85<sup>th</sup> percentiles considering only uncertainty in convergence rate/paleoseismic rate (dashed line).
- Figure 4-17. Contributions of uncertainty in seismic coupling to total uncertainty. Shown are the 15<sup>th</sup> and 85<sup>th</sup> percentiles considering all uncertainties (solid lines) and the 15<sup>th</sup> and 85<sup>th</sup> percentiles considering only uncertainty in seismic coupling (dashed line).
- Figure 4-18. Contributions of uncertainty in magnitude distribution to total uncertainty. Shown are the 15<sup>th</sup> and 85<sup>th</sup> percentiles considering all uncertainties (solid lines) and the 15<sup>th</sup> and 85<sup>th</sup> percentiles considering only uncertainty in magnitude distribution (dashed line).
- Figure 4-19. Peak acceleration hazard from shallow crustal sources. On the left, the 15<sup>th</sup>, 50<sup>th</sup> and 85<sup>th</sup> percentile hazard curves for crustal and subduction zone sources are compared. Shown on the right are the median hazard curves for the various shallow crustal sources.
- Figure 4-20. Contributions to uncertainty in hazard for shallow crustal sources. The solid curves in each plot are the 15<sup>th</sup> and 85<sup>th</sup> percentile curves considering all uncertainties. The left plot shows the median hazard curves obtained using single attenuation relationship. In the center and right plots, the dashed curves are the 15<sup>th</sup> and 85<sup>th</sup> percentile hazard curves considering only uncertainty in maximum magnitude and recurrence rate, respectively.
- Figure 4-21. Hazard curves for 5% damped spectral velocity at periods of 0.15, 0.8 and 2 seconds. Shown are total hazard and hazard from subduction and shallow crustal sources.
- Figure 4-22. 15<sup>th</sup>, 50<sup>th</sup> and 85<sup>th</sup> percentile hazard curves of individual experts for 5% damped spectral velocity at 0.15-second period.

TABLE OF CONTENTS (cont'd)

LIST OF FIGURES  
(continued)

- Figure 4-23. 15<sup>th</sup>, 50<sup>th</sup> and 85<sup>th</sup> percentile hazard curves of individual experts for 5% damped spectral velocity at 0.8-second period.
- Figure 4-24. 15<sup>th</sup>, 50<sup>th</sup> and 85<sup>th</sup> percentile hazard curves of individual experts for 5% damped spectral velocity at 2-second period.
- Figure 4-25. Comparison of experts median hazard curves with aggregate hazard for 5% damped spectral velocity at 0.15, 0.8 and 2 seconds.
- Figure 4-26. Comparison of aggregation procedures for total hazard from subduction zone sources for 5% damped spectral velocity at 0.15, 0.8, and 2 seconds.



## SATSOP SEISMIC HAZARD ANALYSIS

### 1.0 INTRODUCTION

This report documents a probabilistic seismic hazard analysis carried out for the WNP-3 plant site at Satsop, Washington (Figure 1-1). The major components of the study consist of the following:

- Solicitation of expert scientific opinion regarding seismic sources and particularly subduction zone sources that may affect the site.
- Explicit incorporation into the hazard analysis of this scientific understanding and the associated uncertainties.
- Inclusion of the present state of knowledge and uncertainty regarding ground motion attenuation for both crustal and subduction sources.
- Presentation of the hazard results showing relative contributions and sensitivities of the results to the inputs.

Probabilistic seismic hazard analysis (SHA) involves assessments of the probability of earthquake locations, sizes, timing, and associated ground motions, which are coupled with a number of uncertainties. Major components of uncertainty at the Satsop site are due to inaccessibility of the subduction-related seismic sources (precluding conventional fault-specific paleoseismic studies), the relatively short historical observation period of about 130-200 yr (Heaton and Snavely, 1985), scientific uncertainties in the earthquake behavior of the Cascadia subduction zone, and uncertainty in the attenuation of seismic wave energy generated from subduction sources to a site. Therefore, in order to produce a SHA that will withstand intensive scientific and regulatory review, the analysis must capture the present scientific uncertainty in several key tectonic issues such as the seismic capability of the interface between the Juan de Fuca and North American plates.

A complete SHA for the Satsop site must incorporate all known and potential seismic sources that may affect ground motions at the site. This includes potential sources related to subduction. The perception and understanding of subduction in the Pacific Northwest has evolved in the past several

years. Past studies of historical seismicity have led to the conclusion that the interface between the Juan de Fuca and North American plate is either no longer undergoing differential slip (i.e., subduction has ceased) or subduction is occurring aseismically. Improved instrumental seismicity coverage in recent years as well as re-examination of older historical earthquakes has confirmed a virtual lack of thrust-type earthquakes that would be related to interplate displacement. At the same time, studies of high resolution seismic reflection data have shown clear evidence of late Quaternary and Holocene deformation in the young, water-saturated sediments of the outer accretionary wedge offshore, suggesting that plate convergence is still continuing. Offshore and onshore geophysical studies, including the Lithoprobe project through Vancouver Island, have demonstrated that extremely high sedimentation rates have served to bury the Juan de Fuca plate, and, because the plate is relatively young and buried essentially all the way to the Juan de Fuca ridge, the sediments are probably serving to thermally insulate the plate and are themselves heated up.

The confirmation of historical quiescence of the plate interface and increased understanding of other aspects of the Cascadia subduction zone have led to a variety of interpretations of the seismic behavior of the plate interface. The extremes of these interpretations indicate that: 1) the historical record is characteristic of the long-term behavior of the zone and slippage occurs aseismically, or 2) the historical record represents an interseismic period between the occurrence of large interplate thrust earthquakes. A variety of behaviors between these two extremes have also been proposed.

At present, the Cascadia subduction zone appears to be a unique zone in its combination of the youthfulness of the oceanic plate, its relatively low rate of convergence, and lack of interplate historical seismicity. An important issue is whether this behavior is merely a function of our short period of observation or due to true differences with other subduction zones.

To carry out the Satsop SHA, a basic philosophy has been adopted. Those elements of the SHA that are not amenable to resolution in the near-term and with limited available resources should be defined by the current spectrum

of scientific thinking, as represented by expert opinion. Examples of these elements are the seismic activity of the plate interface, the amount of coupling between the plates, and the likely locations of earthquake ruptures. Those elements of the SHA whose uncertainty can be reduced significantly by data collection and analysis efforts are treated differently. In these cases, the Supply System has carried out its own studies and the results supersede previous, more limited, studies. Important examples here are the empirical and numerical studies carried out to estimate ground motions. It became clear in the program that existing published attenuation relationships do not include important recent earthquake recordings (e.g., Mexico and Chile), are not appropriate to the Satsop rock site conditions and are not appropriate to the source-to-site distances of interest. As a result, new relationships were developed for use in the hazard analysis (Appendix D).

The seismic hazard methodology presented herein was developed and implemented after a careful consideration of recent major SHA's involving expert opinion (e.g., those for the eastern U.S. by Lawrence Livermore National Laboratory and the Electric Power Research Institute). We have attempted to build on the strengths of these previous studies in dealing with experts and utilizing their opinions. In addition, we have added our own features to address the differences in the situations between this study and the previous studies. A number of innovations were developed and implemented during this study such as: conducting one-to-one interviews with the experts; documenting the basis for the experts' responses; and dividing the hazard model into several components to allow for more complete representation of uncertainty. A detailed discussion of the methodology is given in the Section 2 of this report.

Because of the large uncertainties associated with a hazard assessment of this kind, extensive sensitivity analyses were carried out to identify those elements of the hazard model that are contributing most to the hazard results and to the total uncertainty in the results. These are useful for identifying the relative significance of various components of the hazard model and determining the effect of uncertainty in these components on the final results.

In sum, we believe we have captured the present scientific and tectonic understanding of the seismic environment in the Satsop site region. The results provide a complete expression of the hazard at the site and the associated uncertainties. As such, they provide a solid basis for evaluating the seismic hazard at the WNP-3 site.

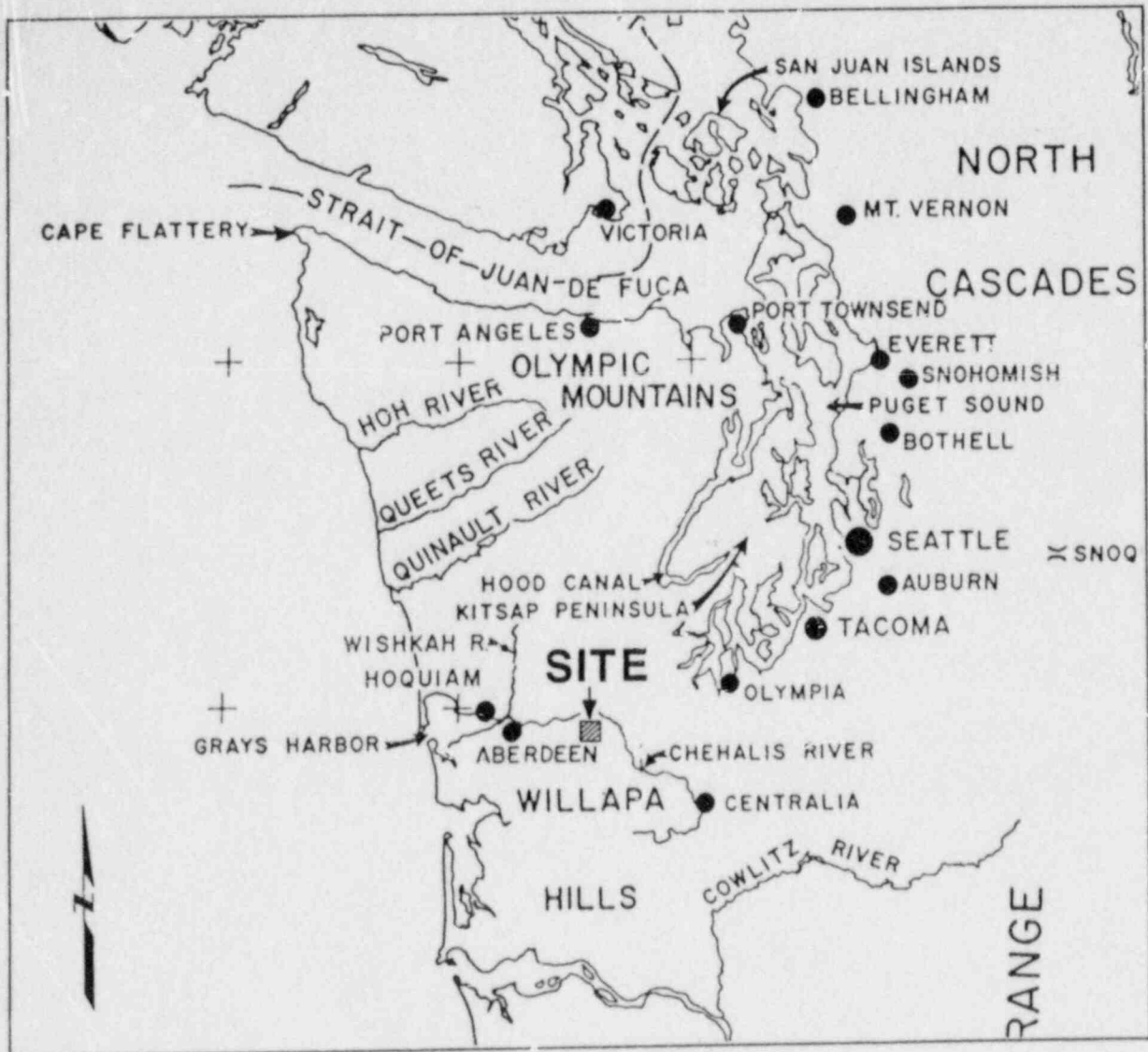


Figure 1-1  
SITE LOCATION MAP  
(from WPPSS, 1982)

## 2.0 APPROACH

### 2.1 Probabilistic Hazard Model

2.1.1 Formulation. Seismic hazard is expressed as the probability that a ground motion parameter,  $Z$  (such as peak ground acceleration, spectral velocity, etc.) will exceed a specified level,  $z$ , during a specified time period,  $t$ . The probability of exceeding a ground motion level at a site can be estimated from the inequality:

$$P(Z > z | t) \leq v(z) \cdot t \quad (2-1)$$

where  $v(z)$  is the frequency or rate at which the level of ground motion parameter  $Z$  exceeds  $z$  at the site. When dealing with the low probability levels of interest in this application,  $v(z) \cdot t$  provides a good, conservative estimate of the hazard. The parameter  $v(z)$  is obtained from the general expression:

$$v(z) = \alpha(m^0) \int_{m^0}^{m^u} \int_0^{\infty} f(m) \cdot f(r) \cdot P(Z > z | m, r) \, dr \, dm \quad (2-2)$$

where  $\alpha(m^0)$  is the frequency of earthquakes above a minimum magnitude of engineering significance,  $m^0$ ;  $f(m)$  is the probability density function for event size between  $m^0$  and a maximum event size,  $m^u$ ;  $f(r)$  is the probability density function for distance to earthquake rupture; and  $P(Z > z | m, r)$  is the probability that, given a magnitude  $m$  earthquake at a distance  $r$  from the site, the ground motion exceeds level  $z$ .

The probability functions contained in Equations 2-1 and 2-2 represent the randomness inherent in the natural phenomena of earthquake generation and seismic wave propagation. For the Cascadia subduction zone one is faced with considerable uncertainty in selecting the appropriate models and model parameters required to apply Equation 2 arising from limited data and/or alternative interpretations of the available data. The approach used in this study explicitly incorporates these uncertainties into the analysis to assess their impact on the estimate of seismic hazard.

The uncertainty in modeling the natural phenomena was incorporated into the hazard analysis through the use of logic trees. The logic tree formulation for seismic hazard analysis (Power et al, 1981; Kulkarni et al, 1984; Youngs et al, 1985; EPRI, 1986; Coppersmith and Youngs, 1986) involves specifying discrete alternatives for states of nature or parameter values and specifying the relative likelihood that each discrete alternative is the correct value or state of the input parameter. The parameter values and their relative likelihoods are usually based on subjective judgment because the available data are too limited to allow a deterministic assessment or a formal statistical analysis.

Figure 2-1 displays the general logic tree format used to represent the seismic hazard model alternatives. The logic tree is laid out to provide a progression from general aspects/hypotheses regarding the characteristics of seismicity and seismic wave propagation in the region to specific input parameters for individual faults and fault segments. The motivation for development of the various levels of the logic tree are discussed below.

2.1.2 Basic Components of Seismic Hazard Model. The seismic hazard model is divided into a number of components, most of which relate to the tectonic characterization of the potential seismic sources. The fourteen experts were responsible for characterizing these components (see Section 3). To help in understanding the hazard model, each component is discussed below.

#### Crustal Geometry

Each expert was asked to provide his interpretation of the three-dimensional geometry of the Cascadia subduction zone. Each expert provided a cross-sectional sketch of one or more possible geometries showing the location of the Juan de Fuca slab and the North American plate. Along-strike variations in geometry (such as changes in slab dip) are also specified. The most common basis for estimating the possible position of the oceanic slab was the distribution of hypocenters of the deeper seismicity beneath Puget Sound, coupled with worldwide analogies to other subduction zones (e.g.,

expected depth required for magma generation may mark the depth to the slab beneath the Cascades).

#### Potential Seismic Sources

The experts were asked to identify all potential seismic sources that could exist in the western Washington region. It was stated to the experts that shallow crustal potential seismic sources would be considered elsewhere in the study, but they were asked to identify those potential sources that might be present in the shallow crust (upper 20 km) but might not have a surface expression. Potential sources were not necessarily limited to those tectonic features that have been associated with seismicity during the historical period. Areal source zones as well as tectonic feature-specific sources could be identified. In general, all of the experts identified two potential seismic sources: 1) an intra-slab source whereby earthquakes are generated within the subducted oceanic slab, and 2) an interface source whereby earthquakes are generated at the interface between the Juan de Fuca and North American plates.

#### Probability of Activity

Each seismic source is associated with an expression of the probability that it is active or seismogenic. Activity is used here to mean that the source is capable of generating tectonically-significant earthquakes. In general, for the subduction-related seismic sources, significant tectonic earthquakes were judged by the experts to be larger than about magnitude 6. (Note that this is not the lower bound magnitude for integration of the hazard calculation, which is discussed in Section 4.) The probability of activity is assessed to be a function of the tectonic role played by a potential source in the present stress regime, and unless that role is expected to change, the probability of activity is independent of time. Thus, "activity" is a binary state (i.e., either "yes" or "no"), and the probability of activity is an expression of the likelihood that the potential source lies in an active state or not. Not included here is the likelihood of earthquake recurrence during any specified time period. This is a function of the recurrence rate, which is a separate component of the seismic hazard model.



The experts considered the probability of activity of the subduction sources (i.e., the intra-slab and interface) to be independent, based largely on observations of subduction zones worldwide.

#### Location of Ruptures

To model the seismic sources for the hazard analysis estimates are made of the three-dimensional location of ruptures for each seismic source. This is an assessment of the geometry of the surface over which future ruptures will occur. For example, an intra-slab seismic source might have the following rupture location characteristics: 1) in cross-section, earthquakes will occur in the upper ten kilometers (brittle portion) of the oceanic slab, 2) the downdip extent will be to depths of about 70 km and updip to the first bend in the slab offshore, 3) the earthquakes larger than magnitude 7 will occur at depths of 50 to 70 km, 4) in map view, the intra-slab seismicity will follow roughly the coastline to accommodate the "corner" near the Canada/ U.S. boundary and will end at the Nootka fault on the north and the Blanco fracture zone on the south, 5) in map view, the relative frequency of earthquakes in the intra-slab source will spatially match that observed in historical seismicity (i.e., higher concentration beneath the Puget Sound/Georgia Strait region than to south or north).

Another aspect of rupture locations that may be specified is that of segmentation of the source. This assessment allows for the possibility that future maximum earthquakes may not rupture the entire maximum dimensions of the source. Possible rupture segment boundaries may be identified and the probability that they will serve as rupture boundaries can also be assessed (e.g., the tear fault in the downgoing slab at a specified location has a 40% chance of serving to stop rupture coming from either direction on the plate interface).

As with all components of the seismic hazard model, alternative hypotheses for the location of ruptures may be given and each can be associated with a relative weight or credibility.

### Maximum Earthquake Magnitude

Each seismic source is associated with a maximum earthquake magnitude that serves as the upper-bound constraint on the recurrence relationship for that source. Maximum magnitudes were often directly assessed by the experts based on the largest historically observed magnitudes or by analogy to other subduction zones. For the plate interface source, many experts indicated that the rupture dimensions, specified previously as part of locations of rupture, provided a reasonable basis for estimating maximum magnitudes. In these cases, the magnitudes were calculated by the elicitation team using the experts' rupture dimensions and the relationship between magnitude and rupture area by Wyss (1979). In general, the magnitudes determined in this manner ranged from 8-3/4 to 9-1/4. In a few instances, the experts specified developing a maximum magnitude estimate from the relationships between plate age, convergence rate, and observed magnitude (Ruff and Kanamori, 1980), resulting in magnitude estimates of about 8.3.

Uncertainty in the maximum magnitude estimate is expressed by the experts in terms of a range of values, a preferred value with associated bounds, or discrete values each associated with a relative weight.

### Convergence Rate

Convergence between the Juan de Fuca and North American plates is considered parallel to the relative plate motion direction. The convergence rate is the relative rate between the two plates, derived in most cases from the absolute plate velocities of each plate. Various investigators have shown that the convergence rate at the Cascadia subduction zone has been decreasing over the past few million years (e.g., Riddihough, 1984). Because we are most interested in the present behavior of the plate boundary, the experts were asked to give convergence rate estimates that are representative of contemporary rates. Often, a broad range of estimates was given, reflecting considerable uncertainty in the rate.

### Seismic Coupling

Seismic coupling ( $\alpha$ ) is defined for this study as the percentage of the total convergence rate that is expected to be released as seismic energy (i.e., ratio between seismic moment rate and convergence rate). Coupling can be estimated from the historical record or from an assumed model. For example, the historical record in the Pacific Northwest shows that virtually no thrust earthquakes larger than magnitude 5 have occurred on the plate interface (i.e., the historical seismic moment rate is very low). If this behavior is judged to be representative of the longer term behavior then seismic coupling would be very low. However, the historical quiescence may be interpreted by some to be the result of a short observation period and actually representative of interseismic quiescence. In this case, the seismic coupling might be assessed to be high (i.e., a close to 1.0). A wide variety of approaches might be considered in arriving at a seismic coupling estimates ranging from detailed studies of the mechanical/thermal properties of subducted sediment to analogies to similar subduction zones worldwide.

### Earthquake Recurrence

Earthquake recurrence or the frequency of occurrence of various magnitude earthquakes is assessed for each seismic source. The experts were asked to specify the preferred method(s) for estimating recurrence including: the use of historical seismicity record, use of seismic moment rate, or geologic data regarding recurrence intervals. To use the historical seismicity record, the three-dimensional area for gathering recurrence statistics is specified as well as the area over which these recurrence rates are assessed to apply. For example, the deep seismicity zone (> 30 km) beneath Puget Sound may be specified to define a recurrence rate per square kilometer. This rate may in turn be said to also be appropriate for the source at this depth north and south of the seismicity zone.

The seismic moment approach to recurrence was used in many cases to define the recurrence for the plate interface. The convergence rate is multiplied by the seismic coupling ( $\alpha$ ) to arrive at a seismic slip rate. To arrive at

a seismic moment rate, the slip rate is multiplied by the total area of the seismic source (defined by the assessed source geometry and location of ruptures) and an assumed rigidity ( $3 \times 10^{11}$  dynes/cm<sup>2</sup>). The use of seismic moment rate to define recurrence has become standard practice for crustal faults (e.g., Anderson and Luco, 1983; Youngs and Coppersmith, 1985a) and appears to be supported by observations of seismic moment release observed for several subduction zones (Peterson and Seno, 1984). To use the resulting seismic moment rate, a recurrence distribution model must be specified that indicates the relative frequency of earthquakes of various magnitudes. The models considered by the experts included: 1) an truncated exponential magnitude distribution based on the familiar form  $\log N = a - bM$ , 2) a characteristic earthquake model of the form given by Youngs and Coppersmith (1985b) and 3) a maximum moment model as described by Wesnousky, et al. (1983).

Some experts used geologic evidence for the recurrence intervals between large earthquakes. Typically this type of data does not provide strong constraints on the size of the earthquakes giving rise to the geologic effect. For this study, we assume that the recurrence intervals apply to magnitudes within one-half magnitude of the maximum. The recurrence distribution model then defines the recurrence rates for smaller magnitudes.

## 2.2 Use of Expert Opinion

Several key tectonic issues (such as the seismogenic capability of the plate interface, the degree of seismic coupling between the plates, earthquake recurrence rates, and the like) are not amenable to resolution within the time frame of this study. Therefore, a decision was made to capture the present understanding and opinions regarding these issues through the use of experts most familiar with them.

In deciding on an appropriate methodology for eliciting expert opinion, careful consideration was given to the strengths and weaknesses of recent large SHA's involving expert opinion (EPRI, 1986; and LLNL, 1985) because the level of uncertainty and the potential for short-term resolution of the issues is comparable.

By considering the attributes of these previous studies as well as the specific requirements for a hazard assessment at the Satsop site, a methodology was developed for utilizing expert opinion. The key attributes of the methodology and the purpose for each are given in Table 2-1, and further discussion is given below.

2.2.1 Panel Selection. The panel selected for the Satsop SHA was intended to span fields of expertise that cover in aggregate the entire range of the hazard model components (e.g., crustal geometry, seismic capability, convergence rate, maximum earthquakes, and earthquake recurrence rate). In addition, it was felt to be desirable to attain a balance of disciplines pertaining to the topic of subduction tectonics and seismicity (e.g., geologists, geophysicists, seismologists, laboratory experimentalists, empirical analysts, etc.). The above considerations required that the total number of experts be relatively large (14) for studies of this kind.

A primary consideration in the selection of experts was that they must have had some experience with the Cascadia subduction zone or allied experience with other subduction zones having similar characteristics. For example, a suitable expert might be a geologist who is carrying-out analytical studies of the seismic behavior of subduction zones that are subducting large amounts of sediments and who is familiar with the accretionary wedge characteristics of the Cascadia zone. Because a large part of the uncertainty associated with the Cascadia zone stems from determining its "uniqueness" relative to other subduction zones, it is important that the experts be familiar with this zone in order to provide as site-specific a hazard model as possible.

Finally, some of the experts have published opinions regarding the seismic behavior of the Cascadia subduction zone. To the extent possible, we achieved a balanced cross-section of opinion in selecting the panel members.

TABLE 2-1

METHODOLOGY FOR CONDUCTING SATSOP SEISMIC HAZARD ANALYSIS

<u>Attribute of Methodology</u>	<u>Purpose</u>
● Large number of experts (14)	● Spectrum of scientific opinion captured
● Experts represent wide variety of disciplines	● Incorporate full range of perspectives and data sets
● No single expert required to address all aspects of hazard model	● Avoid encouraging expert to go beyond area of expertise
● Experts provided with background information and topical reference list	● Encourage a uniform minimal level data base; provide a focus on key issues to SHA
● Experts interviewed individually and opinion not associated with expert by name	● Allow for free expression of opinion; highly focused discussion
● Basis for decisions given and documented	● Allows for a technical evaluation of the responses in terms of the scientific issues driving thinking
● Interview summaries provided to each expert for review	● Ensure accuracy and provide opportunity to change opinion upon reflection
● Hazard model developed as components	● Model is clearer to experts; allows for sensitivity studies
● Full inclusion of uncertainty expressed by experts	● Leads to more complete expression of hazard;

Using the above criteria, a balanced list of experts plus alternates was arrived at. The individuals were then contacted and all agreed to participate, with one exception (who felt that he had little to contribute to this study). The 14 experts were the following:

<u>Expert</u>	<u>Affiliation</u>
John Adams	Canadian Geological Survey
Mark Cloos	University of Texas, Austin
Ron Clowes	University of British Columbia
Daryl Cowan	University of Washington
Robert Crosson	University of Washington
Greg Davis	University of Southern California
Thomas Heaton	U.S. Geological Survey
Thomas Hilde	Texas A & M University
Hiro Kanamori	California Institute of Technology
Vern Kulm	Oregon State University
William McCann	University of Puerto Rico
Thomas Owens	University of Missouri
Robin Riddihough	Canadian Geological Survey
Garry Rogers	Canadian Geological Survey

In the course of discussions with the experts regarding participation in the project, two individuals requested that their responses not be attributed specifically to them by name, lest their response be construed as representing an official position of their institutions. To guard the privacy of all the experts, it was decided to not associate particular opinions with experts by name. Therefore, henceforth in this report, the experts are indicated by number only (e.g., expert #1).

2.2.2 Expert Interview Process. The elicitation of expert opinion for the Satsop hazard analysis occurred through a two-part interview process. The first interview (described in detail below) occurred in the summer of 1986. A second interview, conducted via telephone, was carried out in the fall of

1987. The second interview was a follow-up to the first and was held in light of feedback from the first interview (see Appendix A) and to gauge any change in opinion over the one year time period. Several weeks prior to the interviews, each expert was sent an introductory letter (included in Appendix A) that contained the following: 1) a summary of the purpose of the study, 2) a review of the methods to be used to elicit expert opinion in the interview, 3) a list of questions that are likely to be asked, and 4) a bibliography arranged topically. All of the cited references were made available to the experts at their request. The purpose here was to be sure that all of the experts were made aware of any references that they might not otherwise have come across.

During June and July, 1986, each of the experts was interviewed in his office. Each interview lasted about five hours and was attended by an elicitation team consisting of Dr. Kevin Coppersmith (geologist), Dr. Robert Youngs (hazard analyst), and Dr. Ted Habermann (seismologist). Dr. Robert Winkler (expert opinion elicitation expert) attended the first interview and provided guidance throughout the interview process. Drs. Coppersmith and Youngs were heavily involved in the development and implementation of the EPRI hazard study (EPRI, 1986).

The interviews opened with a short introduction to remind the expert of the purpose of the meeting and to set guidelines for the interview process. Examples of these introductory comments are given below:

- We are using expert judgements because there exist limited or only indirectly relevant "hard" data.
- We are using probabilities to quantify your judgements and uncertainties, but no high-powered statistical treatment is necessary.
- The seismic hazard problem has been broken into component parts to help you think about the problem.
- You may feel more comfortable about some parts of the hazard model than others - that's ok. You may defer on some aspects if you desire.



- What we are attempting to elicit are: 1) one or more interpretations regarding each component of the hazard model, 2) the probabilities associated with each interpretation, and 3) the qualitative basis for your interpretations.
- Try to consider all possible theories and hypotheses, not just "most likely" scenarios.
- Keep the uncertainties in mind in your responses.
- Do not mix values and judgement - we just want your scientific judgement, not your opinion regarding consequences or risk.
- You will have an opportunity to review and revise our summary of this interview.

Included in the introductory comments were descriptions of the major elements of the seismic hazard model and planned methods for incorporating uncertainty, such as the use of logic trees.

During the interview, individual components of the hazard model were discussed separately (e.g., geometry of sources, convergence rate, seismic coupling, etc.).

The experts were encouraged to bring and use any data, maps, reprints, and the like, that they felt were appropriate for explaining their reasoning. Members of the elicitation team recorded in writing the basis for the interpretations (e.g., "the dip of the oceanic slab is  $11^\circ$  based on seismic refraction data, instrumental seismicity, etc."). To define the uncertainty in their estimates, the experts were asked for a range of possible values (e.g., "my preferred value is  $11^\circ$ , but the dip could be as high as  $20^\circ$  or as low as  $9^\circ$ "). Some experts preferred to develop a probability distribution that expressed the uncertainty in their responses (e.g., a normal distribution centered on  $11^\circ$ ). Capturing this uncertainty is important to fully characterize the uncertainty in the hazard assessment.

Asking the experts to provide the basis for their assessments proved to be extremely valuable to understanding the reasoning process involved in arriving at a judgement. It is clear that different types of data are viewed as

being more diagnostic than others depending on the expert. For example, geologic evidence for large earthquakes and their recurrence intervals based on submarine turbidites was believed to be highly conclusive by some experts and merely suggestive or inconclusive by other experts. We believe that asking for their basis helped the experts to sort out the various data sets and to arrive at conclusions. By carefully treating the uncertainty, they were able to qualify the credibility of various interpretations.

In going through the elements of the seismic hazard model on a component-by-component basis, experts were allowed to decline to specify those components that they felt uncomfortable with. It is not surprising that several experts exercised this option given the wide range of fields of expertise involved in a hazard model of this type. In general, however, most experts were able to characterize nearly all components of the model and half provided complete hazard models (see Section 3) and to quantify their uncertainty and confidence in each component.

Overall, the expert interviews were a highly successful part of the project. The experts were well-prepared, open, and willing to express freely their opinions and uncertainties. Following the interviews, written notes were distilled, typed, and sent back to the experts for their review and revision. In general, the changes made were very minor. The interview summaries are given in Appendix A.

As a follow-up to the 1986 interviews, a second set of interviews were carried out in the fall of 1987 via telephone. (The hiatus was due to a change in the focus of the WNP-3 program toward ground motion estimation methodologies.) The second interview had two purposes: 1) to assess whether opinions would change given feedback (discussed below) regarding maximum magnitudes and recurrence, and 2) to allow the experts an opportunity to update their assessments. The feedback consisted of the following: during the course of the interviews, many of the experts had provided source characteristics related to maximum magnitude (e.g., segmentation, interface width) and to earthquake recurrence maximum magnitude or recurrence values. Therefore, in

order for each expert to see the implications of their assessments, the calculated maximum magnitudes and recurrence relationships were provided to each expert prior to the second interview (Appendix A contains this second information package). The interview stepped through the various components of the model as was done the first time, allowing the expert to make any changes that he felt were appropriate. The results were then documented and checked by the experts for accuracy and are given in Appendix A. It is this updated set of expert opinions that are used to calculate the hazard at the Satop site and are discussed in detail in Section 3.

### 2.3 Aggregation of Expert Opinion

The product of the expert interview process was a set of interpretations of the present scientific knowledge concerning the seismic potential of the Cascadia subduction zone. Incorporation of this information into the evaluation of the seismic hazard required aggregation of multiple interpretations into a hazard model that, ideally, represents the combined information of the experts and reflects the current level of uncertainty. The approach used in this study was one of "mechanical" aggregation in which the experts' probability distributions are mathematically combined to arrive at a single distribution representing the uncertainty in the seismic hazard.

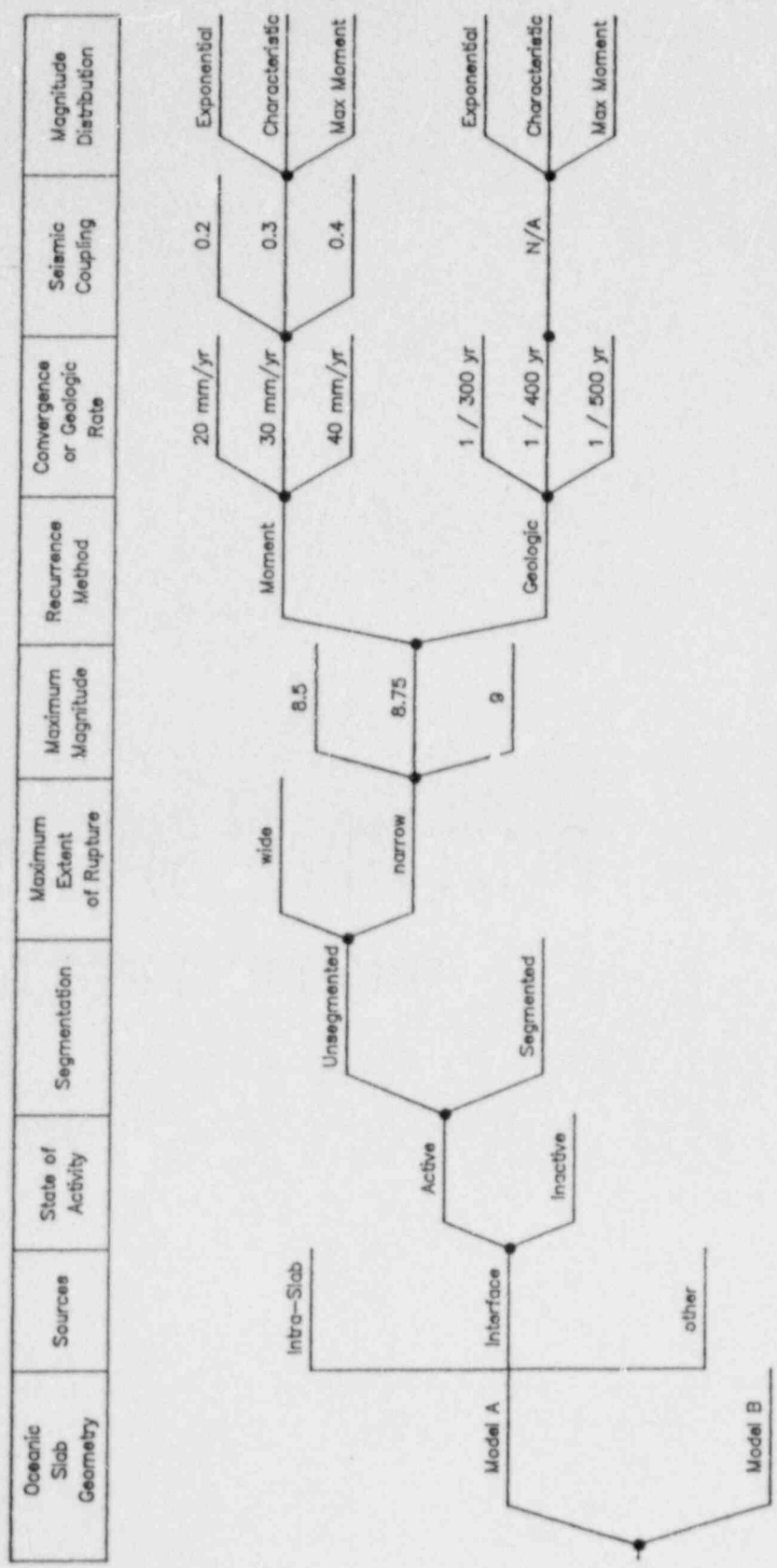
As the assessment of expert opinion was structured to provide information on multiple components of the hazard model the aggregation of these assessments could be done either at the component level or at the hazard level. Component level aggregation would provide a single composite hazard model rather than a set of 14 hazard models. However, because of the sequential nature of the interviewing process, the experts' responses for some questions are conditional on their earlier responses. For example, there was some variation in the seismic sources considered, and later questions are conditional on these sources. When two experts gave different responses on certain questions, aggregating for some later questions would amount to aggregating judgements that were conditional on different sets of assumptions. Therefore, the primary approach to aggregation used in the study was to develop hazard

models for each expert and aggregate the resulting distributions for seismic hazard.

Aggregation at the hazard level raised the problem of experts providing incomplete hazard models because they felt uncomfortable making assessments of particular aspects of the problem. It was judged that the most appropriate way to fill these "gaps" in an individual expert's hazard model was to use an aggregate of the assessments of the other experts. Thus the hazard models of some experts represent, to some extent, a composite hazard model. Accordingly, a secondary analysis was conducted to extend the "gap filling" procedure to full component level aggregation to see how the final hazard estimates differ and to learn more about the state of information regarding each component.

The combining rule for mechanical aggregation used in this study was a simple average with equal weights, both at the component level and at the final hazard level. The simple average was used because there is no compelling reason to assume that one expert is a "better assessor" than another without attempts to calibrate the experts. The simple average also tends to preserve the full distribution of interpretations made by the experts.

FIGURE 2-1. Subduction Zone Hazard Model



### 3.0 SATSOP SEISMIC HAZARD MODEL

This section of the report summarizes the components of the seismic hazard model for the Satsop site. Included here are the "inputs" to the seismic hazard calculations, the results of which are given in Section 4.

The potential future earthquake sources of significance to ground motions at the site can be divided into two groups: those associated with the Cascadia subduction zone and those located in the shallow crustal portion of the North American plate. Seismic hazard models were developed separately for each group of sources as discussed in Section 3.1 for subduction zone sources and 3.2 for shallow crustal sources.

#### 3.1 Subduction Zone Hazard Model

The various seismic source characteristics that were defined for potential subduction zone earthquake sources is given in logic tree format developed to model the subduction zone sources is shown in Figure 3-1. The logic tree progresses from an assessment of the geometry of the subducting slab to assessments of specific analysis parameters for individual sources. The assignment of parameter values and their relative likelihoods for the subduction zone sources was based on the inputs from 14 experts (Section 2.2.2). The individual assessments of each of the experts are documented in Appendix A and are summarized in Table 3-1. As part of this study, site-specific ground motion attenuation relationships were developed based on an analysis of strong motion data including near-field data recorded during several recent earthquakes; this analysis is presented in Appendix D.

3.1.1 Seismic Source Model. As discussed in Section 2.3, the hazard model could be developed by either combining the assessments of all the experts for each parameter (termed "component level" aggregation) to arrive at an aggregated assessment over all experts for each parameter, or by developing a hazard model for each expert based on his individual assessments and then aggregating the computed hazard from the 14 models (termed "hazard level" aggregation). Because many of the assessments of the components were made conditional on other responses (e.g., an assessment of the maximum extent of

interface rupture may be conditional on the assessments made for the geometry of the oceanic slab) the hazard level aggregation approach was judged to be more appropriate. However, as indicated by the blank spaces in Table 3-1, not all of the experts provided a complete set of assessments for all components. Where an individual expert declined to assess a particular component, a distribution of parameter values based on the assessments of the other experts was substituted to complete the hazard model. A supplemental hazard analysis was performed using a composite hazard model constructed from the aggregated distributions for each component presented below.

The component-level distributions for individual parameters were developed on a marginal basis. For example, if an expert has two alternative oceanic slab geometries and for each, he assessed a distribution for maximum magnitude, then his marginal distribution for maximum magnitude would be a combination of the two distributions, each weighted by the probability that the particular slab geometry on which it is based is the correct geometry. The marginal distributions of the experts that made assessments of maximum magnitude could then be aggregated to form a single marginal distribution that could be used to fill gaps in the hazard models of those experts that did not assess maximum magnitude.

The assessments made for each component of the hazard model are summarized below. Included here is a summary of individual experts' assessments for each component as well as the distributions of assessments across all experts for each component. The component-level distributions were used to complete the individual logic trees where necessary and to develop the composite hazard model.

#### Crustal Geometry

All of the experts provided an assessment of the cross sectional geometry of the subducting Juan de Fuca plate. Most of the experts provided only a single assessment consisting of the plate dipping at approximately  $11^\circ$  and extending through the zone of deeper earthquakes lying at depths of 30 km or more beneath the site. Two experts provided a slight modification of the

10° dip consisting of a flat lying slab with a double bend (see cross section for expert 6 in Appendix A as an example). Many of the experts preferred the model recently proposed by Crosson and Owens (1987) that has an arch in the slab along strike. Figure 3-2 presents the aggregate distributions for slab geometry.

#### Seismic Sources

All of the experts identified the Juan de Fuca - North American plate interface and the subducting Juan de Fuca plate as potential sources of thrust and intraslab normal events, respectively. Some experts also identified potential sources in the overlying North American plate. Evaluation of the hazard from these crustal sources was included in the shallow crustal source model described in Section 3.2.

#### Probability of Source Activity

All of the experts made an assessment of the probability that the plate interface and the subducting slab are active or seismogenic (see Section 2.1 for discussion of "activity"). Figure 3-3 shows the distribution of assessments of activity for the intraslab and interface sources. The assessments for the intraslab source are generally at or near unity based on the past record of seismicity. The assessments for the interface range from near zero to near 1.0 with an average of 0.54. The assessments cluster near zero, near 0.5, and near 1.0. It should be noted that the that an adjustment was made to the assessments of experts 4 and 13. As indicated in Table 3-1, column 5, these two experts have probabilities of 0.9 and 0.85, that the maximum magnitudes for the interface is  $M_w$  5 or less. All other experts made the assessment of activity in terms of the probability of the interface being able to generate tectonically significant events ( $M_w > 5$ ). To put the assessments of experts 4 and 13 on a consistent basis they were adjusted to values of 0.075 and 0.0075, respectively, and their maximum magnitude distributions renormalized to include only magnitudes larger than  $M_w$  5. These adjustments were discussed with the experts and they were in agreement.



### Locations of Ruptures

The experts provided assessments on the limits of earthquake ruptures, both along the length of the subduction zone as well as the up dip and down dip extent. Figure 3-4 provides histograms summarizing the responses obtained. Most experts considered the maximum limits of coherent rupture along the interface to be the boundary with the Explorer plate at the Nootka fault zone on the north and the Blanco fracture zone on the south (see Figure 3-5). Several experts considered further segmentation of the interface to have some credibility, with a segment boundary generally in the vicinity of 46°N or segment boundaries on the northern or southern margins of the arch in the slab proposed by Crosson and Owens (1987). The assessments of the minimum depth of rupture along the interface ranged from 5 to 25 km and the maximum depth of rupture ranged from 35 to 60 km. The distributions for minimum and maximum depth of interface rupture shown in Figure 3-4 were used in developing an expert's hazard model if he did not make an assessment.

A majority of the experts stated that they expect the future distribution of intraslab events to follow the observed pattern of historical seismicity with the majority of events occurring generally beneath Puget Sound. Alternatives considered included completely uniform seismicity within the down-going slab or a concentration of larger events at deeper depths. Figure 3-4 shows the aggregate distribution for seismicity distribution. The pattern of historical seismicity generally inferred to lie within the Juan de Fuca plate is shown in Appendix C, Figure C-2.

### Maximum Magnitude

The experts that assessed maximum magnitudes for the interface either made a direct assessment or specified that it be calculated from the maximum rupture dimensions assessed above using the relationship between rupture area and magnitude proposed by Abe (1975) and Kanamori (1977). Their relationship can be written as  $M = \log_{10} (A) + 3.99$ . Regression of published values of  $M_v$  and Area for recent earthquakes holding the slope equal to unity yielded the same relationship between magnitude and rupture area. Twelve experts provided an assessment of maximum magnitude for the interface: seven (58%)

specified the use of maximum rupture dimensions and five (42%) gave a direct assessment of the maximum magnitude on the basis of analogy with other subduction zones or other techniques for magnitude estimation. The aggregate distribution shown in Figure 3-6 is for those five experts who made a direct assessment, and is thus conditional on the direct assessment procedure being the correct procedure. In general, the maximum rupture dimensions specified by the experts resulted in maximum magnitudes of about 9. If an expert did not assess interface maximum magnitude, then the marginal distribution used to represent the aggregated opinion of the other experts consists of 0.58 weight assigned to the magnitude value obtained from the experts assessment of maximum rupture dimensions and 0.42 weight assigned to the conditional distribution based on direct assessment.

The distribution shown at the top of Figure 3-6 has a large probability of 0.38 assigned to a maximum magnitude of 6. As this represents the judgments of two of the experts based on specific reasoning, it is an appropriate distribution for use in component level aggregation. However, it was judged that this assessment is significantly lower than would be obtained from a general population of scientists familiar with subduction zone earthquakes and those experts who did not make any assessment of maximum magnitude for the interface would, nevertheless, be likely to assign a much lower probability to a maximum magnitude of 6. Accordingly, the conditional distribution used for those experts who did not assess maximum magnitude (i.e., the distribution for use in "gap-filling") was modified from that shown at the top of the Figure 3-6 by removing the assessments for very low magnitudes and renormalizing. The resulting distribution is shown in the middle of Figure 3-6.

The maximum magnitude for the intraslab source was assessed by 11 experts on the basis of historical seismicity and analogy with other subduction zones. The aggregated distribution is shown at the bottom of Figure 3-6.

### Earthquake Recurrence Method

All experts who made an assessment of earthquake recurrence preferred to use historical seismicity data to define the recurrence parameters for intraslab events. Appendix C presents recurrence parameters for intraslab events based on an analysis of the seismicity data. These parameters were used for all experts. Recurrence estimates for the plate interface were assessed either on the basis of a moment rate approach or on the basis of geologic evidence for the frequency of large events. In aggregate, the experts favor the moment rate approach slightly more than the use of the geologic data by the ratio 0.54 to 0.46. If an expert did not make an assessment of earthquake recurrence for the interface, then both methods were used with the given weights.

### Geologic Recurrence Rate

Six of the experts chose to base the recurrence estimates for interface events solely or partially on geologic evidence for possible paleoseismic events, primarily the data from coastal subsidence and offshore turbidites. Figure 3-7 presents the aggregated distributions for return period of large interface events. The distributions are centered about an average recurrence interval of about 500 years.

### Convergence Rate

All of the experts made an assessment of convergence rate with most basing the assessment on the rate estimates published by Riddihough (1984), Nishimura and others (1984) and Verplanck and Duncan (1987). Those experts that made a direct assessment generally gave a wide distribution of values with a mean value somewhat lower than the published estimates. Figure 3-8 shows the aggregate distribution for convergence rate estimates.

### Seismic Coupling

Figure 3-8 shows the aggregate distribution of the amount of seismic coupling between the Juan de Fuca and North American plates. Most of the experts gave a wide distribution for the amount of coupling with expert 1 giving a zero/one bimodal distribution. The bases for estimates of coupling were

quite varied and ranged from analogies with other subduction zones to thermal-mechanical modeling of the plate interface.

The product of the plate interface area, the convergence rate and the amount of seismic coupling provide the rate of release of seismic moment. For an interface length of 800 km, a width of 100 km, a convergence rate of 4 cm/yr and an aggregate mean of 0.4 for seismic coupling gives a moment rate of  $3.84 \times 10^{26}$  dyne-cm/yr. Assuming all of the moment is released in magnitude  $8\frac{1}{2}$  events, a moment rate estimate of approximately 200 years would be obtained for the return period of these events.

#### Recurrence Model

Three recurrence models for the form of the magnitude distribution were used for earthquake sources in the analysis: the truncated exponential distribution, the characteristic magnitude distribution, and the maximum moment distribution. Figure 3-9 illustrates the cumulative form of these three distributions and compares how they would estimate the frequency of smaller earthquakes when the absolute level of seismicity is fixed by the frequency of the largest events. Based primarily on the historical absence of small- and moderate-magnitude events, most experts preferred the maximum moment or characteristic models. The aggregated distributions of the experts yielded weights of 0.52, 0.38, and 0.1 for the maximum moment, characteristic, and exponential models, respectively.

3.1.2 Ground Motion Attenuation. Appendix D presents an analysis of strong motion data from subduction zone earthquakes, including data from the recent earthquakes in Chile and Mexico. Two attenuation models were developed representing the uncertainty extrapolation of the empirically based attenuation relationship to magnitudes greater than  $M_w$  8. The two models are designated "S-Cubed" and "Joyner" indicating scaling laws based on the results of ground motion simulations (S-Cubed, 1988) and on theoretical source spectra and random vibration theory (Joyner, 1984). As indicated in Figure 3-9, the S-Cubed model is given greater weight (0.67 vs. 0.33) because it is based on simulation done specifically for ground motions at the WNP-3 site.

### 3.2 Shallow Crustal Hazard Model

The logic tree format developed to model the shallow crustal sources in the North American plate is shown in Figure 3-11. Eleven seismic sources were represented in the hazard analysis, consisting of five sources related to geologic/geophysical features and six distributed area source zones. The maximum magnitude and earthquake recurrence estimates for these crustal sources is presented in Appendix B.

Three recently developed attenuation relationships for ground motions from shallow crustal earthquakes were considered applicable for estimating ground motions at the site from the identified crustal sources. The peak acceleration relationships published by Joyner and Fumal (1985) and Campbell (1987) are based on ground motion data available through 1980 and are considered by their authors to be applicable to both soil and rock sites. The third relationship (Geomatrix Consultants, 1987) is a modified form of that published by Sadigh et al (1986) reflecting analysis of data recorded on rock sites post 1980. The three relationships were given equal weight in the analysis.

TABLE 3-1. SUMMARY OF

EXPERT	OCEANIC SLAB GEOMETRY (DIP)	POTENTIAL SEISMIC SOURCES	PROBABILITY OF ACTIVITY	MAXIMUM MAGNITUDE
#1	Top of deep seismicity	Intra-slab [a]	1.0 [a]	7.25 ( $\pm 0.25$ ) [a]
		Interface [b]	0.35 (0.25-0.5) [b]	Dimensions [b]
#2	Top of deep seismicity	Intra-slab [a]	0.8 [a]	6 - 7 [b]
		Interface [b]	0.4 (0.05-0.2) [b]	
#3	Top of deep seismicity	Intra-slab [a]	1.0 [a]	8 [shallower part of a]
		Interface [b]	0.9 [b]	7½ [deeper part of a] 9 (x ½) [b]
#4	Top of deep seismicity	Intra-slab [a]	1.0 [a]	7 7½ [a]
		Interface [b]	0.075 [b]	3 (0.3) } 4 (0.3) } 5 (0.3) } 1/2 6 (0.09) } 7 (0.07) }
#5	Top of deep seismicity (0.85-0.9) 10° dip (0.10-0.15)	Intra-slab [a]	1.0 [a]	7 [a]
		Interface [b]	0.5 ( $\pm 0.5$ ) [b]	
#6	Top of deep seismicity, single bend (0.3)  Top of deep seismicity, double bend (0.7)	Intra-slab [a]	1.0 [a]	6-3/4 - 7 1/4 [a]
		Interface [b]	0.65 ( $\pm 0.2$ ) [b]	Dimensions [b]
#7	Top of deep seismicity (0.7)	Intra-slab [a]	0.3 ( $\pm 0.2$ ) [b]	Dimension: [b]
		Plate interface [b]		
#8	Top of deep seismicity	Intra-slab [a]	1.0 [a]	Dimensions [b]
		Interface [b]	0.5 (0.25 - 0.75) [b]	
#9	Top of deep seismicity	Intra-slab to 50km depth [a]	0.9 [a]	6.5 (0.1) } 7.0 (0.25) } [a]
		Intra-slab 50 - 75km [b]	1.0 [b]	7.5 (0.55) } 7.8 (0.1) }
		Interface [c]	0.95 $\pm$ 0.05 [c]	7.0 (0.1) } 7.5 (0.8) } [b] 7.8 (0.1) }
		Strike-slip faults in upper plate [d]		
		Accretionary wedge faults [e]	1.0 [d]	Dimensions [c]
		Tears in down-going slab [f]	1.0 [e] 1.0 [f]	7½ [d]  7.5 (0.8) } [e] 8.0 (0.2) }
#10	Top of deep seismicity	Intra-slab [a]	1.0 [a]	7½ (x ½) [a]
		Interface [b]	0.7 (0.6 - 0.9) [b]	Dimensions [b]
#11	Top of deep seismicity	Intra-slab [a]	1.0 [a]	7 - 7½ [a]
		Interface [c]	0.9 (0.8 - 1.0) [b]	Dimensions [b]
		Deep crustal source [c]	1.0 [c]	7½ [c]
#12	Top of deep seismicity	Intra-slab [a]	0.95 - 1.0 [a]	7½ [a]
		Interface [b]	0.9 [b]	9 [b]
#13	Top of deep seismicity	Intra-slab [a]	1.0 [a]	6.5 (0.45) } 7.0 (0.4) }
		Interface [b]	0.0075 [b]	7.5 (0.14) } [a] 8.0 (0.01) }  4 (0.5) } 5 (0.35) } [b] 6 (0.15) }
#14	Top of deep seismicity	Intra-slab [a]	1.0 [a]	7.25 - 7.5 [a]
		Interface [b]	0.35 ( $\pm 0.25$ ) [b]	8.5 ( $\pm 0.5$ ) [b]
		Accretionary wedge [c]	0.7 ( $\pm 0.1$ ) [c]	7 ( $\pm 0.25$ ) [c]
		Tears in slab [d]	0.05 ( $\pm 0.05$ ) [d]	5 [d]

EXPERT INTERVIEWS

CONVERGENCE RATE (MM/YR)	RECURRENCE METHOD	SEISMIC COUPLING (a)	RECURRENCE MODEL	GEOLOGIC RECURRENCE LARGE EARTHQUAKES (YR)
(x 10)	Historical seismicity [a] Moment rate [b]	0 (0.5 - 0.66) 1 (0.5 - 0.33)	Exponential [a] Max. moment given a = 1 [b]	---
35 (0.1) (0.8) (0.1)	Geologic (0.4) [b] Moment rate (0.5) [b]	---	---	430 [b]
(x 19)	Historical seismicity [a] Geologic data [b]	0.66	Exponential [a] Characteristic [b]	500 (400 - 1000) [b]
(0.05) (0.5) (0.4) (0.0%)	Historical seismicity [a] Moment rate [b]	0.05 (0 - 0.15)	Characteristic [b]	---
(24 - 40)	Historical seismicity [a]	---	Exponential [a]	---
17 (0.04) 20 (0.04) 30 (0.4) 40 (0.1) 43 (0.4) 50 (0.02)	Historical seismicity [a] Geologic data (0.75) [b] Moment rate (0.25) [b]	0.6 (x 0.15)	Exponential [a] Exponential (0.2) [b] Characteristic (0.8) [b]	500 - 600 (x 25%) [b]
(x 10)	Historical seismicity [a]	1 (1.0)	Exponential [a] Characteristic (0.5) [b] Maximum moment (0.5) [b]	---
(+7, -10)	---	0.5 (0.2 - 0.7)	---	---
(+ 10)	Historical seismicity [a,b,d,e,f] Geologic data [c]	0.7 - 1.0 (0.54) 0.5 - 0.7 (0.25) 0 (0.01)	Exponential [a,b,d,e,f] Characteristic (0.5) [c] Max. mom. moment (0.5) [c]	500 (x 25%) [c]
5 - 50 (x 19)	Historical seismicity [a] Moment rate [b]	0.3 (0 - 0.5)	Exponential [a,b]	---
(x 10)	Historical seismicity [a,c] Geologic data [b]	---	Exponential [a,c] Maximum moment [b]	500 x 150 [b] x150 [c]
35 (25 - 40)	Historical seismicity [a] Moment rate [b]	0.1 (0.05 - 0.5)	Exponential [a] Maximum moment [b]	500 x 100 [b]
(x 19)	Historical seismicity [a]	0.05 (x 0.05)	Exponential [a]	---
20 (0.05) 30 (0.2) 40 (0.4) 50 (0.3) 50 (0.05)	Historical seismicity [a,c,c'] Moment rate [b]	0.01 (0.4) 0.05 (0.4) 0.10 (0.2) 0.15 (0.15) 0.5 (0.05)	Exponential [a,c,d] Maximum moment [b]	---

TI  
APERTURE  
CARD

Also Available On  
Aperture Card

8803040009-01

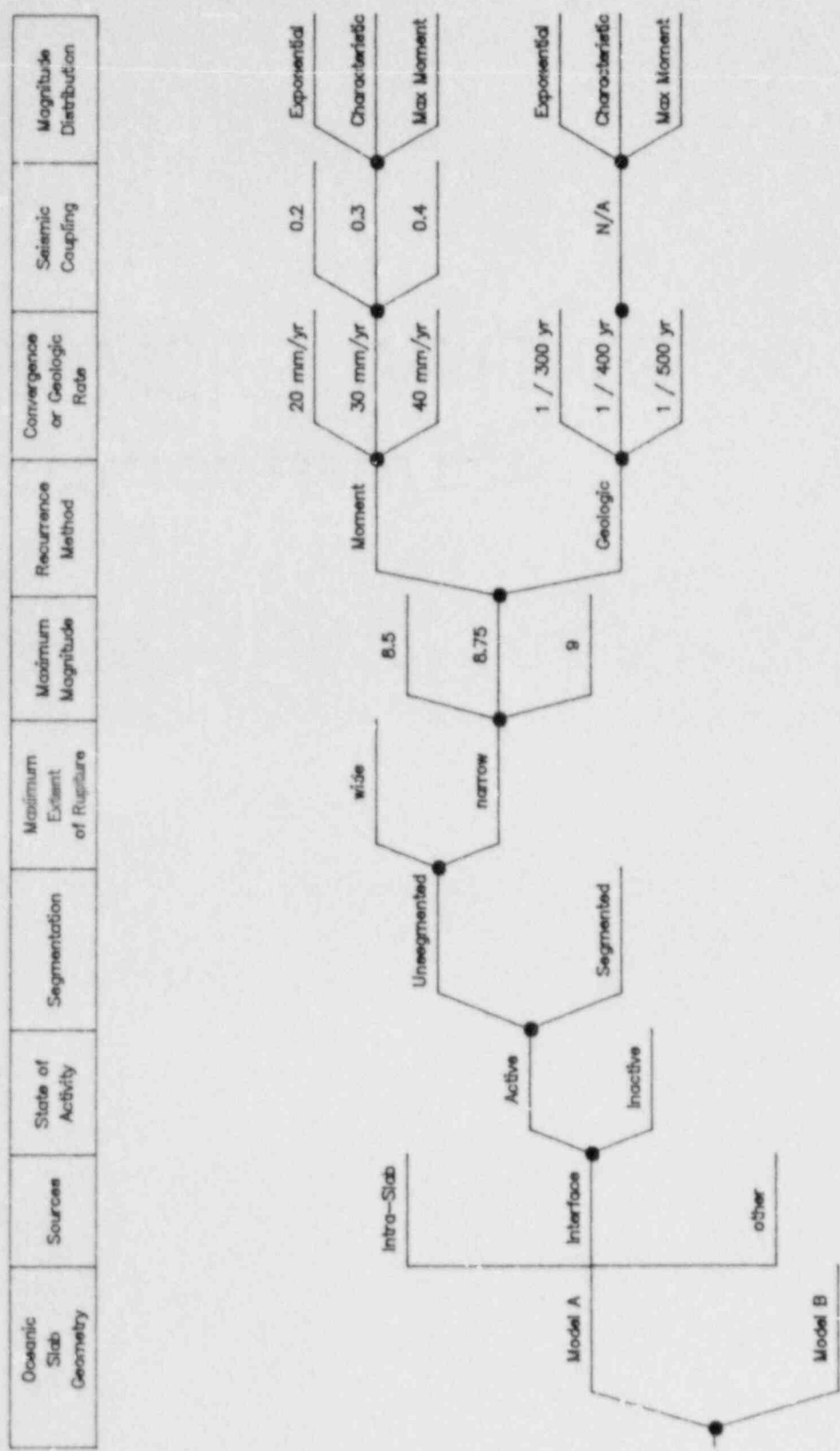
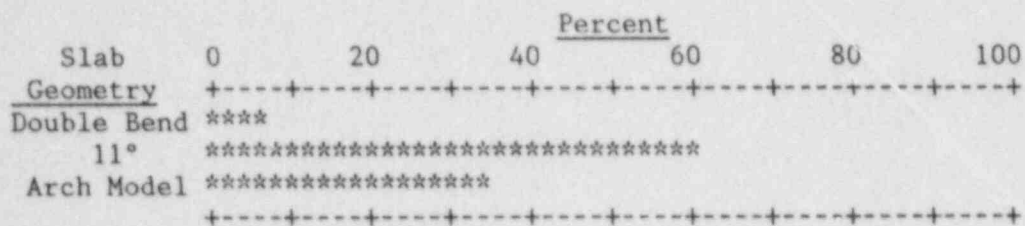


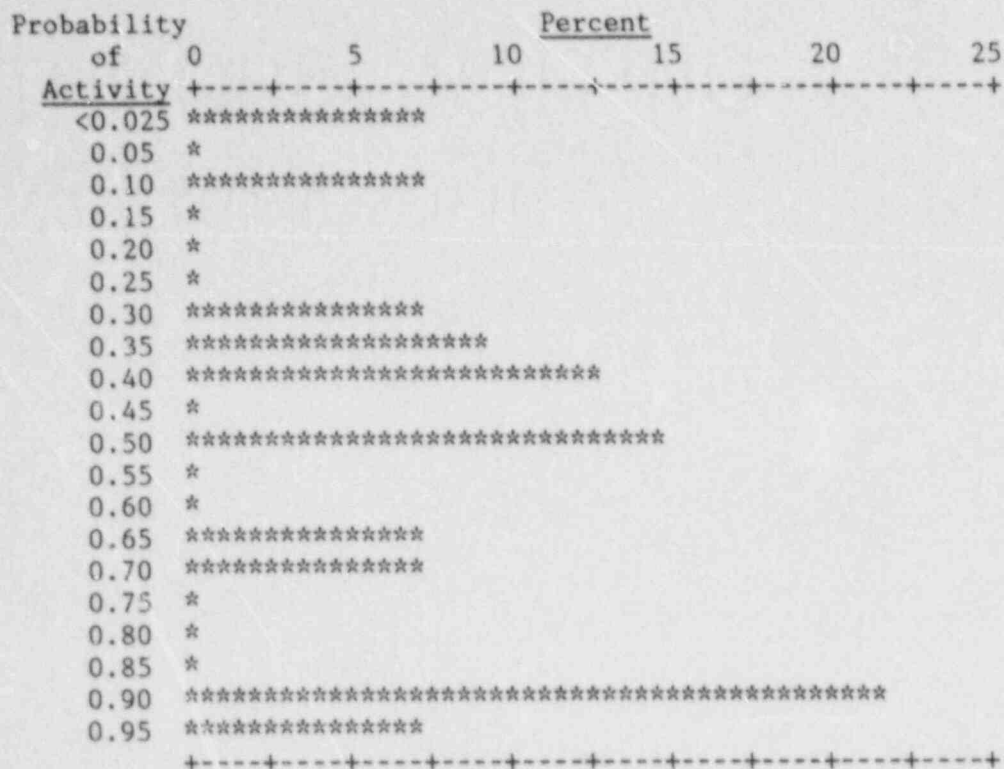
Figure 3-1. Subduction zone sources hazard model.



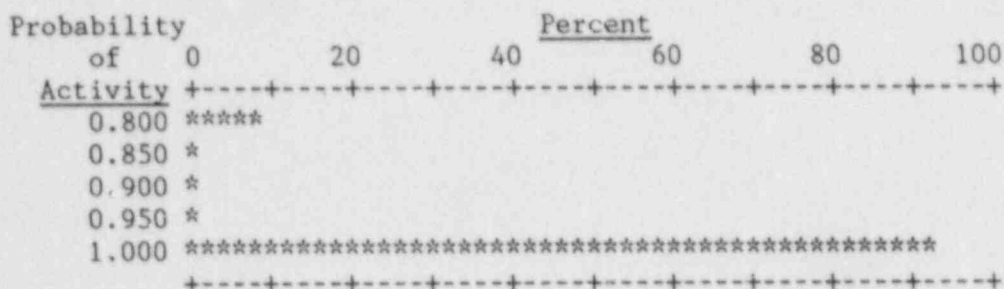


Distribution of 14 experts

Figure 3-2. Aggregate distribution of 14 experts for oceanic slab geometry

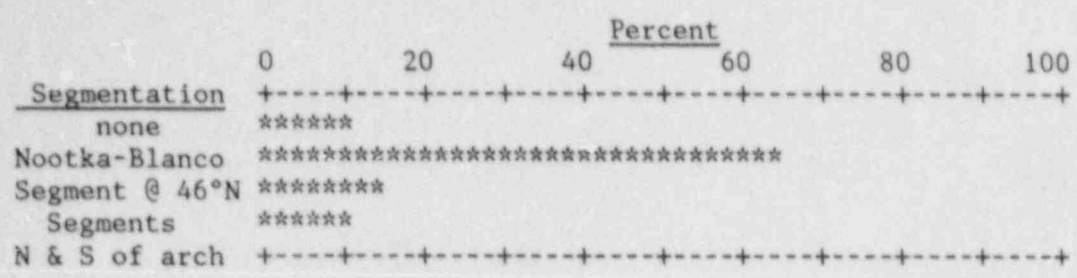


Aggregate distribution of 14 experts for interface activity

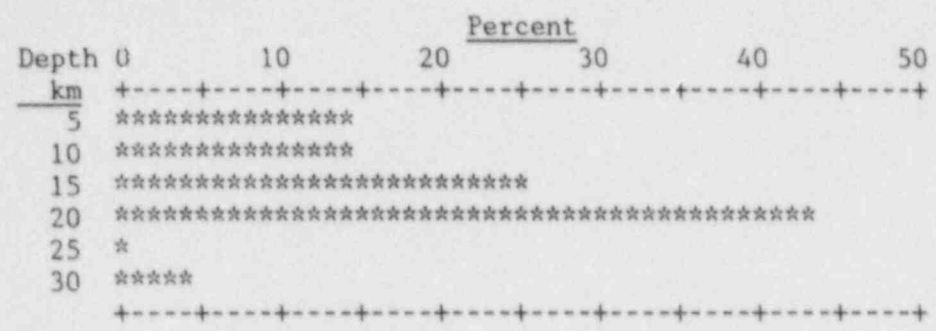


Aggregate distribution of 14 experts for intraslab activity

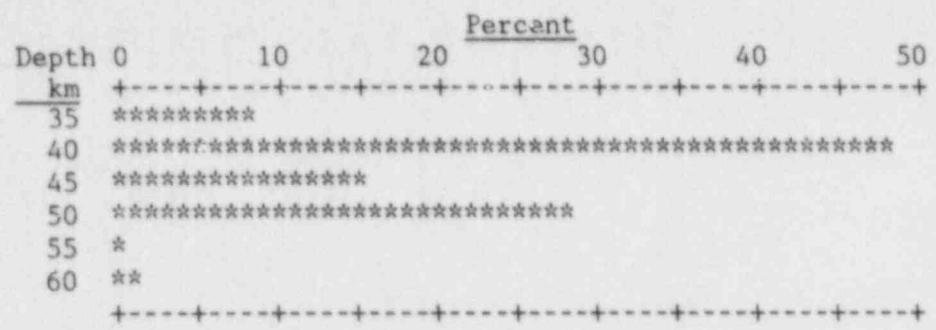
Figure 3-3. Aggregate distribution for probability of activity



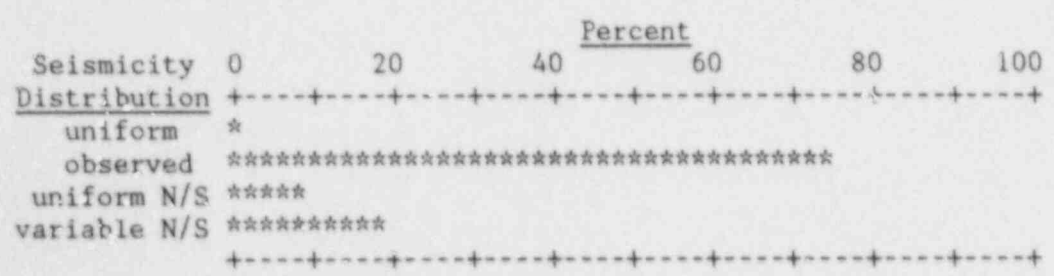
Aggregate distribution of 14 experts for interface segmentation



Aggregate distribution of 14 experts for minimum depth of rupture on interface



Aggregate distribution of 12 experts for maximum depth of rupture on interface



Aggregate distribution of 14 experts for intraslab seismicity distribution

Figure 3-4. Aggregate distributions for location of rupture

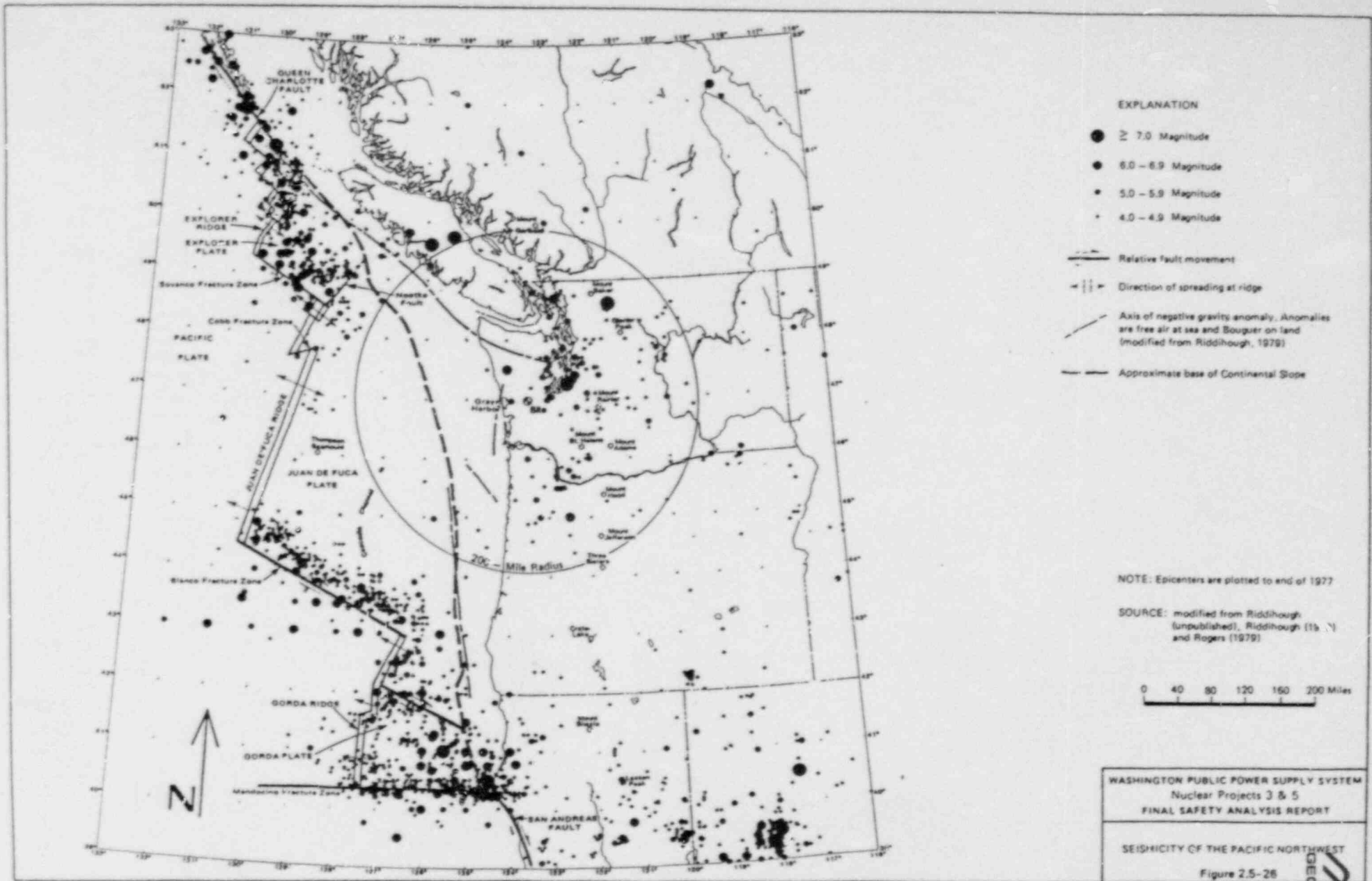
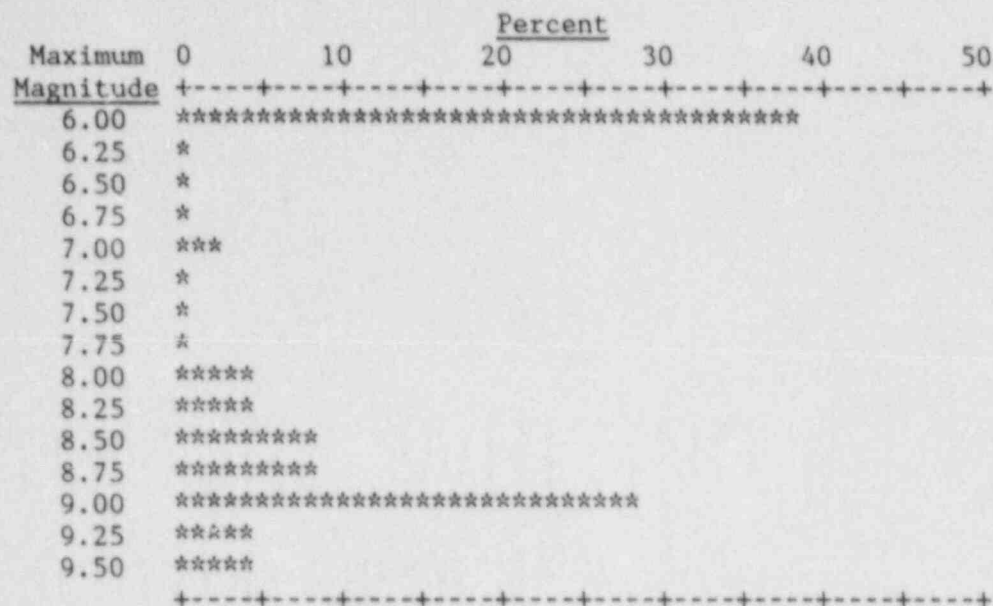
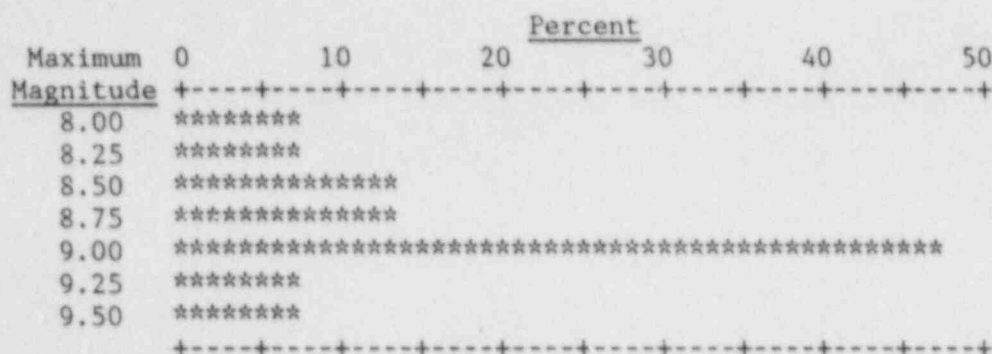


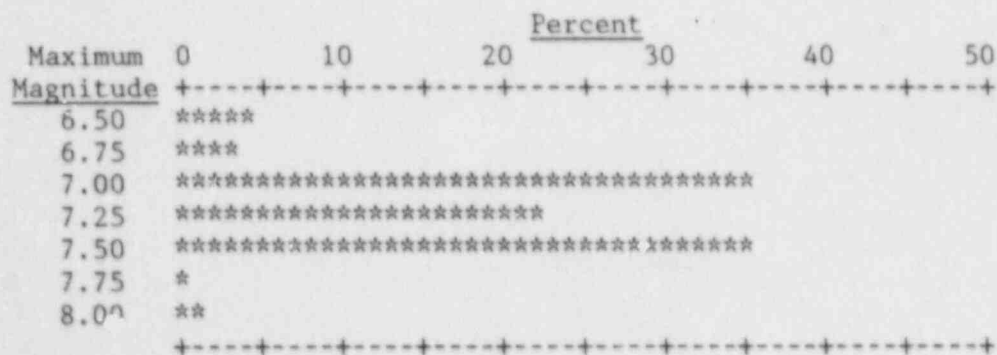
Figure 3-5 Plate Boundaries and Regional Seismicity



Aggregate distribution of 5 experts for directly assessed interface maximum magnitude



Conditional distribution of directly assessed interface maximum magnitude used for "gap filling"



Aggregate distribution of 11 experts for intraslab maximum magnitude

Figure 3-6. Aggregate distributions for maximum magnitude

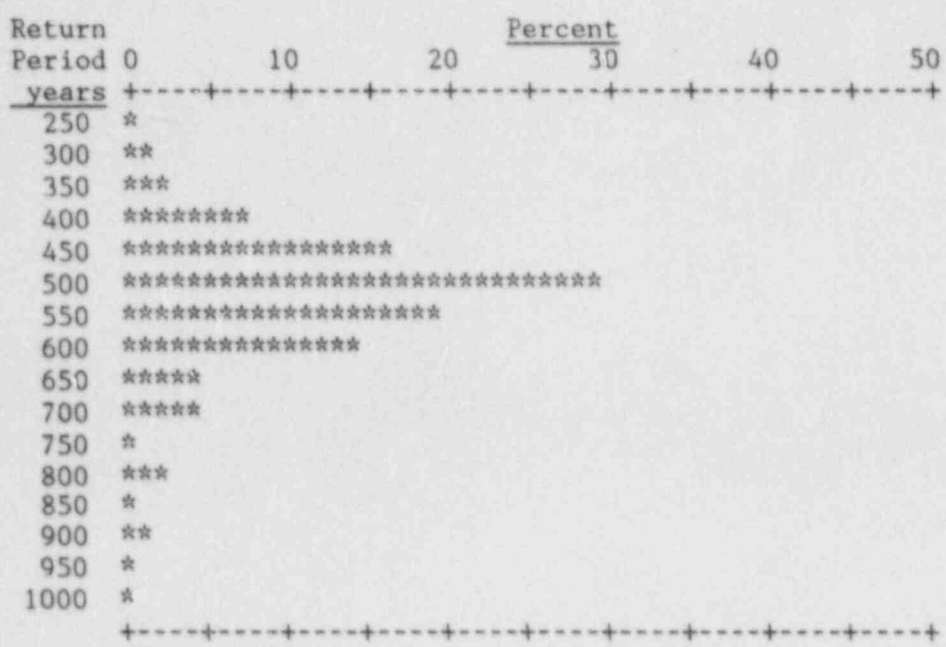
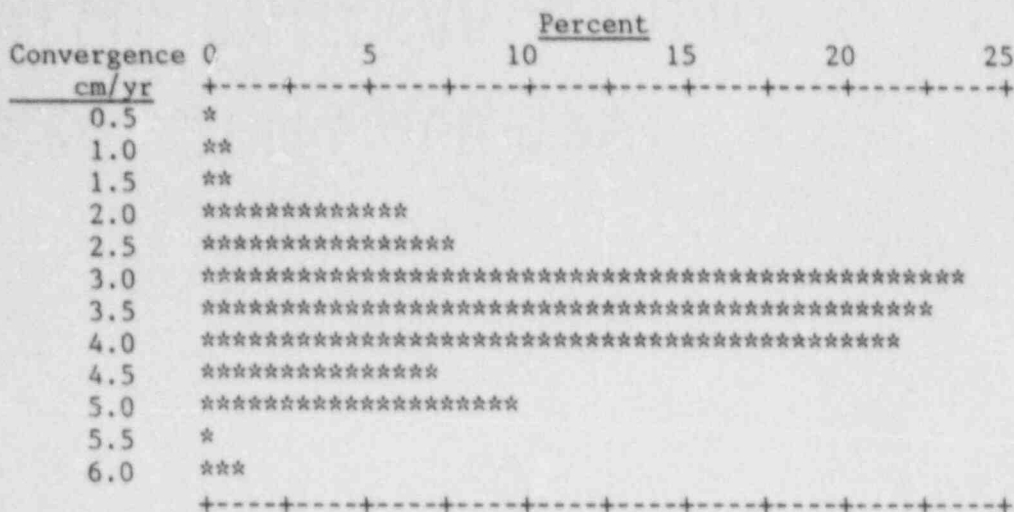
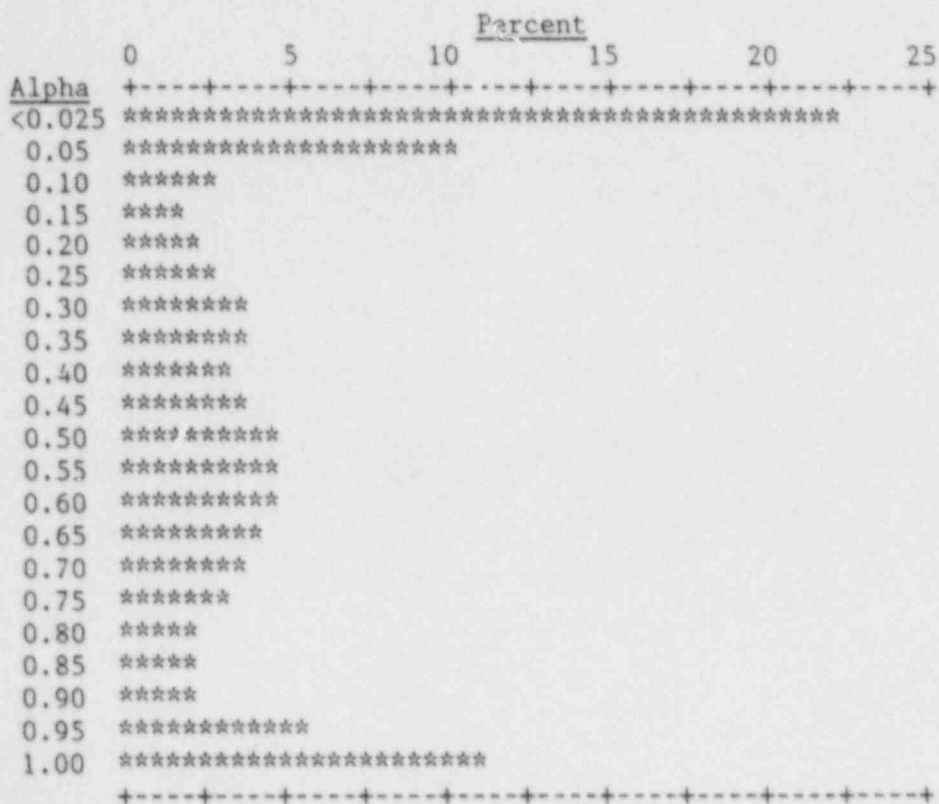


Figure 3-7. Aggregate distribution of 6 experts for return period of large interface earthquakes based on paleoseismic data



Aggregate distribution of 14 experts for convergence rate



Aggregate distribution of 10 experts for alpha

Figure 3-8. Aggregate distributions for moment rate parameters

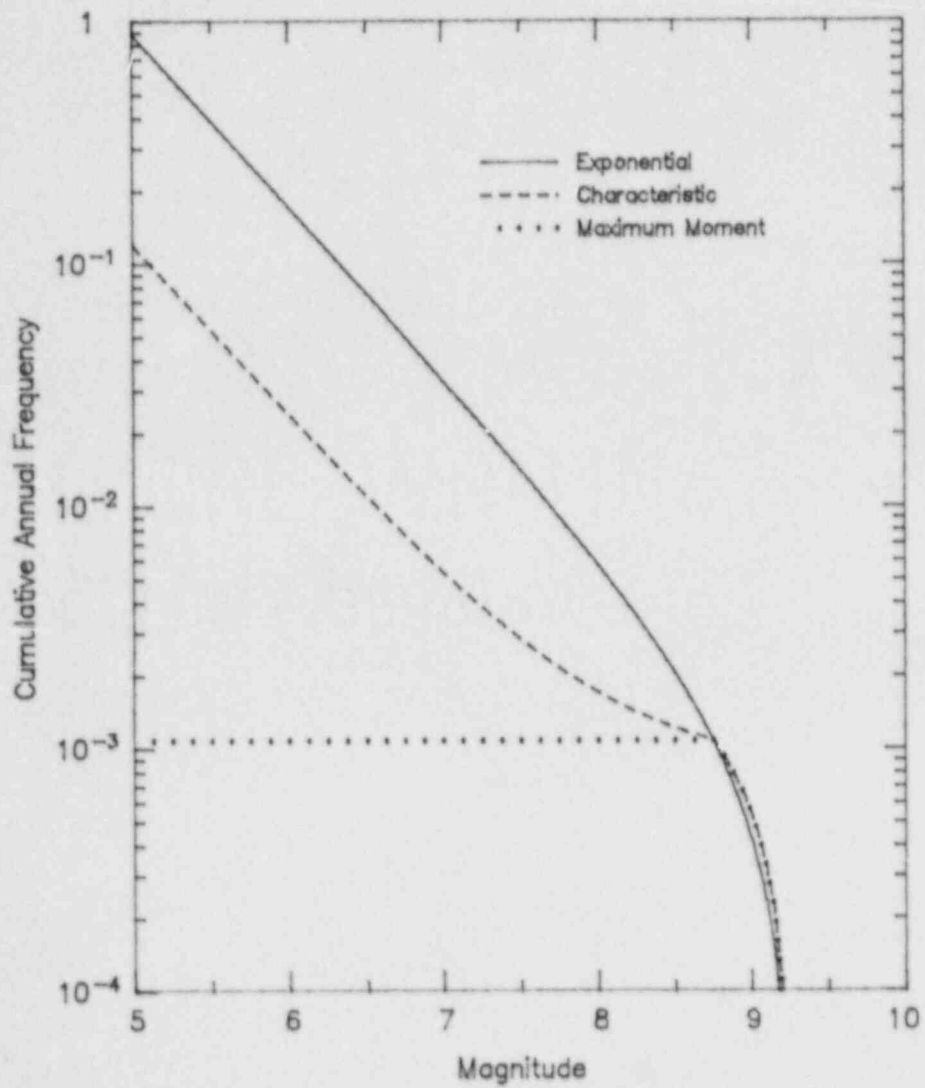


Figure 3-9 Magnitude frequency distributions used in the hazard analysis



Attenuation Model	Oceanic Slab Geometry	Sources	State of Activity	Segmentation	Maximum Extent of Rupture	Maximum Magnitude	Recurrence Method	Convergence or Geologic Rate	Seismic Coupling	Magnitude Distribution
-------------------	-----------------------	---------	-------------------	--------------	---------------------------	-------------------	-------------------	------------------------------	------------------	------------------------

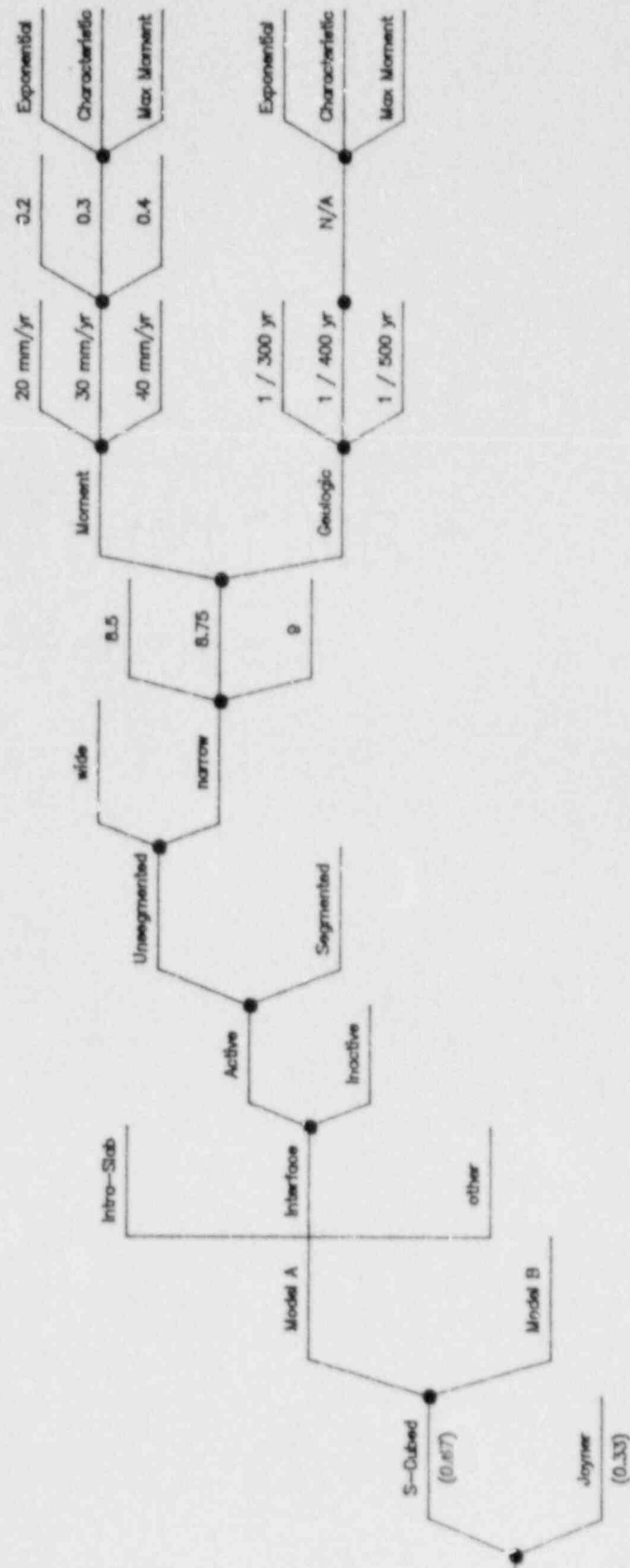


Figure 3-10. Complete subduction zone sources hazard model.

Attenuation Relationship	Sources	Maximum Magnitude	Recurrence Method	Recurrence or Slip Rate
--------------------------	---------	-------------------	-------------------	-------------------------

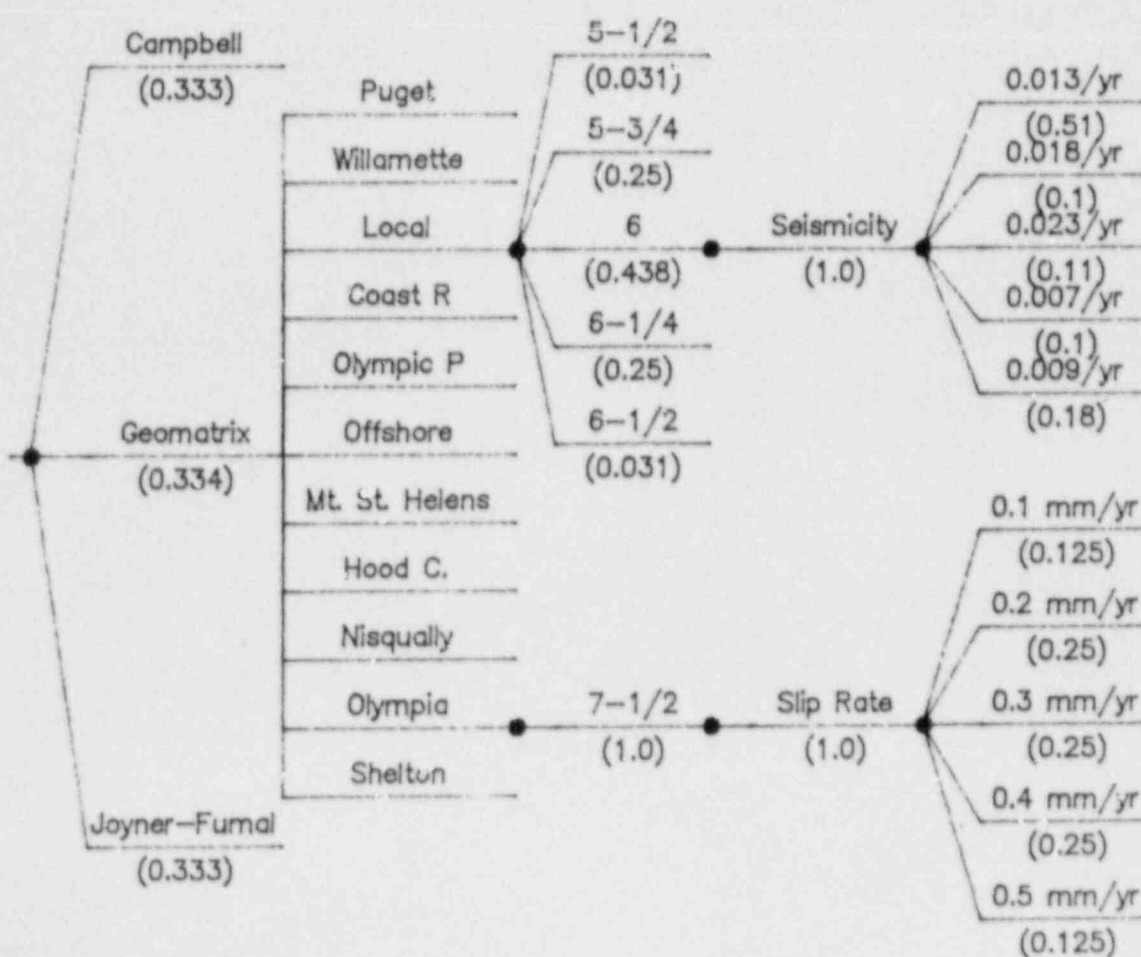


Figure 3-11. Shallow crustal sources hazard model.

## 4.0 ANALYSIS RESULTS

### 4.1 Hazard Computation

Seismic hazard computations were made for each of the hazard model logic trees developed in Section 3 utilizing the formulation given in Section 2. The hazard was computed considering the contributions of earthquakes of magnitude 4.0 and greater for the local shallow crustal sources and magnitude 5.0 and greater for all other sources. The probability density functions for distance to earthquake rupture were developed by modeling earthquake ruptures as rectangular rupture areas distributed over a fault plane. The plate interface and the individual shallow crustal features were modeled as single fault planes with earthquake ruptures distributed over the fault surface. Distributed area sources, including the intraslab source, were modeled as a series of parallel fault planes occupying the volume specified for the source. Spatially variable seismicity rate was modeled by specifying the fraction of the total seismicity that occurs on each fault plane.

The mean rupture area of an event was specified by the following relationships:

$$\text{rupture area} = \exp(2.28M_w - 8.92) \quad (4-1)$$

for interface events, and

$$\text{rupture area} = \exp(2.0M_w - 7.12) \quad (4-1)$$

for all other events. These relationships were developed by linear regression of  $\ln(\text{rupture area})$  on magnitude using the data presented by Abe (1975) and Wyss (1979).

Hazard computations were made for each end branch of the logic trees developed to model the uncertainty in input parameters. The resulting discrete distributions for annual frequency of exceedance of a range of ground motion levels were used to define 15<sup>th</sup>, 50<sup>th</sup> (median) and 85<sup>th</sup> percentile hazard

curves to represent the uncertainty in the exceedance frequency. The computations were made for peak ground acceleration and spectral velocity at periods of 0.15 and 0.8, 2.0 seconds. The periods of 0.15 and 0.8 seconds represent the periods of maximum amplification of spectral acceleration and spectral velocity, respectively, in the response spectrum developed for subduction zone earthquakes (see Appendix D).

#### 4.2 Exceedance Frequency for Peak Ground Acceleration

4.2.1 Total Hazard. Figure 4-1 presents the computed hazard for peak horizontal acceleration. Shown are the 15<sup>th</sup>, 50<sup>th</sup>, and 85<sup>th</sup> percentile hazard curves for the shallow crustal sources, the subduction zone sources, and the combined total hazard. The hazard curves for the subduction zone sources are from an equally weighted aggregate distribution of the 14 expert assessments. As can be seen, the hazard is dominated by potential subduction zone events. The 15<sup>th</sup> and 85<sup>th</sup> percentile curves for the total hazard differ by approximately a factor of 2 at low acceleration levels to a factor of about 10 at high acceleration levels.

Figure 4-2 presents the average contributions to the total hazard from events in various distance and magnitude increments and from various sources for peak accelerations of 0.1, 0.3, and 0.5 g. At low acceleration levels, the hazard results primarily from contributions from the smaller, more frequent events. As the acceleration level increases, the larger magnitude events increasingly dominate the hazard. There is also a major contribution from intraslab events in the magnitude 6 to 7.5 range. The major contribution to the hazard is from events in the distance range of 25 to 65 km corresponding to the closer portions of the plate interface and subducting slab.

The hazard results for the two sets of seismic sources are discussed below.

4.2.2 Subduction Zone Sources. The seismic hazard from the subduction zone sources was computed using the input parameters defined by the 14 experts. The primary approach used in the analysis was to develop a set of input

parameters for each individual expert and then average the resulting 14 hazard distributions to develop an aggregate hazard distribution.

Results for Individual Experts. Hazard models were developed for each of the 14 experts using their individual parameters when they provided a response for a given component and aggregate marginal distributions of the assessments of the other experts when they did not respond. The complexity of the logic trees for the individual experts varied dramatically from a minimum of 15 branches to a maximum of 1000 branches. In general, those experts with large final logic trees did not provide a complete hazard model; the complexity reflects rather the use of the aggregate of the opinions of the other experts for missing components. Hazard computations were performed for each expert's model using the two attenuation models developed in Appendix D.

Figure 4-3 presents the median hazard curves obtained from the logic trees of each expert. The range of median hazard curves spans about one and one-half orders of magnitude. Figure 4-4 shows the 15<sup>th</sup>, 50<sup>th</sup>, and 85<sup>th</sup> percentile hazard curves for each expert. As can be seen, there is generally an order of magnitude difference between each expert's 15<sup>th</sup> and 85<sup>th</sup> percentile hazard curves, which is comparable to the variation between experts shown in Figure 4-3.

Figure 4-5 shows the 15<sup>th</sup>, 50<sup>th</sup>, and 85<sup>th</sup> hazard curves for the two subduction zone sources treated separately for each expert. The solid curves are for the interface source and the dashed curves for the intraslab sources. In many cases, 15<sup>th</sup>, or 15<sup>th</sup> and 50<sup>th</sup> hazard curves are not shown for the interface source, reflecting the assigned probability of the interface being inactive greater than the missing percentile hazard curves. For example, Expert 1 assigned a probability of 0.35 that the interface is active, giving a probability of 0.65 that it is inactive. Thus the 15<sup>th</sup> and 50<sup>th</sup> percentile hazard curves for the interface are zero. Experts 4 and 13 have assigned probabilities less than 0.1 that the interface is active at a magnitude level greater than 5 and thus all three percentile hazard curves are zero.

As can be seen, there is greater variability between experts in the assessment of the hazard from the interface source than the hazard from the intraslab sources.

Aggregated Hazard. As indicated above, the primary approach used to aggregate the assessments of the 14 experts was to form an equal weighted average of the hazard distributions obtained for each expert. Figure 4-6 presents the resulting distribution for exceedance frequency. Shown are the 15<sup>th</sup>, 50<sup>th</sup>, and 85<sup>th</sup> percentile hazard curves for the aggregated distribution (solid curves) as well as the median hazard curves for the 14 experts. The 15<sup>th</sup> and 85<sup>th</sup> percentile hazard curves of the aggregated distributions encompass the median hazard curves of 10 out of 14 experts and an equal number of individual expert medians lie above and below the aggregate median.

Figure 4-7 presents the results of the alternate aggregation approach discussed in Section 2.3. In this approach, the aggregated marginal distributions for each component of the hazard model were used to construct a single composite hazard model logic tree. As shown in Figure 4-7, the composite model hazard curves are very similar to the aggregate hazard curves.

Contributions to Uncertainty. The contributions of uncertainty in various components of the hazard models to the uncertainty in the computed hazard are illustrated in Figures 4-8 through 4-18. Figure 4-8 compares the 15<sup>th</sup> and 85<sup>th</sup> hazard curves considering expert-to-expert variability (dashed lines) with the 15<sup>th</sup> and 85<sup>th</sup> percentile hazard curves representing the total uncertainty. The difference between the 15<sup>th</sup> and 85<sup>th</sup> percentile ranked experts is nearly equal to the difference between the 15<sup>th</sup> and 85<sup>th</sup> percentile curves including all uncertainties. Taking the relative difference in the spread between the 15<sup>th</sup> and 85<sup>th</sup> percentile curves as a measure of the relative difference in the square root of the variance in hazard, the expert-to-expert uncertainty contributes approximately two-thirds of the total variance in hazard.

Figure 4-9 shows the contributions to uncertainty in hazard resulting from uncertainty in modeling subduction zone earthquake ground motions. The plot on the left compares the hazard curves obtained considering both interface and intraslab events and the plot on the right shows the hazard curves considering only the hazard from interface earthquakes. As can be seen, there is only a minimal difference in the two hazard curves reflecting the large contributions to hazard from events below magnitude 8 (Figure 4-2) for which there is no difference in attenuation relationships.

Figures 4-10 through 4-18 present the contributions to the uncertainty in hazard due to the uncertainty in various components of the individual experts hazard models. In each figure the solid lines are the 15<sup>th</sup> and 85<sup>th</sup> percentile hazard curves resulting from the total uncertainty from all components of the hazard model and the dashed curves represent the 15<sup>th</sup> and 85<sup>th</sup> percentile conditional mean hazard curves considering uncertainty only in the component identified in the figure title. (Fractiles of means are shown rather than fractiles of medians because they are more efficient to compute, although they result in a shift away from the median hazard toward the higher percentiles of the distribution). The contributions to the total uncertainty vary from component to component and from expert to expert. For any one component, the width of the distribution shown in Figures 4-10 through 4-18 reflects both the amount of uncertainty in the assessment of the parameter and the sensitivity of the computed hazard to variability in the parameter. For example, the results presented in Figure 4-10 show that the effect of uncertainty in the geometry of the subducting slab on the hazard is small. For most of the experts this results because they selected only a single model for the slab geometry. However, even for those experts who considered alternative geometries, such as experts 1 and 14, the impact on the hazard is relatively small. Alternatively, the results presented in Figure 4-11 indicate that uncertainty in source activity has a significant impact on the uncertainty in hazard. The reason for this large effect was shown previously in Figure 4-5. As indicated in that figure, the hazard from the interface is generally comparable to or higher than the hazard from

the intraslab events, thus the hazard is significantly altered depending on whether or not the interface is seismogenic.

Examination of Figures 4-10 through 4-18 indicate that the major contribution to "within expert" uncertainty is from uncertainty in source activity. The contribution of "within expert" uncertainty to the total uncertainty can be estimated from the results presented in Figures 4-8 and 4-9. The total variance in the hazard is the sum of the expert-to-expert variance, the variance due to uncertainty in modeling the attenuation characteristics, and the average within expert variance. As the expert-to-expert variance was estimated above to be approximately two-thirds of the total variance and the uncertainty in attenuation contributed little to the uncertainty in hazard, the average "within expert" variance is approximately one-third of the total variance.

4.2.3 Shallow Crustal Sources. Figure 4-19 presents the hazard computed for the shallow crustal sources. The plot on the left compares the 15<sup>th</sup>, 50<sup>th</sup>, and 85<sup>th</sup> percentile hazard curves for the shallow crustal sources with those for the subduction zone sources. As can be seen, the median hazard from shallow sources is approximately one and one-half order of magnitude lower than the median for subduction zone sources and the range between the 15<sup>th</sup> and 85<sup>th</sup> percentile curves is greater. Shown on the right in Figure 4-19 are the median hazard curves for the various shallow crustal sources. As indicated by the comparisons in the figure, the hazard from shallow crustal earthquakes is dominated by the local random seismicity source.

Figure 4-20 presents the contributions to the uncertainty in the hazard from shallow crustal earthquakes from uncertainty in selecting the appropriate attenuation relationship, uncertainty in maximum magnitude, and uncertainty in recurrence rate. The uncertainty in hazard is largely due to uncertainty in modeling attenuation with a small contribution from uncertainty in estimating earthquake recurrence rates. The large uncertainty in maximum magnitude for the local random events has little impact.



### 4.3 Exceedance Frequency for Spectral Velocity

Figure 4-21 presents the computed hazard for 5-percent damped spectral velocity at periods of 0.15, 0.8, and 2 seconds. Comparison of these results with the hazard curves for peak acceleration shown in Figure 4-1 indicates that the shallow crustal sources have a similar level of contribution to hazard for spectral accelerations as their contribution to hazard for peak acceleration. Figures 4-22 through 4-24 present the 15<sup>th</sup>, 50<sup>th</sup>, and 85<sup>th</sup> percentile hazard curves for the individual experts, for periods of 0.15, 0.8, and 2 seconds, respectively. As can be seen, the uncertainty in hazard increases somewhat for longer period motions, reflecting greater impact of the uncertainty in the potential for very large events on the plate interface.

The individual expert median hazard curves are compared with the 15<sup>th</sup>, 50<sup>th</sup>, and 85<sup>th</sup> percentile hazard curves for the aggregated distribution in Figure 4-24. As was the case for peak acceleration, the 15<sup>th</sup> and 85<sup>th</sup> percentile hazard curves for the aggregated hazard encompass the median curves for 10 to 11 of the 14 experts. The relative position of the median curves for individual experts is similar to that shown for peak acceleration in Figure 4-3. The results also indicate that the expert-to-expert variability contributes approximately the same proportion of the total uncertainty as was observed for peak acceleration.

Figure 4-26 compares the results for the two approaches used for aggregation. As was the case for peak acceleration, component level aggregation results in similar hazard curves to those obtained using the aggregate of the 14 experts' hazard distribution.

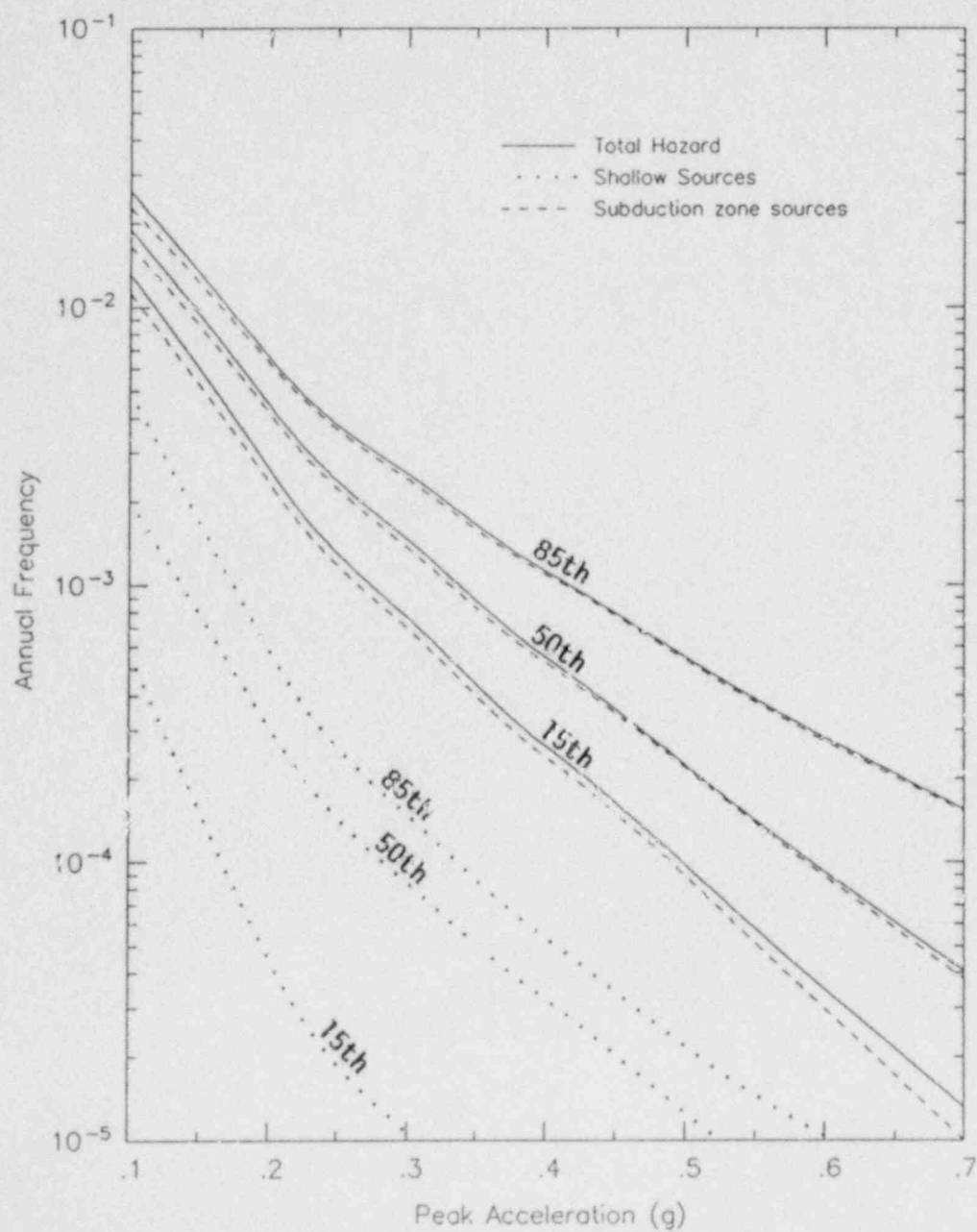


Figure 4-1. Percentile hazard curves for peak horizontal acceleration showing contributions of shallow crustal and subduction zone sources to total hazard.

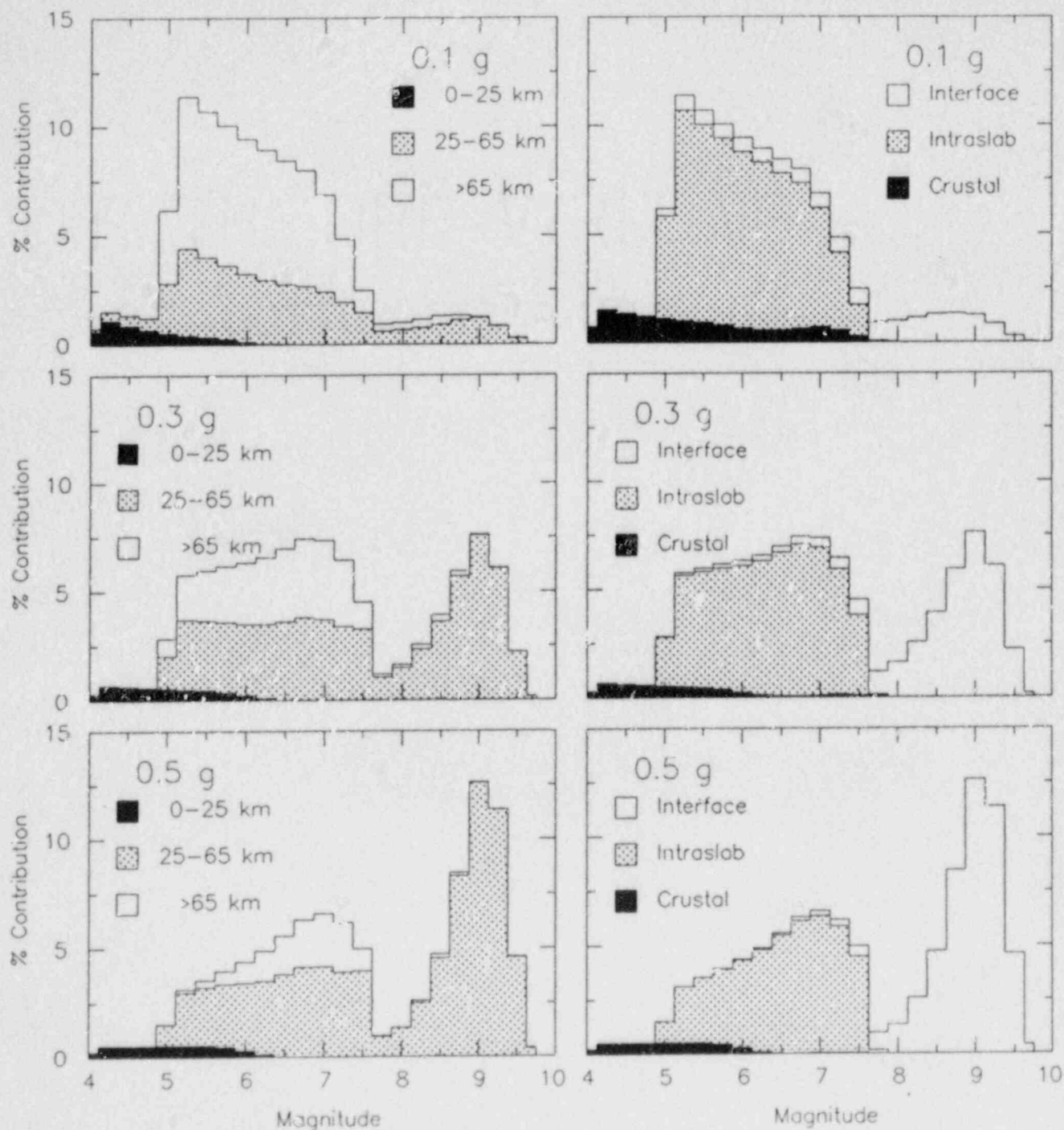


Figure 4-2. Contributions to total hazard shown in terms of magnitude, distance, and source contributions.

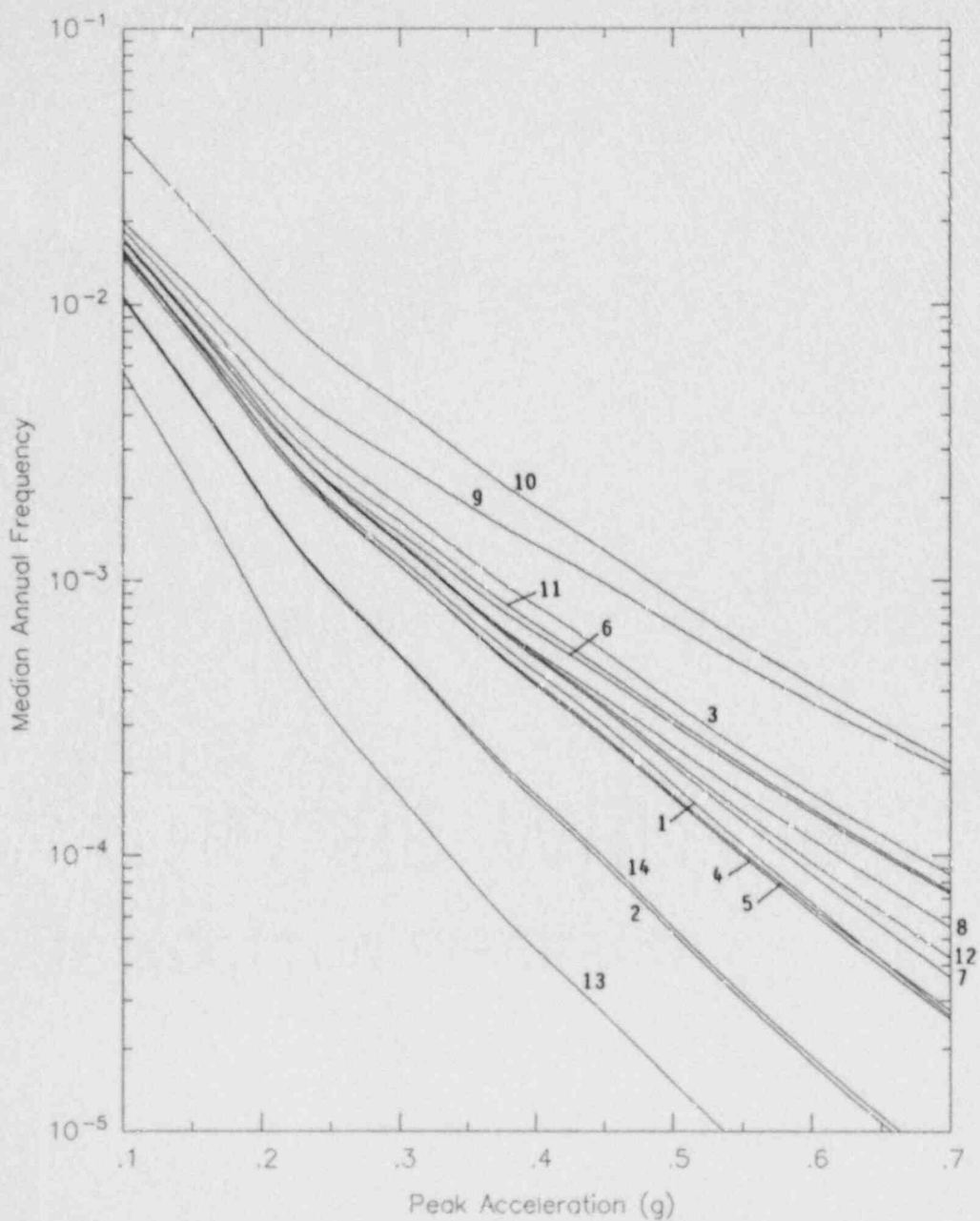


Figure 4-3. Comparison of median hazard curves of individual experts.

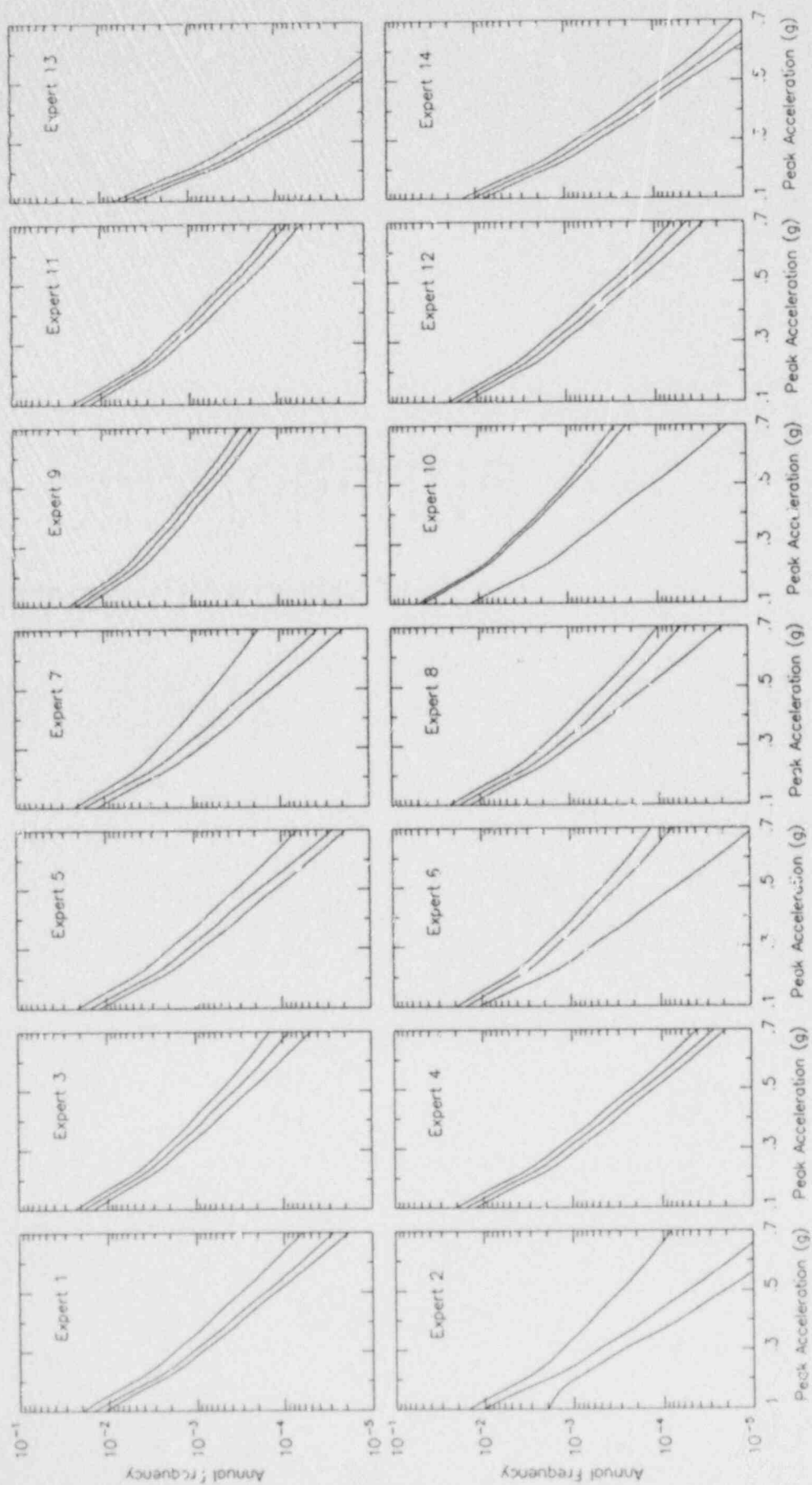


Figure 4-4. 15<sup>th</sup>, 50<sup>th</sup>, and 85<sup>th</sup> percentile hazard curves for individual experts.

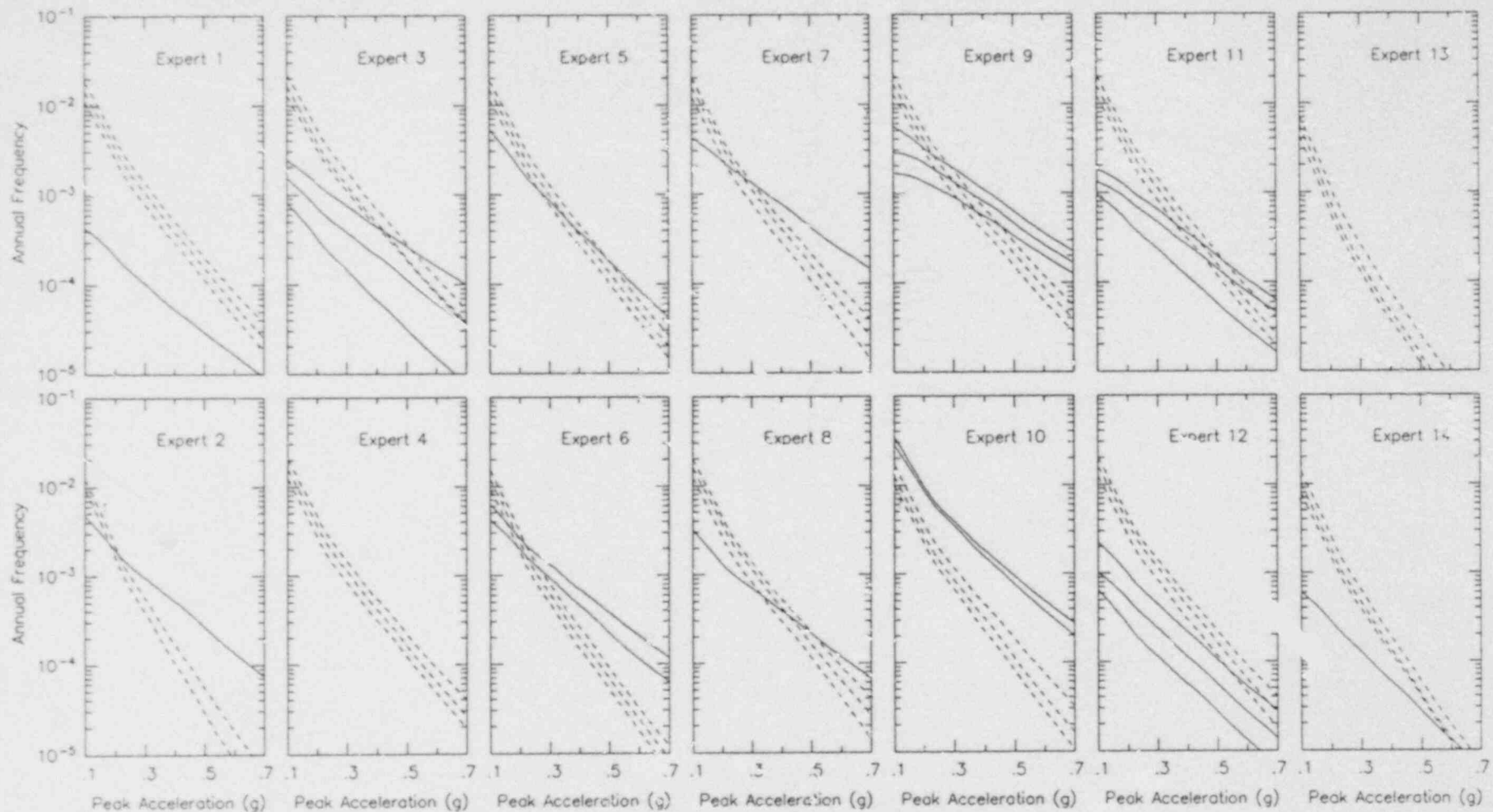


Figure 4-5. 15<sup>th</sup>, 50<sup>th</sup>, and 85<sup>th</sup> percentile curves for interface (solid curves) and intraslab (dashed curves) sources for individual experts.

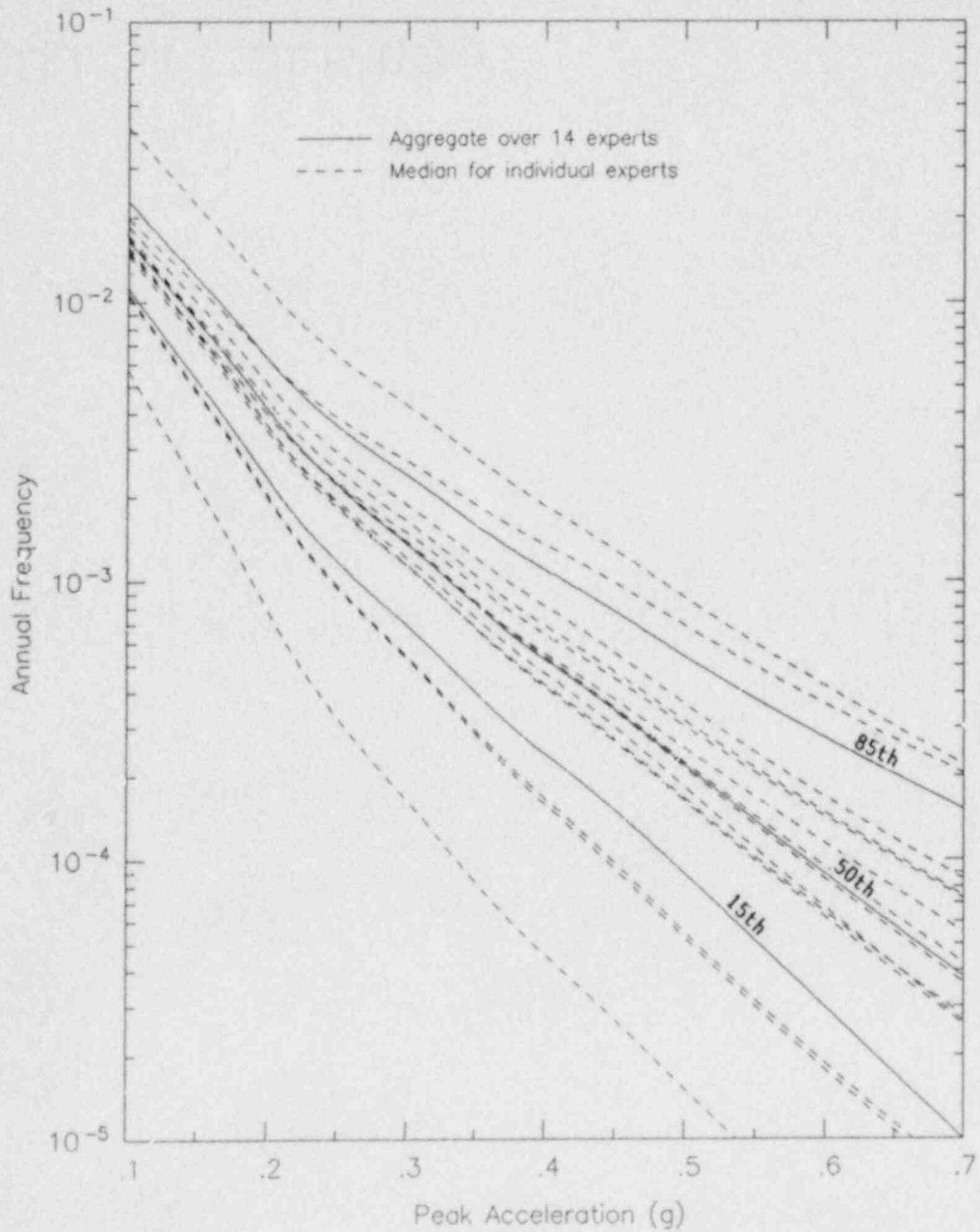


Figure 4-6. Comparison of experts' median hazard curves with aggregate hazard.

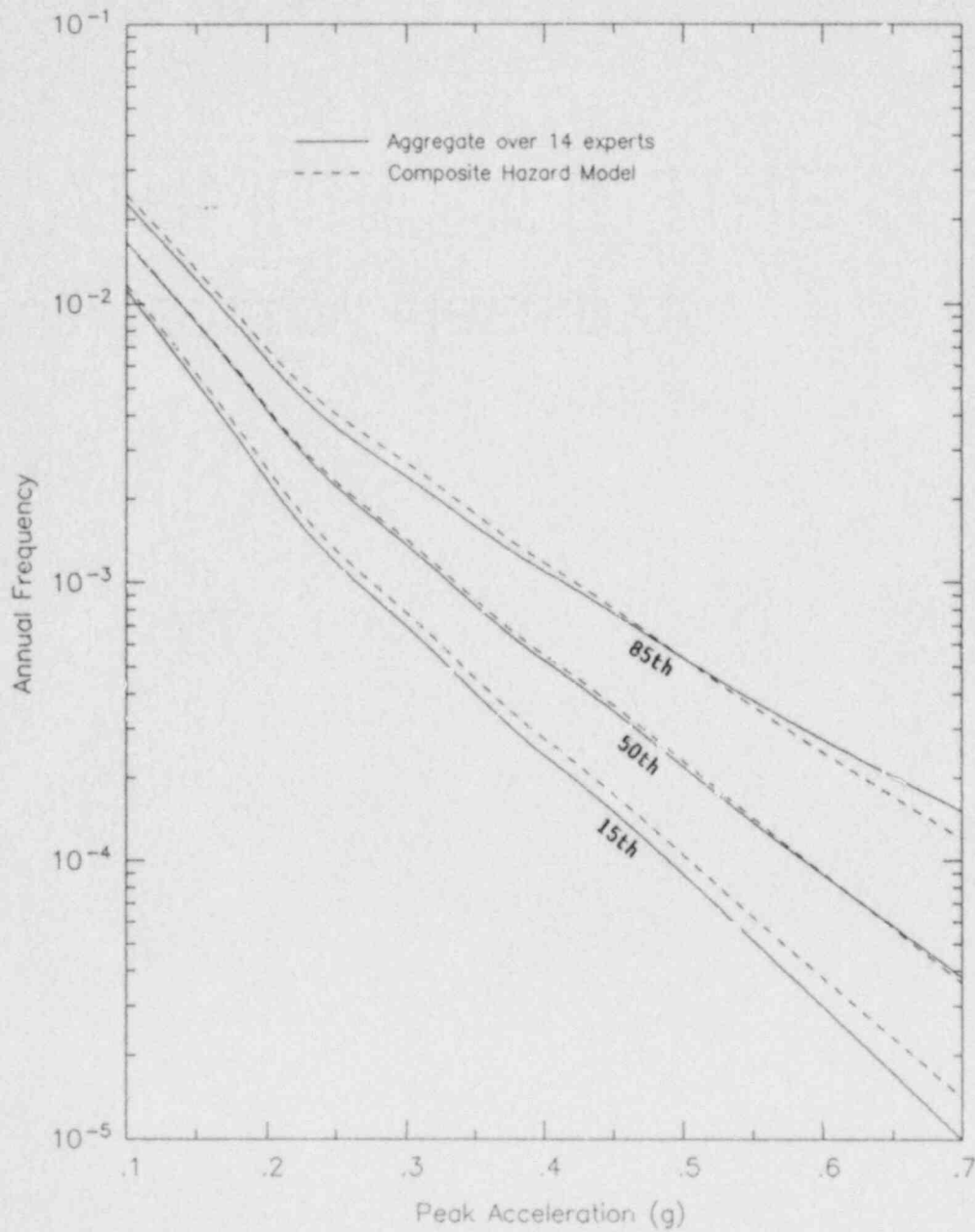


Figure 4-7. Comparison of aggregation procedures for total hazard from subduction zone sources.



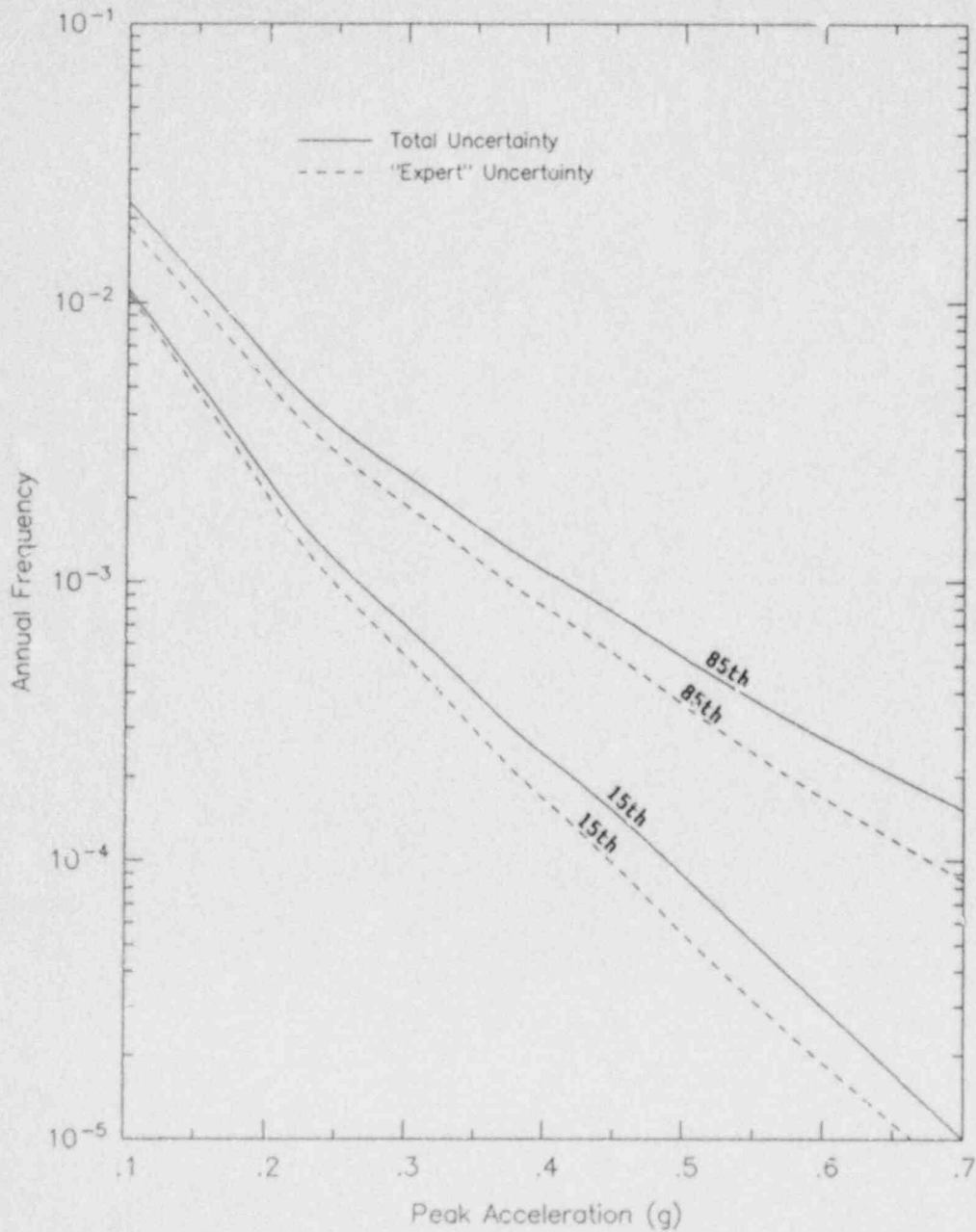


Figure 4-8. Contribution of expert-to-expert uncertainty to total uncertainty.

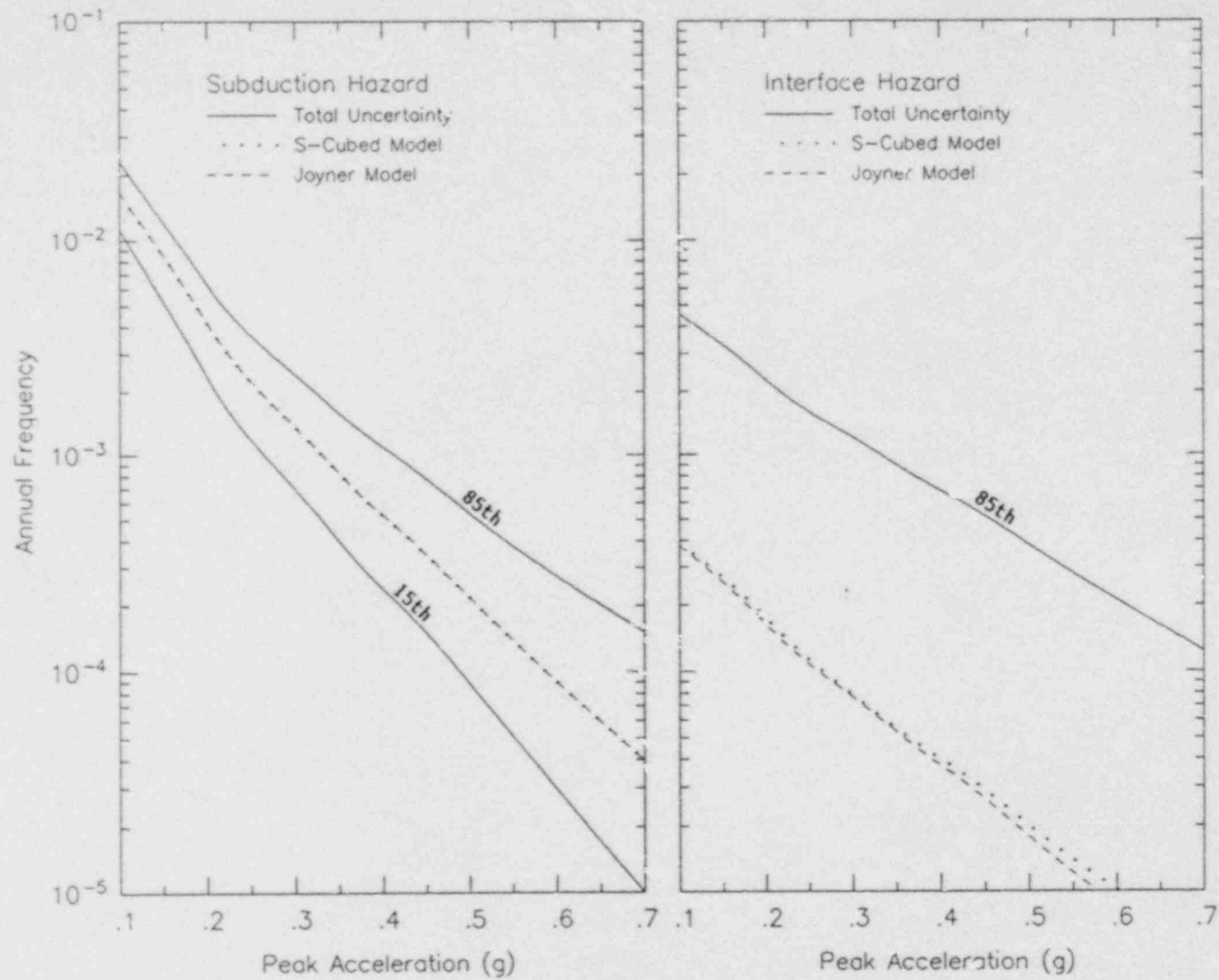


Figure 4-9. Contribution of uncertainty in subduction zone attenuation relationships to total uncertainty.

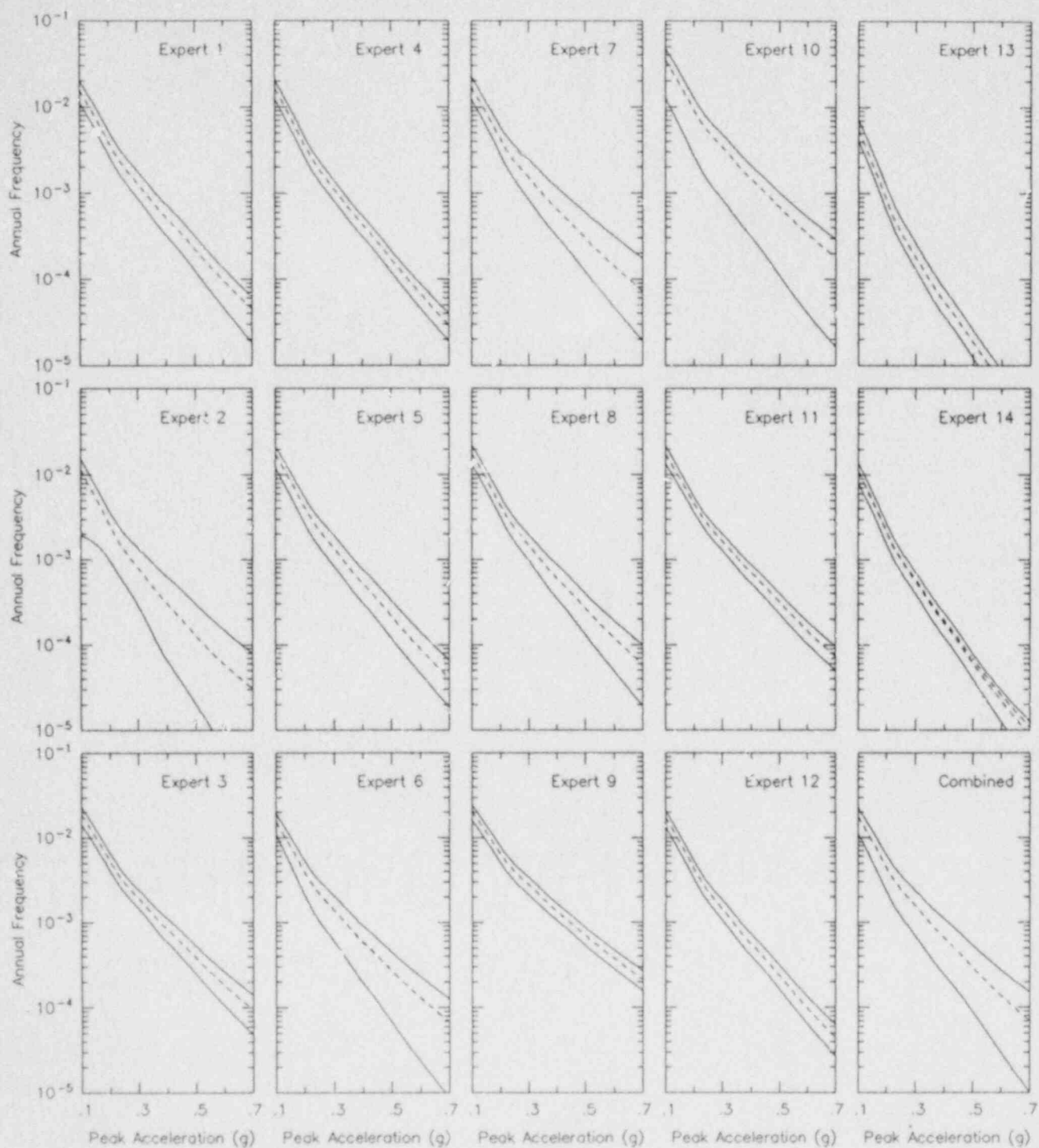


Figure 4-10. Contributions of uncertainty in subducting plate geometry to total uncertainty. Shown are the 15<sup>th</sup> and 85<sup>th</sup> percentiles considering all uncertainties (solid lines) and the 15<sup>th</sup> and 85<sup>th</sup> percentiles considering only uncertainty in plate geometry (dashed line).

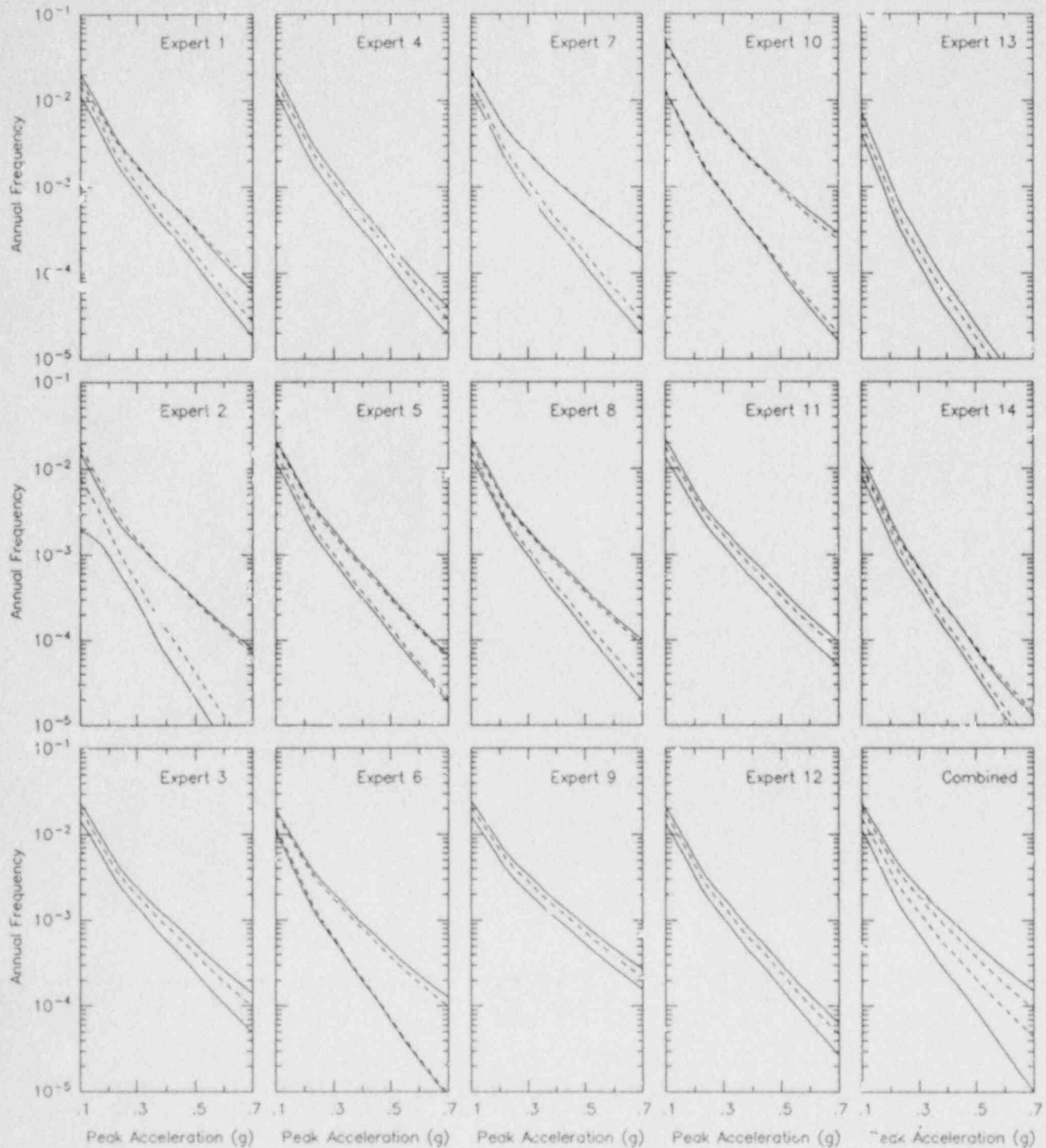


Figure 4-11. Contributions of uncertainty in source activity to total uncertainty. Shown are the 15<sup>th</sup> and 85<sup>th</sup> percentiles considering all uncertainties (solid lines) and the 15<sup>th</sup> and 35<sup>th</sup> percentiles considering only uncertainty in source activity (dashed line).

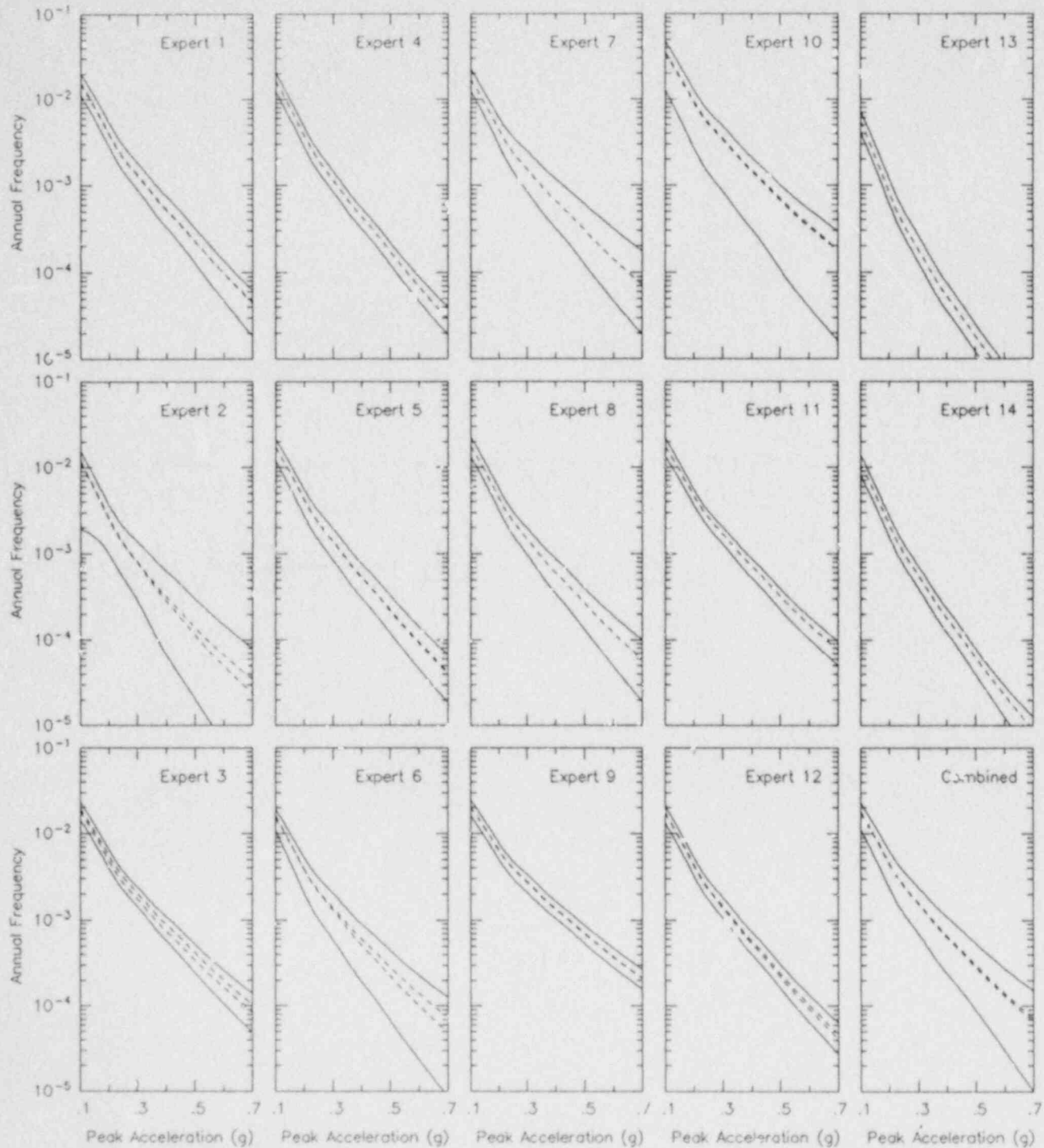


Figure 4-12. Contributions of uncertainty in source segmentation to total uncertainty. Shown are the 15<sup>th</sup> and 85<sup>th</sup> percentiles considering all uncertainties (solid lines) and the 15<sup>th</sup> and 85<sup>th</sup> percentiles considering only uncertainty in source segmentation (dashed line).

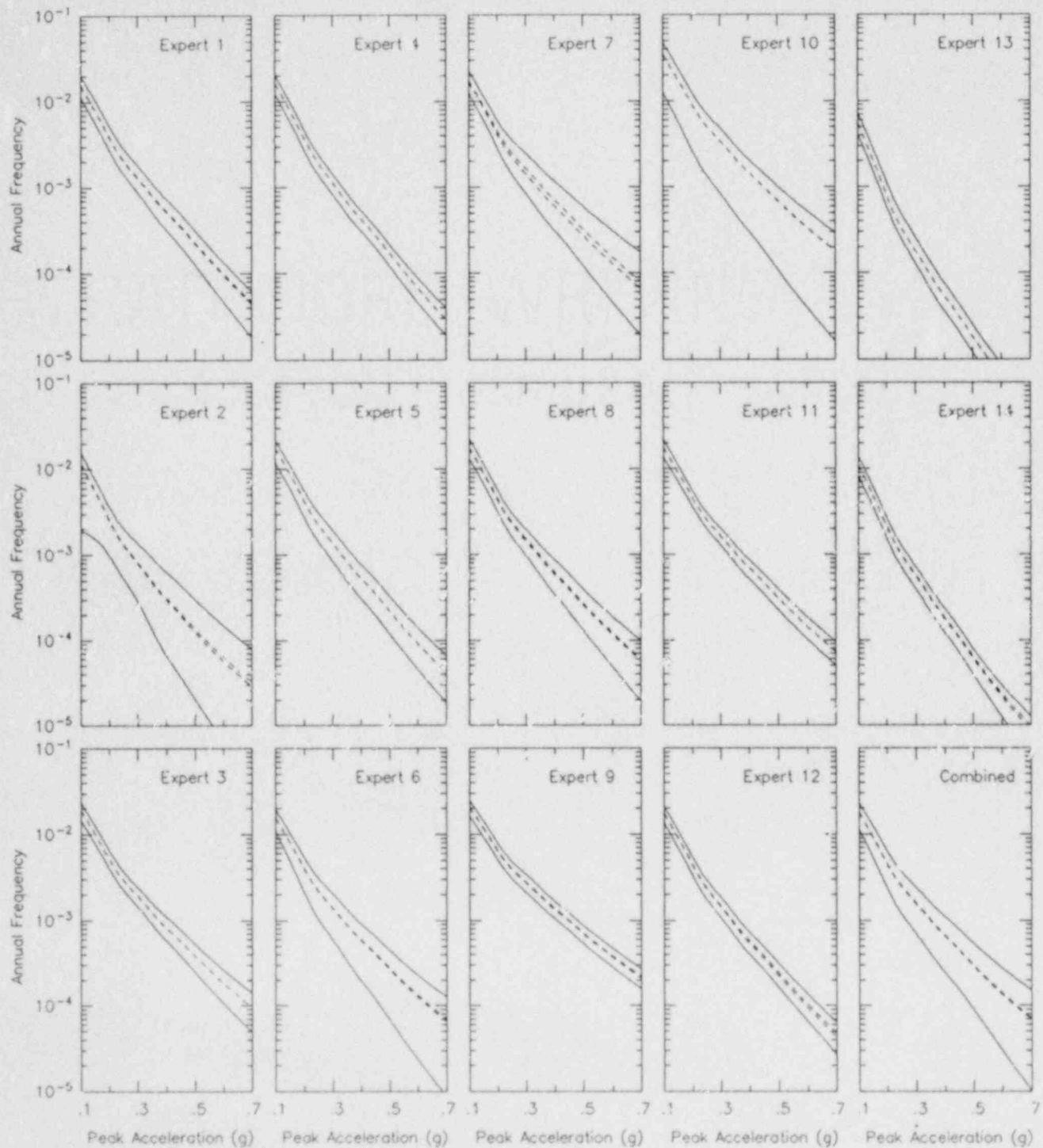


Figure 4-13. Contributions of uncertainty in maximum extent of rupture to total uncertainty. Shown are the 15<sup>th</sup> and 85<sup>th</sup> percentiles considering all uncertainties (solid lines) and the 15<sup>th</sup> and 85<sup>th</sup> percentiles considering only uncertainty in maximum extent of rupture.

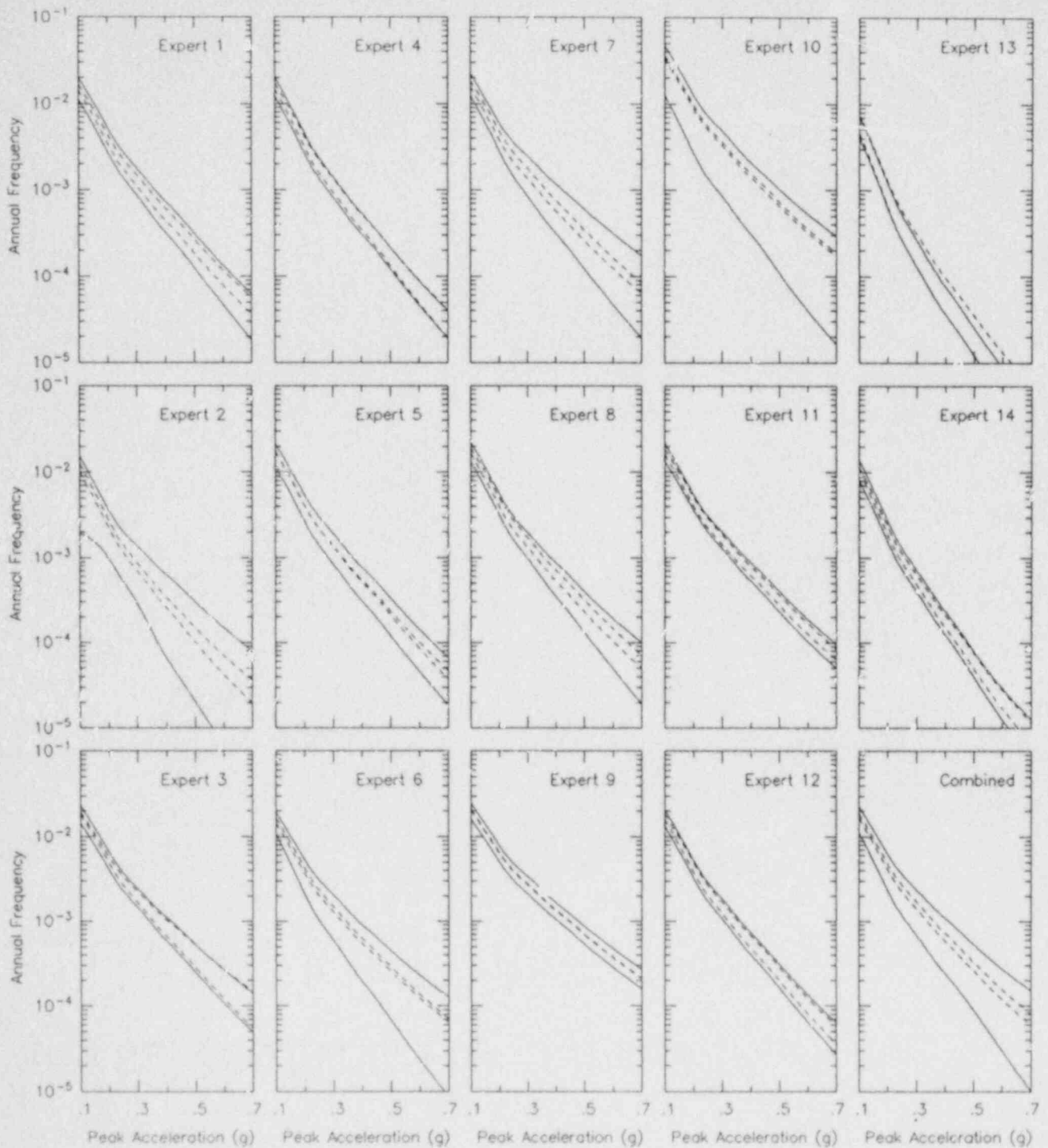


Figure 4-14. Contributions of uncertainty in maximum magnitude to total uncertainty. Shown are the 15<sup>th</sup> and 85<sup>th</sup> percentiles considering all uncertainties (solid lines) and the 15<sup>th</sup> and 85<sup>th</sup> percentiles considering only uncertainty in maximum magnitude (dashed line).

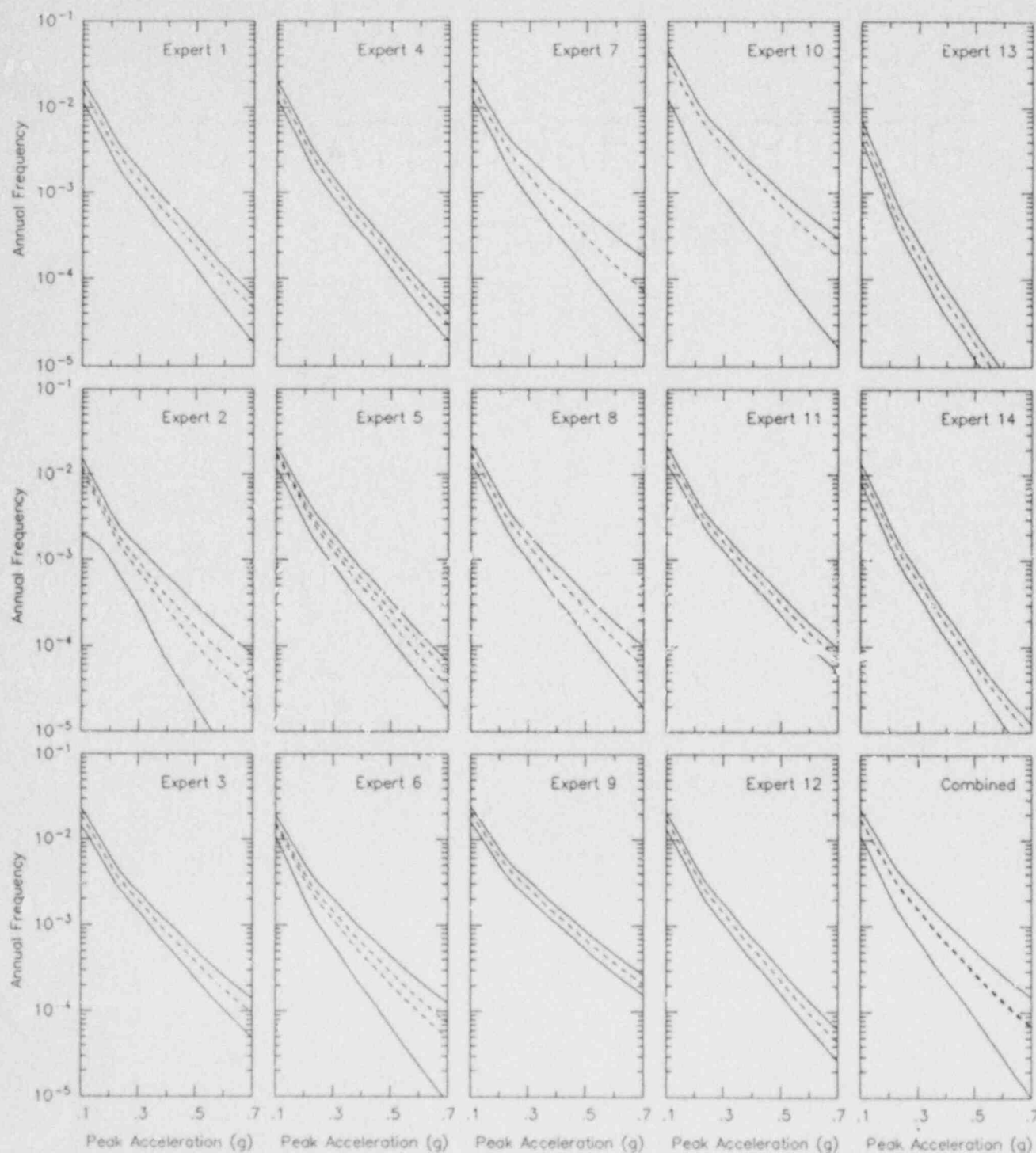


Figure 4-15. Contributions of uncertainty in recurrence method (moment rate vs paleoseismicity) to total uncertainty. Shown are the 15<sup>th</sup> and 85<sup>th</sup> percentiles considering all uncertainties (solid lines) and the 15<sup>th</sup> and 85<sup>th</sup> percentiles considering only uncertainty in recurrence method (moment rate vs paleoseismicity) (dashed line).



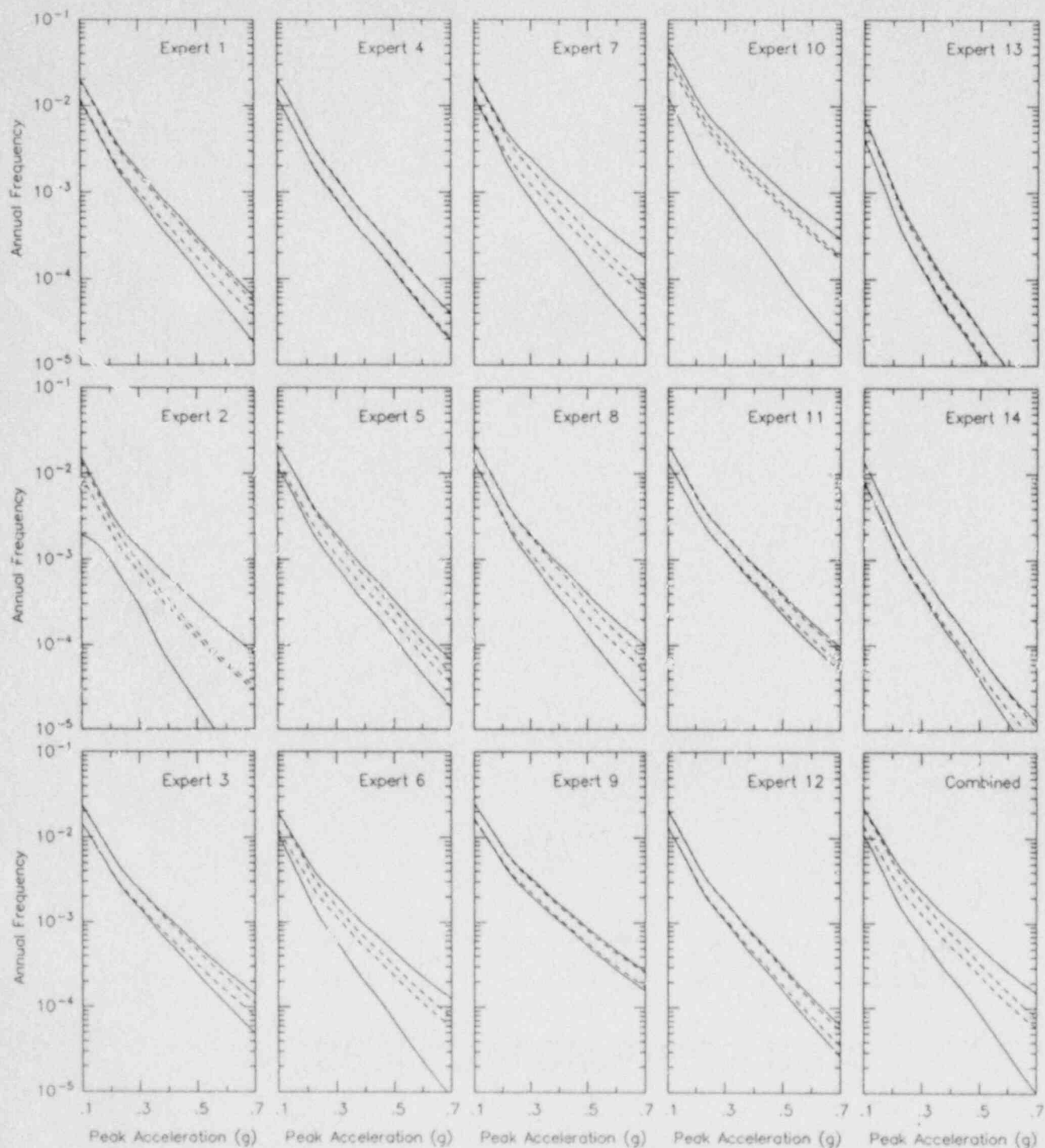


Figure 4-16. Contributions of uncertainty in convergence rate/paleoseismic rate to total uncertainty. Shown are the 15<sup>th</sup> and 85<sup>th</sup> percentiles considering all uncertainties (solid lines) and the 15<sup>th</sup> and 85<sup>th</sup> percentiles considering only uncertainty in convergence rate/paleoseismic rate (dashed line).

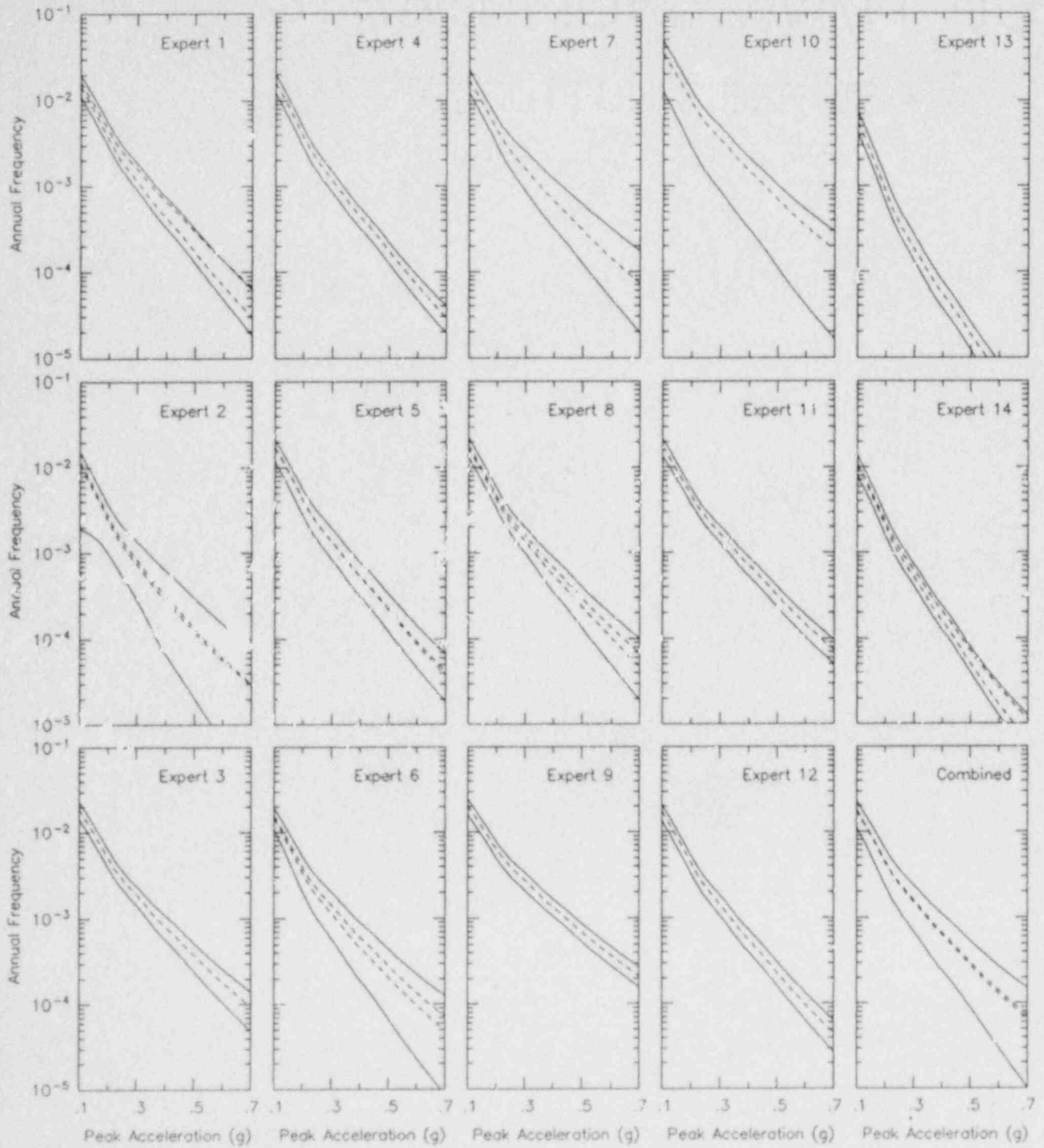


Figure 4-17. Contributions of uncertainty in seismic coupling to total uncertainty. Shown are the 15<sup>th</sup> and 85<sup>th</sup> percentiles considering all uncertainties (solid lines) and the 15<sup>th</sup> and 85<sup>th</sup> percentiles considering only uncertainty in seismic coupling (dashed line).

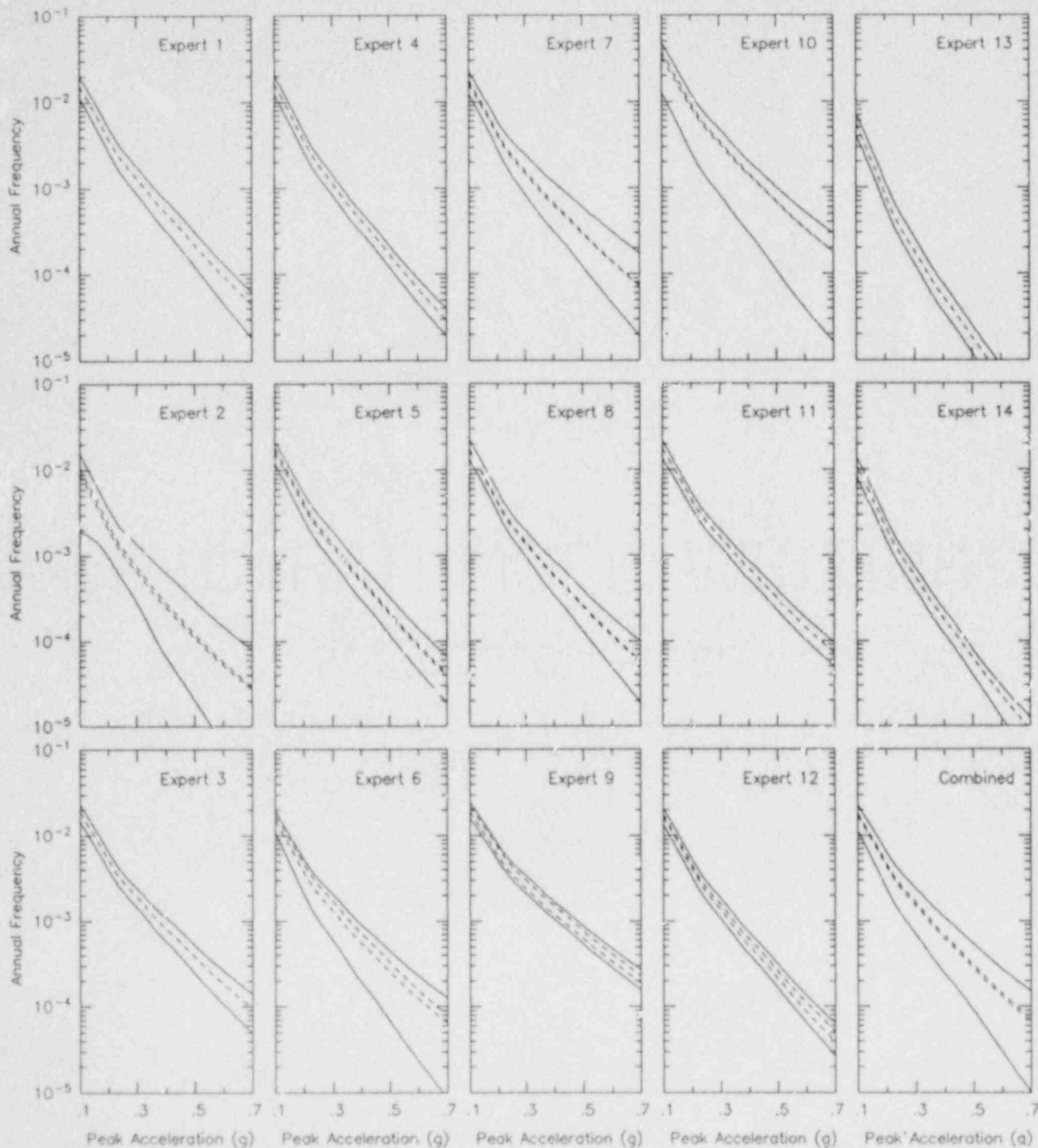


Figure 4-18. Contributions of uncertainty in magnitude distribution to total uncertainty. Shown are the 15<sup>th</sup> and 85<sup>th</sup> percentiles considering all uncertainties (solid lines) and the 15<sup>th</sup> and 85<sup>th</sup> percentiles considering only uncertainty in magnitude distribution (dashed line).

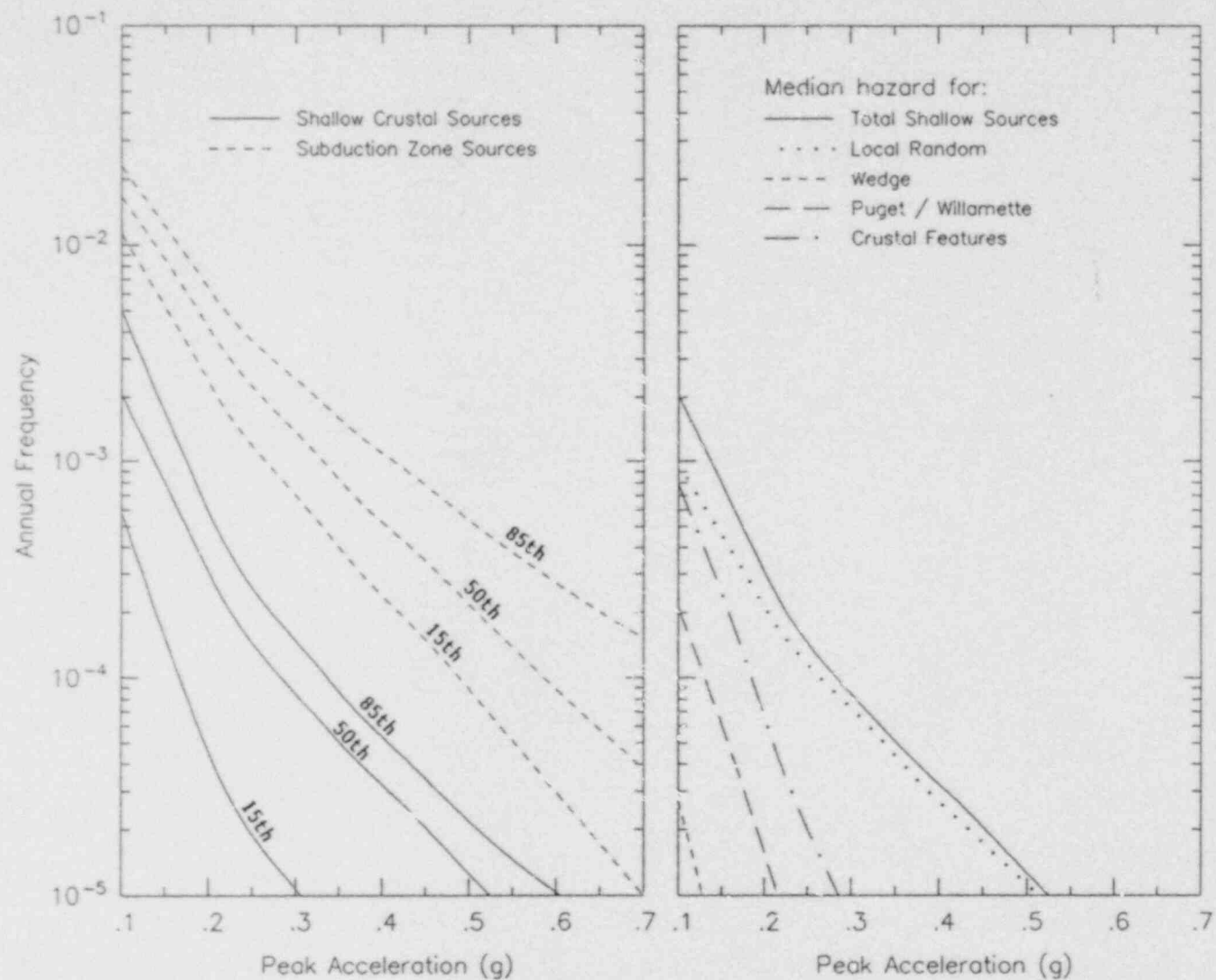


Figure 4-19. Peak acceleration hazard from shallow crustal sources. On the left, the 15<sup>th</sup>, 50<sup>th</sup> and 85<sup>th</sup> percentile hazard curves for crustal and subduction zone sources are compared. Shown on the right are the median hazard curves for the various shallow crustal sources.

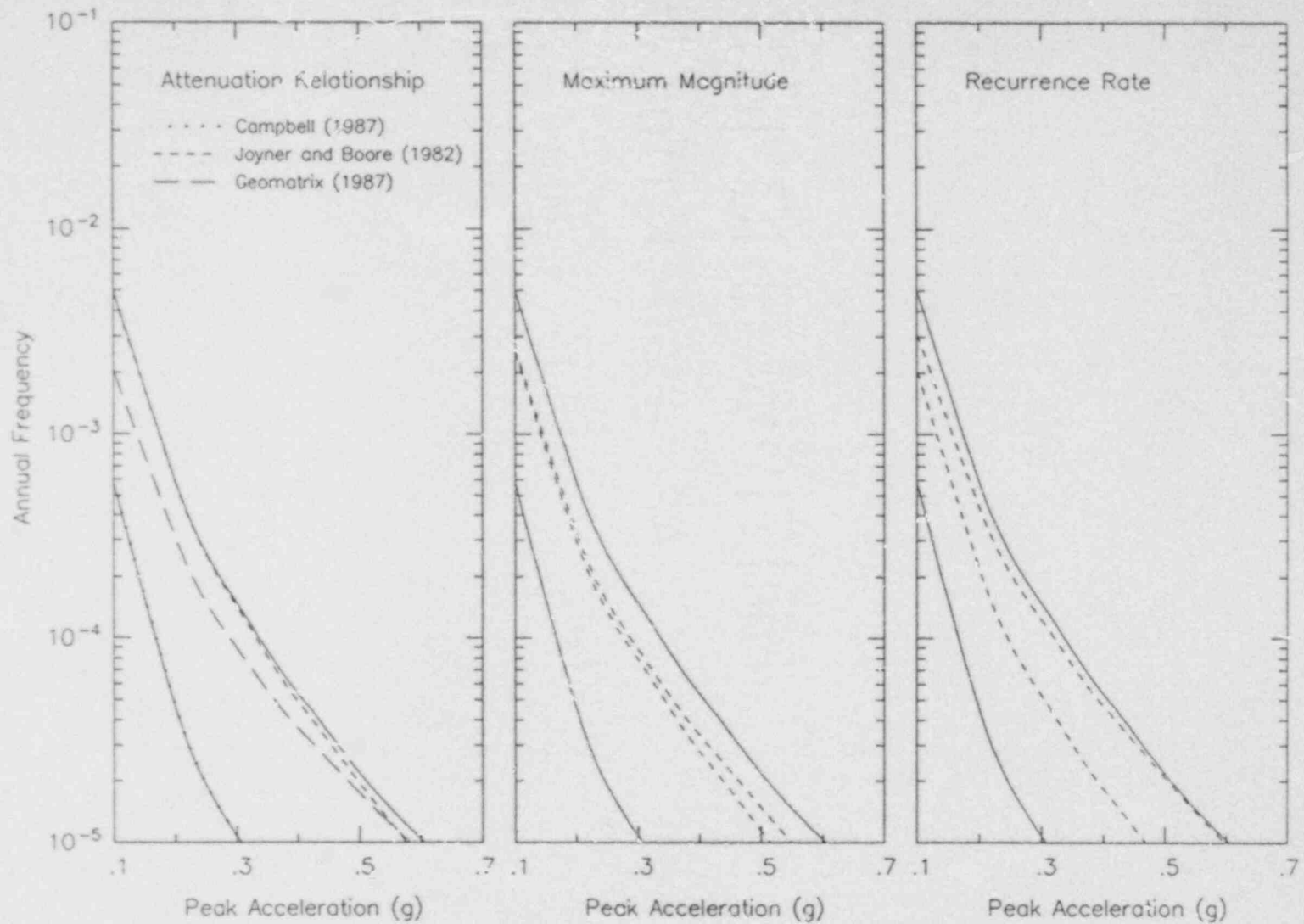


Figure 4-20. Contributions to uncertainty in hazard for shallow crustal sources. The solid curves in each plot are the 15<sup>th</sup> and 85<sup>th</sup> percentile curves considering all uncertainties. The left plot shows the median hazard curves obtained using single attenuation relationship. In the center and right plots, the dashed curves are the 15<sup>th</sup> and 85<sup>th</sup> percentile hazard curves considering only uncertainty in maximum magnitude and recurrence rate, respectively.

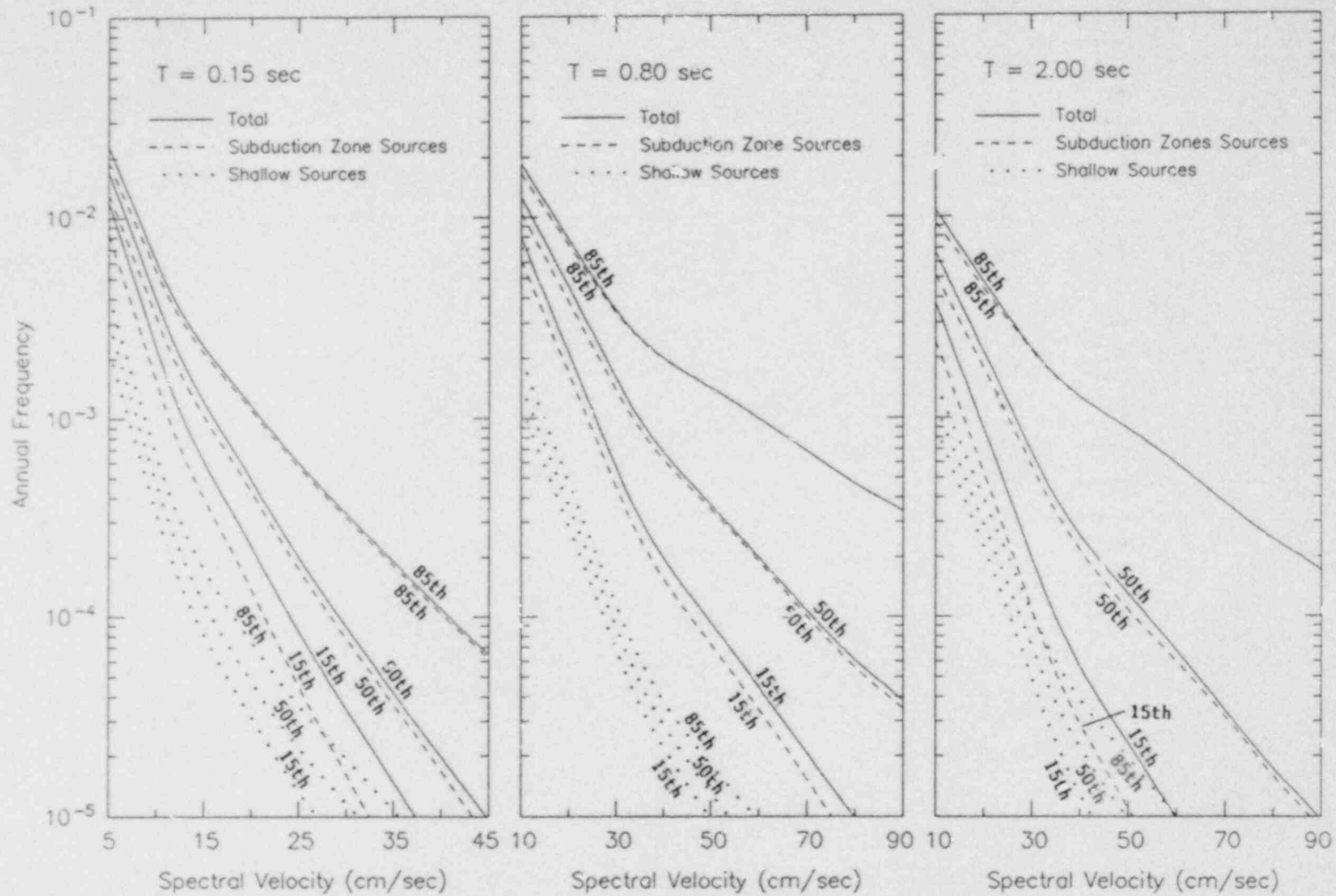


Figure 4-21. Hazard curves for 5% damped spectral velocity at periods of 0.15, 0.8 and 2 seconds. Shown are total hazard and hazard from subduction and shallow crustal sources.

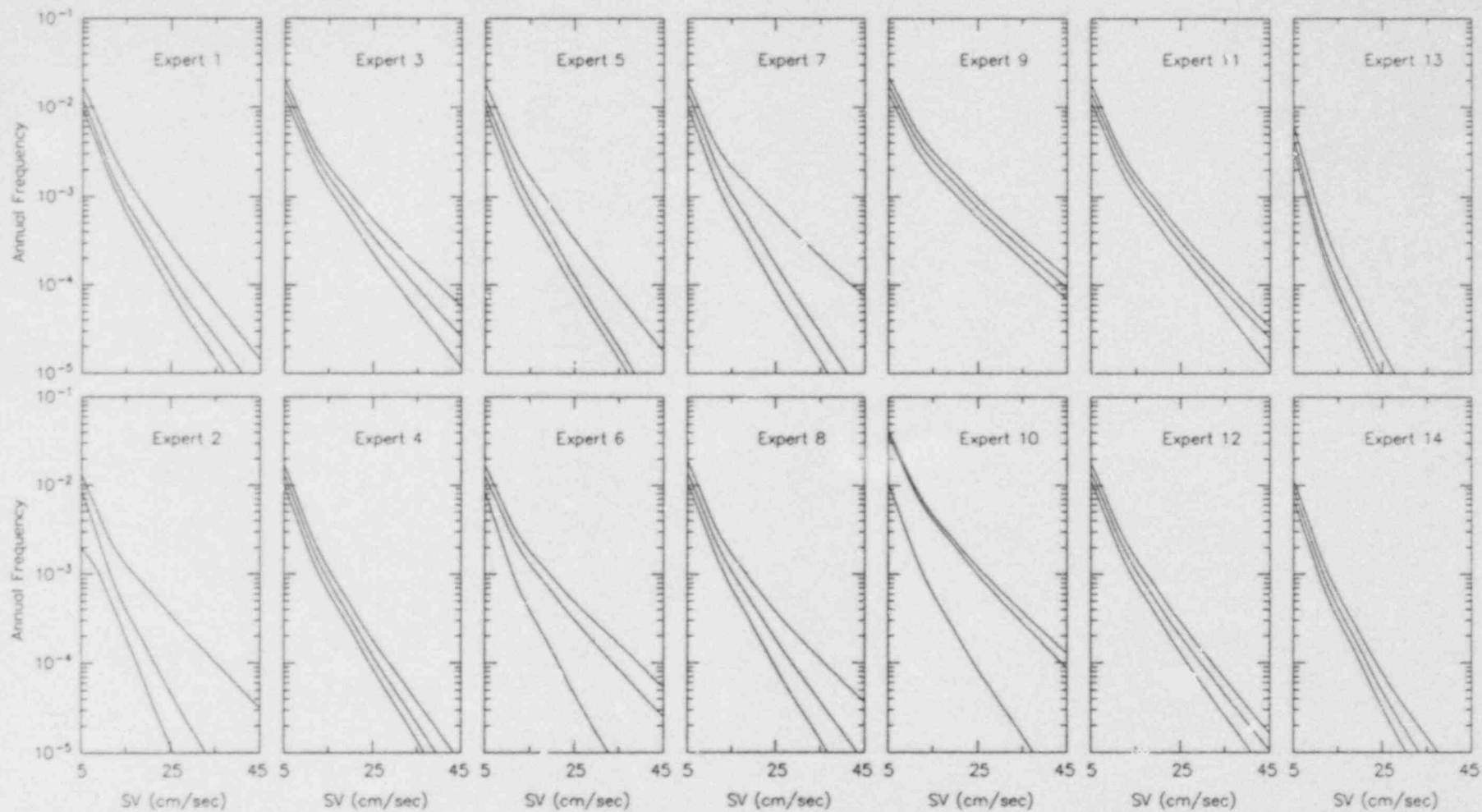


Figure 4-22. 15<sup>th</sup>, 50<sup>th</sup> and 85<sup>th</sup> percentile hazard curves of individual experts for 5% damped spectral velocity at 0.15-second period.

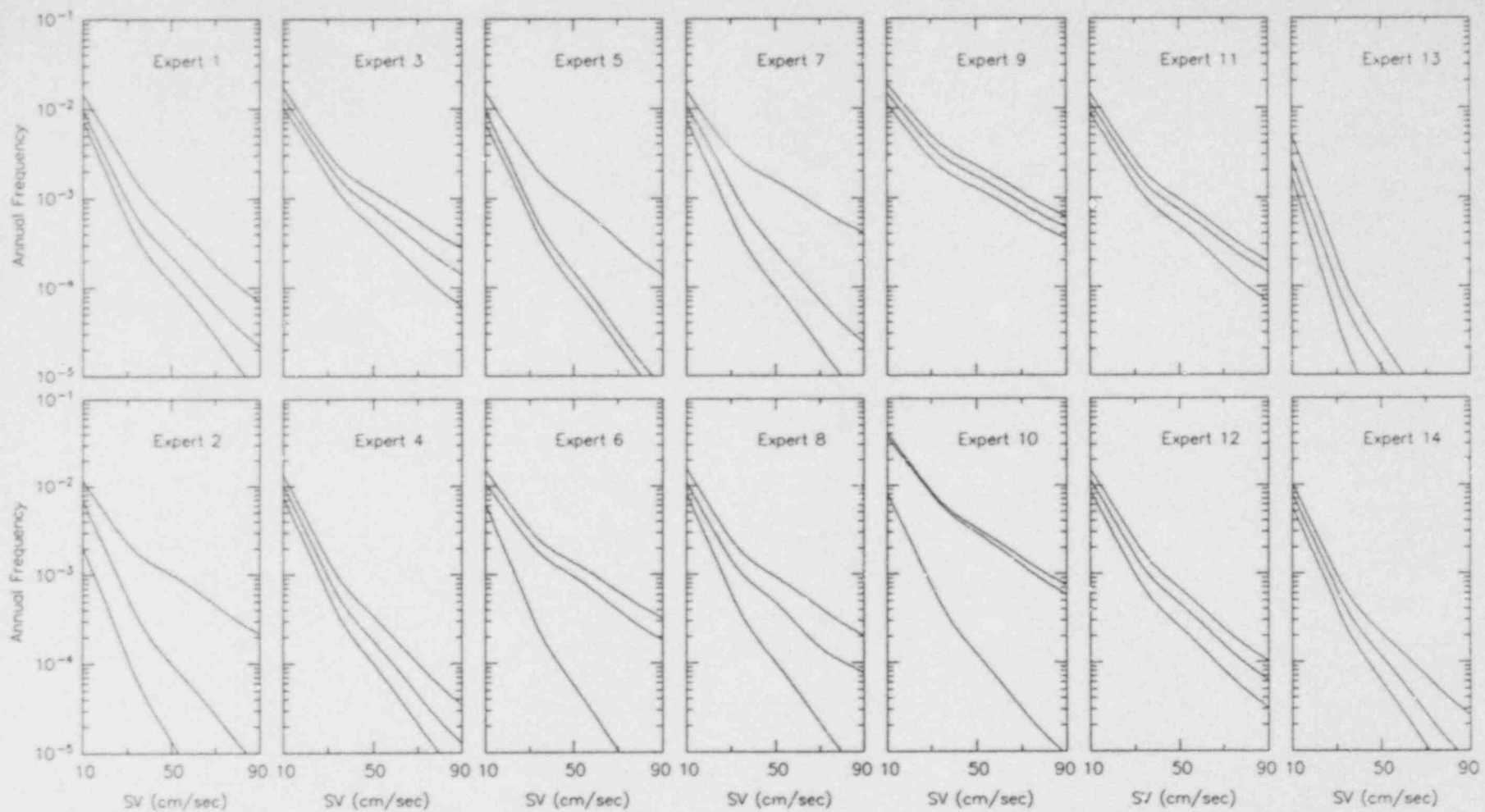


Figure 4-23. 15<sup>th</sup>, 50<sup>th</sup> and 85<sup>th</sup> percentile hazard curves of individual experts for 5% damped spectral velocity at 0.8-second period.



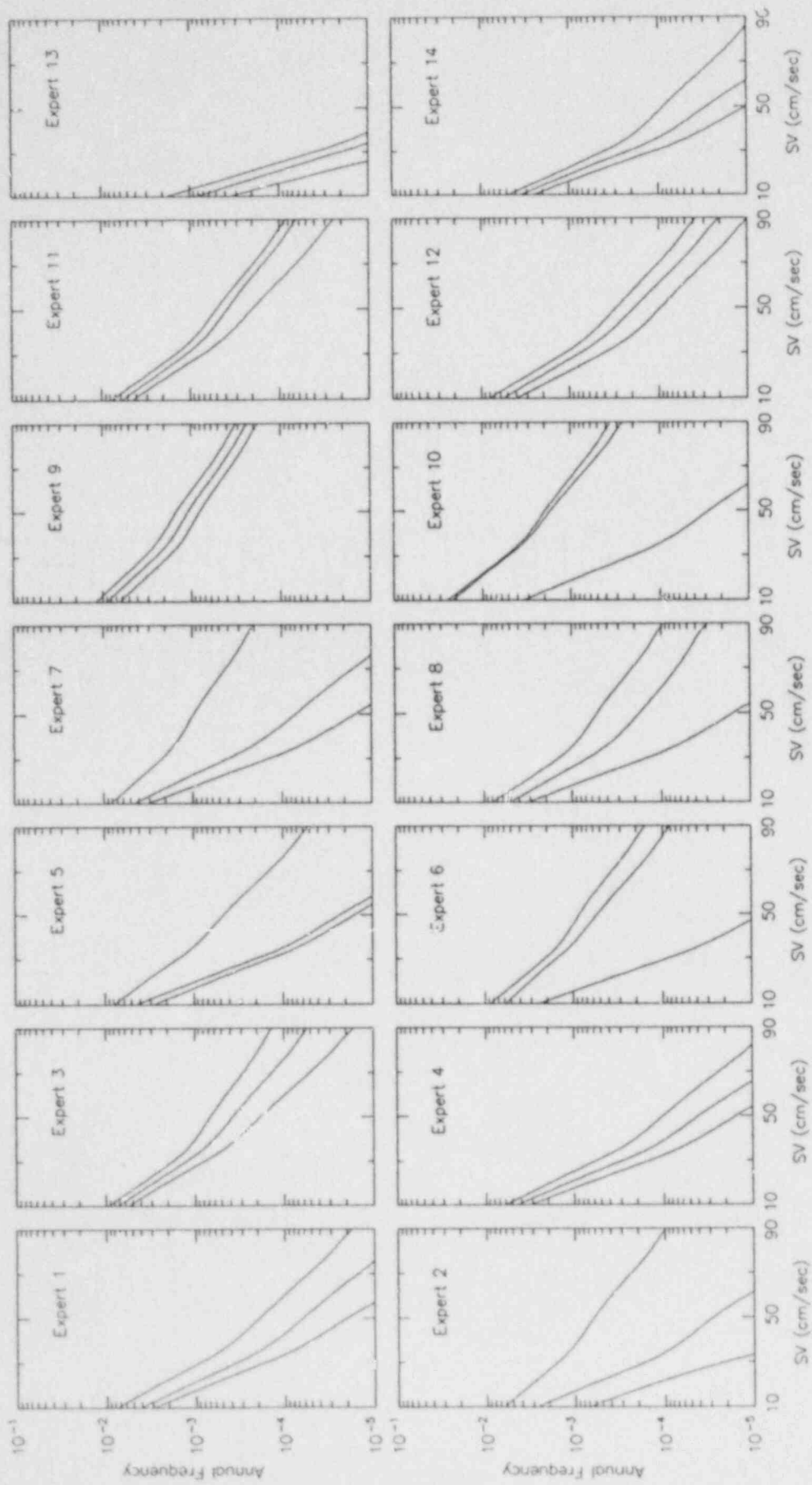


Figure 4-24. 15<sup>th</sup>, 50<sup>th</sup> and 85<sup>th</sup> percentile hazard curves of individual experts for 5% damped spectral velocity at 2-second period.

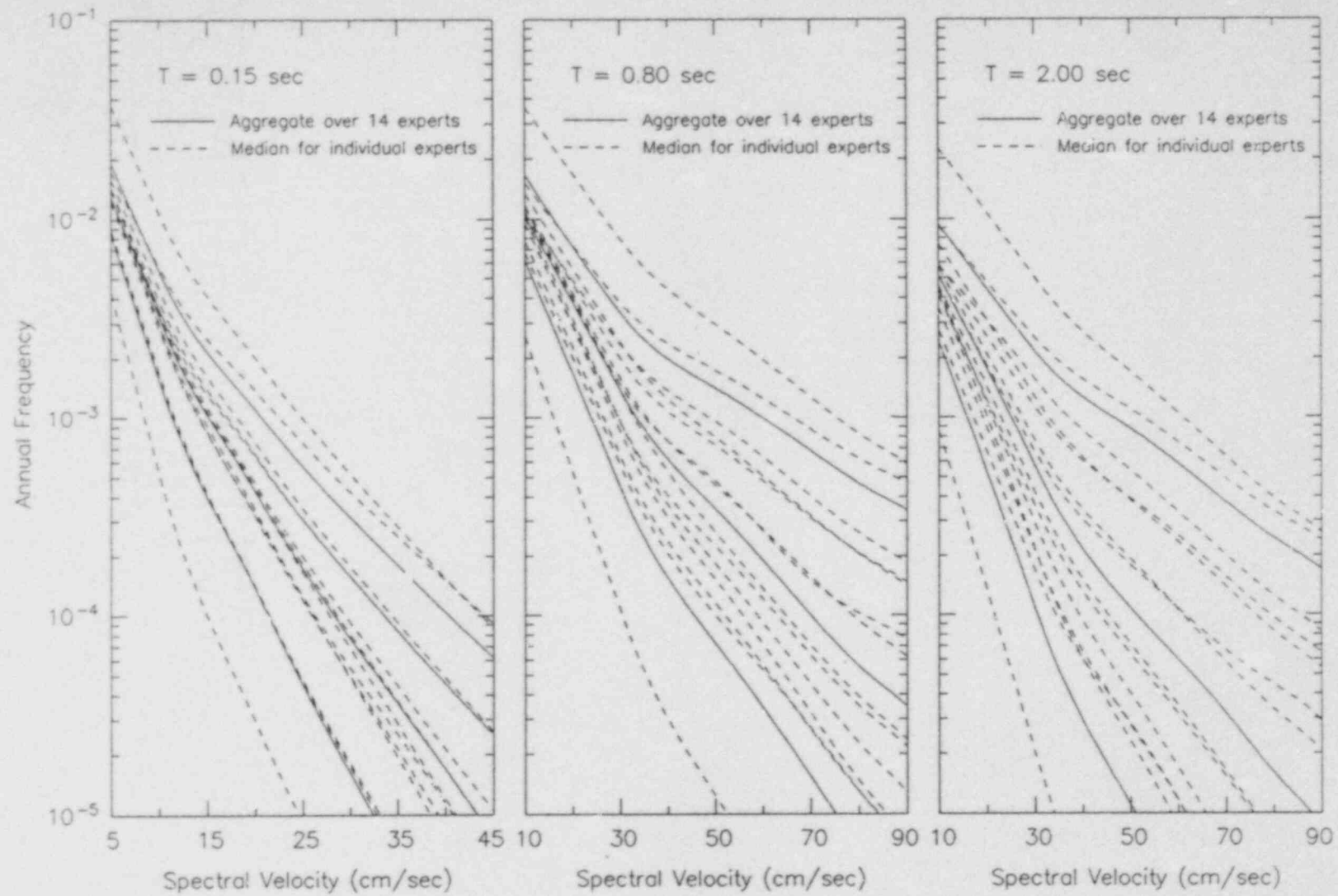


Figure 4-25. Comparison of experts median hazard curves with aggregate hazard for 5% damped spectral velocity at 0.15, 0.8 and 2 seconds.

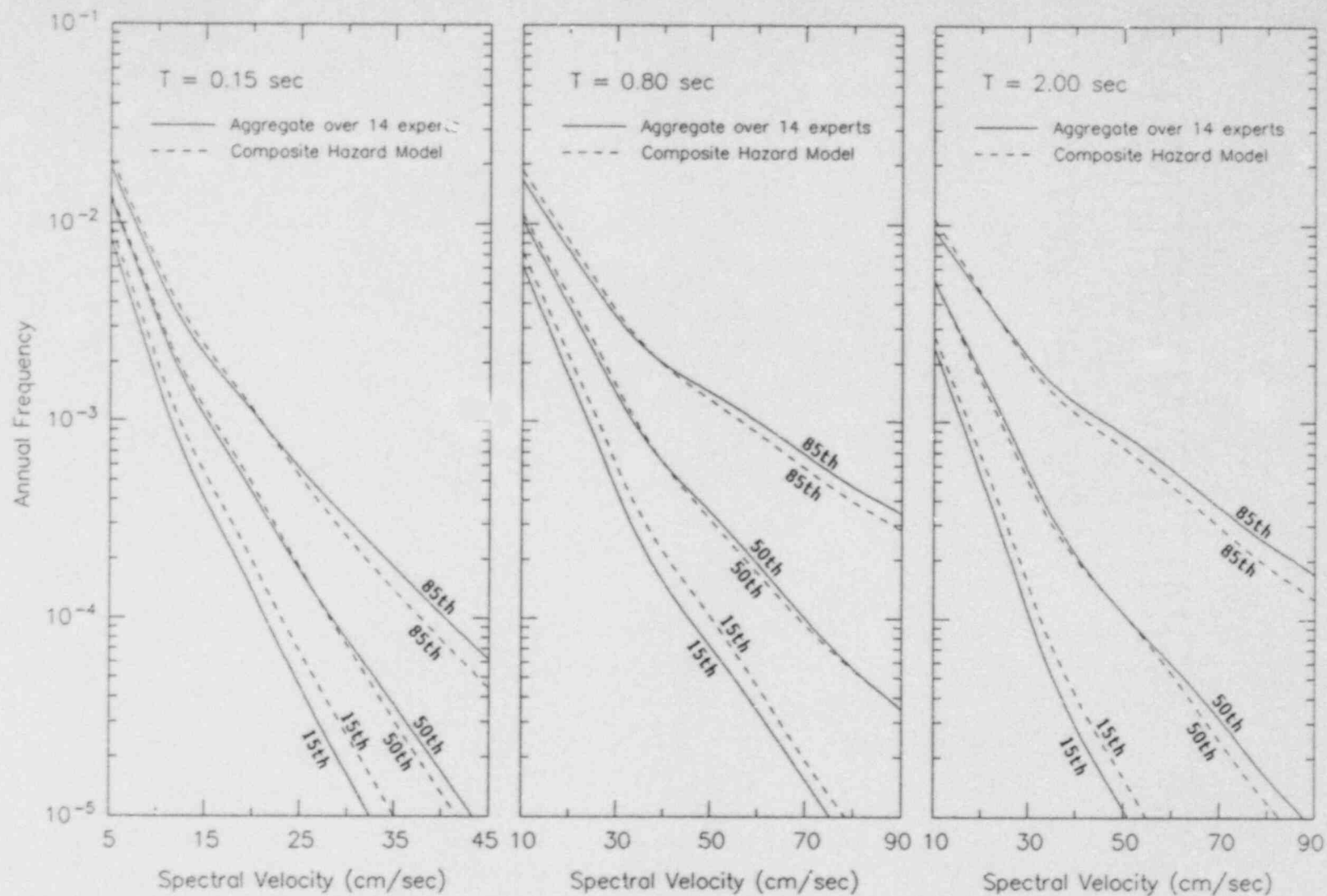


Figure 4-26. Comparison of aggregation procedures for total hazard from subduction zone sources for 5% damped spectral velocity at 0.15, 0.8, and 2 seconds.

REFERENCES

- Abe, K., 1975, Reliable estimation of the seismic moment of large earthquakes: *Journal Physics of the Earth*, v. 23, pp. 386-390.
- Adams, 1984, Active deformation of the Pacific Northwest continental margin: *Tectonics*, v. 3, no. 4, pp. 449-472.
- Anderson, J.G., and Luco, J.E., 1983, Consequences of dip rate constraints on earthquake recurrence relationships: *Bulletin of the Seismological Society of America*, v. 73, pp. 471-496.
- Campbell, K.W., 1987, Predicting strong ground motion in Utah, an evaluation of urban and regional earthquake hazards and risk in Utah: U.S. Geological Survey Professional Paper (in press).
- Coppersmith, K.J., and Youngs, R.R., 1986, Capturing uncertainty in probabilistic seismic hazard assessment within intraplate tectonic environments: *Proceeding, Third U.S. National Conference on earthquake Engineering*, v. 1, pp. 301-312.
- Crosson, R.S., and Owens, T.J., 1987, Slab geometry of the Cascadia subduction zone beneath Washington from earthquake hypocenters and teleseismic converted waves: *Geophysical Research Letters*, v. 14, pp. 824-827.
- Electric Power Research Institute (EERI), 1986, *Seismic hazard methodology for the central and eastern United States, Volume I: Methodology*: EERI Document NP-4726, Vol. I.
- Geomatrix Consultants, 1987, *Empirical ground motions investigations for Pacific Gas and Electric Company, Diablo Canyon Power Plant LTSP*: Report for Pacific Gas and Electric Company, in preparation.
- Heaton, T.H., and Snavely, P.D., 1985, Possible tsunami along the northwestern coast of the United States inferred from Indian traditions: *Bulletin of the Seismological Society of America*, v. 75, pp. 1455-1460.
- Joyner, W.B., 1984, A scaling law for the spectra of large earthquakes: *Bulletin of the Seismological Society of America*, v. 74, pp. 1455-1460.
- Joyner, W.B., and Fumal, T.E., 1985, Predictive mapping of ground motion, in evaluating earthquake hazards in the Los Angeles region: U.S. Geological Survey Professional Paper 1360.
- Kanamori, H., 1977, The energy release in great earthquakes: *Journal of Geophysical Research*, v. 82, pp. 2981-2987.
- Kulkarni, R.B., Youngs, R.R., and Coppersmith, K.J., 1984, Assessment of confidence intervals for results of seismic hazard analysis: *Proceedings of the Eighth World Conference on Earthquake Engineering*, v. 1, pp. 263-270.

- Lawrence Livermore National Laboratory (LLNL), 1985, Seismic hazard characterization of the eastern United States: Vols. I-III, April.
- Nishimura, C., Wilson, D.S., and Hey, R.N., 1984, Pole of rotation analysis of analysis of present-day Juan de Fuca plate motion: *Journal of Geophysical Research*, v. 89, pp. 10,283-10,290.
- Peterson, E.T., and Seno, T., 1984, Factors affecting seismic moment release rates in subduction zones: *Journal of Geophysical Research*, v. 89, pp. 10,233-10,248.
- Power, M.S., Coppersmith, K.J., Youngs, R.R., Schwartz, D.P., and Swan, F.H., III, 1981, Seismic exposure analysis for the WNP-2 and WNP-1/4 Site: Appendix 2.5K to Amendment No. 18 Final Safety Analysis Report WNP-2, for Washington Public Power Supply System, Richland, Washington, September.
- Riddihough, R.R., 1984, Recent movements of the Juan de Fuca plate system: *Journal of Geophysical Research*, v. 89, pp. 6980-6994.
- Ruff, L., and Kanamori, H., 1980, Seismicity and the subduction processes: *Phys. Earth Planet. Int.*, v. 23, pp. 240-252.
- Sadigh, K., Egan, J.A., and Youngs, R.R., 1986, Specification of ground motion for seismic design of long period structures: *Earthquake Notes*, v. 57, no. 1, p. 13.
- S-Cubed, 1988, Ground motion simulations for thrust earthquakes beneath western Washington: Report prepared for Washington Public Power Supply System, July.
- Verplanck, E.P., and Duncan, R.A., 1987, Temporal variations in plate convergence and eruption rates in the western Cascades, Oregon: *Tectonics*, v. 6, pp. 197-209.
- Wesnousky, S., Scholz, C.H., Shinazaki, K., and Matsuda, T., 1983, Earthquake frequency distribution and mechanics of faulting: *Journal of Geophysical Research*, v. 88, pp. 9331-9340.
- Wyss, M., 1979, Estimating maximum expectable magnitude of earthquakes from fault dimensions: *Geology*, v. 7, no. 7, pp. 335-340.
- Youngs, R.R., and Coppersmith, K.J., 1985a, Implications of fault slip rates and earthquake recurrence models to probabilistic seismic hazard estimates: *Bulletin of the Seismological Society of America*, v. 75, pp. 939-964.

Youngs, R.R., and Coppersmith, K.J., 1985b, Development of a fault-specific earthquake recurrence model (abs.): Earthquake Notes, Seismological Society of America, v. 55, p. 16.

Youngs, R.R., Coppersmith, K.J., Power, M.S., and Swan, F.H., III, 1985, Seismic hazard assessment of the Hanford region, eastern Washington State: in Proceedings of the DOE Natural Phenomena Hazards Mitigation Conference, Las Vegas, Nevada, October 7-11, p. 169-176.

## EXPLANATION TO ACCOMPANY

## TABLE 3-1

Table 3-1 summarizes the responses given by the fourteen experts, which are further detailed in Appendix A. A more complete discussion of the components of the seismic hazard model is given in Section 2.1. Each of the columns in Table 3-1 is explained below. Note that blank columns or apparent omissions in the table are the result of the expert declining to characterize these aspects.

Oceanic Slab Geometry

Each of the experts developed a cross-sectional sketch of the geometry of the oceanic slab beneath western Washington. These sketches are included in Appendix A and described verbally in Table 3-1. Alternative models are given along with the relative weight assigned to each, expressed as probabilities summing to unity.

Potential Seismic Sources

The subduction-related potential sources of earthquakes are identified and each is assigned a letter, which is shown in brackets (e.g., "[a]"). These letters are used in subsequent columns to specify which seismic source is being described.

Probability of Activity

Probabilities of activity are given for each potential seismic source, specified by a letter in brackets. Where expressed by the experts, ranges of estimates are given in parentheses. "Activity" is used here to signify capable of generating tectonically significant earthquakes (see Section 2.1).

Maximum Magnitude

Direct assessments of the maximum earthquake magnitude are given for the sources specified in brackets. In some cases, a range of values is given, or a best estimate and uncertainty bounds, or discrete values with relative weights assigned to each value. Where the word "Dimensions" appears, the expert indicated that the rupture dimensions that he specified be used to

## EXPLANATION TO ACCOMPANY TABLE 3-1 (cont'd)

calculate a magnitude (i.e., he did not provide a maximum magnitude estimate directly). See Section 2.1 regarding "location of rupture" to see how the rupture dimensions were estimated.

Convergence Rate

The relative rate of convergence measured parallel to the convergence direction between the North American and Juan de Fuca plates is given in millimeters per year. In some cases, ranges are given or discrete values are given with associated relative weights.

Recurrence Method

The manner in which the experts desired to have the earthquake recurrence rate specified is given in this column. Examples include recurrence based on the historical seismicity record, geologic data for recurrence intervals, or seismic moment rate. The seismic moment rate approach (described in Section 2.1) utilizes the estimates of convergence rate and seismic coupling.

Seismic Coupling ( $\alpha$ )

Seismic coupling is the percentage of the total convergence rate that is expressed seismically. Therefore, if the coupling is very high ( $\alpha = 1.0$ ), then all of the convergence rate will be expressed as earthquakes (i.e., the seismic moment rate from seismicity will be equal to that based on convergence rate). An  $\alpha = 0$  means that convergence is occurring aseismically (i.e., there is no seismic coupling).

Recurrence Model

The recurrence distribution function is specified in this column. Models requested by the experts include an exponential magnitude distribution (i.e.,  $\log N = a - bM$ ); a characteristic magnitude distribution (Youngs and Coppersmith, 1985); and a maximum moment model (Wesnousky, 1983).

Geologic Recurrence for Large Earthquakes

For those cases where geologic data provide a basis for estimating recurrence, an estimate of recurrence intervals for large earthquakes is given. These recurrence intervals were generally judged appropriate for magnitudes at or near the maximum.





Appendices

---

**FINAL REPORT**

**Seismic Hazards Assessment  
for  
WNP-3, Satsop, Washington  
Contract No. C-20453**

Submitted to

**WASHINGTON PUBLIC POWER SUPPLY SYSTEM  
3000 George Washington Way  
Richland, Washington 99352-0968**

---

**Geomatrix Consultants**



Appendices

---

## FINAL REPORT

Seismic Hazards Assessment  
for  
WNP-3, Satsop, Washington  
Contract No. C-20453

Submitted to

WASHINGTON PUBLIC POWER SUPPLY SYSTEM  
3000 George Washington Way  
Richland, Washington 99352-0968

---

Geomatrix Consultants

## APPENDIX A

### DOCUMENTATION OF EXPERT INTERVIEWS

---

This appendix provides documentation of the expert interviews, summarized in Section 3 of the main report. As discussed in detail in Section 2.2.2, the expert interviews occurred in two parts. Phase I consisted of in-person interviews held at the experts' offices during the summer of 1986. The Phase II follow-up interviews were given by telephone in the fall of 1987. In the first case, an Information Package was sent to each expert to explain the objectives of the study and to describe the format. Prior to the follow-up interviews, materials were sent to each expert that summarized their previous assessments and summarized the assessments made by all of the experts. The summaries of their previous assessments included the calculated results (i.e., maximum magnitude and recurrence relationships) derived from their assessments.

The documentation for the expert interviews given here include:

- Information Package sent to the experts prior to the Phase I interviews.
- Phase I responses of individual experts.
- Informational materials sent to the experts prior to the Phase II follow-up interviews. This material includes:
  - Example letter
  - Attachment 1 - Summary of assessments for each expert including calculated results
  - Attachment 2 - Phase I responses of individual expert (presented previously)
  - Attachment 3 - Summary of aggregate expert assessments
  - Attachment 4 - Recent references
  - Attachment 5 - Updated seismicity cross-sections
- Phase II responses of individual experts.

The interview summaries included here are based on written notes taken by members of the elicitation team and are focused on interpretations, uncertainties in each interpretation, and the basis for the responses given. We are not attempting in these summaries to provide a full "defense" of the expert opinions given because most responses are based largely on judgement. We are, however, trying to provide a third party with enough information to understand the key data and interpretations that are driving the experts' opinions. Also, documentation is required because the experts relied to some extent on new unpublished data or work in progress. Note that each expert reviewed his summary for accuracy and the accepted version is given here.

INFORMATION PACKAGE

(Sent Prior to Phase I Interview)

## INFORMATION PACKAGE TO SEND TO SATSOP EXPERTS

Introduction

This information package is intended to provide you with the background and purpose of your involvement in the Satsop Seismic Hazard Analysis.

The problem that we are addressing is: What is the probability of the occurrence of ground motions that would exceed the seismic design basis at the Satsop site? Answering this question requires a probabilistic seismic hazard analysis. We are incorporating the uncertainties that exist regarding the seismic sources that might affect the Satsop site in the source models using probabilistic techniques. We cannot expect to solve the questions regarding earthquake potential in the Pacific Northwest. Therefore, we are making a "snap-shot" of the present state of knowledge using the opinions of experts regarding the nature and seismogenic potential of the Cascadia subduction zone.

The object of this study is to solicit your opinion on the nature of the Cascadia subduction zone thus providing a basis for constructing a source model for the probabilistic seismic hazard analysis. This is a probabilistic study, so ranges of values or weighted values may be given to particular parameters. It is likely that any given expert is not intimately familiar with all aspects of the problem at hand (e.g., one may have knowledge of geophysical constraints on the slab geometry but not of the details of the instrumental seismicity data set). Therefore, we will allow each expert to qualify the responses given relative to his perception of his expertise in the subject area.

The focus of the scientific inquiry is the Cascadia subduction zone--its features, behavior, and seismogenic potential. Inasmuch as analogies to other convergent zones shed light on this margin, the experts may wish to develop such analogies. Please bear in mind, however, that the engineering result of this analysis is a probabilistic ground motion estimate at the Satsop site.

### Basic Elements of a Probabilistic Seismic Hazard Model

The seismic hazard at a site depends on: the location of potential future earthquakes relative to the site; the rate of occurrence of future earthquakes of various sizes; and the attenuation of ground motions with distance. A probabilistic model of the seismic hazard requires 1) characterization of potential earthquake sources in terms of their location and geometry relative to the site; 2) the rate of seismic activity on each source, and the relative frequency of various size events; and 3) characterization of the amplitude of ground motions as a function of source-to-site distance and earthquake size. The latter of these (ground motion attenuation) is not the subject of our concern here. We are focused here on the source model (1 and 2 above), which defines the location and occurrence of seismicity. Further, we are concerned with subduction-related seismic sources only; shallow crustal faults will be modeled separately.

Seismic source modeling techniques for hazard analysis have become increasingly sophisticated in recent years. For example, sources are usually modeled as three-dimensional surfaces, rupture size is constrained by magnitude, the focal depth distribution (rupture nucleation locations) can be specified, fault segments can be modeled, and a variety of recurrence models can be incorporated including renewal or real-time models. In other words, the hazard analysis is capable of effectively modeling virtually any type of earthquake behavior that is believed to be appropriate, and that can be characterized. To account for the uncertainties in the source models, simple probabilistic techniques such as logic trees have been developed that allow for a range of parameter values for any particular characteristic. Each value can be subjectively weighted as to its credibility or likelihood of being the correct value. Simply put, probabilistic approaches do not require that you make a "yes/no" decision; only that you express your expert opinion and the uncertainties associated with it. The probabilistic methods that we will utilize as part of this project are discussed in more detail below.

For this hazard analysis, we are attempting to model any potential seismic sources that are believed by the experts to be associated with the Cascadia subduction zone (e.g., plate interface, intra-slab, accretionary wedge, etc.). Any or all of these features may have some probability of being seismogenic. If there is some finite probability of activity (however small), then the further characterization of the source (its geometry, etc.) can be carried out conditional on the source being seismogenic. Of course, if an element of the subduction zone has no probability of being seismogenic, further characterization is not required.

#### Satsop Site Hazard Analysis

Uncertainties in the seismic hazard of the Cascadia subduction zone stem from the fact that no earthquakes larger than about magnitude 5 have been unequivocally associated with the plate interface. No clear definition of slab geometry can be easily discerned from seismicity data alone (unlike most other convergent margins). Therefore, several essential hazard source characteristics cannot be directly assessed, such as: Is subduction occurring beneath western Washington? What is the geometry of the interface and the slab? If subduction is occurring, what is the degree of seismic coupling between the plates? Why have there been no observed interplate events? How is the maximum earthquake to be evaluated? How is earthquake recurrence to be evaluated? There are no clear answers to these questions but various lines of evidence from geologic, seismologic, and geophysical data can be instrumental in providing constraints that can be included in the hazard model. For example, strain rate (usually fault slip rate) can provide an important constraint on earthquake recurrence (e.g., Anderson, 1979; Anderson and Luco, 1983; Youngs and Coppersmith, 1985). To be useful, one must assess the component of the slip rate that is potential seismic strain energy (i.e., subtract aseismic slip from the total slip). In order to use the relative slip rate (convergence rate) at a subduction zone, it is necessary to estimate the percent seismic coupling. Several studies comparing seismic moment rate (from historical seismicity) with plate convergence rate demonstrate a broad variation in the percent coupling for worldwide subduction zones. Therefore, if the percent seismic

coupling can be estimated for the Cascadia subduction zone, meaningful constraints may be placed on earthquake recurrence. As another example, because this subduction zone is not well expressed from seismicity, we must rely on other data (e.g., refraction studies, broadband data, etc.) to estimate the slab geometry.

#### Probabilistic Approaches to Eliciting Expert Opinion

Many important decision-making problems involve a considerable degree of uncertainty and serious risks associated with that uncertainty. Therefore, it is important to obtain as much information as possible in order to understand and accurately represent the degree of uncertainty concerning events or variables of interest. Often, problems with serious risks are characterized by a lack of directly relevant experimental evidence. The "hard" empirical evidence may be only indirectly relevant (for health risks, consider experiments with new drugs on animals but not on humans) or may be too limited (for seismic risks, consider a limited history of reliable records of seismic activity). As a result, most of the information available is subjective in nature, involving the judgments of experts who presumably will attempt to take into account any "hard" evidence, direct or indirect, that may be available. This is the situation that we face in the Satsop Seismic Hazard Analysis.

To understand and accurately represent the degree of uncertainty concerning events or variables of interest, we must utilize expert judgments and express them in a form useful for communicating and measuring uncertainty. This has been recognized increasingly in recent years and has led to use of experts' probability assessments as important inputs in decision and risk analysis problems. Examples include probability forecasts of rain and other meteorological events, risk assessments of health effects of specific air pollutants, and the recent study of seismic hazards in the Eastern United States by Electric Power Research Institute.

People often think in terms of how likely certain events are but generally do not actually quantify their judgments in terms of probabilities. Yet everyone is exposed to probability statements such as "The probability of



rain tomorrow is 30 percent," "There is a 10 percent chance that the patient will not survive," "The odds are 4-to-1 against the horse winning the race," "The probability of discovering oil if we drill in this location is 5 percent," or "That team has only one chance in one hundred of winning the championship." We are going to ask you to make similar statements about the features, behavior, and seismogenic potential of the Cascadia subduction zone. For example, we will be interested in your probability that the plate interface is seismogenic and your probabilities for different rates of plate convergence.

It is important to emphasize that no background in probability theory is needed, and you will not be asked to perform any fancy manipulation of probabilities. The problem will be broken down logically into small parts so that each question is clear, understandable, and easy to think about. We will use a number of methods to help you translate your judgments into probabilities. Your probabilities will be elicited in an interview session, and the role of the interviewers/analysts is to assist you in thinking about relevant qualitative issues and in representing your knowledge in quantitative terms. The ultimate intent is to wind up with a set of probabilities that accurately reflect your knowledge and uncertainties. It is also useful to obtain an idea of how confident you feel about these probabilities. When you give a probability of, say, 30 percent, we will ask whether you are quite certain about that figure or whether it represents an estimate but you feel that the probability might be lower or higher (for example, it might be as low as 25 percent or as high as 35 percent; or it might be as low as 15 percent or as high as 40 percent). We recognize that it is often difficult to come up with just a single number, and giving a range in addition to the single number provides useful information. Finally, it is important for us to understand your reasoning process and the rationale for the probabilities that are given. Of particular interest are any underlying assumptions or theories that you are considering. Thus, the final outcome of the assessment process should be a set of probabilities, an indication (through ranges of values) of how vague or confident you feel about these probabilities, and the qualitative reasoning behind the probabilities.

Some people tend to feel more comfortable with what they view as "hard" data, such as a set of empirical observations, than with experts' judgmental probabilities, which are viewed by some as representing "softer" data. Detailed evaluations, however, have shown that experts' probabilities can be very stable and reliable. Weather forecasters' probability forecasts provide an example in which the subjective probabilities tend to do at least as well as, and usually better than, probabilistic weather forecasts generated from combinations of statistical and physical models. If the elicitation process is carefully designed, the stability and reliability of the results can be very high. Careful attention to all of an expert's uncertainties is important, just as a full consideration of possible variability related to different sources of sampling or experimental error is vital in empirical research.

To help you represent your judgments most effectively and accurately, we will briefly discuss some factors that you should keep in mind when going through the probability elicitation task. The following four paragraphs provide some suggestions along these lines. It is important that you consider relevant evidence in a systematic and effective manner.

Your probabilities should be based on whatever information is available about the Cascadia subduction zone and what you know about subduction zones elsewhere in the world. It is important to try to consider all of the information and all of the possibilities in terms of features, behavior, and seismogenic potential associated with the Cascadia subduction zone. Think about all scenarios that could possibly be consistent with the information that is available. Do not just focus on a single, "most likely" scenario or on a scenario that stands out in your mind for some reason. Think also of extreme scenarios, even if they are less likely. Consider information that might be inconsistent with a specific theory as well as information that might be consistent with the theory. Try to keep an open mind.

You should also resist any tendency to place greater weight on pieces of information seen first or last. Early information can influence the way you think about a problem and the way you interpret and react to later information. On the other hand, the most recent information seen is most accessible in your memory and may have undue influence on your judgments for that reason. Review all of the available information, again trying to keep an open mind.

Be sure to keep in mind the uncertainties associated with data and other information. The reliability and accuracy of information vary considerably, and you should be careful not to overestimate reliability or accuracy and to ignore uncertainties.

Finally, do not confuse values with judgments. We are interested in your scientific appraisal of probabilities concerning possible seismic sources associated with the Cascadia subduction zone. The costs associated with seismicity in view of the location of the Satsop site are a separate issue. In giving your probabilities, you should just be considering the likelihood of certain events, not the potential consequences associated with those events.

As noted above, your probabilities will be elicited in an interview session, which will last about one-half day. The session will begin with a brief introduction to uncertainty and probability to familiarize you with the basic notions of quantifying judgments in terms of probabilities. Next, we will discuss the Cascadia subduction zone, reviewing available evidence and obtaining some of your qualitative judgments concerning the features, behavior, and seismogenic potential of the Cascadia subduction zone. Then we will ask you to quantify your judgments and to provide certain probabilities in a systematic manner. The interviewers/analysts will assist you in this process of assessing probabilities. As the interview proceeds, you may think of aspects of the problem you had not recalled earlier. At any point, you can reconsider and change earlier probabilities. After the probability assessment process is completed, we

will review both the qualitative judgments and the quantitative probabilities. After the interview, we will prepare a summary of the information obtained and send it to you so that you can see if it accurately reflects your judgments. At that time, you can make any modifications that seem appropriate. As we have mentioned, the ultimate intent is to wind up with a set of probabilities, together with an indication of the degree of confidence in the probabilities and a qualitative discussion of relevant factors, to accurately reflect your knowledge and uncertainties. In documenting our study, interpretations from all the experts will be aggregated for the analysis and particular interpretations will not be attributed to individual experts.

#### Some Likely Questions

The following is a list of some likely questions to give you a feel for the type of information that we will ask about during the interview.

1. What does the geometry of the plate margin beneath Western Washington look like? We will give you a graph and ask you to sketch possible models for this geometry. Then we would like you to assign probabilities to these models.
2. Consider the rate of plate convergence normal to the North American/Juan de Fuca plate boundary. What is the probability that this rate of convergence is less than 10 mm/year? What is the probability that it is between 10 and 20 mm/yr? Between 20 and 30 mm/yr? Between 30 and 40 mm/yr? Between 40 and 50 mm/yr? Greater than 50 mm/yr?
3. What are the possible seismic sources associated with subduction?
4. For the Cascadia subduction zone, what is the probability that each possible seismic source is seismogenic (active)?
5. If the plate interface has some probability of being seismogenic, what are the updip and downdip constraints (minimum and maximum depths) on the seismically coupled part of the interface? We will ask for values and probabilities regarding the updip and downdip constraints.
6. What is the probability that the plate boundary is laterally segmented? If it is segmented, where do you think the segment boundaries are? What is the probability that fault rupture will start/stop at these segment boundaries?

7. What is the longest rupture that may occur along the plate interface? We will ask about the probabilities of ruptures of various lengths.
8. If the plate interface has some chance of being a capable seismic source, what is your best estimate of the percent seismic coupling between the plates? (Seismic coupling is defined here as the percent of the convergence rate that is released as seismic energy; coupling may be a function of the historical observations or of an assumed model). What is the probability of less than 10 percent seismic coupling? What is the probability of between 10 and 30 percent seismic coupling? Between 30 and 50 percent? Greater than 50 percent?
9. Do you have direct estimate of earthquake recurrence for the plate interface? If so, express this as a recurrence interval for particular magnitude events or as a recurrence relationship of the form  $\log N = a - bm$ .
10. We will ask questions like those in 5, 6, 7, and 9 with reference to intraplate seismicity, accretionary prism seismicity, and any other possible seismic sources.

These questions are just intended to give you some idea of the type of information that is of interest. During the interview session, terms will be defined precisely and clarification will be provided as needed.

BIBLIOGRAPHY

The following references provide a representative sampling of the published data and interpretations pertinent to this study.

Geometry of Cascadia Subduction Zone

- Atwater, T., 1970, Implications of plate tectonics for the Cenozoic tectonic evolution of western North America, *Bull. Geol. Soc. Am.*, 81, 3513-3536.
- Crosson, R.S., 1976, Crustal structure modeling of earthquake data 2. Velocity structure of the Puget Sound region, Washington, *J. Geophys. Res.*, 81, 3047-3054, 1976.
- Crosson, R.S., 1986, Where is the subducting slab beneath the Pacific Northwest, (abs.), *Earthquake Notes*, 1986 SSA Meeting, Charleston, South Carolina.
- Dickenson, W.R., 1970, Relations of andesites, granites, and derivative sandstones to arc-trench tectonics, *Rev. Geophys.*, 8, 813-860.
- Ellis, R.M., et al., 1983, The Vancouver Island Seismic Project: A COCRUST onshore-offshore study of a convergent margin: *Canadian Journal of Earth Sciences*, v. 20, pp. 719-741.
- Henderson, M., Crosson, R.S., and T.J. Owens, 1985, Seismic structures from inversion of teleseismic wave forms on the Washington continental margin, *EOS, Trans. Am. Geophys. Un.*, 66, 987.
- Hendrickson, M.A., 1986, The determination of seismic structure from teleseismic P waveforms on the Washington Continental Margin: unpub. Masters Thesis, U. of Washington, 74 p.
- Kanasewich, E.R., Clowes, R.M., Green, A.G., Spencer, C., and C.J. Yorath, 1984, Lithoprobe I: Results of deep crustal vibroseis reflection program on Vancouver Island, *EOS*, 65, 989 (abs.).
- Langston, C.A., 1977, Corvallis, Oregon, crustal and upper mantle receiver structure from teleseismic P and S waves, *Bull. Seism. Soc. Am.* 67(3), 713-724.
- Langston, C.A., and D.F. Blum, 1977, The April 29, 1965 Puget Sound earthquake and the crustal and upper mantle structure of western Washington, *Bull. Seism. Soc. Am.*, 67, 693-711.
- Langston, C.A. 1979, Structure under Mt. Rainier, Washington, inferred from teleseismic body waves, *J. Geophys. Res.* 84(B9), 4949-4762.

- Langston, C.A., 1981, Evidence for the subducting lithosphere under southern Vancouver Island and western Oregon from teleseismic P wave conversions, *J. Geophys. Res.*, 86 (B5), 3857-3866.
- McKenzie, D., and B. Julian, 1971, The Puget Sound, Washington, earthquake and the mantle structure beneath the northwestern United States, *Bull. Geol. Soc. Am.*, 82, 3519-3524.
- McMechan, G.A., and G.D. Spence, 1983, P-wave velocity structure of the earth's crust beneath Vancouver Island: *Canadian Journal of Earth Science*, v. 20, pp. 742-752.
- Michaelson, C.A., 1983, Three-Dimensional velocity structure of the crust and upper mantle of Washington and Oregon, University of Washington Geology Dept., M.S. Thesis.
- Michaelson, C.A., and C.S. Weaver, 1986, Upper mantle structure from teleseismic P wave arrivals in Washington and northern Oregon: *J. Geophys. Res.*, v. 91, no. B2, p. 2077-2094.
- Owens, T.J., Hendrickson, M., and R.S. Crosson, 1986, Constraints on the subduction geometry beneath western Washington using broadband teleseismic P-waveform modeling, (abs.), *Earthquake Notes*, 57, 1986 SSA Meeting, Charleston, South Carolina.
- Riddihough, R.P., 1979, Gravity and structure of an active margin: British Columbia and Washington: *Canadian Journal of Earth Sciences*, v. 16, pp. 350-362.
- Rohay, A.C., 1982, Crust and mantle structure of the North Cascade Range Washington, Univ. of Wash., Seattle, Washington, Ph.D. Thesis.
- Spence, G.D., Clowes, R.M., and R.M. Ellis, 1985, Seismic structure across the active subduction zone of western Canada: *Journal of Geophysical Research*, v. 90, pp. 6754-6772.
- Taber, J.J., 1983, Crustal Structure and Seismicity of the Washington Continental Margin, Ph.D. Thesis University of Washington, Seattle, WA.
- Weaver, C.S., and C.A. Michaelson, 1983, Segmentation of the Juan de Fuca plate and volcanism in the Cascade range: (abs.), *EOS*, v. 64, p. 886.
- Yorath, C.J., Green, A.G., Clowes, R.M., Brown, A.S., Brandon, J.T., Kanasewich, E.R., Hyndman, R.D., and C. Spencer, 1985, Lithoprobe, southern Vancouver Island: seismic reflection sees through Wrangellia to the Juan de Fuca plate: *Geology*, v. 13, p. 759-762.
- Zervas, C.E., and R.S. Crosson, 1986, Pn observation and interpretation in Washington: *Bull. Seis. Soc. Am.*, v. 76, no. 2, p. 521-546.

### Seismicity of the Pacific Northwest

- Crosson, R.S., 1972, Small earthquakes, structure, and tectonics of Puget Sound area, Bull. Seismol. Soc. Amer., 62, 1133-1171.
- Crosson, R.S., 1983, Review of seismicity in the Puget Sound region from 1970-1978: a brief summary: in J.C. Yount and R.S. Crosson (eds.) Earthquake Hazards of the Puget Sound Region, U.S. Geological Survey Open File Report 83-15, pp. 6-18.
- Heaton, T.H., and P.D. Snavely, Jr., 1985, Possible tsunami along the northwestern coast of the United States inferred from Indian traditions: Bulletin of the Seismological Society of America, v. 75, pp. 1455-1460.
- Rogers, G.C., 1983, Seismotectonics of British Columbia: unpublished Ph.D. dissertation, University of British Columbia, 247 p.
- Rogers, G.C., 1985, Seismicity and seismic potential of Canada's western margin (abs.): The 23rd General Assembly of International Association of Seismology and Physics of the Earth's Interior, v. 1, p. 53.
- Taber, J.J. and S.W. Smith, 1985, Seismicity and focal mechanisms associated with the subduction of the Juan de Fuca plate beneath the Olympic Peninsula, Washington: Bulletin of the Seismological Society of America, v. 75, pp. 237-249.
- Washington Public Power Supply System (WPPSS), 1982, Final safety analysis report - Supply System nuclear project no. 3, volume 3.
- Weaver, C.S., and S.W. Smith, 1983, Regional tectonic and earthquake hazard implications of a crustal fault zone in southwestern Washington: Journal of Geophysical Research, v. 88, pp. 10,371-10,384.
- Yellin, T.S., 1982, The Seattle earthquake swarms and Puget Basin focal mechanisms and their tectonic implications: unpublished M.Sc. Thesis, University of Washington, 96 p.

### Plate Convergence in the Pacific Northwest

- Chase, R.L., Tiffin, D.L., and J.W. Murray, 1975, The western Canadian continental margin, in Canada's Continental Margins and Offshore Petroleum Exploration, Canadian Society of Petroleum Geologists in association with the Geological Association of Canada, Calgary, Alberta, Canada, pp. 701-721.
- Nishimura, C., Wilson, D.S., and R.N. Hey, 1984, Pole of rotation analysis of analysis of present-day Juan de Fuca plate motion: Journal of Geophysical Research, v. 89, pp. 10,283-10,290.



- Riddihough, R.P., 1977, A model for recent plate interactions off Canada's west coast, *Can. J. Earth Sci.*, Vol. 14, pp. 384-396.
- Riddihough, R.P., 1981, Absolute motions of the Juan de Fuca plate system: resistance to subduction?: (abs.), *EOS*, v. 62, p. 1035.
- Riddihough, R.P., 1984, Recent movements of the Juan de Fuca plate system *J. Geophys. Res.*, 89, 6980-6994.

#### General References Regarding Seismic Coupling

- Adams, J., 1984, Active deformation of the Pacific Northwest continental margin, *Tectonics*, 3(4), 449-472.
- Ando, M., and E.I. Balasz, 1979, Geodetic evidence of aseismic subduction of the Juan de Fuca plate: *Journal of Geophysical Research*, v. 84, pp. 3023-3027.
- Christensen, D., and L. Ruff, 1983, Outer rise earthquakes and seismic coupling: *Geophysical Research Letters*, v. 10, pp. 697-700.
- Davis, G.A., Coombs, H.A., Crosson, R.S., Kelleher, J.A., Tillson, D.D., and W.A. Keil, 1984, Juan de Fuca/North American Plate convergence: seismic or aseismic subduction? Report prepared for Washington Public Power Supply System, Nuclear Project No. 3, August, 1984, 40 p.
- Heaton, T.H., and H. Kanamori, 1984, Seismic potential associated with subduction in the northwestern United States: *Bulletin of the Seismological Society of America*, v. 79, pp. 933-941.
- Hyndman, R.D., and D.H. Weichert, 1983, Seismicity and Rates of Relative Motion on the Plate Boundaries of Western North America, *Geophys. J. R. Astr. Soc.*, Vol. 72, pp. 59-82
- Kanamori, H., 1977, Seismic and aseismic slip along subduction zones and their tectonic implications: in M. Talwani and W.C. Pitman, III (eds.), Island Arcs, Deep Sea Trenches and Back-Arc Basins, Maurice Ewing Series I, pp. 173-174, AGU, Washington, D.C.
- LeFevre, L.V., and K.C. McNally, 1985, Stress distribution and subduction of aseismic ridges in the middle America subduction zone: *Journal of Geophysical Research*, v. 90, pp. 4495-4510.
- McCann, W.R., and C.R. Sykes, 1984, Subduction of aseismic ridges beneath the Caribbean plate: implications for the tectonics and seismic potential of the northeastern Caribbean; *J. Geophys. Res.*, v. 89, p. 4493-4519.
- Peterson, E.T., and T. Seno, 1984, Factors affecting seismic moment release rates in subduction zones: *Journal of Geophysical Research*, v. 89, pp. 10,233-10,248.

- Reilinger, R., and J. Adams, 1982, Geodetic evidence for active landward tilting of the Oregon and Washington coastal ranges: *Geophys. Res. Letters*, v. 9, no. 4, p. 401-403.
- Ruff, L., and H. Kanamori, 1980, Seismicity and the subduction processes: *Phys. Earth Planet. Int.*, v. 23, pp. 240-252.
- Savage, J.C., Lisowski, M., and W.H. Prescott, 1981, Geodetic strain measurements in Washington: *Journal of Geophysical Research*, v. 86, pp. 4929-4940.
- Stein, S., Wiens, D.A., Engeln, J.F., and K. Fiyita, 1986, Comment on "Subduction of aseismic ridges beneath the Caribbean plate: implications for the tectonic and seismic potential of the northeastern Caribbean: *J. Geophys. Res.*, v. 91, no. B1, p. 784-786.
- Woodward-Clyde Consultants (WCC), 1984, Juan de Fuca Plate Comparison, report prepared for Washington Public Power Supply System WPPSS, Richland, WA.

General References Regarding Subduction Pertinent to the Cascadia Zone

- Cande, S.C., and R.B. Leslie, 1986, Late Cenozoic tectonics of the southern Chile trench: *J. Geophys. Res.*, v. 91, no. B1, p. 471-496.
- Kanamori, H., 1981, The nature of seismicity patterns before major earthquakes: in D.W. Simpson and P.G. Richards (eds.), Earthquake Prediction, an International Review, Maurice Ewing Series IV, pp. 1-19, AGU, Washington, D.C.
- Kelleher, J., and W. McCann, 1976, Buoyant zones, great earthquakes, and unstable boundaries of subduction: *Journal of Geophysical Research*, v. 81, pp. 4885-4896.
- Kelleher, J., and J. Savino, 1975, Distribution of the seismicity before large strike slip and thrust-type earthquakes: *Journal of Geophysical Research*, v. 80, pp. 260-271.
- Lay, T., Kanamori, H., and L. Ruff, 1982, The asperity model and the nature of large subduction zone earthquakes: *Earthquake Prediction Research*, v. 1, pp. 3-71.
- Mogi, K., 1979, Two kinds of seismic gaps: *Pure Applied Geophysics*, v. 117, pp. 1172-1186.
- Sacks, I.S., 1983, The subduction of young lithosphere: *Journal of Geophysical Research*, v. 14, pp. 3355-3366.
- Scholl, D.W., 1974, Sedimentary sequences in the north Pacific trenches: in C. Turk and L. Drake (eds.), The Geology of Continental Margins, Springer-Verlag, New York, pp. 493-504.

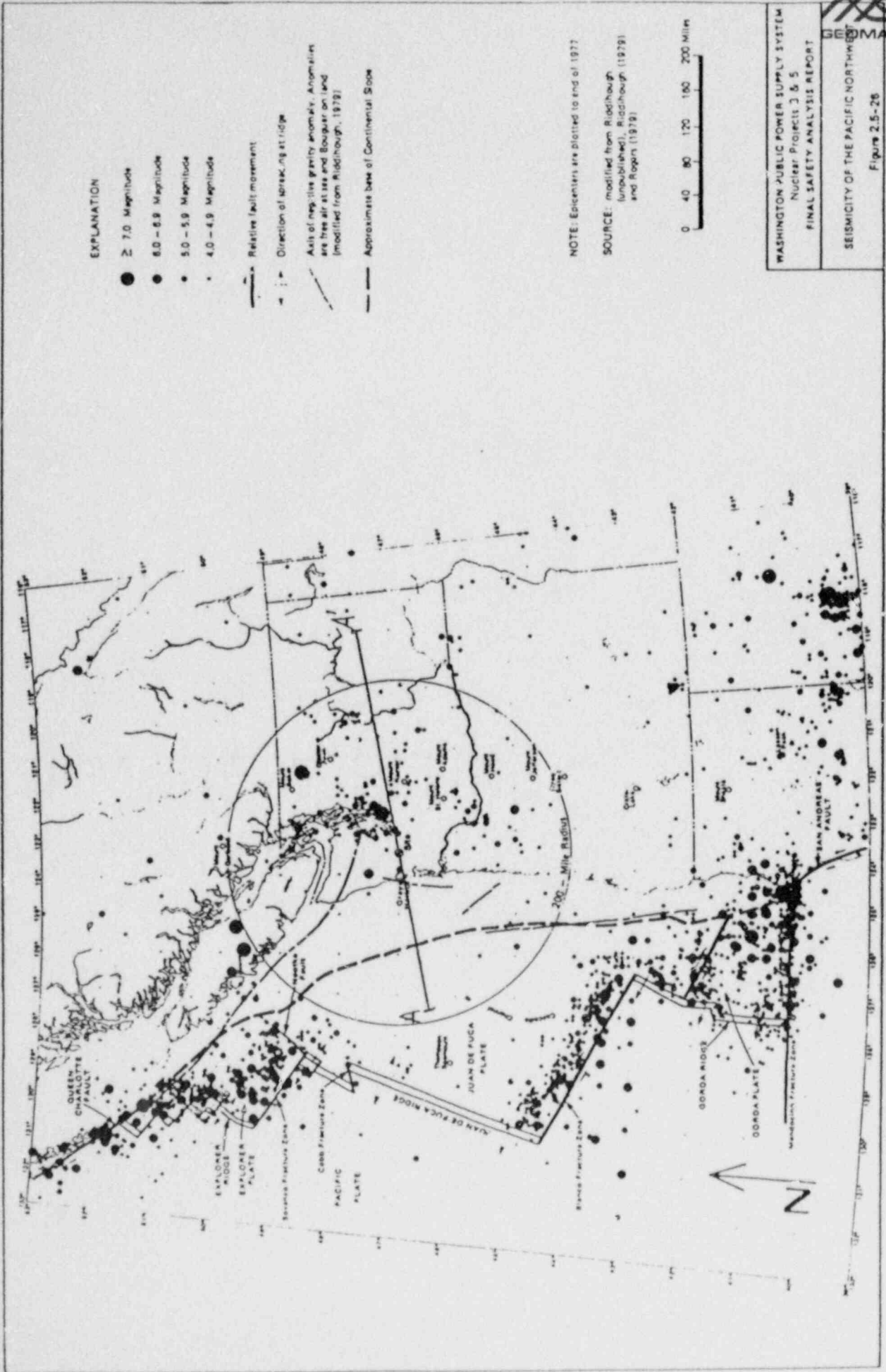
- Seno, T., Shimazaka, K., Somerville, P., Sudo, K., and T. Eguchi, 1980, Rupture process of the Miyagi-oki, Japan, Earthquake of June 12, 1978. *Physics of the Earth and Planetary Interiors*, v. 23, pp. 39-61.
- Uyeda, S., and H. Kanamori, 1979, Back-arc opening and the mode of subduction: *Journal of Geophysical Research*, v. 84, pp. 1049-1061.
- Von Huene, R., 1974, Modern trench sediments: in C. Burk and L. Drake (eds.), *The Geology of Continental Margins*, Springer-Verlag, New York, pp. 493-504.
- Yokoyura, T., 1981, On subduction dip angles: *Tectonophysics*, v. 77, pp. 63-77.

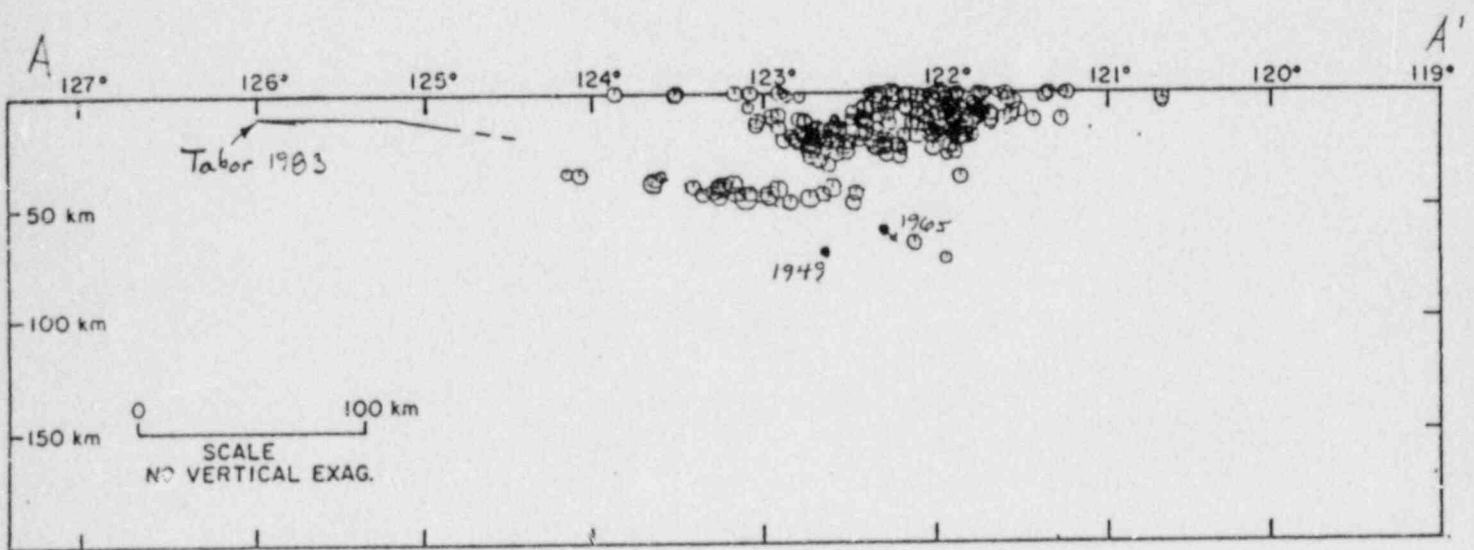
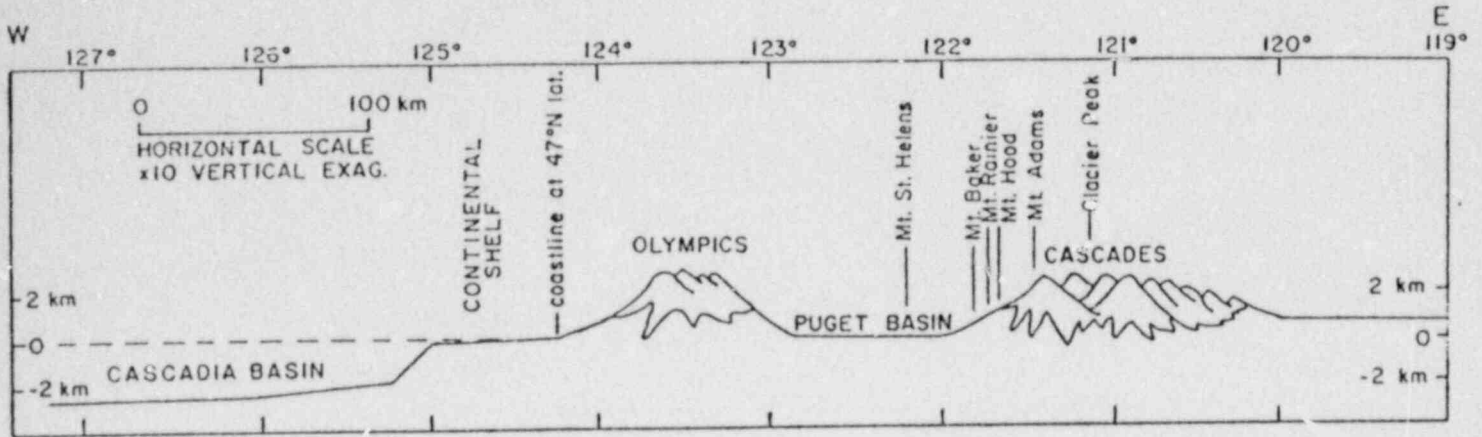
#### General References Regarding Earthquake Recurrence and Maximum Earthquake Assessment

- Anderson, J.E., 1979, Estimating the seismicity from geological structure: *Bull. Seis. Soc. Am.*, v. 69, p. 163-185.
- Anderson, J.G., and J.E. Luco, 1983, Consequences of slip rate constraints on earthquake recurrence relations: *Bulletin of the Seismological Society of America*, v. 73, pp. 471-496.
- Schwartz, D.P., and K.J. Coppersmith, 1984, Fault behavior and characteristic earthquakes: examples from the Wasatch and San Andreas faults: *Journal of Geophysical Research*, v. 89, pp. 5681-5698.
- Schwartz, D.P., Coppersmith, K.J., and F.H. Swan, III, 1984, Methods for assessing maximum earthquakes: *Proceedings of the Eighth World Conference on Earthquake Engineering*, San Francisco, California, Vol. 1, pp. 279-285.
- Youngs, R.R., and K.J. Coppersmith, 1985, Implications of fault slip rates and earthquake recurrence models to probabilistic seismic hazard estimates: *Bulletin of the Seismological Society of America*, v. 75, pp. 939-964.

#### Geology Related to Subduction in the Pacific Northwest

- Connard, G., Couch, R.W., Roy, J., and S. Kulm, 1983, Heat flow: Atlas of the Ocean Margin Drilling Program, Western Washington-Oregon Continental Margin, and Adjacent Ocean Floor, Region V, Joint Oceanographic Institutions, Inc., Marine Science International, Woods Hole, MA, 1 map sheet plus text.
- Kulm, L.D., 1983, Western Washington/Oregon Juan de Fuca Project: unpublished draft report for Washington Public Power Supply System, 35 p.
- Kulm, L.D., and R.W. Embly, 1983, Contrasting tectonic-sedimentologic styles along the convergent Juan de Fuca plate boundary: *EOS*, . 64, p. 828.





PHASE I RESPONSES OF INDIVIDUAL EXPERTS

PHASE I  
RESPONSES BY EXPERT #1



Geometry

Credibilities associated with geometries sketched on cross-section provided:

10° dip with double bend	0.20
15° dip	0.50
25°	0.30

The basis for these are:

- The refraction data of Taber are good near the hinge area; his 10° dip east of the hinge is constrained by only two stations and a dip of 15° appears to be reasonable using his data.
- The deep seismicity does not define a dip of more than a couple degrees; the T-axes of focal mechanisms are not as systematically oriented as suggested by Taber and Smith.
- The 25° dip is consistent with depth of high velocity layer of Langston from the Longmire station and the proper depths for magma generation.
- The Pn data suggest that the 6 - 7.8 km/sec transition has essentially no dip and the 8.1 km/sec velocity is not seen, although it is well-determined to the west offshore.
- The velocity inversion of broad band data suggest dips of greater than 10° and most likely about 15°.
- Recent work by Canadian investigators suggest 15° dip.

Convergence Rate

30 mm/yr normal convergence (+10 mm/yr) based on analyses by Riddihough and Nishimura et al. These studies show that the rate has been decreasing over the past several years.

Seismic Sources and Activity

Potential seismic sources are:

Intra-slab

Interface

"deep events" above Juan de Fuca plate for 15° and 25° dip models (remnant plate?)

Probability that the intra-slab source is seismogenic:

Given a dip of  $10^{\circ}$ : 1.0 based on occurrence of 1965, 1949 events

Given a dip of  $15^{\circ}$  -  $25^{\circ}$ : 1.0 for deep zone (which may be remnant slab); 0.10 - 0.15 for deep slab because of lack of current seismicity down to magnitude 2

Probability that the interface is seismogenic:

40% (ranging from 25% to less than 50%) based on:

- Complete absence of thrust earthquakes that would be associated with stress buildup on the interface
- The unusual nature of the margin relative to other margins globally
- Adams turbidite data suggest possibility of large earthquakes, as perhaps will Brian Atwater subsidence data
- Jim Savage most recent strain data does not see strain accumulation across Puget Basin, but may be shear strain accumulation across Strait of Juan de Fuca

### Location of Rupture

Intra-slab source:

$10^{\circ}$  dip model:

Eastern limit at about  $122^{\circ}$  because of age, depth, and temperature of plate

Western limit for most of seismicity at about  $124^{\circ}$  based on observed drop-off of seismicity and the effect of the accretionary wedge although could have mag 4 to 5 events all the way to the ridge

95% of the seismicity would be expected between  $122^{\circ}$  and  $124^{\circ}$

$15^{\circ}$  -  $25^{\circ}$  models:

Expect the seismicity to be above about 50 km but have little basis for estimating

The remnant slab source would not expect it to be restricted in lateral extent to the Puget Sound region

For all models, the observed seismicity provides a reasonable basis for the relative frequency of earthquake occurrence along strike



Interface source:

Downdip extent should be at about 40 to 50 km depth based on pressure and temperature

Updip extent to within about 50 km of the slab hinge point (toe of the continental slope at  $125^{\circ}$ ); above this would be in weaker materials of the accretionary wedge

Along-strike representation of the interface is poorly constrained.

- Michaelson and Weaver inversion is subject to considerable uncertainties, no alternative models were tested
- 20% likelihood that the M & W boundary segments the interface
- The ends of the Juan de Fuca plate (Nootka fault zone and Blanco fracture zone) should be segment boundaries.

Maximum Earthquake Magnitude

Intra-slab source ( $10^{\circ}$  dip) or remnant slab source ( $15^{\circ}$  -  $25^{\circ}$  dips):

7.25 ( $\pm 0.25$  with 7.25 slightly preferred) based on largest historical events and constraints from thickness of brittle slab

Intra-slab source ( $15^{\circ}$  -  $20^{\circ}$  dips)

5 - 6 based on observed events offshore

Interface:

Maximum dimensions (given above) provide reasonable maximum magnitude constraint

Ruff and Kanamori relationship is not very applicable to the Juan de Fuca plate because off edge of distribution

Seismic Coupling and Earthquake Recurrence

Uncertainty is seismic coupling represented by a bimodal distribution; which says that the interface is either nearly entirely aseismic or is nearly completely locked.

The probability mass near  $\alpha = 0$  and  $\alpha = 1$  ranges from 0.5 - 0.5 to 0.66 - 0.33, respectively.

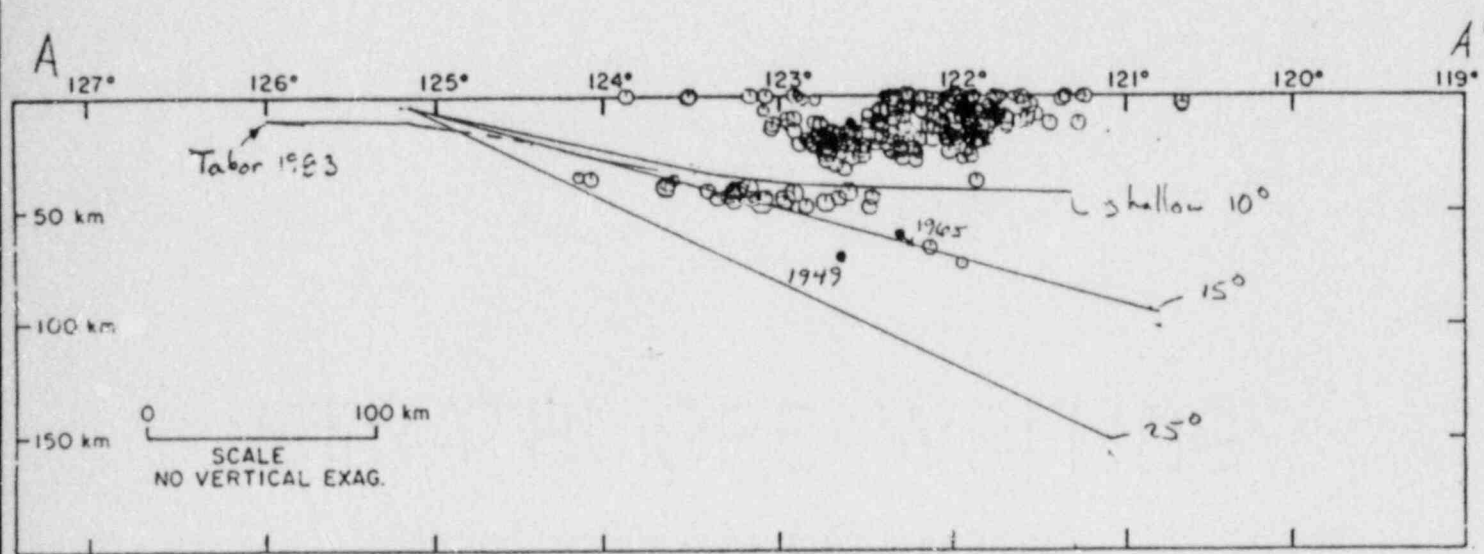
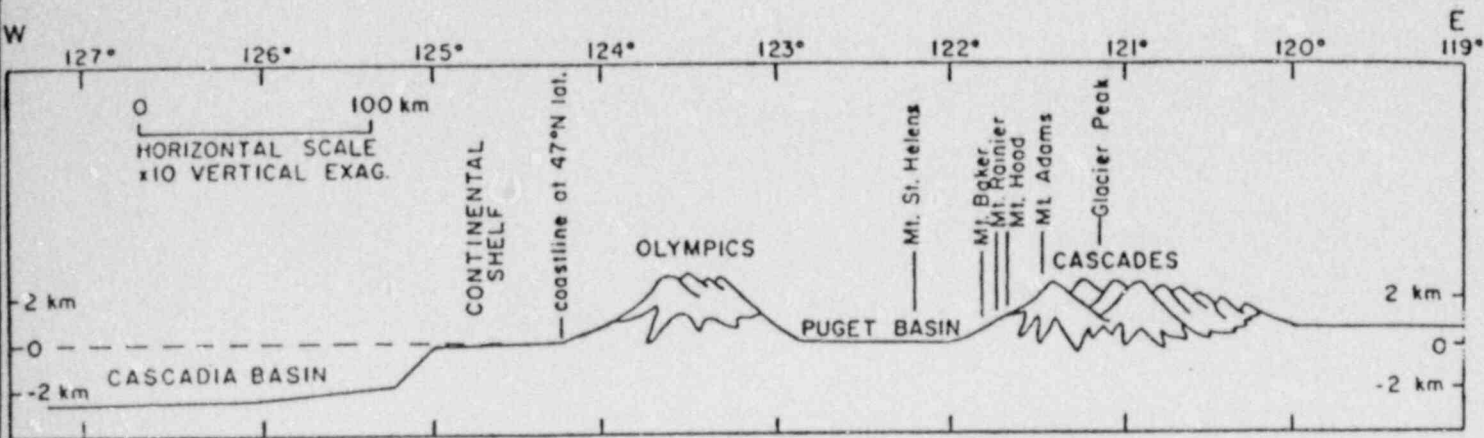
The basis for this assessment is the following:

- If the coupling were  $\alpha = 0.5$ , one would expect to see small to moderate magnitude thrust earthquakes in the region surrounding the imminent rupture; no such events have been observed.

- There appears to be no known analog subduction zone that is completely locked; this would imply a maximum moment recurrence model (i.e., essentially no other events besides the largest magnitudes)
- The strain data will be very important to assessing whether a very low  $\alpha$  (aseismic slip) is occurring; at present, uniform strain accumulation does not appear to be occurring.

Paleoseismic indicators (e.g., turbidites, Atwater subsidence data) suggest longer recurrence intervals (500 - 1,000 yr); due to present uncertainties, these data should only be used as a basis for comparison.

For intraplate and remnant slab sources, use historical seismicity for recurrence estimation.



EXPERT #1

Three configurations:

- shallow 10° with double bend
- 15°
- 25°

PHASE I  
RESPONSES FROM EXPERT #2



Geometry

Basis for geometry sketched on cross-section provided:

- Refraction results by McClain beneath the continental slope show a 5 - 10° dip to the slab
- Seismicity data constrain the slab location beneath Puget Sound
- A steepening beneath Puget Sound (as suggested by Michaelson and Weaver, 1986) gets the slab to proper depths for magma generation beneath the Cascade. This also agrees with work by Langston.

Note that the boundary sketched is the oceanic crust/mantle boundary (oceanic Moho) with the top of plate located as indicated.

Convergence Rate

A distribution of values is provided:

15 mm/yr	10%
20 - 25 mm/yr	80%
30 mm/yr	10%

(Note that these are orthogonal rates of convergence.)

Based on estimates made by Duncan and Verplanek, Riddihough, Engebretson, and Jurdy.

Seismic Sources and Activity

Potential seismic sources are:

Intra-slab  
Interface

Probability that the intra-slab source is seismogenic:

60-70% based on occurrence of historical seismicity and uncertainty in location of 1949 and 1965 earthquakes

Probability that the interface is seismogenic:

80% (+5%, -10%) based on:

- McClain's refraction results show 4 - 4.5 cm/sec crust against the oceanic crust.

- The isotherms and heat flow suggest that well-cemented dewatered rocks should be present.
- Low-grade metamorphism and reduction would be expected (based on McClain's work).

### Location of Rupture

#### Intra-slab source:

The upper 10-15 km of oceanic crust is expected to be the brittle (seismogenic) part of the slab.

The updip extent should be at about 123 longitude (near the bend in the plate).

The downdip extent is uncertain; but 80-90% of the large earthquakes would be expected near the deeper bend in the plate.

#### Interface:

The updip extent of rupture lies approximately beneath the coastline based on:

- This is western extent of Oligocene-Miocene volcanic rocks. Interface between Eocene volcanics and sedimentary Oligocene-Miocene accretionary wedge.
- The subducted sediments have undergone low-grade metamorphism and have had the fluids squeezed out, low porosity, and zero permeability.

The downdip extent of rupture cannot be assessed with confidence.

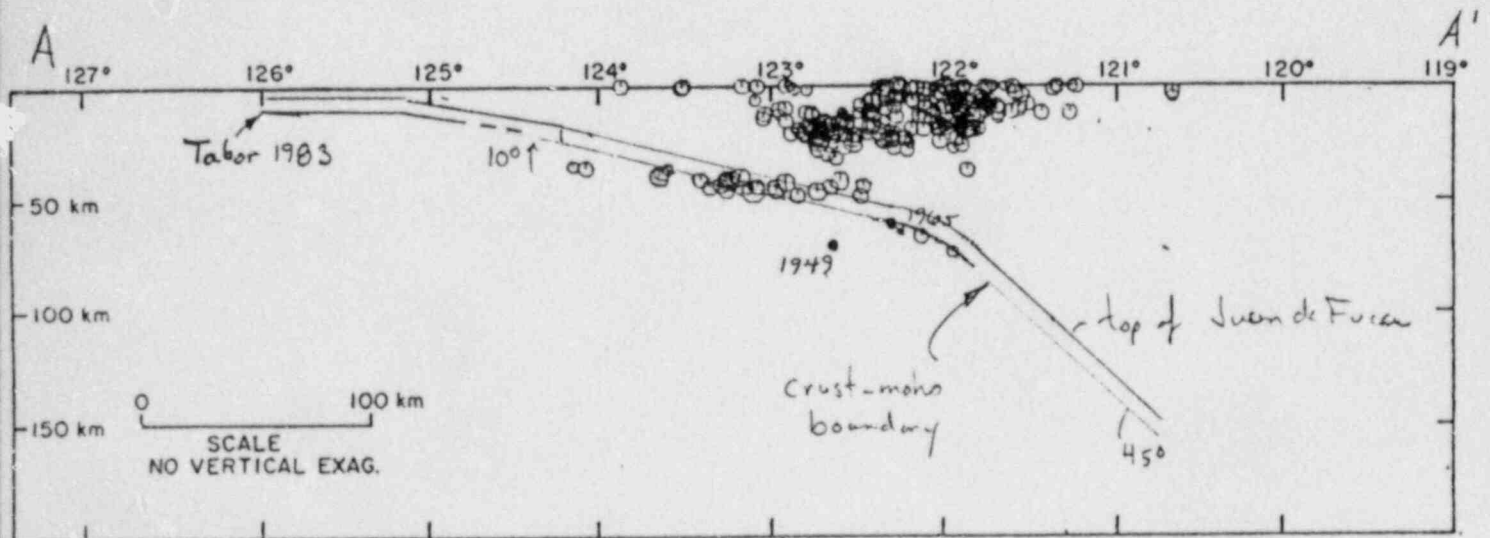
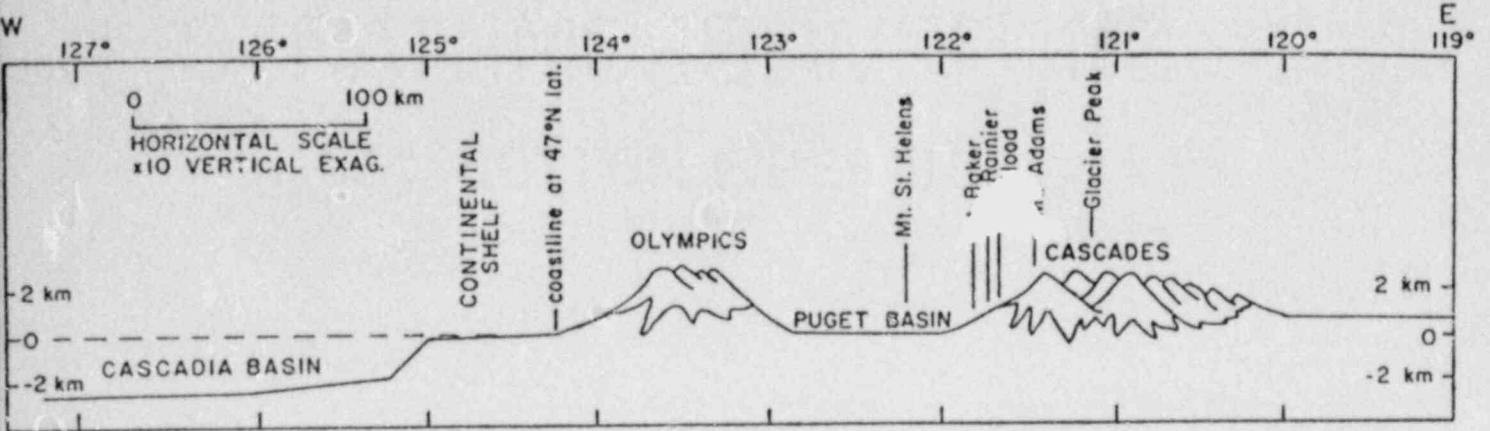
Along-strike segmentation of the interface is difficult because morphologic evidence would be obscured by the thick sediments and no deep reflection lines have been run parallel to the margin to look for sub-sediment morphologic changes. Between  $46^{\circ}$  and  $47^{\circ}$  lat. lies a free-air and Bouguer gravity low that may represent a segment (following <sup>W</sup> model of Kelleher et al.). Confidence level in this segment is 40% (+10%, -30%).

### Earthquake Recurrence

30% confidence is given to the Adams turbidite interpretation because:

- The cause of the turbidites could be sediment loading at the slope, storm activity, or seismic triggering

- Recurrence intervals of hundreds of years seems reasonable for this margin due to sediment loading because the shelf is over 35 km wide.
- More work is needed to verify that the thickness of the hemipelagic clays is consistent among turbidites to verify that recurrence intervals are regular.



EXPERT #2

PHASE I  
RESPONSES BY EXPERT #3

Geometry

Basis for the geometry sketched on cross-section attached:

- Focal mechanisms of the deeper seismicity, including the 1965 event, are normal suggesting they lie within the slab.
- Langston's analysis of converted phases above the 1965 events shows a low velocity zone that is inferred to be a layer of subducted sediments.
- No opinion is given regarding the location of the slab beneath the Cascades.

Convergence Rates

40 mm/yr (+19 mm/yr) based on the analyses of Nishimura et al. This rate appears to be compatible with rates on major structures to the north and south such as the Queen Charlotte fault and the San Andreas fault. The 40 mm/yr is based on an average rate over 700,000 yr. No data exists to determine shorter-term rates. Shortening rates given by Adams (25 mm/yr) are probably not true crustal shortening rates or would expect to see large mountain ranges like the Transverse Ranges.

Seismic Sources and Activity

Potential seismic sources are the following:

- Intra-slab source
- Plate interface
- Faults in accretionary wedge (analogy is made to seismogenic faults in the wedge such as that giving rise to the 1945 Mikawa earthquake, which experienced surface rupture. It is assumed that this type of source will be modelled by the known crustal faults in the site area and/or by a random crustal source).

Probability that the potential sources are seismogenic:

Intra-slab: 1.0 based on the historical occurrence of the 1965 and 1949 events, which are inferred to be intra-slab events.

Interface: 0.6 based on the following:

- If the interface were creeping, one would expect to see more small magnitude ( $M < 6$ ) thrust events.
- It would be unusual on a global basis for the margin to be completely quiet seismically, especially along its entire length.



- Global comparisons of plate age, convergence rate, etc., suggest that the Cascadia zone should be seismogenic.
- The probability may be as high as 80% if geologic evidence for large events is further supported; or it may be less than 50% if other analogous margins can be shown to be aseismic.

#### Locations of Rupture

**Intra-slab:** (Distribution for likelihood of earthquake occurrence shown on cross-section.) Two most likely locations are the outer rise and where they have occurred historically. Although very few outer rise events have occurred historically, they would be expected by analogy to other margins. In map view, the relative likelihood of intra-slab earthquake occurrence can be modelled either by the pattern of observed seismicity or by an assumption of a uniform distribution. Both of these models are given an equal weight of 50%.

**Interface:** (Distribution for likelihood of earthquake occurrence shown on cross-section.) Basis for this distribution is global analogies to where seismic radiation typically occurs. In map view, the Blanco fracture zone and the Nootka fault zone, which mark the ends of the Juan de Fuca plate probably serve as segment boundaries. No strong evidence exists for segmentation within the plate, although it is possible for the interface to rupture along a length that is shorter than the entire 700 km-long margin.

#### Maximum Earthquake Magnitudes

**Intra-slab:** 7-1/2 in the deeper part of the slab.  
8 in the shallow part; based on global analogy (Sumba, Rat Island)

**Interface:** 9 (+1/2) based primarily on maximum rupture dimensions and analogy to the 1960 Chile earthquake.

#### Recurrence-Related Parameters

**Intra-slab:** The historical seismicity provides a reasonable basis for estimating recurrence.

**Interface:**

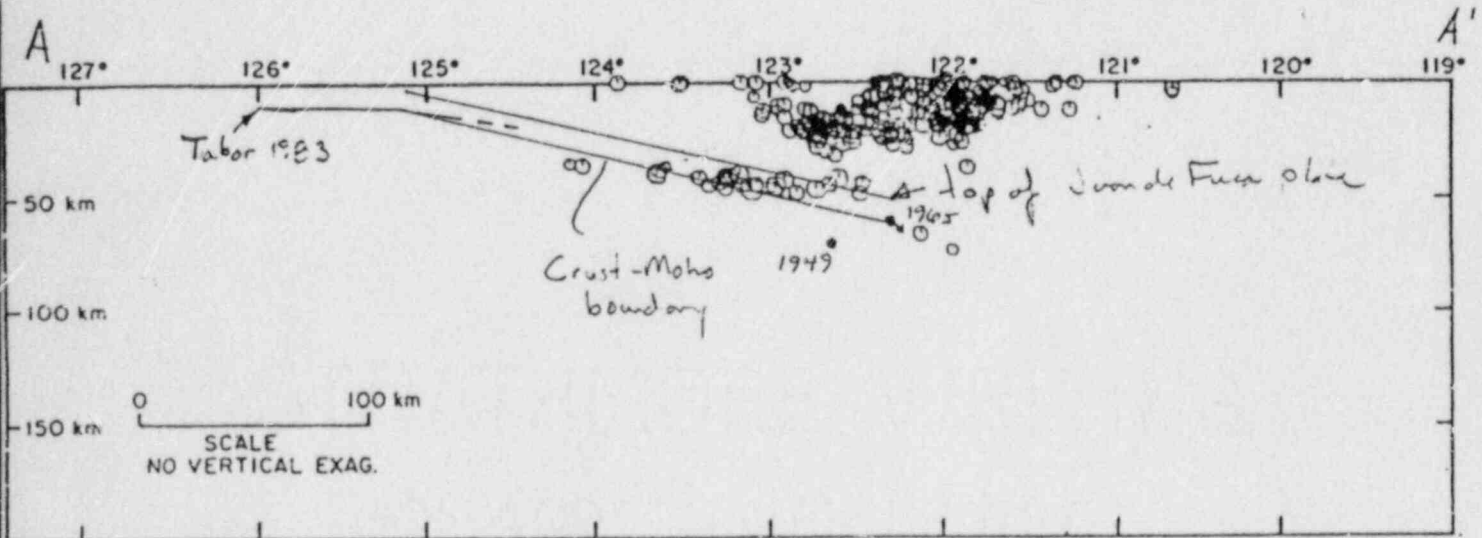
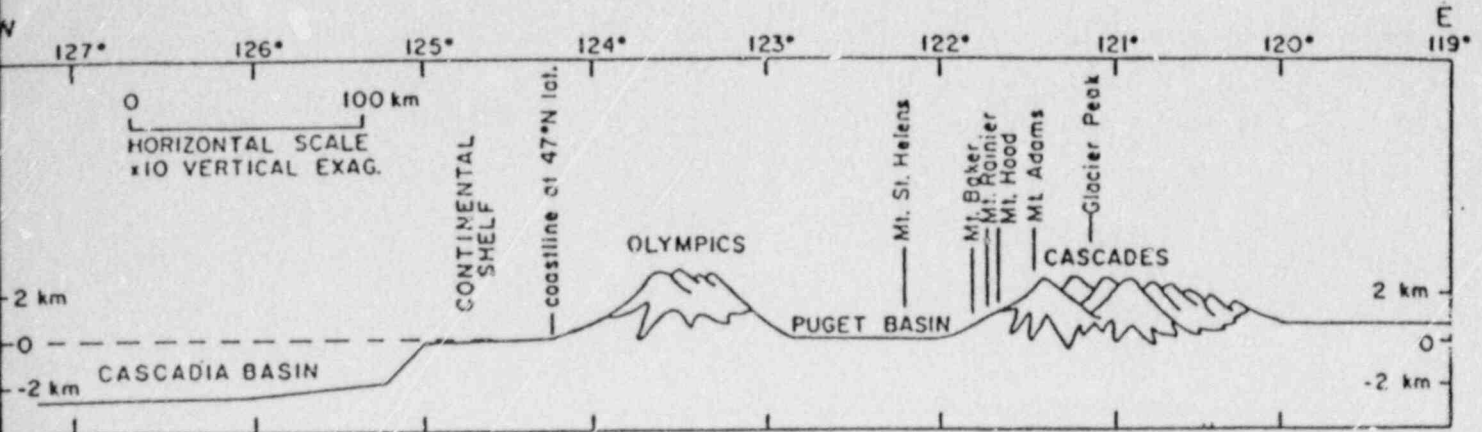
Recurrence intervals may range from 200 to 20,000 yrs with a preferred value of about 400 yr based on:

- Recurrence from offshore turbidites appears to be about 400 - 500 yr.

- Preliminary evidence for subsidence by Atwater suggests recurrence intervals longer than 1,000 yr, as do recurrence data in Alaska.
- Historical data suggest that at least 150 yr and probably 200 yr have elapsed since the last major earthquake.

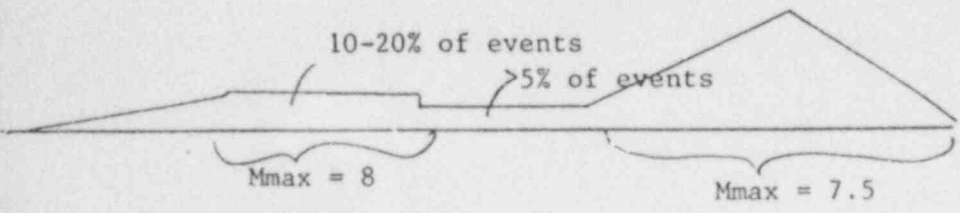
A characteristic earthquake recurrence model is considered to be appropriate to explain the absence of moderate size events. The range of the characteristic magnitude should be 8 - 9.

Seismic coupling (see distribution) is given an expected value of 0.66 based on global analogies and Kanamori's age vs. coupling relationship. The value is less than 1.0 because post-seismic creep probably accommodates a considerable amount of total convergence. Earthquake recurrence on the interface should be based primarily on the recurrence interval date (given above) and the seismic coupling estimate used as a secondary check on these estimates.

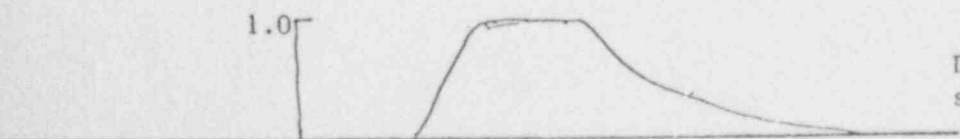


EXPERT #3

Cross-Section



Location Distribution for Intraslab events



Distribution for prob that section of interface will rupture in event

PHASE I  
RESPONSES BY EXPERT #4

Geometry

Basis for geometry sketched on cross-section provided:

- Should be 100-125 km beneath volcanics based on global analogs
- Shallow dip is consistent with young hot plate and slow convergence
- The refraction data by Taber offshore are good

[Note that we have reinterpreted your drawing to reflect the fact that the Taber (1983) line represents the top of oceanic Moho, not top of the oceanic plate (see attached).]

Convergence Rate

A distribution of rates was given:

1 cm/yr	0.05
2 cm/yr	0.50
3 cm/yr	0.40
4 cm/yr	0.05

The basis for this estimate is:

- Comparison with other margins
- Presence of the volcanic arc
- Presence and number of earthquakes
- Global plate reconstructions

It is noted that uncertainties in these rates may result from the breaking up of the Juan de Fuca plate.

Seismic Sources and Activity

Two potential seismic sources are identified:

- plate interface
- intra-slab

Probability that the intra-slab source is seismogenic:

- 1.0 based on historical occurrence of 1965 and 1949 events, which are inferred to be intraplate events

Probability that the interface source is seismogenic:

0.75 (+0.25) based on the evidence that the rocks are being stressed near the interface, as witnessed by the small-magnitude intra-slab events

(Note that "seismogenic" here is interpreted to be applicable down to magnitudes as small as M3).

#### Location of Rupture

Intra-slab source:

Seismicity within the slab would be expected to occur within the upper 20 km; 90% within 5-15 km. The upper 5 km is probably weaker and unable to support large earthquakes, but could be the location of aftershocks. The weakness is probably due to the intermixing of sediments with basalts in the upper part of the slab.

Along strike, a higher concentration of seismicity might be expected where they have occurred historically (low confidence in this assessment).

Interface:

The downdip extent would be at about 40 km based on:

- Globally, maximum depths are typically about 60 km, but because this is a young plate and has a slow convergence rate, a shallower depth is expected
- The presence of intra-slab events at depths of 40 km suggests that the rocks can support earthquakes at these depths

The updip extent lies at about 20 km depth based on:

- Analogies to other subduction zones
- This lies at about the eastern edge of the accretionary prism

Along strike, the boundary with the Explorer Plate (Nootka fault zone) and the Gorda Plate (Blanco fracture zone) should be barriers to interface rupture with a confidence level of 50% (+45%).

#### Maximum Earthquake Magnitude

Intra-slab source:

Uniform distribution between magnitude 7 - 7-1/2.

Interface:

3	30%
4	30%
5	30%
6	9%
7	1%

Seismic Coupling and Recurrence

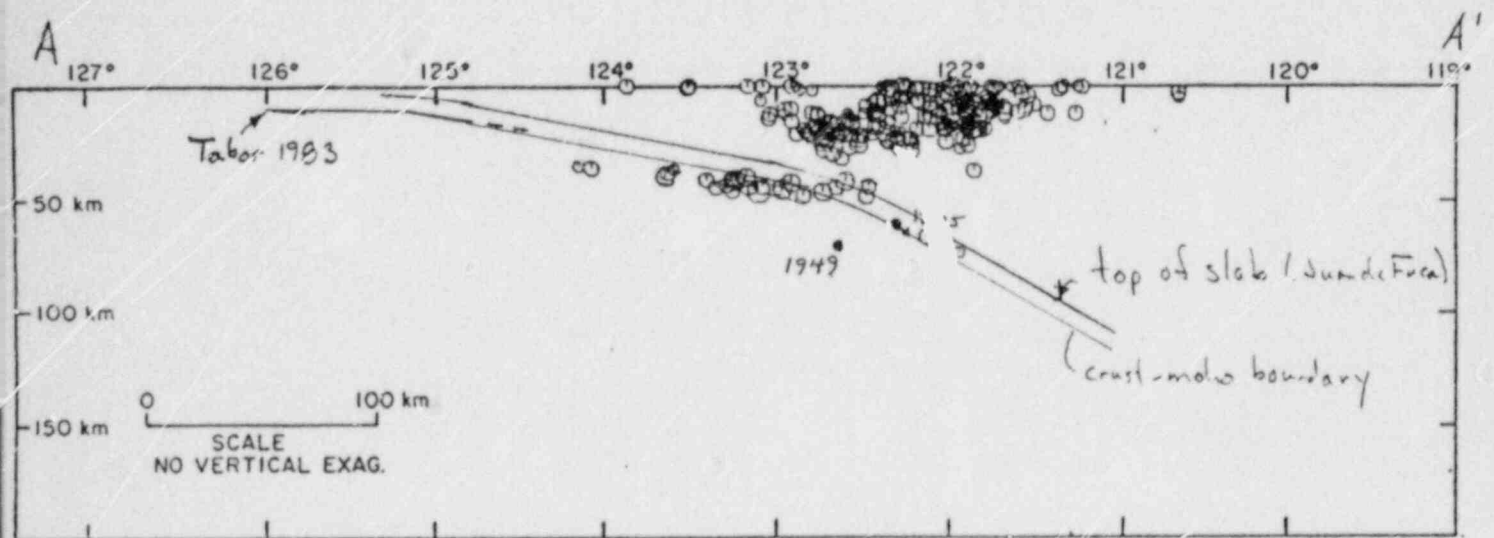
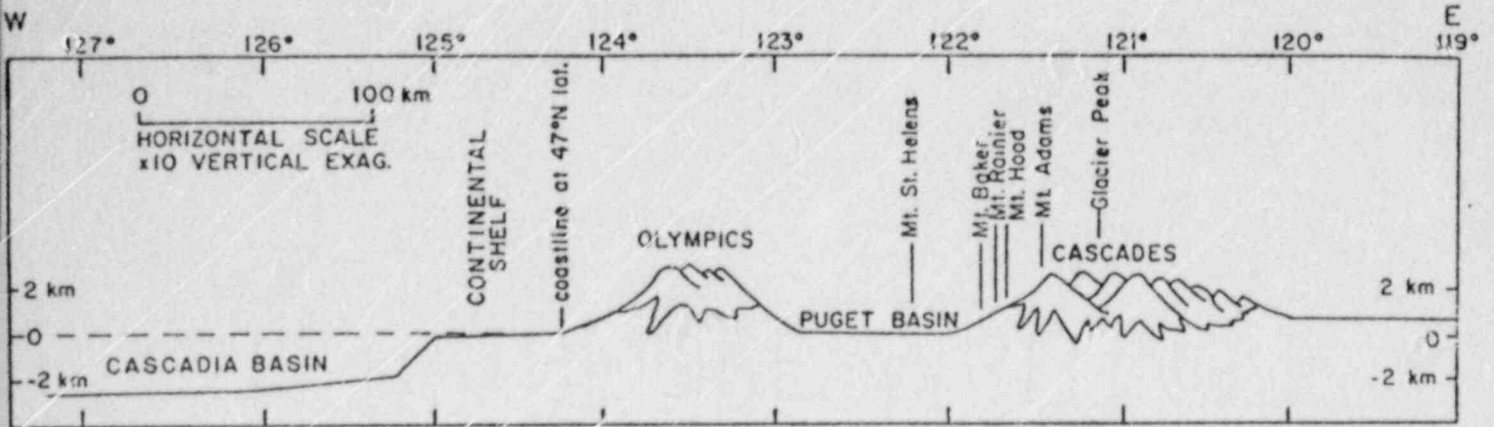
Intra-slab source:

Use of historical seismicity to define recurrence seems to be reasonable (low confidence in this assessment).

Interface:

$\alpha = 0.05$  (+0.15, -0.05) with 80% weight at 0.05.

based on global analysis to other subduction zones such as Barbados and southernmost Chile.



EXPERT #4

PHASE I  
RESPONSES BY EXPERT #5

Geometry

The following weights are given to the geometries sketched on the cross-sections provided:

Model A (gradually increasing slab dip):	75 - 80% ( $\pm .1 - .15$ )
Model B (shallow dip):	20 - 25% ( $\pm .1 - .15$ )

based on:

- To reach magma generation depths, need to be at about: 100 km beneath Mt. Ranier
- The hypocenters for the deeper seismicity do not define a dip
- Taber's refraction data allow slab dips above  $11^\circ$
- Waveform modeling by Owens suggests dips of about  $15 - 20^\circ$  are likely at about  $123.5^\circ$
- Model A is consistent with Michaelson and Weaver's  $45^\circ$  dips to east and with appropriate magma depths

Convergence Rate

40 (+0, -15) mm/yr based on:

- Riddihough analyses of plate reconstructions
- The internal deformation occurring in the Explorer and Gorda plates suggests that the Juan de Fuca plate is changing character from an actively subducting plate to one that is passive and less rigid.
- The convergence rates lack resolution and are averaged over the past million years; a decrease in convergence rate has been noted. Therefore, the average rate over this period should represent the maximum rate.

Seismic Sources and Activity

Potential seismic sources are the following:

- Intra-slab
- Plate interface



Probability that the sources are seismogenic:

Intra-slab: 1.0 based on the historical occurrence of the 1949 and 1965 earthquakes which can be attributed to the slab

Interface:  $0.5 \pm 0.5$  based on:

- Heaton and Hartzell make a good case for the possibility of large earthquake occurrence
- Convergence is taking place but there have been no historical thrust earthquakes
- It is rare to have an aseismic young plate
- All of the evidence is circumstantial rather than definitive; therefore, a large uncertainty is assigned
- Juan de Fuca tending toward behavior similar to Explorer and Gorda plates

Location of Rupture

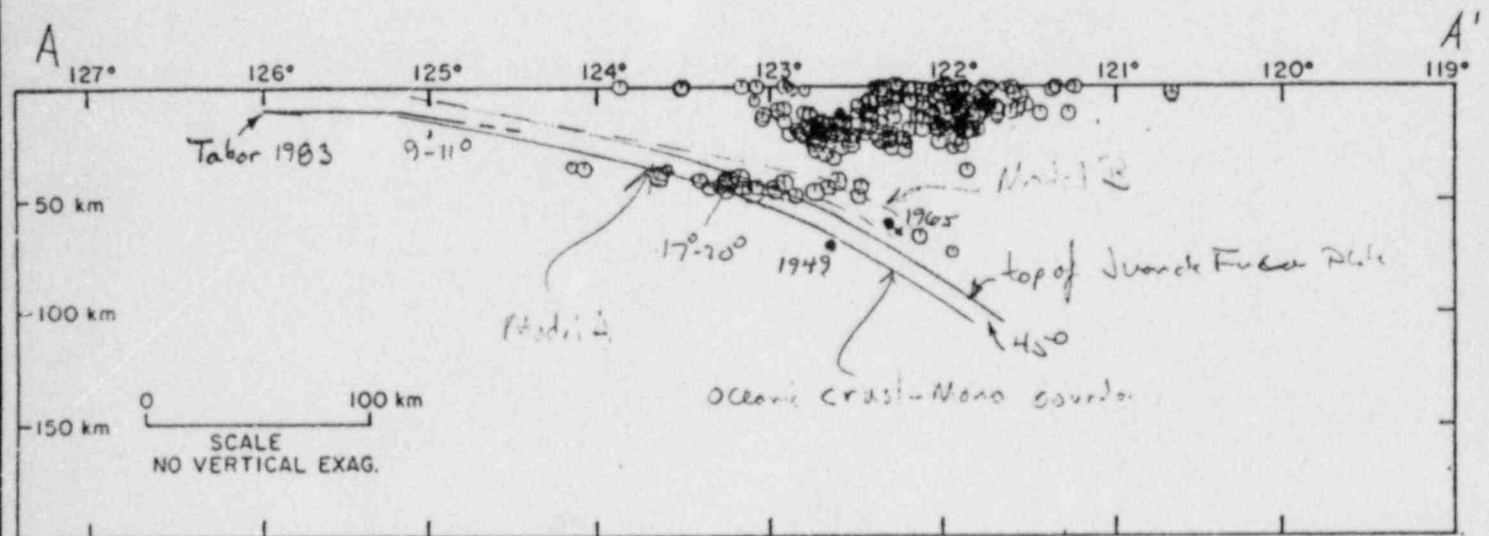
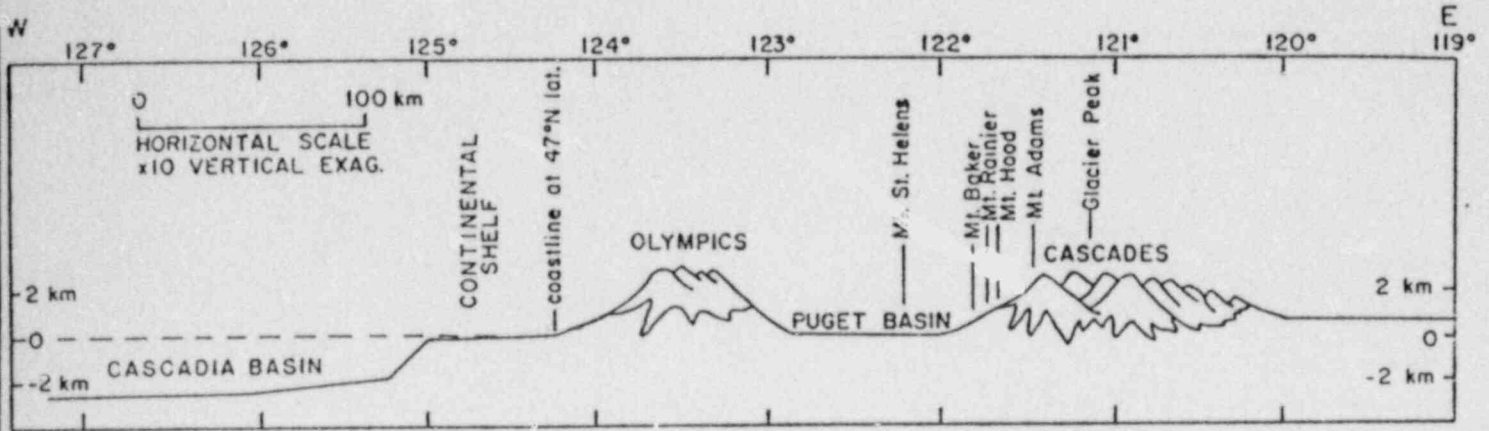
Intra-slab: In cross-section, the upper 6 - 8 km of the slab is expected to be seismogenic. Downdip seismicity is not expected east of Mt. Ranier. The updip extent is essentially at the coastline based on the seismicity data and the youthfulness of the slab. In map view, the historical seismicity record can provide a basis for the relative frequency of earthquake occurrence; with the slab corner model of Rogers, a possible explanation for the localization of Puget Sound seismicity.

Interface: The downdip extent of the seismogenic interface should be at about  $123.5^\circ$  where the continental Moho lies against the interface. Updip, the interface should extend to the eastern boundary of the accretionary prism essentially at the coastline. Along strike, the boundaries with the Explorer and Gorda plates should be segment boundaries based on the different behavior of these other plates. Segmentation within the Juan de Fuca plate cannot be assessed with any confidence.

Maximum Magnitudes and Earthquake Recurrence

Intra-slab: The historical record and analogies to intra-slab earthquakes globally suggest that M7 is a reasonable maximum magnitude. The historical seismicity record provides a reasonable basis for assessing earthquake recurrence on this source.

Interface: The characteristics of the Juan de Fuca plate suggest that it is unlikely that it would behave coherently in a single earthquake rupture, but a maximum magnitude estimate can not be made with any confidence. Recurrence on the interface cannot be made with any confidence.



EXPERT #5

PHASE I  
RESPONSES BY EXPERT #6

Geometry

Basis for geometry sketched on cross-section provided:

- Taber's refraction data in the offshore region are good
- The slab should be about 100 km beneath Mt. Ranier to reach proper magmatic depths
- Seismicity data show down-dip tensional mechanisms, which is typical of intra-slab seismicity. The plunge of the t-axis of the 1965 earthquake is from teleseismic data and, therefore, not as affected by local structure as the mechanisms from the local network data.

The relative weight given to the geometry models shown are:

Model A	70% $\pm$ .05	based on T-axis of focal teleseismic data
Model B	30% $\pm$ .05	based on seismicity distribution

Convergence Rates

Minimum convergence rate is 13 mm/yr, which is Savage's compression rate based on geodetic data. This value is given a weight of 0.1. 40 mm/yr is given a weight of 75% based on global reconstructions. It is unlikely that rates are higher than this because there are no large forces (slab pull), the ridge has recently realigned, and the pole shifts show that the rate is slowing down.

Following distribution given:

<u>Rate</u>	<u>Probability</u>
10 - 20 mm/yr	0.04
20 - 30 mm/yr	0.04
30 - 40 mm/yr	0.4
40 - 43 mm/yr	0.1
43 - 50 mm/yr	0.4
50 - 50 mm/yr	0.02

Seismic Sources and Activity

Potential seismic sources are the following:

- Intra-slab source
- Plate interface
- Upper plate above Blanco fracture zone (because of distance to site, this source is not considered further)

Probability that these potential sources are seismogenic:

Intra-slab: 100% based on historical seismicity data

Interface: 65% ( $\pm 15\%$ ) based on the young age of the slab as compared to other subduction zones, the convergence rate is slowing down meaning that it is being resisted, and resistance is giving rise to a rotation of the ridge and change in pole location.

#### Location of Rupture

Intra-slab: Earthquakes should be confined to the upper 10-15 km of the slab. In cross-section, they may occur 75 km ( $\pm 25$  km) west of the free-air low (trench) down to a maximum depth of 75 km. 75% ( $\pm 15\%$ ) of the  $M \geq 6$  earthquakes would be expected in the bend region and where they have been observed historically. The relative rate should decrease to the west by the square root of the distance.

Interface: The downdip extent of the seismogenic interface should be about 45 km ( $\pm 5$  km) depth. Updip extent is at a depth of about 20 km, which is essentially the end of the crust in the overlying plate. Hypocenters for earthquakes below M7 may occur randomly over the interface, but above M7 they are expected to nucleate toward the base of the interface.

Along strike, segment boundaries to interface rupture and their credibility, are the following: Blanco fracture zone ( $50\% \pm 25\%$ ), Savanco fracture zone (no probability given), major change in the free-air gravity at  $46^\circ$  ( $25\% \pm 25\%$ ). The probability of a rupture breaking more than a single segment boundary is low (10%).

#### Maximum Earthquake Magnitudes

Intra-slab: Uniform distribution between 6-3/4 and 7-1/4 based on historical record.

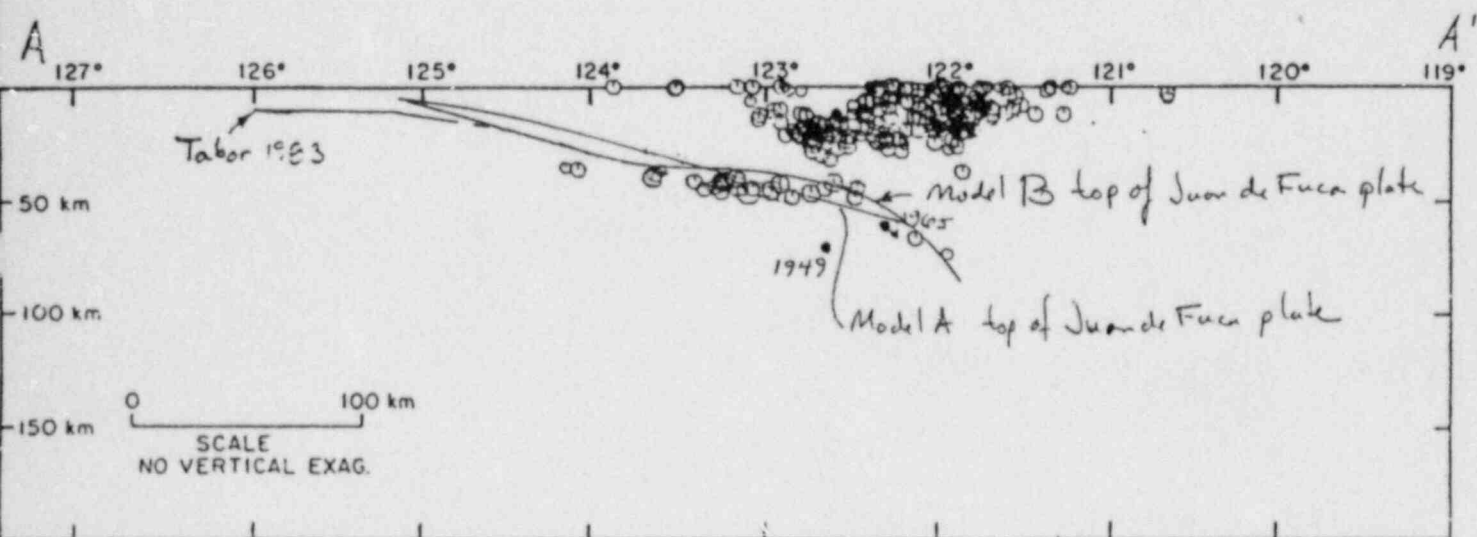
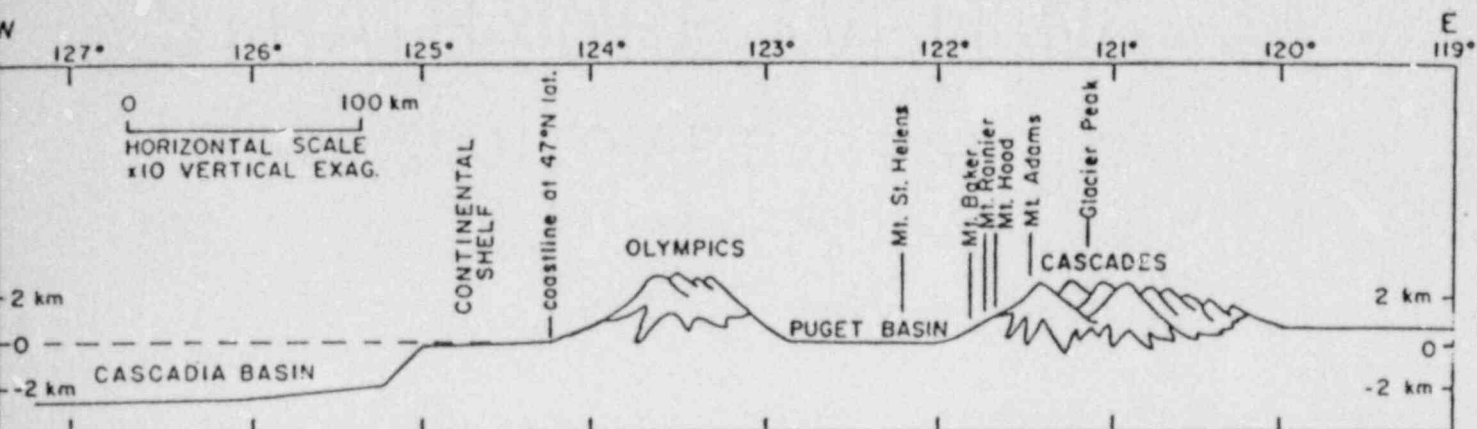
Interface: Use rupture dimensions given.

#### Recurrence-Related Parameters

Coupling:  $\alpha = 0.6 \pm 0.15$  (uniform) based on dip angle (low dip = high  $\alpha$ ), young age, and rate of convergence.

Interface recurrence: should weigh equally estimates based on moment rate with Adam's paleoseismic estimates

Intra-slab recurrence: use historical seismicity



EXPERT #6

Note: Cross-section redrawn to reflect that the offshore line labeled Tabor 1983 is the crust-Moho boundary, not the top of slab.

PHASE I  
RESPONSES BY EXPERT #7

Geometry

Basis for geometry sketched in cross-section provided:

- Refraction data in the offshore, gravity data, and depths required for magma generation suggest the general geometry given.
- "Knee-bend" beneath Puget Sound may be due to phase changes in the slab, changes in the absolute velocities of the slab, or the bulldozer effect as the slab goes under continental crust. Knee-bends are relatively common in downgoing slabs.
- EMSLAB data beneath Vancouver Island also support this model

Convergence Rate

42 mm/yr ( $\pm$  10 mm/yr) as published by Riddihough (JGR, 1984). The rate between the Juan de Fuca and Pacific plates is very well known, but because the Pacific-North America rate is uncertain, so is the Juan de Fuca-North America rate. Bear in mind that these convergence rates are averaged over geologic time periods and that the instantaneous rate is not known.

Potential Seismic Sources and Activity

Intra-slab source

Plate interface

Probability that potential sources are seismogenic:

Intra-slab: (no estimate given)

Interface: 0.3 ( $\pm$ 0.2) (see discussion under Recurrence-Related Parameters for basis)

Locations of Rupture

Intra-slab: Seismogenic part of slab should be upper 20 km based on age of the plate. The locations of earthquakes within the slab should approximate the distribution observed from historic seismicity data. The observed concentration beneath the Puget trough region may be due to 1) phase changes brought about because the slab is going into the mantle faster to the north, or 2) a "corner" in the slab that is accommodated by phase changes into the slab.

**Interface:** (low confidence in this assessment). One would expect the contact zone to be to the west of the Coast Ranges and to be very narrow due to the underplating occurring along the margin. The true amount of compression occurring along the margin is a function of the position of the first slab bend, the trench roll-back velocity, and the absolute velocity of the upper plate. Along strike, the Nootka fault zone and the Blanco fracture zone are likely segment boundaries. Tears or other segment boundaries that could relate to plate interaction are not evident in the Juan de Fuca plate.

#### Maximum Earthquake Magnitudes

**Intra-slab:** no estimate given.

**Interface:** (low confidence in this assessment). A rupture of the entire plate (Nootka to Blanco fracture zone) seems to be the maximum rupture possible but have little basis for suggesting this is the case.

#### Earthquake Recurrence-Related Parameters

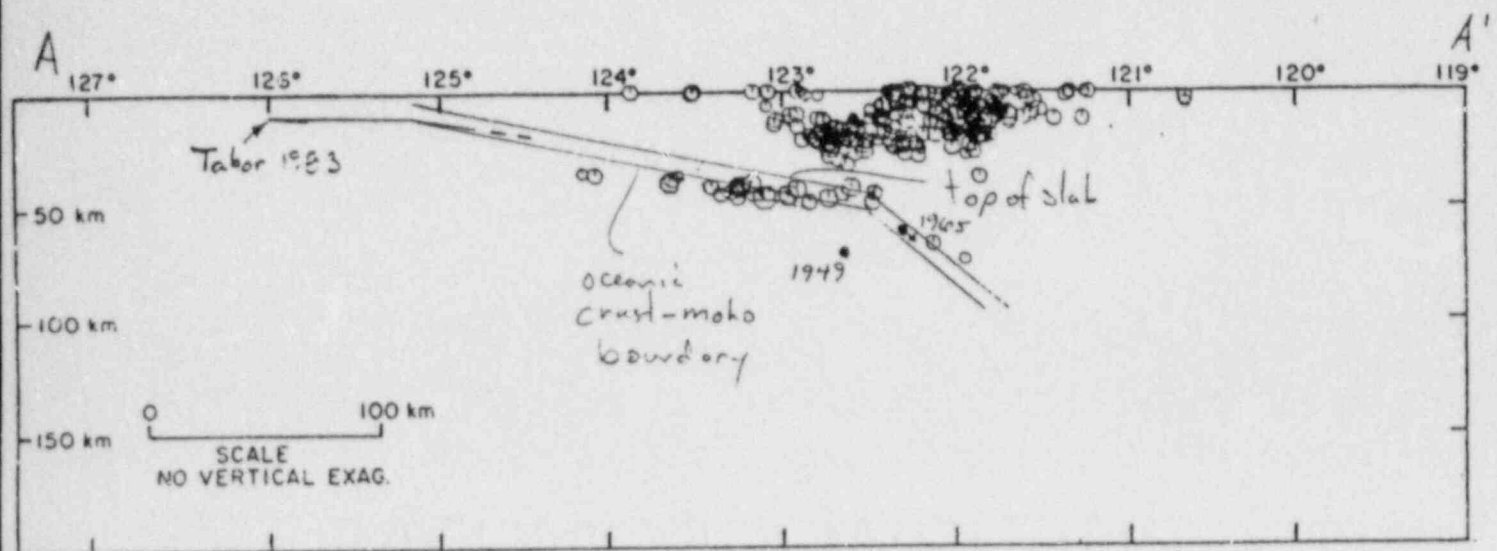
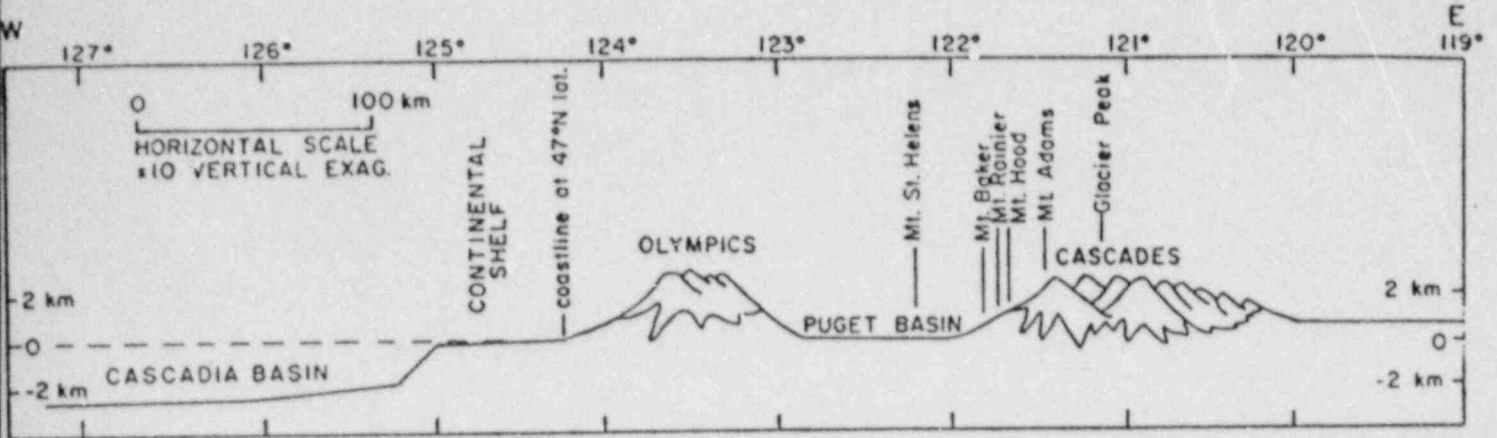
**Intra-slab:** Historical seismicity provides a reasonable basis for estimating intra-slab recurrence.

**Interface:** The behavior of the Cascadia subduction zone suggests that the interface is totally locked ( $\alpha = 1.0$ ) or totally lubricated ( $\alpha = 0$ ), but not in between. The relative weight given to these models are the following:

0	0.7 ( $\pm 0.2$ )
1.0	0.3 ( $\pm 0.2$ )

Preference for the aseismic condition is based on the lack of historical thrust earthquakes, the steady uplift observed from the leveling data, and the good evidence for extensive sediment subduction and underplating seen in the Vancouver Island geophysical work. No independent estimates of recurrence are given.





EXPERT #7

PHASE I  
RESPONSES BY EXPERT #8

Geometry

Basis for geometry sketched on cross-section provided

- Slab geometries determined from seismic refraction, seismic reflection, seismicity, and other data.
- The same general model for slab beneath Vancouver I. should apply to Washington because have same age of plate, sediment supply, etc.
- Velocity models used for earthquake locations in southwest Canada are based on new refraction results (1983 on).

Convergence Rate

40 mm/yr (+ 10-15%) based on the Riddihough analysis. Note that he finds a decrease in rate through the last several million years. His results are probably best for the more northerly parts of the Juan De Fuca plate, which is most appropriate for the present study.

Seismic Sources and Activity

Potential seismic sources are identified:

Intra-slab source

Plate interface

Probability that the potential sources are seismogenic:

Intra-slab: 1.0 based on historic seismicity

Interface: range of 0.25 to 0.75 with preference for 0.4 to 0.5 on the following basis: The probability should be greater than 0 because we see evidence of a sole thrust in the refraction and reflection data. The "E" zone seen in the Lithoprobe results, appears to act as a zone of decoupling, which is highly affected by fluids and sediments. The latest results show that the top of the slab is below the E zone by 1 to 1.5 sec and is, therefore, separated from the E zone. The relationship between E zone and current subducting plate is not totally clear.

### Location of Rupture

Intra-slab: Earthquakes would be expected in the upper 8-10 Km of the slab. In cross-section, the eastern extent should be at about 70 Km depth based on the seismicity data, heat flow data, and magnetotelluric data. To west, intra-slab earthquakes may occur to the toe of the slope ( $125^\circ$  west) where the slab first bends. In map view, the relative frequency of earthquake occurrence should approximate that observed historically (i.e. higher concentration in Puget Sound region) due to a probable corner of the plate in this area.

Interface: Seismogenic part of the interface should be limited updip at about  $124.5^\circ$ - $125^\circ$  where the high velocity unit (above  $E_1$ ) pinches out. Downdip the interface should extend to about  $123^\circ$  where continental mantle would come in contact with the slab. Along strike, the Nootka fault zone would be expected to act as a segment boundary since reflection and refraction data show that it is a major boundary and crustal earthquakes are associated with the fault zone.

### Maximum Earthquake Magnitudes (low confidence in this assessment)

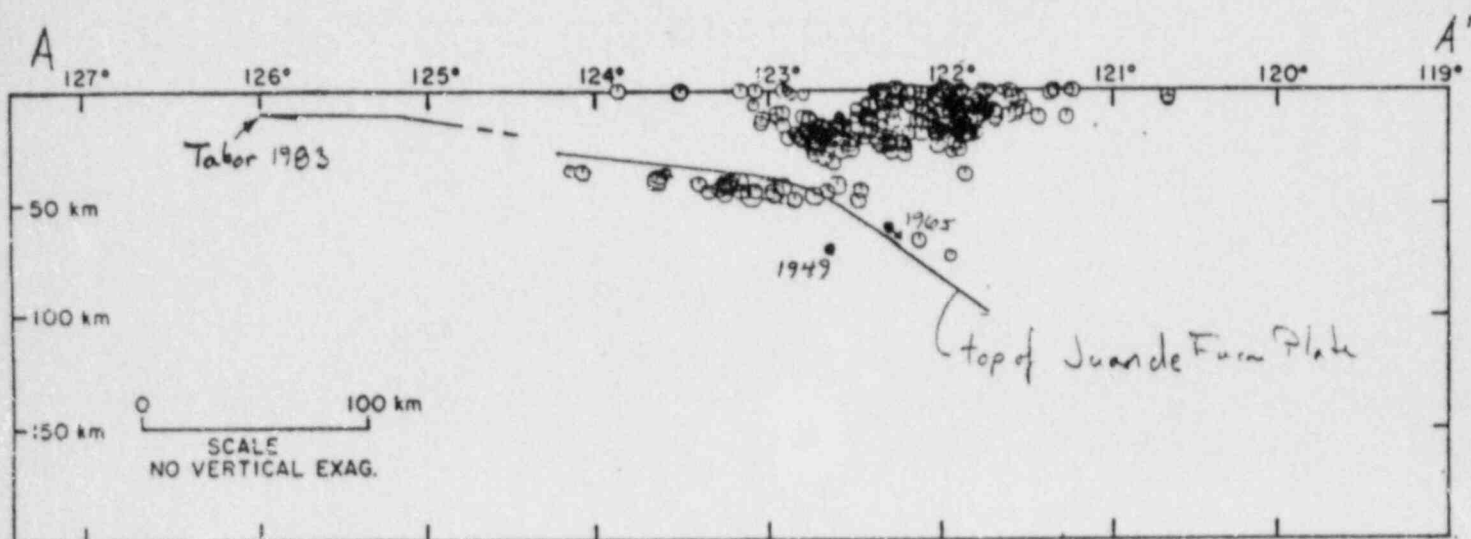
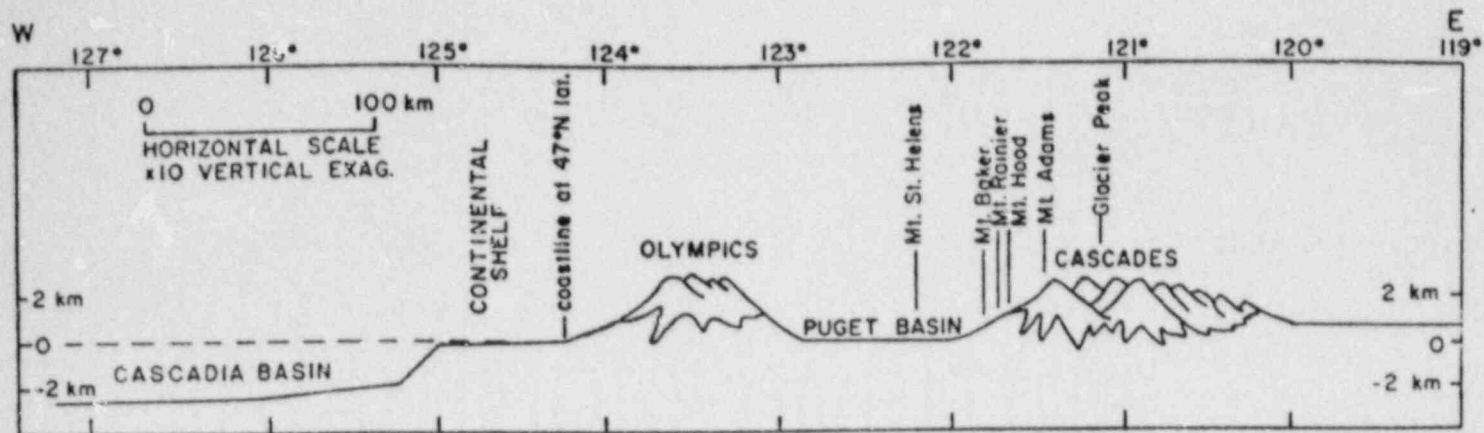
Intra-slab: no estimate, but note that it is a young plate with critical geotherm ( $500^\circ\text{C}$ ) limiting vertical rupture dimension to  $< 8$  km.

Interface: Reasonable to use maximum rupture dimensions.

### Recurrence Related Parameters

Intra-slab: No estimate.

Interface: Seismic coupling estimated at 25% (range 20% - 50% based on evidence for imbricated deformation. Underplating or subcretion is taking place including sediments and perhaps some of the oceanic plate. As a result of imbrication, the thickness of the sediments actually increases down the interface. This type of deformation is expected to give rise to aseismic behavior or only small earthquakes.



EXPERT #8

PHASE I  
RESPONSES BY EXPERT #9

Geometry

Basis for the geometry sketched on the cross-section provided:

- The hypocentral locations and focal mechanisms of the deeper seismicity beneath the Puget Sound region suggest that these events are occurring within the upper part of the downgoing slab
- The depths required for magma generation provide a suggestion of bending of the slab
- The cut-off of seismicity downdip in the slab is due to a change in the physical properties of the slab

Convergence Rate

42  $\pm$  10 mm/yr based on studies by Riddihough. This rate is consistent with shortening rates of 25 mm/yr based on onshore and offshore deformation analyses by Adams.

Seismic Sources and Activity

Potential seismic sources are the following:

- Intra-slab source(S) A,B.
- Plate interface
- Deep intra-slab source \*C\* (not considered further because probable lack of significance to hazard at site)
- Strike-slip faults within upper plate (such as the St. Helens zone) east of 123°
- Accretionary wedge faults (a generic fault(s) west of 123°)
- Tears in the down-going slab

Probability that these potential sources are seismogenic:

Intra-slab A 0.9

Intra-slab B 1.0

Intra-slab: 10% in deeper portion below 600° geotherm (east of about 121-122°) \*C\*.

Interface: The following distribution is specified:

<u>p (seismogenic)</u>	<u>relative weight</u>
90 - 100%	0.75
80 - 90%	0.24
0	0.01

This distribution is for the probability of generating large earthquakes ( $M \geq 8$ ) and is based on worldwide analogies suggesting that it would be unusual for this margin to be aseismic, the turbidites offshore suggest possible large earthquakes, the stress provinces suggest a large locked area, onshore deformation confirms active convergence, and terrace, tilt and geodetic data.

Tears: if the slab is segmented by tear faults, 100% likely they would be seismogenic above 600° geotherm.

Accretionary wedge faults: 100% that a fault in this region is seismogenic based on the M 5.3 1904 earthquake

Strike-slip zone(s): 100% that a fault of this type is seismogenic based on the 1946 Vancouver Island event, which had a strike-slip mechanism. These zones may be the result of the obliqueness of the convergence vector.

Locations of Rupture

Intra-slab: the seismogenic part of the slab should be the upper 10 km. The pattern of historical seismicity provides a reasonable basis for estimating the relative frequency of earthquake occurrence along strike and downdip.

Interface: two models of the location of the seismogenic interface in cross-section

124.7° - 122.7°	80% likelihood
124.7° - 122°	20% likelihood

Preference is given to the first model because 122.7° is the margin between the Puget Basin and the Olympics as well as close to the Weaver and Smith stress boundary. In map view, the interface may be segmented at the Blanco fracture zone and the Nootka fault zone (80% likelihood). Additional possible segment at the Michaelson and Weaver segment boundary; which is also near a change in observed crustal stress (20%; +30%, -20% likelihood). The margin is narrower in southern Oregon.

Accretionary wedge faults: seismogenic faults should lie between about 123° and 124.5° above the interface. To the west of 124.5° deformation occurs aseismically in soft sediments. Analysis by Adams suggest that the rate of deformation decreases to the east within the accretionary wedge.

Tears in slab: most likely location would be northern Oregon (see segmentation of interface dicussion above).

Strike slip faults: between the western edge of the Puget Trough to the central Cascades; at the eastern boundary of the stress province of Weaver and Smith.

Maximum Earthquake Magnitude

Intra-slab (shallow part, "A"): the following distribution is given:

6.5	0.1
7.0	0.25
7.5	0.55
8.0	0.1

based on worldwide analogies and the age of the oceanic crust.

Intra-slab (deep part, "B"):

7.0	0.1
7.5	0.8
8.0	0.i

based on the historical seismicity record and the thickness of the brittle part of the slab (10 km).

Interface: Use the rupture lengths developed earlier to assess Mmax. Favor large rupture based on turbidite data, locked zone from focal mechanisms.

Accretionary wedge: Use the following distribution

7.5	0.8
8.0	0.2

based on dimensional arguments.

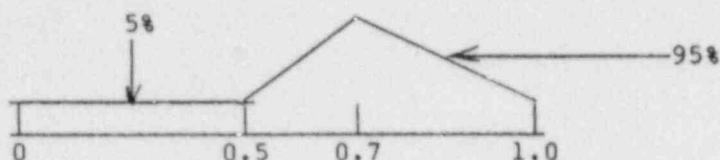
Strike-slip faults: ~ 7-1/2 based on Weaver and Smith's assessment for the St. Helens zone.

Earthquake Recurrence-Related Parameters

Intra-slab "A": use worldwide data to determine seismicity of this age ocean floor.

Intra-slab "B": Use historical seismicity data to constrain recurrence for intra-slab sources.

Interface: Primary basis for recurrence on the interface is the 430 yr (+25%) recurrence interval derived from the turbidite data. Seismic coupling may serve as a basis for comparison and should have the following distribution:



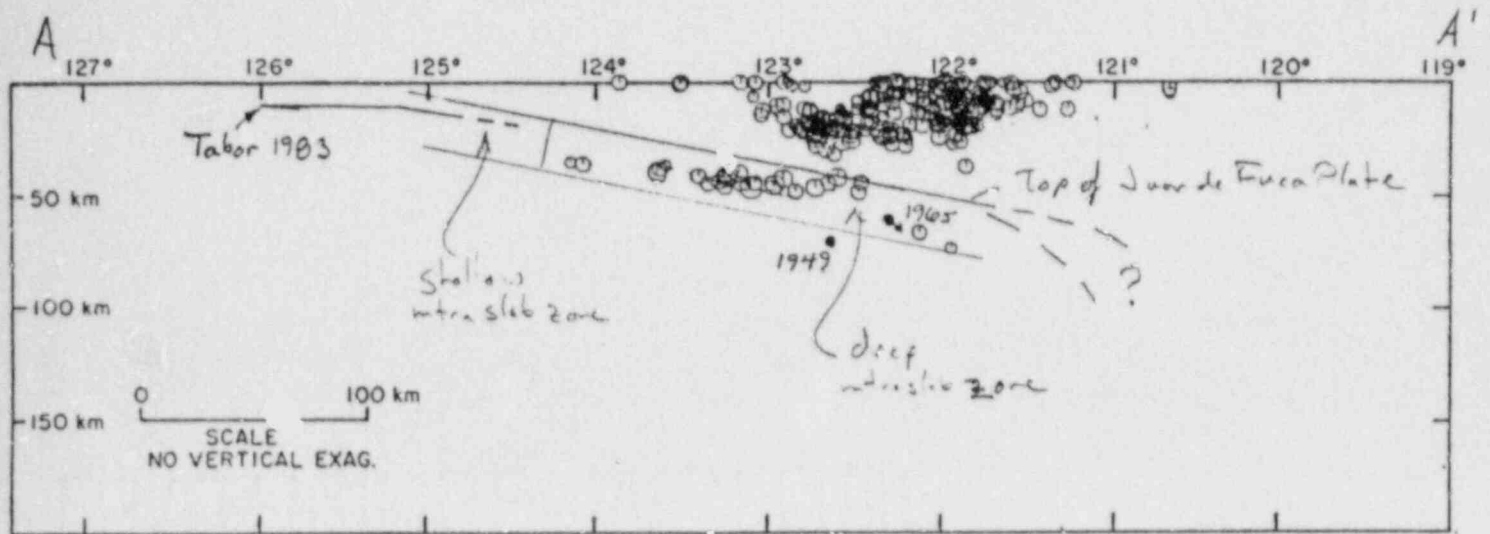
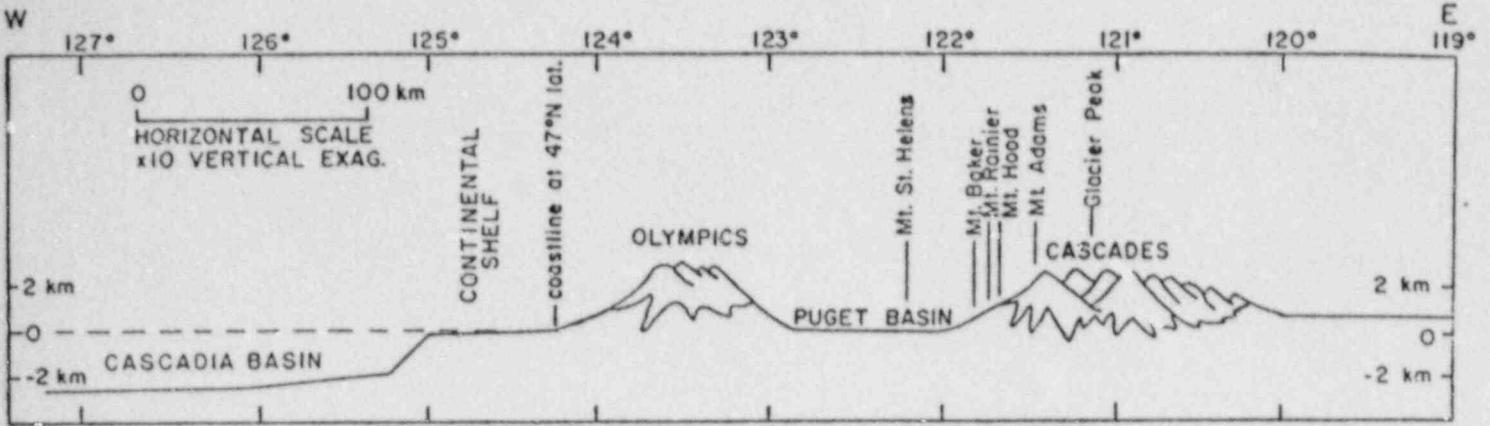
- Coupling is believed to be high based on the evidence for deformation in the overlying plate in the onshore and offshore; and the tide gauge and terrace deformation suggest that their zero isobases have the same positioned relation as at the Shikoku I, Japan.

Tears: Should already be included by intra-slab seismicity.

Accretionary wedge: Use historical seismicity data for recurrence.

Strike slip faults: Use Weaver and Smith's earthquakes for the St. Helens zone and compare the total rate for the strike slip region with this rate.





EXPERT #9

### Geometry

Basis for geometry sketched on cross-section provided:

- Focal mechanisms for the 1949 and 1965 earthquakes, as well as those for the smaller magnitude events are primarily extensional, thus they likely lie within the upper part of the subducting slab.
- Increasing dip to the east is required to attain magmatic generation depths and is in agreement with the T-axis of the 1965 earthquake.
- T-axes for the smaller magnitude seismicity are not very well-resolved from the available data. They do not have to coincide with slab dip as they are likely controlled by local structure.
- Waveform modeling studies, such as those by Crosson and Owens, that suggest steeper slab dips are tentative at the present time.

### Convergence Rates

35 - 50 mm/yr (+19 mm/yr) based on global studies such as that by Nishimira et al. Uncertainty is 95% confidence level of Nishimira. Note that these rates are averaged over the past 1 my and any more recent changes in rate can not be determined from available data. Offshore and onshore deformation rates are somewhat lower than 35 - 50 mm/yr.

### Seismic Sources and Activity

Potential seismic sources are the following:

- Intra-slab source
- Plate interface
- Accretionary wedge: (Example of this type of source is the 1945 Mikawa earthquake, which was accompanied by surface rupture and to have recurrence intervals of about 10,000 years. It is assumed that this type of source will be modeled by the known crustal faults in the site region and/or as a random crustal source.)

Probability that the potential sources are seismogenic:

Intra-slab: 1.0 based on the occurrence of the 1965 and 1949 events which are inferred to be intra-slab events.

Interface: 0.7 (0.6 to ~0.9) based on the following:

- No other subduction zones show complete absence of thrust earthquakes.

- Comparison with other margins in terms of plate age, convergence rate, etc., suggests large thrust events are possible.
- Rivera plate (1932 event and aftershocks) and southern end of 1960 Chile rupture are examples of young plates that have had thrust events.
- Southernmost Chile is as quiet as the Cascadia zone but it has recently subducted a ridge - more analogous to coastal California.
- Preseismic compression can be expressed by compressional outer rise events; very preliminary analysis of the 5.1 event off Oregon suggests that it does not appear to be a compressional event.
- There is some evidence that 1949 and 1965 type of events occur at subduction zones which are strongly (seismic) coupled.

#### Locations of Rupture

- Intra-slab: Elastic part of slab should be the upper 10-20 km based on the age of the plate. The larger intra-slab events ( $M > 6$ ) should occur below depths of 30 km and as deep as 60 km, which is the approximate maximum depth of the historical events. In map view, the observed deeper seismicity has a nonuniform distribution but this may be due to differences in detection capability, particularly from Washington to Oregon. A 50% weight is given to modelling the intra-slab seismicity according to the historical distribution; and a 50% weight is given to a uniform distribution.
- Interface: Downdip extent of seismogenic interface should be at depth of about 30-40 km based on global analogies. Updip extent should be to about the trench (long.  $125^\circ$ ) based on OBS studies in Japan. The Blanco fracture zone and Nootka fault zone should serve as segment boundaries to interplate rupture. The evidence for internal segmentation of the Juan de Fuca plate is weak.

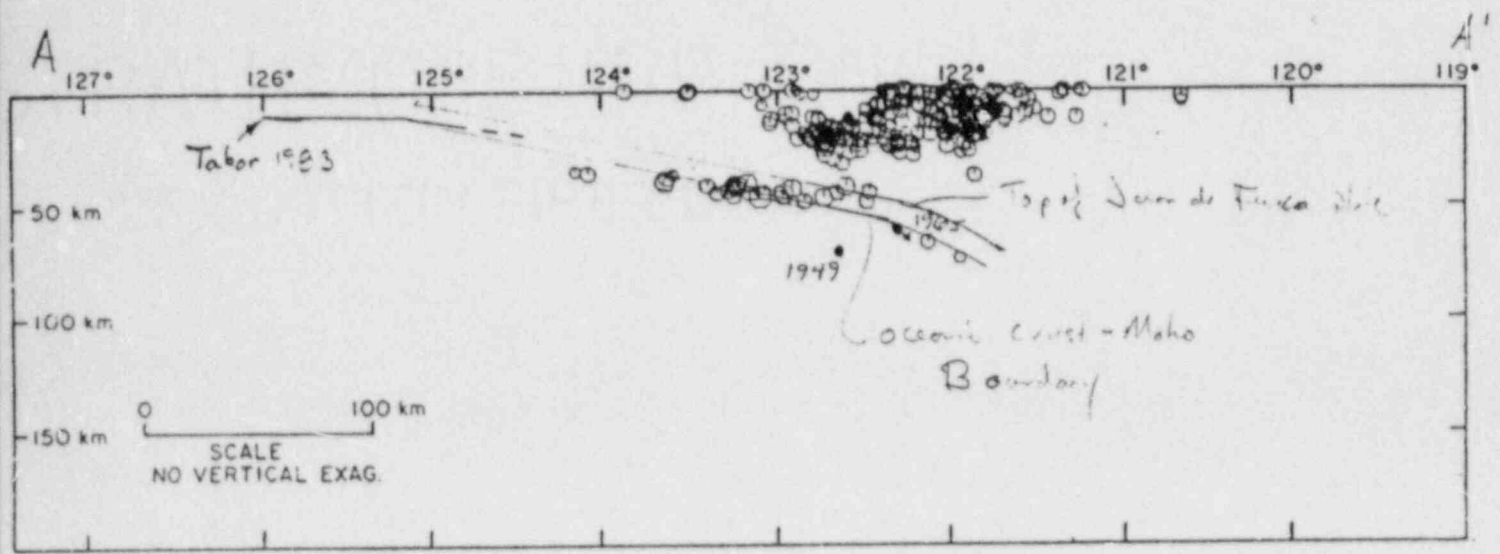
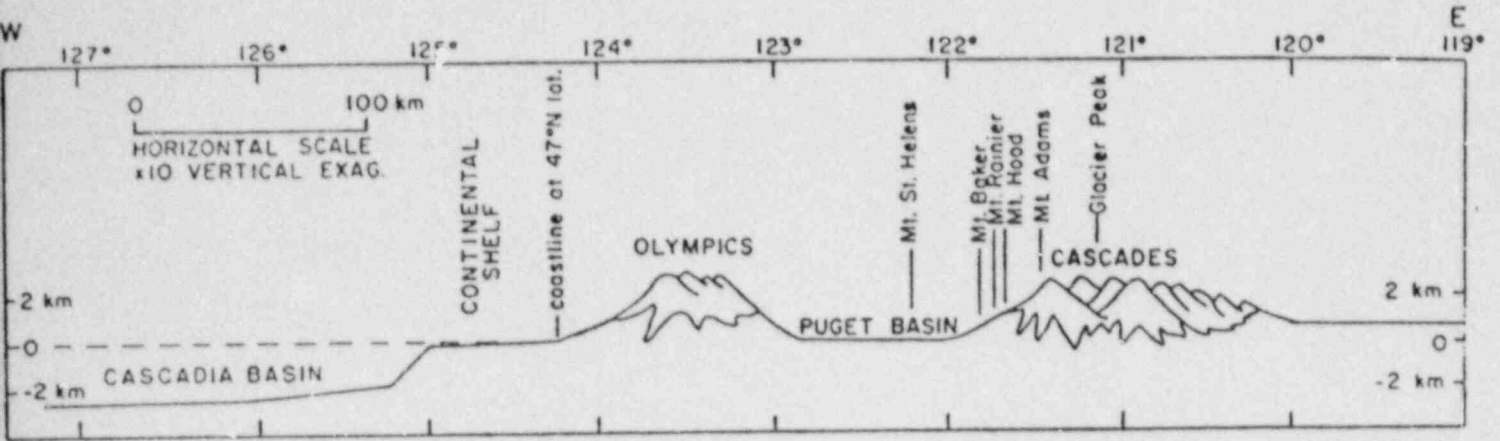
#### Maximum Earthquake Magnitudes

- Intra-slab:  $7-1/4$  ( $\pm 1/4$ ) based on the young slab age and the size of the 1949 event.
- Interface: Use two approaches and assign a 50% weight to each:
1. Rupture dimensions as specified above.
  2. Age vs. convergence rate vs. magnitude relationships of Ruff and Kanamori. (Note that this relationship arrives at essentially a moment rate, not necessarily the maximum magnitude.)

Recurrence-Related Parameters

Intra-slab: The historical seismicity data set provides a reasonable basis for assessing earthquake recurrence.

Interface: Seismic coupling on the interface is estimated to be 30% (with a maximum range of greater than 0% to less than 50% ) based on the plate age vs. coupling relationship of Kanamori and Astiz. This relationship shows a decrease in coupling for progressively younger plates, that are younger than 20 my. Tsunami and turbidite data suggest that the recurrence interval for large interface events should be longer than 150 yr. Use the seismic coupling estimate as the primary constraint on recurrence, with the 150 yr estimate as a check.



EXPERT #10

PHASE I  
RESPONSES BY EXPERT #11



Geometry

Basis for geometry sketched on cross-section provided

- Focal mechanisms for deep events beneath Puget Sound and the Georgia Strait indicate normal faulting; essentially no thrusting.
- These events should be near the upper part of the slab based on temperature constraints
- T-axes of the 1965 and 1976 events are about 30° and support the increase in dip to the east; the depth necessary for magma generation also support a steeper dip as well as theoretical considerations of buoyancy due to phase changes
- The hinge in the slab near the coastline is supported by seismicity data along the Canadian margin
- Lithoprobe results combined with seismicity data are similar to the geometry shown

Convergence Rate

42 mm/yr ( $\pm 10$ )

Based on the analyses of Riddihough

Note that the evidence suggests that the rate is decreasing and the most recent rates are averaged over the past 1/2 million years. Therefore the contemporary rate may be less than 42 mm/yr.

Seismic Sources and Activity

Potential seismic sources are identified:

Intra-slab source

Interface source

Deep crustal source (that may not be identified at the surface)

Probability that the potential sources are seismogenic:

Intra-slab: 1.0 based on historic seismicity

Interface: 0.9 (.8 to 1) based on analogy to other subduction zones such as southern Chile. If the margins were aseismic it would be anomalous implying special conditions and we don't see evidence for this.

Deep crustal source: The source of 1946 Vancouver Island event is the type of event for this source. Although the 1946 event was coincident with the Beaufort fault zone, it apparently had no aftershocks (suggesting a deep crustal source) and a focal mechanism that does not appear to be consistent with an intra-slab source. If such a source exists, its probability of activity is 1.0.

#### Location of Rupture

Intra-slab: within the upper 10 km of the slab. Updip and downdip extent based on high concentration of instrumental seismicity. Large events in depth range 40 to 70 km (east of 124°). Earthquakes up to about M5 might be expected to west of about 124° based on the youth of the plate, historical seismicity, and analogies. Along strike, use distribution of observed seismicity to define the location and relative rate of intra-slab seismicity.

Interface: In cross-section the seismogenic part of the interface is expected to be west of the intersection of the continental Moho with the slab at about 123°, and west about 100 km to beneath the top of the continental slope. Along strike the Nootka fault zone and Blanco fracture zone are expected to act as segment boundaries separating the Juan de Fuca plate from the Explorer and Gorda plates respectively. The Michaelson and Weaver proposed segment boundary is very unlikely because there is no evidence for it in the seismicity data (i.e., similar boundaries identified in other subduction zones are seismogenic). No other segment boundaries are evident.

Deep crustal source: Above 30 km depth anywhere within the upper plate along the entire margin.

#### Maximum Earthquake Magnitudes

Intra-slab: 7 - 7-1/2 (slight preference for 7-1/2) based on historical seismicity and thickness of seismogenic part of slab.

Interface: Maximum magnitude should be based on dimensions of rupture (given above). Ruff and Kanamori relationship does not have direct applicability to this margin except to infer that large earthquakes are possible.

Deep crustal source: 7-1/2 based on size of 1946 event (7.3) and the fact that a large event would likely result in surface rupture.

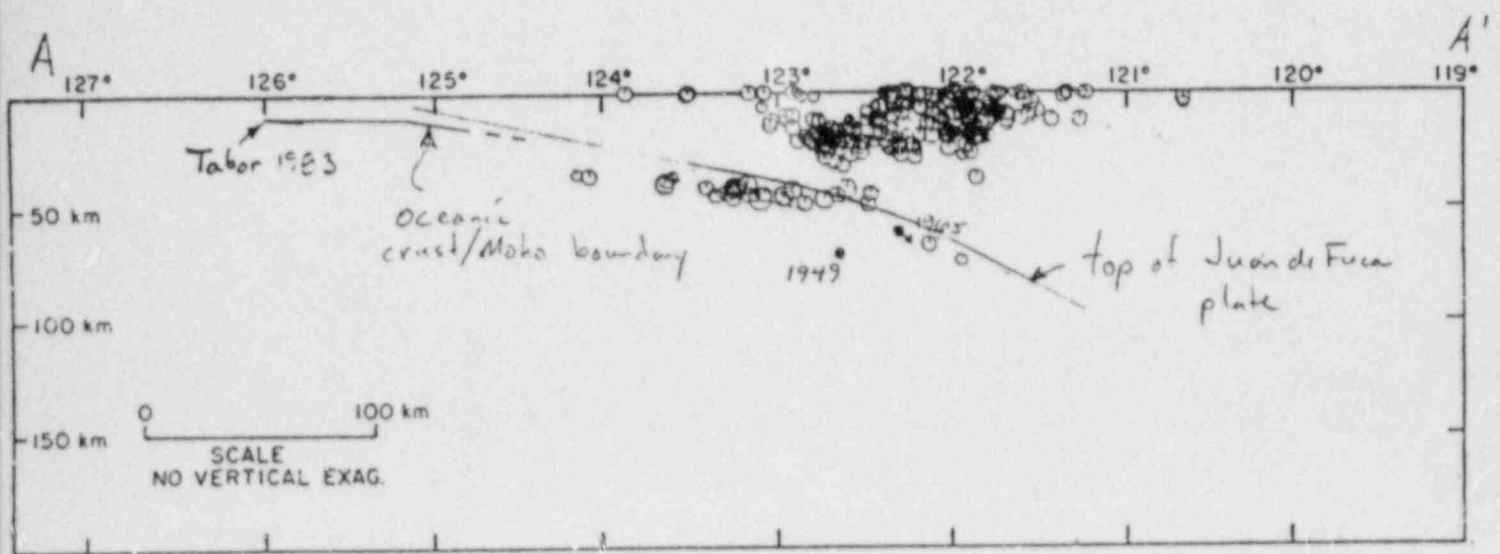
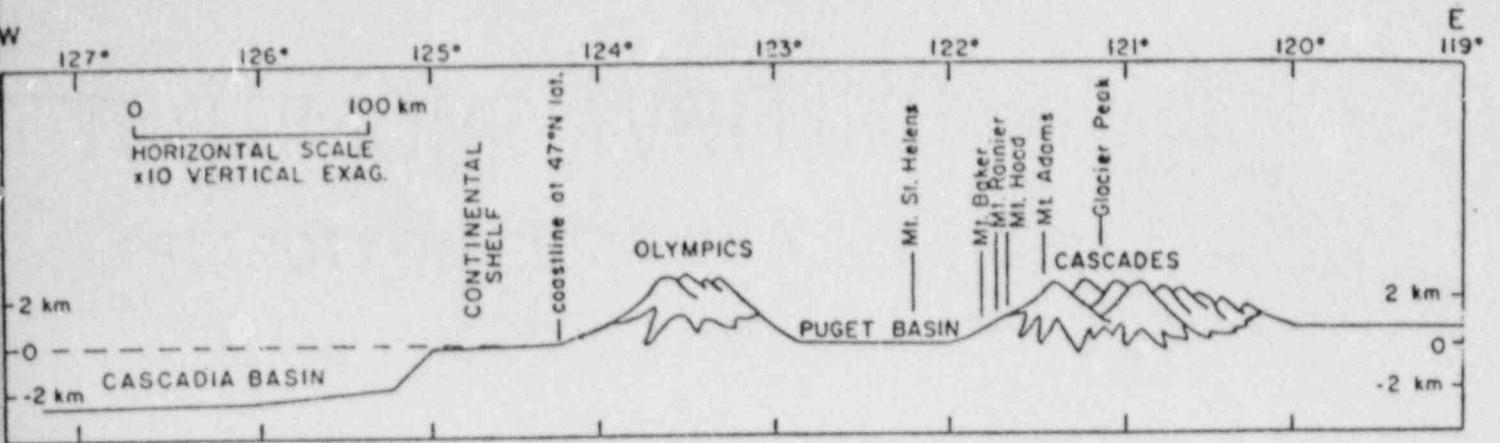
### Recurrence Related Parameters

Interface: Recurrence intervals for large earthquakes ( $\geq 8-1/2$ ) should be a minimum of 300 years based on historical observation of quiescence and Adams recurrence from turbidite data. Because of the essential absence of thrust events, a characteristic earthquake or maximum moment recurrence model is appropriate (as opposed to an exponential magnitude distribution).

Intra-slab: Use seismicity data to estimate earthquake recurrence.

Deep crustal source: From historical record, recurrence interval for M7 should be minimum of 150 yr.





EXPERT #11

PHASE I  
RESPONSES BY EXPERT #12



Geometry

Basis for the two geometries sketched on the cross-section provided:

- Taber's refraction data and seismicity data provide principal basis
- The presence and position of the volcanic arc argues for steepening and against flattening of the slab
- Steeper slab models (e.g., Crosson) must be confirmed by positive velocity evidence for existence of the slab at greater depth

Relative confidence in the two models is the following:

Progressive steeping model 0.8

Flattening model 0.2

Convergence Rate

3 - 3.5 cm/yr (with a 60% likelihood); ranging from 2.5 to 4 cm/yr

Based on Riddihough analyses and Atwater vector solutions

Seismic Sources and Activity

Two potential seismic sources are identified:

Intra-slab source  
Interface source

Probability that the intra-slab source is seismogenic:

95 - 100% based on historical seismicity (with some uncertainty due to the mechanism and location of these events).

Probability that the interface is seismogenic:

20% (with a range of 10% to 40%) based on:

- No thrust events have been observed along the entire length of the margin
- Global analog subduction zones are seismogenic
- 1949 or 1965 earthquakes may have occurred on the interface, although they were more likely intra-slab events

### Location of Rupture

#### Intra-slab source:

The historical seismicity record provides a reasonable basis for the location and relative frequency of earthquake occurrence, both down-dip and along strike. The seismogenic part of the slab is 6 - 10 km thick. 0.05 probability that future locations are completely random.

#### Interface source:

Downdip extent of rupture is at about 50 km depth where the slab comes into contact with continental mantle. Updip extent is probably limited by eastern extent of underplating; but this location is uncertain.

Segmentation of the interface along strike probably occurs at the Juan de Fuca-Explorer plate boundary and, to the south, with the Gorda plate. There is a 30% likelihood that the change in orientation of the volcanic trend at southern Vancouver Island represents a segment boundary.

### Maximum Earthquake Magnitude

#### Intra-slab source:

The largest historical events (1949, 1965) probably provide a basis for the maximum events but there is a 20% chance that the maximum event could be larger.

#### Interface:

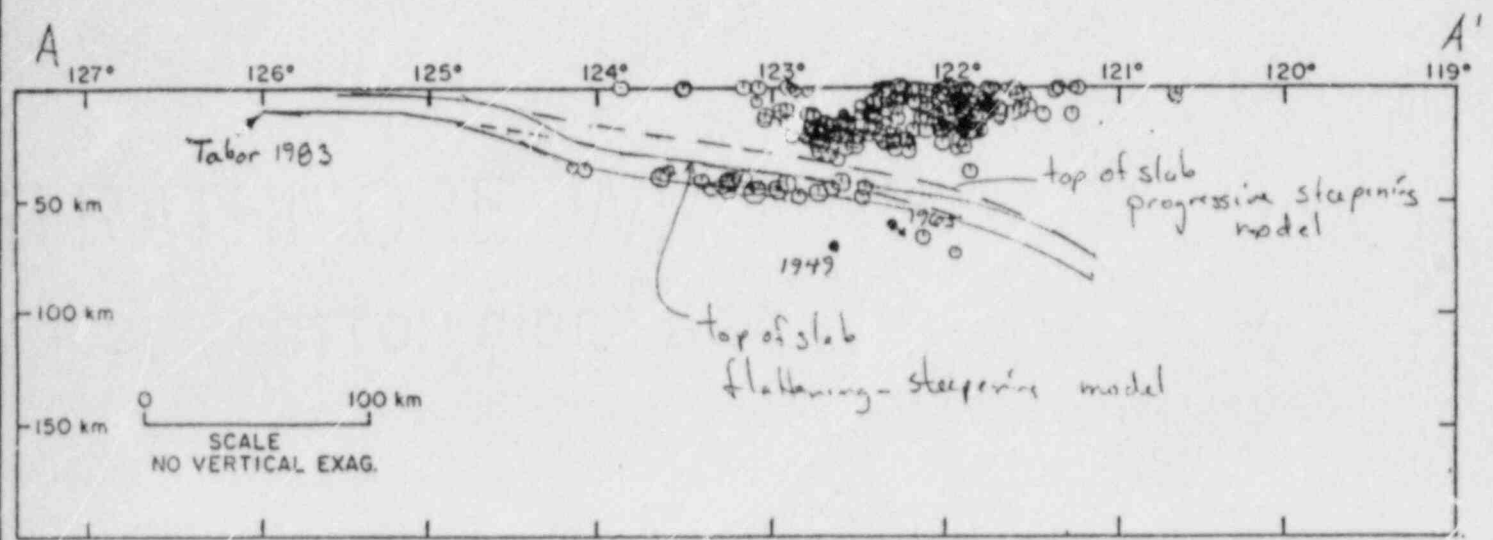
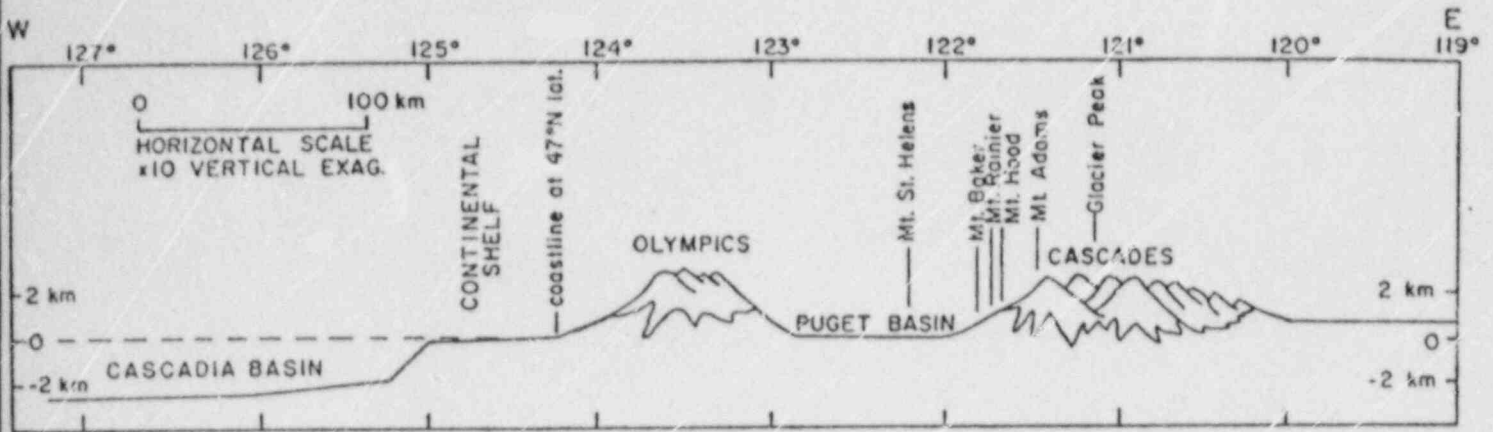
No real basis for making assessment.

### Seismic Coupling and Earthquake Recurrence

Seismic coupling ( $\alpha$ ) estimates to be between 0.05 and 0.5 with a preferred value of 0.1; there is an 80% likelihood that  $\alpha$  lies between 0.05 and 0.15.

The basis for the coupling estimate is a consideration of all types of data related to subduction including the historical seismicity record, back-arc spreading, slab age and dip; sediment accretion of underplating; Chilean vs. Mariannas type behavior, etc. The geologic evidence tends to favor low coupling along the Cascade zone. Coupling and convergence rates provide a reasonable basis for estimating earthquake recurrence along the interface.

The historical seismicity record may be used to estimate recurrence on the intra-slab source.



### Geometry

Basis for geometry sketched on cross-section provided:

- Deeper hypocenters are separated from shallower events
- Depths of some events (e.g., 1965) are too deep for interface events
- Normal focal mechanisms are typical of top of slab extension and graben formation seen within slabs worldwide
- Magma source depths are typically about 100 km, but this is a thin, hot slab so depth constraint not strong
- Would not expect piece of young thin plate to break off and stay seismically active

Note that we have reinterpreted your drawing to reflect the fact that the Tabor (1983) line represents the transition to oceanic Moho, not top of oceanic plate (see attached).

### Convergence Rate

43 ± mm/yr

Based on analysis of Nichimura et al. (1984)

In agreement with evidence of deformation and accretion offshore.

### Seismic Sources and Activity

Two potential seismic sources:

- plate interface
- intra-slab

Probability that intra-slab source is seismogenic

80% (+ about 10%): based on occurrence of deeper seismicity with normal mechanisms and on the estimated age of this slab and the convergence rate.

Probability the interface source is seismogenic

5% ± 5%: Based on fact that essentially all deep events down to magnitudes less than 3 do not show thrust mechanisms, but show down-dip tension consistent with intra-slab seismicity.

Historical record also precludes interface events.

### Location of Rupture

#### Intra-slab source:

- 90% of the moderate-to-large events will occur between 50 and 80 km depth due to age of the plate, maximum downdip tension, possible bending of plate
- In map view, may expect higher concentrations where have had them historically (e.g., Puget Sound region); perhaps due to fabric resulting from extension of Savanco and other Explorer Plate fracture zones into this area

#### Interface source:

- Seismogenic portion will extend from east of accretionary wedge (15-20 km depth) to depths of 40-50 km; accretionary wedge not sufficiently strong to store seismic energy; 40-50 km cut-off depth consistent with worldwide cases and the age/rate of Juan de Fuca plate
- Segment boundaries generally at boundary with Explorer Plate and with Gorda plate

### Maximum Magnitude

#### Intra-slab source: the following magnitudes and associated probabilities:

- Stated values 6-1/2 (80%  $\pm$  10%), 7 (70%  $\pm$  10%), 7-1/2 (25%  $\pm$  10%), 8 (1%) translate to: 6-1/2 (0.45), 7 (0.4), 7-1/2 (0.14), 8 (0.01)
- Based on historical seismicity and age and rate of subducting slab

#### Interface:

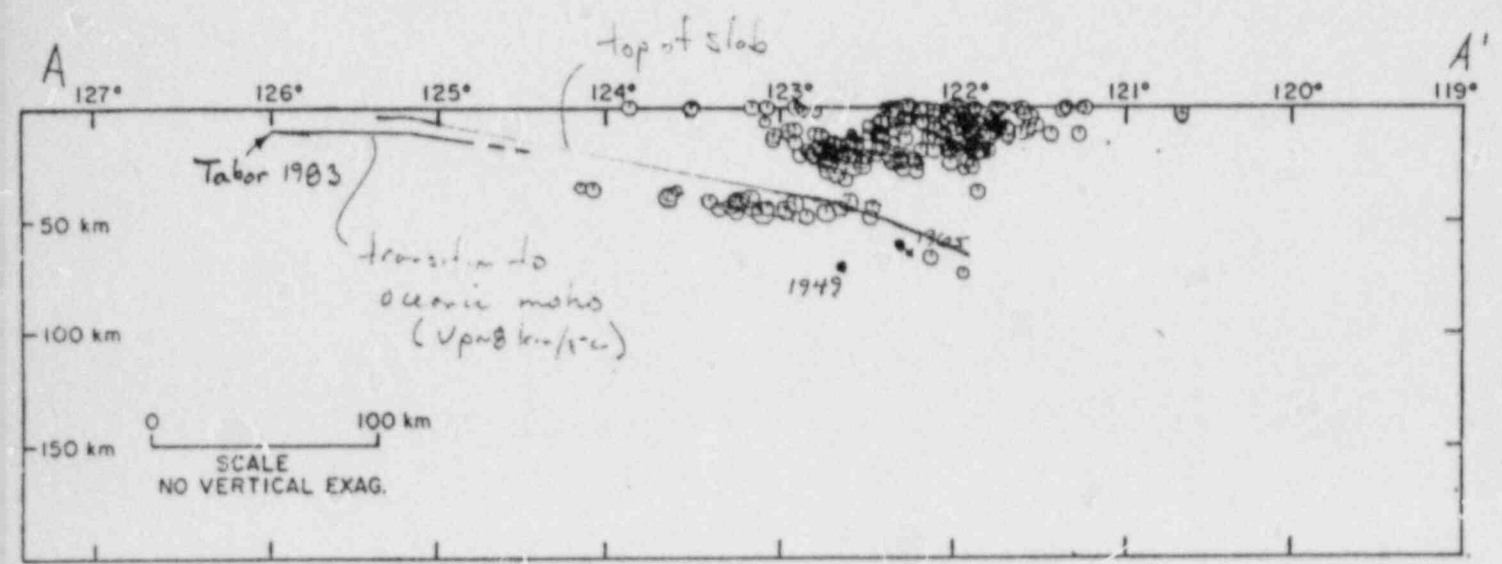
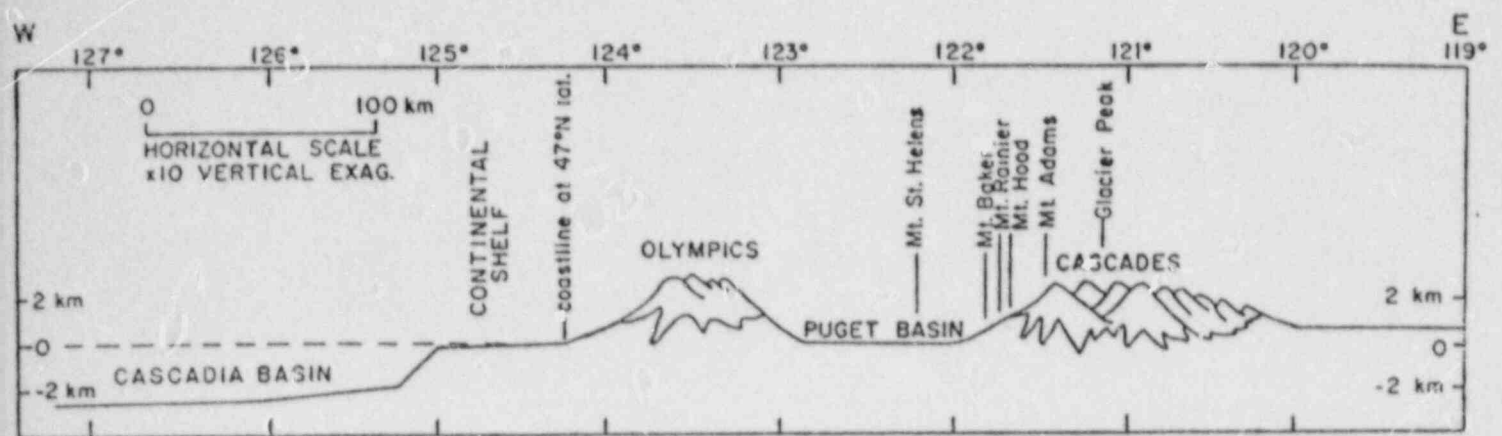
- Stated values 4 (35%), 5 (25%), 6 (10%) translate to: 4 (0.5), 5 (0.35), 6 (0.15)
- Based on young hot plate, slow convergence and correlation to worldwide subduction zones and large amount of sediments that may be contained between plates.

### Coupling

- Seismic coupling: 5% ( $\pm$  5%)
- Based on the young age, low convergence rate; the large amount of sediment being subducted; even with accretion, a large amount of sediment is being subducted

### Recurrence

- Intra-slab - use historical seismicity



PHASE I  
RESPONSES BY EXPERT #14



Geometry

Basis for geometries given on cross-section provided:

- Depth to magma generation should be 100-125 km and used locations beneath Mr. Ranier.
- The deeper earthquakes beneath Puget Sound do not appear to be North American plate earthquakes; either they are within the Juan de Fuca plate or in a remnant slab.

Two models are given:

- Model A (shallow slab dip): based on assumption that deep earthquakes are occurring within the upper part of the oceanic slab. This is compatible with the extensional focal mechanisms of the small events as well as the 1949 and 1965 earthquakes.
- Model B (shallow and steeply-dipping interfaces): based on Crosson's and Owens' inversion results calling for a steeper dip to the Juan de Fuca slab. Note that this model does not assume that the deep seismicity beneath the Puget Sound is in the North American plate, but that it is occurring in a wedge between two interfaces.

Relative preference is given to Model B, and it is given a weight of 65% (+15%).

Convergence Rate

On the basis of published estimates such as those by Riddihough and Nishimura et al., the following distribution is given:

> 50 mm/yr	0.05
40 - 50 mm/yr	0.30
30 - 40 mm/yr	0.40
20 - 30 mm/yr	0.20
10 - 20 mm/yr	0.05

Seismic Sources and Activity

The following potential seismic sources are identified, as a function of geometric model:

Model A

- Intra-slab source
- Interface source
- Accretionary wedge faults
- Tears in the down-going slab



The probability that each of the potential seismic sources are seismogenic is the following:

Model A

- Intra-slab: 1.0 due to occurrence of 1949 and 1965 events
- Interface: 0.35 ( $\pm 0.15$ ) based on:
  - Seismic quiescence is marked and no thrust earthquakes have occurred
  - The thermal history of the Juan de Fuca plate strongly suggests that the plate is very hot due to blanketing of the plate very near the ridge; the sediments prevent convective loss of heat as well as water circulation; therefore, the plate has a very young thermal age
  - Relatively low rate of convergence
  - Analogy to other subduction zones suggest that some possibility exists for interface earthquakes and very long recurrence intervals.
- Accretionary wedge fault: 70% ( $\pm 10\%$ )
  - There are many known faults between the coast and the trench showing young displacement, some may be seismogenic
- Tear in slab: given that a tear exists, probability of it being seismogenic is 0.05 ( $\pm 0.05$ ) based on:
  - To function as a later tear fault, different movement rates of the slab would be needed and there is no evidence for this.
  - For dip-slip, would require large differences in slab age and this is not the case.

Model B

- Shallow interface: 0.25 ( $\pm 0.15$ )
  - lower than Model A because would expect a lower strain rate and less likelihood for stick-slip behavior
- Deep interface: 0.3 ( $\pm 0.1$ )
  - lower than shallow interface in Model A because it would be deeper and hotter; absence of observed seismicity
- Deep intra-slab: 0.1 based on absence of observed seismicity

- Shallow intra-slab (Model A) would be remnant slab (Model B) with the probability of seismogenic the same (1.0)
- Accretionary prism and tear fault the same as Model A.

### Location of Rupture

#### Model A

Intra-slab: Seismogenic thickness of slab is about 10 km

- In cross-section, intra-slab events will occur between  $124^{\circ}$  longitude on the west to 70 km slab depth (about  $122^{\circ}$  on the east).
- 80-90% of the larger earthquakes ( $M \geq 5$ ) would be expected in the slab bend area, where the 1947 and 1965 events occurred.
- Along-strike distribution should reflect the relatively higher rates of occurrence where they have occurred historically, which is also the location of the change in trend of the plate.

Interface: In cross-section, the seismogenic part of the interface would be expected to be between the trench axis ( $125^{\circ}$ ) on the west to a depth of about 50km on the east (at the bend). 50 km is the typical maximum depth of thrust events on subduction zones worldwide.

- Along strike, segment boundaries would be expected at the northern and southern ends of the Juan de Fuca plate (about  $44^{\circ}$  and  $49^{\circ}$  latitude).
- A low probability ( $0.2 \pm 0.15$ ) is given to the likelihood that the Juan de Fuca plate interface is internally segmented. Major differences in slab geometry (such as proposed by Michaelson and Weaver) would be expressed in the volcanic axis and they aren't. If a segment boundary exists, it would be coincident with the southern cutoff of seismicity south of Puget Sound and on strike with the northeasterly convergence direction.

Accretionary wedge: potential seismogenic faults would be expected between the coastline and halfway down the continental slope, with the highest likelihood at the shelf/slope break.

#### Model B

Shallow interface and shallow intra-slab (remnant slab) same location in cross-section as Model A. Along strike, the shallow interface and remnant slab do not extend south of Puget Sound zone of seismicity.

Deep Interface: In cross sections, extends from trench to depth of 50 km; same lateral constraints as Model A.

Deep intra-slab: Location of rupture is not known.

Tear: If a tear exists, it would most likely be at the segment boundary described above.

### Maximum Earthquakes

#### Model A

Interface: 8 ( $\pm 0.5$ ) (0.66 weight between 7.5 and 8); dimensional arguments that give estimates of magnitude 9 are not applicable to the Cascadia subduction zone due primarily to different strain rates.

Intra-slab: 7.25 - 7.5, which is slightly larger than historical observation (1949, 1965).

Accretionary wedge: 7 ( $\pm 0.25$ ). The occurrence of earthquakes in the wedge is localized by accretionary processes (fluid pressures, etc.) and the expected seismogenic area is limited.

#### Model B

Shallow interface: 7.25 ( $\pm 0.25$ ) less than Model A because of slower strain rates resulting in different rheology.

Accretionary wedge and remnant slab (shallow intra-slab) same as Model A.

Deep interface: .75 for 7.5 to 8, .25 for 8 to 8.5

Deep intra-slab: No basis for estimate.

Tear fault: 5. There is no need for either significant strike-slip or dip-slip displacement in the slab.

### Recurrence-Related Parameters

#### Model A

Intra-slab: The historical seismicity record provides a reasonable basis for estimating recurrence.

Interface: (Fairly low confidence in estimating seismic coupling)

- High heat flow, low convergence rate suggest that the plate should have a very young thermal age..
- Seismic coupling estimated at 10% ( $\pm 5\%$ ) based on Kanamori relation between slab age and coupling.

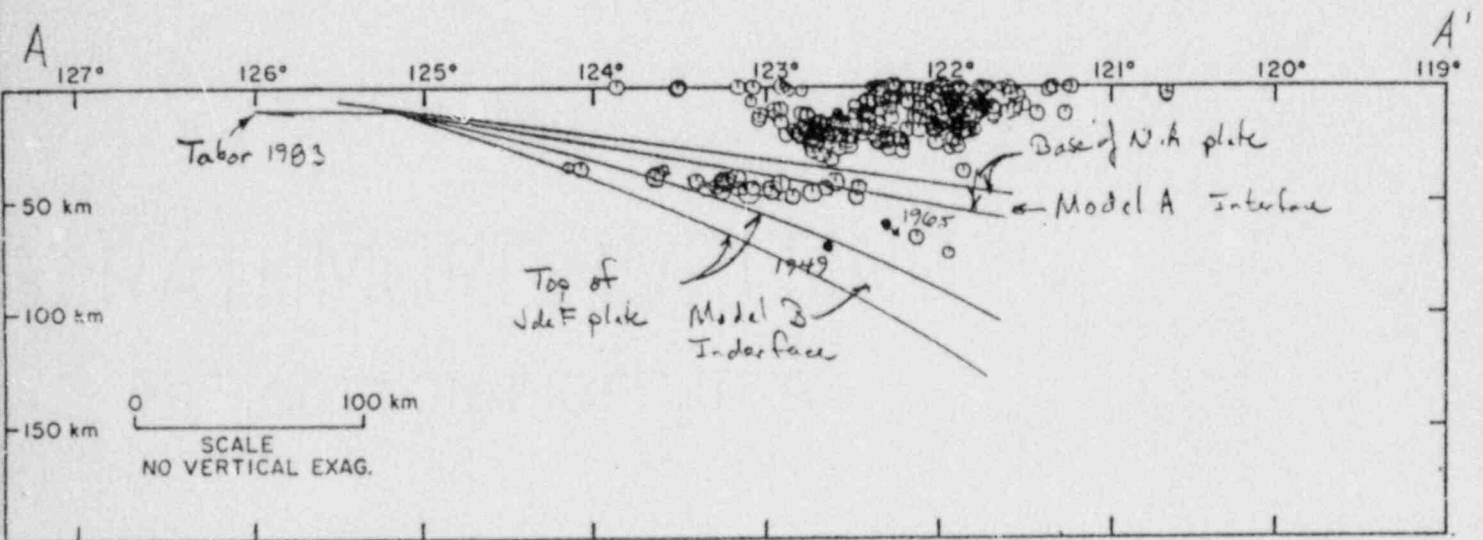
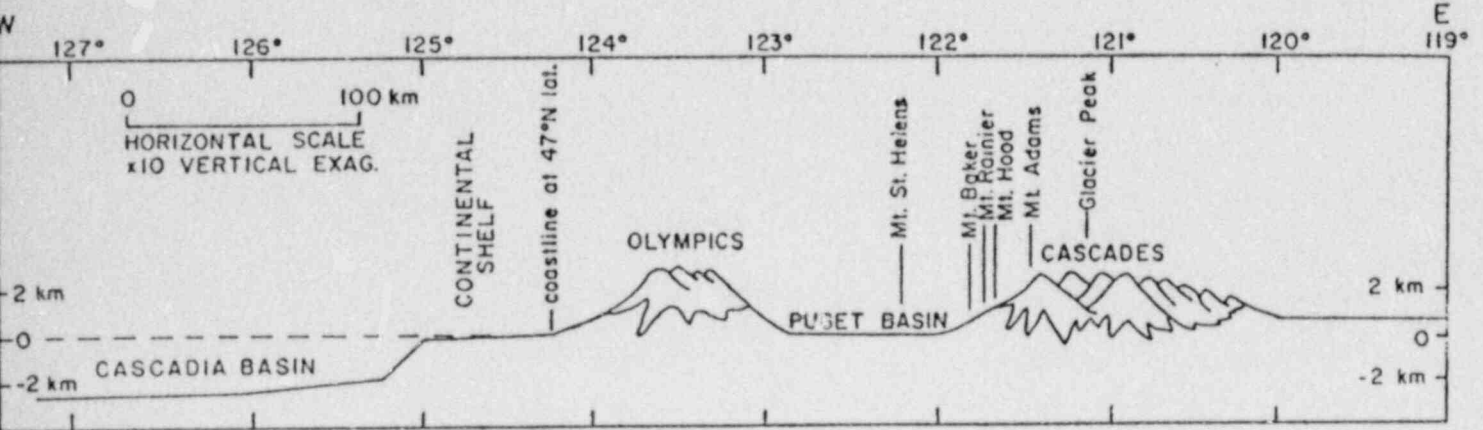
- For interface recurrence, use coupling and maximum earthquake estimates.

#### Model B

Shallow and deep interfaces: Coupling value of Model A is appropriate but convergence rate should be partitioned between the upper and lower interfaces with a ratio of 1:1 to 1:6, respectively (preference at 3:1).

Accretionary wedge: Adams finds about 25 mm/yr of shortening in the accretionary wedge; an estimated 5% may be expected to be released as seismic energy.

Assuming that the plate interface is seismogenic (by either Model A or Model B), a maximum moment recurrence model is appropriate.



EXPERT #14

PHASE II

INFORMATIONAL MATERIALS  
SENT TO EXPERTS PRIOR TO FOLLOW-UP INTERVIEW

SAMPLE LETTER SENT TO EXPERTS

September 18, 1987  
Project 1133A-1.4

Prof. \_\_\_\_\_

Subject: Satsop, Washington Seismic Hazard Analysis

Dear \_\_\_\_\_:

Many apologies for the long delay in getting back to you concerning the subject study. The past several months can be summarized by the following. The tectonic assessments for the hazard analysis were completed at the end of November, 1986. The results of this analysis essentially provide a quantification of the probability of occurrence of various magnitude earthquakes on various seismic sources. The next step of the hazard analysis specifies the level of ground motion at the site given these earthquakes. For these predictions, ground motion attenuation relationships are required that describe the rate of ground motion amplitude variation with distance as a function of magnitude. These relationships are readily available for shallow crustal earthquake sources. However, relationships for subduction zones, particularly for sites within 30 km, potentially directly above the plate interface, magnitudes  $\geq 8$ , and on rock sites have not been previously developed. As a result, several months of the project were devoted to ground motion analysis.

The ground motion analysis has included the development of appropriate empirical attenuation relationships. Considerable effort was focused on developing a data set of close-in, rock site recordings for both intraplate and interface earthquakes. Here, data from the 1985 Chile and Mexico earthquakes have proven invaluable. The preliminary results of this effort were presented at SSA in April, 1987 (Youngs et al, Seis. Res. Ltr., v. 58, p. 29, 1987). The ground motion-related studies were completed in July of this year.

So at present, we are equipped to carry out a full hazard analysis for the Satsop site. We are, however, concerned that during the intervening time, the opinions of one or more of the experts may have changed in light of recent studies. In addition, we feel that it may be useful for each expert to see the calculated results of his assessments and to re-examine his assessments in light of those given by all of the experts. As a result, we are asking you to review the attached materials and to participate in a telephone interview aimed at identifying any changes in your previous assessment.

The materials attached to this letter are the following:

Attachment 1. A summary of your assessments (referred to by your expert number). This summary includes not only the direct assessments given by you (e.g., probability of activity), but also the calculated results of your assessments. For example, you may have specified that the maximum magnitude on the plate interface be calculated from the dimensions of rupture; Attachment 1 shows the magnitude values that result from these dimensions. As another example, you may have specified that earthquake recurrence be calculated from the convergence rate, seismic coupling, and a particular recurrence model. The calculated recurrence relationships based on these specifications are given in Attachment 1. Please review these results and their associated uncertainties. Bear in mind that it is possible to change either the parameters or the calculated results (e.g., recall that maximum magnitude or recurrence intervals could be assessed directly). Attachment 1 (along with the cross-sections in Attachment 5) will provide the basis for the present reassessment.

Attachment 2. A detailed summary of the assessments given by all of the experts. These are the individual assessments (each checked for accuracy) given by the experts. These are important because they provide the scientific bases for the conclusions drawn. You will find yours according to your expert number. Please bear in mind that these summaries reflect opinions given in 1986 and are subject to modification.

Attachment 3. Overall summary and analysis of expert assessments. This attachment summarizes the range of expert opinion given for the parameters of interest to the hazard analysis. This document may help provide a context for your responses, although no attempt has been made to call out individual expert opinions. Again, please remember that these assessments are subject to change.

Attachment 4. Recent references related to the Cascadia subduction zone. The papers attached have either come into print or have been accepted for publication since our last meeting. Also included are the abstracts of papers that we are aware of that have been submitted for publication. Copies of these papers are not yet available, subject to acceptance for publication.

Attachment 5. Seismicity cross-sections. As an aid in evaluating your assessments of crustal geometries, we are providing updated seismicity cross-sections. The uncertainty in hypocentral location is given by the error bars. The cross-section of particular importance for this analysis is Cross-section F, which passes through the site.



Prof. \_\_\_\_\_  
September 14, 1987  
Page 3



The procedure that we will follow for the reassessments will consist of the following. Please review the attached materials, paying particular attention to your previous assessments, their calculated results, and the assessments made by others. We will call you in the near future to set up an appointment for a telephone interview, which will occur in late September or early October. During the interview, we will step through your assessments and the associated uncertainties and ask you for any changes. As was done previously, we will make out best attempt to record both your assessments and the basis for them. Our record will then be sent to you for review to ensure accuracy.

Once again, we apologize for the long delay in following up on this hazard assessment. As far as we know, it is one of the largest seismic hazard analyses involving expert opinion that has yet been undertaken. Your participation is invaluable and greatly appreciated. We are pleased to offer a \$250 honorarium as a small expression of thanks for your efforts on this phase. As promised, the complete Satsop Seismic Hazard Analysis will be provided to you upon completion.

We look forward to speaking with you soon.

Best regards,

Kevin J. Coppersmith  
Project Manager

dla

Attachments

ATTACHMENT 1

Summary of Phase I Assessments for Each Expert  
Including Calculated Results

Expert 1  
SUMMARY OF MODEL PARAMETERS

Slab Geometry:

Three dips: Model A - 10° (0.2)  
 Model B - 15° (0.5)  
 Model C - 25° (0.3)

Convergence rate:

3G ±10 mm/yr

The resulting distribution for convergence rate mm/yr is

percent:	0	10	20	30	40	50
prob	mm/yr	+-----+-----+-----+-----+-----+-----+				
0.050	20.00	*****				
0.300	25.00	*****				
0.300	30.00	*****				
0.300	35.00	*****				
0.050	40.00	*****				
prob	value	+-----+-----+-----+-----+-----+-----+				

Sources and probability of activity:

Model A - Interface 0.4 (0.25 - < 0.5)  
 Intraslab 1.0

Models B and C - Interface 0.4 (0.25 - < 0.5)  
 Intraslab (Juan de Fuca) 0.1 - 0.15  
 "deep zone" beneath Puget Sound 1.0

Maximum extent of rupture on interface:

Updip - toe of continental slope  
 Downdip - depth of 40 to 50 km (equal weights)  
 Along strike - Nootka to Blanco (0.8)  
 Nootka to Blanco segmented at 46°N (0.2)

Interface Maximum Magnitude:

Use maximum rupture dimensions

Model A - unsegmented area	=	134400 to 160000 km <sup>2</sup>	M <sub>w</sub>	9.25
segmented area	=	67200 to 80000 km <sup>2</sup>	M <sub>w</sub>	9.0
Model B - unsegmented area	=	76000 to 92000 km <sup>2</sup>	M <sub>w</sub>	9.0
segmented area	=	38000 to 46000 km <sup>2</sup>	M <sub>w</sub>	8.75
Model C - unsegmented area	=	28800 to 38400 km <sup>2</sup>	M <sub>w</sub>	8.5-8.75
segmented area	=	14400 to 19200 km <sup>2</sup>	M <sub>w</sub>	8.25-8.5

Interface Earthquake Recurrence:

Use moment rate approach with:

 $\text{moment rate} = \text{convergence rate} * \alpha * \text{interface area}$ 
 $\alpha = 0.05$  (0.58) or  $0.95$  (0.42)

use "maximum moment" magnitude distribution

Attached Figure 1 shows the resulting distribution of recurrence estimates for interface events. Maximum event magnitude is assumed to be uniformly distributed in the range of the expected maximum magnitude given above  $\pm 0.25$  magnitude units. Repeat times for maximum events range from 300 to 20,000 years. Figure 2 shows the effect of choice of  $\alpha$  on recurrence estimates for Model A. The remaining variation in recurrence estimates shown in Figure 2 reflect the effects of variations in convergence rate and maximum magnitude.

Location of intraslab events:

Model A - 95% between 122°W and 124°W

 Models B and C - "deep zone" between 122°W and 124°W  
 intraplate shallower than 50 km

Along strike - match observed relative frequency

Intraslab Maximum Magnitude

 Model A and "deep zone" for Models B and C -  $7.25 \pm 0.25$   
 resulting distribution

prob	value	0	10	20	30	40	50
0.300	7.000	*****					
0.400	7.250	*****					
0.300	7.500	*****					

Models B and C - 5 to 6 uniform distribution

Intraslab Earthquake Recurrence:

Historical seismicity used to compute a- and b-values for exponential model. For intraslab events in Models B and C, the seismicity rate was estimated from offshore events within the Juan de Fuca plate away from the spreading centers and fracture zones. Figure 3 shows the recurrence relationship used for the intraslab events in Model A and the deep zone in Models B and C. This curve is based on all recorded events not inferred to lie within the North American plate. Figure 4 shows the recurrence relationship for the offshore Juan de Fuca plate used to model the intraslab recurrence for Models B and C.

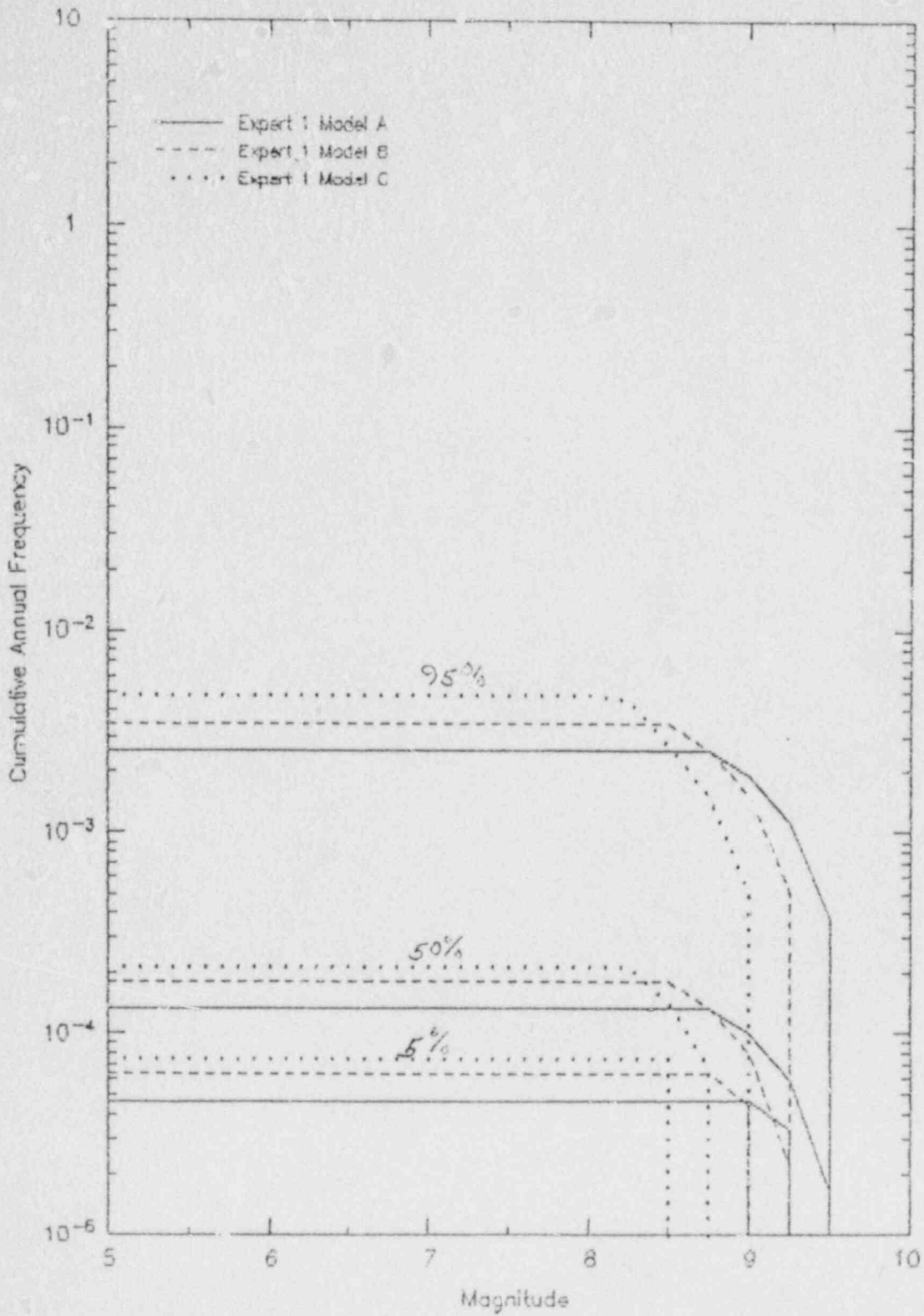


Figure 1 Estimated recurrence distribution for Expert 1

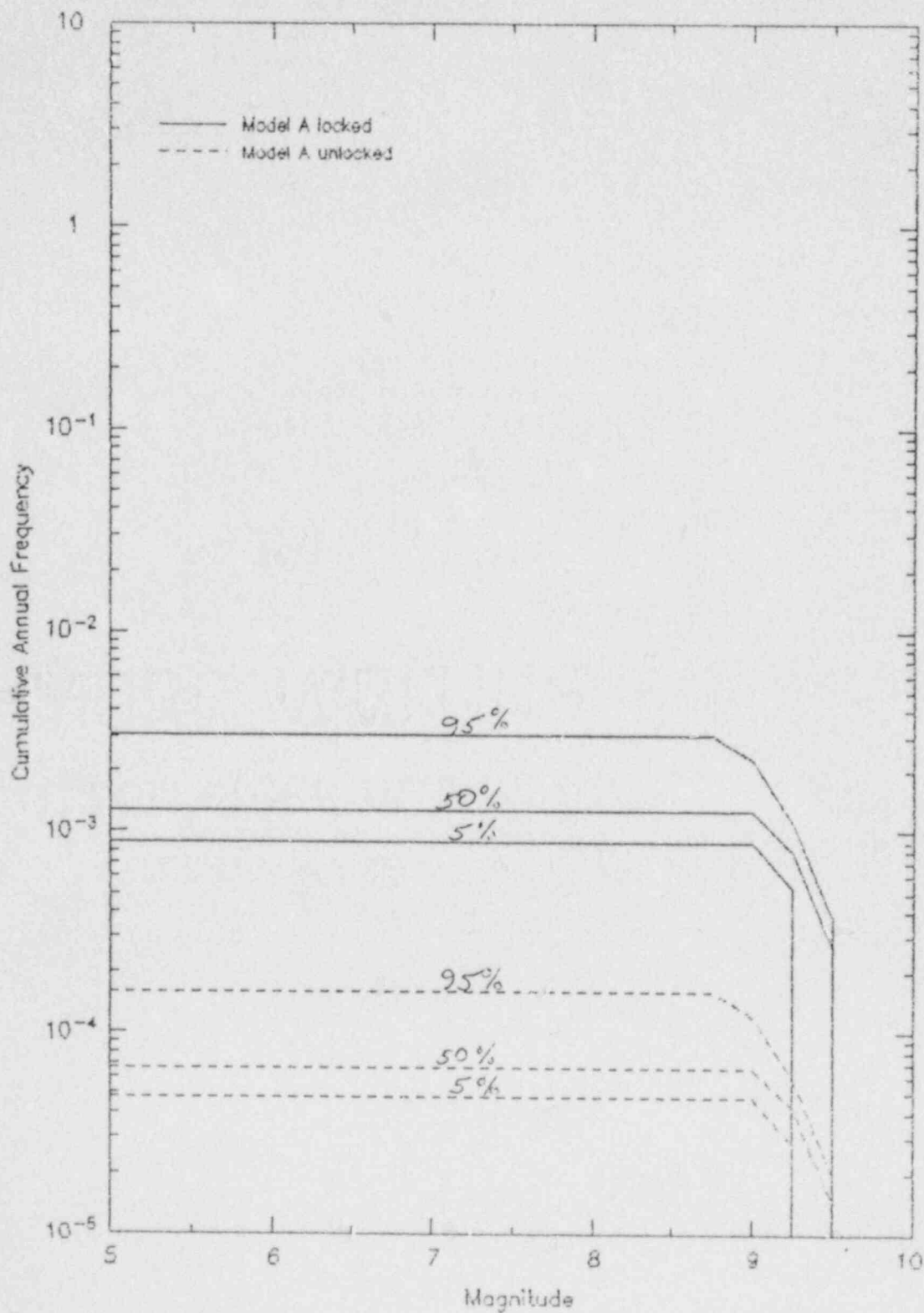


Figure 2 Effect of Alpha for Expert 1

FIGURE 3 B-value -  
Deep Zone

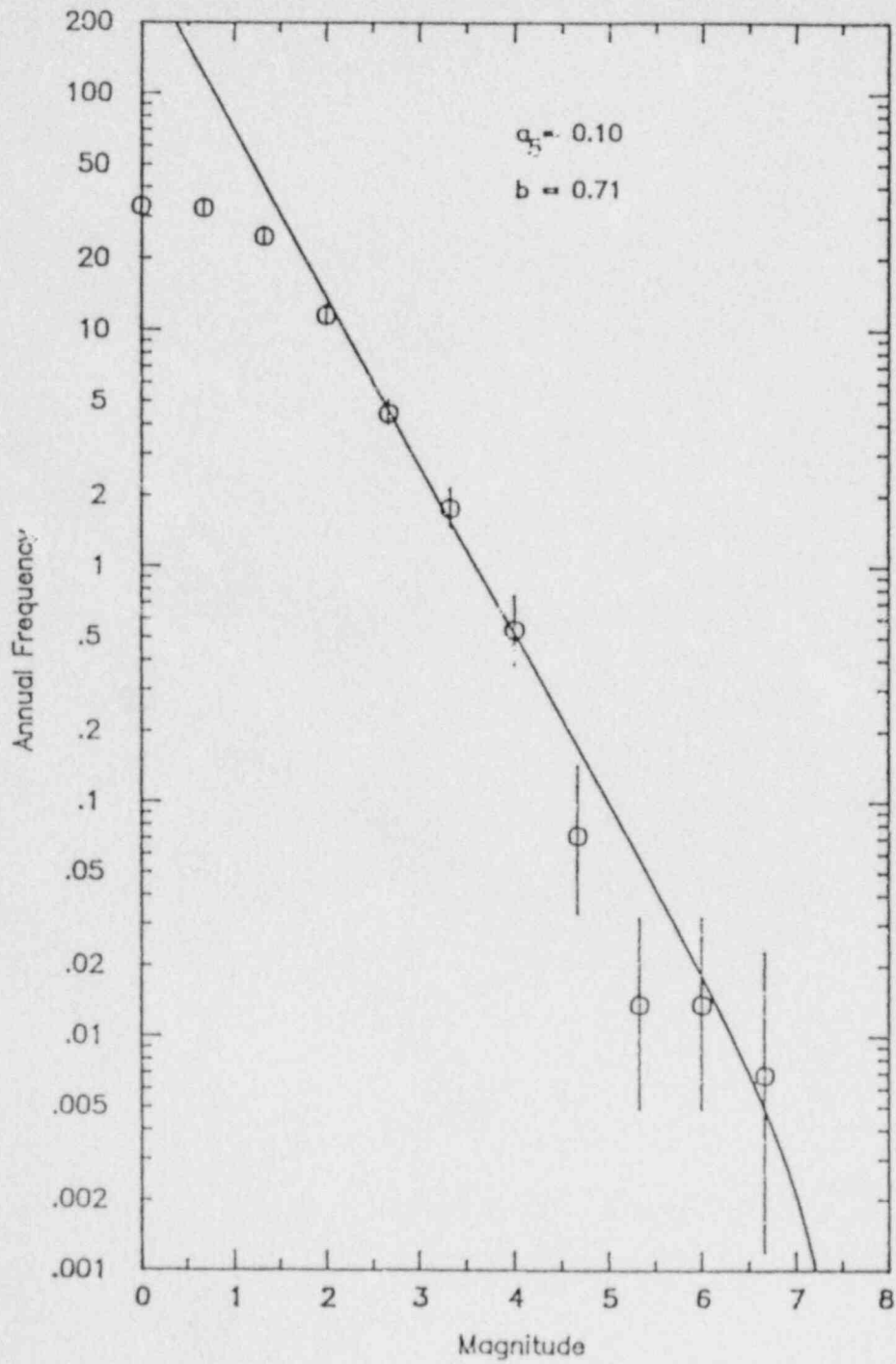
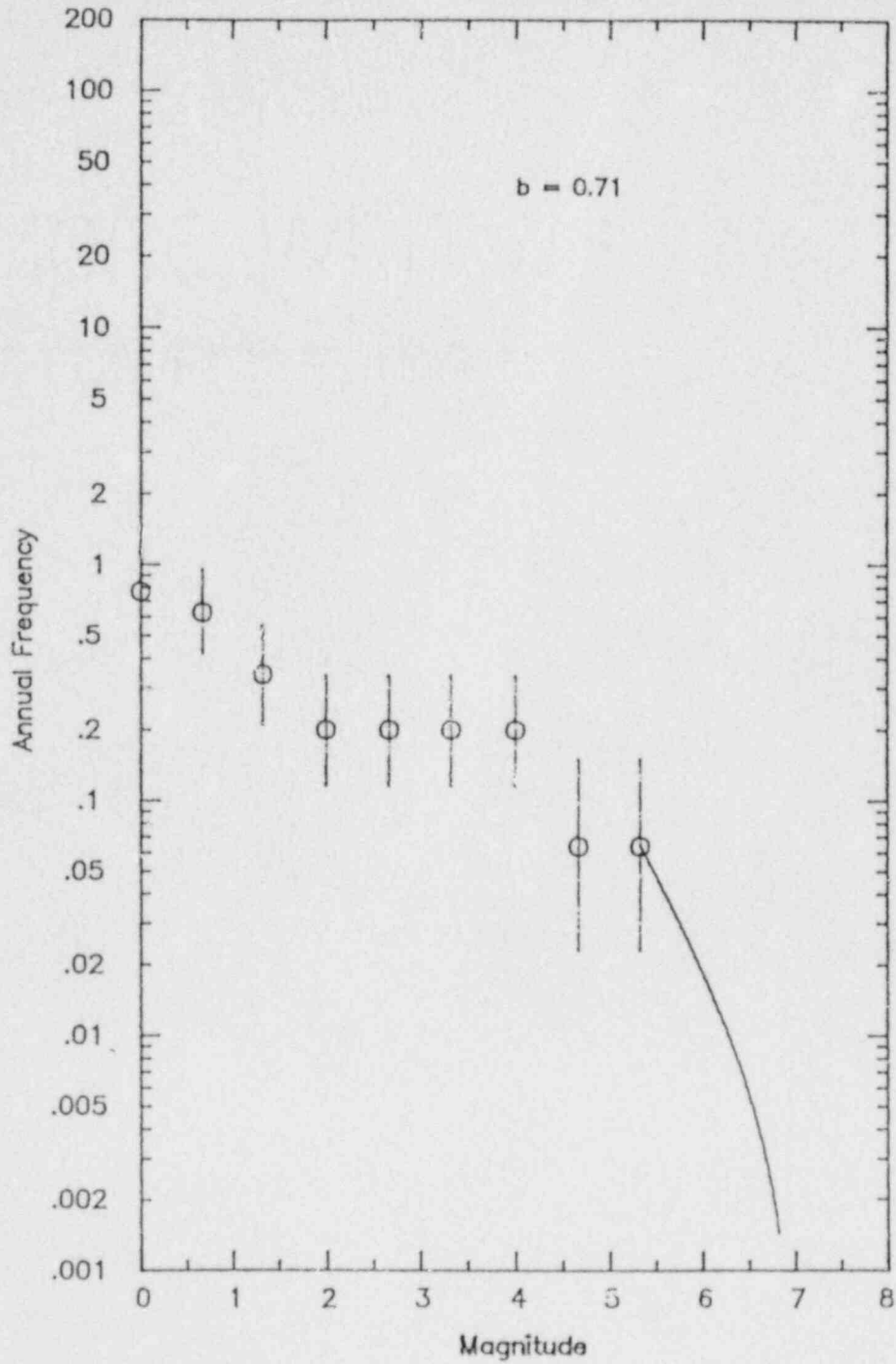


FIGURE 4 B-value -  
Off Shore





Expert 2  
SUMMARY OF MODEL PARAMETERS

Slab geometry:

Approximately 10° dip through deep seismicity

Convergence rate:

15 to 30 mm/yr with the following distribution

	percent:	0	10	20	30	40	50
prob	ma/yr	+---+---+---+---+---+---+---+---+					
0.100000	15.00	*****					
0.400000	20.00	*****					
0.400000	25.00	*****					
0.100000	30.00	*****					
prob	value	+---+---+---+---+---+---+---+---+					

Sources and probability of activity:

Interface 0.8 (0.7-0.85)  
 Intraslab 0.6 - 0.7

Maximum extent of rupture on interface:

Updip - coastline  
 Downdip - not assessed, use AGGREGATE distribution  
 for maximum depth of rupture (km)

	percent:	0	10	20	30	40	50
prob	d (km)	+---+---+---+---+---+---+---+---+					
0.083	30.00	*****					
0.250	35.00	*****					
0.317	40.00	*****					
0.125	45.00	*****					
0.225	50.00	*****					
		+---+---+---+---+---+---+---+---+					

Along strike - Nootka to Blanco (0.6)  
 Nootka to Blanco segmented at 46°N (0.4)

Interface maximum magnitude:

Not assessed - use AGGREGATE distribution  
 a) 0.55 weight assigned to estimate from maximum rupture area  
 unsegmented model - rupture area 64800 to 133600 -  $M_w$  9-9.25  
 segmented model - rupture area 32400 to 66800 -  $M_w$  8.75-9

b) 0.45 weight assigned to following distribution

prob	Mmax	percent: 0	10	20	30	40	50
0.073333	7.50	*****					
0.073333	7.75	*****					
0.073333	8.00	*****					
0.390000	8.25	*****					
0.098333	8.50	*****					
0.083333	8.75	*****					
0.083333	9.00	*****					
0.083333	9.25	*****					
0.041667	9.50	*****					

Combining a) and b) the distribution over all maximum rupture geometries is

prob	Mmax	percent: 0	10	20	30	40	50
0.033000	7.50	****					
0.033000	7.75	****					
0.033000	8.00	****					
0.175500	8.25	*****					
0.044250	8.50	*****					
0.180500	8.75	*****					
0.329000	9.00	*****					
0.153000	9.25	*****					

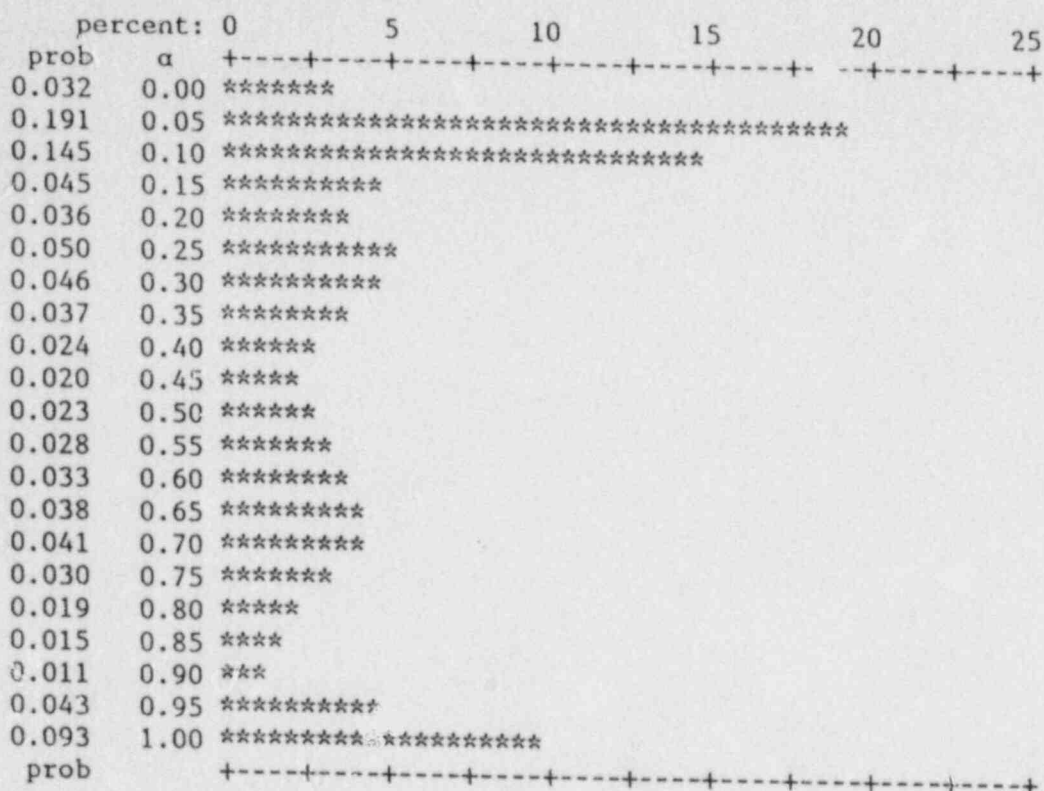
Interface earthquake recurrence:

- 0.3 weight assigned to geologic estimate of 430 (±25%) yrs
- 0.7 weight assigned to moment rate approach

$$\text{moment rate} = \text{convergence rate} * \alpha * \text{interface area}$$

Assessed distribution for convergence rate mm/yr is give above

alpha not assessed - use AGGREGATE distribution of experts



Magnitude distribution model not assessed - use AGGREGATE assessment of the experts  
 exponential (0.23)  
 characteristic (0.41)  
 maximum moment (0.36)

Figure 1 shows the resulting distribution of recurrence estimates. Figure 2 shows the effect of variation in maximum magnitude on recurrence estimated using the moment rate approach, and Figure 3 shows the effect of choice of magnitude distribution model on recurrence estimates.

The earthquake recurrence relationships shown in Figure 1 can be summarized in terms of return periods for events of various sizes as follows:

Magnitude M	Return Period (yrs) for events of magnitude ≥ M		
	5th percentile	50th percentile	95 percentile
5	7000	20	0.4
6	7000	75	2
7	7000	275	6
8	-	630	60
9	-	10000	400

Location of intraslab events:

Updip extent - 123°W  
 Downdip uncertain but 80 - 90 % near bend at 122°W  
 Along strike - variation not assessed, use aggregate opinion  
     0.9 variable matching observed seismicity pattern  
     0.1 uniform along strike

Intraslab Maximum Magnitude:

Not assessed - use following AGGREGATE distribution

prob	Mmax	percent
0.041	6.60	*****
0.030	6.75	****
0.355	7.00	*****
0.219	7.25	*****
0.345	7.50	*****
0.000	7.75	*
0.010	8.00	**
prob		+

Intraslab earthquake recurrence:

Not assessed - use historical seismicity. Figure 4 shows recurrence relationship for deep earthquakes assumed to be occurring within downgoing slab. This curve is based on all recorded events not inferred to lie within the North American plate.

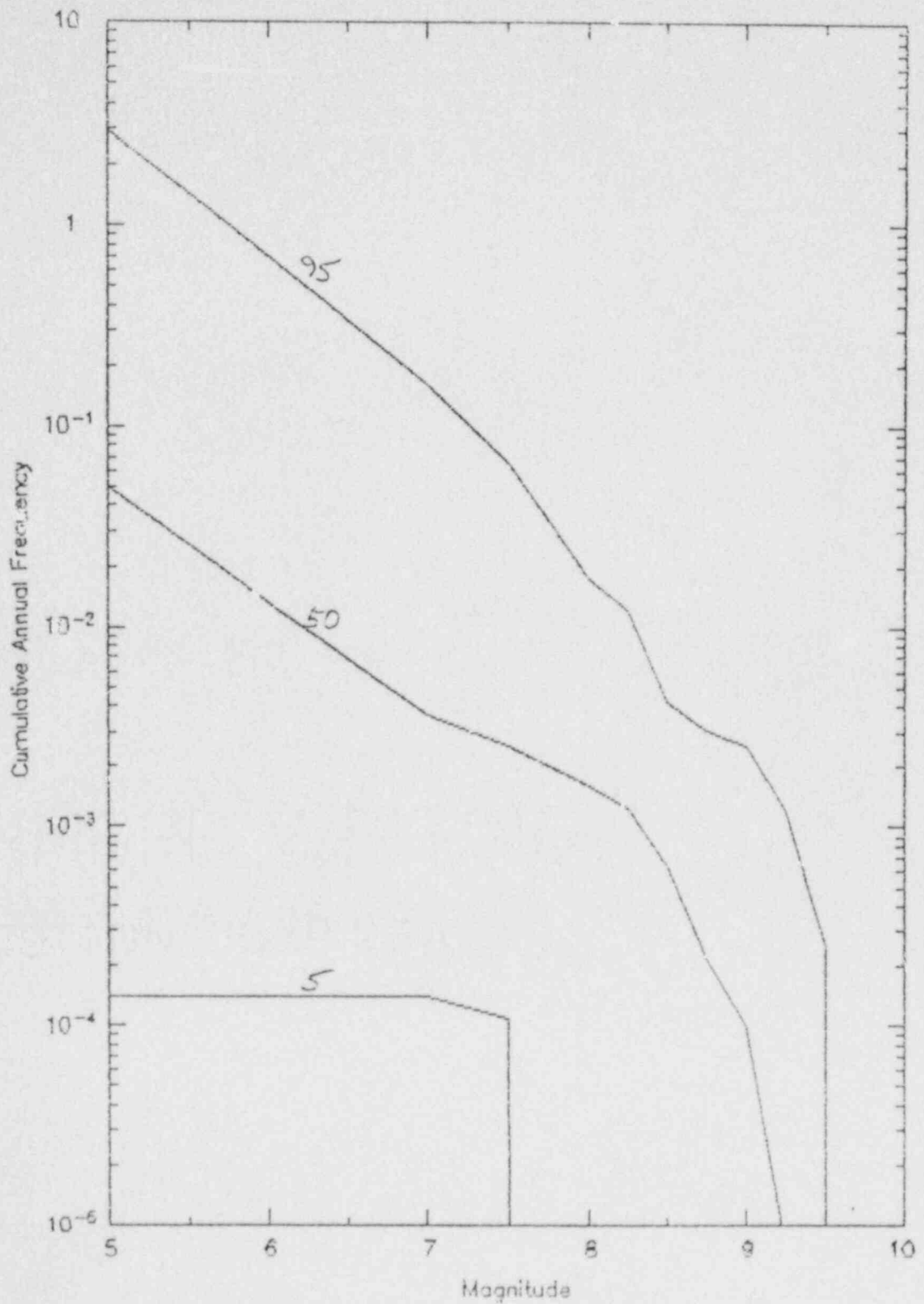


Figure 1 Estimated recurrence distribution for Expert 2

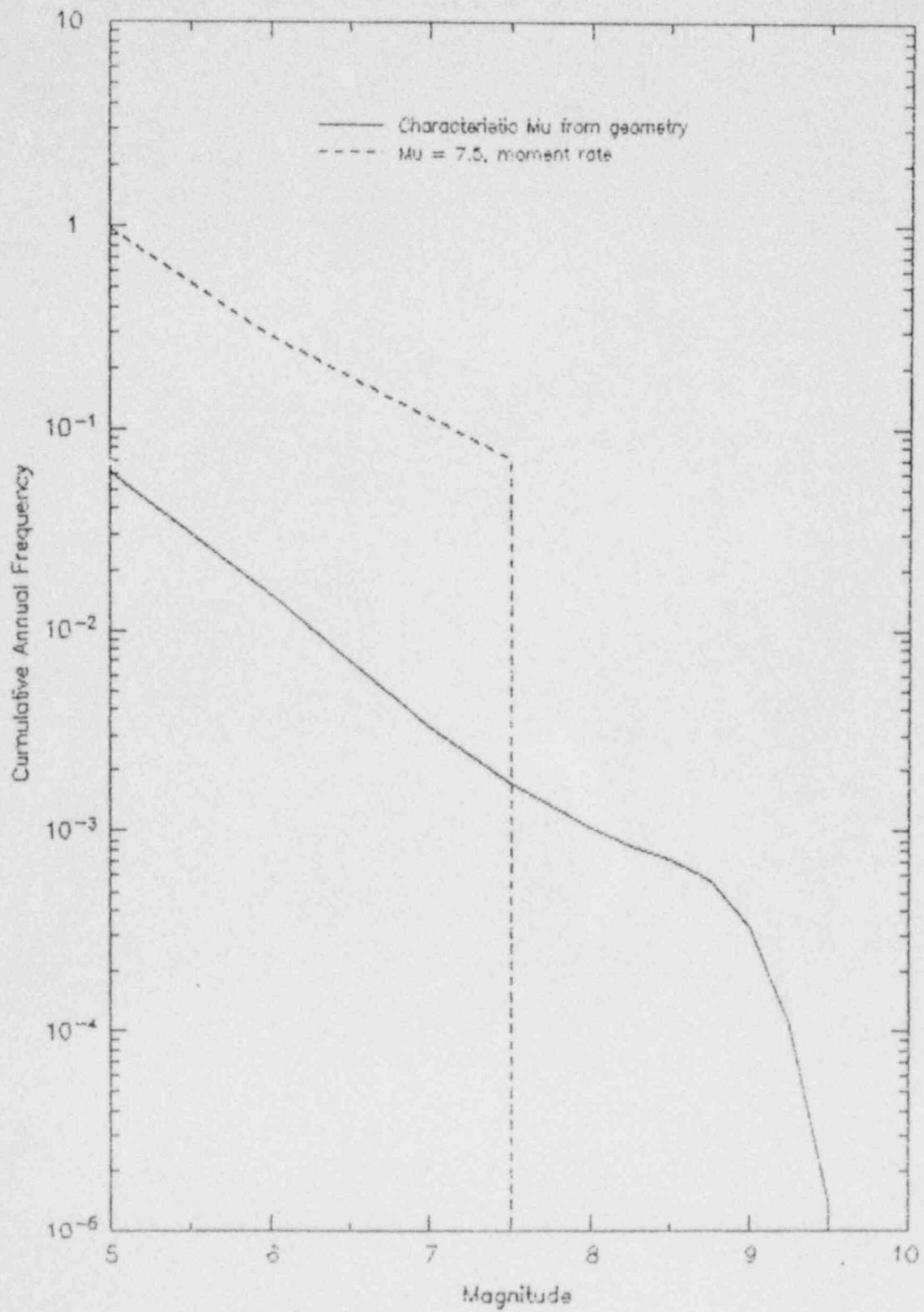


Figure 2 Effect of Max Magnitude for Expert 2

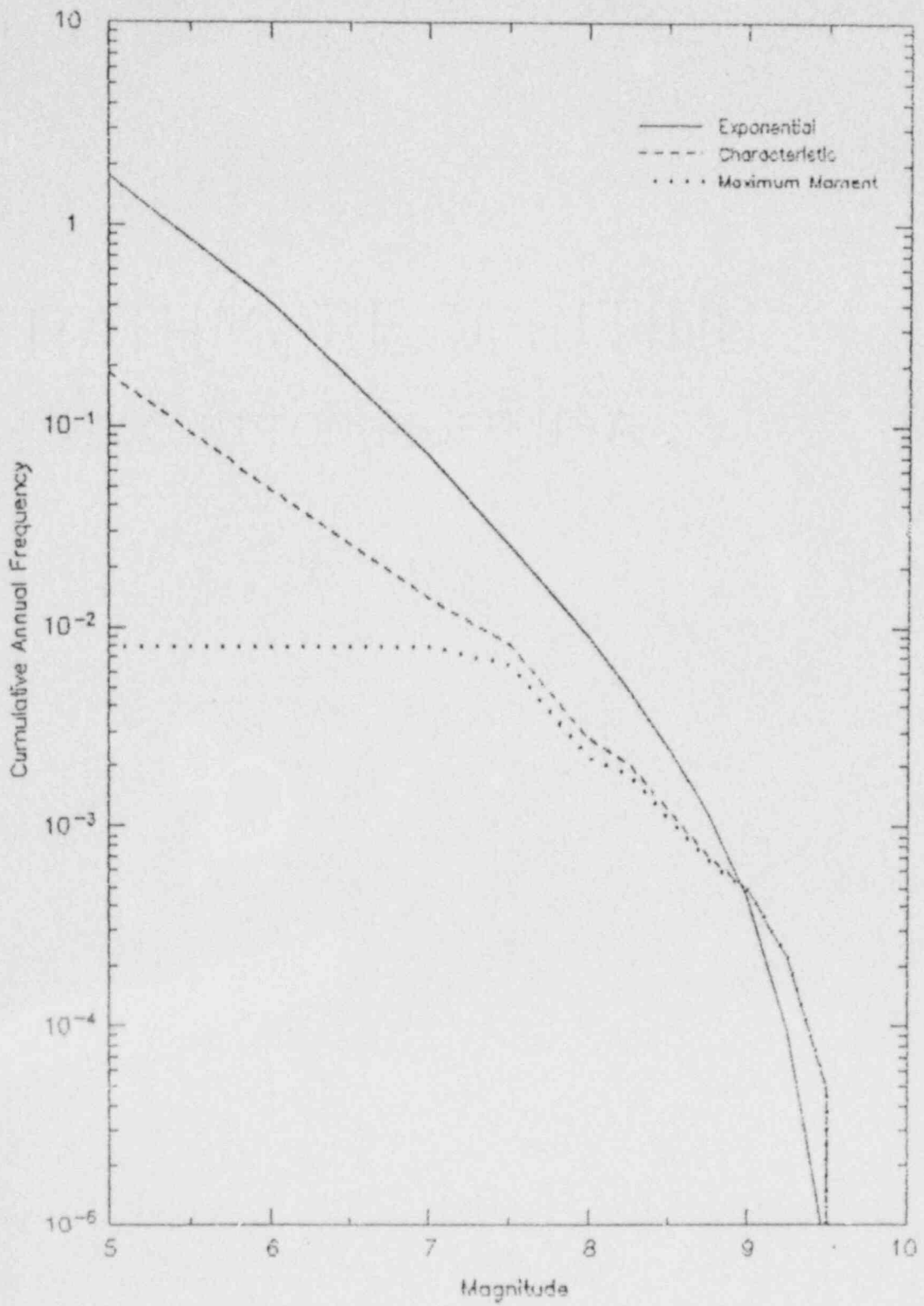
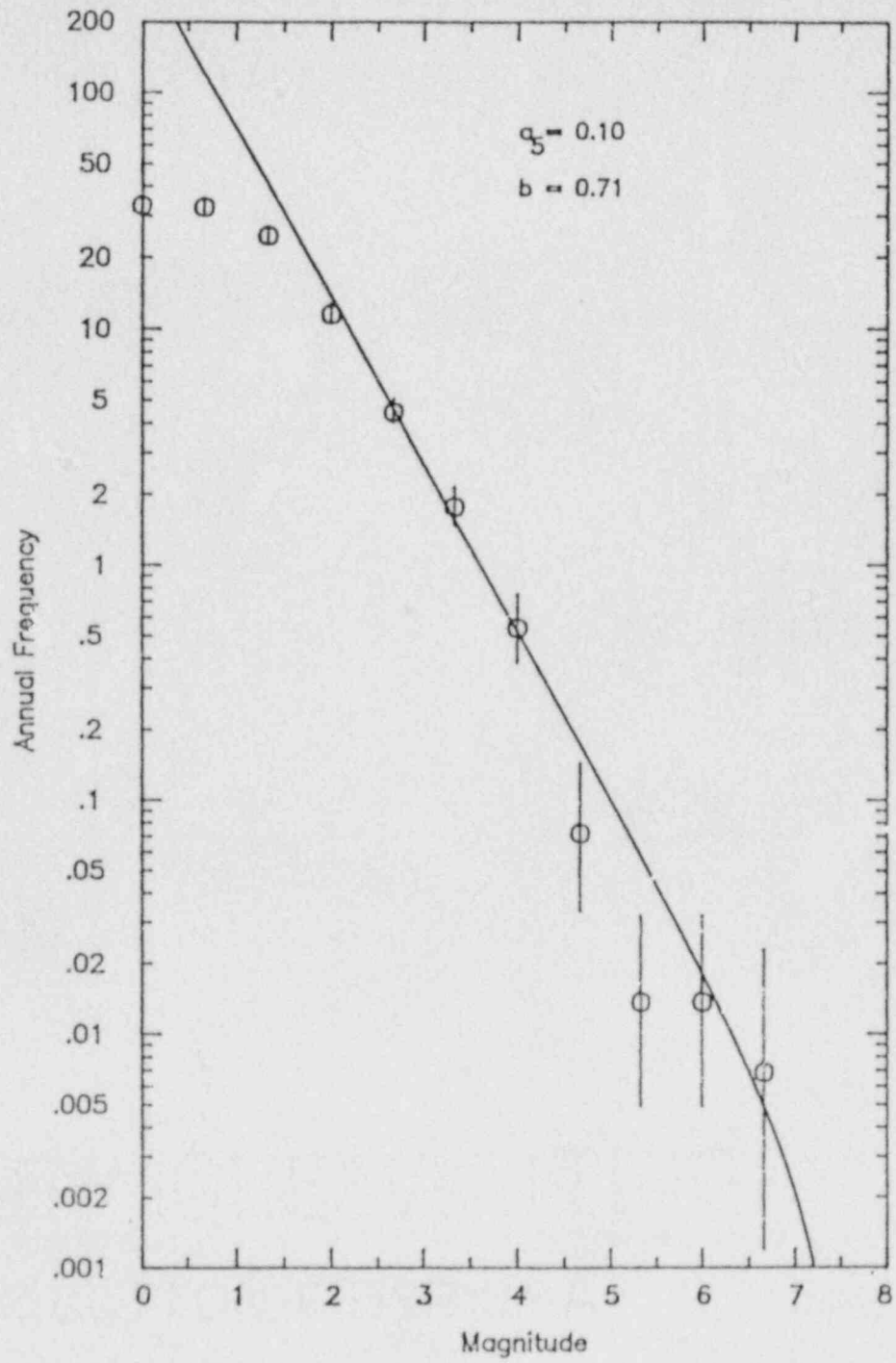


Figure 3 Effect of magnitude distribution model for Expert 2

FIGURE 4 B-value -  
Deep Zone





Expert 3  
SUMMARY OF MODEL PARAMETERS

Slab Geometry:

Approximately 10° through deep seismicity

Convergence rate:

40 ±19 mm/yr

The resulting distribution for convergence rate mm/yr is

	percent:	0	10	20	30	40	50
prob	mm/yr	+-----+-----+-----+-----+-----+-----+-----+					
0.050000	20.00	*****					
0.300000	30.00	*****					
0.300000	40.00	*****					
0.300000	50.00	*****					
0.050000	60.00	*****					
prob		+-----+-----+-----+-----+-----+-----+-----+					

Sources and probability of activity:

Interface 0.6

Intraslab 1.0

Maximum extent of rupture on interface:

Updip - minimum depth 5 km

Downdip - maximum depth 45 km (resulting width 200 km)

Along strike - Nootka to Blanco

Interface Maximum Magnitude:

directly assessed according to following distribution

	percent:	0	10	20	30	40	50
prob	Mmax	+-----+-----+-----+-----+-----+-----+					
0.125000	8.50	*****					
0.250000	8.75	*****					
0.250000	9.00	*****					
0.250000	9.25	*****					
0.125000	9.50	*****					
prob		+-----+-----+-----+-----+-----+-----+					

Interface Earthquake Recurrence:

Use geological assessment according to following distribution:

prob	years	percent: 0	5	10	15	20	25
0.006940	200.00	**					
0.055560	300.00	*****					
0.103300	400.00	*****					
0.104170	500.00	*****					
0.097220	600.00	*****					
0.090280	700.00	*****					
0.083330	800.00	*****					
0.076390	900.00	*****					
0.069440	1,000.00	*****					
0.062500	1100.00	*****					
0.055560	1200.00	*****					
0.048610	1300.00	*****					
0.041670	1400.00	*****					
0.034720	1500.00	*****					
0.027780	1600.00	*****					
0.020830	1700.00	*****					
0.013890	1800.00	****					
0.006940	1900.00	**					
0.000870	2000.00	*					

(moment rate approach used as check with :

 $\text{moment rate} = \text{convergence rate} * \alpha * \text{interface area}$ 

 for  $\alpha = 0.66$  and  $M_{\text{max}} = 9$ , return period = 333 yrs)

use "characteristic" magnitude distribution

Attached Figure 1 shows the resulting distribution of recurrence estimates for interface events. Figure 2 shows the effect of  $M_{\text{max}}$  on recurrence estimates. The earthquake recurrence estimates shown in Figure 1 can be summarized in terms of return period for events of various sizes as follows:

Magnitude M	Return Period (yrs) for events of Magnitude $\geq M$		
	5th percentile	50th percentile	95 percentile
5	21	7	2
6	87	30	8
7	364	132	41
8	1050	430	166
9	-	1320	340

Location of intraslab events:

10 to 20 % near outer rise

5 % at intermediate depths

remainder in deep zone of observed seismicity

Along strike - match observed relative frequency

Intraslab Maximum Magnitude:

Mmax = 7.5 in deeper part of slab

= 8.0 in shallow part

Intraslab Earthquake Recurrence:

Historical seismicity used to compute a- and b-values for exponential model. Figure 3 shows the recurrence relationship used for the intraslab events. This curve is based on all recorded events not inferred to lie within the North American plate.

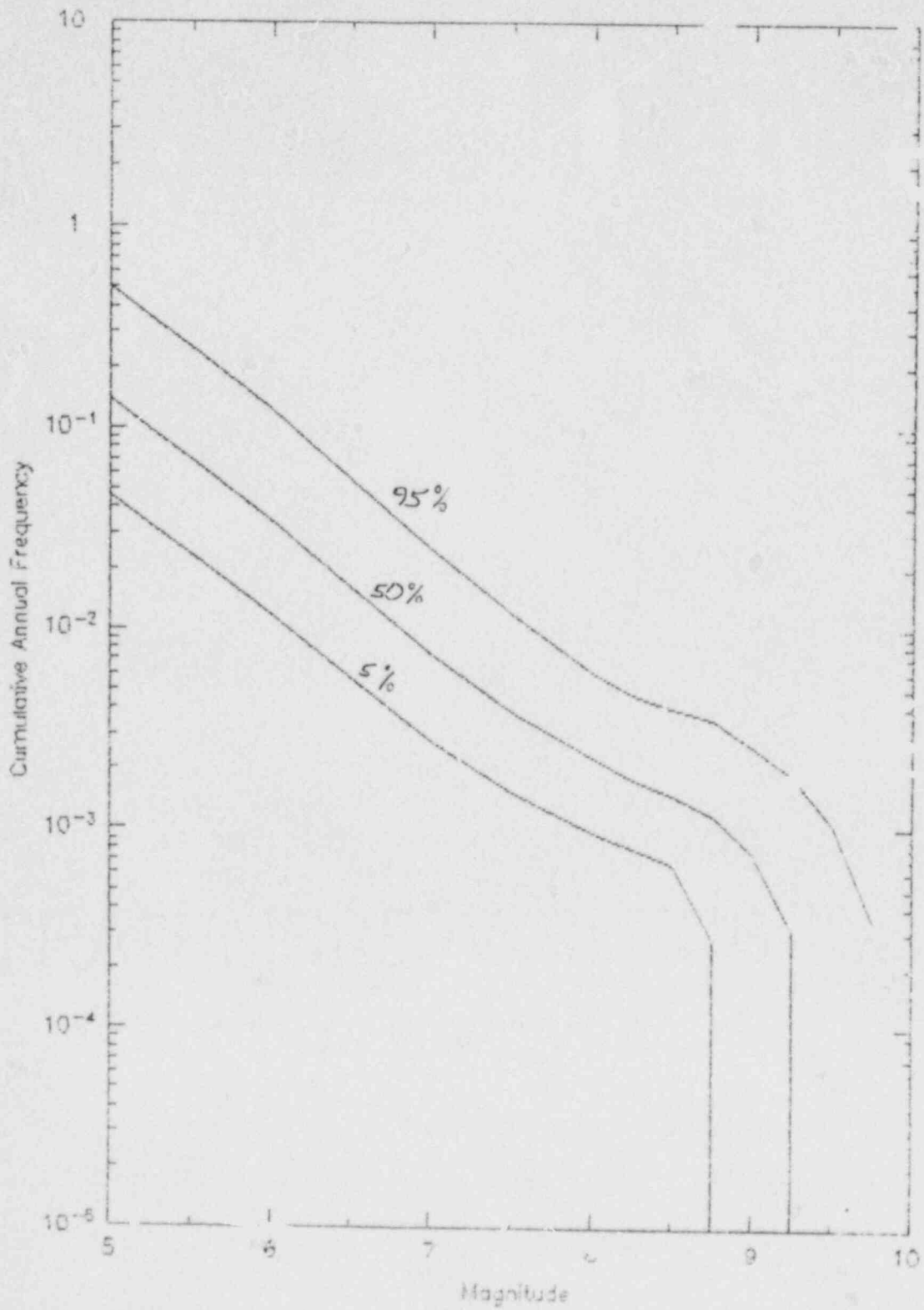


Figure 1 Estimated recurrence distribution for Expert 3

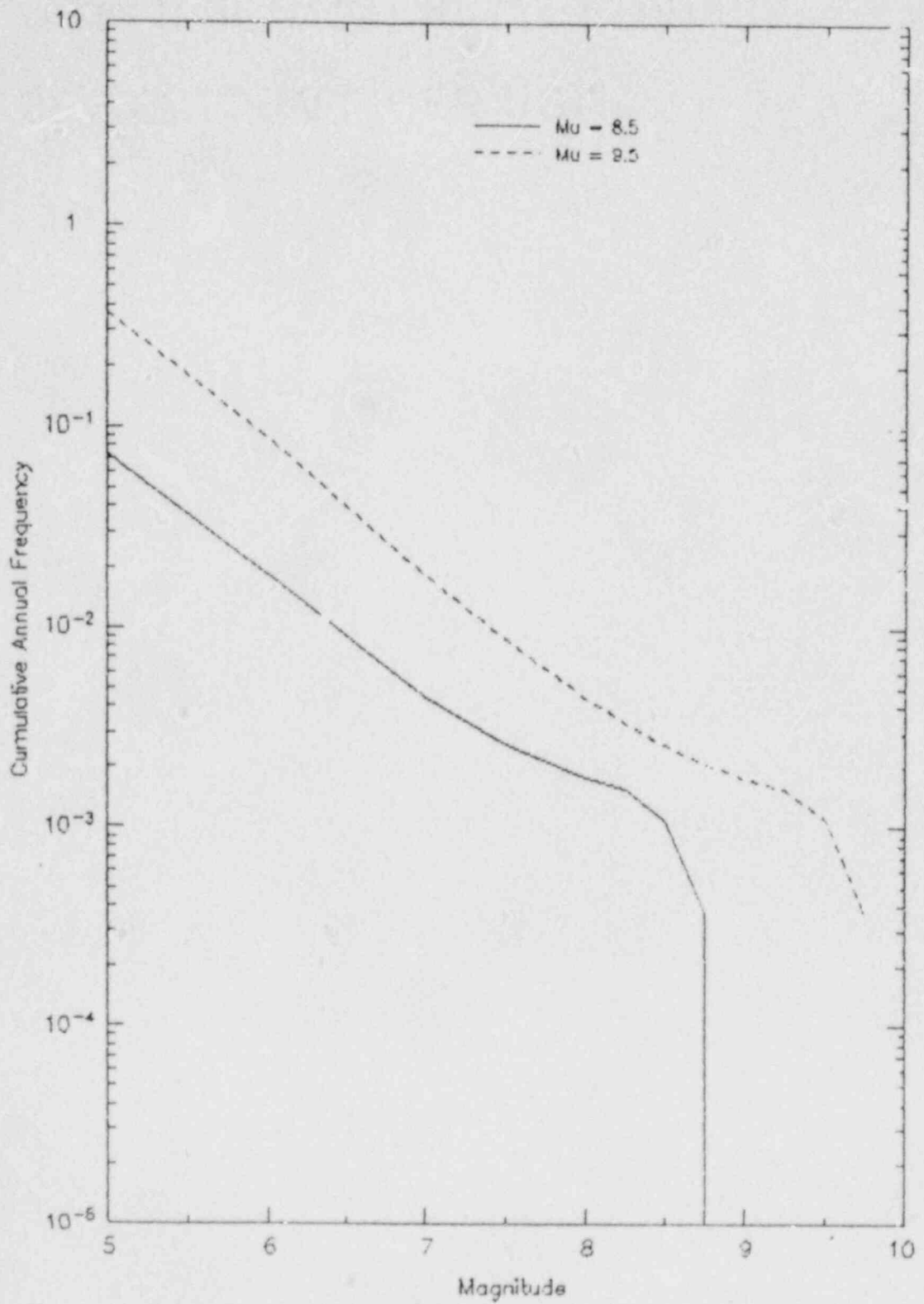
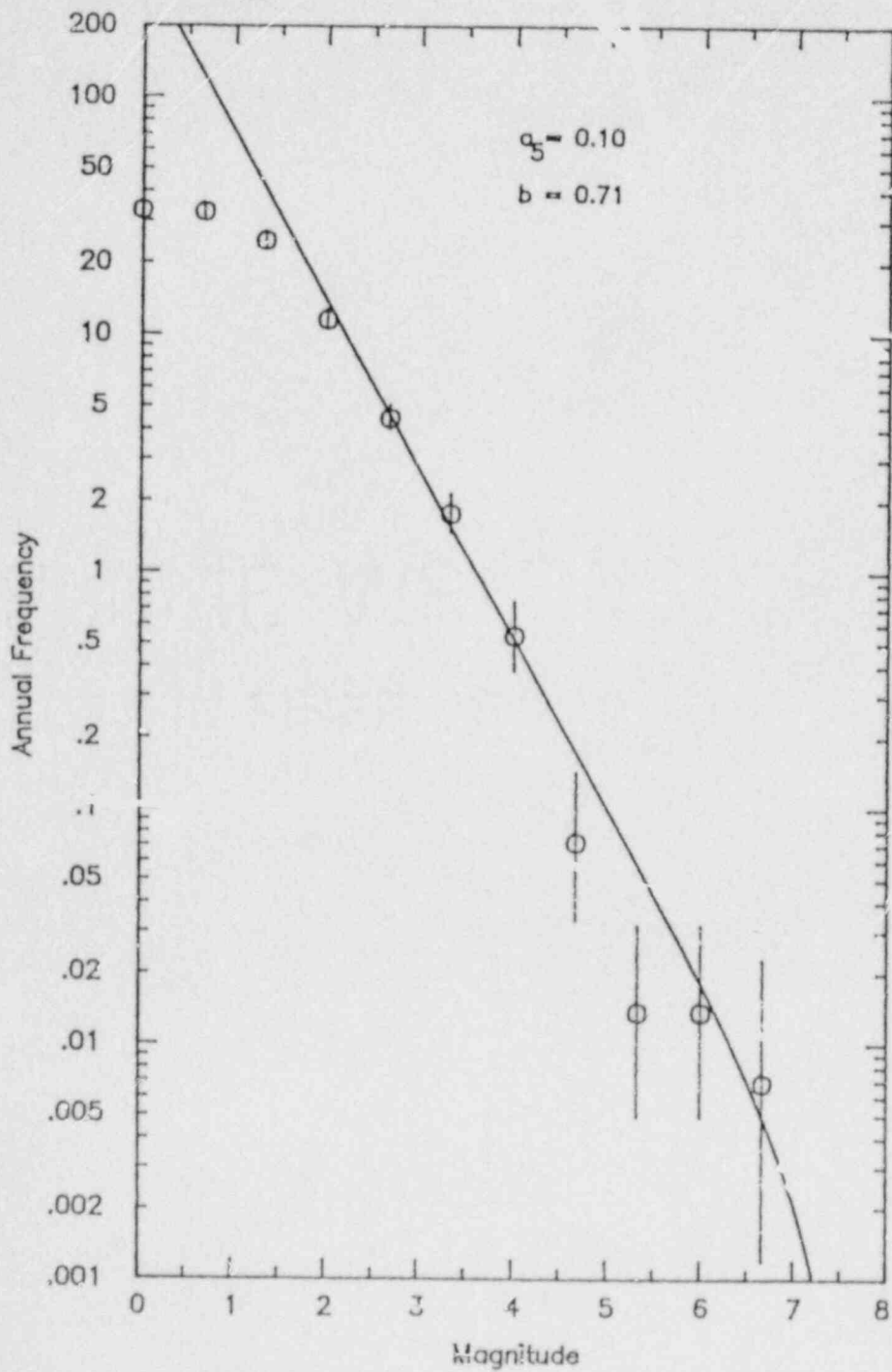


Figure 2 Effect of max magnitude for Expert 3

FIGURE 3 B-value -  
Deep Zone



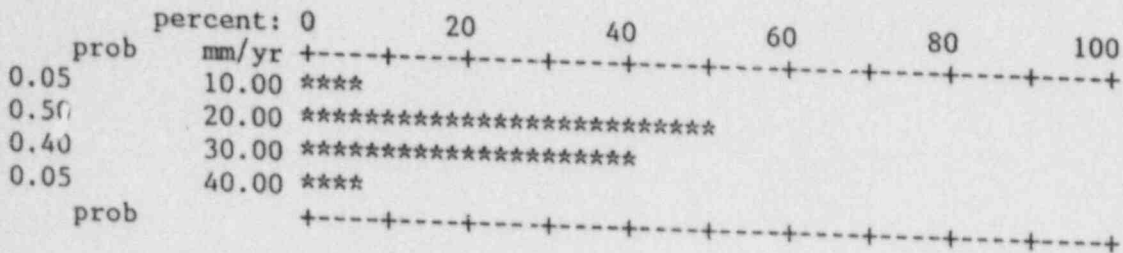
Expert 4  
SUMMARY OF MODEL PARAMETERS

Slab geometry:

Approximately 10° dip through deep seismicity

Convergence rate:

Following distribution assessed



Sources and probability of activity:

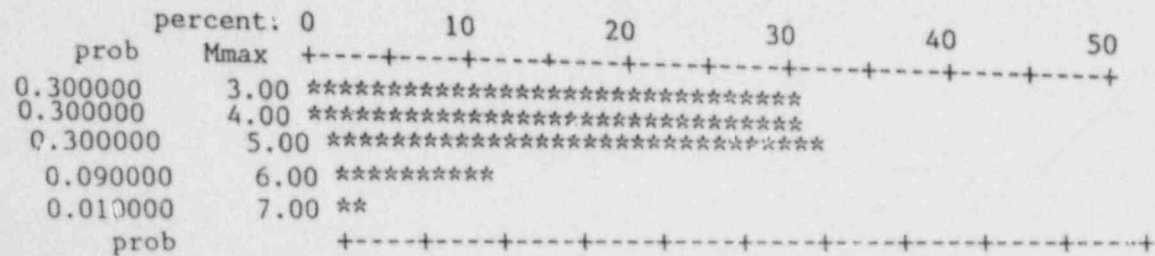
Interface 0.75 ( $\pm 0.25$ ) renormalized to 0.075 for events > M 5.0  
 Intraslab 1.0

Maximum extent of rupture on interface:

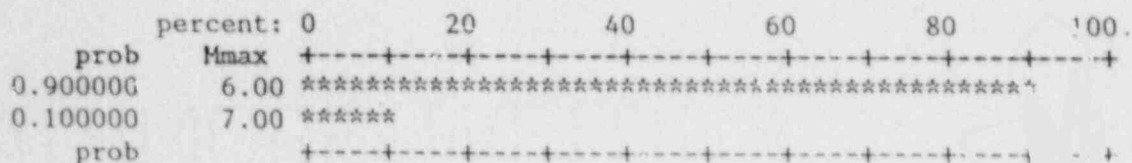
Updip - 20 km depth  
 Downdip - 40 km depth  
 Along strike - Nootka to Blanco barrier to rupture (0.5)

Interface maximum magnitude:

Assessed distribution



Renormalized distribution for events > mag 5



Interface earthquake recurrence:

use moment rate approach

$$\text{moment rate} = \text{convergence rate} * \alpha * \text{interface area}$$

Assessed distribution for convergence rate mm/yr is give above  
alpha assessed as follows

	percent: 0	20	40	60	80	100
prob	+-----+-----+-----+-----+-----+-----+-----+					
0.050000	0.00	****				
0.800000	0.05	*****				
0.050000	0.10	****				
0.050000	0.15	****				
0.050000	0.20	****				
prob	+-----+-----+-----+-----+-----+-----+-----+					

Magnitude distribution model not assessed - use AGGREGATE assessment of the experts

- exponential (0.23)
- characteristic (0.41)
- maximum moment (0.36)

Figure 1 shows the resulting distribution of recurrence estimates, Figure 2 shows the effect of variation in magnitude distribution model on recurrence estimated using the moment rate approach.

The earthquake recurrence relationships shown in Figure 1 can be summarized in terms of return periods for events of various sizes as follows:

Magnitude M	Return Period (yrs) for events of Magnitude ≥ M		
	5th percentile	50th percentile	95 percentile
5	10	0.3	0.06
6	15	0.6	0.5
7	-	-	51



Location of intraslab events:  
 Use observed seismicity pattern

Intraslab Maximum Magnitude:  
 Assessed distribution as follows:

	percent:	0	10	20	30	40	50
prob	Mmax	+-----+-----+-----+-----+-----+-----+-----+					
0.330000	7.00	*****					
0.340000	7.25	*****					
0.330000	7.50	*****					
prob		+-----+-----+-----+-----+-----+-----+-----+					

Intraslab earthquake recurrence:  
 Use historical seismicity. Figure 3 shows recurrence relationship for deep earthquakes assumed to be occurring within downgoing slab. This curve is bases on all recorded events not inferred to lie within the North American plate.

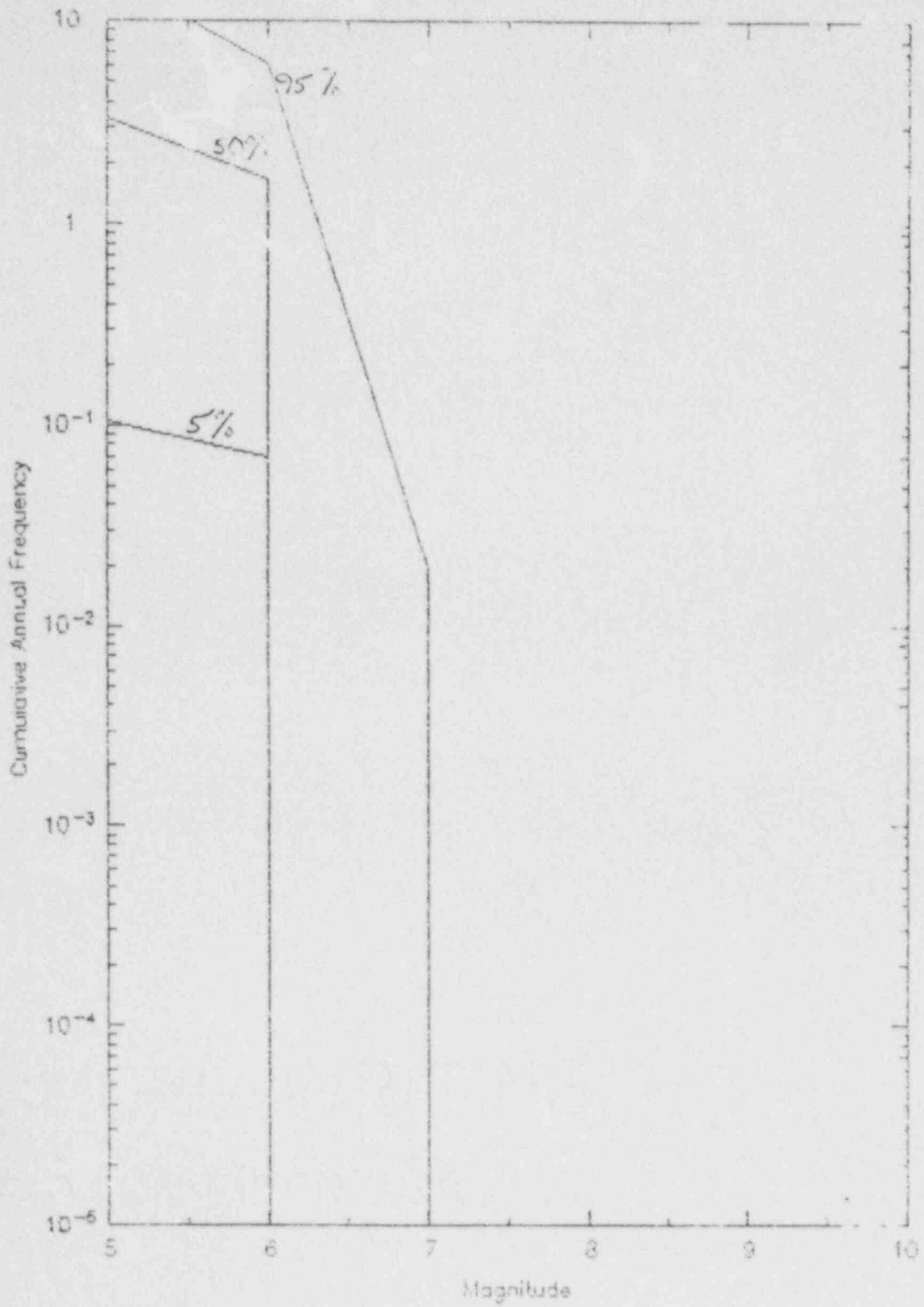
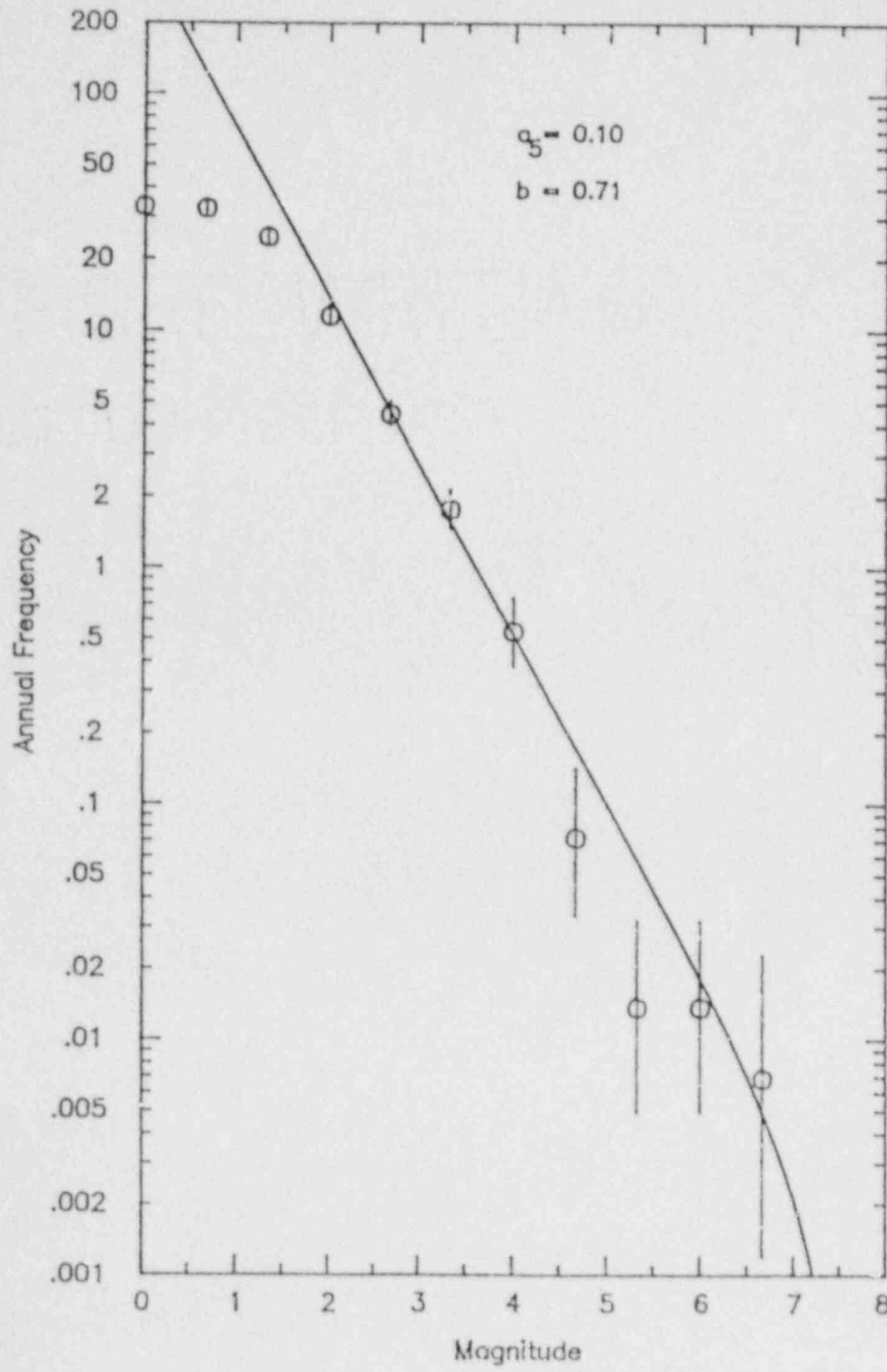


Figure 1 Estimated recurrence distribution for Expert 4

FIGURE 3 B-value -  
Deep Zone



Expert 5  
SUMMARY OF MODEL PARAMETERS

Slab geometry:

Model A - gradually increasing dip approximately 17° below site (0.75-0.80)  
 Model B - approximately 10° dip through deep seismicity (0.20-0.25)

Convergence rate:

25 to 40 mm/yr with the following distribution

prob	mm/yr	percent: 0	10	20	30	40	50
0.028	25.00	****					
0.222	30.00	*****					
0.444	35.00	*****					
0.306	40.00	*****					

Sources and probability of activity:

Interface 0.5 (±0.5)  
 Intraslab 1.0

Maximum extent of rupture on interface:

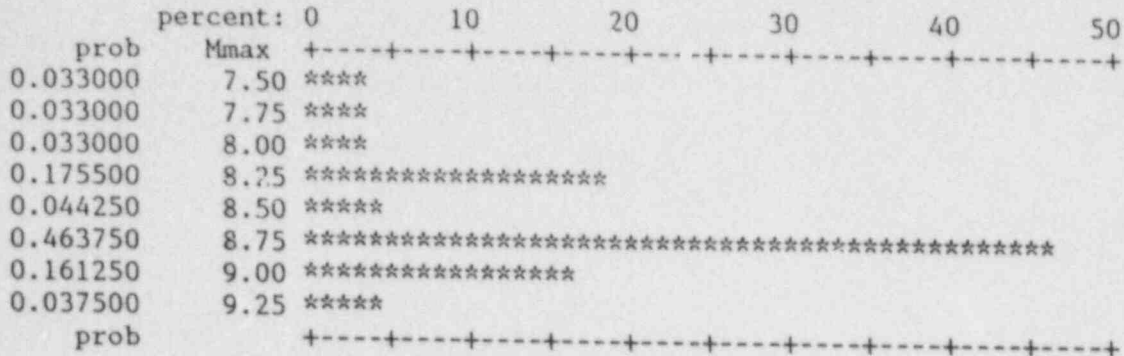
Updip - coastline  
 Downdip - 123.5°W longitude  
 Along strike - Nootka to Blanco

Interface maximum magnitude:

Not assessed - use AGGREGATE distribution  
 a) 0.55 weight assigned to estimate from maximum rupture area  
     Model A - rupture area 43200 -  $M_w$  8.75  
     Model B - rupture area 64000 -  $M_w$  9  
 b) 0.45 weight assigned to following distribution

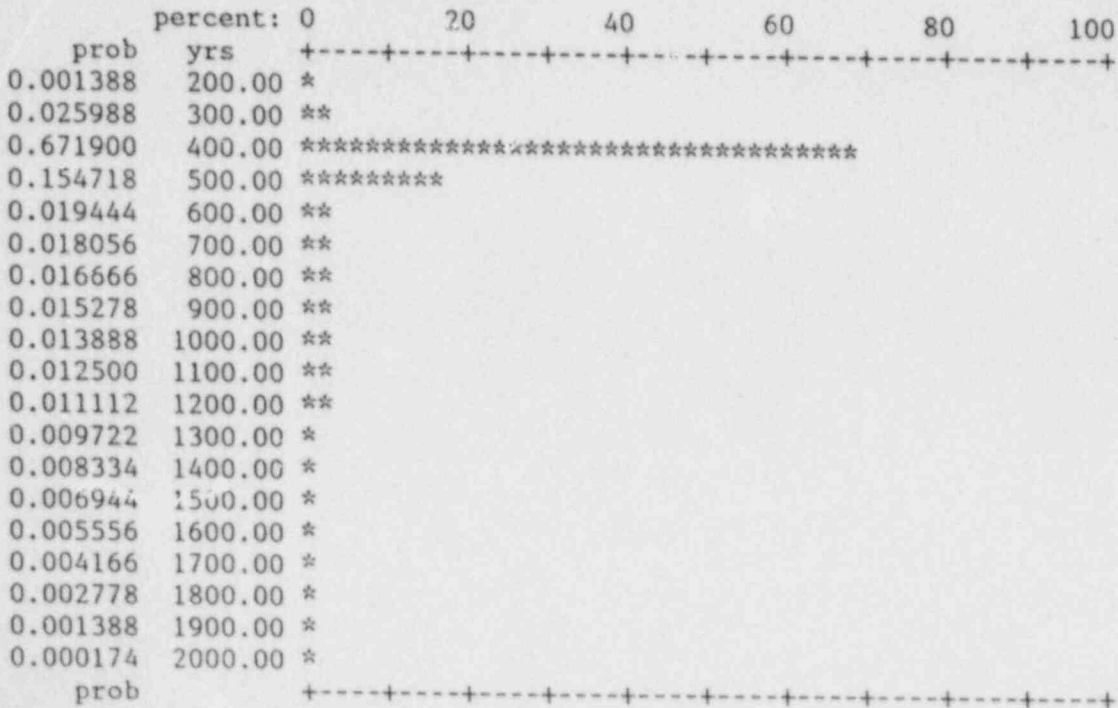
prob	Mmax	percent: 0	10	20	30	40	50
0.073333	7.50	*****					
0.073333	7.75	*****					
0.073333	8.00	*****					
0.390000	8.25	*****					
0.098333	8.50	*****					
0.083333	8.75	*****					
0.083333	9.00	*****					
0.083333	9.25	*****					
0.041667	9.50	*****					

Combining a) and b) the distribution over all maximum rupture geometries is



Interface earthquake recurrence:

Not assessed - use AGGREGATE distribution of other experts as follows:  
 0.48 weight assigned to following AGGREGATE distribution of geological estimates of return period for large events

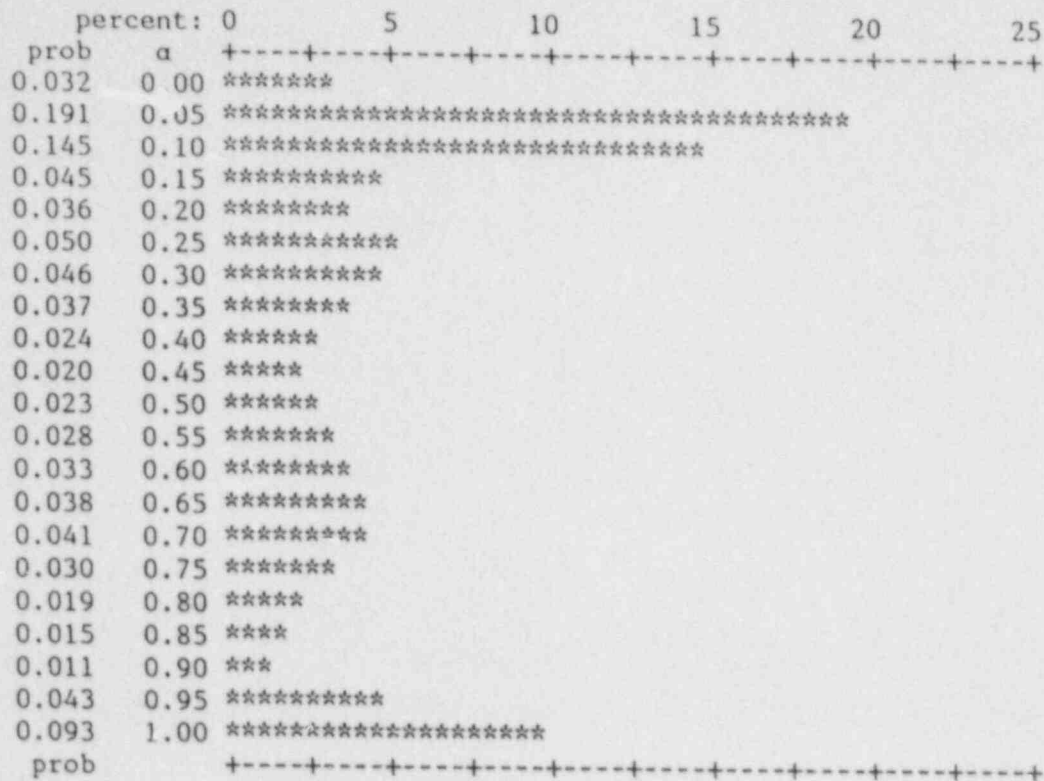


0.52 weight assigned to moment rate approach

$$\text{moment rate} = \text{convergence rate} * a * \text{interface area}$$

Assessed distribution for convergence rate mm/yr is give above

alpha not assessed - use AGGREGATE distribution of experts



Magnitude distribution model not assessed - use AGGREGATE assessment of the experts  
 exponential (0.23)  
 characteristic (0.41)  
 maximum moment (0.36)

Figure 1 shows the resulting distribution of recurrence estimates, Figure 2 shows the effect of variation in maximum magnitude on recurrence estimated using the moment rate approach, Figure 3 shows the effect of choice of magnitude distribution model on recurrence estimates, and Figure 4 shows the effect of slab geometry on the recurrence estimates.

The earthquake recurrence relationships shown in Figure 1 can be summarized in terms of return periods for events of various sizes as follows:

Magnitude M	Return Period (yrs) for events of Magnitude ≥ M		
	5th percentile	50th percentile	95 percentile
5	4200	17	0.4
6	4200	63	2
7	5250	240	9
8	-	480	60
9	-	12000	540

Location of intraslab events:

Updip extent - coastline

Downdip extent - Mt. Ranier

Along strike - match observed seismicity pattern

Intraslab Maximum Magnitude:

Magnitude 7

Intraslab earthquake recurrence:

Use historical seismicity. Figure 5 shows recurrence relationship for deep earthquakes assumed to be occurring within downgoing slab. This curve is based on all recorded events not inferred to lie within the North American plate.

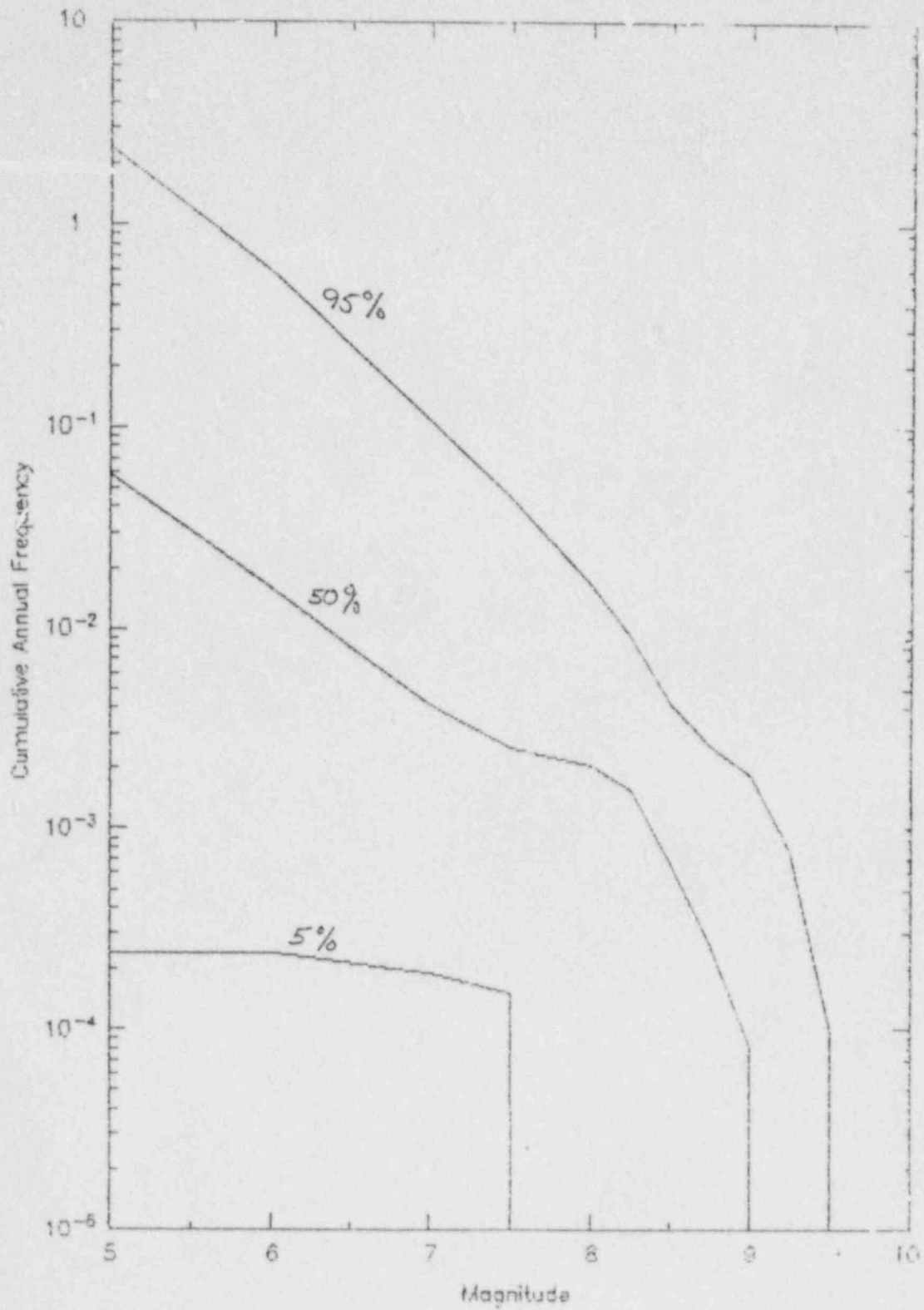


Figure 1 Estimated recurrence distribution for Expert 5



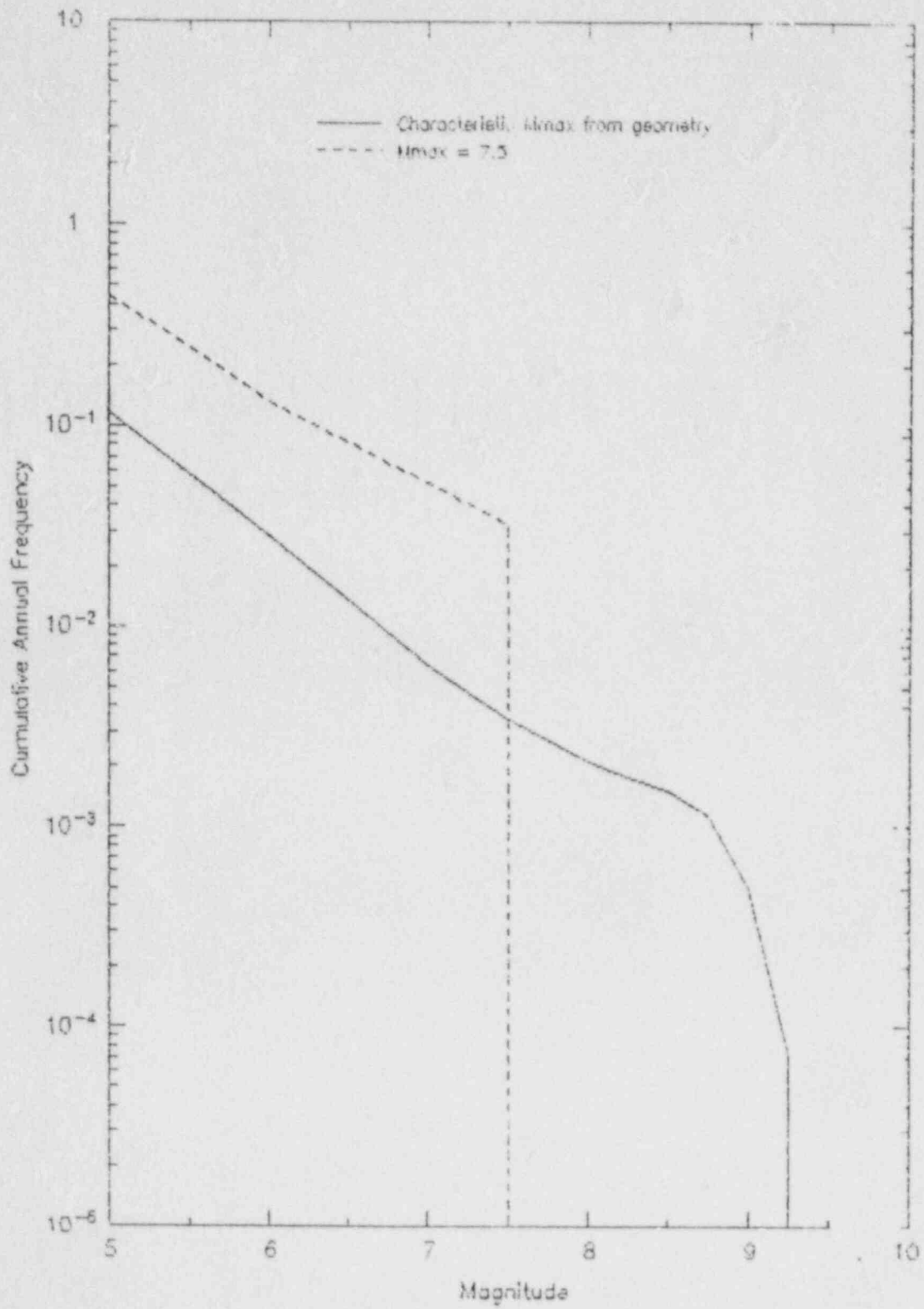


Figure 2 Effect of Max Magnitude for Expert 5

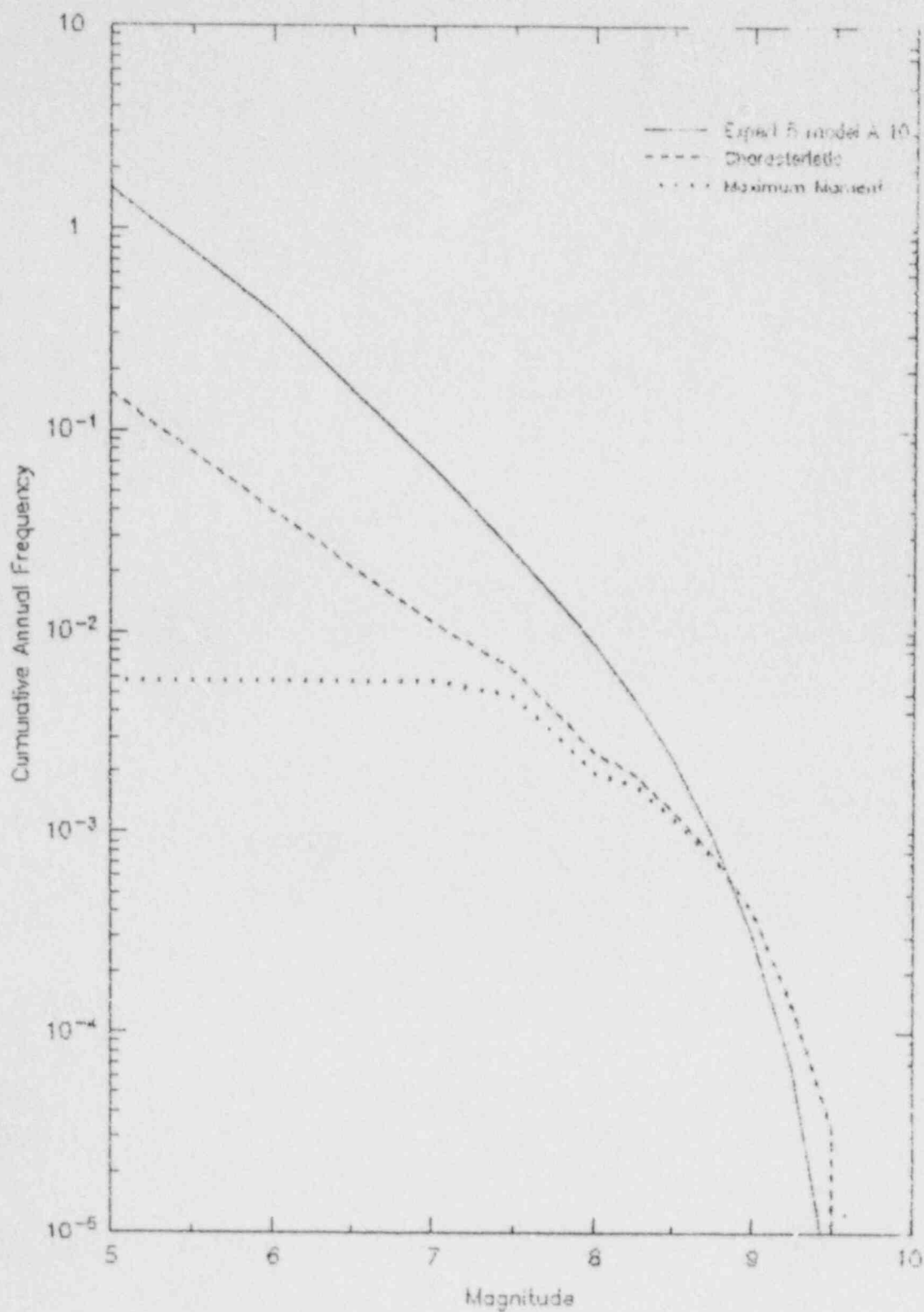


Figure 3 Effect of magnitude distribution model for Expert 5

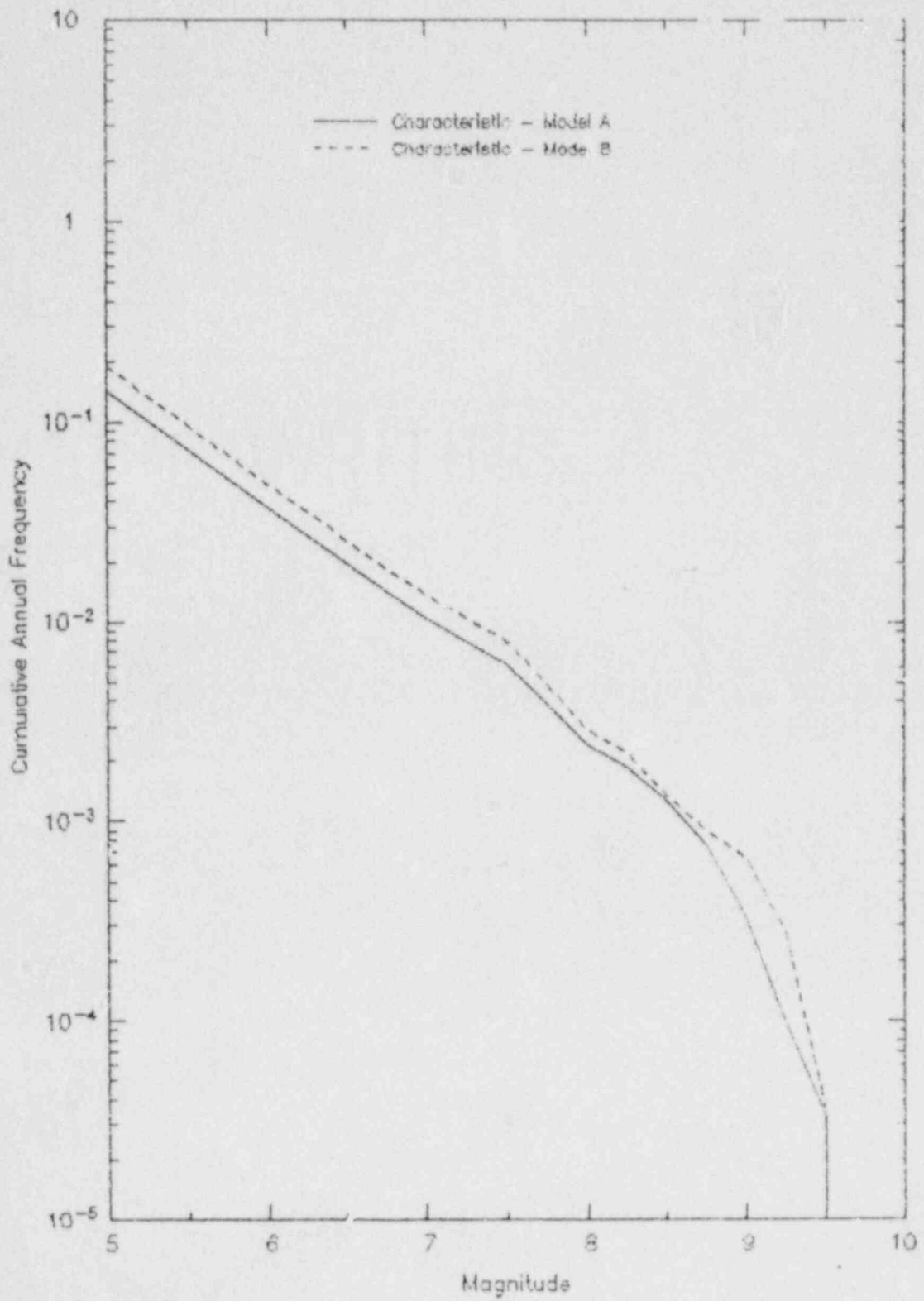
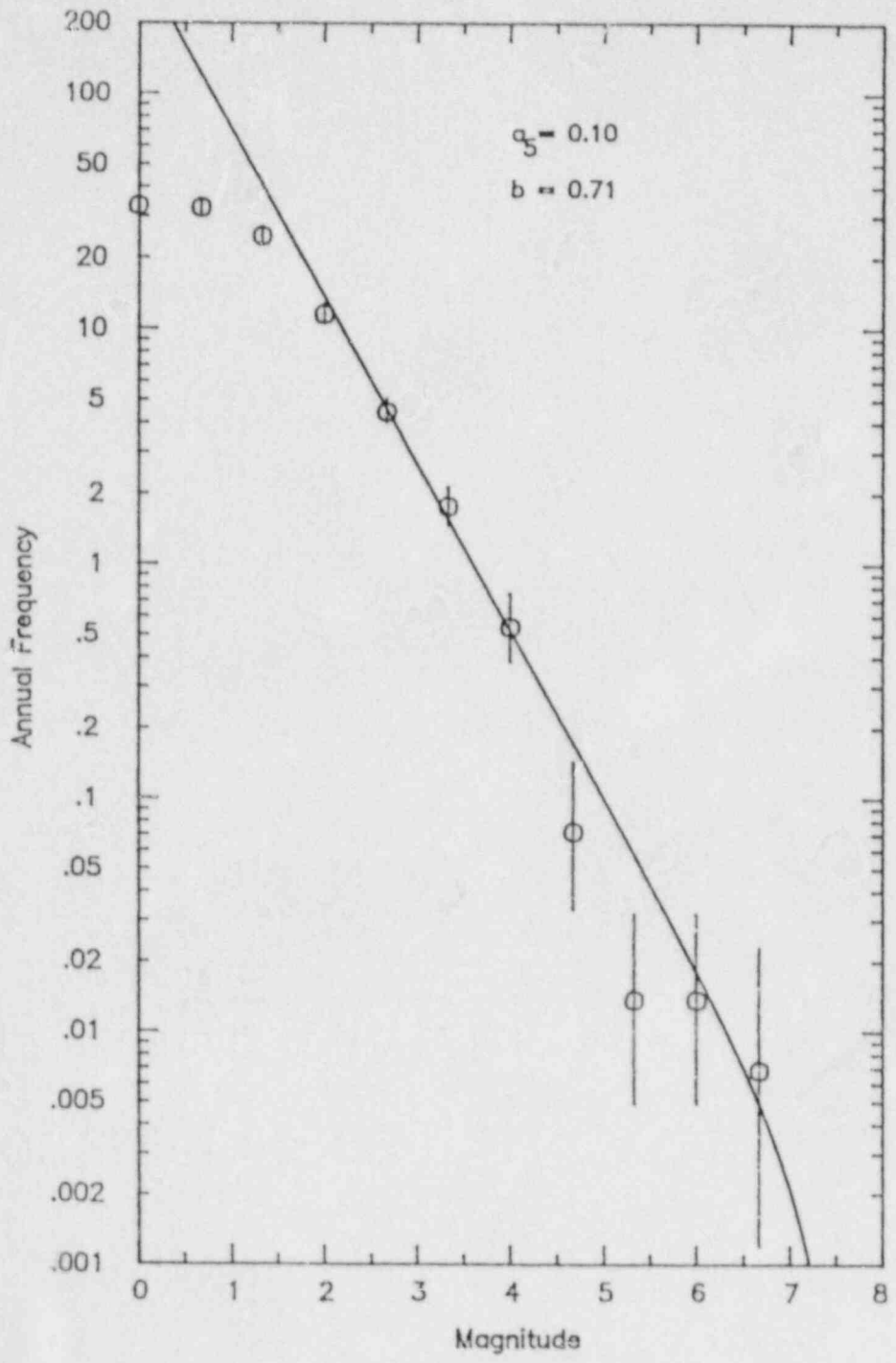


Figure 4 Effect of slab geometry for Expert 5

FIGURE 5 B-value -  
Deep Zone



Expert 6  
SUMMARY OF MODEL PARAMETERS

Slab Geometry:

Model A - 10° through deep seismicity (0.70 ±0.05)  
 Model B - 10° with double bend through deep seismicity (0.30 ±0.05)

Convergence rate:

10 to 60 mm/yr with the following distribution:

	percent:	0	10	20	30	40	50
prob	mm/yr	+-----+-----+-----+-----+-----+-----+-----+					
0.010	10.00	**					
0.020	15.00	***					
0.020	20.00	***					
0.020	25.00	***					
0.110	30.00	*****					
0.200	35.00	*****					
0.183	40.00	*****					
0.274	45.00	*****					
0.143	50.00	*****					
0.010	55.00	**					
0.005	60.00	**					
prob		+-----+-----+-----+-----+-----+-----+-----+					

Sources and probability of activity:

Interface 0.65 (±0.15)  
 Intraslab 1.0

Maximum extent of rupture on interface:

Updip - depth 20 km  
 Downdip - depth of 45 km (±5)  
 Along strike - Nootka to Blanco (0.5)  
                   Entire plate (0.5)

Interface Maximum Magnitude:

Use maximum rupture dimensions  
 Model A - unsegmented area = 157500 km<sup>2</sup> M<sub>w</sub> 9.25  
           segmented area = 120000 km<sup>2</sup> M<sub>w</sub> 9.25  
 Model B - unsegmented area = 210000 km<sup>2</sup> M<sub>w</sub> 9.5  
           segmented area = 160000 km<sup>2</sup> M<sub>w</sub> 9.25

Interface Earthquake Recurrence:

Use moment rate approach with weight (0.5)  
 moment rate = convergence rate\*α\*interface area  
 convergence rate distribution given above



$\alpha$  assessed according to following distribution

prob	$\alpha$	0	5	10	15	20	25
0.083	0.45	*****					
0.167	0.50	*****					
0.167	0.55	*****					
0.167	0.60	*****					
0.167	0.65	*****					
0.167	0.70	*****					
0.082	0.75	*****					

Use geologic estimate of 430  $\pm$ 25% with weight (0.5)

Magnitude distribution - exponential (0.6)  
 - characteristic (0.4)

Attached Figure 1 shows the resulting distribution of recurrence estimates for interface events. Maximum event magnitude is assumed to be uniformly distributed in the range of the expected maximum magnitude given above  $\pm$  0.25 magnitude units. Figure 2 shows the effect of magnitude distribution model on recurrence estimates, Figure 3 shows the effect of uncertainty in segmentation, and Figure 4 shows the effect of slab geometry.

The earthquake recurrence relationships shown in Figure 1 can be summarized in terms of return periods for various sizes as follows:

Magnitude M	Return Period (yrs) for events of Magnitude $\geq$ M		
	5th percentile	50th percentile	95 percentile
5	9	1	0.2
6	37	4	0.7
7	182	21	3
8	675	118	20
9	1860	525	200

Location of intraslab events:

- Updip - 75 km west of trench
- Downdip - depth of 75 km 75% of mag>6 near bend
- Along strike - match observed relative frequency

Intraslab Maximum Magnitude:

Uniform distribution 6.75 to 7.25

Intraslab Earthquake Recurrence:

Historical seismicity used to compute a- and b-values for exponential model. Figure 5 shows the recurrence relationship used for the intraslab events in Model A and the deep zone in Models B and C. This curve is based on all recorded events not inferred to lie within the North American plate.

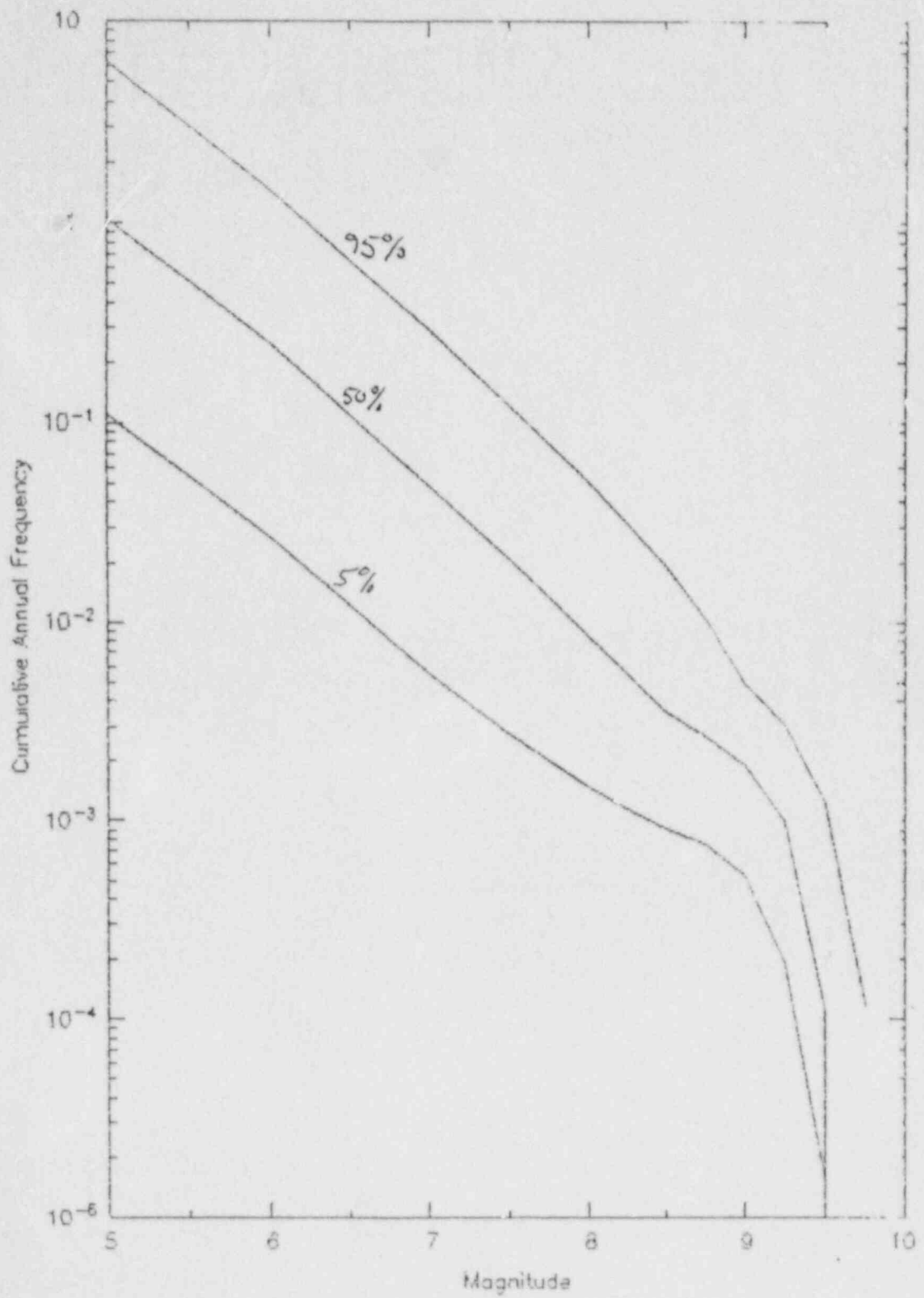


Figure 1 Estimated recurrence distribution for Expert 6

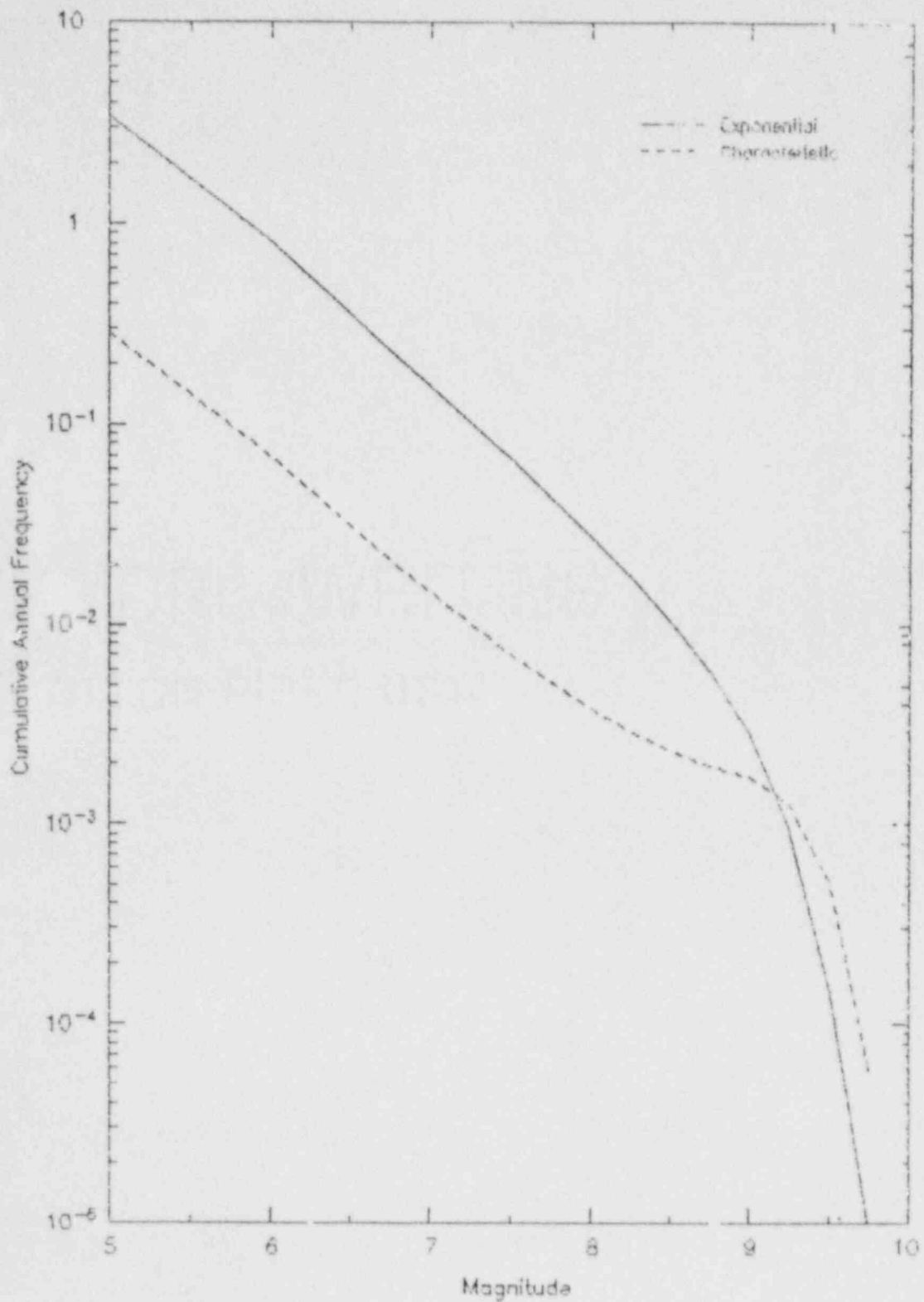


Figure 2 Effect of magnitude distribution model for Expert 6



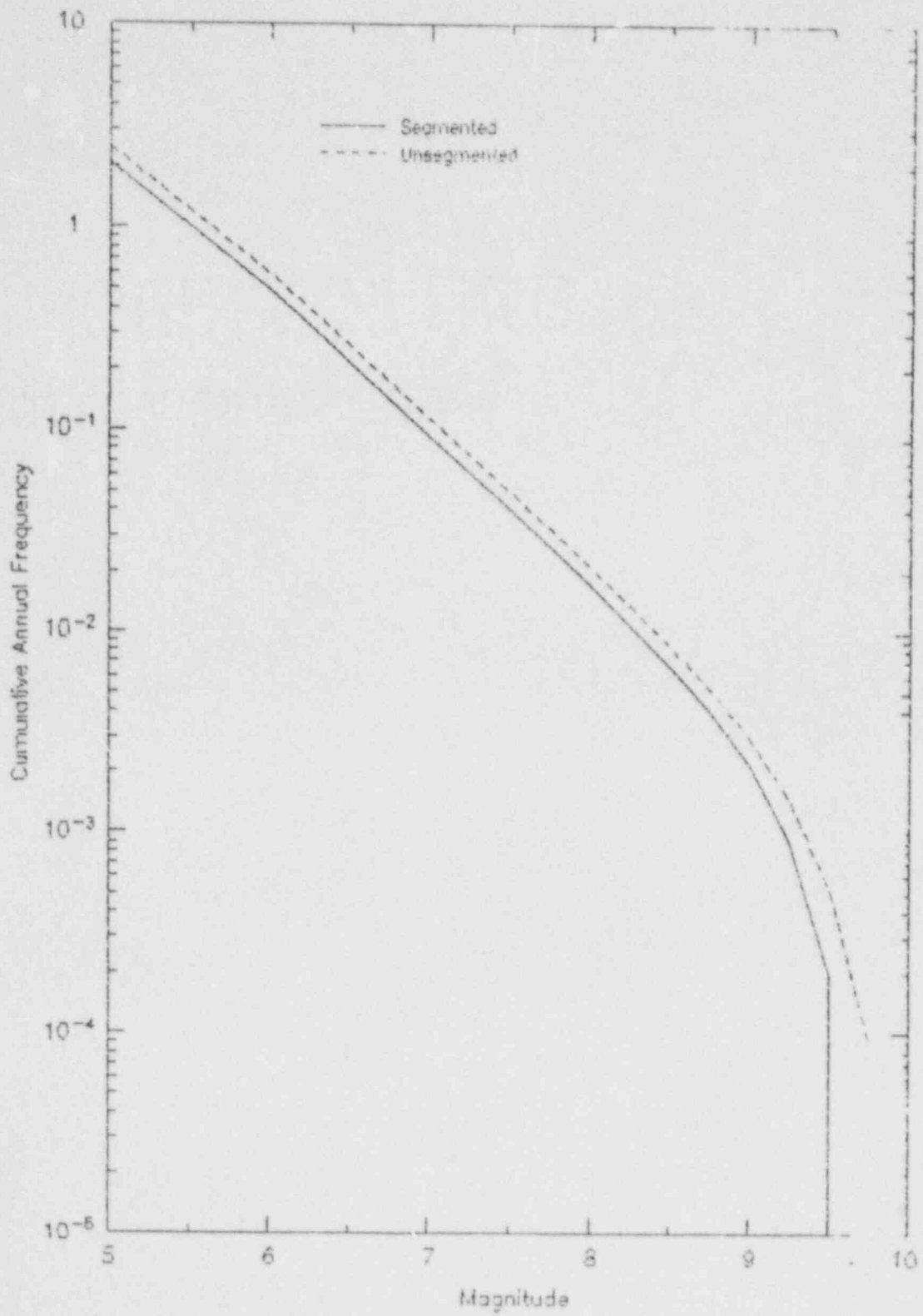


Figure 3 Effect of segmentation for Expert 6

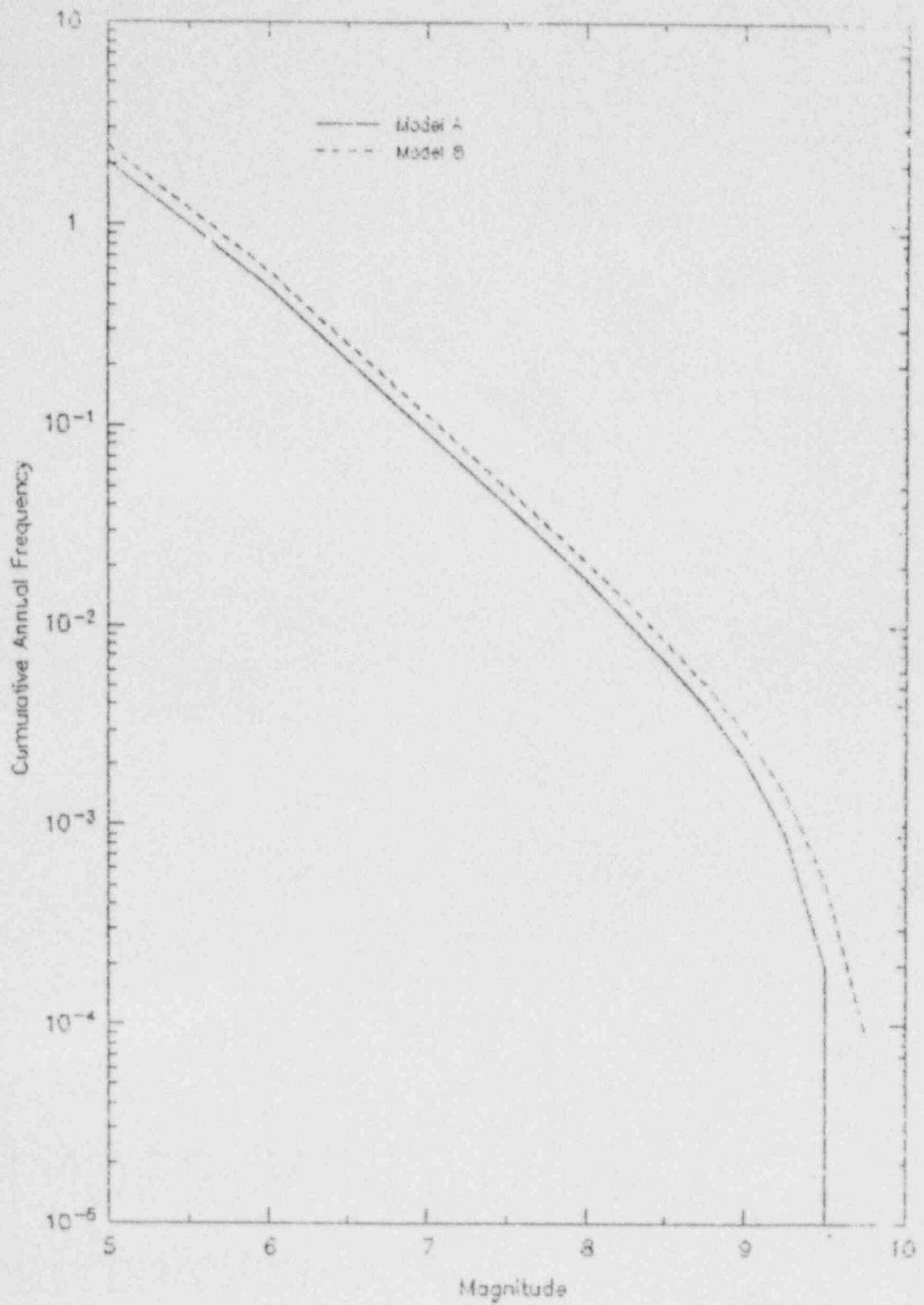
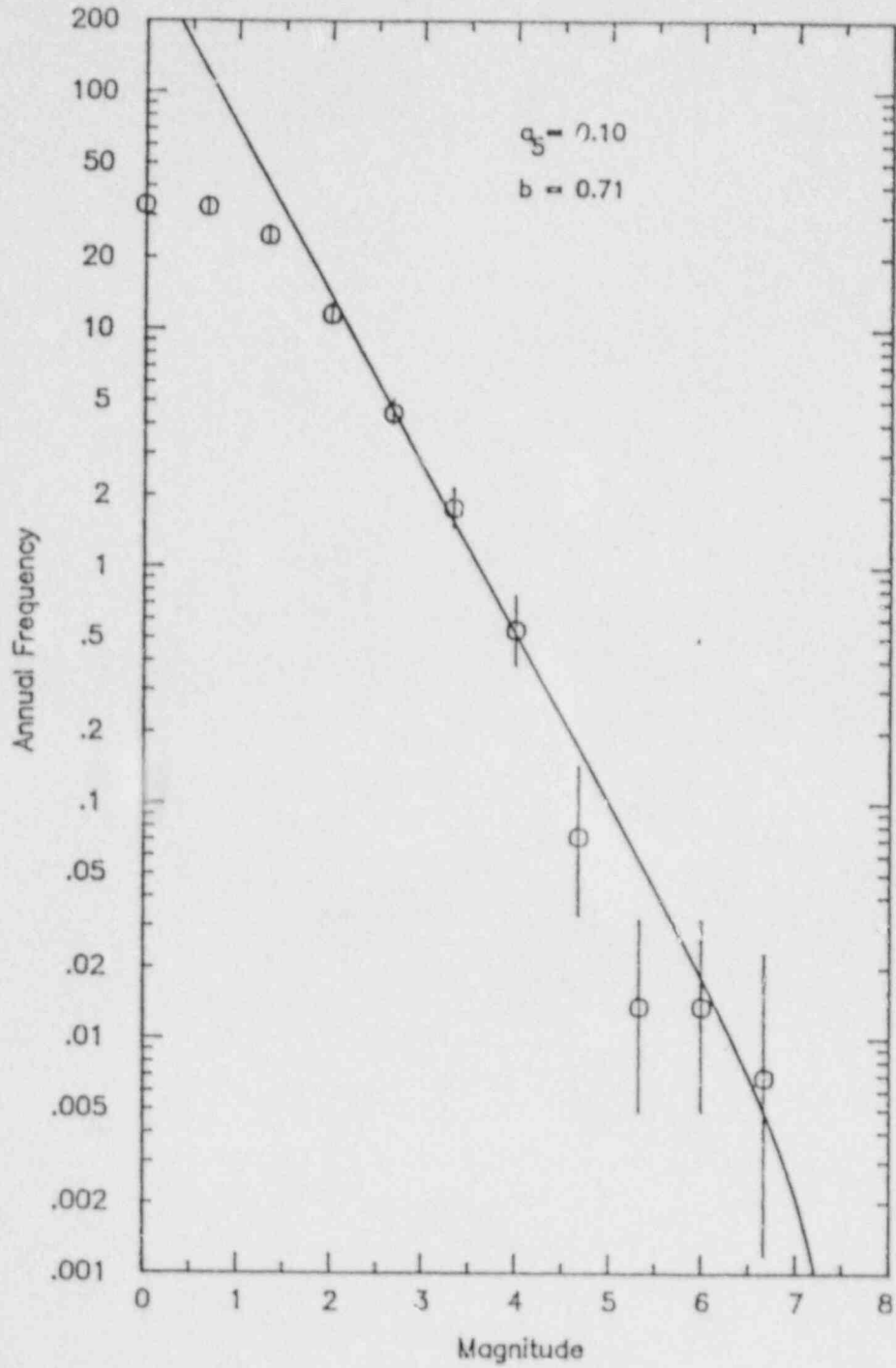


Figure 4 Effect of slab geometry for Expert 6

FIGURE 5 B-value -  
Deep Zone



Expert 7  
SUMMARY OF MODEL PARAMETERS

Slab geometry:

Approximately 10° dip through deep seismicity

Convergence rate:

42 ±10 mm/yr with the following distribution

	percent:	0	10	20	30	40	50
prob	mm/yr	+-----+-----+-----+-----+-----+-----+-----+-----+					
0.05	30.00	*****					
0.30	35.00	*****					
0.30	40.00	*****					
0.30	45.00	*****					
0.05	50.00	*****					
prob		+-----+-----+-----+-----+-----+-----+-----+-----+					

Sources and probability of activity:

Interface 0.3 (±0.2)

Intraslab not assessed - use AGGREGATE assessment of 0.96

Maximum extent of rupture on interface:

Updip - depth of 15 to 20 km (equal weights)

Downdip - coast ranges depth 30 km

Along strike - Nootka to Blanco

Interface maximum magnitude:

Use maximum rupture area

rupture area 44000 to 68000 -  $M_w$  8.75-9

Interface earthquake recurrence:

Use moment rate approach

moment rate = convergence rate \*  $\alpha$  \* interface area

Assessed distribution for convergence rate mm/yr is give above

alpha assessed as 1.0 (conditional on source active)

Magnitude distribution model not assessed - use AGGREGATE assessment of the experts

exponential (0.23)

characteristic (0.41)

maximum moment (0.36)

Figure 1 shows the resulting distribution of recurrence estimates and Figure 2 shows the effect of choice of magnitude distribution model on recurrence estimates.

The earthquake recurrence relationships shown in Figure 1 can be summarized in terms of return periods for events of various sizes as follows:

Magnitude M	Return Period (yrs) for events of Magnitude $\geq$ M		
	5th percentile	50th percentile	95 percentile
5	630	6	0.4
6	630	22	2
7	630	100	9
8	630	310	60
9	13400	1400	533

Location of intraslab events:

Updip , downdip, and along strike - match observed seismicity pattern

Intraslab Maximum Magnitude:

Not assessed - use following AGGREGATE distribution

prob	Mmax	percent: 0	10	20	30	40	50
0.041	6.60	*****					
0.030	6.75	****					
0.355	7.00	*****	*****	*****	*****	*****	*****
0.219	7.25	*****	*****	*****	*****	*****	*****
0.345	7.50	*****	*****	*****	*****	*****	*****
0.000	7.75	*					
0.010	8.00	**					

Intraslab earthquake recurrence:

Use historical seismicity. Figure 3 shows recurrence relationship for deep earthquakes assumed to be occurring within downgoing slab. This curve is based on all recorded events not inferred to lie within the North American plate.

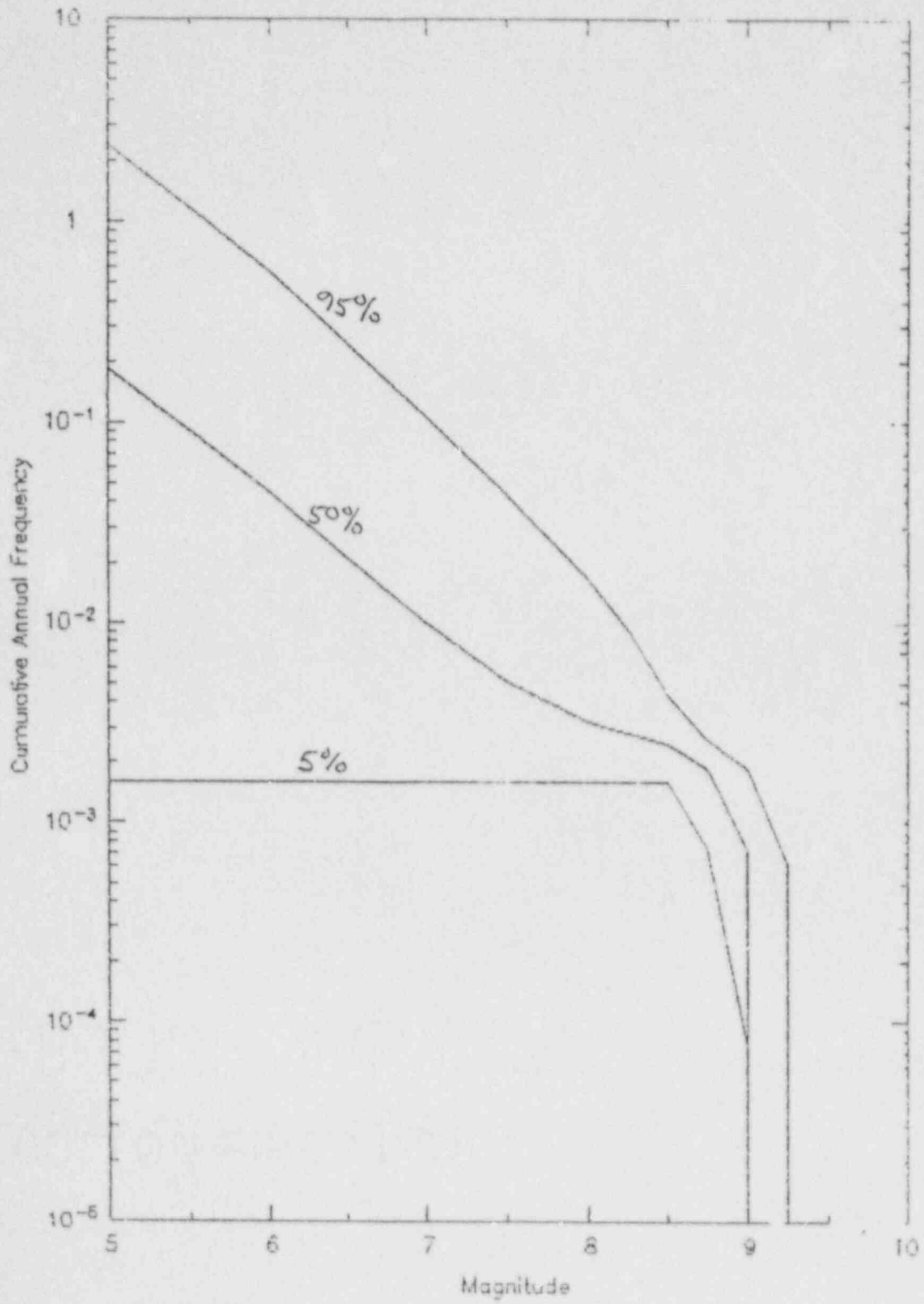


Figure 1 Estimated recurrence distribution for Expert 7

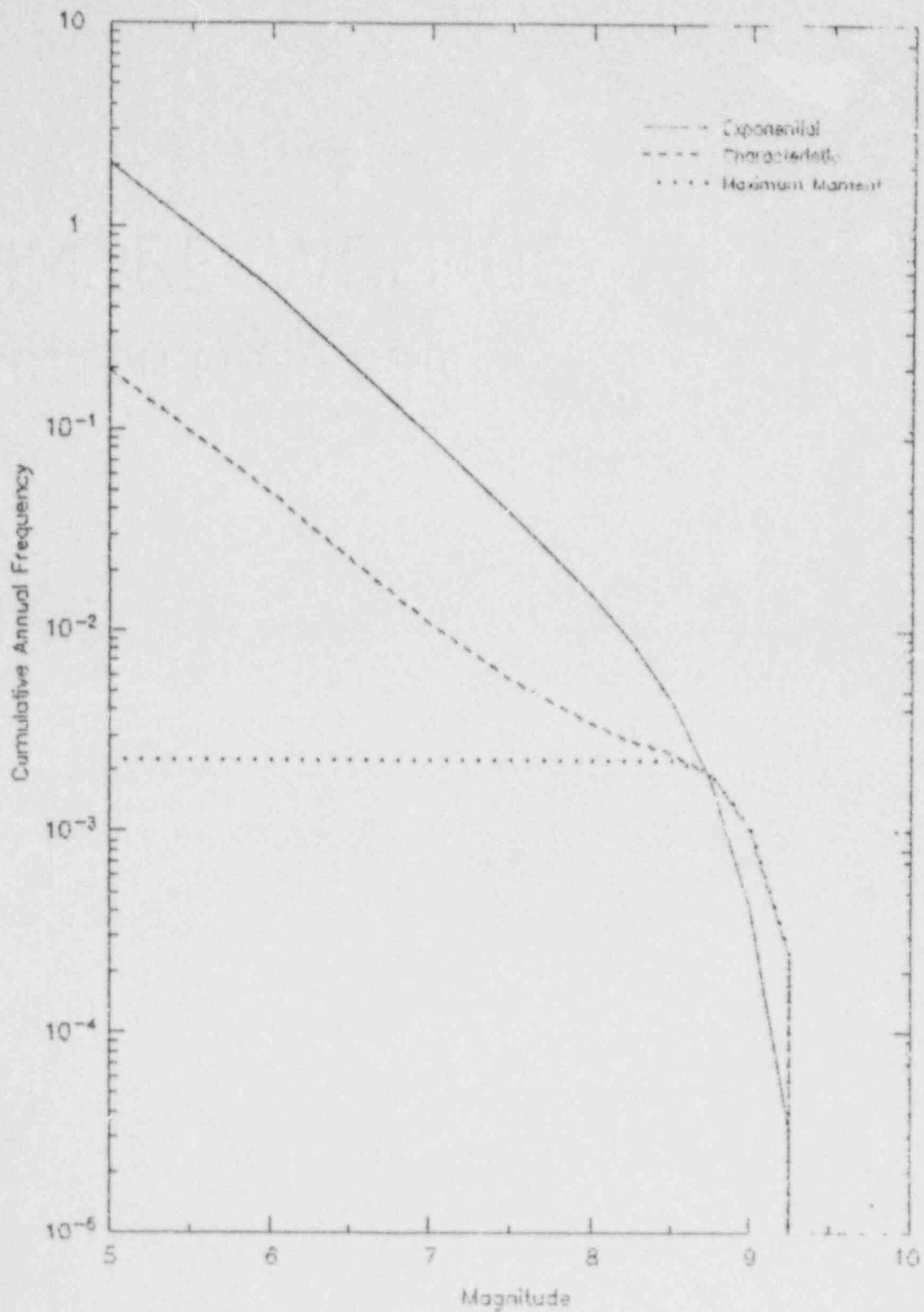
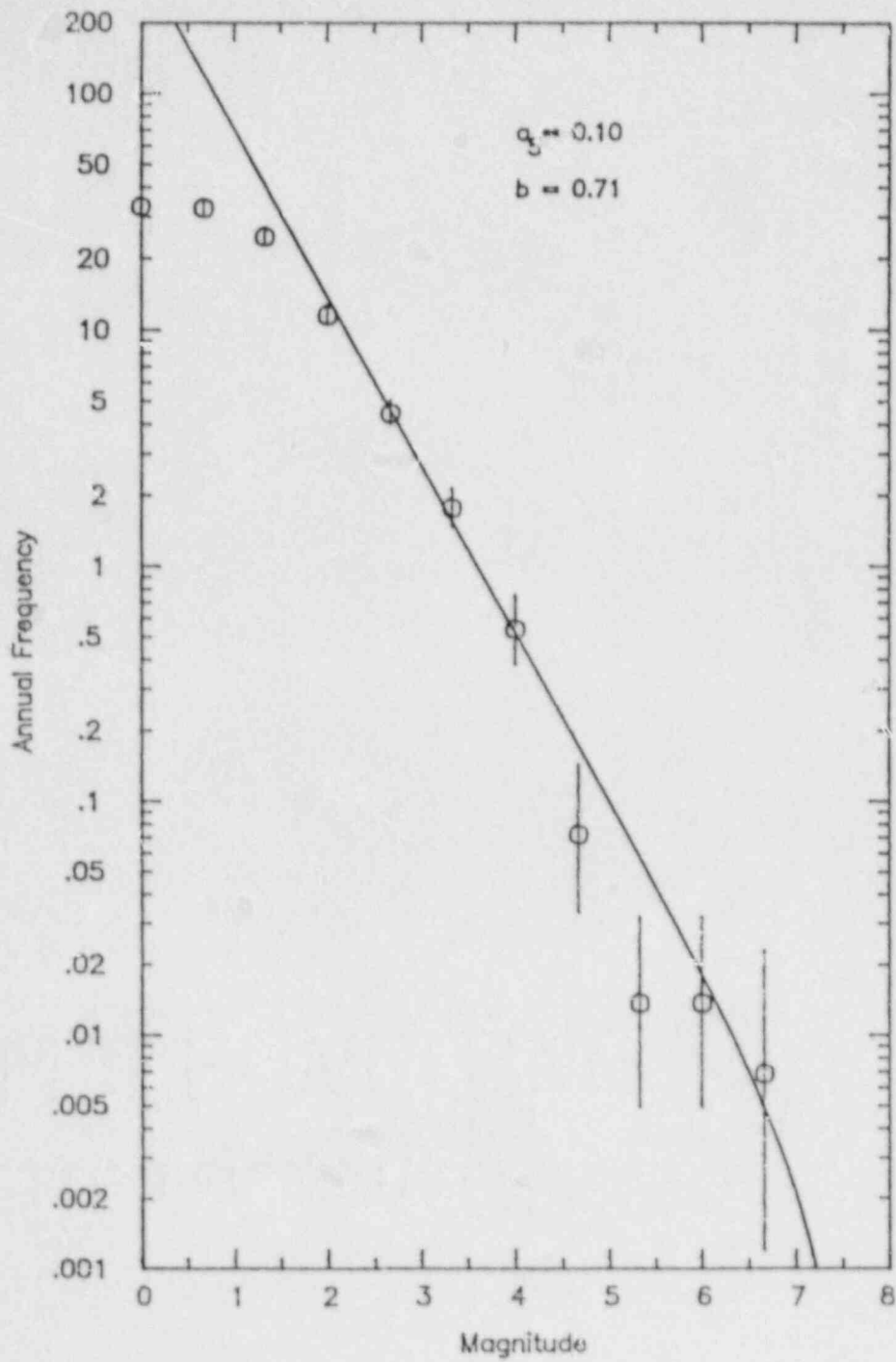


Figure 2 Effect of magnitude distribution model for Expert 7

FIGURE 3 B-value -  
Deep Zone





Expert 8  
SUMMARY OF MODEL PARAMETERS

Slab geometry:

Approximately 10° dip through deep seismicity

Convergence rate:

42 ±10 mm/yr with the following distribution

	percent:	0	10	20	30	40	50
prob	mm/yr	+-----+-----+-----+-----+-----+-----+-----+					
0.05	30.00	*****					
0.30	35.00	*****					
0.30	40.00	*****					
0.30	45.00	*****					
0.05	50.00	*****					
prob		+-----+-----+-----+-----+-----+-----+-----+					

Sources and probability of activity:

Interface 0.45 (0.25-0.75)

Intraslab 1.0

Maximum extent of rupture on interface:

Updip - 124.5°W to 125°W (equal weights)

Downdip - 123° W

Along strike - Nootka to Blanco

Interface maximum magnitude:

Use maximum rupture area

rupture area 89600 to 119200 -  $M_w$  9-9.25

Interface earthquake recurrence:

Use moment rate approach

moment rate = convergence rate \*  $\alpha$  \* interface area

Assessed distribution for convergence rate mm/yr is give above

alpha assessed according to following distribution

	percent:	0	10	20	30	40	50
prob	$\alpha$	+-----+-----+-----+-----+-----+-----+-----+					
0.017860	0.15	***					
0.142860	0.20	*****					
0.260710	0.25	*****					
0.228570	0.30	*****					
0.171430	0.35	*****					
0.114290	0.40	*****					
0.057140	0.45	*****					
0.007140	0.50	**					
prob		+-----+-----+-----+-----+-----+-----+-----+					

Magnitude distribution model not assessed - use AGGREGATE assessment of the experts

- exponential (0.23)
- characteristic (0.41)
- maximum moment (0.36)

Figure 1 shows the resulting distribution of recurrence estimates and Figure 2 shows the effect of choice of magnitude distribution model on recurrence estimates.

The earthquake recurrence relationships shown in Figure 1 can be summarized in terms of return periods for events of various sizes as follows:

Magnitude M	Return Period (yrs) for events of Magnitude $\geq$ M		
	5th percentile	50th percentile	95 percentile
5	2500	14	0.3
6	2500	57	1
7	2500	270	6
8	2500	500	36
9	4400	1700	380

Location of intraslab events:

- Updip - 125°W
- Downdip - 70 km depth
- Along strike - match observed seismicity pattern

Intraslab Maximum Magnitude:

Not assessed - use following AGGREGATE distribution

prob	Mmax	percent: 0	10	20	30	40	50
0.041	6.60	*****					
0.030	6.75	****					
0.355	7.00	*****					
0.219	7.25	*****					
0.345	7.50	*****					
0.000	7.75	*					
0.010	8.00	**					
prob		+-----+	+-----+	+-----+	+-----+	+-----+	+-----+

Intraslab earthquake recurrence:

Not assessed - use historical seismicity. Figure 3 shows recurrence relationship for deep earthquakes assumed to be occurring within downgoing slab. This curve is based on all recorded events not inferred to lie within the North American plate.

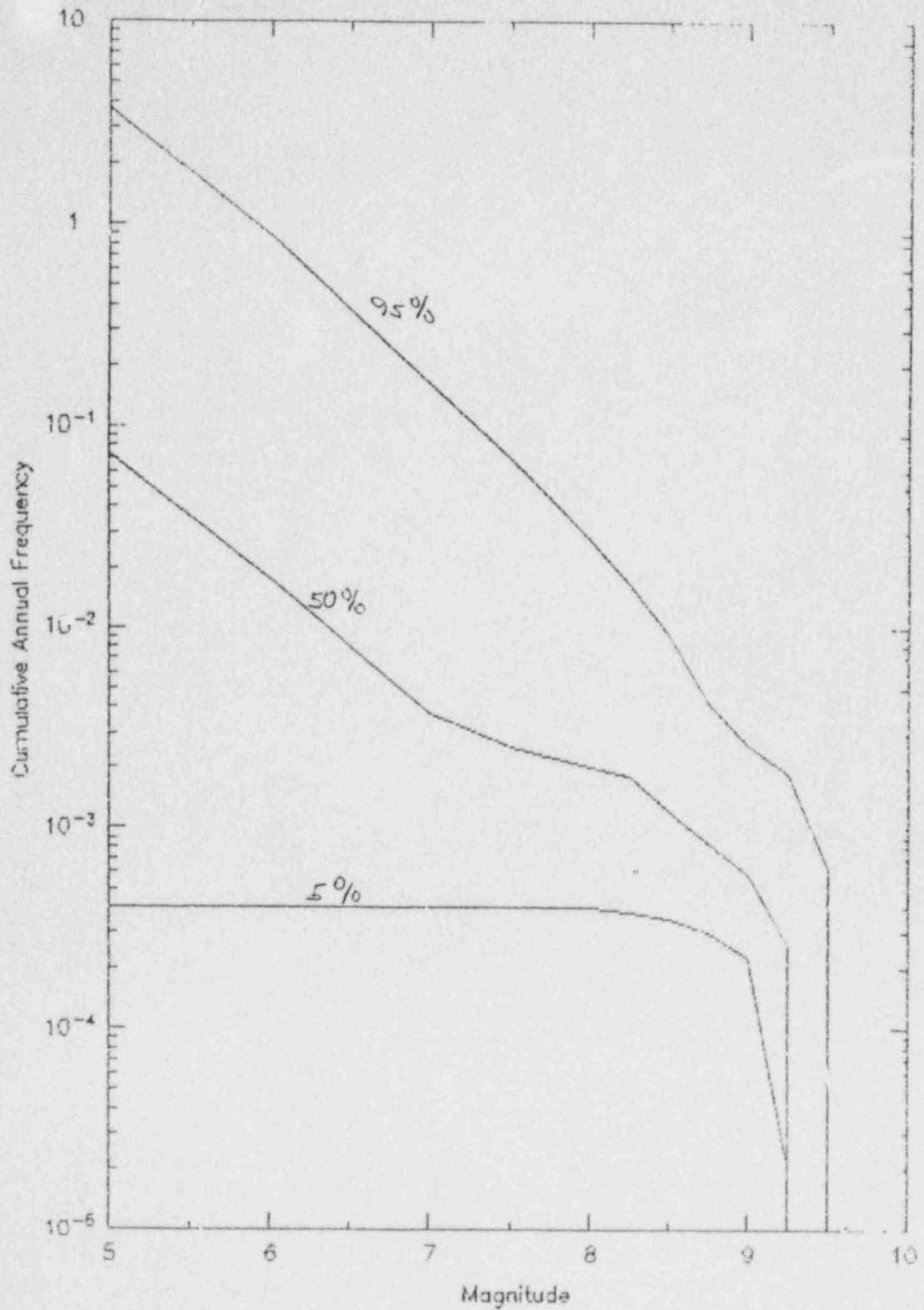


Figure 1 Estimated recurrence distribution for Expert 3

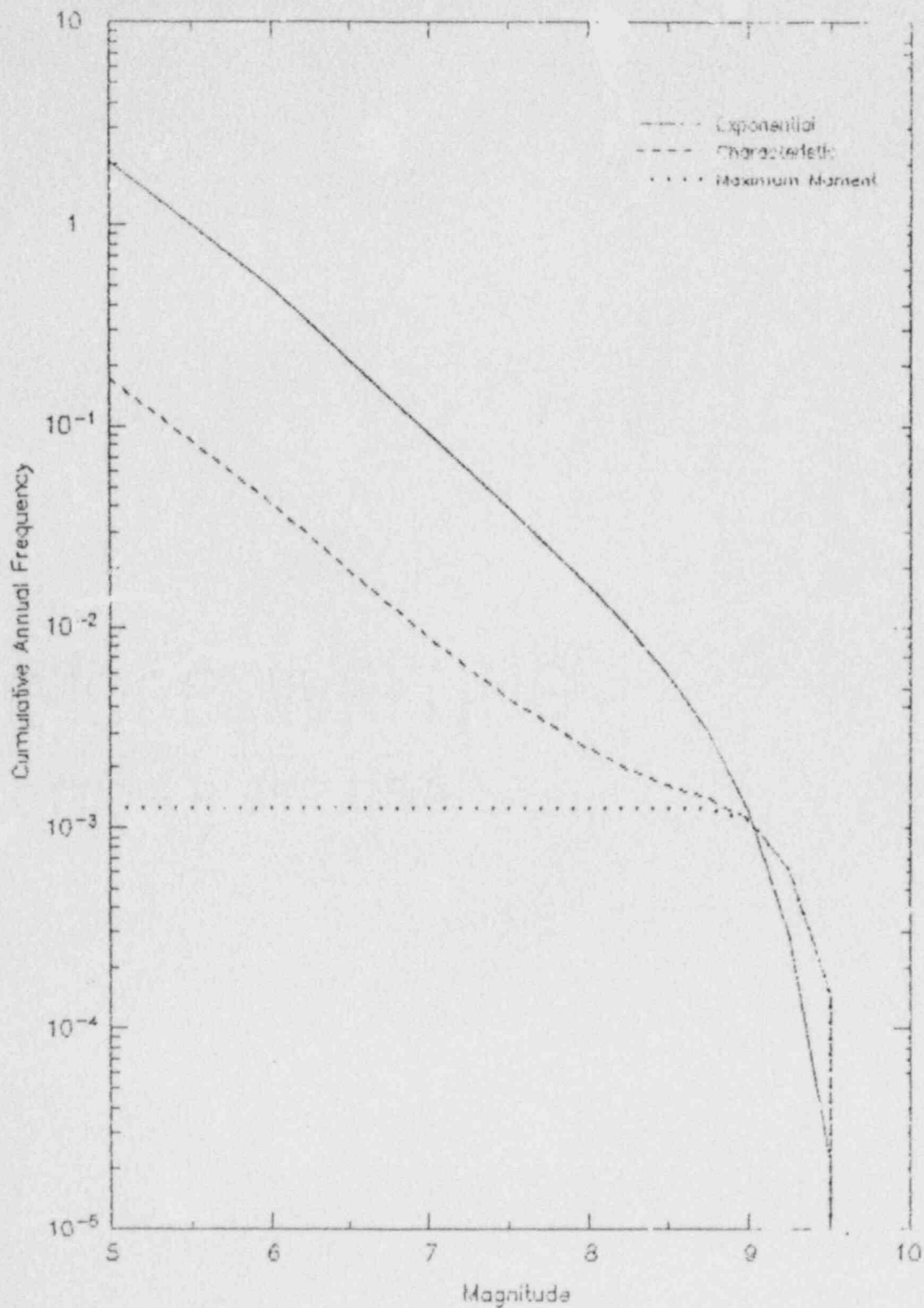
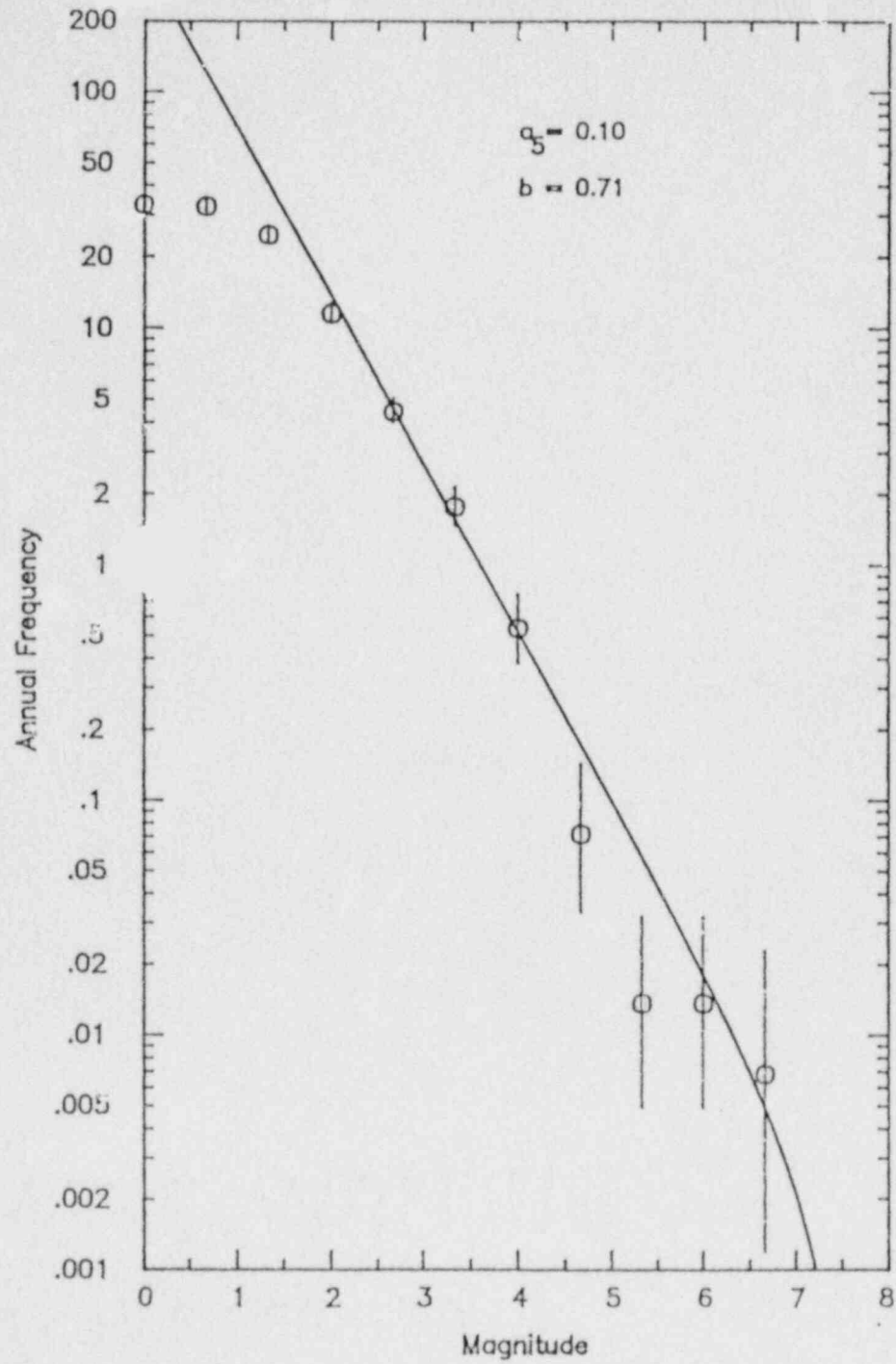


Figure 2 Effect of magnitude distribution model for Expert 8

FIGURE 3 B-value -  
Deep Zone



Expert 9  
SUMMARY OF MODEL PARAMETERS

Slab geometry:

Approximately 10° dip through deep seismicity

Convergence rate:

42 ±10 mm/yr with the following distribution

	percent:	0	10	20	30	40	50
prob	mm/yr	+-----+	+-----+	+-----+	+-----+	+-----+	+-----+
0.05	30.00	*****					
0.30	35.00	*****	*****	*****	*****	*****	*****
0.30	40.00	*****	*****	*****	*****	*****	*****
0.30	45.00	*****	*****	*****	*****	*****	*****
0.05	50.00	*****					
prob		+-----+	+-----+	+-----+	+-----+	+-----+	+-----+

Sources and probability of activity:

Interface 0.92 (0.8-1.0)  
 Intraslab shallow 0.9  
 Intraslab deep 1.0

Maximum extent of rupture on interface:

up/down dip extent - 124.7°W to 122.7°W (0.8)  
                                   124.7°W to 122.0°W (0.2)  
 Along strike - Entire Zone (0.2)  
                                   Nootka to Blanco (0.6)  
                                   Nootka to Blanco segmented at 46°N (0.2)

Interface maximum magnitude:

Use maximum rupture area  
 Entire zone - rupture area           178800 to 241200 - M<sub>w</sub> 9.5  
 Nootka - Blanco                       119200 to 160800 - M<sub>w</sub> 9.25  
 Nootka - Blanco segmt at 46°N   59600 to 80400 - M<sub>w</sub> 9.0

Interface earthquake recurrence:

Use geological estimate of 430 yrs (±25%)  
 Use characteristic magnitude distribution model

Figure 1 shows the resulting distribution of recurrence estimates. The earthquake recurrence relationships shown in Figure 1 can be summarized in terms of return periods for events of various sizes as follows:

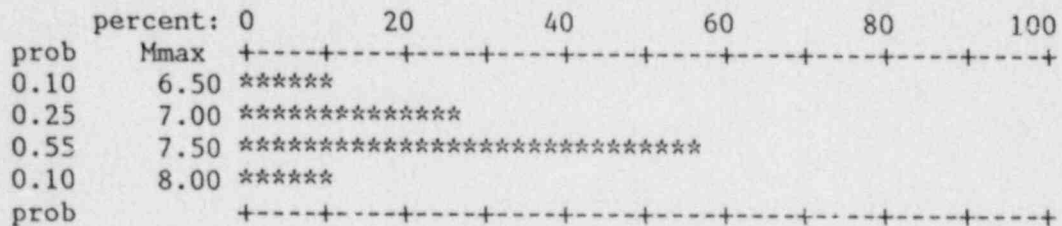
Magnitude M	Return Period (yrs) for events of Magnitude $\geq$ M		
	5th percentile	50th percentile	95 percentile
5	4	3	2
6	17	11	7
7	77	53	32
8	256	427	132
9	600	427	330

Location of intraslab events:

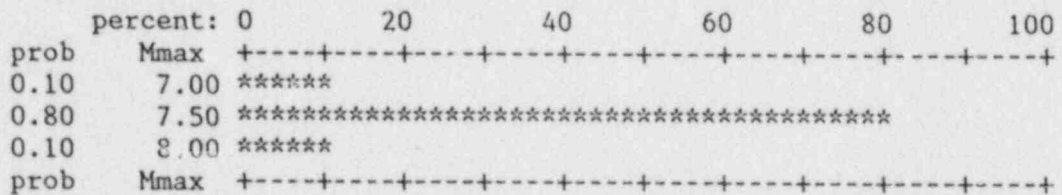
Match observed seismicity pattern up/down dip and along strike

Intraslab Maximum Magnitude:

Shallow zone use following distribution



Deep zone use following distribution



Intraslab earthquake recurrence:

Use historical seismicity. Figure 2 shows recurrence relationship for deep zone. This curve is based on all recorded events not inferred to lie within the North American plate. Figure 3 shows the recurrence relationship for the shallow zone based on the offshore recordings within the Juan de Fuca plate.

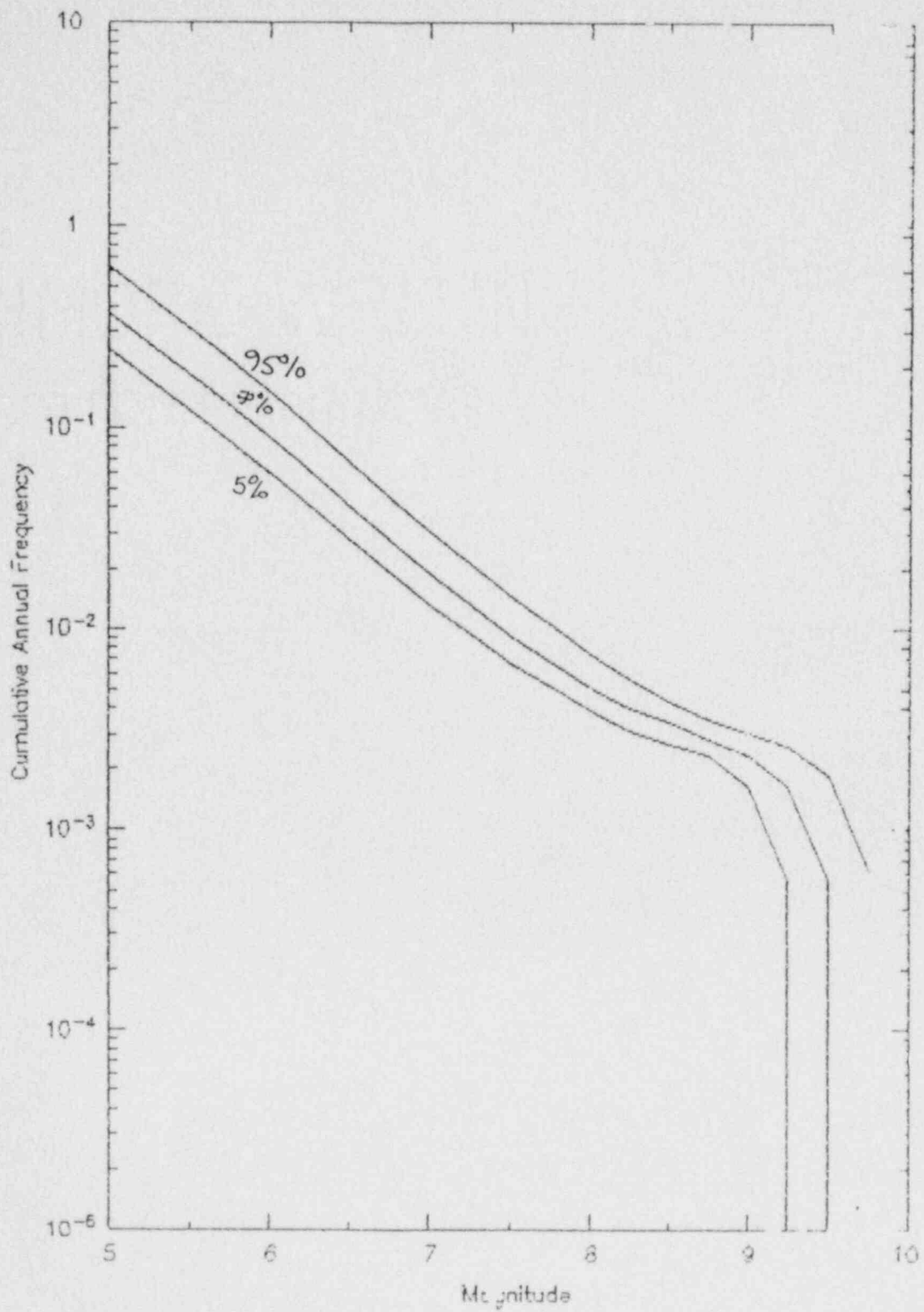


Figure 1 Estimated recurrence distribution for Expert 9



FIGURE 2 B-value - used for deep intraplate  
Deep Zone

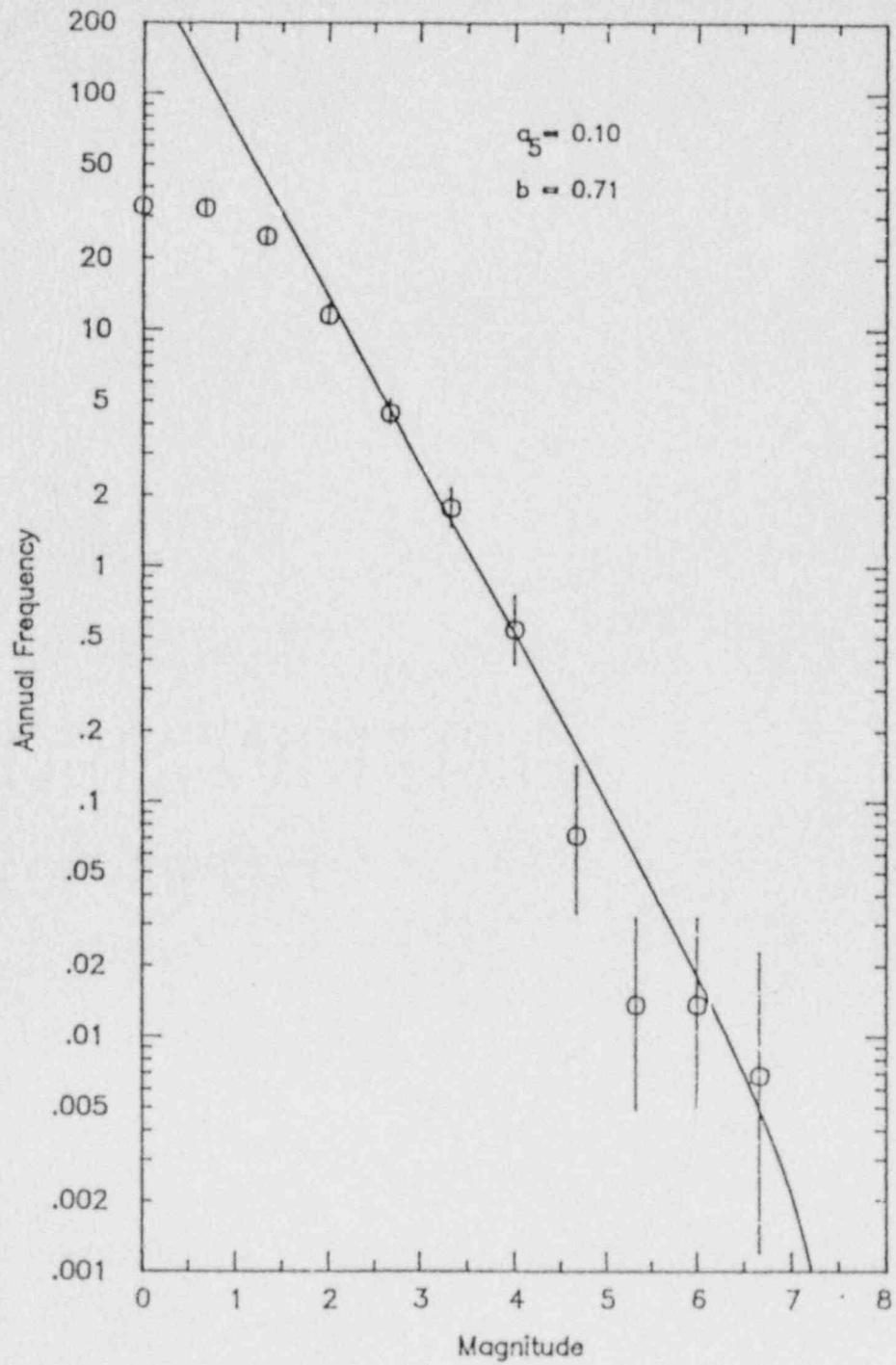
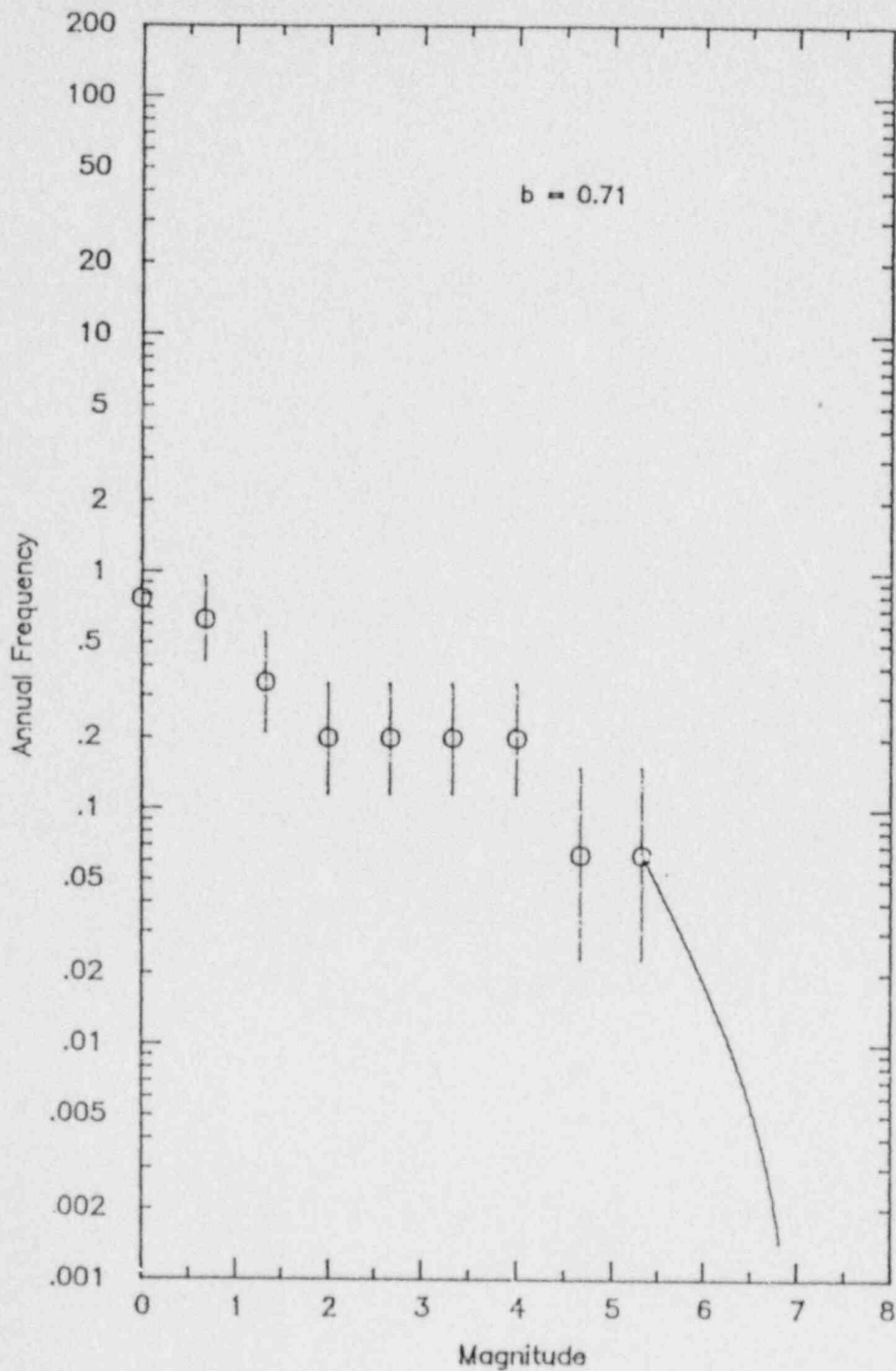


FIGURE 3 B-value - Off Shore used for shallow intraplate



Expert 10  
SUMMARY OF MODEL PARAMETERS

Slab geometry:

Approximately 10° dip through deep seismicity

Convergence rate:

35 - 50 mm/yr with the following distribution

	percent:	0	10	20	30	40	50
prob	mm/yr	+-----+	+-----+	+-----+	+-----+	+-----+	+-----+
0.25	35.00	*****					
0.25	40.00	*****					
0.25	45.00	*****					
0.25	50.00	*****					
prob	e	+-----+	+-----+	+-----+	+-----+	+-----+	+-----+

Sources and probability of activity:

Interface 0.7 (0.6-0.9)  
 Intraslab 1.0

Maximum extent of rupture on interface:

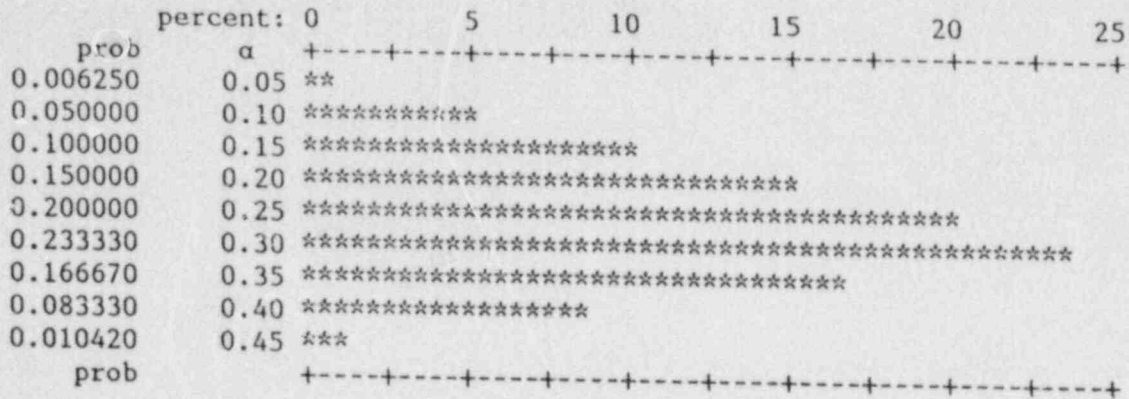
up dip - 125°W  
 down dip - 30 to 40 km depth  
 Along strike - Nootka to Blanco

Interface maximum magnitude:

Maximum rupture area - weight 0.5  
 rupture area 116000 -  $M_w$  9.25  
 Age versus convergence rate -  $w$  weight 0.5  
 $M_w$  8.3

Interface earthquake recurrence:

Use moment rate approach  
 moment rate = convergence rate \*  $\alpha$  \* interface area  
 Convergence rate specified above  
 $\alpha$  specified by following distribution



Use exponential magnitude distribution model

Figure 1 shows the resulting distribution of recurrence estimates and Figure 2 shows the effect of maximum magnitude on earthquake recurrence. The earthquake recurrence relationships shown in Figure 1 can be summarized in terms of return periods for events of various sizes as follows:

Magnitude M	Return Period (yrs) for events of Magnitude ≥ M		
	5th percentile	50th percentile	95 percentile
5	4	1	0.2
6	17	5	1
7	88	27	6
8	500	170	61
9	-	-	1930

Location of intraslab events:

- Large events occur in depth range 30 to 60 km
- Along strike - 0.5 weight to observed seismicity pattern
- 0.5 weight to uniform distribution

Intraslab Maximum Magnitude:

7.25 ±0.25

Intraslab earthquake recurrence:

Use historical seismicity. Figure 3 shows recurrence relationship for deep zone. This curve is based on all recorded events not inferred to lie within the North American plate.

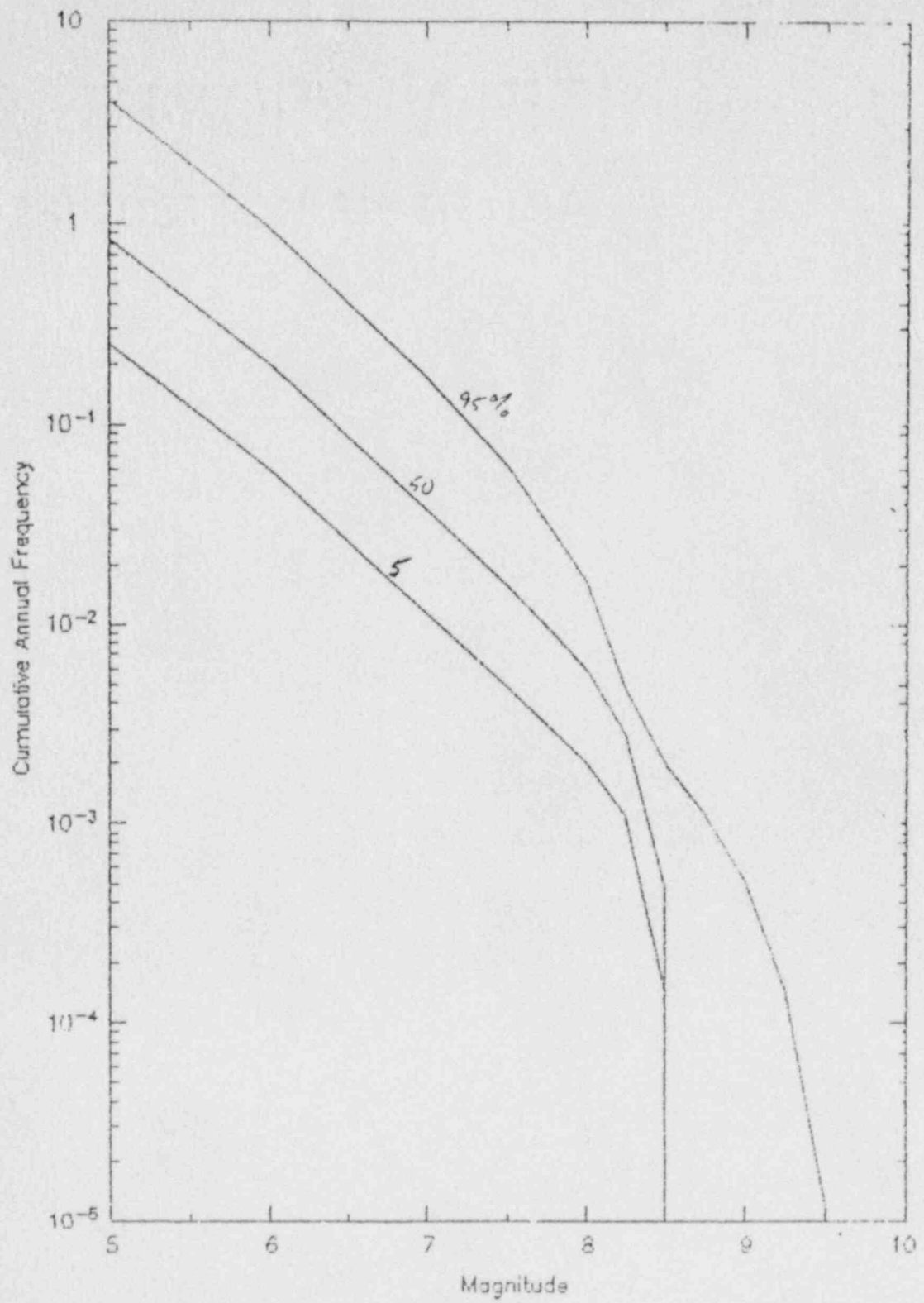


Figure 1 Estimated recurrence distribution for Expert 10

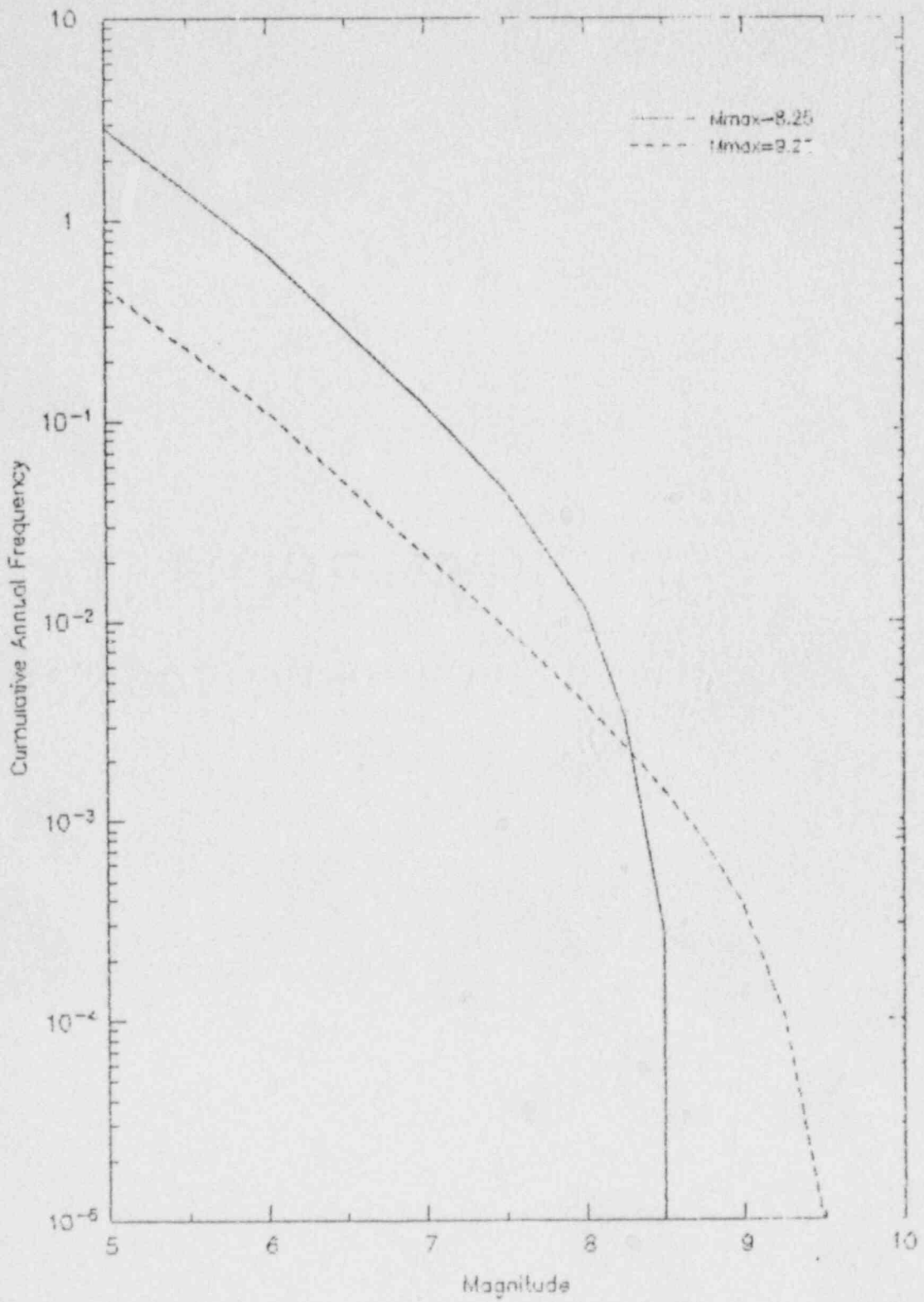
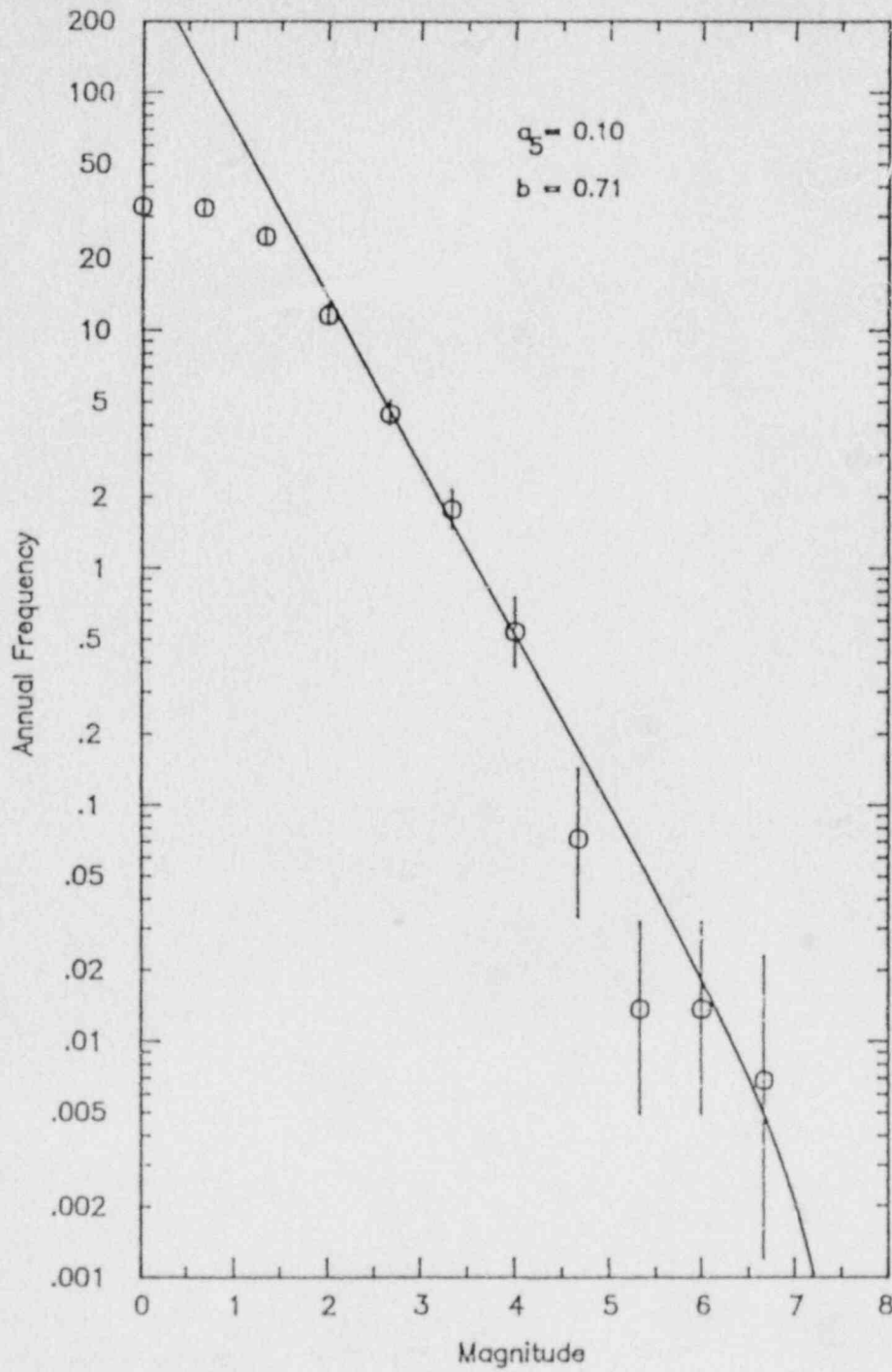


Figure 2 Effect of Maximum magnitude for Expert 10

FIGURE 3 B-value -  
Deep Zone



Expert 11  
SUMMARY OF MODEL PARAMETERS

Slab geometry:

Approximately 10° dip through deep seismicity

Convergence rate:

42 ±10 mm/yr with the following distribution

	percent: 0	10	20	30	40	50
prob	mm/yr	+---+---+---+---+---+---+---+				
0.05	30.00	*****				
0.30	35.00	*****				
0.30	40.00	*****				
0.30	45.00	*****				
0.05	50.00	*****				
prob		+---+---+---+---+---+---+---+				

Sources and probability of activity:

Interface 0.9 (0.8-1.0)

Intraslab 1.0

Maximum extent of rupture on interface:

up dip extent - top of continental slope

down dip extent - 123°W

Along strike - Entire Zone (0.09)

Nootka to Blanco (0.91)

Interface maximum magnitude:

Use maximum rupture area

Entire zone - rupture area 122400 -  $M_w$  9.25

Nootka - Blanco rupture area 81600 -  $M_w$  9

Interface earthquake recurrence:

Use geological estimate of 430 yrs (±25%)

Use characteristic magnitude distribution model

Figure 1 shows the resulting distribution of recurrence estimates. The earthquake recurrence relationships shown in Figure 1 can be summarized in terms of return periods for events of various sizes as follows:

Magnitude M	Return Period (yrs) for events of Magnitude ≥ M		
	5th percentile	50th percentile	95 percentile
5	5	4	3
6	19	15	11
7	85	68	51
8	284	227	177
9	670	533	400



Location of intraslab events:

Match observed seismicity pattern up/down dip and along strike. Large events in depth range 40 to 70 km.

Intraslab Maximum Magnitude:

Use following distribution

	percent:	0	10	20	30	40	50
prob	Mmax	+-----+-----+-----+-----+-----+-----+-----+-----+					
0.30	7.00	*****					
0.33	7.25	*****					
0.37	7.50	*****					
prob		+-----+-----+-----+-----+-----+-----+-----+-----+					

Intraslab earthquake recurrence:

Use historical seismicity. Figure 2 shows recurrence relationship for deep zone. This curve is based on all recorded events not inferred to lie within the North American plate.

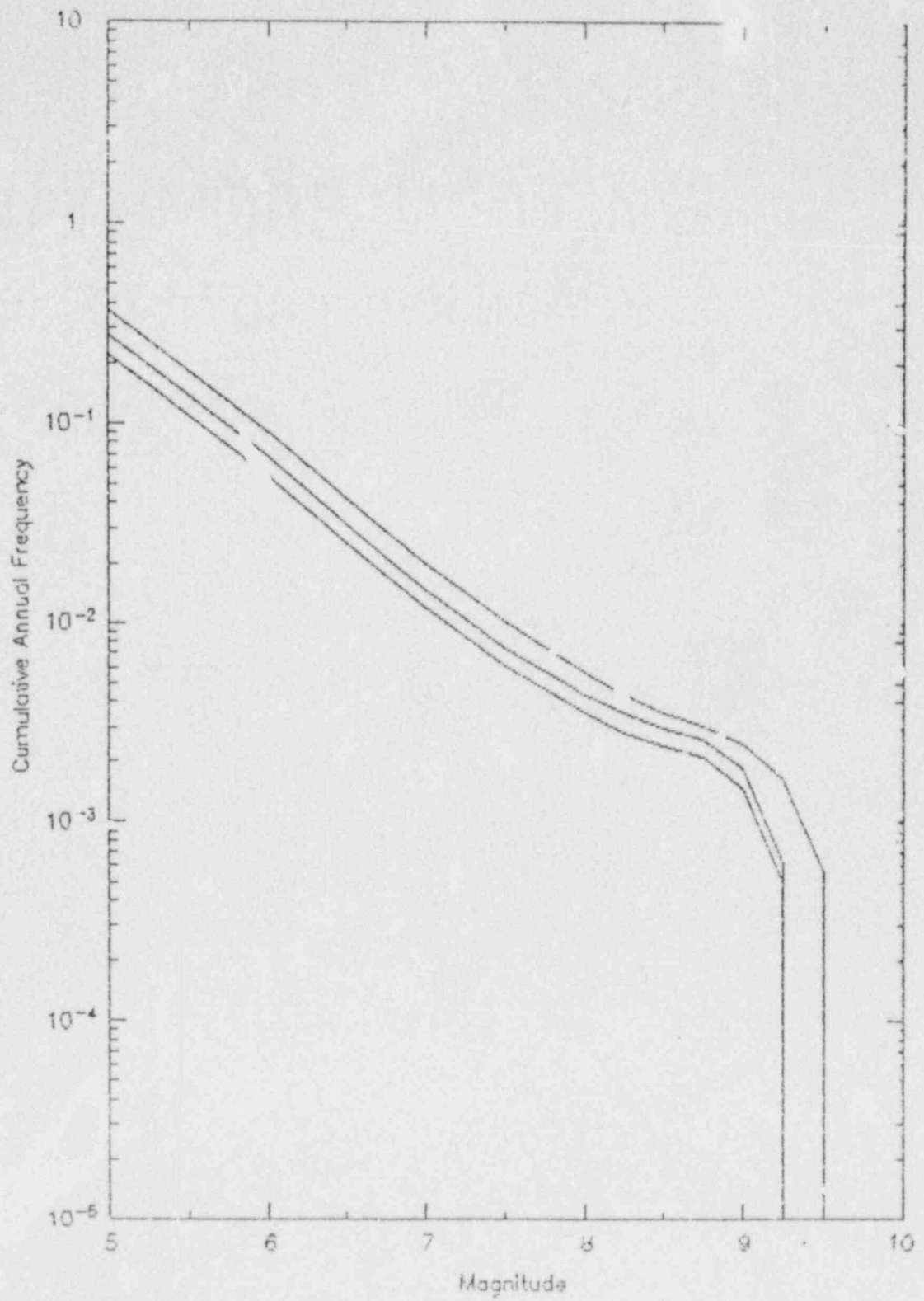
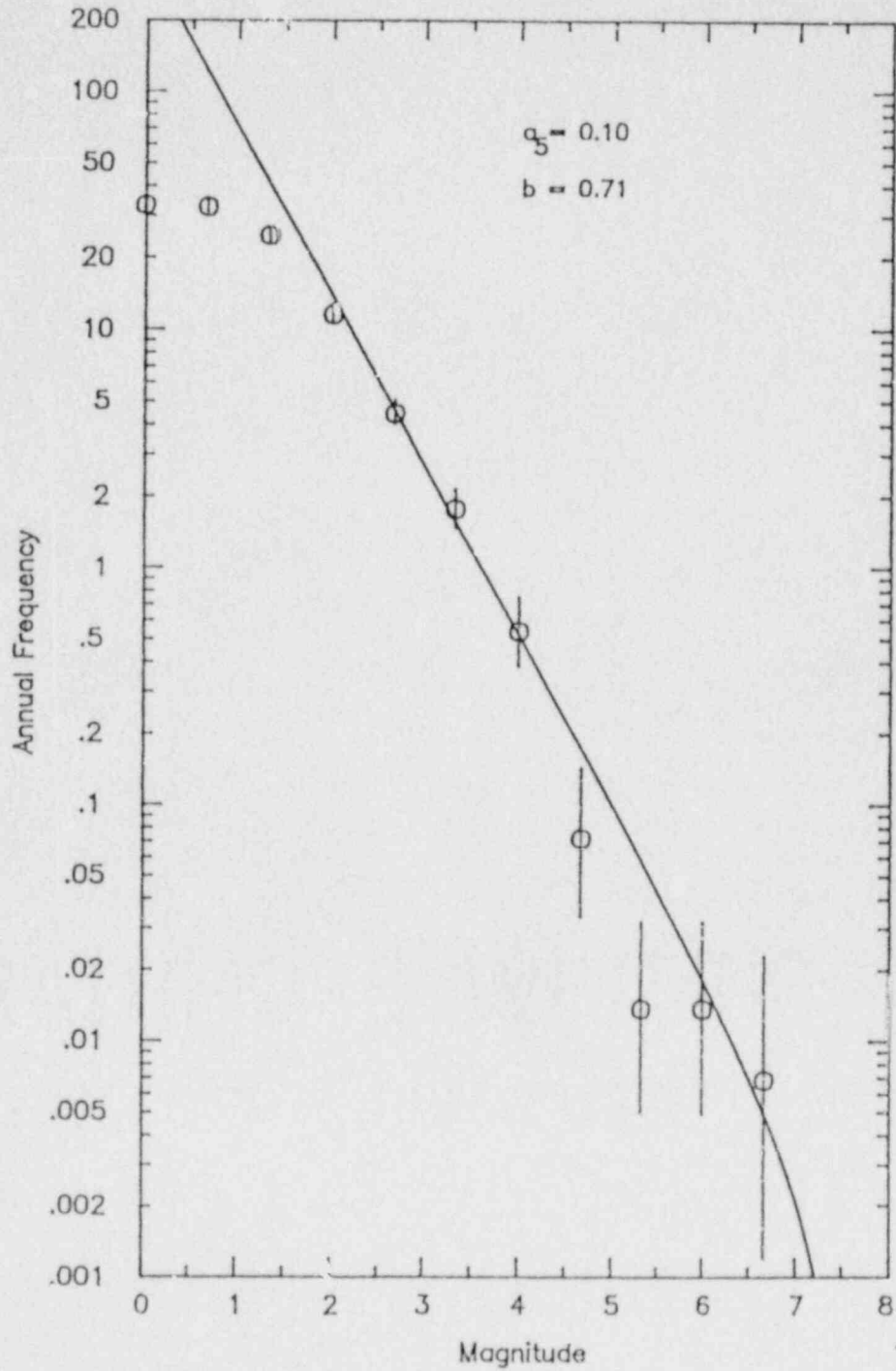


Figure 1 Estimated recurrence distribution for Expert 1.

FIGURE 2 B-value -  
Deep Zone



Expert 12  
SUMMARY OF MODEL PARAMETERS

Slab geometry:

Model A - approximately 10° dip through deep seismicity (0.80)

Model B - approximately 10° dip with reverse bend (0.20)

Convergence rate:

25 to 40 mm/yr with the following distribution

	percent:	0	10	20	30	40	50
prob	mm/yr	+-----+-----+-----+-----+-----+-----+-----+-----+					
0.200000	25.00	*****					
0.300000	30.00	*****					
0.300000	35.00	*****					
0.200000	40.00	*****					
prob		+-----+-----+-----+-----+-----+-----+-----+-----+					

Sources and probability of activity:

Interface 0.2 (0.1-0.4)

Intraslab 0.95-1.0

Maximum extent of rupture on interface:

Updip - eastern extent of underplating - 15 to 20 km depth (equal weight)

Downdip - 50 km depth

Along strike - Nootka to Blanco (0.7)

Nootka to Blanco segmented at tip of Vancouver I (0.3)

Interface maximum magnitude:

Not assessed - use AGGREGATE distribution

a) 0.55 weight assigned to estimate from maximum rupture area

Model A - unsegmented area 106400 to 124800 -  $M_w$  9.25

segmented area 86450 to 101400 -  $M_w$  9 to 9.25

Model B - unsegmented area 138400 to 161600 -  $M_w$  9.25

segmented area 112450 to 131300 -  $M_w$  9.25

b) 0.45 weight assigned to following distribution

	percent:	0	10	20	30	40	50
prob	$M_{max}$	+-----+-----+-----+-----+-----+-----+-----+-----+					
0.073333	7.50	*****					
0.073333	7.75	*****					
0.073333	8.00	*****					
0.390000	8.25	*****					
0.098333	8.50	*****					
0.083333	8.75	*****					
0.083333	9.00	*****					
0.083333	9.25	*****					
0.041667	9.50	*****					
prob		+-----+-----+-----+-----+-----+-----+-----+-----+					

Combining a) and b) the distribution over all maximum rupture geometries is

	percent:	0	20	40	60	80	100
prob	Mmax	+-----+-----+-----+-----+-----+-----+-----+					
0.033000	7.50	***					
0.033000	7.75	***					
0.033000	8.00	***					
0.175500	8.25	*****					
0.044250	8.50	***					
0.037500	8.75	***					
0.103500	9.00	*****					
0.521500	9.25	*****					
prob	Mmax	+-----+-----+-----+-----+-----+-----+-----+					

Interface earthquake recurrence:

Use moment rate approach

moment: rate = convergence rate \*  $\alpha$  \* interface area

Assessed distribution for convergence rate mm/yr is give above

assessed distribution for alpha

	percent:	0	20	40	60	80	100
prob	$\alpha$	+-----+-----+-----+-----+-----+-----+-----+					
0.100000	0.05	*****					
0.600000	0.10	*****					
0.127550	0.15	*****					
0.048980	0.20	***					
0.040820	0.25	***					
0.032650	0.30	***					
0.024490	0.35	**					
0.016330	0.40	**					
0.008160	0.45	*					
0.001020	0.50	*					
prob		+-----+-----+-----+-----+-----+-----+-----+					

Magnitude distribution model not assessed - use AGGREGATE  
 assessment of the experts  
 exponential (0.23)  
 characteristic (0.41)  
 maximum moment (0.36)

Figure 1 shows the resulting distribution of recurrence estimates, Figure 2 shows the effect of variation in maximum magnitude on recurrence estimated using the moment rate approach, Figure 3 shows the effect of choice of magnitude distribution model on recurrence estimates, and Figure 4 shows the effect of slab geometry on the recurrence estimates.

The earthquake recurrence relationships shown in Figure 1 can be summarized in terms of return periods for events of various sizes as follows:

Magnitude M	Return Period (yrs) for events of Magnitude $\geq$ M		
	5th percentile	50th percentile	95 percentile
5	10000	42	1
6	10000	148	5
7	10000	427	17
8	-	1950	170
9	-	10500	3160

Location of intraslab events:

Updip, downdip extent, and along strike  
 0.95 weight - match observed seismicity pattern  
 0.05 weight - uniform

Intraslab Maximum Magnitude:

Not assessed - use AGGREGATE assessment of other experts

prob	Mmax	percent: 0	10	20	30	40	50
0.041	6.50	*****					
0.030	6.75	****					
0.355	7.00	*****	*****	*****	*****	*****	*****
0.219	7.25	*****	*****	*****	*****	*****	*****
0.345	7.50	*****	*****	*****	*****	*****	*****
0.000	7.75	*					
0.010	8.00	**					
prob		+-----+	+-----+	+-----+	+-----+	+-----+	+-----+

Intraslab earthquake recurrence:

Use historical seismicity. Figure 5 shows recurrence relationship for deep earthquakes assumed to be occurring within downgoing slab. This curve is based on all recorded events not inferred to lie within the North American plate.

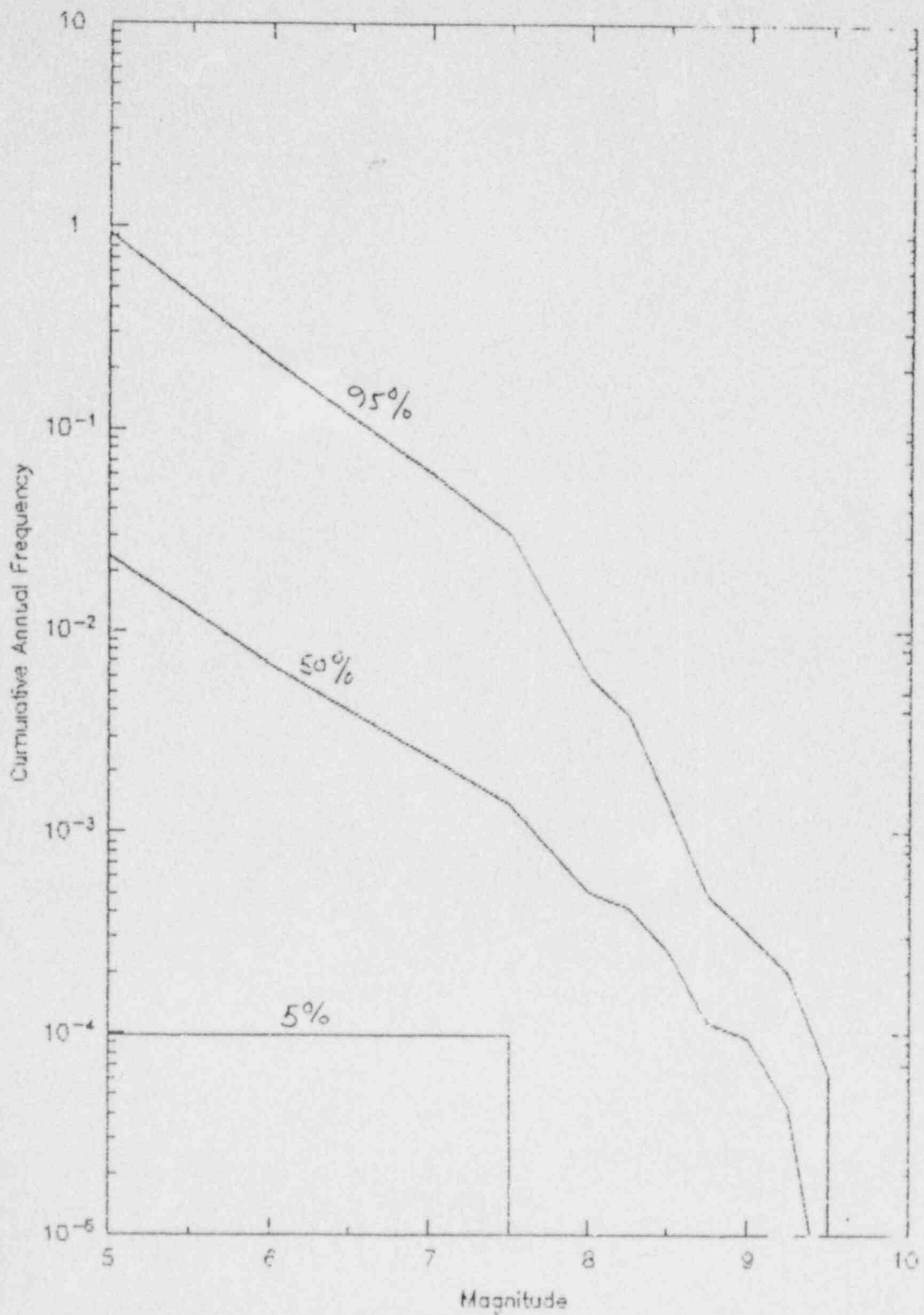


Figure 1 Estimated recurrence distribution for Expert 12

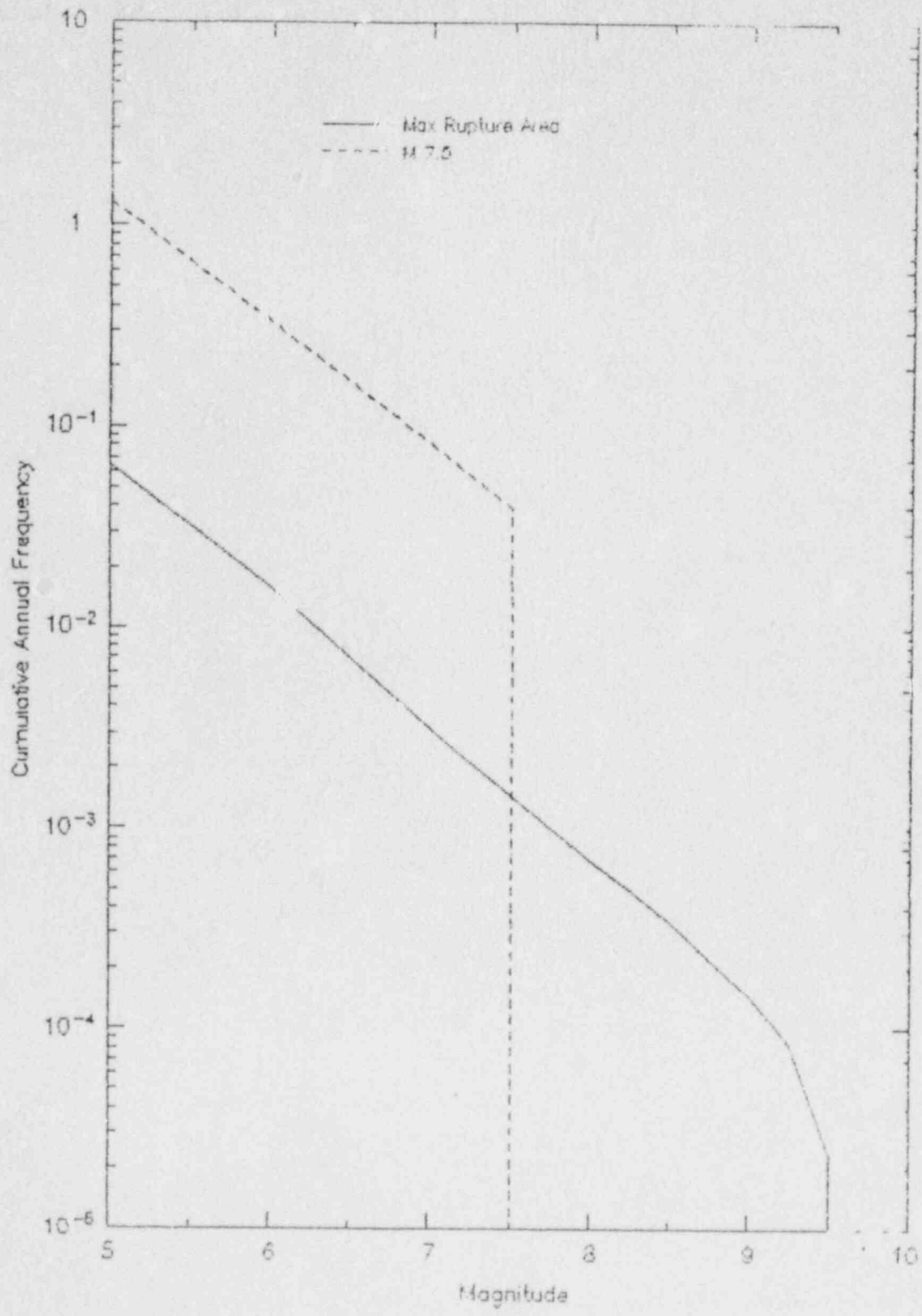


Figure 2 Effect of Max Magnitude for Expert 12



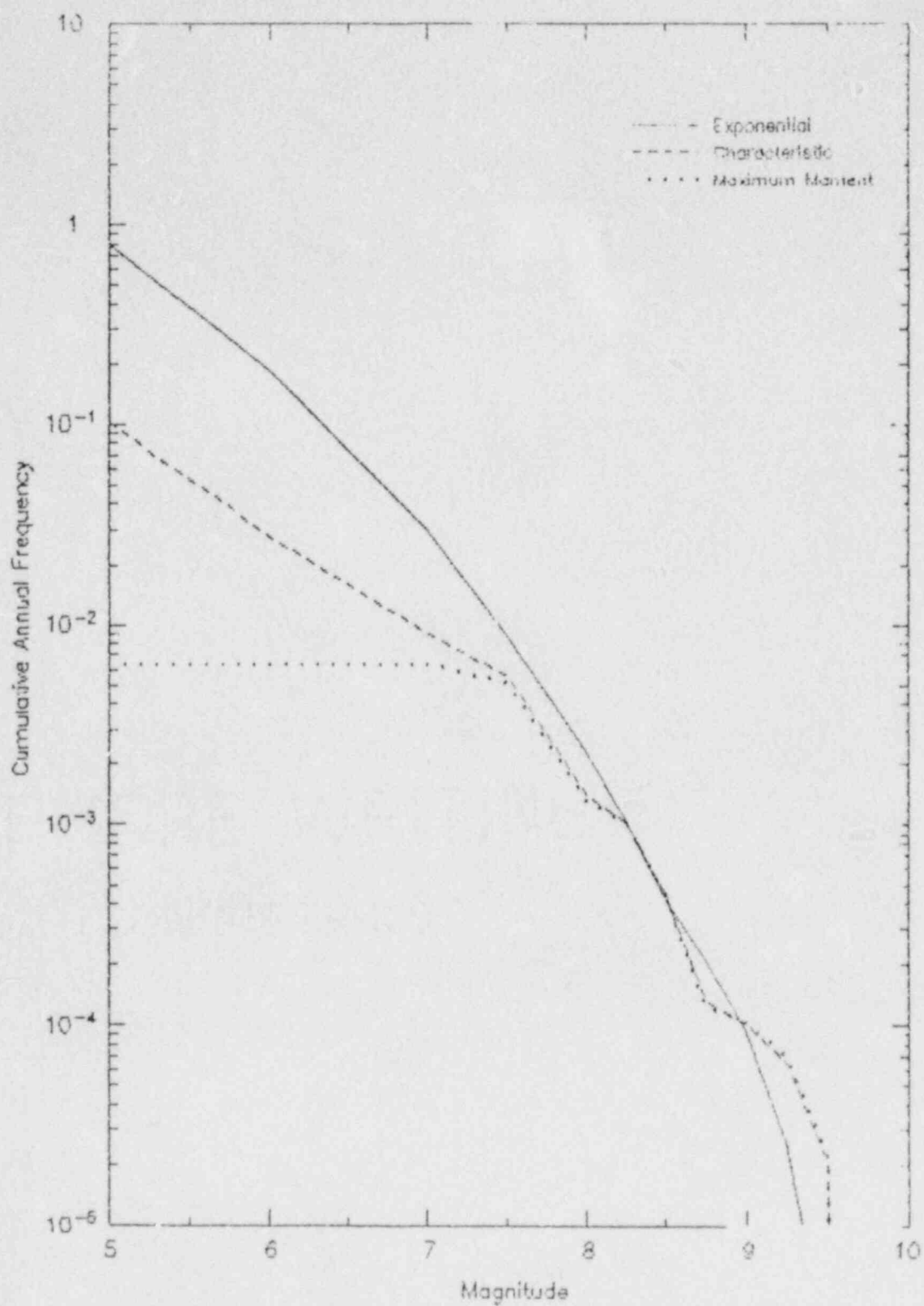


Figure 3 Effect of magnitude distribution model for Expert 12

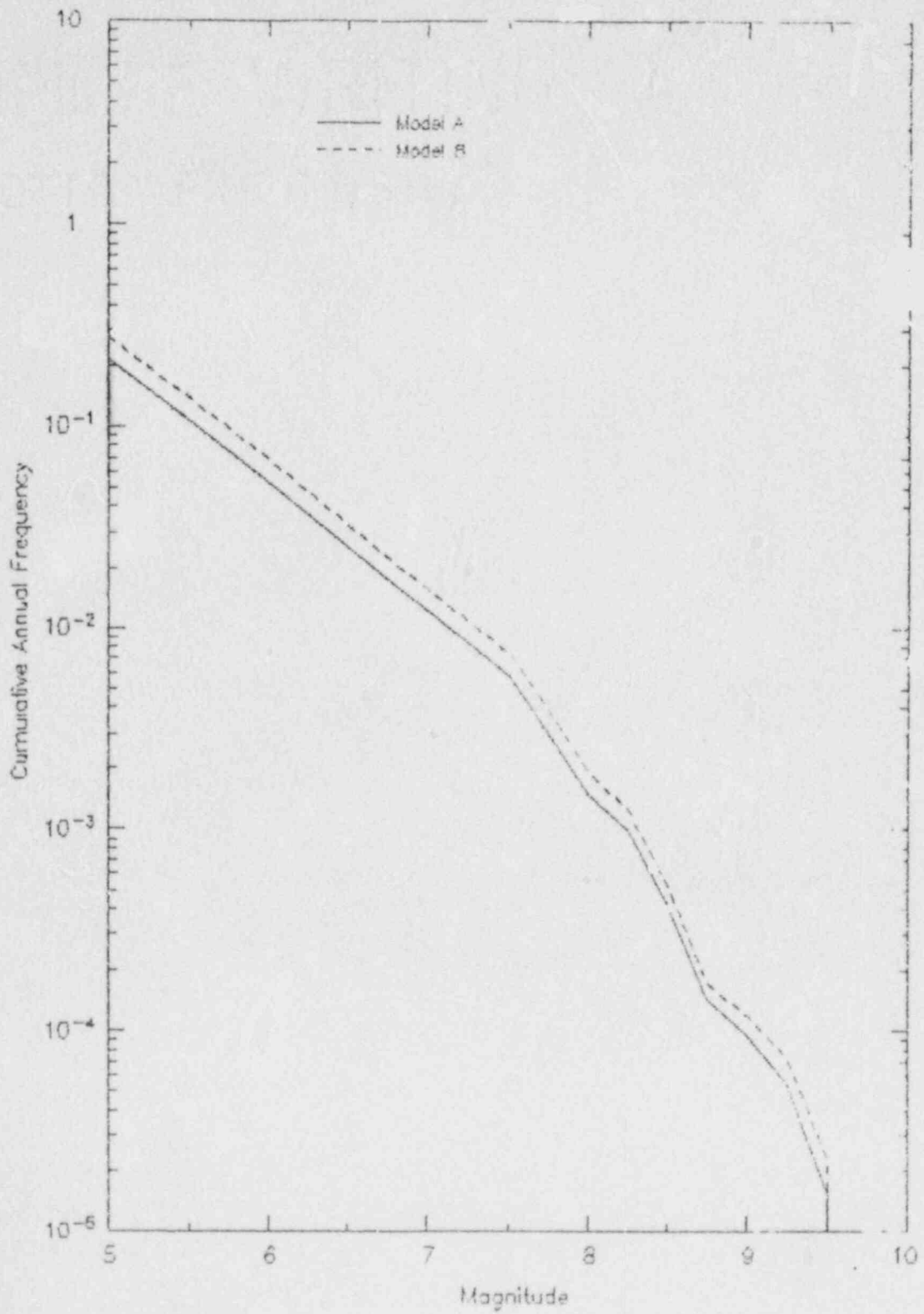
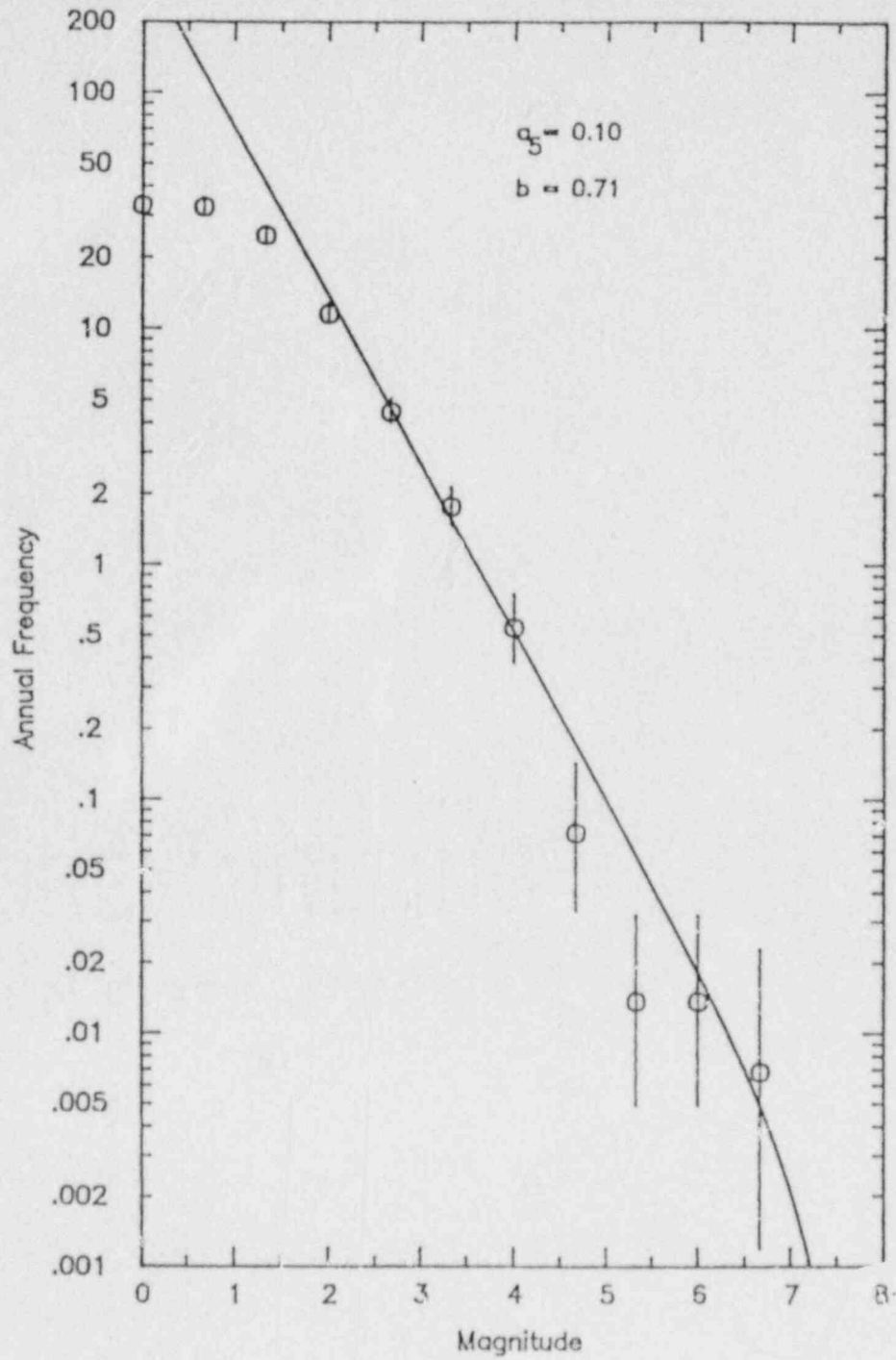


Figure 4 Effect of slrb geometry for Expert 12.

FIGURE 5 B-value -  
Deep Zone



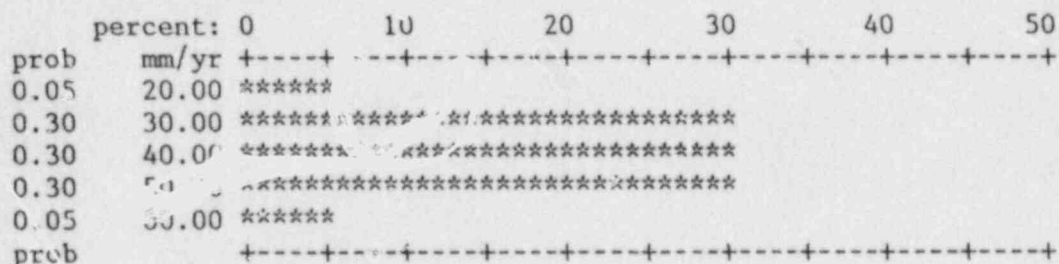
Expert 13  
SUMMARY OF MODEL PARAMETERS

Slab geometry:

Approximately 10° dip through deep seismicity

Convergence rate:

Following distribution assessed



Sources and probability of activity:

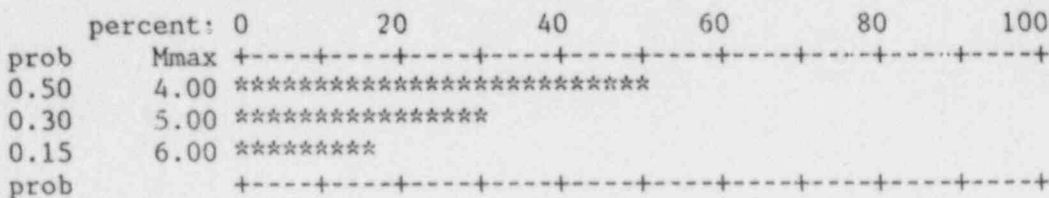
Interface 0.05 (±0.05) renormalized to 0.0075 for events > M 5.0  
 Intraslab 0.8 (±0.1)

Maximum extent of rupture on interface:

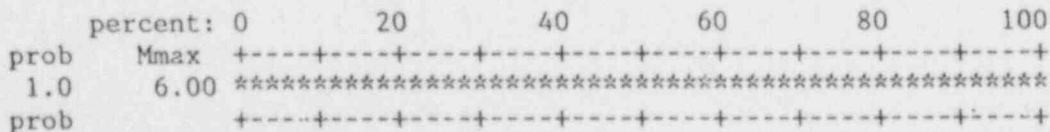
Updip - 15 to 20 km depth  
 Downdip - 40 to 50 km depth  
 Along strike - Nootka to Blanco

Interface maximum magnitude:

Assessed distribution



Renormalized distribution for events > mag 5



Interface earthquake recurrence:

Not assessed - use moment rate approach as Mmax to small to produce geological evidence

moment rate = convergence rate \*  $\alpha$  \* interface area

Assessed distribution for convergence rate mm/yr is give above  
alpha assessed as follows

	percent:	0	10	20	30	40	50
prob	$\alpha$	+-----+-----+-----+-----+-----+-----+					
0.30	0.001	*****					
0.40	0.050	*****					
0.30	0.100	*****					
prob		+-----+-----+-----+-----+-----+-----+					

Magnitude distribution model not assessed - use AGGREGATE assessment  
of the experts

- exponential (0.23)
- characteristic (0.41)
- maximum moment (0.36)

Figure 1 shows the resulting distribution of recurrence estimates, Figure 2 shows the effect of variation in magnitude distribution model on recurrence estimated using the moment rate approach.

The earthquake recurrence relationships shown in Figure 1 can be summarized in terms of return periods for events of various sizes as follows:

Magnitude M	Return Period (yrs) for events of Magnitude $\geq$ M		
	5th percentile	50th percentile	95 percentile
5	1	0.1	0.02
6	3	0.4	0.1
7	-	-	-

Location of intraslab events:

Use observed seismicity pattern, 90% of large events in 50 to 90 km depth range

Intraslab Maximum Magnitude:

Assessed distribution as follows:

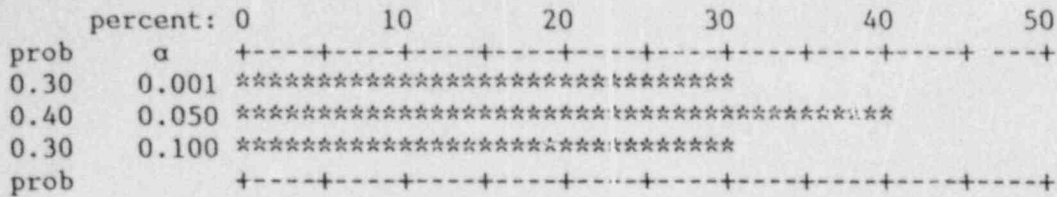
	percent:	0	10	20	30	40	50
prob	Mmax	+-----+-----+-----+-----+-----+-----+					
0.45	6.50	*****					
0.40	7.00	*****					
0.14	7.50	*****					
0.01	8.00	**					
prob		+-----+-----+-----+-----+-----+-----+					

Intraslab earthquake recurrence:

Use historical seismicity. Figure 3 shows recurrence relationship for deep earthquakes assumed to be occurring within downgoing slab. This curve is based on all recorded events not inferred to lie within the North American plate.



Assessed distribution for convergence rate mm/yr is give above  
alpha assessed as follows



Magnitude distribution model not assessed - use AGGREGATE assessment  
of the experts

- exponential (0.23)
- characteristic (0.41)
- maximum moment (0.36)

Figure 1 shows the resulting distribution of recurrence estimates, Figure 2 shows the effect of variation in magnitude distribution model on recurrence estimated using the moment rate approach.

The earthquake recurrence relationships shown in Figure 1 can be summarized in terms of return periods for events of various sizes as follows:

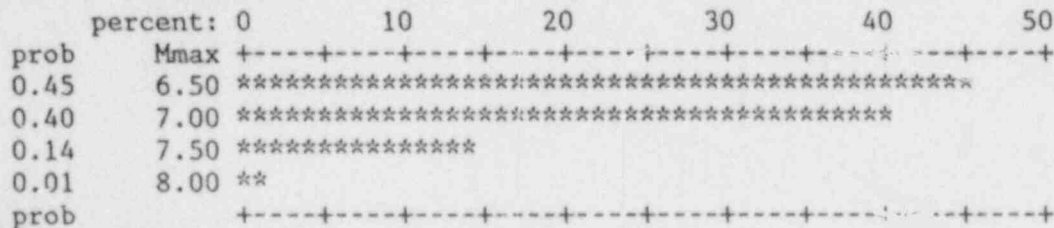
Magnitude M	Return Period (yrs) for events of Magnitude ≥ M		
	5th percentile	50th percentile	95 percentile
5	1	0.1	0.02
6	3	0.4	0.1
7	-	-	-

Location of intraslab events:

Use observed seismicity pattern, 90% of large events in 50 to 90 km depth range

Intraslab Maximum Magnitude:

Assessed distribution as follows:



Intraslab earthquake recurrence:

Use historical seismicity. Figure 3 shows recurrence relationship for deep earthquakes assumed to be occurring within downgoing slab. This curve is based on all recorded events not inferred to lie within the North American plate.

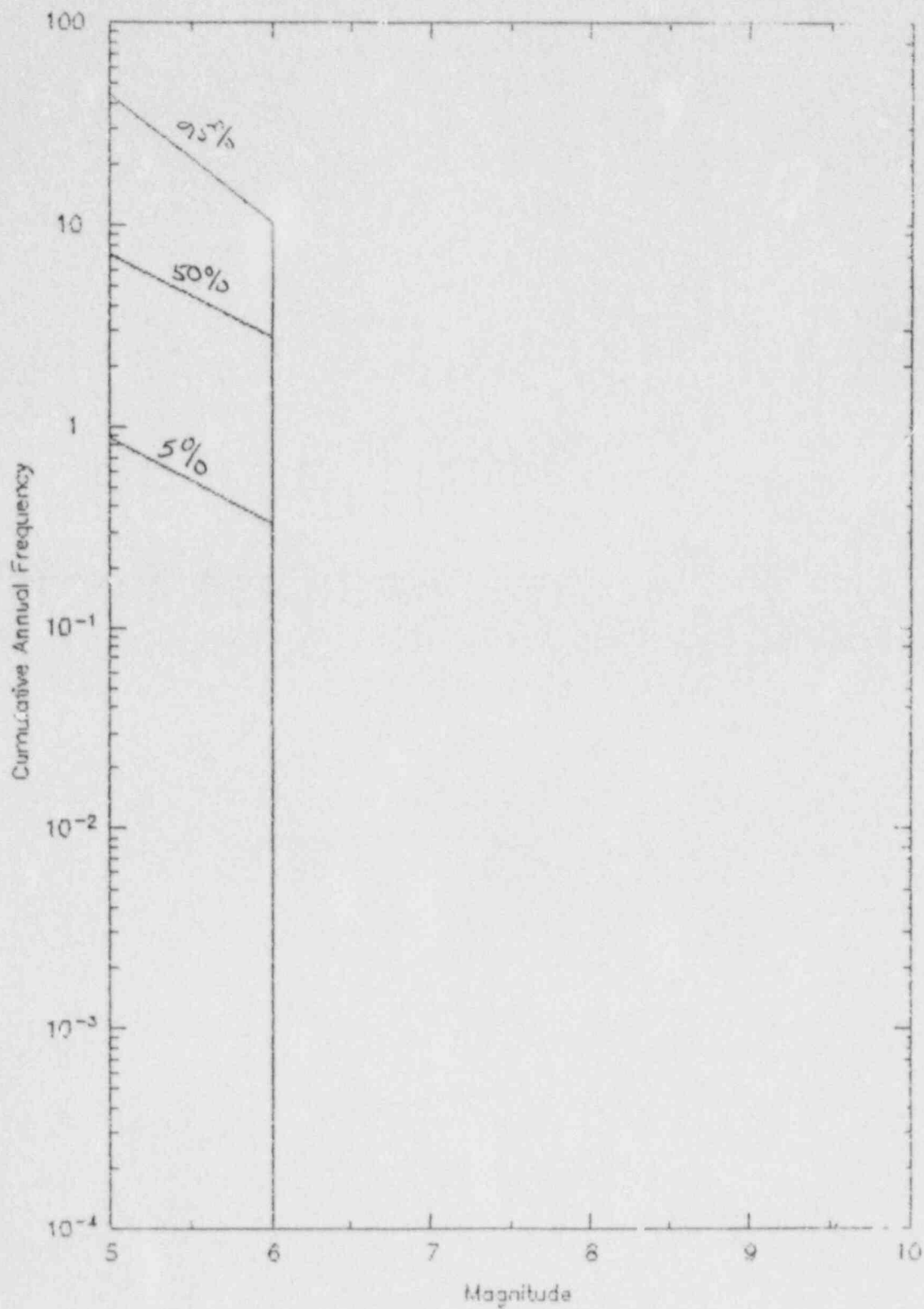


Figure 1 Estimated recurrence distribution for Expert 13

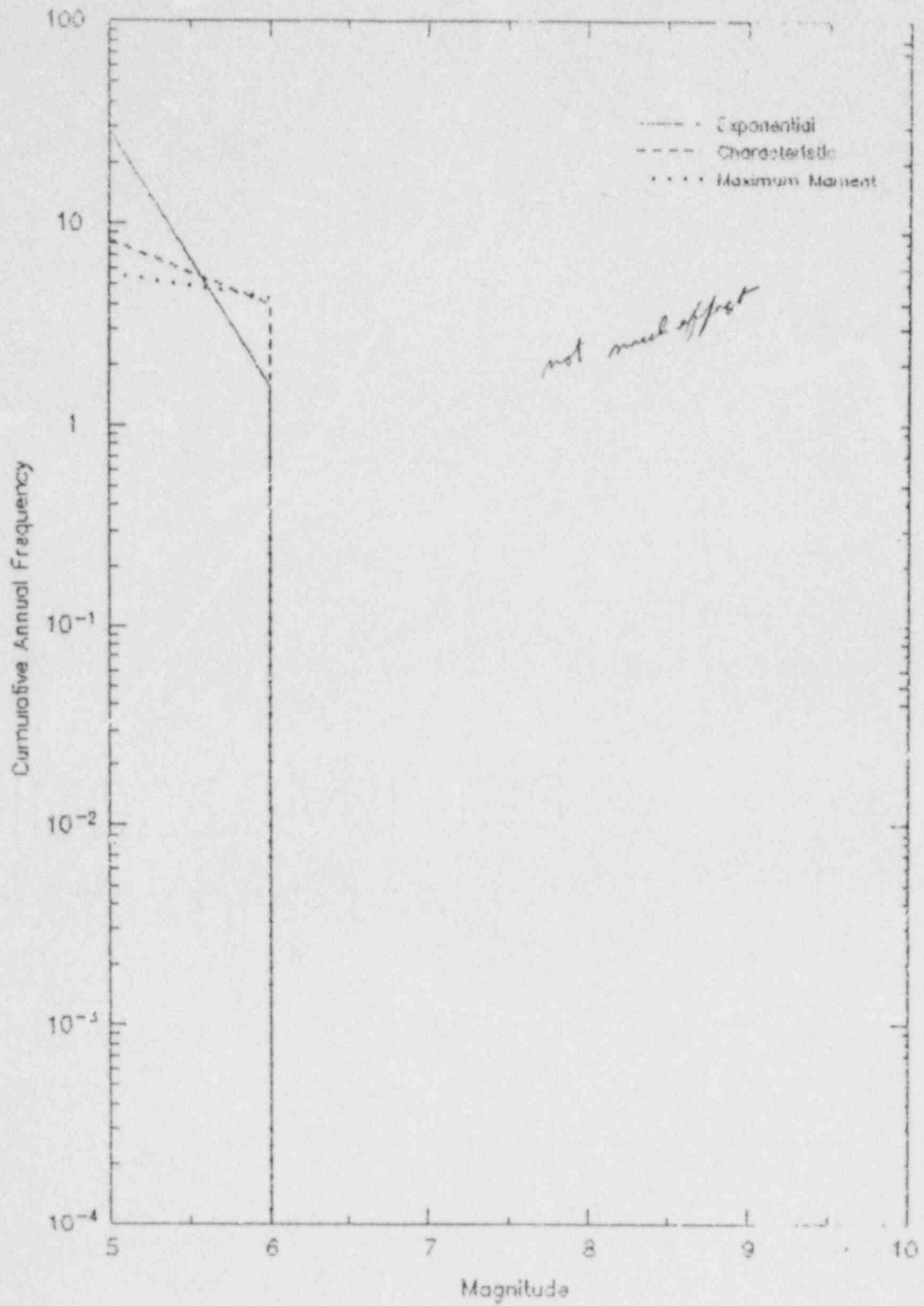
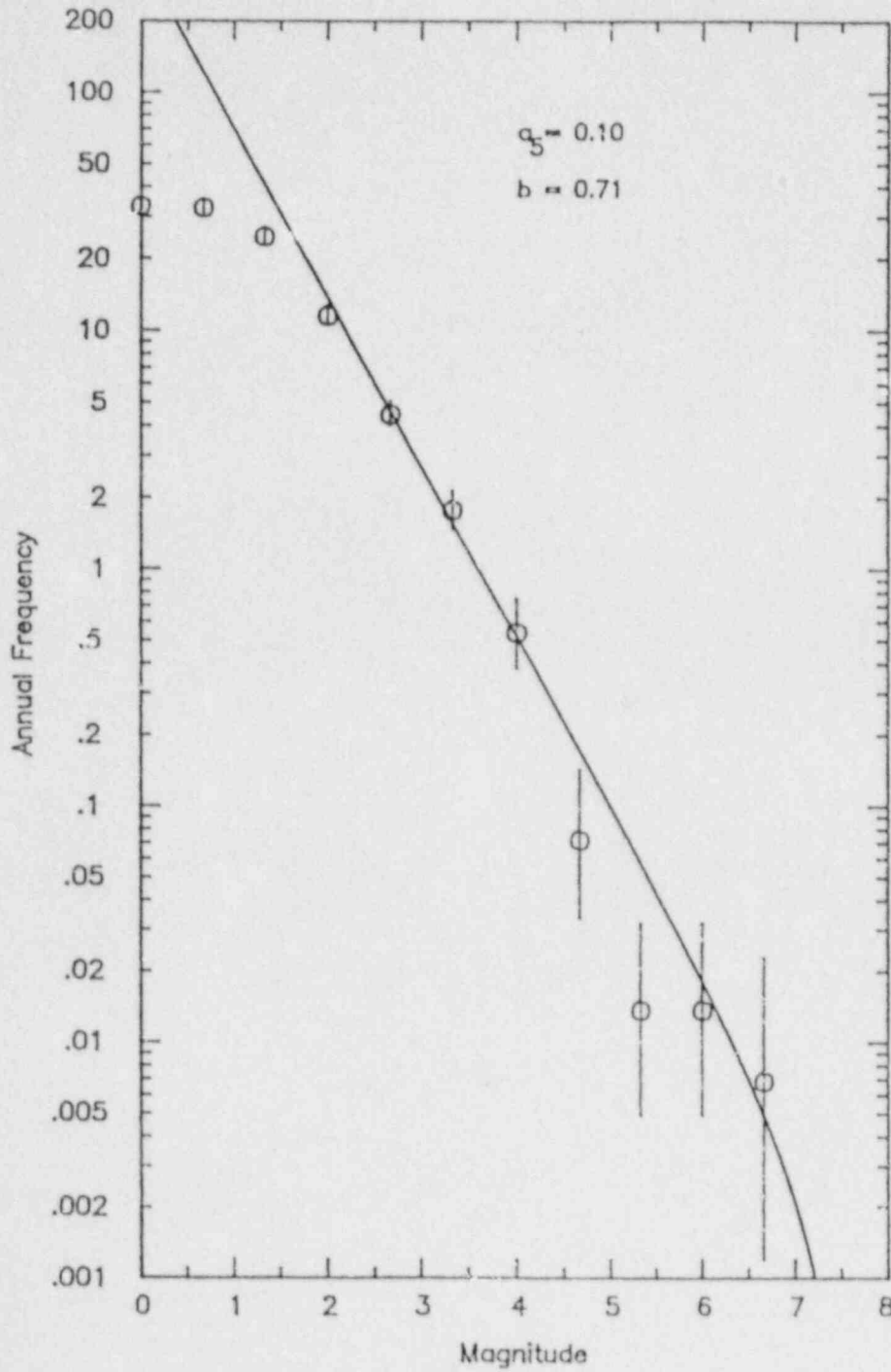


Figure 2 Effect of magnitude distribution model for Expert 13



FIGURE 3 B-value -  
Deep Zone



Expert 14  
SUMMARY OF MODEL PARAMETERS

Slab Geometry:

Two dips:           Model A - 9° to 10° (0.35)  
                           Model B - 20 to 25° (0.65)

Convergence rate:

The assessed distribution for convergence rate mm/yr is

	percent:	0	5	10	15	20	25
prob	mm/yr	+-----+-----+-----+-----+-----+-----+-----+					
0.012500	10.00	****					
0.025000	15.00	*****					
0.062500	20.00	*****	*****				
0.100000	25.00	*****	*****	*****			
0.150000	30.00	*****	*****	*****	*****		
0.200000	35.00	*****	*****	*****	*****	*****	
0.175000	40.00	*****	*****	*****	*****	*****	
0.150000	45.00	*****	*****	*****	*****	*****	
0.100000	50.00	*****	*****	*****	*****	*****	
0.025000	55.00	*****					
prob		+-----+-----+-----+-----+-----+-----+					

Sources and probability of activity:

Model A - Interface 0.35 ( $\pm 0.15$ )  
                   Intraslab 1.0

Model B - Shallow Interface 0.25 ( $\pm 0.15$ )  
                   Deep Interface 0.3 ( $\pm 0.1$ )  
                   Intraslab (Juan de Fuca) 0.1  
                   "deep zone" beneath Puget Sound 1.0

Maximum extent of rupture on interface:

Model A - Updip at 125°  
                   Downdip at depth of 50 km  
                   Along strike - Nootka to Blanco (0.8)  
   Nootka to Blanco segmented at 47°N (0.2)

Model B - Updip at 125° both interfaces  
                   Downdip at depth of 50 km both interfaces  
                   Along strike - Nootka to Blanco (0.8)  
   Nootka to Blanco segmented at 47°N (0.2)  
                   shallow interface exists only north of 47°N

Interface Maximum Magnitude:

Shallow interface - 8 ( $\pm 0.25$ ) Model A, 7.25 ( $\pm 0.25$ ) Model B resulting  
                   in following distribution

	percent:	0	10	20	30	40	50
prob	Mmax	+-----+-----+-----+-----+-----+-----+-----+-----+					
0.214500	7.00	*****					
0.221000	7.25	*****					
0.291500	7.50	*****					
0.077000	7.75	*****					
0.077000	8.00	*****					
0.059500	8.25	*****					
0.059500	8.50	*****					
prob		+-----+-----+-----+-----+-----+-----+-----+-----+					

Deep interface - 8 (±0.25) Model B resulting in following distribution

	percent:	0	5	10	15	20	25
prob	Mmax	+-----+-----+-----+-----+-----+-----+-----+					
0.220000	7.50	*****					
0.220000	7.75	*****					
0.220000	8.00	*****					
0.170000	8.25	*****					
0.170000	8.50	*****					
prob		+-----+-----+-----+-----+-----+-----+-----+					

Interface Earthquake Recurrence:

Use moment rate approach with:

moment rate = convergence rate\* $\alpha$ \*interface area  
 $\alpha$  assessed according to following distribution

	percent:	0	20	40	60	80	100
prob	$\alpha$	+-----+-----+-----+-----+-----+-----+-----+					
0.200000	0.05	*****					
0.600000	0.10	*****					
0.200000	0.15	*****					
prob		+-----+-----+-----+-----+-----+-----+-----+					

Use "maximum moment" magnitude distribution

Attached Figure 1 shows the resulting distribution of recurrence estimates for interface events. Maximum event magnitude is assumed to be uniformly distributed in the range of the expected maximum magnitude given above ± 0.25 magnitude units. Figure 2 shows the effect of choice of maximum magnitude on recurrence estimates and Figure 3 shows the differences between Model A and Model B.

The recurrence estimates shown in Figure 1 can be summarized in terms of return period for various size events as follows

Magnitude M	Return Period (yrs) for events of Magnitude $\geq$ M		
	5th percentile	50th percentile	95 percentile
5	260	33	8
6	260	33	8
7	260	34	8
8	-	427	60

Location of intraslab events:

Model A - between 122°W and 124°W

Model B - "deep zone" between 122°W and 124°W

Along strike - match observed relative frequency  
for Model B "deep zone" exists only north of 47°N

Intraslab Maximum Magnitude:

Model A and "deep zone" for Model B - 7.25 to 7.5

Model B - not assessed

Intraslab Earthquake Recurrence:

Historical seismicity used to compute a- and b-values for exponential model. For intraslab events in Model B the seismicity rate was estimated from offshore events within the Juan de Fuca plate away from the spreading centers and fracture zones. Figure 4 shows the recurrence relationship used for the intraslab events in Model A and the deep zone in Model B. This curve is based on all recorded events not inferred to lie within the North American plate. Figure 5 shows the recurrence relationship for the offshore Juan de Fuca plate used to model the intraslab recurrence for Model B.

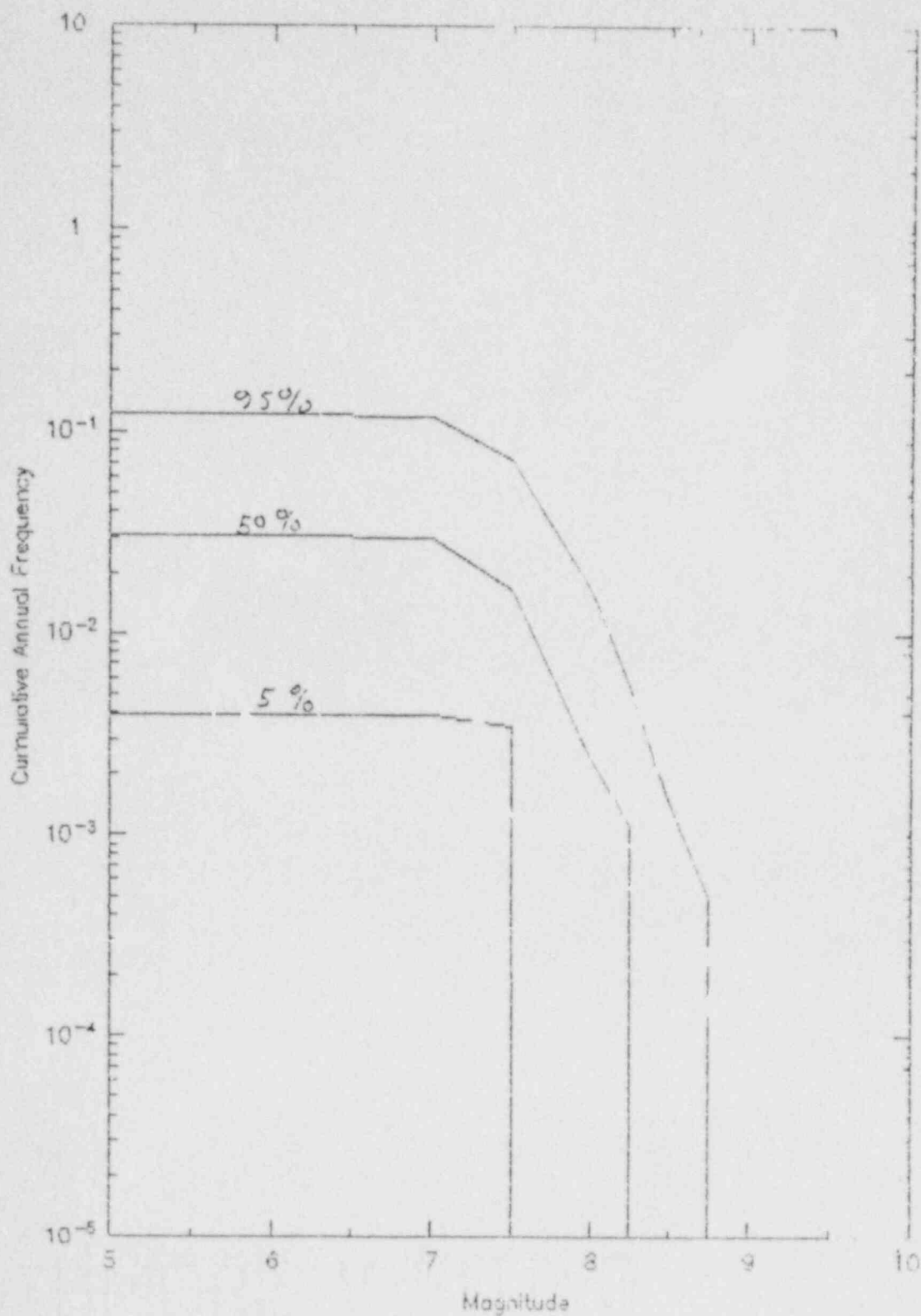


Figure 1 Estimated recurrence distribution for Expert 14

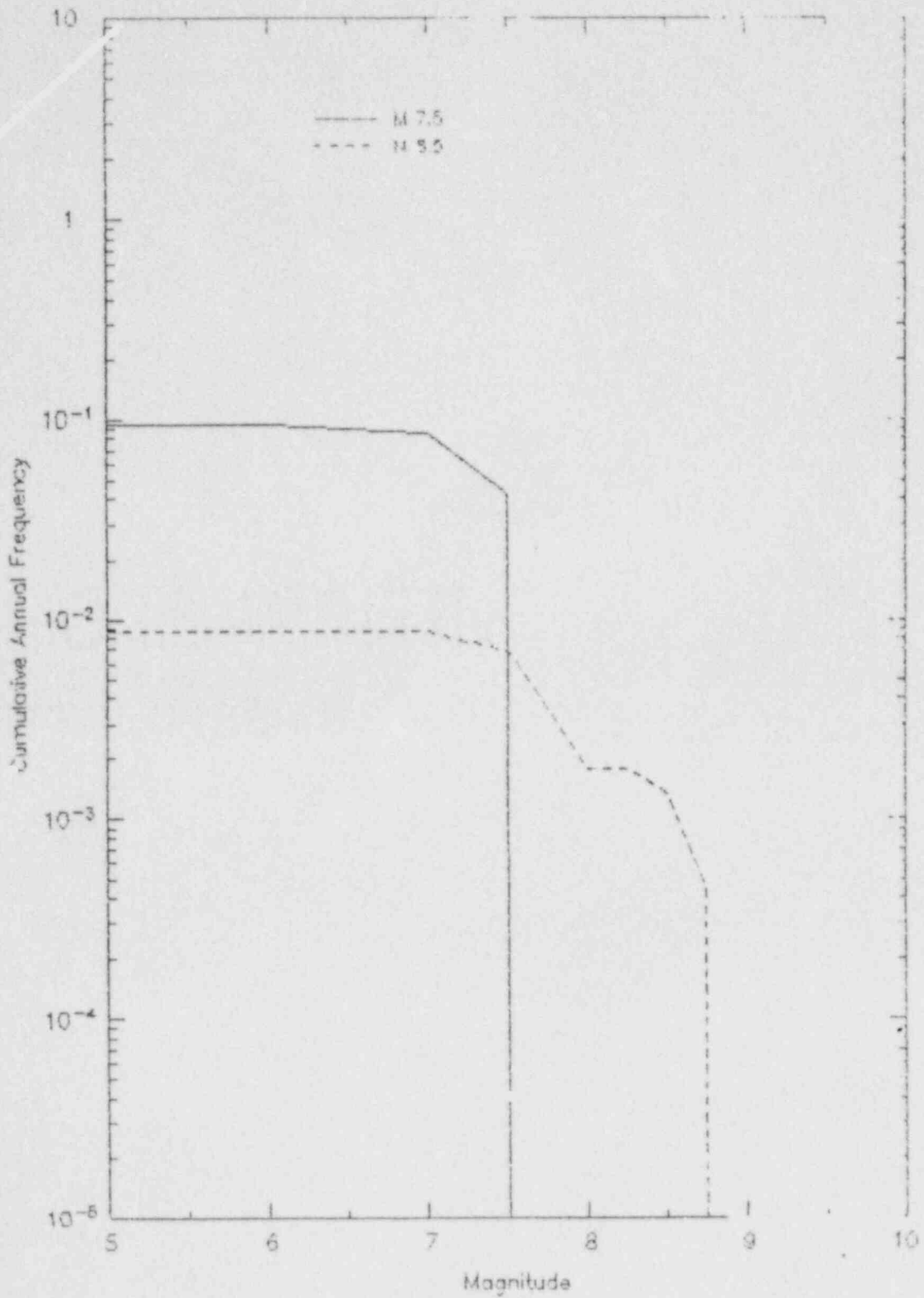


Figure 2 Effect of Max Magnitude for Expert 14

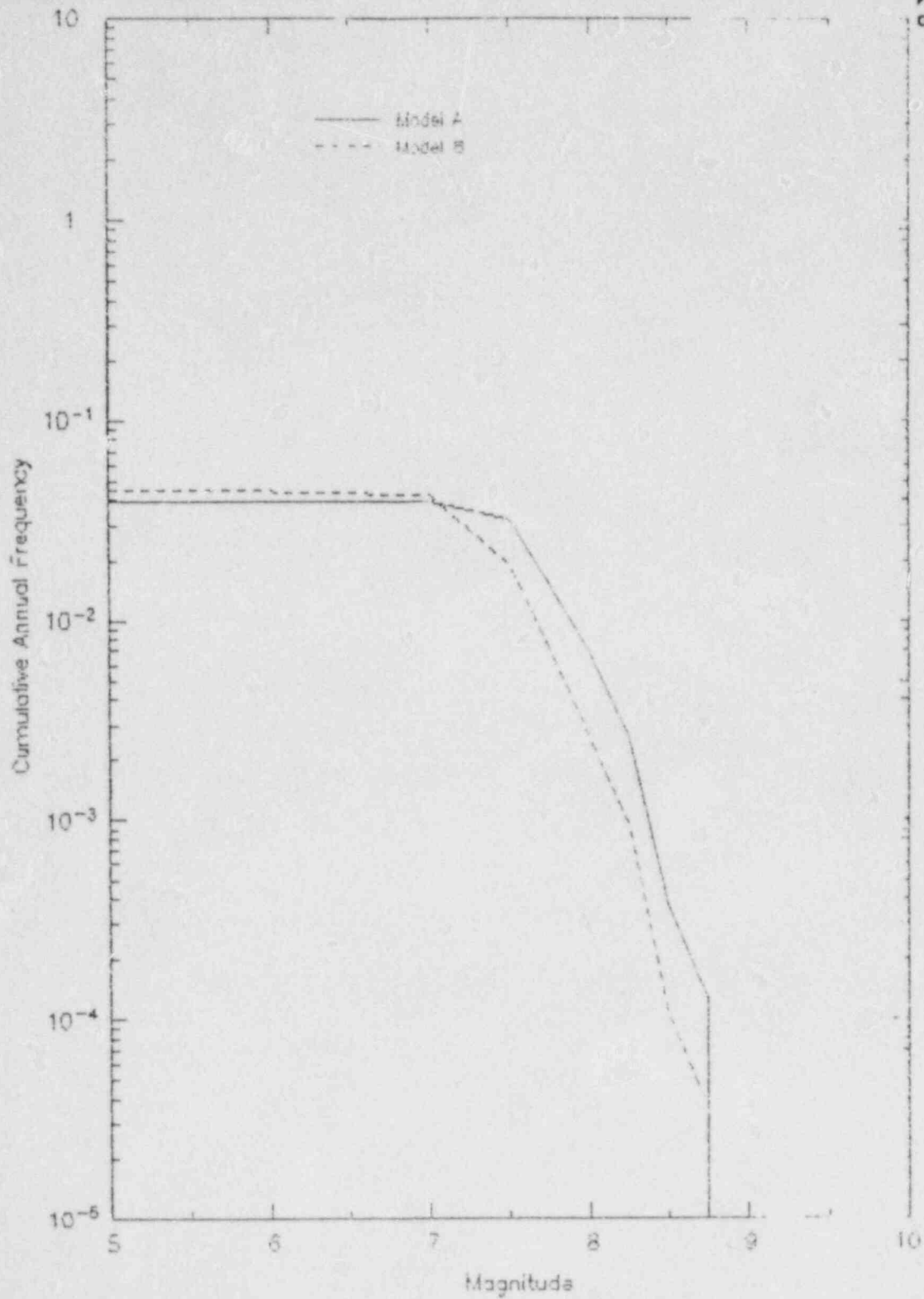


Figure 3 Effect of slab geometry for Expert 14

FIGURE 4 B-value -  
Deep Zone

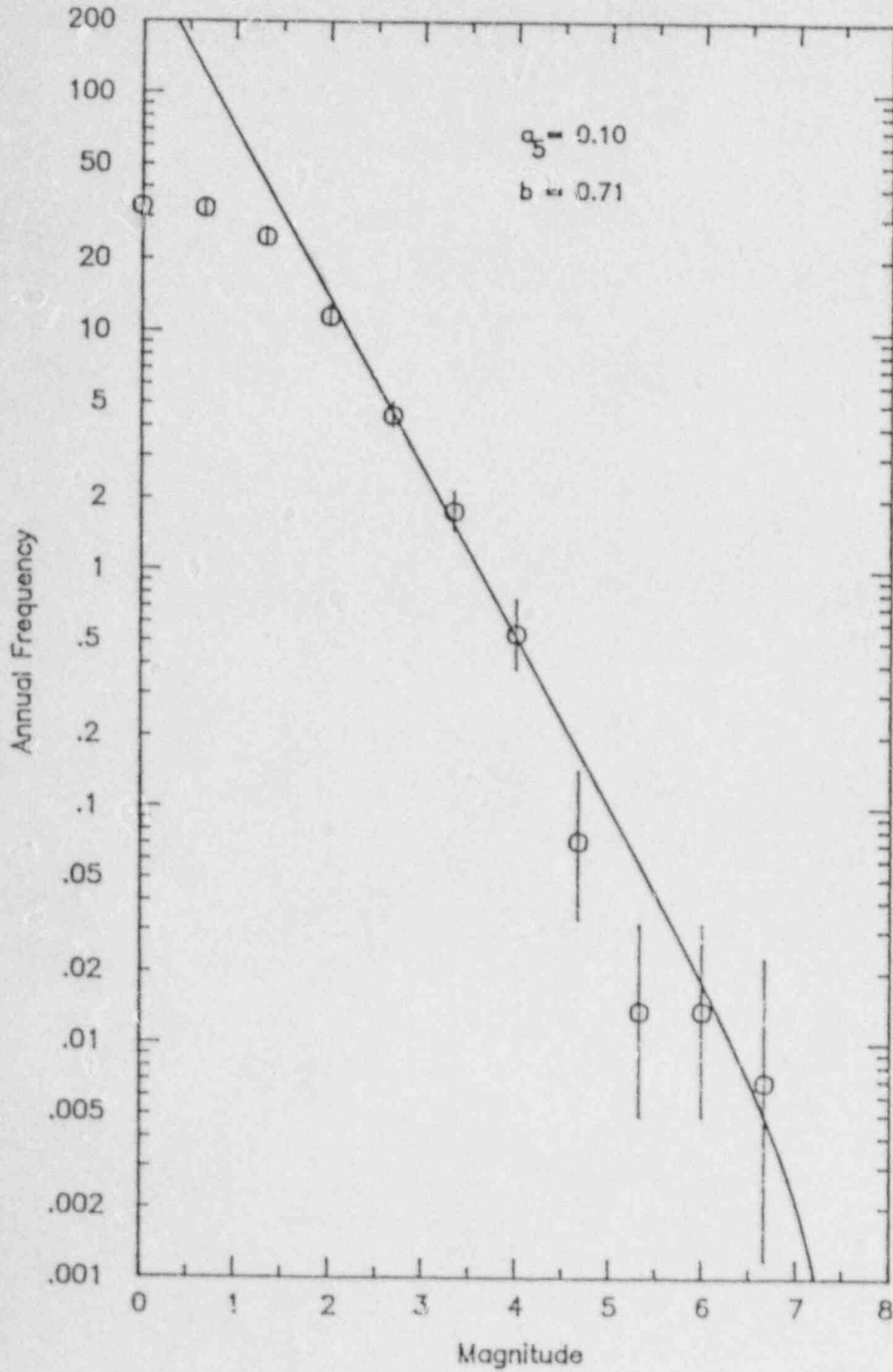
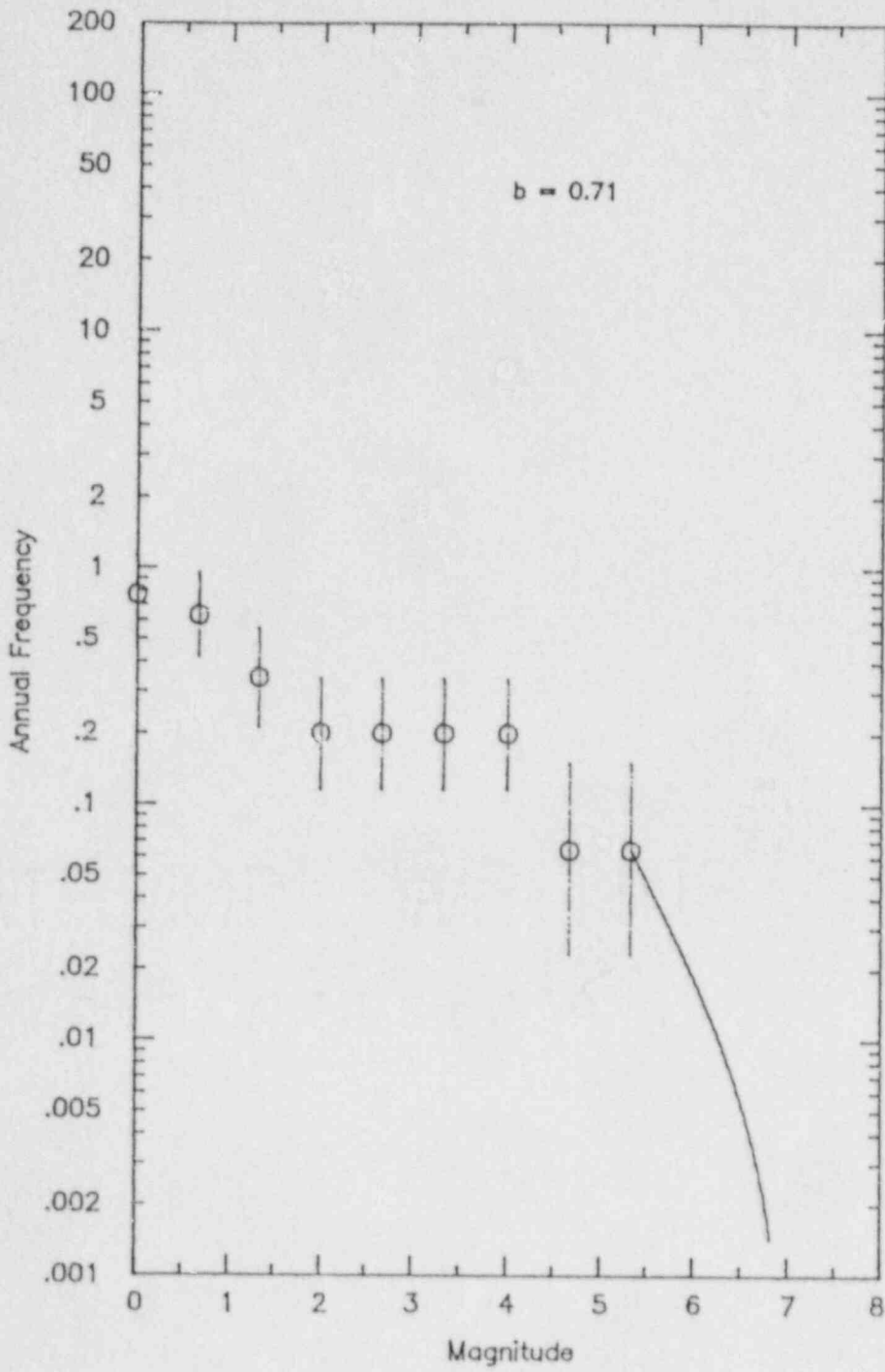




FIGURE 5 B-value -  
Off Shore



ATTACHMENT 2

Assessments Made by Individual Experts

(These are the Phase I assessments  
included previously in this  
appendix.)

ATTACHMENT 3

Summary of Aggregate Expert Assessments

SUMMARY OF EXPERT ASSESSMENTS  
FOR SUBDUCTION ZONE SEISMIC SOURCES

The logic tree format developed to model the subduction zone sources is shown in Figure 3-1. The logic tree progresses from an assessment of the geometry of the subducting slab to assessment of specific analysis parameters for individual sources. The assignment of parameter values and their relative likelihoods for the subduction zone sources was based on the inputs from 14 experts. The individual assessments of each of the experts are documented in Appendix A and are outlined in Table 3-1. The assessments made for each component of the hazard model are summarized below.

Crustal Geometry

All of the experts provided an assessment of the cross sectional geometry of the subducting Juan de Fuca plate. Most of the experts provided only a single assessment consisting of the plate dipping at approximately  $10^\circ$  and extending through the zone of deeper earthquakes lying at depths of 30 km or more beneath the site. Three experts provides alternative geometeries consisting of a more steeply dipping interface with a possible remnant slab or secondary interface in the vicinity of the observed deep seismicity. Two experts provided a slight modification of the  $10^\circ$  dip consisting of a flat lying slab with a double bend (see cross section for expert 6 in Appendix A as an example). Figure 3-2 presents the aggregate distributions for slab geometry.

Seismic Sources

All of the experts identified the Juan de Fuca - North American plate interface and the subducting Juan de Fuca plate as potential sources of thrust and intraslab normal events, respectively. Several experts also identified potential sources in the overlying North American plate. Evaluation of the hazard from these crustal sources was included in the shallow crustal source model.

### Probability of Source Activity

All of the experts made an assessment of the probability that the plate interface and the subducting slab are seismogenic. Figure 3-3 shows the distribution of assessments of activity for the intraslab and interface sources. The assessments for the intraslab source are generally at or near unity based on the past record of seismicity. The assessments for the interface range from near zero to near 1.0 with a nearly uniform distribution and an equal weighted average of 0.49. It should be noted that that an adjustment was made to the assessments of experts 4 and 13. As indicated in Table 3-1, column 5, these two experts have probabilities of 0.9 and 0.85, that the maximum magnitudes for the interface is  $M_w$  5 or less. All other experts made the assessment of activity in terms of the probability of the interface being able to generate tectonically significant events ( $M_w > 5$ ). To put the assessments of activity of experts 4 and 13 on a consistent basis they were adjusted to values of 0.075 and 0.0075, respectively, and their maximum magnitude distributions renormalized to include only magnitudes larger than  $M_w$  5.

All but two of the experts assigned a value of unity to the probability that the intraslab source, as represented by the deep zone of seismicity is active.

### Location of Ruptures

The experts provided assessments on the limits of earthquake ruptures, both along the length of the subduction zone as well as the up dip and down dip extent. Figure 3-4 provides histograms summarizing the responses obtained. Most experts considered the maximum limits of coherent rupture along the interface to be the boundary with the Explorer plate at the Nootka fault zone on the north and the boundary with the Gorda plate at the Blanco fracture zone on the south (see Figure 3-5). Several experts considered further segmentation of the interface to have some credibility, with a segment boundary generally in the vicinity of  $46^\circ$ N. The assessed minimum depth of rupture along the interface ranged from 5 to 25 km and the maximum depth of rupture ranged from 35 to 50 km.

A majority of the experts stated that they expect the future distribution of intraslab events to follow the observed pattern of historical seismicity with the majority of events occurring generally beneath Puget Sound. Alternatives considered included completely uniform seismicity within the down-going slab or a concentration of larger events at deeper depths. Figure 3-4 shows the aggregate distribution for seismicity distribution.

#### Maximum Magnitude

The experts that assessed maximum magnitudes for the interface either made a direct assessment or specified that it be calculated from the maximum rupture area assessed above using the relationship proposed by Wyss (1979). The ten experts that provided an assessment of maximum magnitude for the interface were nearly evenly split (0.55, 0.45: one expert using both methods) between the use of maximum rupture dimensions and a direct assessment of the maximum magnitude on the basis of analogy with other subduction zones or other techniques for magnitude estimation. The aggregate distribution shown in Figure 3-6 is for those who made a direct assessment, and is thus conditional on the direct assessment procedure being the correct procedure. If an expert did not assess interface maximum magnitude, then the marginal distribution used to represent the aggregated opinion of the other experts consists of 0.55 weight assigned to the magnitude value obtained from the experts assessment of maximum rupture dimensions and 0.45 weight assigned to the conditional distribution bases on direct assessment.

The distribution shown at the top of Figure 3-6 has a large probability of 0.38 assigned to a maximum magnitude of 6. As this represents, the judgments of two of the experts based on specific reasoning, it is an appropriate distribution for use in component level aggregation. However, it was judged that this assessment is significantly lower than would be obtained from a general population of scientists familiar with subduction zone earthquakes and those experts who did not make any assessment of maximum magnitude for the interface would, nevertheless, be likely to assign a much lower probability to a maximum magnitude of 6. Accordingly, the conditional distribution used for those experts who did not assess maximum magnitude was modified from that shown at the top of the Figure 3-6 by removing the

assessments for very low magnitudes and renormalizing. The resulting distribution is shown in the middle of Figure 3-6.

The maximum magnitude for the intraslab source was assessed by 11 experts on the basis of historical seismicity and analogy with other subduction zones. The aggregated distribution is shown at the bottom of Figure 3-6.

#### Earthquake Recurrence Method

All experts who made an assessment of earthquake recurrence preferred to use historical seismicity data to define the recurrence parameters for intraslab events. These parameters were used for all experts. Recurrence estimates for the plate interface were assessed either on the basis of a moment rate approach or on the basis of geologic evidence for the frequency of large events. In aggregate, the experts favor the moment rate approach slightly more than the presently available geologic data by the ratio 0.58 to 0.42. If an expert did not make an assessment of earthquake recurrence for the interface, then both methods were used with the given weights.

#### Geologic Recurrence Rate

Five of the experts chose to base the recurrence estimates for interface events solely or partially on geologic evidence for possible paleoseismic events, primarily the data on turbidites. Figure 3-7 presents the aggregated distributions for return period of large interface events. The distributions are tightly clustered about the estimate of 430 years given by Adams (1985).

#### Convergence Rate

All of the experts made an assessment of convergence rate with most basing the assessment on the rate estimates published by Riddihough (1984) and Nishimura and others (1984). Those experts that made a direct assessment generally gave a wide distribution of values with a mean value somewhat lower than the published estimates. Figure 3-8 shows the aggregate distribution for convergence rate estimates.

### Seismic Coupling

Figure 3-8 shows the aggregate distributions of the amount of seismic coupling between the Juan de Fuca and North American plates. Most of the experts gave a wide distribution for the amount of coupling with expert J giving a zero/one bimodal distribution.

The combination of the plate interface area, the convergence rate and the amount of seismic coupling provide the rate of release of seismic moment. For an interface length of 800 km, an average width of 150 km, a convergence rate of cm/yr and an aggregate mean of 0.4 for seismic coupling gives a moment rate of  $5.76 \times 10^{26}$  dyne-cm/yr. Assuming all of the moment is released in magnitude 9 events, a moment rate estimate of approximately 700 years would be obtained for the return period of these events.

### Recurrence Model

Three recurrence models for the form of the magnitude distribution were used for interface events in the analysis: the truncated exponential distribution, the characteristic magnitude distribution, and the maximum moment distribution. Figure 3-11 illustrates the cumulative form of these three distributions and compares how they would estimate the frequency of smaller earthquakes when the absolute level of seismicity is fixed by the frequency of the largest events. The aggregated distributions of the experts yielded probabilities of 0.23, 0.41, and 0.36 for the exponential, characteristic, and maximum moment models, respectively.



Expert	Oceanic Slab Geometry (Dip)	Potential Seismic Sources	Probability of Activity	Max Magn
#1	Top of deep seismicity (0.2) 15° dip (0.5) 25° dip (0.3)	Intra-slab [a]	1.0 [a]	7.25 (±0.25)
		Interface [b]	0.4 (0.25 - 0.5) [b]	Dimensions [b]
		"Deep events" (for 15° & 25° dips) [c]	1.0 [c]	7.25 (±0.25)
		Deep slab (for 15° & 25° dips) [d]	0.1 - 0.15 [d]	5 - 6 [d]
#2	Top of deep seismicity	Intra-slab [a]	0.6 - 0.7 [a]	
		Interface [b]	0.8 (0.7 - 0.85) [b]	
#3	Top of deep seismicity	Intra-slab [a]	1.0 [a]	8 (shallow part)
		Interface [b]	0.6 (0.5 - 0.8) [b]	7-1/2 [deep]
				9 (± 1/2) [b]
#4	Top of deep seismicity	Intra-slab [a]	1.0 [a]	7 - 7-1/2 [a]
		Interface [b]	0.75 (±0.25) [b]	3 (0.3)
				4 (0.3)
				5 (0.3)
				6 (0.09)
				7 (0.01)
#5	Top of deep seismicity (0.2 - 0.25) 17° - 20° dip (0.75 - 0.8)	Intra-slab [a]	1.0 [a]	7 [a]
		Interface [b]	0.5 (±0.5) [b]	
#6	Top of deep seismicity, single bend (0.7)  Top of deep seismicity, double bend (0.3)	Intra-slab [a]	1.0 [a]	6-3/4 - 7-1/4
		Interface [b]	0.65 (±0.15) [b]	Dimensions [b]
#7	Top of deep seismicity (0.7)	Intra-slab [a]		
		Plate interface [b]	0.3 (±0.2) [b]	Dimensions [b]
#8	Top of deep seismicity	Intra-slab [a]	1.0 [a]	Dimensions [b]
		Interface [b]	0.4 - 0.5 (0.25 - 0.75) [b]	
#9	Top of deep seismicity	Intra-slab to 50km depth [a]	0.9 [a]	6.5 (0.1)
		Intra-slab 50 - 75km [b]	1.0 [b]	7.0 (0.25)
		Interface [c]	0.9 - 1.0 (0.75)	7.5 (0.55)
		Strike-slip faults in upper plate [d]	0.8 - 0.9 (0.24) 0 (0.01)	8.0 (0.1)
		Accretionary wedge faults [e]	1.0 [d]	7.0 (0.1)
		Tears in down-going slab [f]	1.0 [e]	7.5 (0.8)
				8.0 (0.1)
			Dimension: [c]	
			7-1/2 [d]	
			7.5 (0.8)	
			8.0 (0.2)	
#10	Top of deep seismicity	Intra-slab [a]	1.0 [a]	7-1/4 (±1/4) [a]
		Interface [b]	0.7 (0.6 - 0.9) [b]	Dimensions (0.5) 8.3 (0.5)
#11	Top of deep seismicity	Intra-slab [a]	1.0 [a]	7 - 7-1/2 [a]
		Interface [b]	0.8 (0.8 - 1.0) [b]	Dimensions [b]
		Deep crustal source [c]	1.0 [c]	7-1/2 [c]
#12	Top of deep seismicity, single bend (0.8) Top of deep seismicity, double bend (0.2)	Intra-slab [a]	0.95 - 1.0 [a]	7-1/4 [a]
		Interface [b]	0.2 (0.1 - 0.4) [b]	
#13	Top of deep seismicity	Intra-slab [a]	0.8 (±0.1) [a]	6.5 (0.45)
		Interface [b]	0.05 (±0.05) [b]	7.0 (0.4)
			7.5 (0.14)	
			8.0 (0.01)	
			4 (0.5)	
			5 (0.35)	
			6 (0.15)	
#14	Top of deep seismicity (0.35) Steeper dip (0.65)	Intra-slab (shallow dip model) [a]	1.0 [a]	7.25 - 7.5 [a]
		Interface (shallow dip model) [b]	0.35 (±0.15) [b]	8 (±0.5) [b]
		Shallow interface (steep dip model) [c]	0.25 (±0.15) [c]	7.25 (±0.25) [c]
		Deep interface (steep dip model) [d]	0.3 (±0.1) [d]	7.5 - 8 (0.75)
		Remnant slab (steep dip model) [e]	1.0 [e]	8 - 8.5 (0.25)
		Deep intra-slab (steep dip model) [f]	1.0 [f]	7.25 - 7.5 [a]
		Accretionary wedge [g]	0.7 (±0.1) [g]	7 (±0.25) [g]
		Tears in slab [h]	0.05 (±0.05) [h]	5 [h]

OF EXPERT INTERVIEWS

Latitude	Convergence Rate (mm/yr)	Recurrence Method	Seismic Coupling ( $\alpha$ )	Recurrence Model	Geologic Recurrence Large Earthquakes (yr)
a)	30 ( $\pm 10$ )	Historical seismicity [a, c]	$\sim 0$ (0.5 - 0.66)	Exponential [a, b]	--
b)		Moment rate [b]	$\sim 1$ (0.5 - 0.33)	Max. moment given $\alpha = 1$ [b]	
c)					
	15 (0.1) 20 - 25 (0.8) 30 (0.1)	Geologic (0.3 confidence) [b]	--	--	$\sim 430$ [b]
part of a)	40 ( $\pm 19$ )	Historical seismicity [b]	0.66	Exponential [a]	400 (200 - 2,000) [b]
		Geologic data [b]		Characteristic [b]	
	10 (0.05) 20 (0.5) 30 (0.4) 40 (0.05)	Historical seismicity [a]	0.05 (0 - 0.15)	--	--
b)					
	40 (25 - 40)	Historical seismicity [a]	--	Exponential [a]	--
a)	10 - 20 (0.04) 20 - 30 (0.04) 30 - 40 (0.4) 40 - 43 (0.1) 43 - 50 (0.4) 50 - 60 (0.02)	Historical seismicity [a] Geologic data (0.5) [b] Moment rate (0.5) [b]	0.6 ( $\pm 0.15$ )	Exponential [a] Exponential (0.5) [b] Characteristic (0.4) [b]	430 [b]
	42 ( $\pm 10$ )	Historical seismicity [a]	1 (1.0)	Exponential [a]	--
	40 ( $\pm 10 - 15\%$ )	--	0.25 (0.2 - 0.5)	--	--
	42 ( $\pm 10$ )	Historical seismicity [a,b,d,e,f] Geologic data [c]	0.7 (0.5 - 1.0)	Exponential [a,b,d,e,f] Characteristic [c]	430 ( $\pm 25\%$ ) [c]
	35 - 50 ( $\pm 19$ )	Historical seismicity [a] Moment rate [b]	0.3 (0 - 0.5)	Exponential [a,b]	--
[b]					
	42 ( $\pm 10$ )	Historical seismicity [a,c] Geologic data [b]	--	Exponential [a,c] Characteristic [b]	$\geq 300$ [b] $\geq 150$ [c]
	30 - 35 (25 - 40)	Historical seismicity [a] Moment Rate [b]	0.1 (0.05 - 0.5)	Exponential [a]	--
	43 ( $\pm 19$ )	Historical seismicity [a]	0.05 ( $\pm 0.05$ )	Exponential [a]	--
	10 - 20 (0.05) 20 - 30 (0.2) 30 - 40 (0.4) 40 - 50 (0.3) $\geq 50$ (0.05)	Historical seismicity [a,e,f] Moment rate [b,c,d,g]	0.1 ( $\pm 0.05$ )	Exponential [a,e,f] Max. moment [b,c,d,g]	--
[d]					

TI  
APERTURE  
CARD

Also Available On  
Aperture Card

8803040009-02

## EXPLANATION TO ACCOMPANY

TABLE 3-1

Table 3-1 summarizes the responses given by the fourteen experts, which are further detailed in Appendix A. A more complete discussion of the components of the seismic hazard model is given in Section 2.1. Each of the columns in Table 3-1 is explained below. Note that blank columns or apparent omissions in the table are the result of the expert declining to characterize these aspects.

Oceanic Slab Geometry

Each of the experts developed a cross-sectional sketch of the geometry of the oceanic slab beneath western Washington. These sketches are included in Appendix A and described verbally in Table 3-1. Alternative models are given along with the relative weight assigned to each, expressed as probabilities summing to unity.

Potential Seismic Sources

The subduction-related potential sources of earthquakes are identified and each is assigned a letter, which is shown in brackets (e.g., "[a]"). These letters are used in subsequent columns to specify which seismic source is being described.

Probability of Activity

Probabilities of activity are given for each potential seismic source, specified by a letter in brackets. Where expressed by the experts, ranges of estimates are given in parentheses. "Activity" is used here to signify capable of generating tectonically significant earthquakes (see Section 2.1).

Maximum Magnitude

Direct assessments of the maximum earthquake magnitude are given for the sources specified in brackets. In some cases, a range of values is given, or a best estimate and uncertainty bounds, or discrete values with relative weights assigned to each value. Where the word "Dimensions" appears, the

expert indicates that the rupture dimensions that he specified be used to calculate a magnitude (i.e., he did not provide a maximum magnitude estimate directly). See Section 2.1 regarding "location of rupture" to see how the rupture dimensions were estimated.

#### Convergence Rate

The relative rate of convergence measured parallel to the convergence direction between the North American and Juan de Fuca plates is given in millimeters per year. In some cases, ranges are given or discrete values are given with associated relative weights.

#### Recurrence Method

The manner in which the experts desired to have the earthquake recurrence rate specified is given in this column. Examples include recurrence based on the historical seismicity record, geologic data for recurrence intervals, or seismic moment rate. The seismic moment rate approach (described in Section 2.1) utilizes the estimates of convergence rate and seismic coupling.

#### Seismic Coupling ( $\alpha$ )

Seismic coupling is the percentage of the total convergence rate that is expressed seismically. Therefore, if the coupling is very high ( $\alpha = 1.0$ ), then all of the convergence rate will be expressed as earthquakes (i.e., the seismic moment rate from seismicity will be equal to that based on convergence rate). An  $\alpha = 0$  means that convergence is occurring aseismically (i.e., there is no seismic coupling).

#### Recurrence Model

The recurrence distribution function is specified in this column. Models requested by the experts include an exponential magnitude distribution (i.e.,  $\log N = a - bM$ ); a characteristic magnitude distribution (Youngs and Coppersmith, 1985); and a maximum moment model (Wesnousky, 1983).

Geologic Recurrence for Large Earthquakes

For those cases where geologic data provide a basis for estimating recurrence, an estimate of recurrence intervals for large earthquakes is given. These recurrence intervals were generally judged appropriate for magnitudes at or near the maximum.

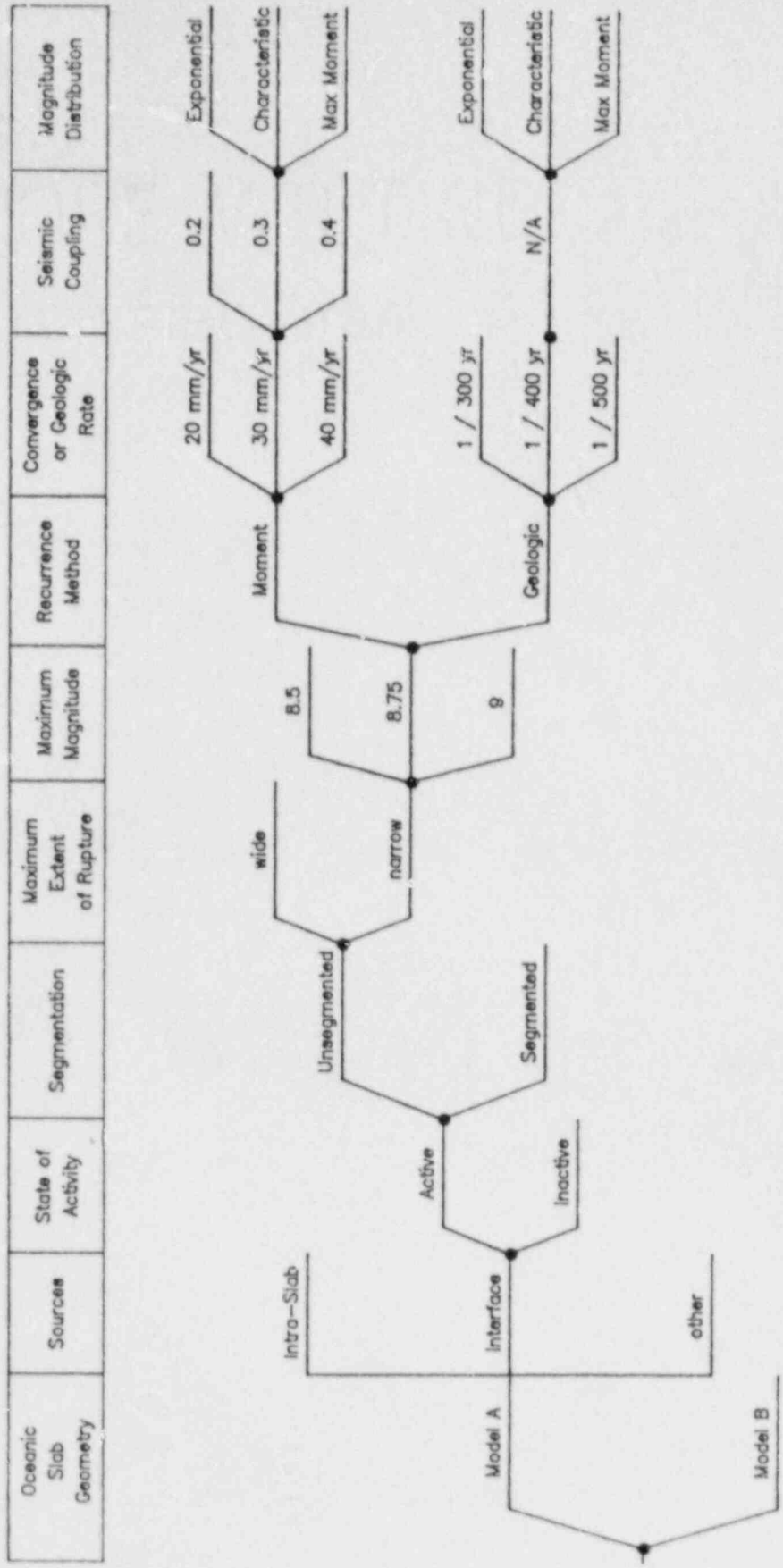
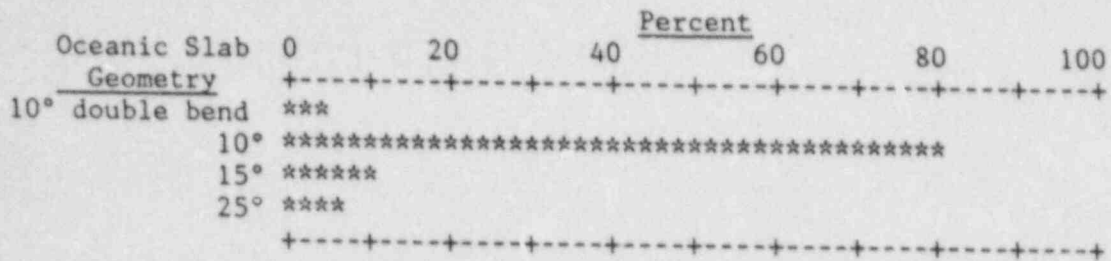
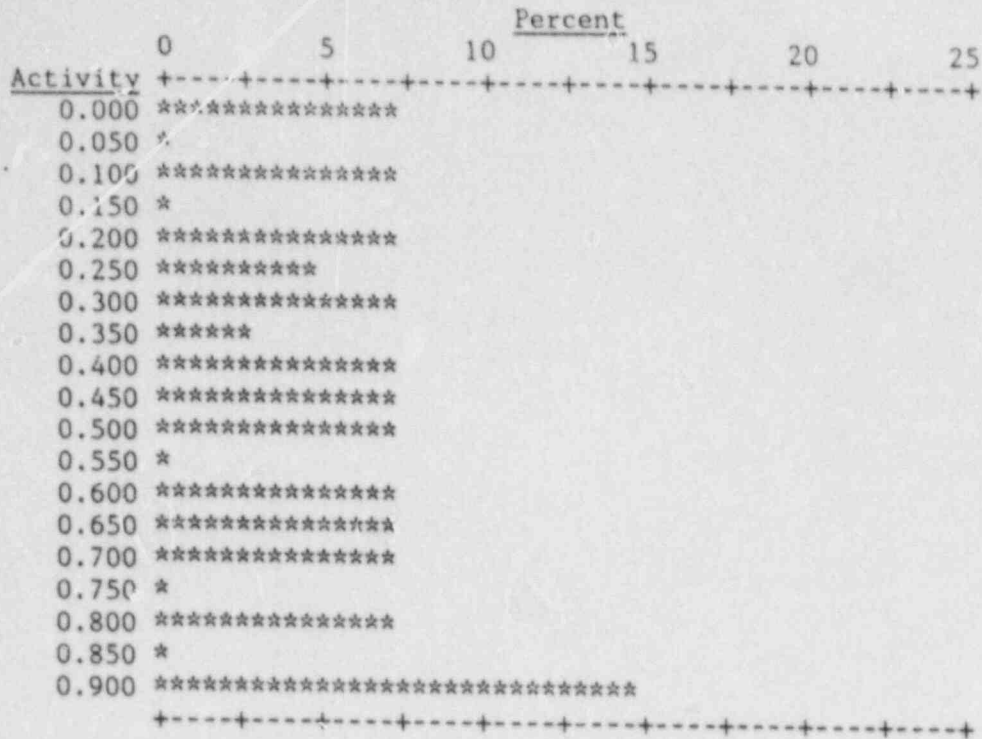


Figure 3-1 Subduction Zone Sources Hazard Model

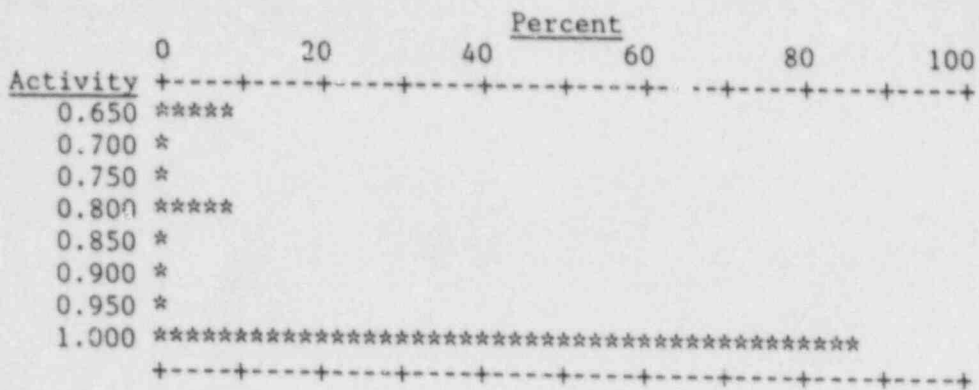


Distribution of 14 experts

Figure 3-2 Aggregate Distribution for Slab Geometry



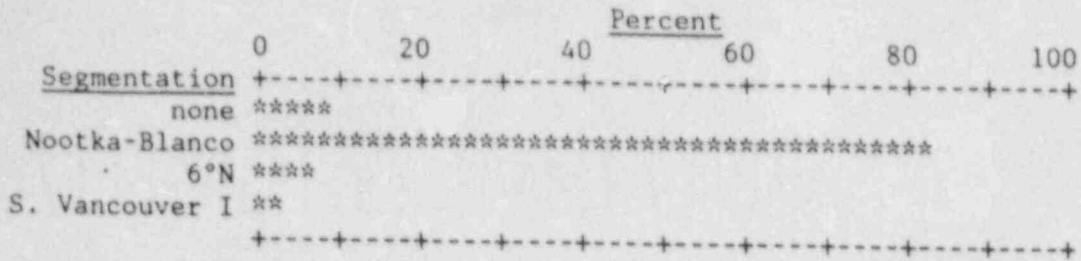
Distribution of 14 experts for interface activity



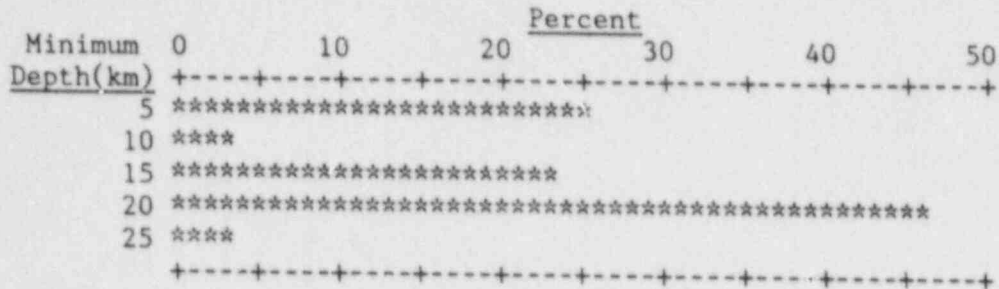
Distribution of 14 experts for intraslab/deep zone activity

Figure 3-3 Aggregate Distributions for Probability of Activity

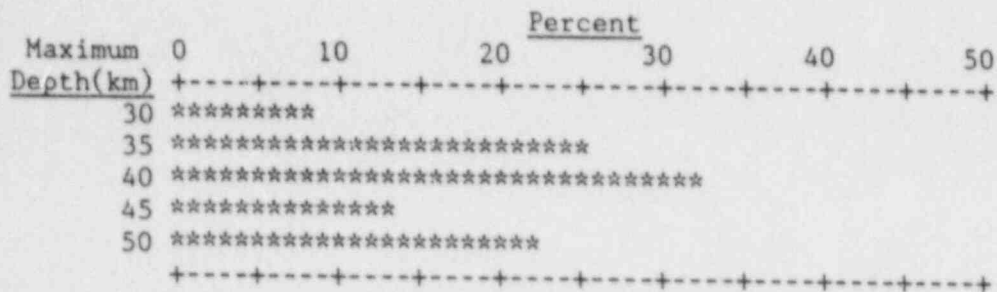




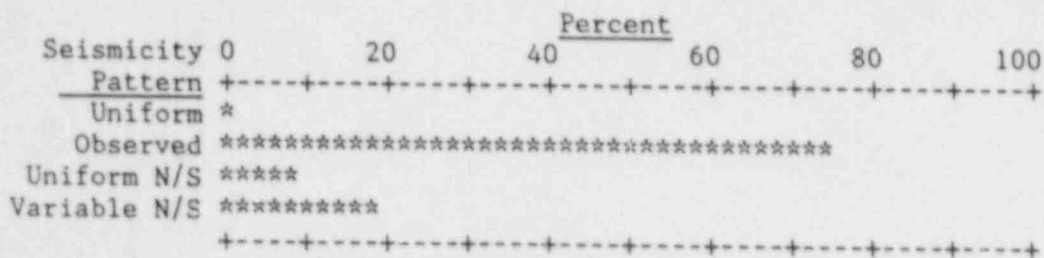
Distribution of 14 experts for interface segmentation



Distribution of 12 Experts for Minimum Depth of Rupture on Interface



Distribution of 12 Experts for Maximum Depth of Rupture on Interface



Distribution of 14 for Intraslab Seismicity Pattern

Figure 3-4 Aggregate Distribution For Location of Rupture

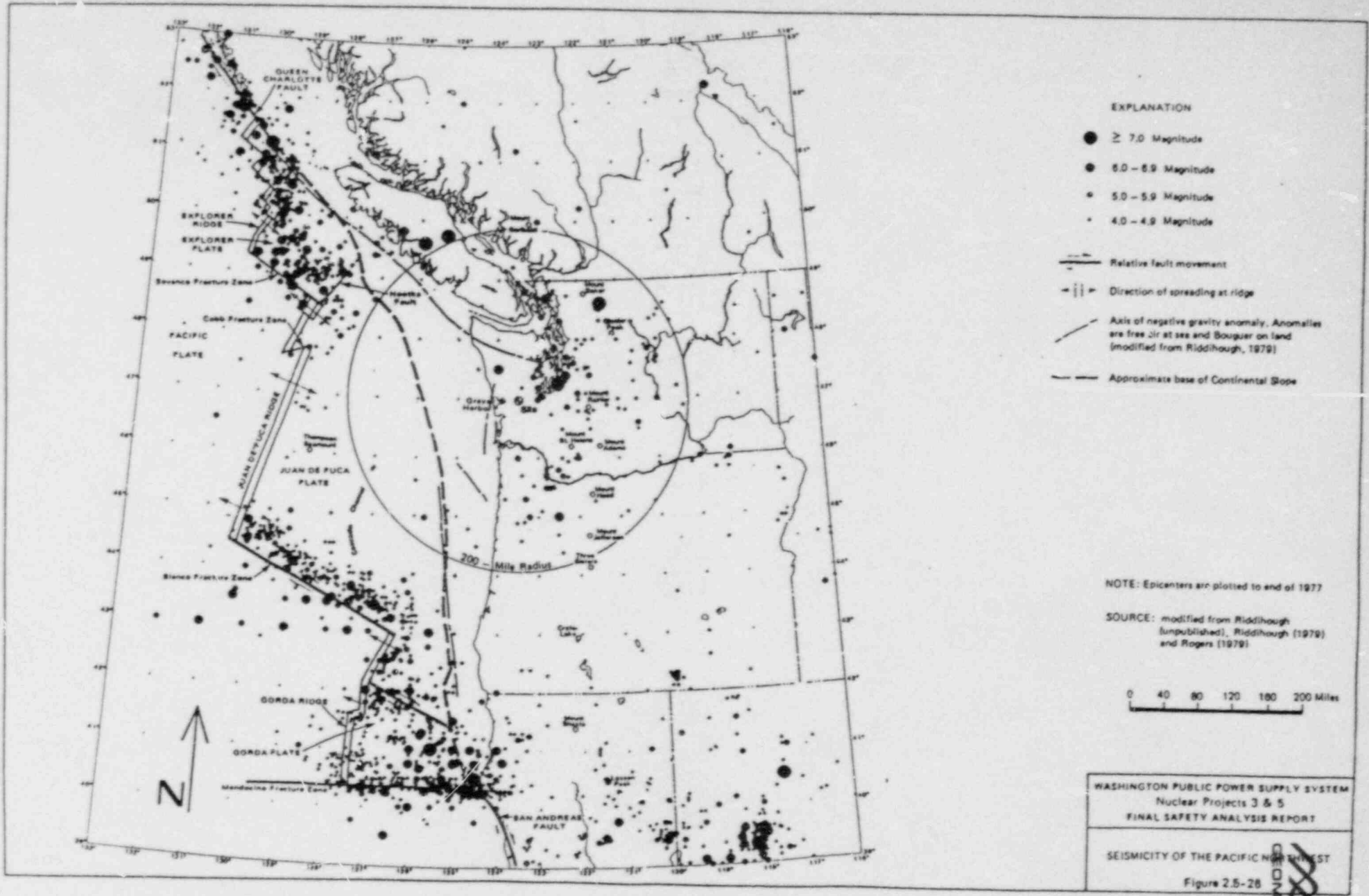
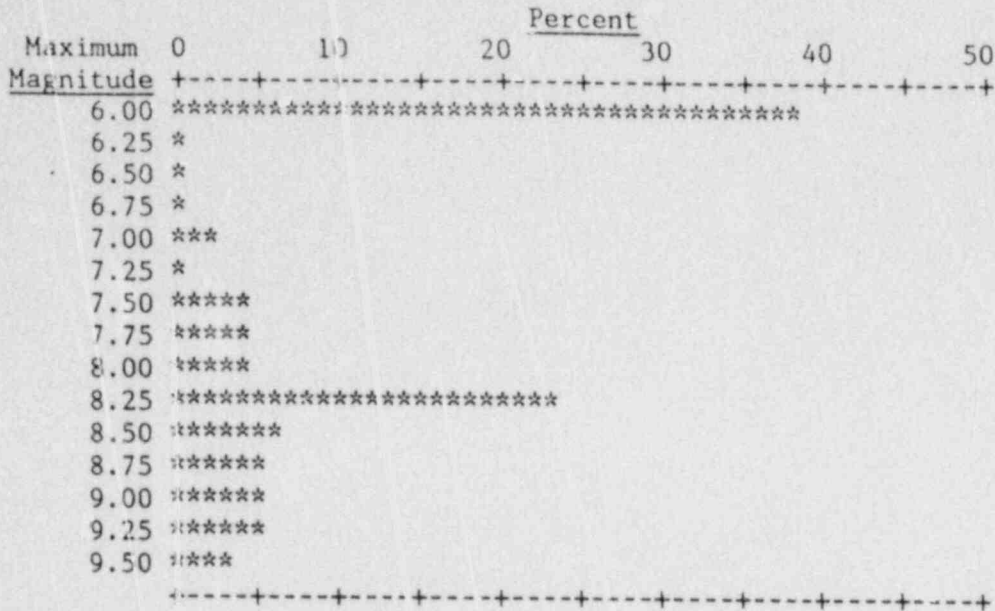
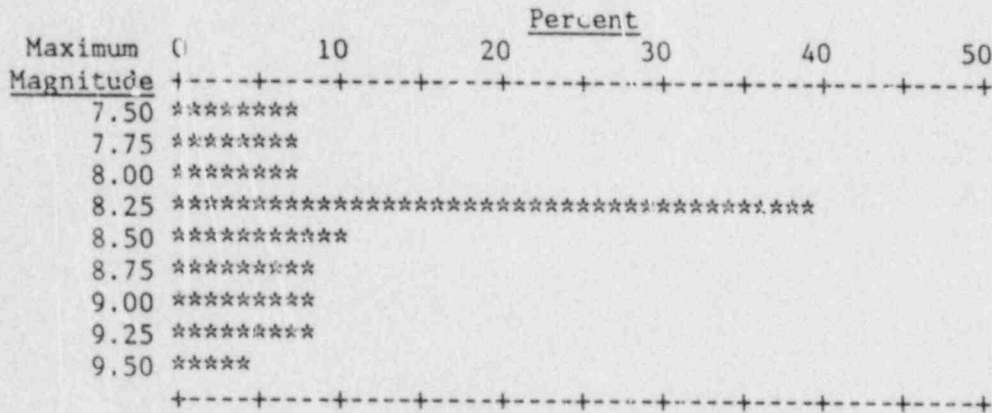


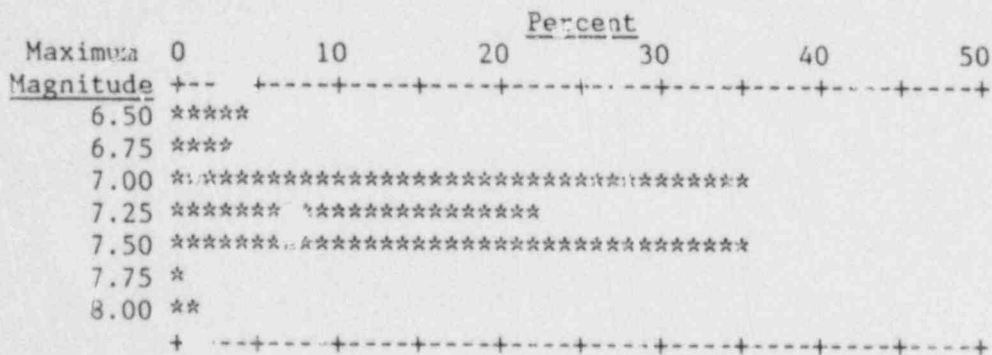
Figure 3-5 Plate Boundaries and Regional Seismicity



Conditional distribution of 5 experts for interface maximum magnitude used for component level aggregation

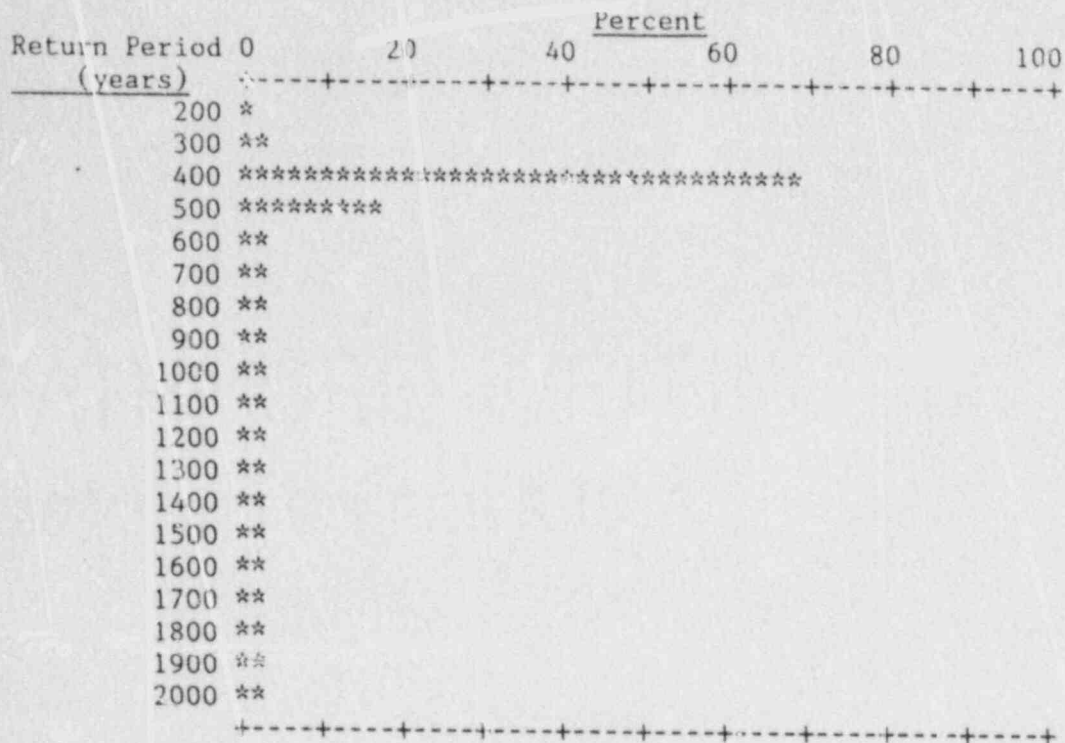


Conditional distribution for interface maximum magnitude used for "gap filling"



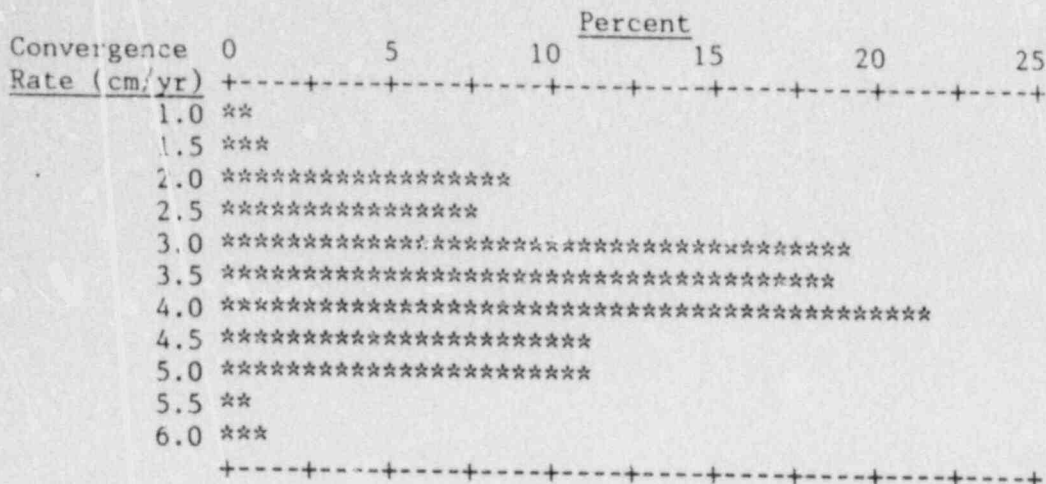
Distribution of 11 experts for intraslab maximum magnitude

Figure 3-6 Aggregate Distributions For Maximum Magnitude

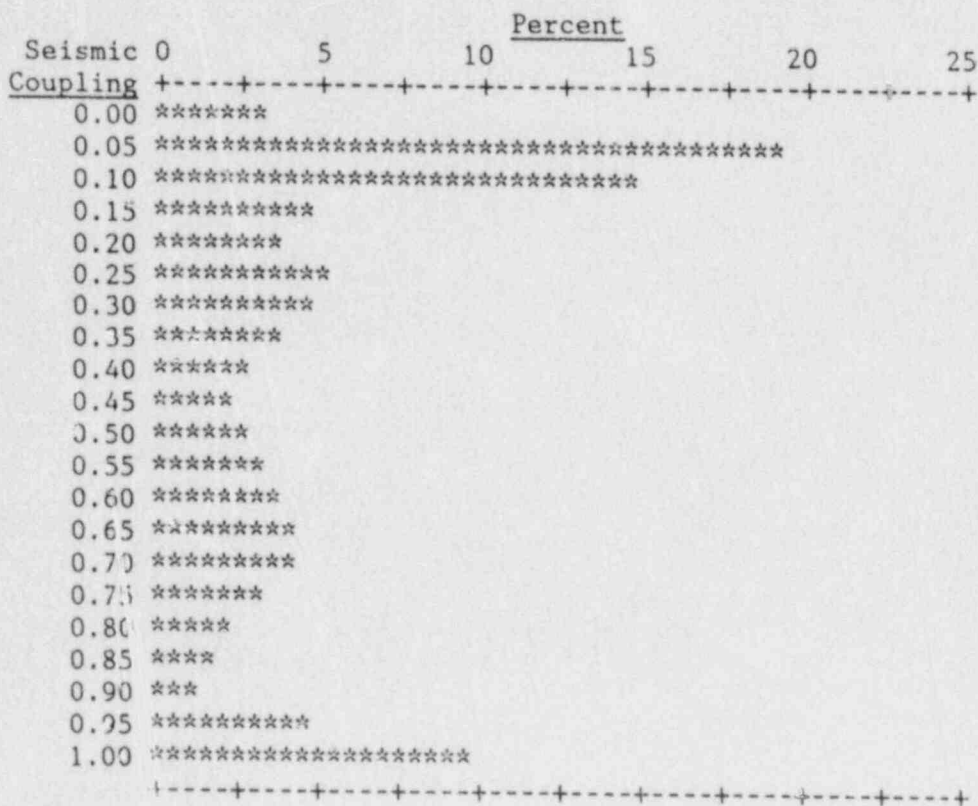


Distribution of 5 experts

Figure 3-7 Aggregate Distribution Return period of Large Magnitude Events Based on Geological Data



Distribution of 14 experts for convergence rate



Distribution of 11 experts for seismic coupling

Figure 3-8 Aggregate Distribution For Moment Rate Recurrence Parameters

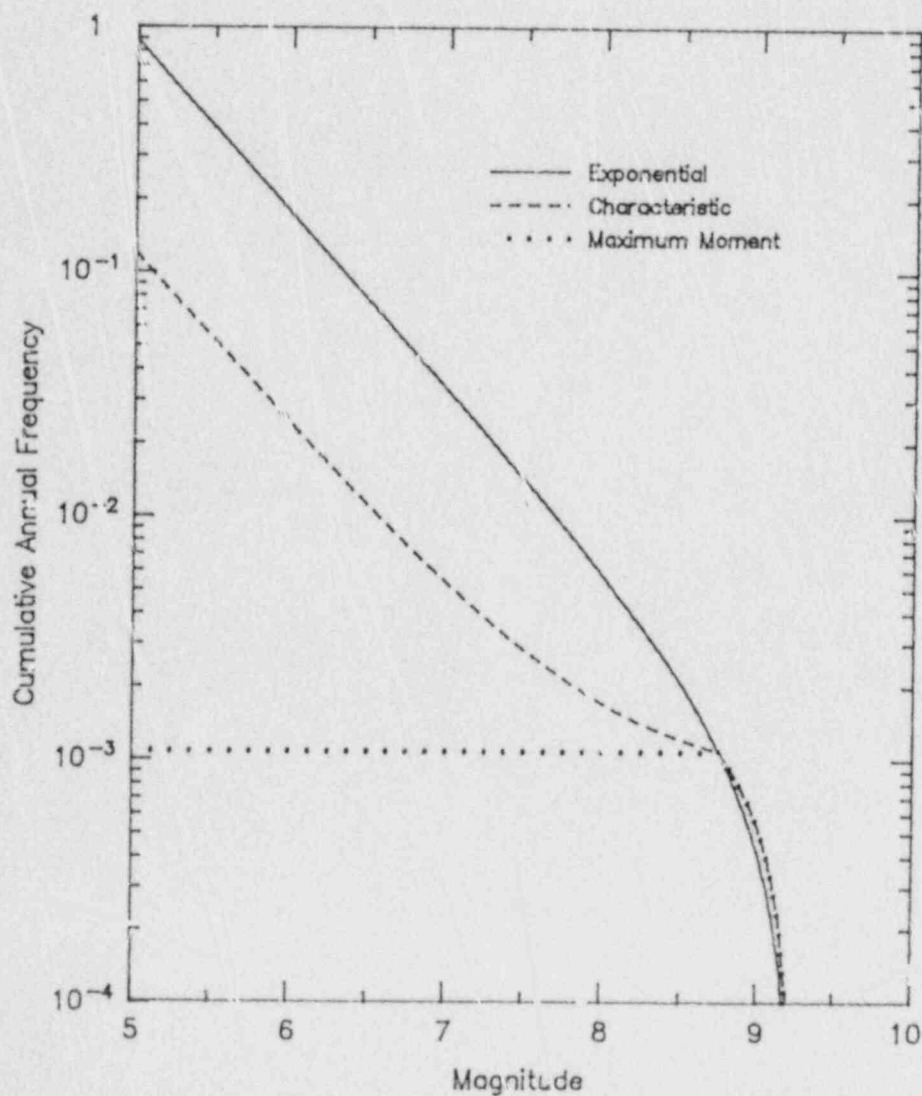


Figure 3-9 Magnitude Frequency Distributions Used in the Analysis

ATTACHMENT 4

Recent references

[Note to readers of Appendix A: Reprint copies of the following references were supplied to the experts. Their citations are given below.]

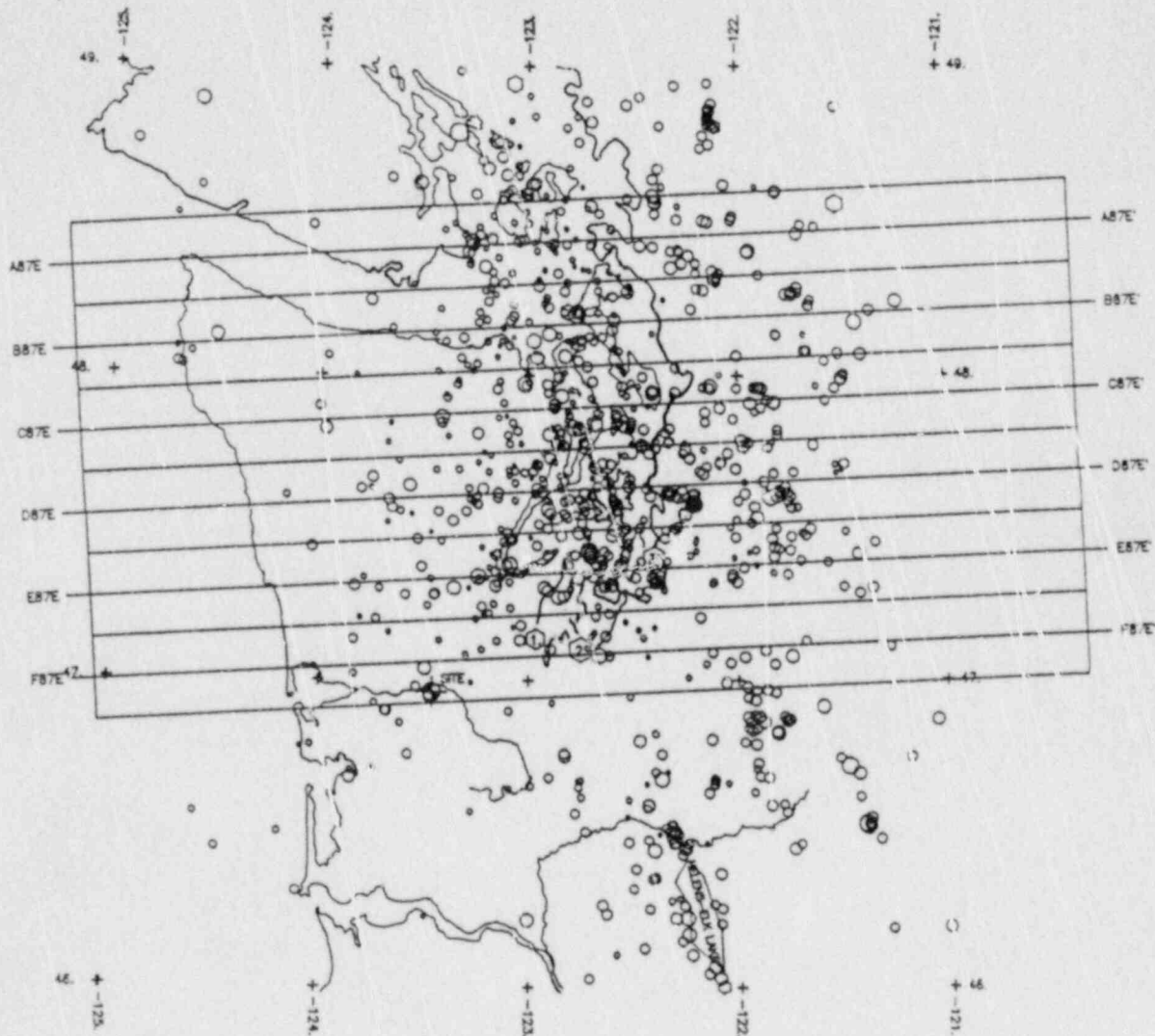
- Atwater, B.F., 1987, Evidence for great Holocene earthquakes along the outer coast of Washington state: *Science*, v. 236, p. 942-944.
- Crosson, R.S., and Owens, T.J., 1987, Slab geometry of the Cascadia subduction zone beneath Washington from earthquake hypocenters and teleseismic converted waves: *Geophysical Research Letters*, v. 14, p. 824-827.
- Ellis, M.A., 1986, Structural morphology and associated strain in the central Cordillera (British Columbia and Washington): Evidence of oblique tectonics: *Geology*, v. 14, p. 647-650.
- Heaton, T.H., and Hartzell, S.H., 1987, Earthquake hazard on the Cascadia subduction zone: *Science*, v. 236, p. 162-168.
- Owens, T.J., Crosson, R.S., and Hendrickson, M.A., 1988, Constraints on the subduction geometry beneath western Washington from broadband teleseismic waveform modelling: preprint submitted to *Bulletin of the Seismological Society of America*.
- Spence, W., 1986, Origins of stresses at the Cascadia subduction zone, U.S. Pacific Northwest: (abs.), *EOS*, v. 67, p. 1115.
- Sammis, C.G., Davis, G.A., and Crosson, R.S., 1988, A case for stable sliding in the Cascadia subduction zone: preprint submitted to *Tectonics*.
- Verplanck, E.P., and Duncan, R.A., 1987, Temporal variations in plate convergence and eruption rates in the western Cascades, Oregon: *Tectonics*, v. 6, p. 197-209.
- West, D.O., McCrumb, D.R., and Kiel, W.A., 1987, Geomorphology, convergent margins and earthquakes: in *Proceedings of the Fifth Symposium on Coastal and Ocean Management*, Seattle, Washington, May 1987, v. 4, p. 3320-3331.
- West, D.O., and McCrumb, D.R., 1988, Characteristics of subduction zone coastline uplift and implications regarding the nature of Cascadia subduction zone tectonics: preprint submitted to *Geology*.



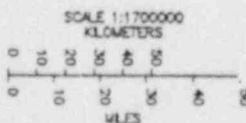
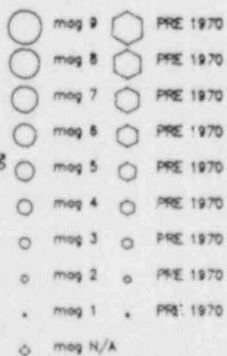
ATTACHMENT 5

Updated Seismicity Cross-Sections

WASHINGTON SEISMICITY  
 UNIVERSITY OF WASHINGTON INSTRUMENTAL DATA (1970-1986) & (DEEP PRE 1970 DATA)  
 (0-30 km MAG>2.5) (30-100 km MAG>1.0)  
 EXCLUDING (MT. ST. HELENS-ELK LAKE ZONE)  
 CROSS SECTION ORIENTATION (NORTH 87 EAST)



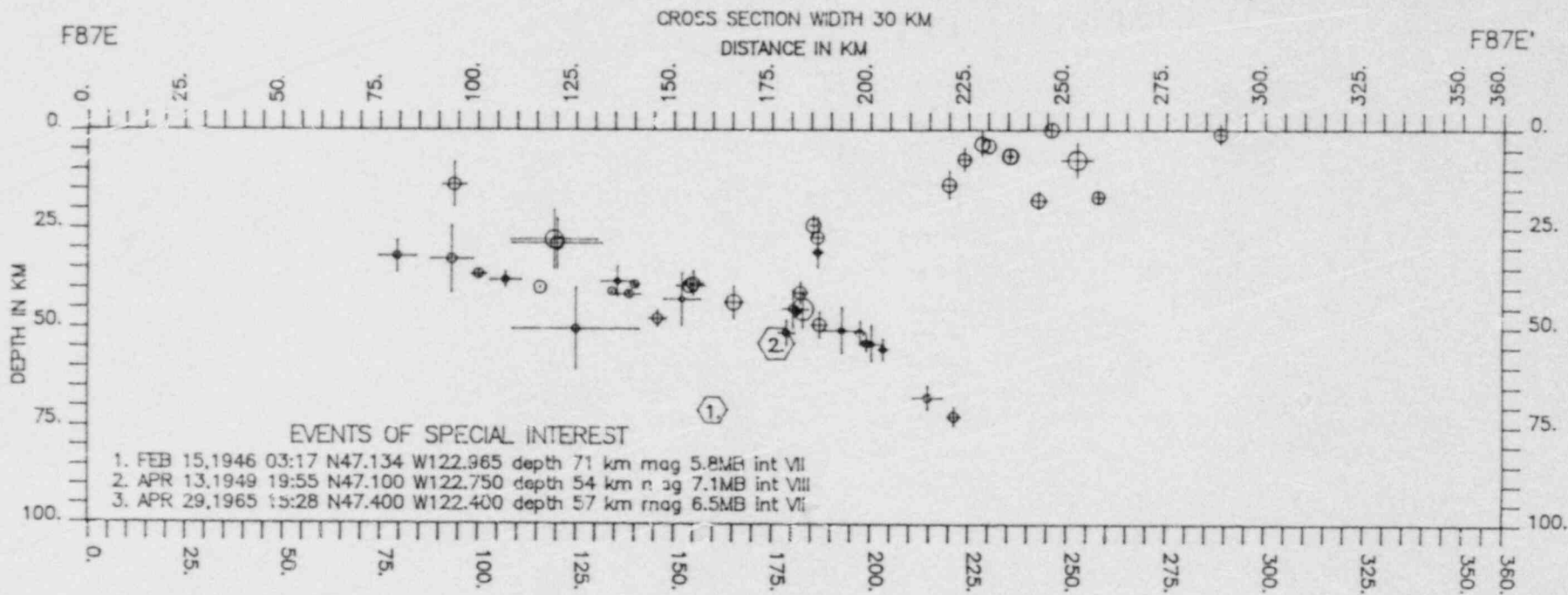
MAGNITUDE SCALE

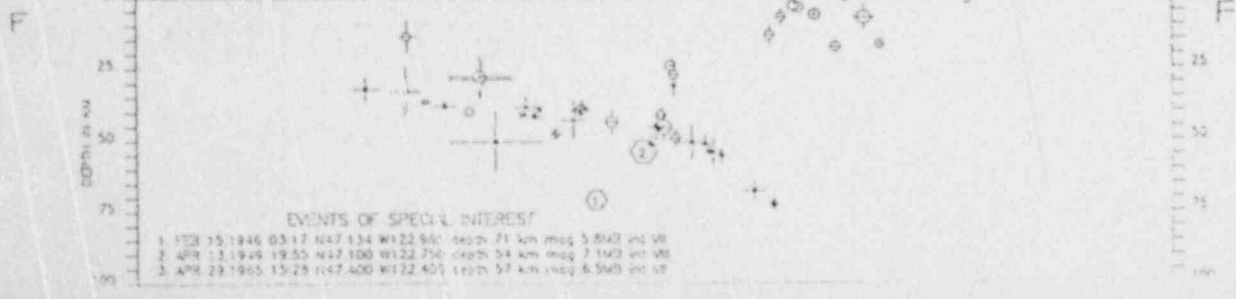
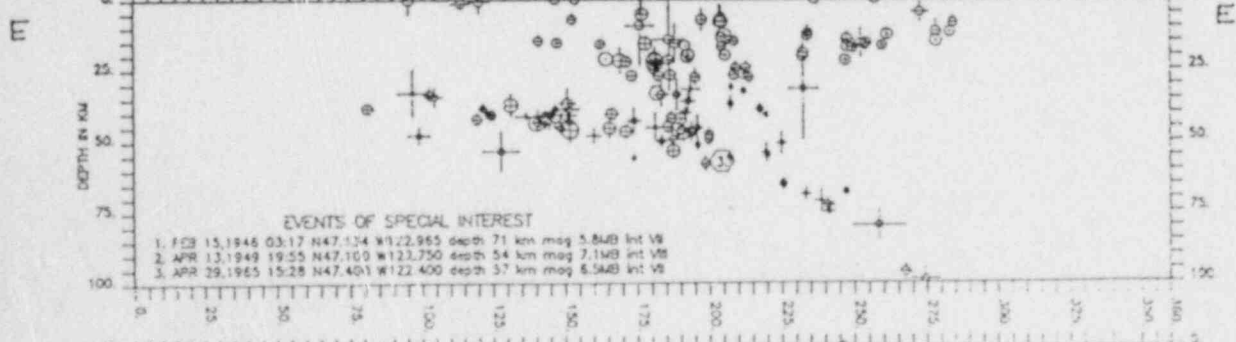
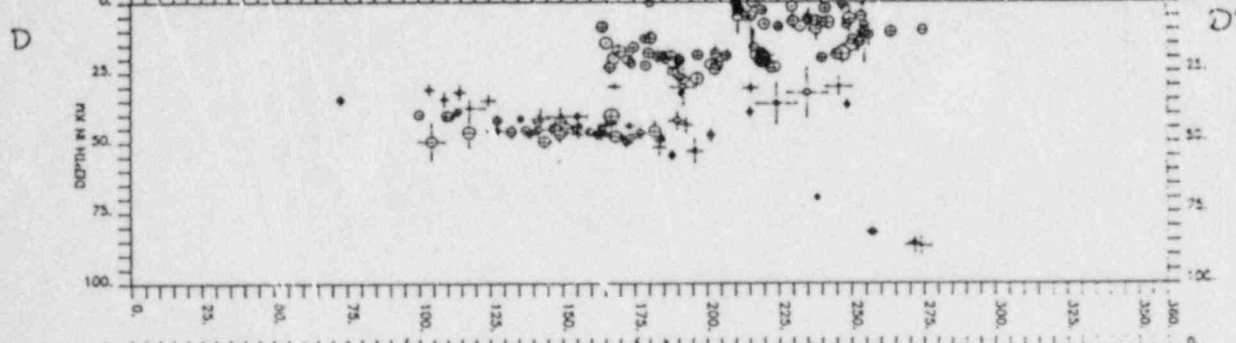
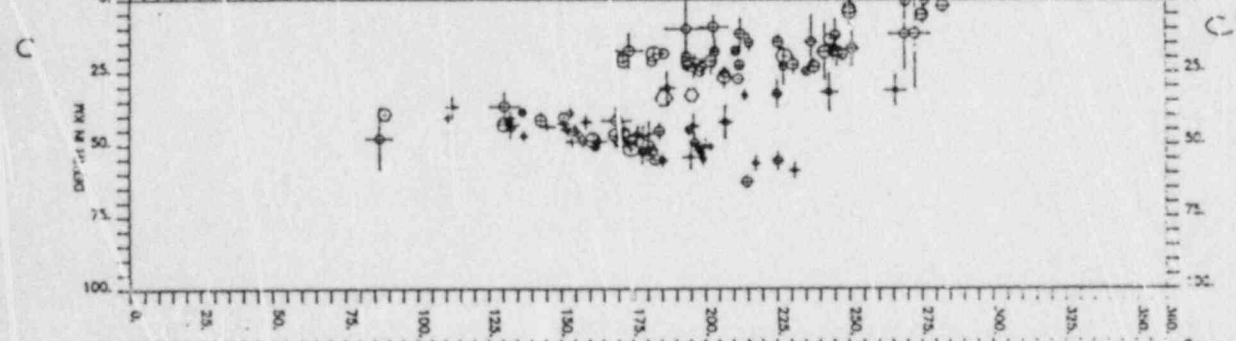
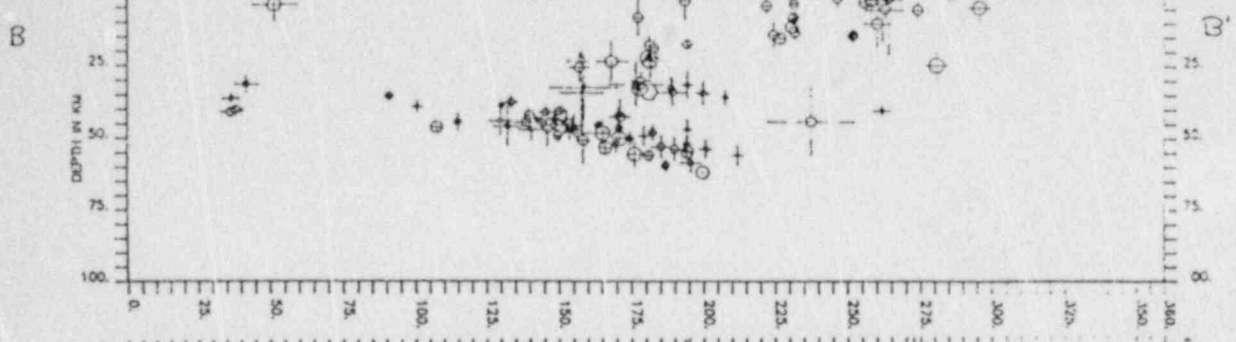
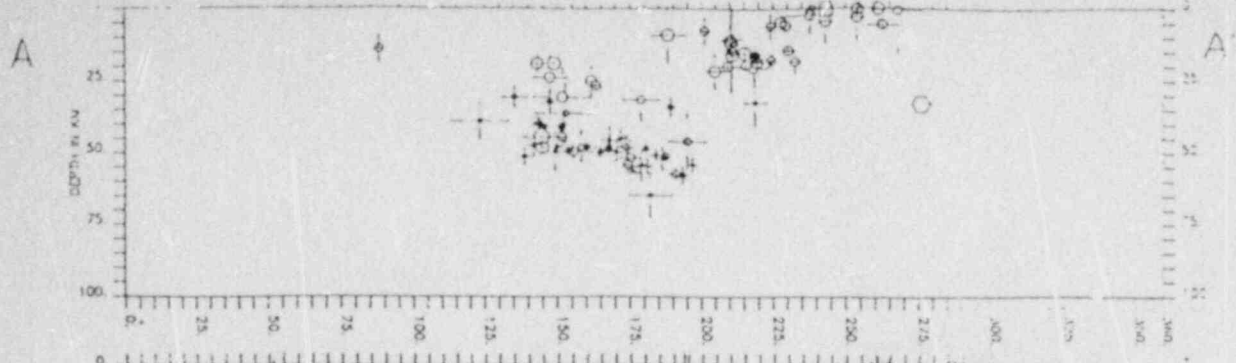


EVENTS OF SPECIAL INTEREST

1. FEB 15, 1948 03:17 N47.134 W122.965 depth 71 km mag 5.8MB int VI
2. APR 13, 1949 19:55 N47.100 W122.750 depth 54 km mag 7.1MB int VII
3. APR 29, 1963 15:28 N47.400 W122.400 depth 57 km mag 6.5MB int VI

UNIVERSITY OF WA INSTRUMENTAL DATA (1970-1986) & (DEEP PRE 1970 DATA)





PHASE II RESPONSES OF INDIVIDUAL EXPERTS

## PHASE I I

### RESPONSES BY EXPERT # 1

Note: This summary includes significant changes made to the Phase I assessments. If no change was indicated and/or previously made arguments still apply, the reader is directed to the Phase I summaries.

#### Geometry

A single model of slab geometry is adopted, that of Crosson and Owens (1987). This model suggests that the slab is arched along strike. The arch explains the observed or interpreted differences in slab dip beneath southern Vancouver Island, Central Puget Sound, and northern Oregon. The change in slab dip at 47° latitude, interpreted by Michaelson and Weaver to be a "tear", is probably the southern edge of the arch.

#### Convergence Rate

No change. Recent work by Verplanck and Duncan confirms that rates have been decreasing over the past several million years.

#### Seismic Sources and Activity

Intra-slab: Located at position of deep seismicity beneath Puget Sound

- No change in probability of activity
- "Deep events" source is no longer considered a third seismic source

#### Interface

- Probability of activity: 0.35 (.25-.50) based essentially on the same arguments given in Phase I. Geologic evidence for large earthquake is not definitive and modeling studies suggest that the interface may be aseismic.

### Location of Rupture

Interface: use geometry of Crosson and Owens (1987) directly. Updip extent unchanged, downdip extent at 40-50 km (2:1 relative likelihood)

- 0.6 : 47°N to Blanco fracture zone segmentation
- 0.4 : Nootka fault zone to Blanco segmentation
- based on arch creating a likely barrier/segmentation point to rupture

Intra-slab: no change

### Maximum Earthquake Magnitude

Interface: no change, use maximum rupture dimensions given in Phase II

Inter-slab: no change

### Seismic Coupling and Earthquake Recurrence

No change in coupling ( $\alpha$ )

#### Interface

- use a maximum moment recurrence model with a uniform distribution between magnitude 8 and 9. Absence of moderate to small thrust events supports this model. The evidence for an arch in the slab suggests more structural complexity and, therefore, a greater likelihood that a range of magnitudes from 8 to 9 should occur, rather than just the largest magnitude.

## PHASE II

### RESPONSES BY EXPERT #2

Note: This summary includes significant changes made to the Phase I assessments. If no change was indicated and/or previously made arguments still apply, the reader is directed to the Phase I summaries.

#### Geometry

Essentially unchanged;  $5^\circ$  at the leading edge, about  $10^\circ$  to the bend, steeper thereafter.

#### Convergence Rate

25 mm/yr	0.1
30-35	0.8
40	0.1

These are total convergence rates. Basis for assessments as given in Phase I.

#### Probability of Activity

Intra-slab: 0.8 based on historical seismicity record

Interface: 0.4 (0.05, 0.2); lower probability is suggested by recent studies by Sammis and Davis showing the thermal character of the slab and overlying sediments.

#### Location of Rupture

No change



### Maximum Earthquake Magnitude

interface: no change (i.e., use aggregate distribution) except the maximum magnitude should not be as small as 6-7.

### Interface Earthquake Recurrence

Relative weight given to methods for assessing recurrence.

Geologic data 0.4

Moment rate 0.6

Uncertainties exists in the data used to specify both models.

PHASE II

RESPONSES BY EXPERT #3

Note: This summary includes significant changes made to the Phase I assessments. If no change was indicated and/or previously made arguments still apply, the reader is directed to the Phase I summaries.

Geometry

No change

Convergence Rate

No change

Seismic Sources and Activity

Intra-slab: no change

Interface: 0.9

- based on Atwater geologic data and similar ongoing work in Oregon. This probability is less than 1.0 because we have not actually observed a large historical interface earthquake.

Location of Rupture

No change

Maximum Earthquake Magnitude

No change

Recurrence-Related Parameters

Intra-slab: no change

Interface: use of characteristic earthquake model whose characteristic magnitude is one unit wide (e.g., 8 to 9 for  $M_{max}$  of 9)

- Recurrence intervals: preferred value of 500 yr, ranging from 400 yr to 1000 yr based on new Atwater data showing five events in the past 2800 yr.
- The occurrence of moderate events implied by the characteristic model is okay despite historical absence because many of these events may occur as aftershocks.

## PHASE II

### RESPONSES BY EXPERT # 4

Note: This summary includes significant changes made to the Phase I assessments. If no change was indicated and/or previously made arguments still apply, the reader is directed to the Phase I summaries.

#### Geometry

No change. Use constant dip from Puget Sound south to Blanco rather than variable dip model of Crosson and Owens.

#### Convergence Rate

No change.

#### Seismic Sources and Activity

No change. Agree with approach used to evaluate probability of interface events of magnitude  $> 5.0$ .

#### Location of Rupture

No change. Rupture for interface events can extend to shallower depths as low high-frequency-energy slip events.

#### Maximum Earthquake Magnitude

No change. Agree with renormalized distribution conditional on events being larger than magnitude 5.0, which results in probability of activity of 0.075.

#### Seismic Coupling and Earthquake Recurrence

Interface: should be reduced so that return period for magnitude 5 interface events is about 25 years on the average to match observed record (no documented interface events). Use characteristic recurrence model as absence of interface events suggests a suppressed rate for lower magnitude events.

Intraslab: No change.

## PHASE II

### RESPONSES BY EXPERT #5

Note: This summary includes significant changes made to the Phase I assessments. If no change was indicated and/or previously made arguments still apply, the reader is directed to the Phase I summaries.

#### Geometry

Model A: Revise old Model A to use variable model of Crosson and Owens (1987) as model fits many of the observed interpretations of slab geometry along strike. Weight 0.85 to 0.9.

Model B: Planar slab dipping  $\sim 10^\circ$  through seismicity. A weight 0.10-0.15 - represents possibility Model A is wrong.

#### Convergence Rate

No change. However, the modeled distribution in Phase I has too much weight on 40 mm/yr. 30 to 35 mm/yr more probable (0.7) range still 25 to 40. Verplanck and Duncan (1987) give estimate of 32 mm/yr.

#### Seismic Sources and Activity

No change.

#### Location of Rupture

Interface: No change on up-dip and down-dip. Revised along strike as follows:

Model A: Nootke to Blanco segmented north and south of arch at latitudes  $46^\circ\text{N}$  and  $49^\circ\text{N}$  (weight 0.75). Nootke to Blanco segmented only south of arch at latitude  $46^\circ\text{N}$  (weight 0.25).

Model B: Nootke to Blanco (1.0)

- If arch exists it should act to constrain rupture to zones of similar geometry. If arch does not exist - no basis for segmentation.

Intraslab: No change.

Maximum Earthquake Magnitude

No change. Approach used in Phase I appears reasonable.

Seismic Coupling and Earthquake Recurrence

Interface: No change on approach. However, the return periods estimates for magnitude 6 or greater events should be at least 30 to 40 years (minimum of 20) based on 1949 and 1965 being intraslab events.

Intraslab: No change.

## PHASE II

## RESPONSES BY EXPERT #6

Note: This summary includes significant changes made to the Phase I assessments. If no change was indicated and/or previously made arguments still apply, the reader is directed to the Phase I summaries.

Geometry

The relative weight given to Models A and B are the following:

Model A: 0.7

Model B: 0.3

Model A is preferred because updated seismicity data appear to be reliable. Model B allows for the possibility that the hypocenters are mislocated.

Convergence Rate

The revised convergence rate distribution is the following:

0-10 mm/yr	0.04
10-20	0.04
20-30	0.4
30-40	0.1
40-43	0.4
43-50	0.02

The central value of about 35 mm/yr is supported by Verplank and Duncan's work showing the rate to be slowing down through time and changing orientation.

Probability of Activity

Intra-slab: no change

Interface:  $0.65 \pm 0.2$

The uncertainty is slightly larger than Phase I. Based on geologic evidence by Atwater, including evidence for sands that may have been deposited by tsunamis.

#### Location of Rupture

Intra-slab: no change

Interface: alternative maximum lengths of rupture are:

Nootka fault zone to Blanco fracture zone	0.75
Nootka to change in free-air gravity at $46^{\circ}\text{N}$	0.25

The Crosson and Owens evidence for an arch in the slab suggests that segmentation is likely.

#### Recurrence-Related Parameters

Intra-slab: no change

Interface: no change in seismic coupling ( $\alpha$ )

A recurrence interval of 500-600 yr ( $\pm 25\%$ ) is assessed by recent geologic studies.

Earthquake recurrence for the interface should be based 75% on geologic data and 25% on seismic moment rate.

The relative weight to be given to the size distribution models is:

Characteristic earthquake model	0.8
Exponential model	0.2

Because we have not seen moderate-to-small magnitude earthquakes in the historical record, the recurrence interval for a  $M_6$  interface event should be  $50 \pm 20$  yr.



PHASE II

RESPONSES BY EXPERT #7

Note: This summary includes significant changes made to the Phase I assessments. If no change was indicated and/or previously made arguments still apply, the reader is directed to the Phase I summaries.

Geometry

No change: updated hypocentral cross-sections further support down-dip bend in slab as well as arching along strike.

Convergence Rate

No change: recent studies such as Verplanck and Duncan support decrease in rate up to present.

Sources and Probability of Activity

No change (see "recurrence" below for discussion of geodetic data vv. interface activity)

Location of Rupture

Intra-slab: no change

Interface: updip extent at 10-15 km depth; a lot of deformation is occurring offshore but we don't know if any of it is seismogenic

Maximum Earthquake Magnitude

No change; it should be remembered that this is a very young plate

Recurrence-Related Parameters

Intra-slab: no change

Interface:

- No change in coupling ( $\alpha$ )
- When one examines the geodetic data, one sees shortening parallel to the convergence direction but decreasing in magnitude from west to east. This may suggest that the strain is due to the accretion of sediments onto the North American plate. Such a process may be aseismic but may still be responsible for the coastal subsidence inferred by Atwater.
- The models for interface recurrence may range from a maximum moment model to a characteristic earthquake model whereby the recurrence interval for a M6 event is at least 50 yr.

## PHASE II

### RESPONSES BY EXPERT #8

Note: This summary includes significant changes made to the Phase I assessments. If no change was indicated and/or previously made arguments still apply, the reader is directed to the Phase I summaries.

#### Geometry

Use the slab geometry given by Crosson and Owens, which suggests variability in slab dip along strike. Slab geometries from reflection and seismicity beneath southern Vancouver Island, which indicate a dip of approximately  $13^\circ$ , also support this variability along strike, as well as a bend in the slab downdip.

#### Convergence Rate

38 mm/yr (+5, -10) based on Riddihough, Verplank and Duncan evidence that the convergence rate has been decreasing through time.

#### Probability of Activity

Intra-slab: no change

Interface: 0.5 (0.25-0.75) based on consideration of both geologic studies suggesting prehistoric large earthquakes and studies suggesting aseismic behavior. Neither appear to be conclusive. Note that underplating is probably occurring and thereby taking up some of the differential plate motion.

#### Location of Rupture

Intra-slab: no change

Interface: at latitude of site, no change; at latitude of S. Vancouver Island, updip extent at the first bend in the slab; downdip to about  $122.5^\circ$ .

No change along strike, although uncertain whether rupture will extend through the bend.

#### Recurrence-Related Parameters

Seismic coupling ( $\alpha$ ) is assessed to be 0.5 (0.2-0.7), based on the following. Recent seismic reflection and refraction studies beneath Vancouver Island have identified what is likely the plate interface (reflector F) and it is fairly distinct discontinuity that is on the order of 100's of meters thick. It was previously thought that the reflector was the imbricated zone representing the interface and that F was the oceanic Moho.

A possible interpretation is that the E zone, which is a relative wide zone of imbrication and thrusting, is an older interface zone. At the present time, the F zone, which is sharper and more continuous appears to be the interface, suggesting less imbrication and, perhaps, a more coherent interface than previously existed.

The remainder of recurrence parameters are left to the aggregate distribution. It should be noted, however, that the recurrence of moderate-to-large earthquakes should be a minimum of hundreds of years, based on the historical absence of these events.

PHASE II

RESPONSES BY EXPERT #9

Note: This summary includes significant changes made to the Phase I assessments. If no change was indicated and/or previously made arguments still apply, the reader is directed to the Phase I summaries.

Geometry

No change

Convergence Rate

No change (note that Riddihough indicates changes in rate along the strike of the subduction zone)

Seismic Sources and Activity

Intra-slab: no change

Interface:  $0.95 \pm 0.05$ ; consistent with John Adams' evidence for turbidities along over 500 km of length of the subduction zone

Accretionary wedge faults, tears in slab, strike-slip faults: no change

Location of Rupture

Intra-slab: no change

Interface:	<u>Relative Weight</u>	<u>Segmentation</u>
	0.1	no segmentation
	0.1	Nootka - Blanco
	0.8	Nootka - Mendocino

- based on the fact that the same number of turbidities are seen north of and 50-100 km south of the Blanco fracture zone

Maximum Earthquake Magnitude

Intra-slab (shallow part, "A" and deep part "B"): no change except replace M8 with 7.8 based on expected source dimensions.

Interface: no change (use rupture dimensions, given above, which will result in magnitude of Mw 9.25-9.5)

Seismic Coupling and Earthquake Recurrence

Intra-slab: no change

Interface: primary basis for interface recurrence continues to be geologic evidence for recurrence intervals from the turbidities offshore. The estimate is 500 yr  $\pm$  25% based on an average of 13 turbidities deposited since the Mazama ash deposition. 25% is judged to be one standard deviation.

Recurrence models should be:

Maximum moment 0.5  
Characteristic earthquake 0.5

For the characteristic earthquake model, the recurrence for a M6 earthquake should be a minimum of 100 yr based on the historical record. A uniform distribution should be used between 100 yr recurrence and the absence of M6 earthquakes implied by a maximum moment model. The range of the characteristic earthquake should be one-half magnitude unit.

Seismic coupling, which should not be used for recurrence estimation, should have the following distribution:

<u><math>\alpha</math></u>	<u>Weight</u>
0.7-1.0	0.54
0.5-0.7	0.25
0	0.01

PHASE II

RESPONSES BY EXPERT #10

Note: This summary includes significant changes made to the Phase I assessments. If no change was indicated and/or previously made arguments still apply, the reader is directed to the Phase I summaries.

Geometry

No change

Convergence Rate

No change

Sources and Probability of Activity

No change

Location of Rupture

Intra-slab: no change

Interface: downdip extent of rupture estimated at depth  $50 \pm 10$  km based on the observation that the in 1985 Chile earthquake rupture extended to deeper than 40 km.

Maximum Earthquake Magnitude

Intra-slab: No change

Interface: Use rupture area only.

Recurrence-Related Parameters

Intra-slab: no change.

Interface: assessment of coupling is unchanged

slab movement rate from  $\alpha$  and convergence rate is  
 $800 \text{ km} \times 200 \text{ km} \times 5 \times 10^{11} \text{ dyne/cm}^2 \times 4 \text{ cm/yr} \times 0.3 = 5.8 \times 10^{26} \text{ dyne cm/yr}$

- Moment rate from  $M_w' = 8.4$  is equal to  
 $10^{**} (1.2 * 8.4 + 18.2) \times 8/100 = 1.5 \times 10^{27}$  dyne cm/yr
- Use  $M_w$  to compute moment rate
- Geologic data regarding recurrence intervals provide only a loose constraint on recurrence
- Exponential behavior may not occur until after major event.



## PHASE II

### RESPONSES BY EXPERT #11

Note: This summary includes significant changes made to the Phase I assessments. If no change was indicated and/or previously made arguments still apply, the reader is directed to the Phase I summaries.

#### Geometry

No change

#### Convergence Rate

No change

#### Sources and Probability of Activity

No change

#### Location of Rupture

Intra-slab: no change

Interface: rather than the Blanco fracture zone, the southern extent of rupture should be at the middle of the Gorda plate, where we have a change in the spreading rate at the ridge.

#### Maximum Earthquake Magnitude

No change

#### Recurrence-Related Parameters

Inter-slab: no change

Interface: earthquake recurrence intervals for large events should be 500+ 150 yr based primarily on J. Adams evidence for turbidites

- a maximum moment recurrence model is appropriate vv. the historical record. Use a one-magnitude unit width for characteristic magnitude.

## PHASE II

### RESPONSES BY EXPERT #12

Note: This summary includes significant changes made to the Phase I assessments. If no change was indicated and/or previously made arguments still apply, the reader is directed to the Phase I summaries.

#### Geometry

A progressively steepening model is favored having a bend offshore and another bend downdip at about  $122.5^\circ$  at the latitude of the site. The deeper bend is indicated by the seismicity data as well as the requirement that the slab attain magmatic generation depths of 100-150 km beneath the Cascades.

#### Probability of Activity

Inter-slab: no change

Interface: the interface is assessed to be composed of essentially two elements: the interface between the slab and overlying material, and a listric fault zone that would exist within the accretionary wedge. The probability that these two sources are active is 0.9. If active, the distribution of events is approximately 50%, 50%.

#### Location of Rupture

Intra-slab: no change

Interface: the downdip extent is unchanged. The updip extent is controlled by mechanical properties and should be at about  $123.5-124^\circ$ . Along strike, the likelihood of segmentation at southern Vancouver Island is increased to 0.5 based on the Crosson and Owen evidence for an arch in the slab, as well as a change in the trend of the volcanic arc.

Accretionary wedge: the zone would merge with and be listric to the plate interface at  $123.5-124^\circ$  and would reach the surface to the west of the coastline (to provide the possibility of being tsunamigenic). Along-strike segmentation would be the same as the plate interface.

#### Maximum Earthquake Magnitude

Intra-slab: no change

Interface: A direct assessment of magnitude 9 is given based on Atwater's evidence for subsidence. This estimate would also apply to the accretionary wedge source.

#### Earthquake Recurrence-Related Parameters

Interface: Recurrence intervals for magnitude  $7\frac{1}{2}$  or larger earthquakes is assessed at 500 ( $\pm 100$ ) yr based primarily on Atwater's data, and supported by Adams turbidite data. In the recurrence relationship, a uniform distribution is given between a  $7\frac{1}{2}$  to  $8\frac{1}{2}$  and the relative likelihood between a  $7\frac{1}{2}$  to  $8\frac{1}{2}$  event and a 9 event is 90% and 10% respectively. A maximum moment size distribution model is preferred (weighted  $> 0.5$ ), but the aggregate distribution may be used provided this model is given a weight of 0.5 or better.

PHASE II

RESPONSES BY EXPERT #13

Note: This summary includes significant changes made to the Phase I assessments. If no change was indicated and/or previously made arguments still apply, the reader is directed to the Phase I summaries.

Geometry

No change

Convergence Rate

No change

Sources and Probability of Activity

Intra-slab: 1.0 given the historical record

Interface: no change

Location of Rupture

No change

Maximum Earthquake Magnitude

No change

Recurrence-Related Parameters

Inter-slab: no change

Interface: assessment of coupling ( $\alpha$ ) is unchanged but this does not provide an appropriate constraint on earthquake recurrence

- Based on the absence of thrust events in historical record and the evidence from magnetotellurics data showing a thick sequence of subducted sediments, the recurrence interval for M5 earthquake should be about 50-100 yr.

## PHASE II

## RESPONSES BY EXPERT #14

Note: This summary includes significant changes made to the Phase I assessments. If no change was indicated and/or previously made arguments still apply, the reader is directed to the Phase I summaries.

Geometry

Use slab geometry implied by recent studies of Crosson and Owens, including the arch in the slab along strike. The previous "model B" is abandoned.

Convergence Rate

No change

Location of Rupture

Intra-slab: no change

Interface: Updip extent at coastline with weaker materials in wedge west of this point. Downdip 40 to 50 km based on worldwide analogies. The morphology of the coast (uplifted marine terraces, etc.) suggests differences north and south of the Columbia River, as does the southern limit of deep seismicity in subducting plate farther inland and the probable change in North American plate stress state (based on different pattern in Washington and Oregon of Quaternary volcanism). Therefore, a segmentation point near this location is believed likely. The abrupt northern cutoff in the upper- and lower-plate seismicity and the change in trend of the subduction zone argue for segmentation near the south end of Vancouver Island (Strait of Juan de Fuca).

Segmented: 0.85 (Nootka to Blanco segmented at south end of Vancouver Island at Columbia River)

Unsegmented: 0.15 (Nootka to Blanco)

Probability of Activity

Intra-slab: no change

Interface: the probability of activity is a function of the segmentation

Unsegmented:  $p(\text{activity}) = 0.35 \pm 0.25$

Segmented:  $p(\text{activity north of Columbia River both segments})$   
 $= 0.4 \pm 0.2$

$p(\text{activity south of Columbia River}) = 0.2 \pm 0.2$

This is based on the fact that no Holocene terraces are present along the Oregon coast and that the large estuaries are present along the Washington coast. Note that these estimates are essentially equivalent to those of Phase I except the uncertainty ranges are larger due to the recent studies that support both seismic and aseismic subduction.

#### Maximum Earthquake Magnitude

Intra-slab: no change

Interface:  $8.5 \pm 0.5$  based to some extent on rupture dimensions

#### Recurrence-Related Parameters

Intra-slab: no change

Interface: the following distribution is given for seismic coupling

<u><math>\alpha</math></u>	<u>Weight</u>
0.01	0.2
0.05	0.4
0.10	0.2
0.15	0.15
0.5	0.05

Low coupling is indicated by the studies of Sammis that show that the thermal age of the Juan de Fuca plate is very young ( $< 8\text{Ma}$ ) due to thermal insulation by sediment blanketing. Low coupling is supported by the Kanamori and Astiz relation between plate age and coupling. A coupling of 0.5 is very unlikely because we have not observed small-magnitude interface events.

## APPENDIX B

## CHARACTERIZATION OF SHALLOW CRUSTAL SEISMIC SOURCES

## B.1 INTRODUCTION

The seismic hazard analysis for the Satsop site considers all possible sources of seismicity that may affect ground motions at the site. The potential sources related to subduction were identified by the expert panel. Discussed here are the potential seismic sources in the shallow crust (upper 25 km) in the site region. The shallow sources were identified and characterized based on extensive studies conducted for the site as part of site characterization by the Washington Public Power Supply System.

The investigations for the PSAR and FSAR (Appendix 2.5F) as well as for the NRC Geosciences Review Questions (Questions 231.1 through 231.7, submitted in June, 1986) address the capability of the faults and structures in the site locality (the area within about 16 km of the site and locally to more than 40 km from the site). This information provides insight into the tectonic evolution and non-capability of the shallow crustal structures in the vicinity of the site. The characteristics of the structures in the site locality are discussed below.

Studies conducted for the WNP-3 PSAR (WPPSS, 1974) and FSAR (WPPSS, 1982) resulted in the identification of five potential seismic sources in the Puget-Willamette Trough of the shallow crust of the North American plate east of the site. Four of the potential sources are geophysical lineaments defined primarily by linear gravity gradients associated spatially with shallow crustal seismicity of the Puget Trough and with interpreted displacements of Quaternary sediments underlying the Puget Sound region. The fifth potential source is defined by a linear zone of seismicity near Mt. St. Helens. The general characteristics of the potential shallow crustal seismic sources are presented in Table B-1.

For purposes of this seismic hazard analysis, several other seismic source zones were identified to account for regional earthquake sources that might affect ground motions at the site as well as to account for possible "unidentified" seismic sources in the site locality. Figure B-1 shows a plot of the North American plate seismicity and shows the boundaries of the seismic source zones used in the hazard analysis.

## B.2 DESCRIPTION OF POTENTIAL SHALLOW CRUSTAL SEISMIC SOURCES

Given here is a general description of the various potential crustal seismic sources. This is followed by a summary of the characteristics of each source that are important to the hazard analysis (i.e., maximum magnitude and earthquake recurrence).

### B.2.1 Sources Related to Geologic/Geophysical Features

B.2.1.1 Olympia Lineament. The Olympia lineament is well-defined by a northwest-trending 80 to 90 mgal linear gravity anomaly located at the southern end of Puget Sound, northeast of the site (Response to Question 231.7; WPPSS, 1982). The steepness of the anomaly diminishes abruptly to the northwest as it approaches the Hood Canal lineament and also to the southeast. The Olympia lineament delineates the southwestern margin of the Puget Sound tectonic subprovince and is drawn coincident with the northeasternmost exposures of the Crescent Basalt on the northeastern flank of the Black Hills (WPPSS, 1982).

The Olympia lineament is 35 km northeast of the site at its closest approach and is about 88 km long. The character of the gravity anomaly would suggest that the lineament may represent a northeast-dipping normal fault that juxtaposes thick Quaternary sediments underlying Puget Sound against the basaltic bedrock of the Black Hills. The length of the lineament (88 km) is defined by the length of the gravity anomaly and constrained by geologic evidence at the ends of the lineament that suggests that it does not extend beyond its defined length (Response to Question 231.7; WPPSS, 1982). Exposed Miocene and older formations along the projection of the lineament at either end have not been displaced and late Eocene volcanics beyond the southeast end do not exhibit displacement (in terms of the sense or the amount) consistent with the mapped portion of the Olympia lineament.

The Olympia lineament is considered to be a capable fault because of its spatial association to other steep, linear gravity gradients beneath Puget Sound that have been interpreted to be active normal faults (Response to Question 231.7, WPPSS, 1982; Rogers, 1970; Danes et al., 1965). The thickness of unconsolidated deposits mapped across the lineament (Hall and Othberg, 1974) suggest between 120 and 240 m of normal fault displacement along the Olympia lineament during the Pleistocene. The age of the base of the unconsolidated Pleistocene deposits is interpreted to be from 500,000 to 1.8 million years old. Thus, there has been approximately 120 to 240 m of normal displacement across the Olympia lineament in the past 500,000 to 1.8 million years.

B.2.1.2 Shelton Lineament. The Shelton lineament is poorly expressed on the gravity data for the Puget Sound region and it was initially identified and located by Rogers (1970) on the basis of limited geophysical and geomorphic data (WPPSS, 1982). The lineament trends northeast for a distance of about 48 km from its junction with the Olympia lineament where it is 35 km from the site at its closest approach. The Shelton lineament terminates at its southwestern end against the Olympia lineament whose gravity gradient is undisturbed and where the exposures of Crescent Basalt in the Black Hills are similarly undisturbed. To the northeast, the length of the lineament is constrained by undisplaced Tertiary volcanics and intrusives across its projection.

The Shelton lineament is considered to be a capable normal fault, dipping to the northwest, based on its spatial relationship to the set of steep gravity



gradients that exist under Puget Sound and have been interpreted to be active (WPPSS, 1982; Rogers, 1970; Danes et al., 1965). The change in thickness of unconsolidated Pleistocene deposits across the lineament (Hall and Othberg, 1974) would suggest from 240 to 360 m of normal slip in the past 500,000 to 1.8 million years.

**B.2.1.3 Hood Canal Lineament.** The Hood Canal lineament is well-expressed on the gravity data for the Puget Sound region as a northeast-trending linear anomaly and it is also well-expressed topographically as seen in the linear nature of Hood Canal. It separates the Puget Trough tectonic sub-province on the east from the Olympic Mountains on the west.

The Hood Canal lineament is interpreted to be an east-dipping normal fault. The lineament is about 45 km north-northwest of the site at its closest approach where it joins the northwest termination of the Olympia lineament. The length of the Hood Canal lineament (96 km) is constrained at its southwest end because the geologic data along a postulated southwest extension do not support the existence of a major structure such as the lineament and the gravity data to the southwest are not consistent in sense or magnitude to support such an extension (WPPSS, 1982).

The Hood Canal lineament is interpreted to represent a capable normal fault based on its association to other gravity anomalies under Puget Sound that have been interpreted to be active normal faults (WPPSS, 1982; Rogers, 1970; Danes et al., 1965). Danes et al. (1965) suggest there have been at least 3900 m of apparent vertical displacement across the lineament. Based on the change in thickness of unconsolidated Pleistocene deposits across the lineaments (Hall and Othberg, 1974) from 240 to 480 m of normal slip is interpreted to have occurred in the past 500,000 to 1.8 million years.

**B.2.1.4 Nisqually Lineament.** The Nisqually lineament, as defined by Rogers (1970), is located subparallel to and about 13 to 18 km northeast of the Olympia lineament (WPPSS, 1982). The lineament is not well-defined on the regional gravity data for Puget Sound and it appears to be part of the shallow gradient of the north-east base of the broad linear anomaly that describes the Olympia lineament. Rogers (1970) identified that lineament on the basis of limited gravity and geomorphic evidence (WPPSS, 1982).

The Nisqually lineament is interpreted to be a northeast-dipping normal fault. It is 53 km northeast of the site at its closest approach. Its length of 80 km is constrained at the northwest end where it terminates against undisturbed Eocene Crescent volcanics and to the southeast against Miocene and older volcanics (WPPSS, 1982). The Nisqually lineament is interpreted to be capable because of its spatial association to other gravity anomalies under Puget Sound that have been considered to be active (WPPSS, 1982; Rogers, 1970; Danes et al., 1965). Changes in the thickness of unconsolidated Pleistocene deposits across the lineament (Hall and Othberg, 1974) would suggest between 120 and 240 m of normal displacement in the past 500,000 to 1.8 million years.

B.2.1.5 Mt. St. Helens Seismic Zone. The Mt. St. Helens seismic zone is defined by a north-northwest-trending alignment of earthquakes that extends about 96 km from just south of Mt. St. Helens to the southeast corner of Puget Sound (Weaver and Smith, 1983; WPPSS, 1982; Beaulieu and Peterson, 1981; Weaver and Smith, 1981). The zone is about 70 km east of the site at its closest approach. The seismic zone is identified on the basis of earthquakes ( $M_c > 2.8$ ) that occurred from mid-1970 to February 15, 1981 (Beaulieu and Peterson, 1981). The largest earthquake was  $M_c$  5.5 and all of the events were less than 20 km in depth (Beaulieu and Peterson, 1981; Weaver and Smith, 1981). Focal mechanisms suggest right-lateral strike-slip motion (Weaver and Smith, 1983). Estimates of the potential maximum magnitude for the Mt. St. Helens seismic zone by Beaulieu and Peterson (1981) indicate that  $M_s$  7.2 is a conservative maximum earthquake while  $M_s$  6.2 is a more reasonable maximum event for the zone.

#### B.2.2 Regional Seismic Source Zones

Several regional seismic source zones were identified that account for earthquake sources that cannot be identified as faults or localized geologic/geophysical structures. The source zones are shown in Figure B-1 and are discussed below.

The Puget Lowlands source zone is defined by the structurally defined Puget trough and the concentration of seismicity in this area. This source zone is distinguished from the Willamette Trough source zone to the south on the basis of a significantly lower level of seismicity to the south. The Olympic Peninsula source zone is tectonically distinct from surrounding tectonic provinces by the presence of Tertiary volcanics and differences in the level of seismicity from the Puget Lowlands to the east and the offshore region to the west. The Coast Range source zone is characterized tectonically as the older (late Tertiary) part of the accretionary wedge complex and is marked by significantly lower levels of seismicity than the Willamette Trough zone to the east. The Offshore zone extends as far west as the oceanic trench and consists of the younger parts of the accretionary wedge. This zone is marked by very low levels of seismicity.

#### B.2.3 Seismic Sources in the Site Locality

B.2.3.1 Faults in the Site Locality. In general, the structure of the site locality (32 km radius) site is characterized by northwest-trending folds and faults (Response to Questions 231.1 and 231.2; WPPSS, 1982). The faults occur as part of a regional, rectilinear northwest and east-northeast-trending pattern where the majority of the northwest-trending faults are steeply east-dipping reverse-slip and the east-northeast-trending faults are high-angle normal-slip or strike-slip. The reverse faults are oriented parallel to the major folds and considered to be genetically related to folding. The development of this pattern appears to have been the result of northeast-directed near-horizontal compression associated with late Tertiary subduction of the Farallon plate beneath the North American plate and development of an accretionary wedge (Response to Question 231.2).

The capability of more than forty faults at the site and within the site locality (including faults to almost 50 km from the site) was evaluated for the PSAR studies, studies leading to the FSAR, and studies in response to NRC review questions (Response to Question 231.1; WPPSS, 1982, Appendix 2.5F; WPPSS, 1974). The capability evaluations consisted of documenting the displacement history of each fault based on the age of the oldest features not disturbed by the fault or by genetic association of the fault with nearby faults for which the age of most recent displacement could be determined. The evaluations utilized several Quaternary features and stratigraphy (e.g., relict erosion surfaces, glacio-fluvial deposits, deep weathering profiles, paleosols) with ages from Holocene (10,000 years old) to early Pleistocene (1.8 million years old) to establish the ages of most recent movement (WPPSS, 1982).

Based on field studies that included detailed geologic mapping and mapping of more than 50 trenches, the faults in the site locality have been shown or interpreted to be not capable (Response to Question 231, 1986; NRC, 1985; WPPSS, 1982; WPPSS, 1974). These studies and evaluations indicate:

1. The faults in the site locality formed before and during a period of late Tertiary deformation that ceased by early Pleistocene.
2. The area containing the faults has been tectonically stable (with respect to folding and fault displacement) since early Pleistocene. This is evident in accordant summits of relict erosion surfaces, undisturbed deep weathering profiles, and the undisturbed and parallel nature of Pleistocene glacio-fluvial terrace surface profiles that cross the trends of the folds and faults.
3. A number of faults in the site locality are overlain by undisturbed early to late Pleistocene deposits. The resolution of these findings varies from less than one centimeter for detailed trenching to 1 to 5 m for detailed and reconnaissance level mapping, respectively.
4. In no case is there evidence to suggest that faults in the site locality have been tectonically active during the Holocene or Pleistocene.

The faults and folds in the site locality are interpreted to have formed in a subduction zone accretionary complex during the Tertiary (Response to Questions 231.1 and 231.2). They initiated as shallow-dipping thrusts in the accretionary prism and were rotated to more steeply dipping orientations as new sediment was added to the front with continued subduction. As the accretionary complex built seaward with the addition of new sediment at the accretionary front, the older sediments and thrust faults entered a progressively more stable tectonic environment. The seaward migration of the active accretionary complex has resulted in the site now being located some 180 km east of the zone of current deformation. This general model of abandonment of active faulting and propagation of deformation seaward is documented by

Moore and Byrne (1987). Consequently, although the faults in the site locality were most likely formed as the result of subduction and accretion, they are now much removed from that setting and should no longer be expected to be active.

B.2.3.2 Possible Unidentified Seismic Sources in Site Locality. For the probabilistic seismic hazard analysis, consideration is given to the possibility of local "unidentified" crustal seismic sources that may have escaped detection during the detailed studies in the site locality. This source is modeled in the hazard analysis as a randomly located source within 32 km of the site.

### B.3 SHALLOW CRUSTAL SEISMIC SOURCE CHARACTERISTICS

Based on the data and interpretations summarized above, each potential seismic source was characterized by those parameters required for the seismic hazard analysis: closest distance to the site, maximum magnitude, slip rate (if known), and earthquake recurrence. These parameters are given in Table B-2.

#### B.3.1 Maximum Magnitude

The maximum magnitude for the sources related to geologic/geophysical features are those developed in WPPSS (1982, Appendix 2.5J). The maximum magnitude for the Puget Lowlands and Willamette Trough source zones was assessed to be 7.5, which is similar to that assessed for the lineaments within the trough. The maximum magnitudes for both the Olympic Peninsula and Coast Range source zones are assessed to be  $5\frac{1}{2}$  -  $7\frac{1}{2}$ .  $5\frac{1}{2}$  is slightly larger than the largest historically-observed event in these zones;  $7\frac{1}{2}$  is the size of the largest earthquakes observed in other tectonically-analogous accretionary wedges and is allowed by the variable level of geologic resolution of mapping at more remote parts of these source zones. The maximum magnitude assessed for the offshore source zone is  $5\frac{1}{2}$  - 6, based on the fact that this is the young part of the accretionary wedge and analogous regions at other subduction zones show similar maximum events.

The maximum earthquake associated with the site locality source zone (within 32 km) is a function of the historical seismicity and the resolution of geologic studies. The historical and instrumental record of seismicity shows that the largest shallow crustal earthquakes within the landward part of the accretionary wedge are less than magnitude 4 (WPPSS, 1982). Recent analysis of the 1904 earthquake by Rogers (1983) shows that it was about magnitude 5 and located in the western Puget Sound region, and not on the western Olympic Peninsula as previously reported. Because of the relatively short period of the historical record, this maximum observed magnitude may not be an appropriate maximum for the seismic source.

As discussed previously in this appendix, the level of resolution of geologic studies in the site locality ranges from less than one centimeter in trench exposures, to about one meter in areas of detailed mapping, to about five meters in areas of reconnaissance-level mapping. Simply stated, the

resolution is the maximum amount of cumulative deformation (either fault displacement or folding) that could escape detection in the geologic studies. In general, the Quaternary deposits and geomorphic surfaces that exist in the site locality are a few hundred thousand to over one million years old (WFPSS, 1984; Figure 2.5F-53). For example, the terraces along the Chehalis River, which show no evidence of fault displacement or tilting, are estimated to be about 320,000 yr old. Given the antiquity of the deposits, a fault generating repeated large-magnitude displacements and/or associated folding would be expected to be detected in the geologic investigations. Because of the long time period represented by the Quaternary deposits and surfaces, only very small deformations (few tens of centimeters per event) with probable long repeat times (tens to hundreds of thousands of years) could escape geologic expression within the resolution. It is estimated that the maximum size of these events would be about  $6 \pm \frac{1}{2}$ , based on existing correlations of displacement with magnitude.

### B.3.2 Earthquake Recurrence

Slip rates were used to develop recurrence relationships for the geologic/geophysical sources based on the seismic moment rate approach (Anderson and Luco, 1983; Youngs and Coppersmith, 1985). The recurrence relationship for all of the seismic source zones are estimated based on the recurrence relationships from the seismicity record extrapolated to the maximum magnitude. As indicated in Section C.3 and Figures C-19 through C-24, distributions of recurrence relationships are used in the analysis to quantify the uncertainty in estimating recurrence based on the seismicity catalogs. Figure B-2 compares the mean recurrence rates for the various shallow crustal sources. In developing the recurrence relationships for the geophysical lineaments on the basis of slip rate, the b-value was assumed to be the same as obtained for the Puget Lowlands.

TABLE B-1

 POTENTIAL SHALLOW CRUSTAL SEISMIC SOURCES  
 RELATED TO GEOLOGIC/GEOPHYSICAL FEATURES

<u>Structure</u>	<u>Closest Distance to Site, km</u>	<u>Sense of Displacement</u>
Olympia Lineament	35	Normal
Shelton Lineament	35	Normal
Hood Canal Lineament	45	Normal
Nisqually Lineament	53	Normal
Mt. St. Helens Seismic Zone	70	Strike-slip

TABLE B-2

## SHALLOW CRUSTAL SEISMIC SOURCE CHARACTERISTICS

<u>Potential Source</u>	<u>Closest Distance to Site (km)</u>	<u>Maximum Magnitude (Ms)</u>	<u>Slip Rate (mm/yr)</u>
Olympia Lineament	35	7.4	0.07 - 0.48
Shelton Lineament	35	7.2	0.13 - 0.72
Hood Canal Lineament	45	7.5	0.13 - 0.96
Nisqually Lineament	53	7.4	0.07 - 0.48
Mt. St. Helens Seismic Zone	70	6.2 - 7.2	*
Puget Lowlands Source Zone	35	7.5	*
Willamette Trough Source Zone	35	7.5	*
Olympic Peninsula Source Zone	40	5½ - 7½	*
Coast Ranges Source Zone	32	5½ - 7½	*
Offshore Source Zone	54	5½ - 6	*
Site Locality Source Zone	0	6 ± ½	*

\*Recurrence assessed from historical seismicity record presented in Appendix C, Figures C-19 and C-24, and shown in Figure B-2.

## REFERENCES

- Anderson, J.G., and Luco, J.E., 1983, Consequences of slip rate constraints on earthquake recurrence relations: *Bulletin of the Seismological Society of America*, v. 73, p. 471-496.
- Beaulieu, J.D., and Peterson, N.V., 1981, Seismic and volcanic hazard evaluation of the Mount St. Helens area, Washington, relative to the Trojan Nuclear Site, Oregon: State of Oregon, Department of Geology and Mineral Industries Open-File Report O-81-9.
- Danes, Z.F., Borno, M.M., Brau, E., Gilham, W.D., Hoffman, T.F., Johansen, L., Jones, M.A., Malfait, B., Masten, J., and Teague, G.O., 1965, Geophysical investigations of the southern Puget Sound area, Washington: *Journal of Geophysical Research*, v. 70, p. 5573-5580.
- Hall, J.B., and Oehberg, K.L., 1974, Thickness of unconsolidated sediments, Puget Lowland, Washington: State of Washington, Division of Geology and Earth Resources Geologic Map GM-12.
- Moore, J.C., and Byrne, T., 1987, Thickening of fault zones: a mechanism of melange formation in accreting sediments: *Geology*, v. 15, p. 1040-1043.
- Nuclear Regulatory Commission (NRC), 1985, Draft Safety Evaluation Report, Washington Public Power Supply System Nuclear Project No. 3, Docket No. 50-508, November.
- Rogers, W.P., 1970, A geological and geophysical study of the central Puget Sound Lowland: Ph.D. Thesis, University of Washington, Seattle, Washington, 123 p.
- Rogers, G.C., 1983, Seismotectonics of British Columbia: Ph.D. dissertation, University of British Columbia, 247 p.
- Washington Public Power Supply System (WPPSS), 1974, WPPSS Nuclear Project Nos. 3 and 5, Preliminary Safety Analysis Report, Section 2.5 Geology and Seismology, Docket-STN-50508 and -50509.
- Washington Public Power Supply System (WPPSS), 1982, WPPSS Nuclear Project 3, Final Safety Analysis Report, 2.5 Geology and Seismology: Washington Public Power Supply System, Richland, Washington.
- Weaver, C.S., and Smith, S.W., 1981, St. Helens seismic zone: A major crustal fault zone in western Washington: Abstract, *Transactions of the American Geophysical Union, EOS*, v. 62, p. 699.

Weaver, C.S., and Smith, S.W., 1983, Regional tectonic and earthquake hazard implications of a crustal fault zone in southwestern Washington: *Journal of Geophysical Research*, v. 88, no. 13, p. 10,371-10,383.

Youngs, R.R., and Coppersmith, K.J., 1985, Implications of fault slip rates and earthquake recurrence models to probabilistic seismic hazard estimates: *Bulletin of the Seismological Society of America*, v. 75, p. 939-964.



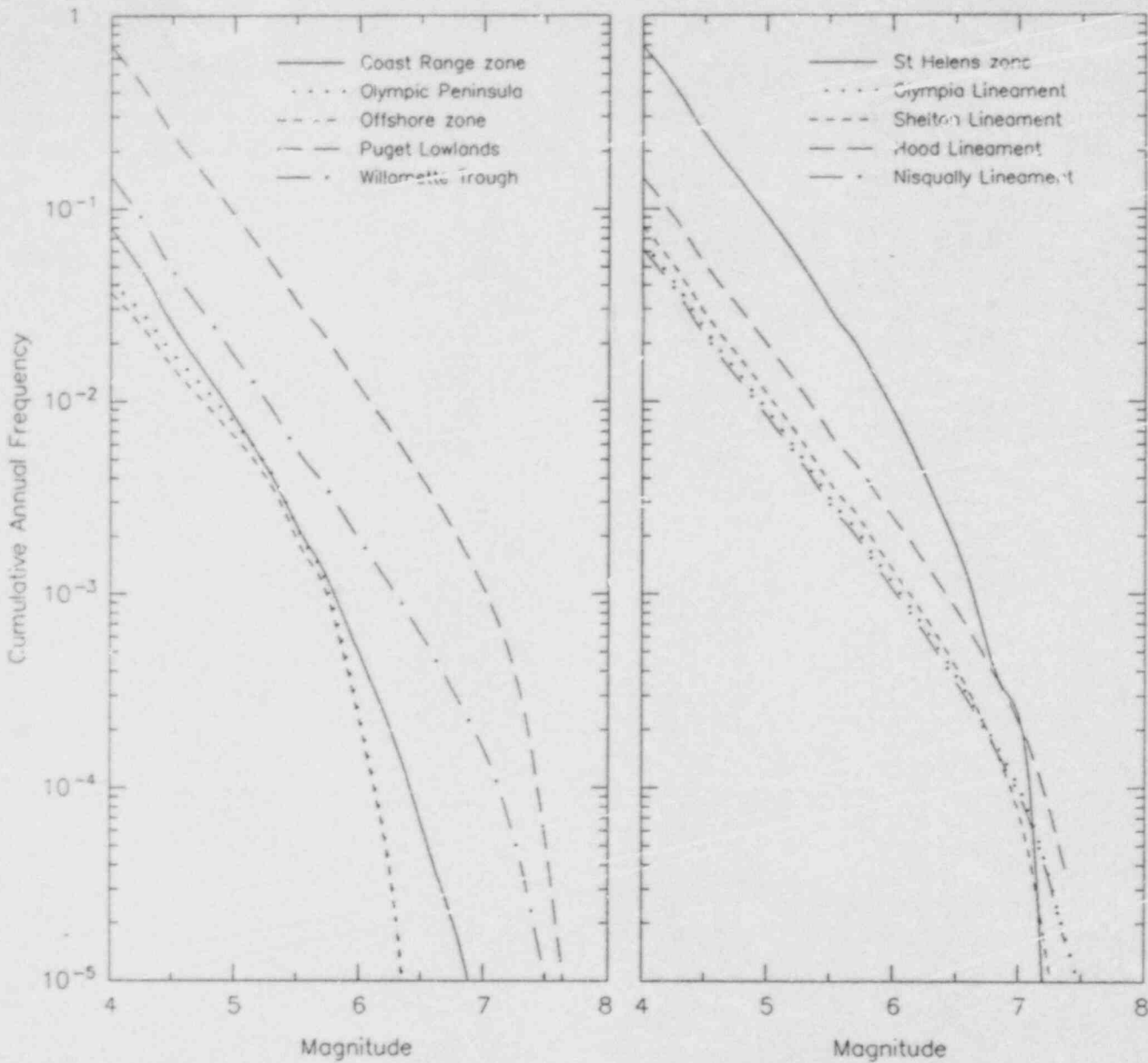


Figure B-2. Mean recurrence relationships for crustal sources.

WASHINGTON SEISMICITY  
SHALLOW SOURCE ZONES  
(MAG > 2.5)  
(St. Helens Zone events not plotted)

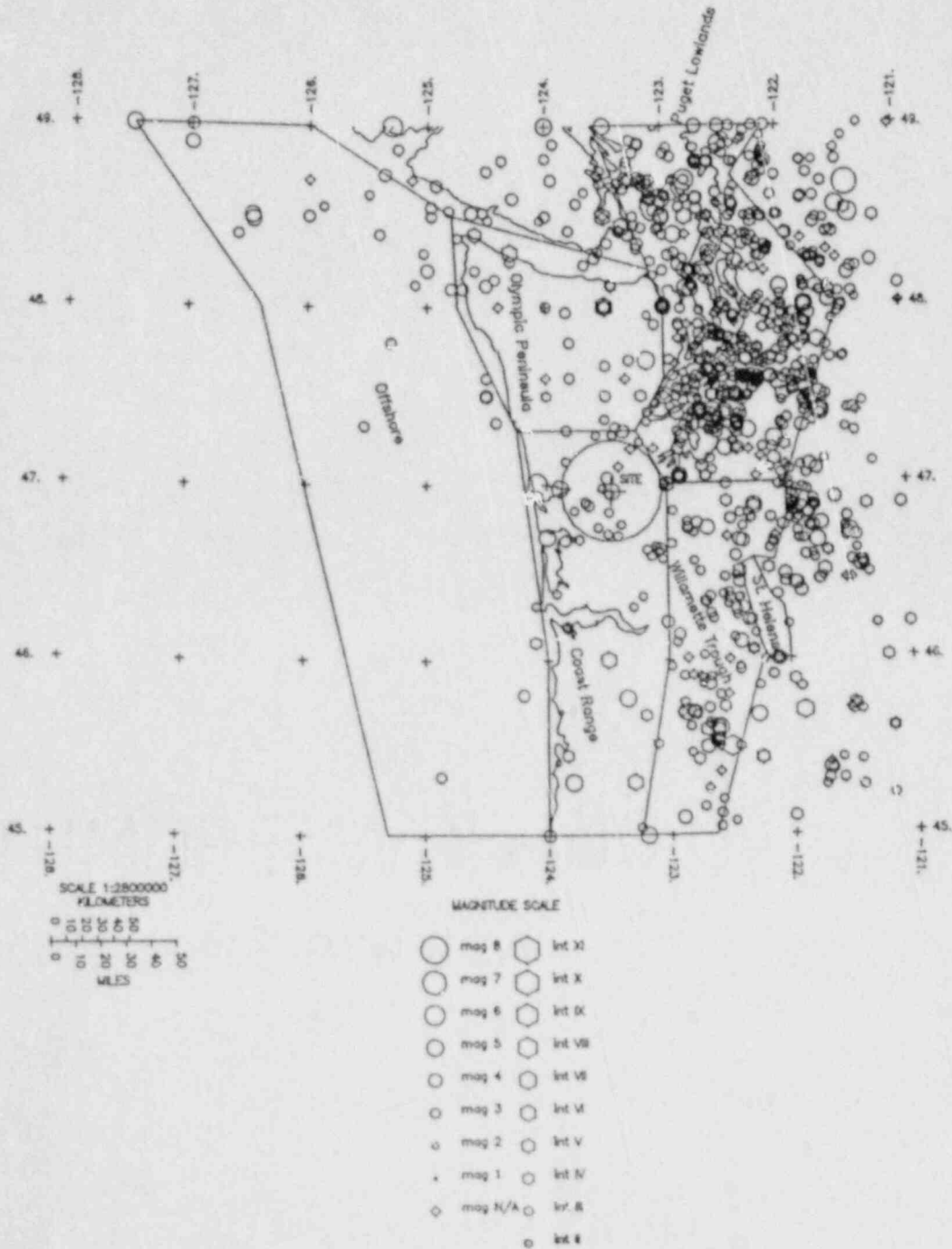


Figure B-1. North American crustal seismicity and source zones.

## APPENDIX C

## CATALOG EVALUATION AND RECURRENCE RATES

The earthquake catalog used in the seismic hazard evaluation of the WNP-3 site was compiled from four major data sources. For the historical period of coverage (1827-1969) three catalogs were combined. The Decade of North American Geology (DNAG) catalog (in preparation) was the primary source of information for this period since it contains the most recent data on historical seismicity in Washington State, and has been thoroughly reviewed by the University of Washington staff. The (DNAG) catalog, however, reports only those events in magnitude and time intervals for which the authors feel the historical record is complete. These magnitude thresholds are as follows (Ruth Ludwin personal communication):

prior to 1917 mag 5.75  
 1917 - 1939 mag 5.25  
 1940 - 1955 mag 4.75  
 1956 - 1964 mag 4.25  
 1965 - 1969 mag 3.75  
 1970 - 1986 mag 2.50

In an effort to provide as complete an earthquake catalog as possible, data from two other catalogs were combined with the DNAG catalog. These additional sources were the earthquake catalog reported in the WNP-3 FSAR (WPPSS, 1982) and the Rasmussen (1967) listing of historical earthquakes, as updated by Linda Nosen (University of Washington Geophysics Program, unpublished listing). If no magnitudes were listed for an event, then a local magnitude was estimated using the relationship  $M_L = 2/3 I_o + 1$  (Gutenberg and Richter, 1956).

For the period of instrumental coverage from 1970 to April, 1987, the University of Washington Catalog was the primary data source. Additional events included in the DNAG catalog but not present in the University of Washington listing were also needed. Although most of the earthquakes reported by the University of Washington for the period (1970 - 1986) are also included in the DNAG catalog, data from the University of Washington was used preferentially because the DNAG catalog lists only the largest of all magnitudes reported by a number of sources for a particular event rather than a consistent magnitude scale. The University of Washington, on the other hand, has gone to considerable effort to ensure the consistency of the reported data, particularly with regard to reported magnitude. The magnitudes are reported as coda length magnitude,  $M_c$ , which has been calibrated to be equivalent to  $M_L$  (Crosson, 1972).

Figures C-1 and C-2 present epicentral plots of the catalogs. Figure C-1 shows those events of magnitude 2.5 or greater located in the North American plate (all events east of the trench axis with reported focal depths of 30 km or less). Figure C-2 shows those events of magnitude 1.0 or greater that lie within the subducting Juan de Fuca plate.

## C-2 EVALUATION OF CATALOG COMPLETENESS

The catalog compiled for this study was subdivided into seven geographical regions corresponding to the physiographic provinces defined in the WNP-3 FSAR. Figures C-1 and C-2 show the boundaries of these regions. For the North American plate, the regions are the Puget Lowlands, the Willamette Trough, the Mt. St. Helens seismic zone, the Olympic Peninsula, the Coast Range, and the Offshore zone.

Figure C-3 shows the completeness intervals for earthquake reporting in Washington that have been estimated by Stepp (1972) and Rogers (1983), and for the DNAG catalog as indicated above. These intervals reflect various changes in seismicity reporting for the region, which include: establishment of regularly published newspapers in the 1850's; opening of the Victoria, British Columbia seismograph station in 1898 (Rogers, 1983); systematic reporting of earthquake data by ISS beginning in 1917; addition of US postmasters to earthquake questionnaire canvass in 1929 (Stepp, 1972); and establishment of the University of Washington seismograph network in 1970. The University of Washington has estimated detection thresholds for the region at approximately magnitude 2 for the period 1970 through 1974 and approximately magnitude 1.5 for the period 1975 through 1984 (University of Washington, 1985).

The catalog completeness in the study region was evaluated for each of the zones identified in Figures C-1 and C-2. Figures C-4 through C-10 present plots of the observed frequency of occurrence of events in different magnitude intervals as a function of time before the present (April 1, 1987), with the observed frequency equal to the number of events observed in the last T years divided by T. The magnitude intervals were chosen to correspond to magnitudes estimated using unit intensities in the Gutenberg and Richter (1956) intensity-magnitude relationship for intensity II and greater. Each figure shows two plots, one for all events in the zone (left-hand plot) and one for independent events (right-hand plot) identified by applying empirical criteria for defining dependent events (foreshocks and aftershocks) described below. The plot for independent events removes the effects of large temporal clusters of earthquakes whose presence results in deviations from the assumed model for earthquake recurrence of independent Poisson arrivals.

The resulting completeness estimates are:

## Date after which Events are Considered Completely Reported

Magnitude Range	Puget Lowlands	Willamette Trough	Coast Range	Olympic Peninsula	Offshore Zone	Deep Zone
1.5-2.0	07/1980	07/1980	07/1980	07/1980	07/1980	07/1980
2.0-2.7	01/1970	07/1980	07/1980	07/1980	07/1980	01/1970
2.7-3.3	01/1970	01/1970	07/1980	07/1980	07/1980	01/1970
3.3-4.0	01/1950	01/1950	01/1970	01/1970	07/1980	01/1970
4.0-4.7	01/1950	01/1950	01/1950	07/1950	07/1980	01/1950
4.7-5.3	01/1930	01/1930	01/1950	01/1950	07/1980	01/1950

The July 1980 date was chosen to reflect the major increase in the coverage of the University of Washington's seismograph network that occurred in the first half of 1980. As there are too few events in the catalog to evaluate completeness for events greater than magnitude 5, the completeness intervals proposed by Rogers (1983) were used. The completeness periods for the Mount St. Helens zone are assumed to be the same as those listed above for the Willamette Trough.

The results for the onshore regions are in general agreement with the periods of completeness listed above. As can be seen, the installation of the University of Washington network in 1970 represents an abrupt boundary before which there were very few events reported below magnitude 4. The frequency versus time for the Mt. St. Helens seismic zone (Figure C-9) is complicated by numerous changes in instrumentation as well as continuing volcanic activity. The present level of complete detection appears to be about magnitude 1.5 to 2 for all of the zones except the offshore zone where the level of detection is magnitude 3 or greater.

### C.3 EARTHQUAKE RECURRENCE

Earthquake recurrence relationships were developed for each of the provinces identified in Figures C-1 and C-2. The recurrence relationships are based on the maximum likelihood method developed by Weichert (1980) and on the completeness intervals denoted above. The recurrence relationships are in the form of a truncated exponential distribution for the occurrence of independent earthquakes. Dependent events in the catalog (foreshocks and aftershocks) were identified using empirical criteria for the size in time and space of main shock-foreshock-aftershock sequences published by Arabasz and Robinson (1976), Gardner and Knopoff (1974), and Uhrhammer (1986). Figure C-11 shows the relationship between magnitude and the size of the time and distance windows specified by the three criteria. As Arabasz and Robinson (1976) present only temporal criteria for aftershock identification, a spatial criteria based on earthquake rupture size was defined using the data presented in Wyss (1979). The catalogs of independent events obtained using the three sets of criteria differ significantly only for events less than magnitude 4.0 and only for the Puget Lowlands, Willamette Trough, and St. Helens zones.

Figures C-12 through C-18 show the recurrence relationships developed for each of the zones. Each figure shows the cumulative earthquake frequencies obtained using all events and the cumulative frequency of independent events as determined by the three criteria for identifying dependent events shown in Figure C-11 when there are significant differences in the catalogs. A truncated exponential recurrence relationship was fit to each data set using the maximum likelihood technique developed by Weichert (1980). The relationship was fit to the data for magnitude 2.0 and larger as it appears that smaller magnitudes currently are not reported completely in many of the zones. A minimum magnitude of 1.5 was used for the Juan de Fuca plate zone and a minimum magnitude of 2.67 was used for the Offshore zone. The fitted recurrence relationships are shown in Figures C-12 through C-18 and the

recurrence relationship parameters are summarized in Table C-1. In general, the recurrence relationships for independent events have lower b-values and, correspondingly, higher estimates for the rate of larger events. As indicated in Figure C-17, approximately 90 percent of the events that have occurred in the Mount St. Helens zone can be classified as dependent events.

As indicated in Figures C-12 through C-18 and in Table C-1, there is significant uncertainty in assessing the earthquake recurrence rates for many of the zones because of the limited seismicity catalogs. This uncertainty was quantified by developing a joint distribution for  $N(m^0)$  and b-value using the relative likelihood of various parameter values given the observed seismic history (see Bender, 1983). This distribution was discretized into five recurrence relationships for use in the hazard analysis. Figures C-19 through C-25 show the resulting discrete recurrence relationships used to model the uncertainty in defining earthquake recurrence rates for each of the zones.

#### REFERENCES

- Arabasz, W.J., and Robinson, R., 1976, Microseismicity and geologic structure in the northern South Island, New Zealand: *New Zealand Journal of Geology and Geophysics*, v. 19, no. 2, p. 561-601.
- Bender, B., 1983, Maximum likelihood estimation of b-values for magnitude grouped data: *Bulletin of the Seismological Society of America*, v. 53, p. 831-852.
- Crosson, R.S., 1972, Small earthquakes, structure, and tectonics of the Puget Sound region: *Bulletin of the Seismological Society of America*, v. 62, no. 5, p. 1133-1171.
- Gardner, J.K., and L. Knopoff, 1974, Is the sequence of earthquakes in Southern California, with aftershocks removed, Poissonian: *Bulletin of the Seismological Society of America*, v. 64, no. 5, p. 1363-1367.
- Gutenberg, B., and C.F. Richter, 1956, Earthquake magnitude, intensity, energy, and acceleration: *Bulletin of the Seismological Society of America*, v. 46, p. 105-145.
- Rasmussen, N.H., 1967, Washington State earthquakes, 1840 through 1965: *Bulletin of the Seismological Society of America*, v. 57, p. 463-476.
- Stepp, J.C., 1972, Analysis of completeness of the earthquake sample in the Puget Sound area and its effect on statistical estimates of earthquake hazard: *Proceedings of the International Conference on Microzonation*, v. 2, p. 897-910.
- Urhammer, R.A., 1986, Characteristics of northern and central California seismicity (abs.): *Earthquake Notes*, v. 57, no. 1, p. 21.

Washington Public Power Supply System (WPPSS), 1982, WPPSS Nuclear Project 3, Final Safety Analysis Report, 2.5 Geology and Seismology: Washington Public Power Supply System, Richland, Washington.

Weichert, D.H., 1980, Estimation of the earthquake recurrence parameters for unequal observation periods for different magnitudes: Bulletin of the Seismological Society of America, v. 70, no. 4, p. 1337-1346.

Wyss, M., 1979, Estimating maximum expected magnitude of earthquakes from fault dimensions: Geology, v. 7, no. 7, p. 336-340.

TABLE C-1. EARTHQUAKE RECURRENCE PARAMETERS

Zone	Parameter*	All Events	Criteria 1	Criteria 2	Criteria 3
Coast	$N(m^0)$	3.8( $\pm 0.5$ )	3.7( $\pm 0.5$ )	3.5( $\pm 0.5$ )	3.0( $\pm 0.4$ )
Ranges	b	0.995( $\pm 0.094$ )	0.988( $\pm 0.094$ )	0.967( $\pm 0.094$ )	0.913( $\pm 0.093$ )
Olympic	$N(m^0)$	0.64( $\pm 0.22$ )	0.64( $\pm 0.22$ )	0.64( $\pm 0.22$ )	0.64( $\pm 0.22$ )
Peninsula	b	0.664( $\pm 0.151$ )	0.664( $\pm 0.151$ )	0.664( $\pm 0.151$ )	0.664( $\pm 0.151$ )
Offshore	$N(m^0)$	0.08( $\pm 0.04$ )	0.08( $\pm 0.04$ )	0.08( $\pm 0.04$ )	0.08( $\pm 0.04$ )
Zone	b	0.903( $\pm 0.565$ )	0.903( $\pm 0.130$ )	0.903( $\pm 0.565$ )	0.903( $\pm 0.565$ )
Mt. St.	$N(m^0)$	1223( $\pm 30.1$ )	131( $\pm 11.6$ )	68.6( $\pm 8.3$ )	27.9( $\pm 4.5$ )
Helens	b	0.683( $\pm 0.012$ )	1.053( $\pm 0.066$ )	1.010( $\pm 0.086$ )	0.654( $\pm 0.074$ )
Puget	$N(m^0)$	24.3( $\pm 0.8$ )	20.9( $\pm 0.7$ )	17.5( $\pm 0.5$ )	11.1( $\pm 0.5$ )
Lowlands	b	0.922( $\pm 0.024$ )	0.898( $\pm 0.025$ )	0.867( $\pm 0.026$ )	0.723( $\pm 0.025$ )
Willamette	$N(m^0)$	10.7( $\pm 0.9$ )	9.5( $\pm 0.8$ )	8.3( $\pm 0.8$ )	6.2( $\pm 0.6$ )
Trough	b	0.955( $\pm 0.056$ )	0.925( $\pm 0.057$ )	0.930( $\pm 0.061$ )	0.804( $\pm 0.058$ )
Juan de	$N(m^0)$	1.3( $\pm 0.08$ )	1.3( $\pm 0.08$ )	1.3( $\pm 0.08$ )	1.3( $\pm 0.08$ )
Fuca	b	0.596( $\pm 0.030$ )	0.596( $\pm 0.030$ )	0.596( $\pm 0.030$ )	0.596( $\pm 0.030$ )

\* $N(m^0)$  = annual number of events  $\geq M_L$  2/10,000 km<sup>2</sup> for all zones except offshore which is  $\geq M_L$  2.7/10,000 km<sup>2</sup> and Juan de Fuca which is  $\geq M_L$  1.5/10,000 km<sup>2</sup>



WASHINGTON SEISMICITY  
SHALLOW SOURCE ZONES  
(MAG > 2.5)  
(St. Helens Zone events not plotted)

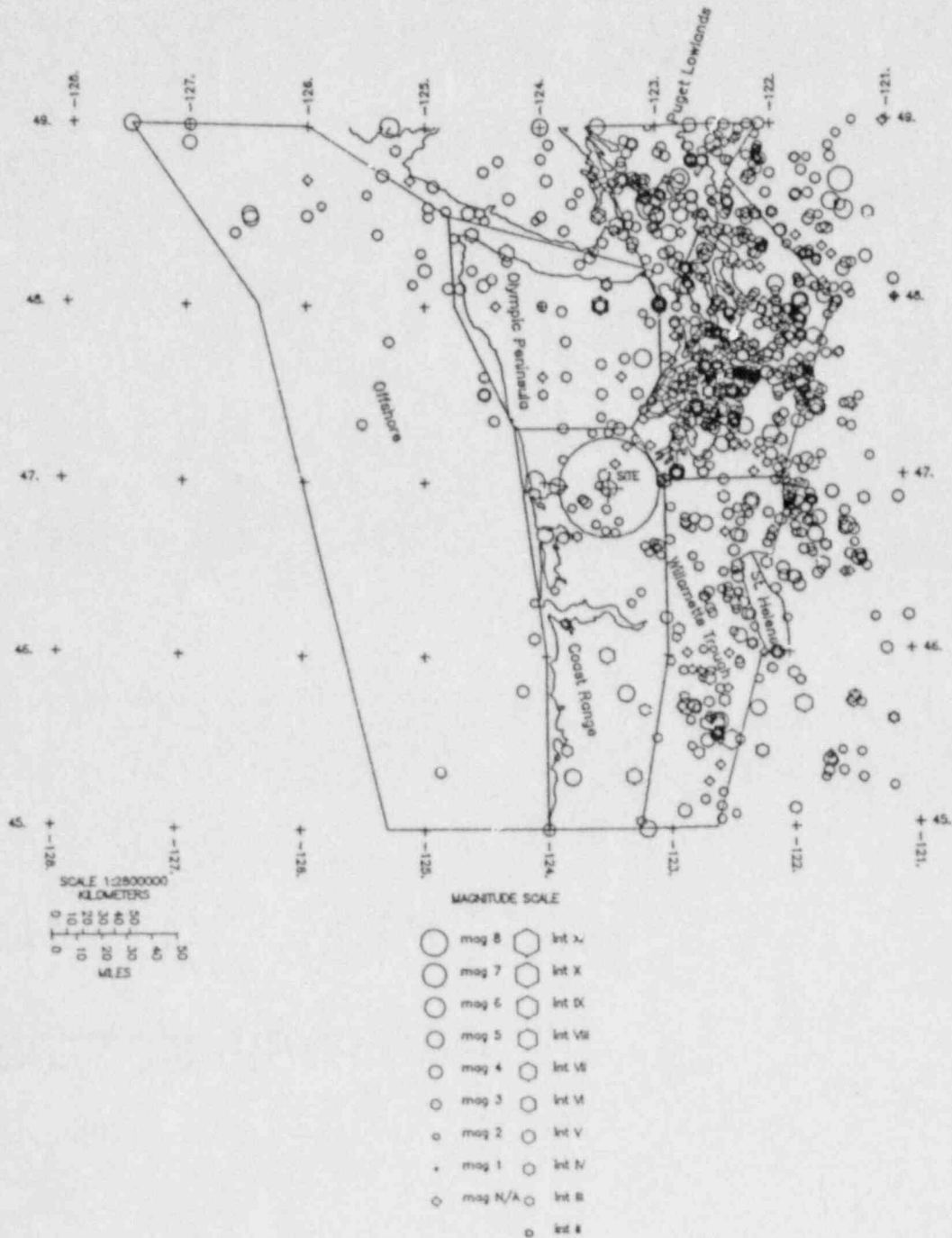


Figure C-1. North American crustal seismicity and source zones.

WASHINGTON SEISMICITY  
DEEP SEISMICITY  
(MAG>1.0)

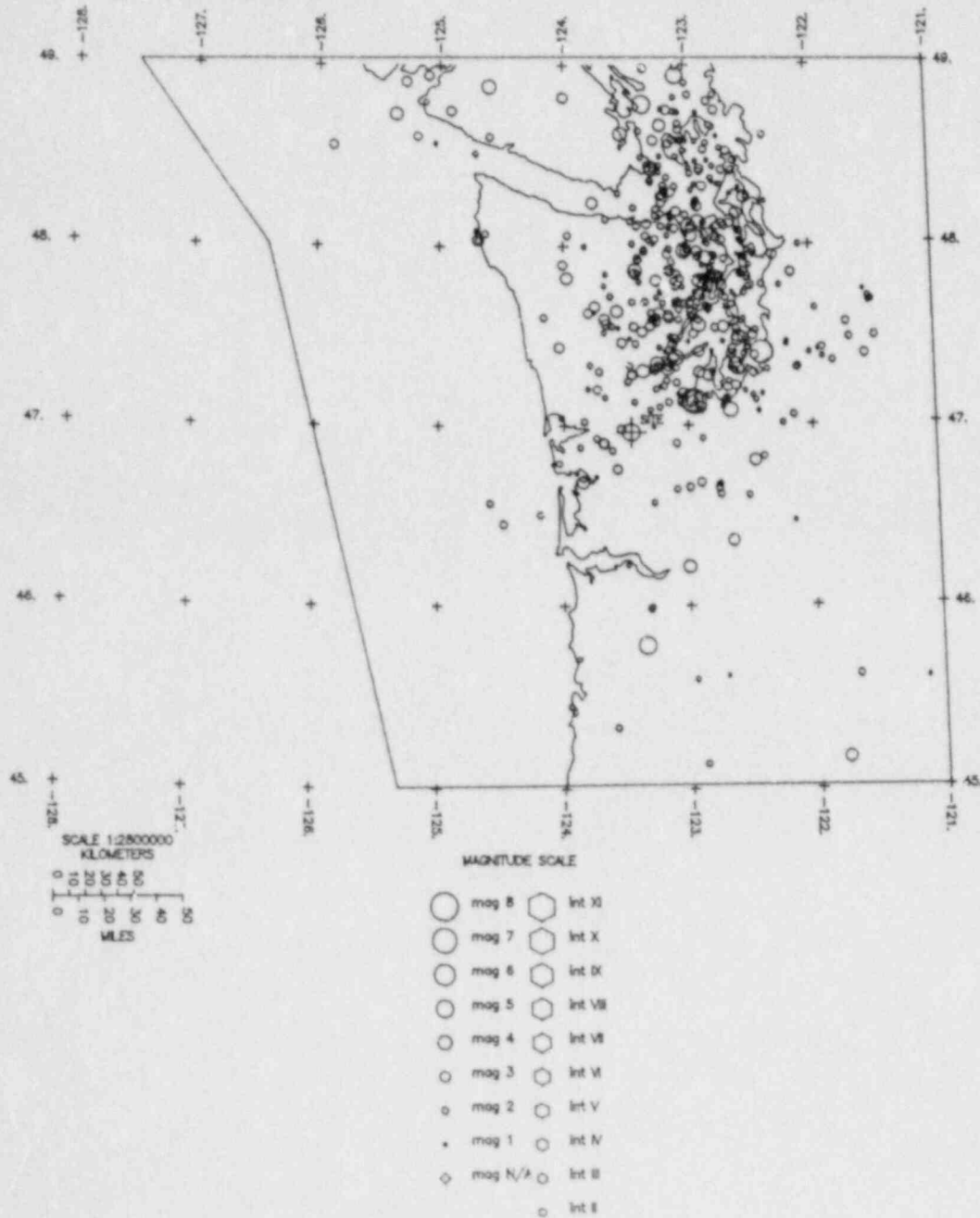


Figure C-2. Subducting Juan de Fuca Plate Seismicity.

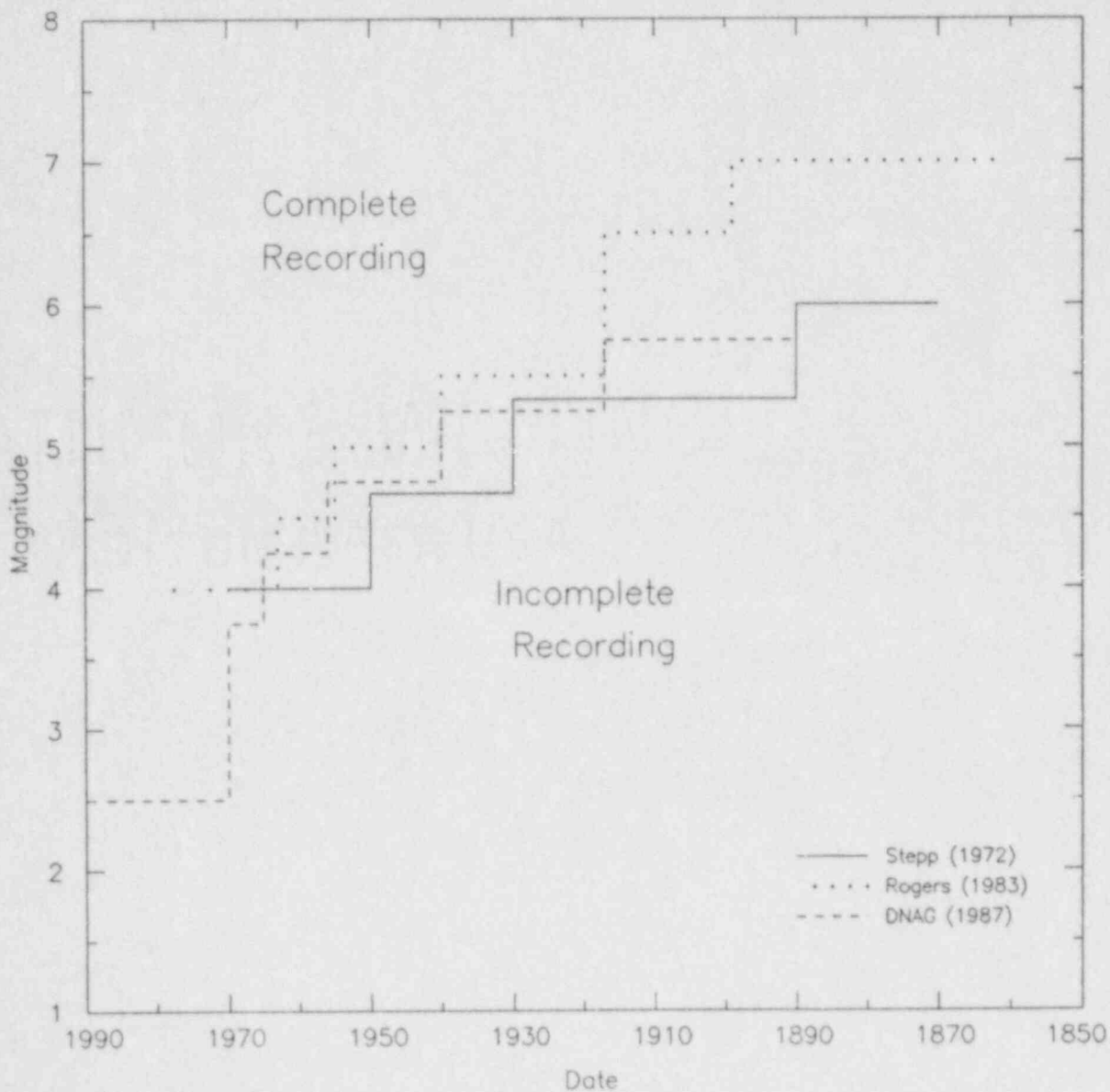


Figure C-3. Catalog completeness estimates for western Washington State.

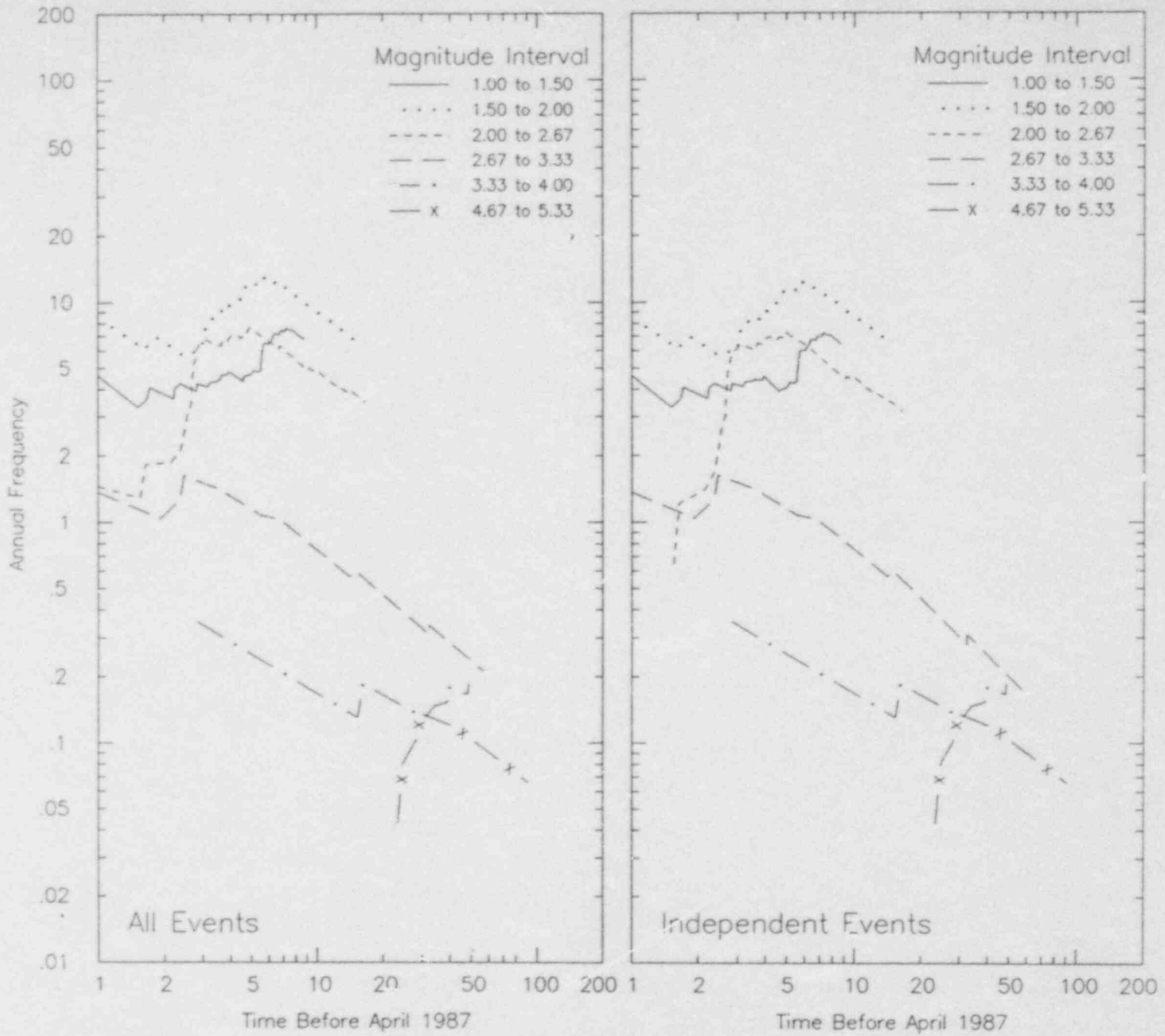


Figure C-4. Earthquake frequency vs time before present for Coast Range zone.

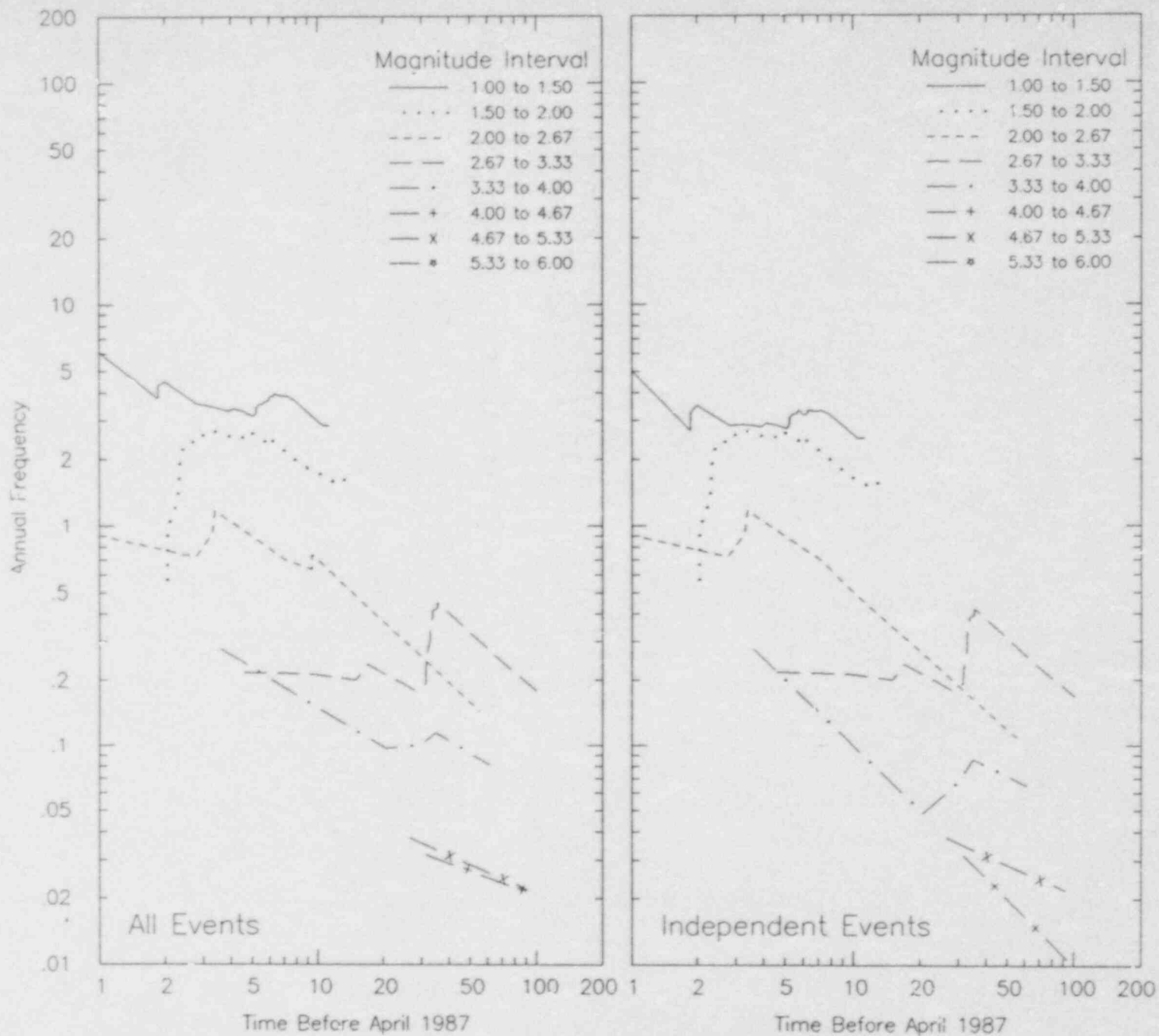


Figure C-5. Earthquake frequency vs time before present for Olympic Peninsula zone.

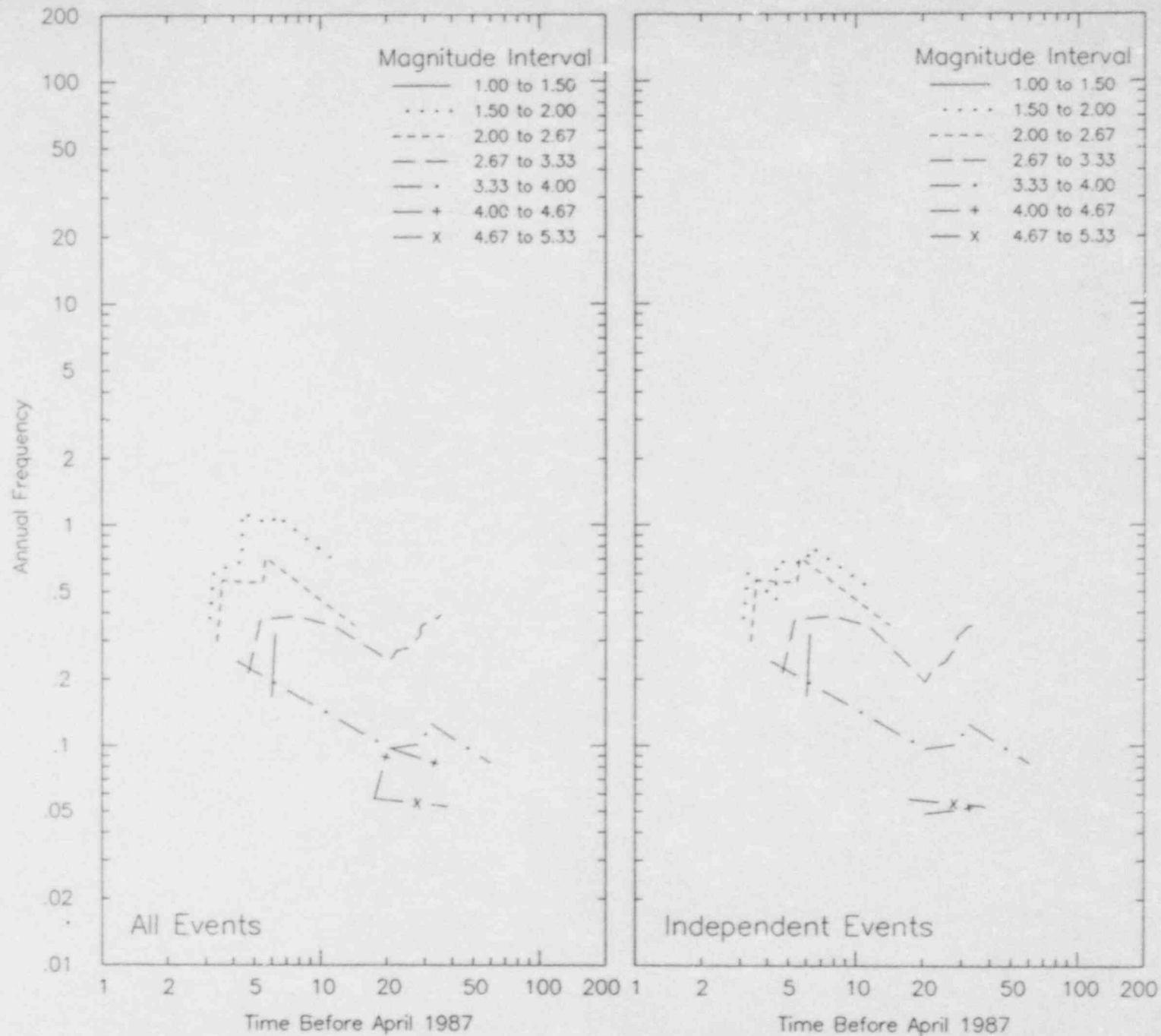


Figure C-6. Earthquake frequency vs time before present for Offshore zone.

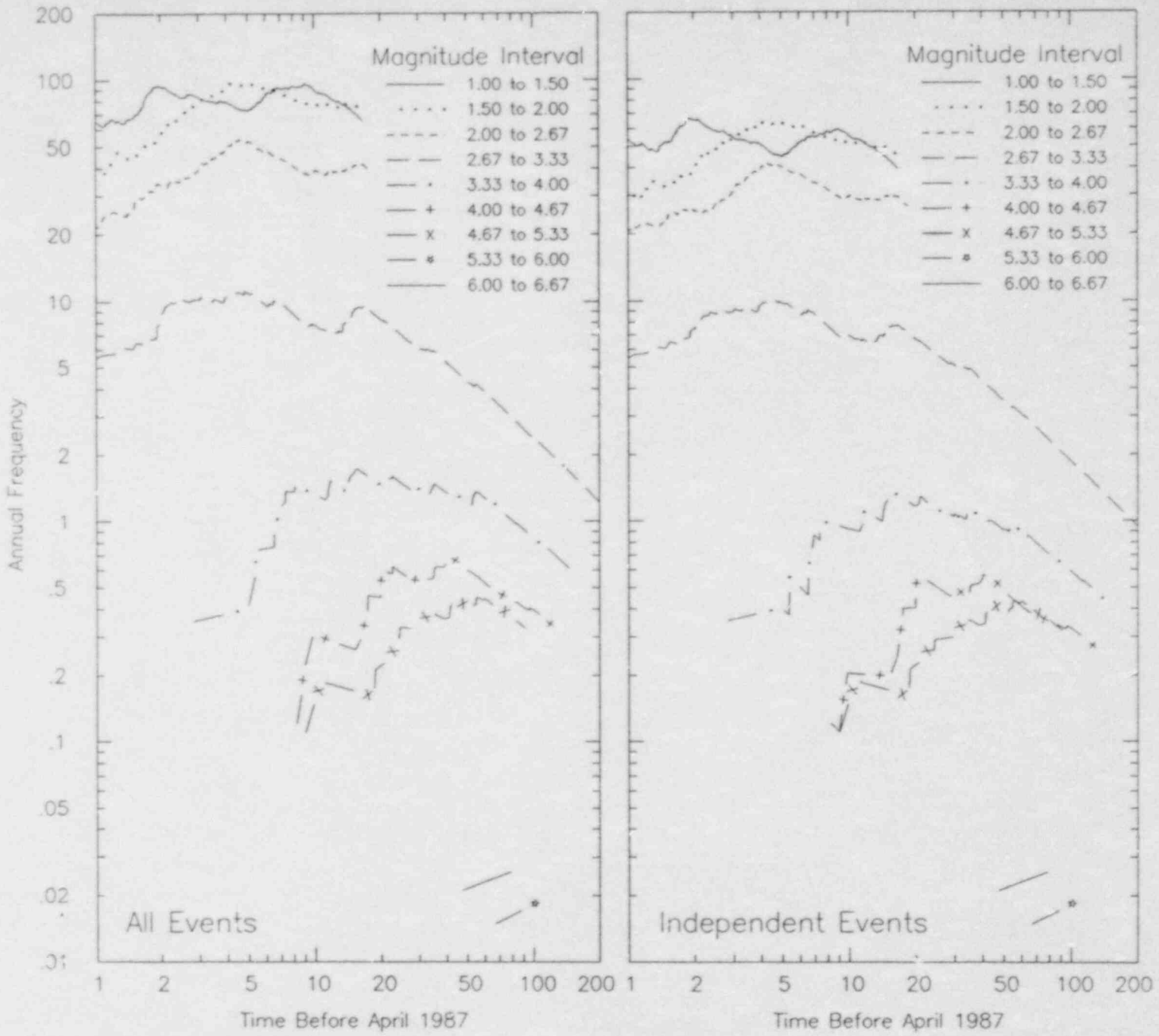


Figure C-7. Earthquake frequency vs time before present for Puget Lowlands.

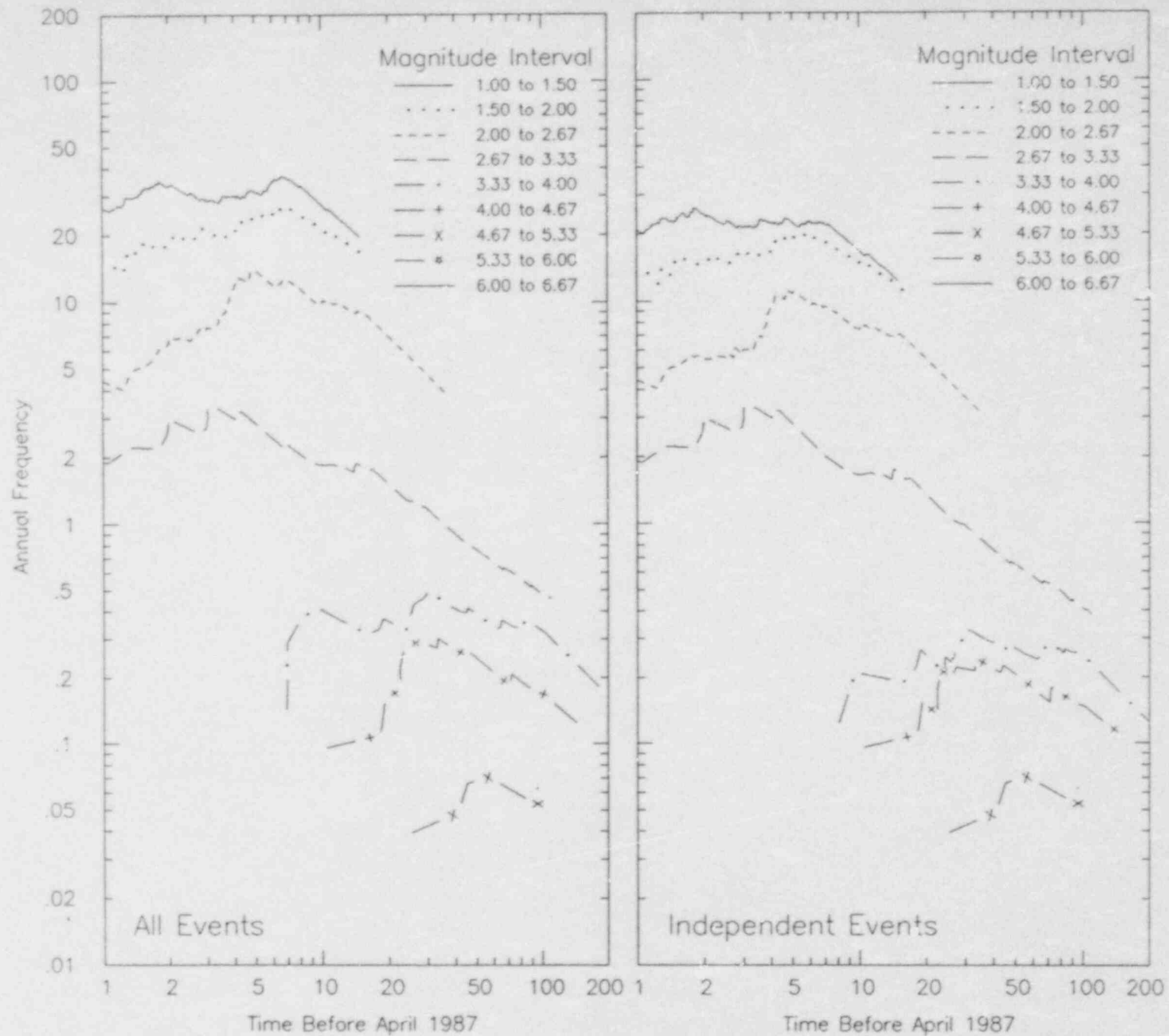


Figure C-8. Earthquake frequency vs time before present for Willamette Trough.



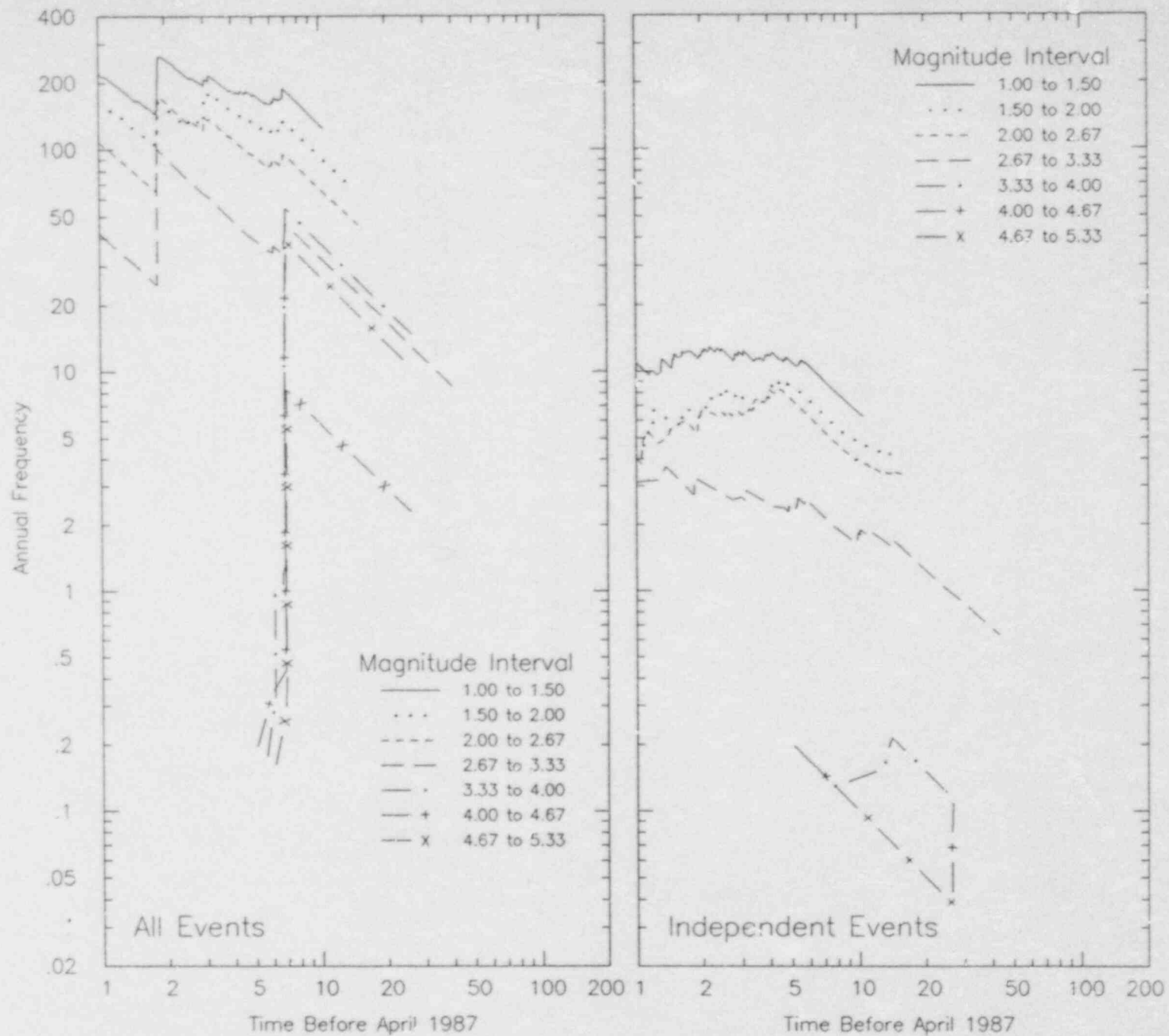


Figure C-9. Earthquake frequency vs time before present for St. Helens zone.

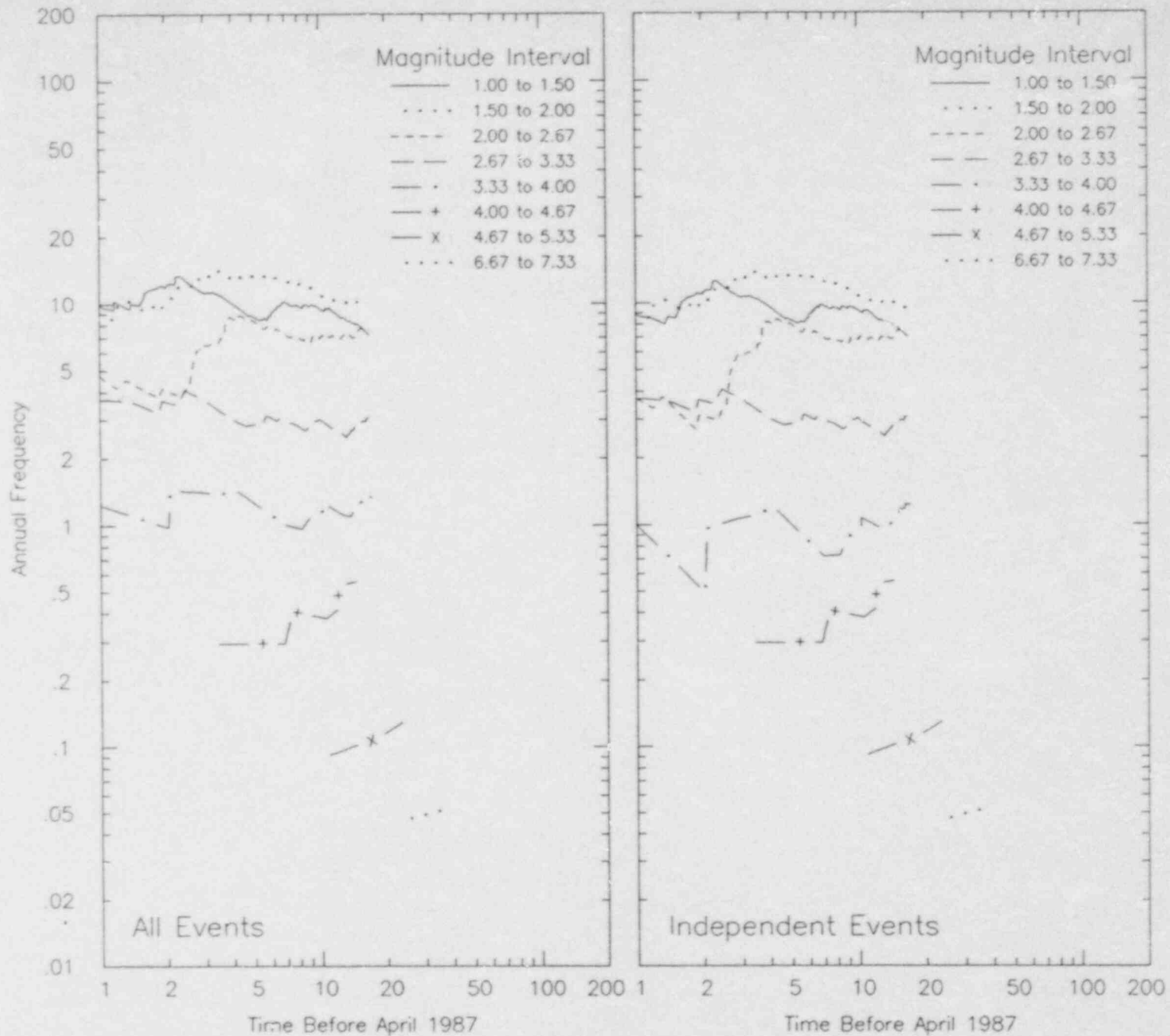


Figure C-10. Earthquake frequency vs time before present for subducting Juan de Fuca plate.

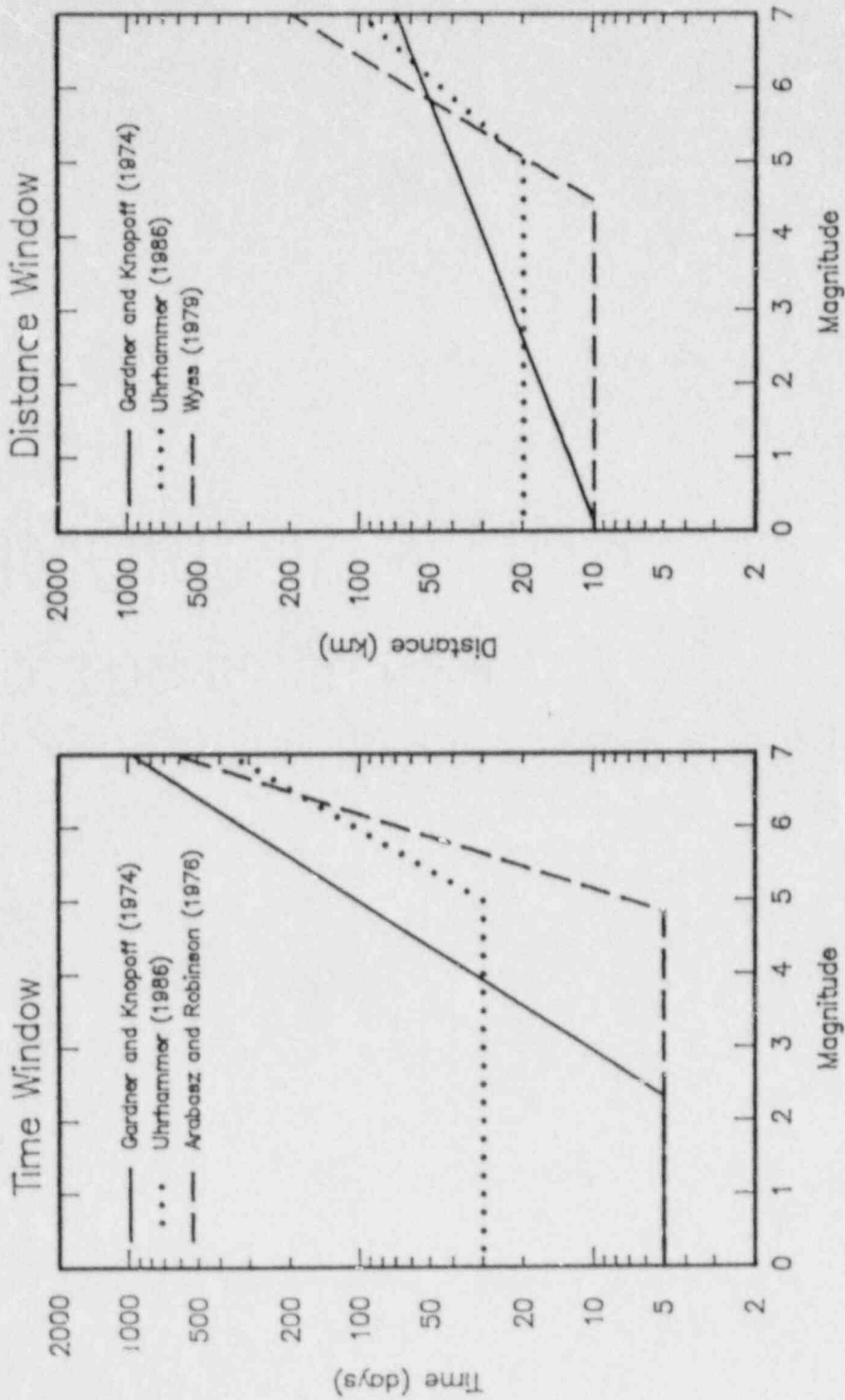


Figure C-11. Empirical criteria used to identify dependent events in earthquake catalogs.

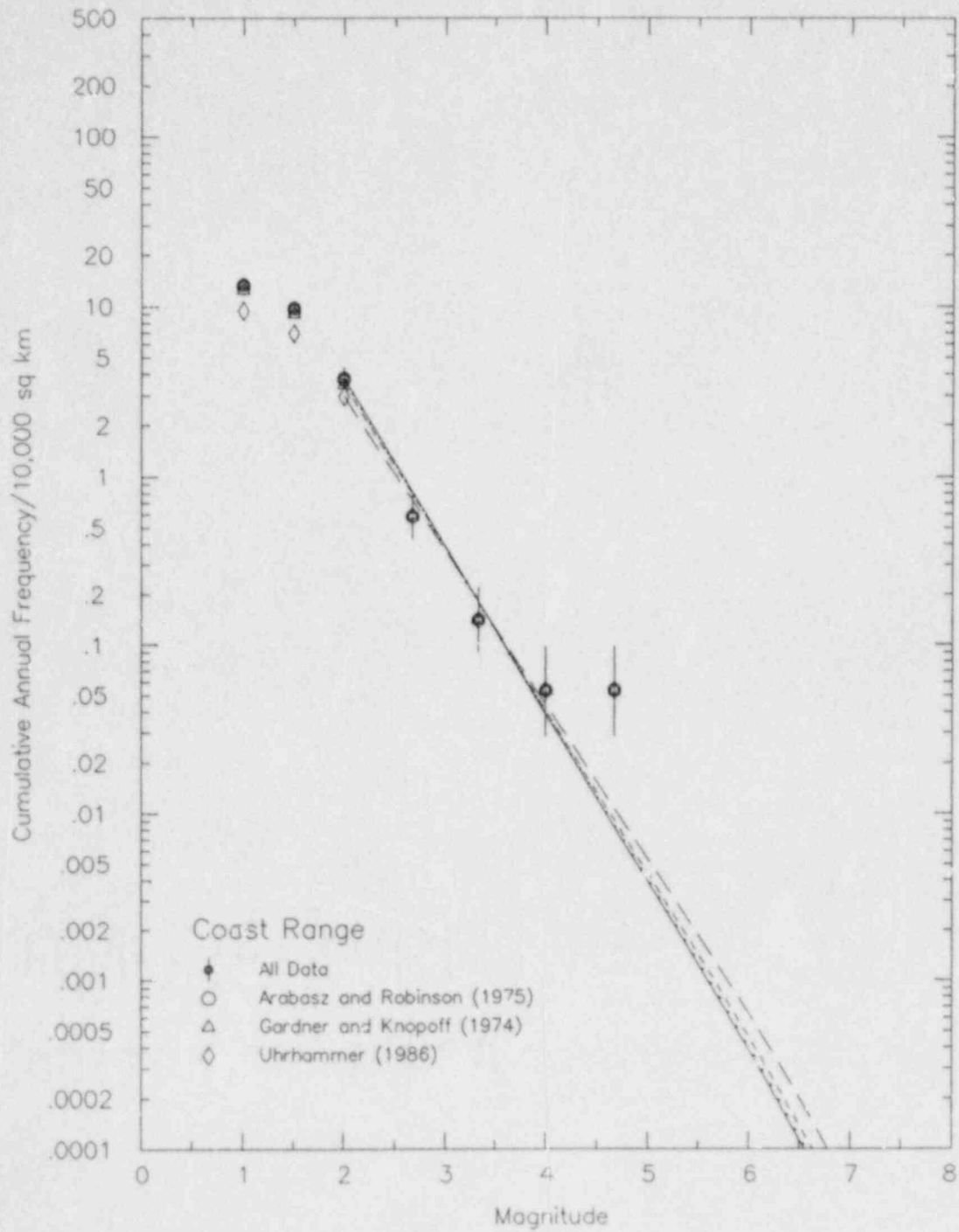


Figure C-12. Maximum likelihood earthquake recurrence relationships for Coast Range zone.

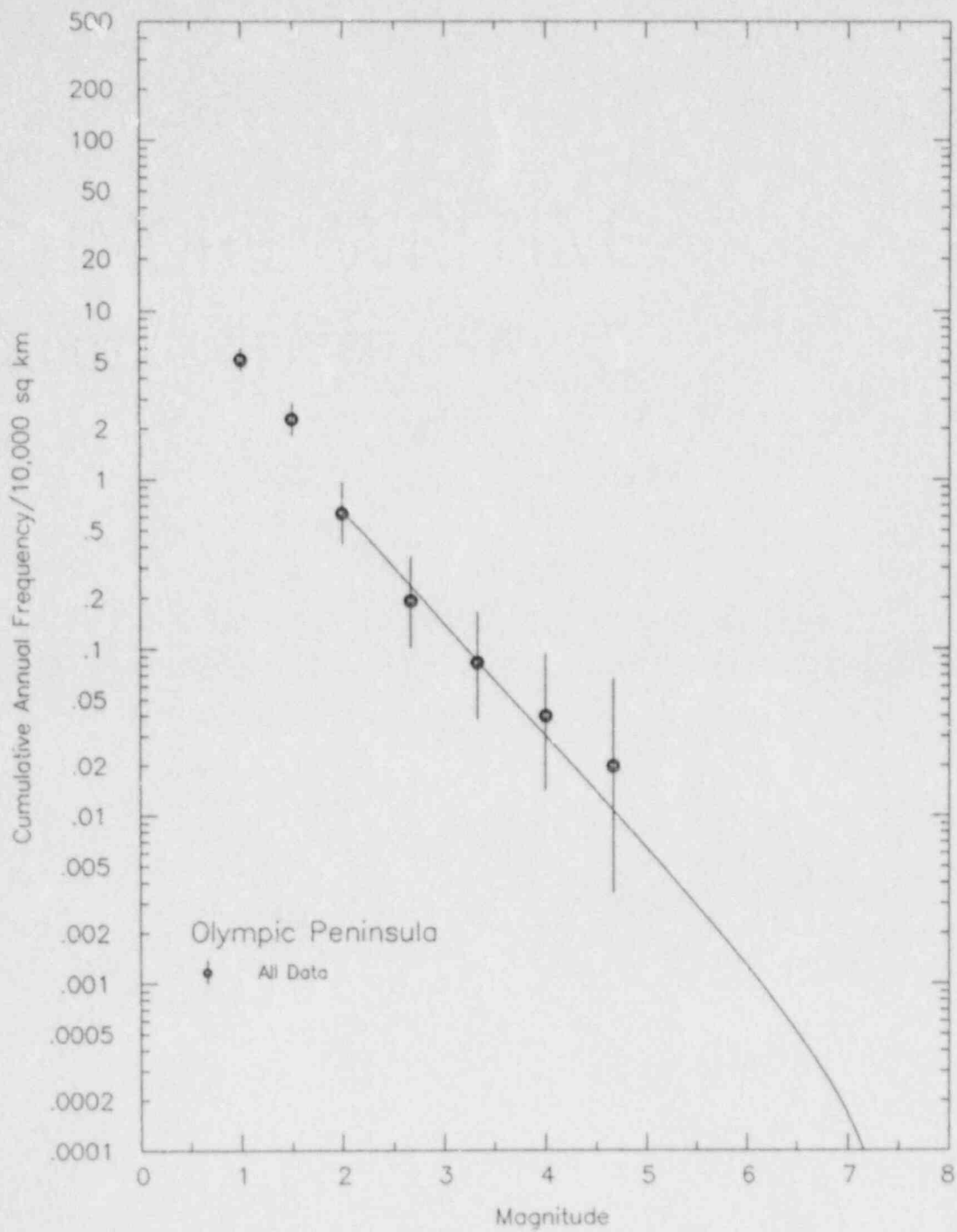


Figure C-13. Maximum likelihood earthquake recurrence relationship for Olympic Peninsula.

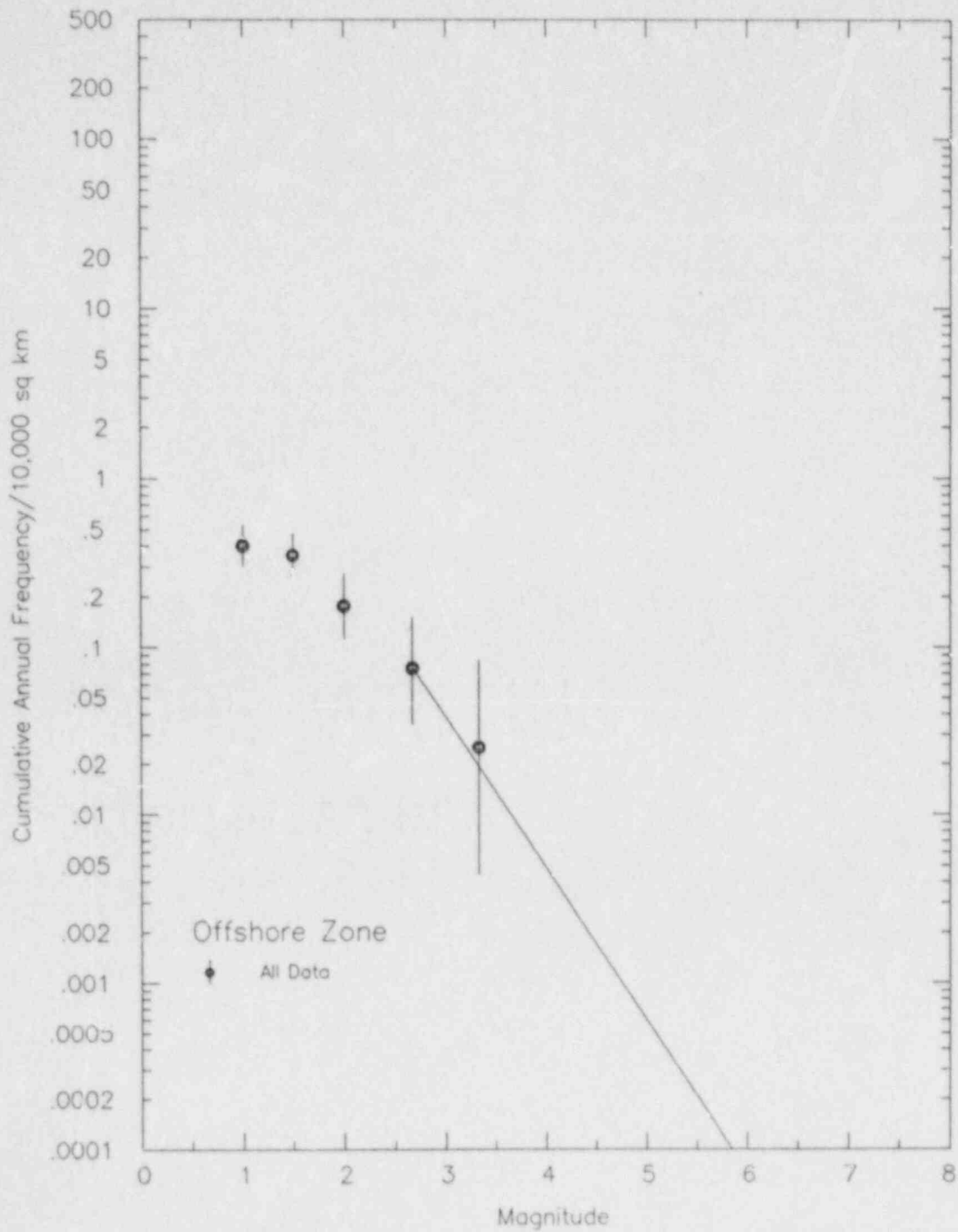


Figure C-14. Maximum likelihood earthquake recurrence relationship for Offshore zone.

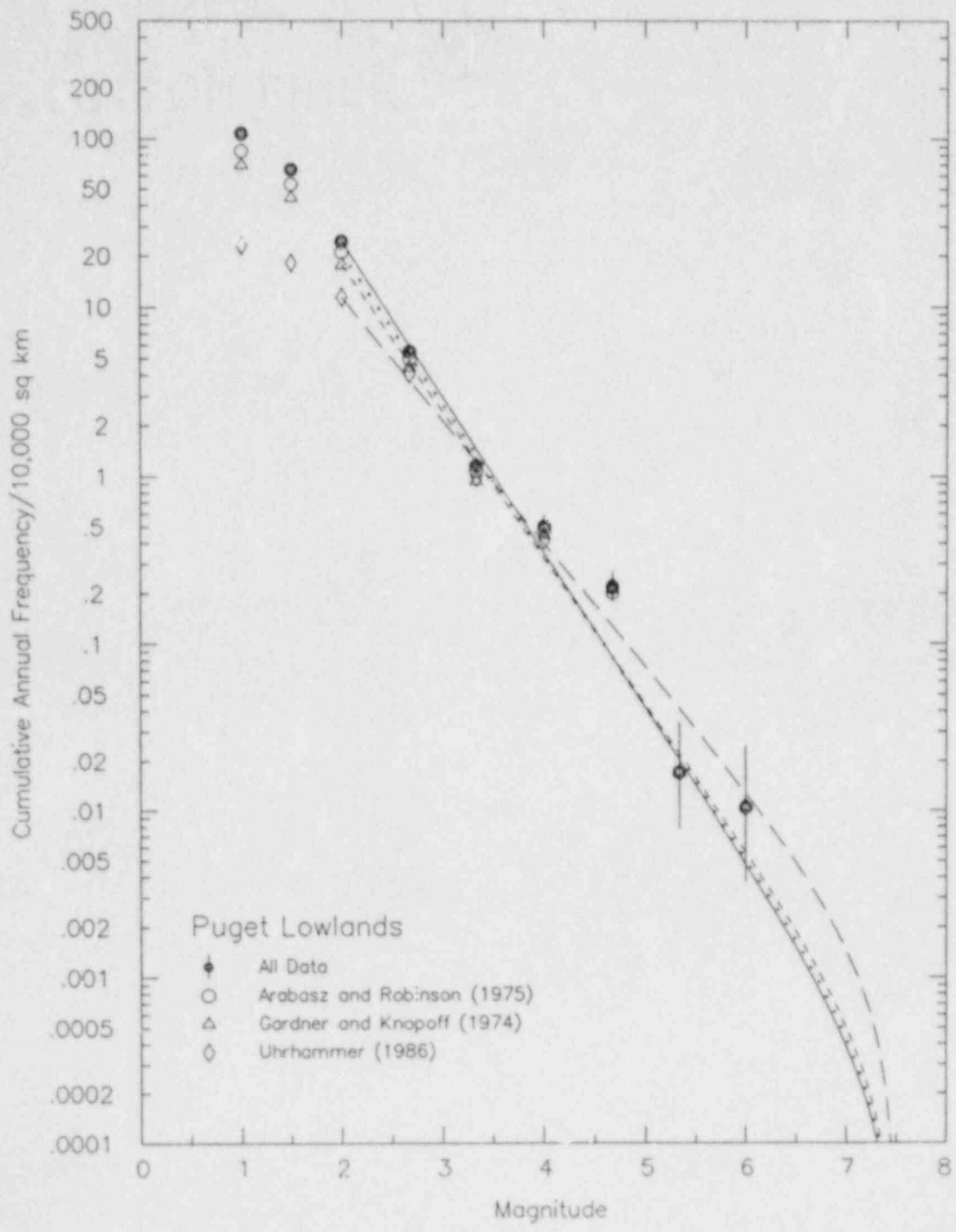


Figure C-15. Maximum likelihood earthquake recurrence relationships for Puget Lowlands.

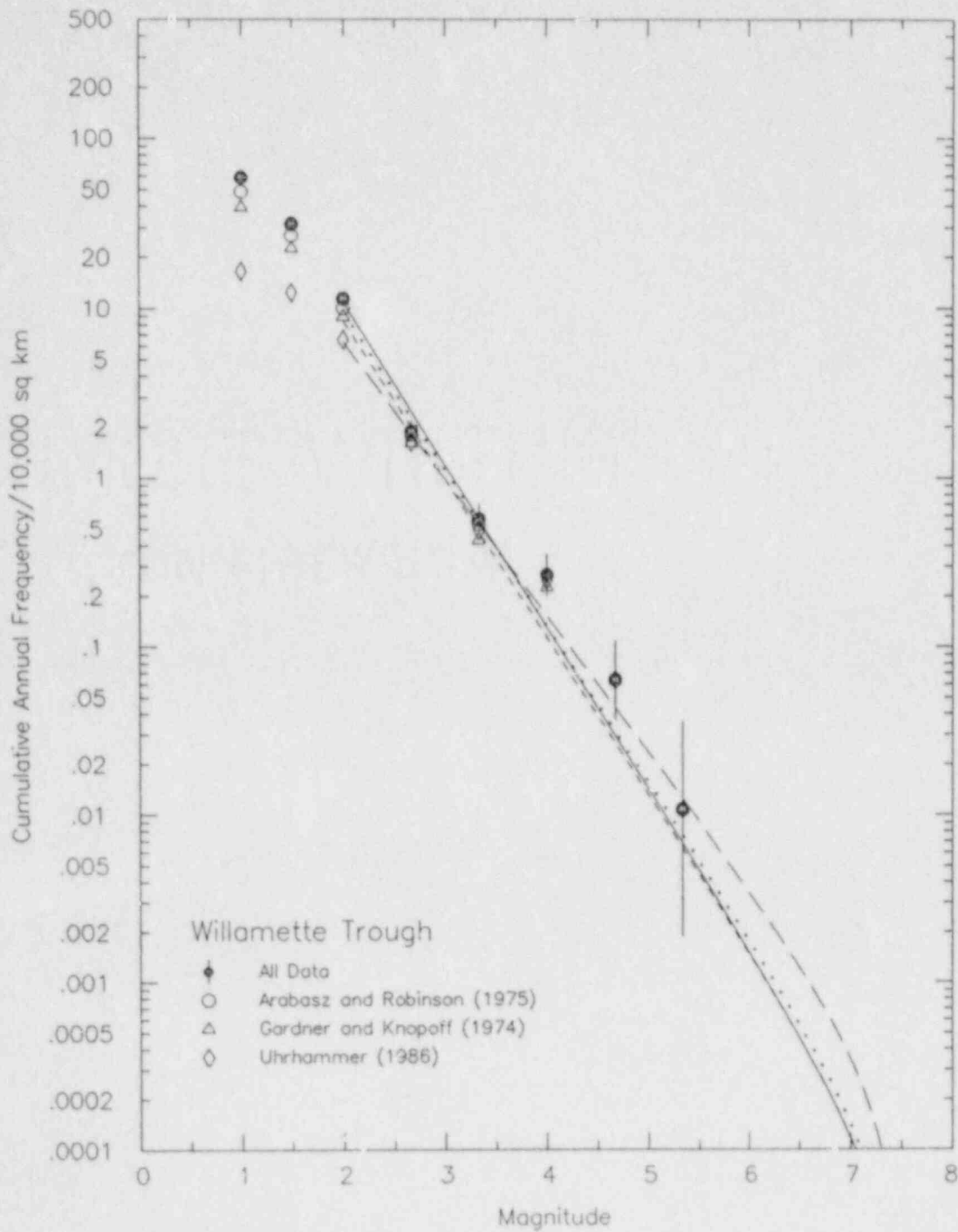


Figure C-16. Maximum likelihood earthquake recurrence relationships for Willamette Trough.



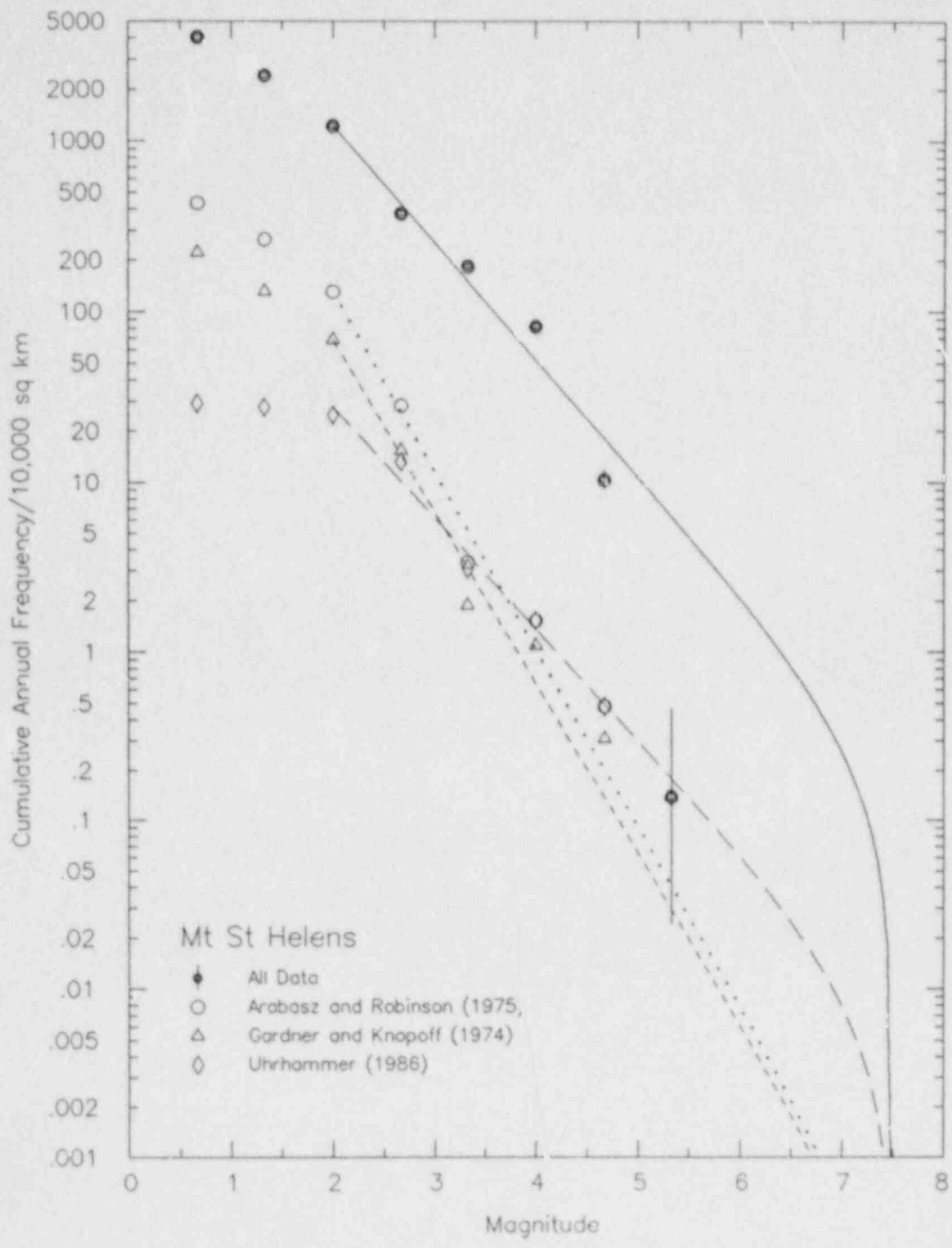


Figure C-17. Maximum likelihood earthquake recurrence relationships for St. Helens zone.

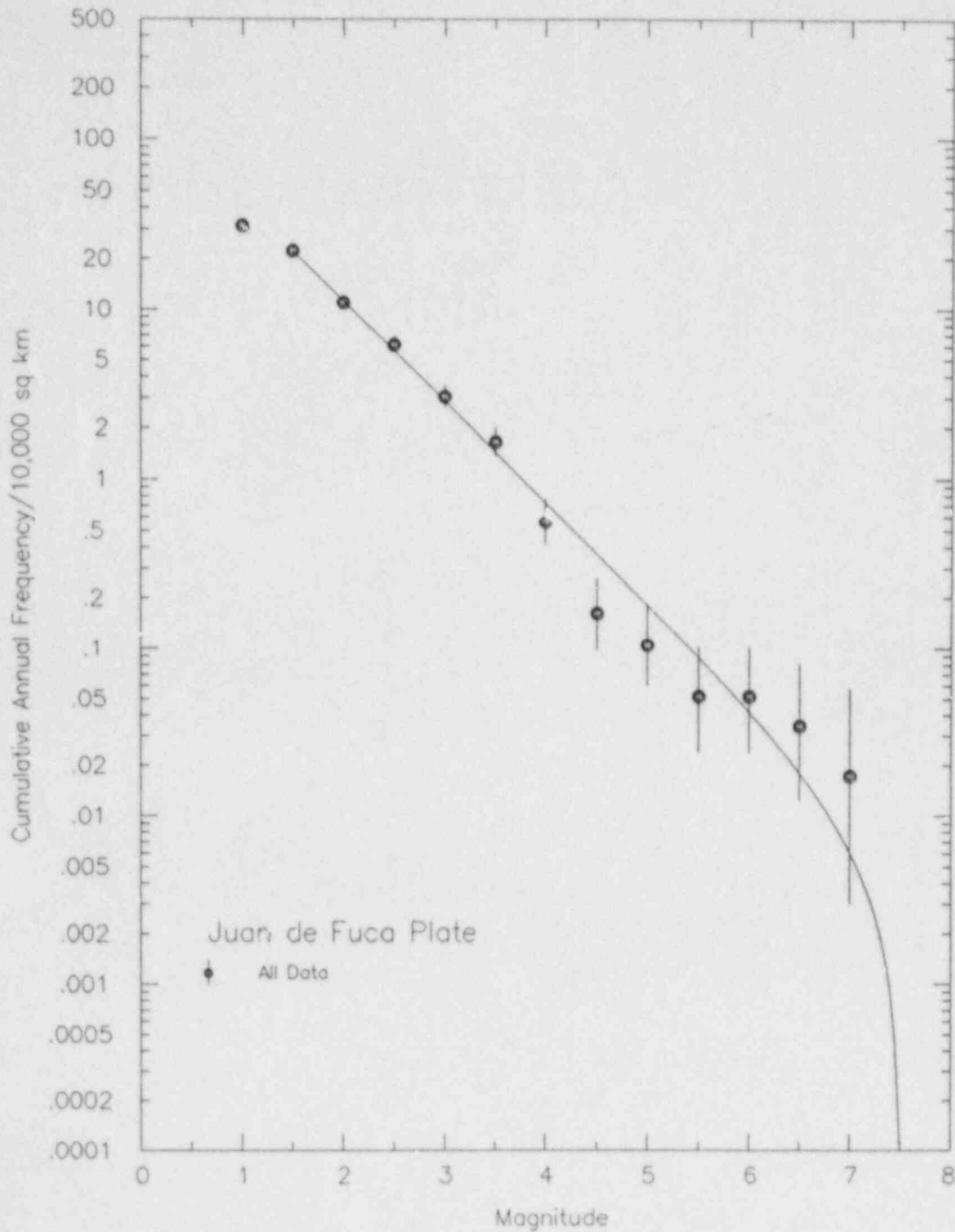


Figure C-18. Maximum likelihood earthquake recurrence relationship for subducting Juan de Fuca plate.

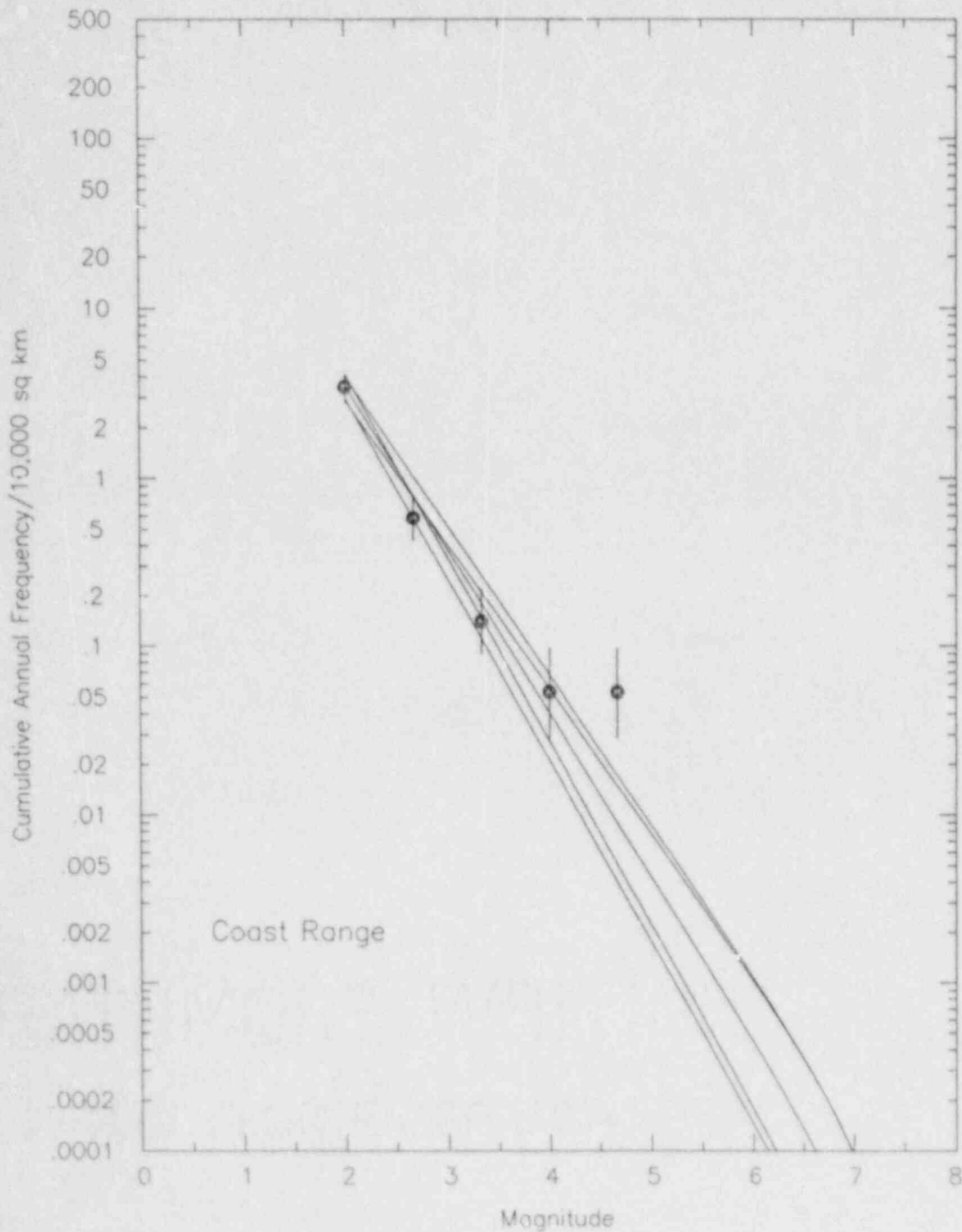


Figure C-19. Distribution of recurrence relationships for Coast Range zone used in hazard analysis.

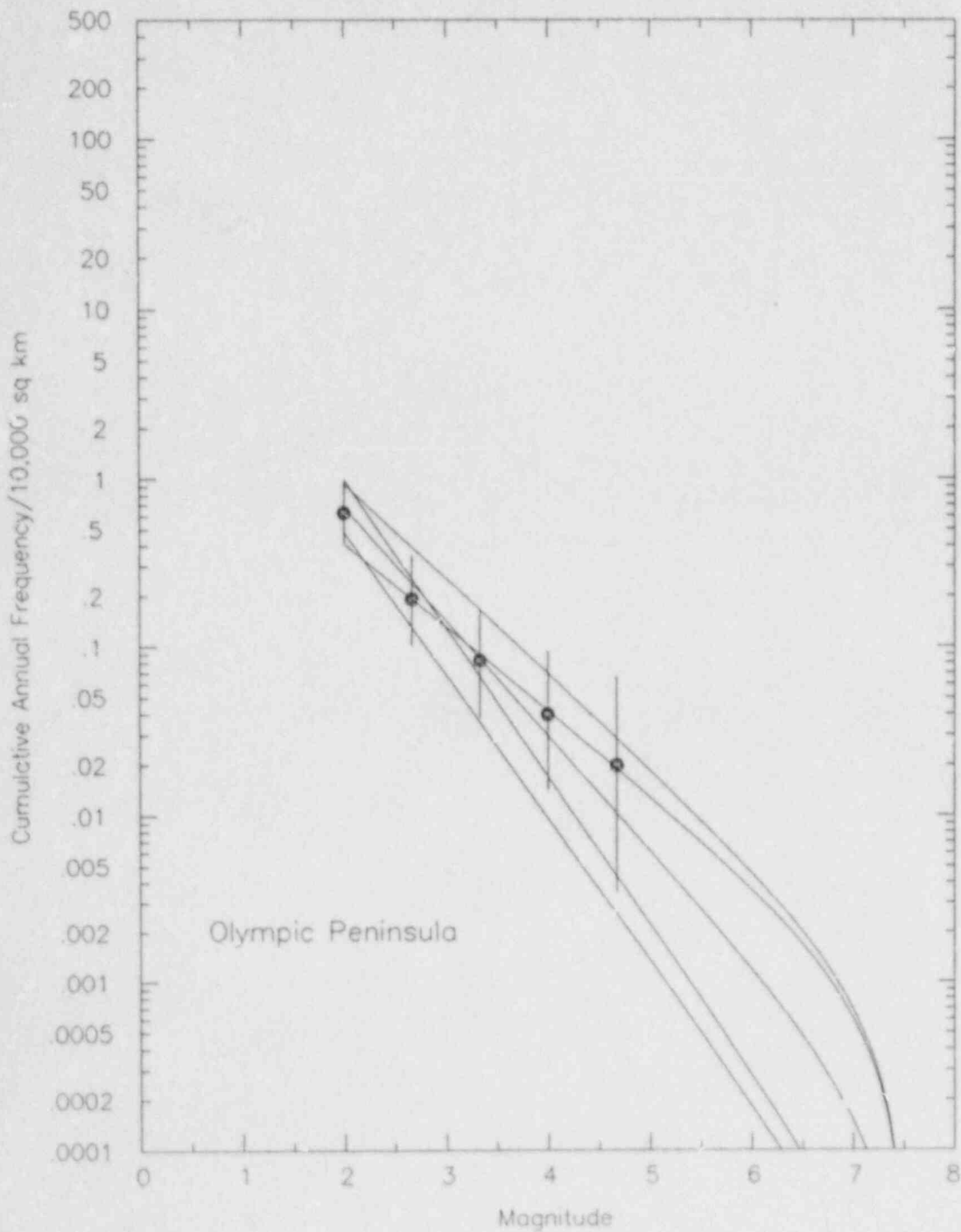


Figure C-20. Distribution of recurrence relationships for Olympic Peninsula used in hazard analysis.

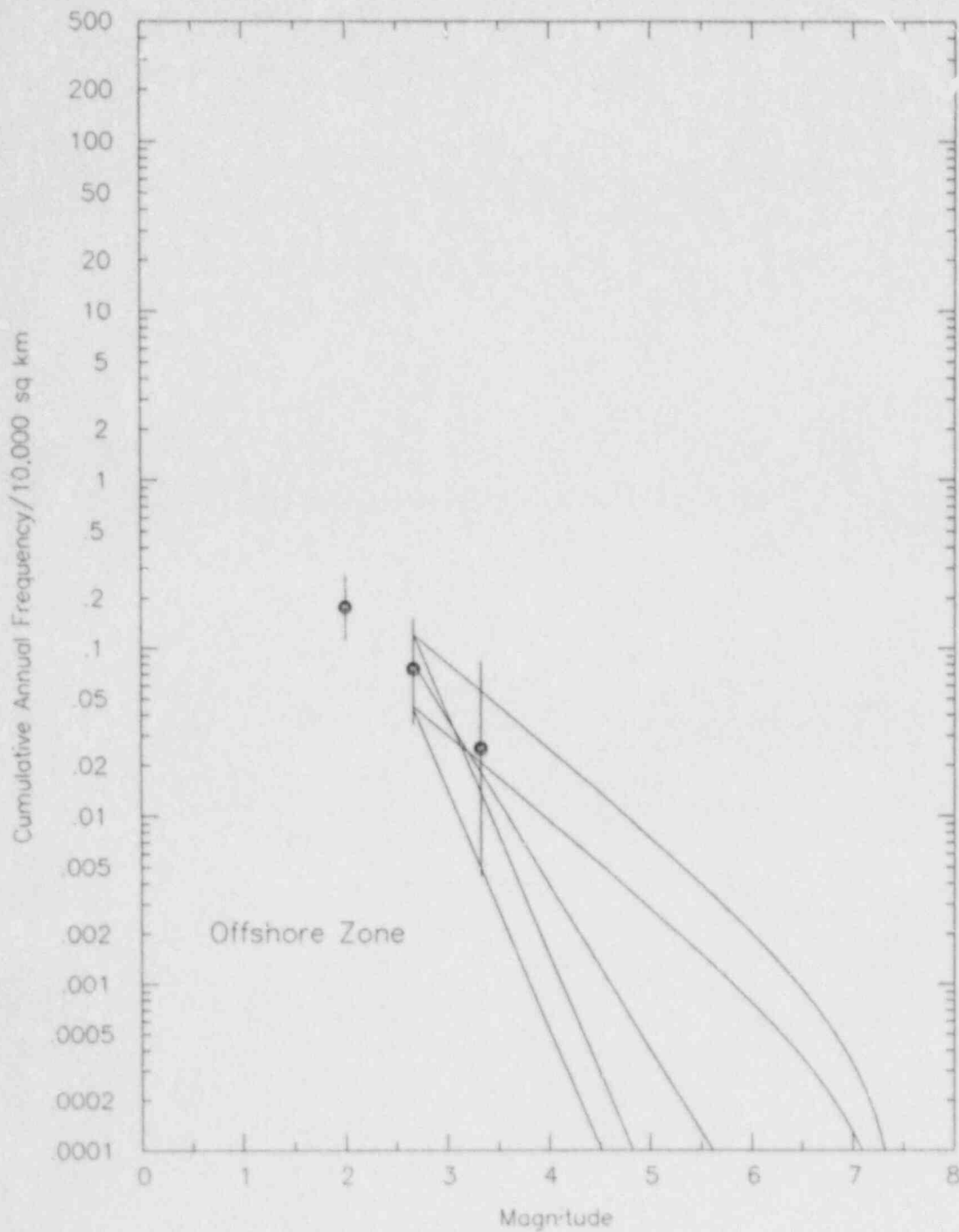


Figure C-21. Distribution of recurrence relationships for Offshore zone used in hazard analysis.

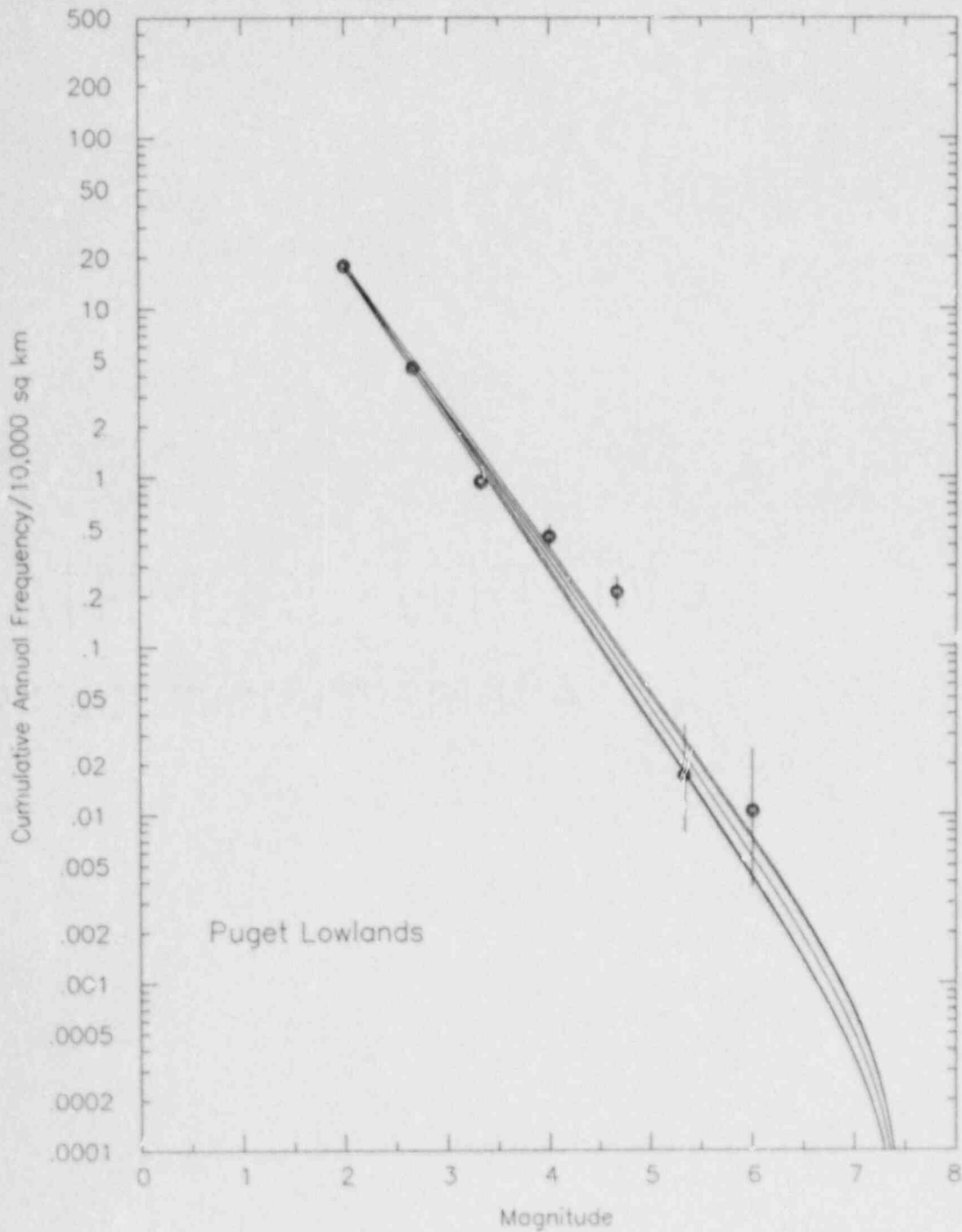


Figure C-22. Distribution of recurrence relationships for Puget Lowlands used in hazard analysis.

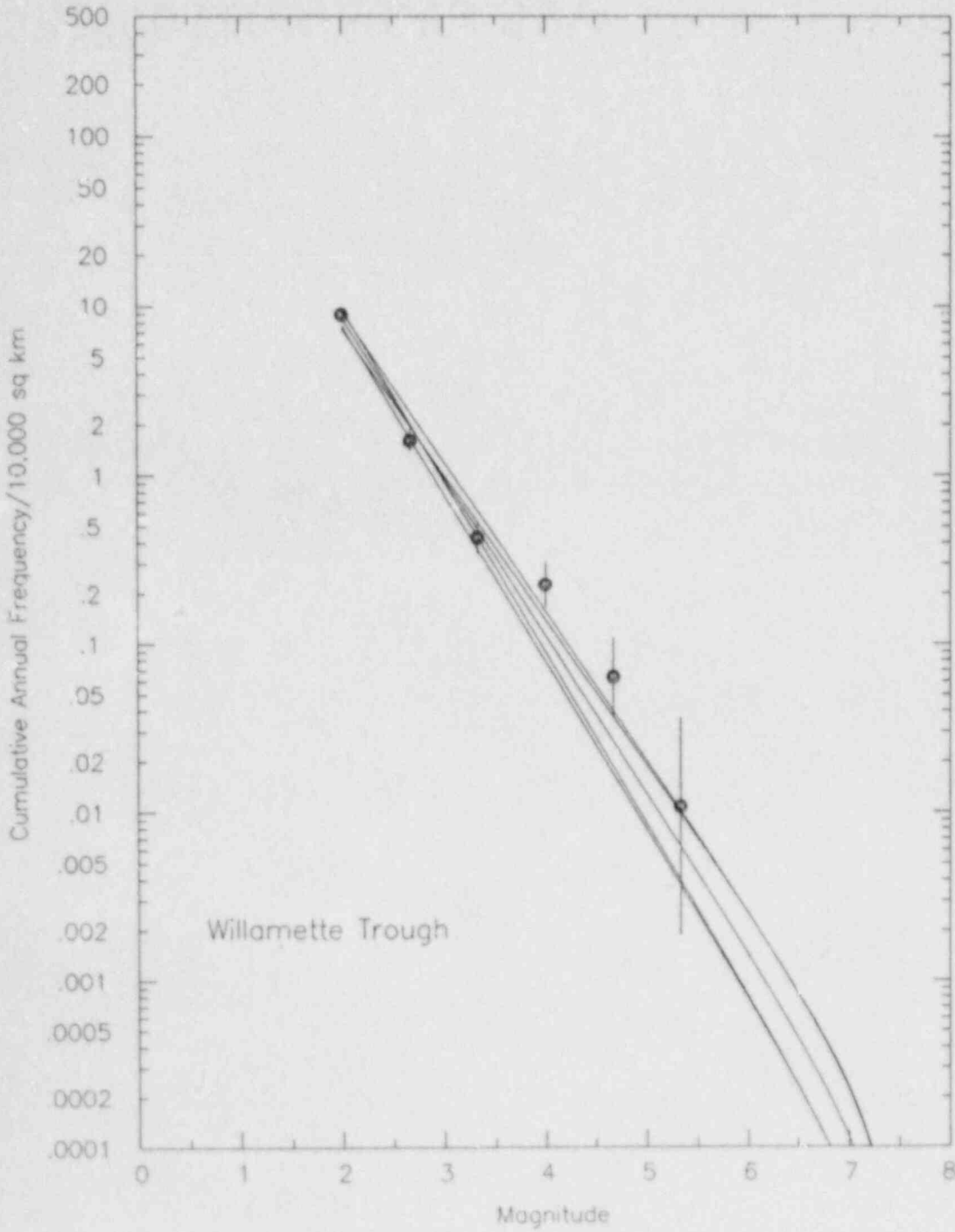


Figure C-23. Distribution of recurrence relationships for Willamette Trough used in hazard analysis.

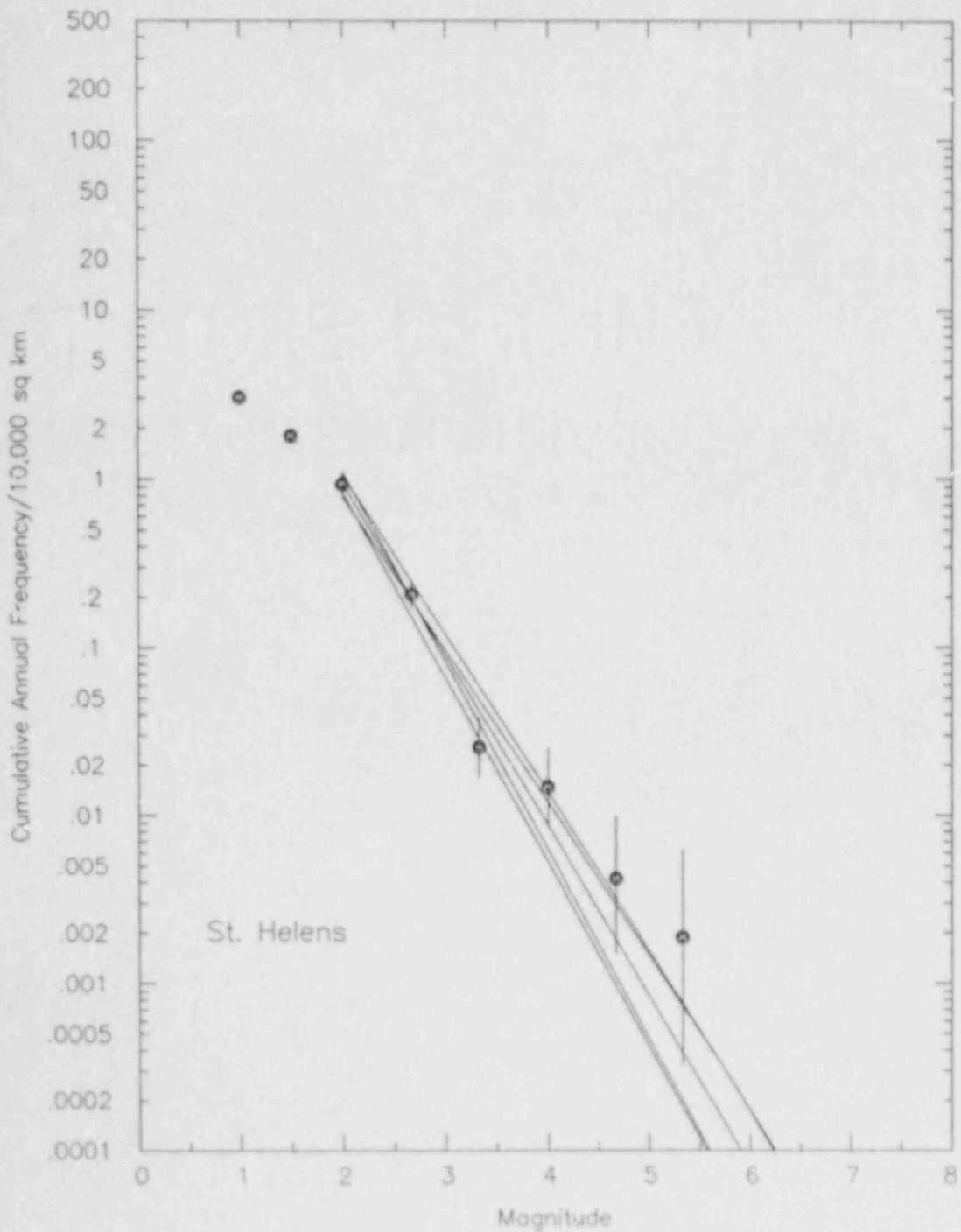


Figure C-24. Distribution of recurrence relationships for St. Helens zone used in hazard analysis.



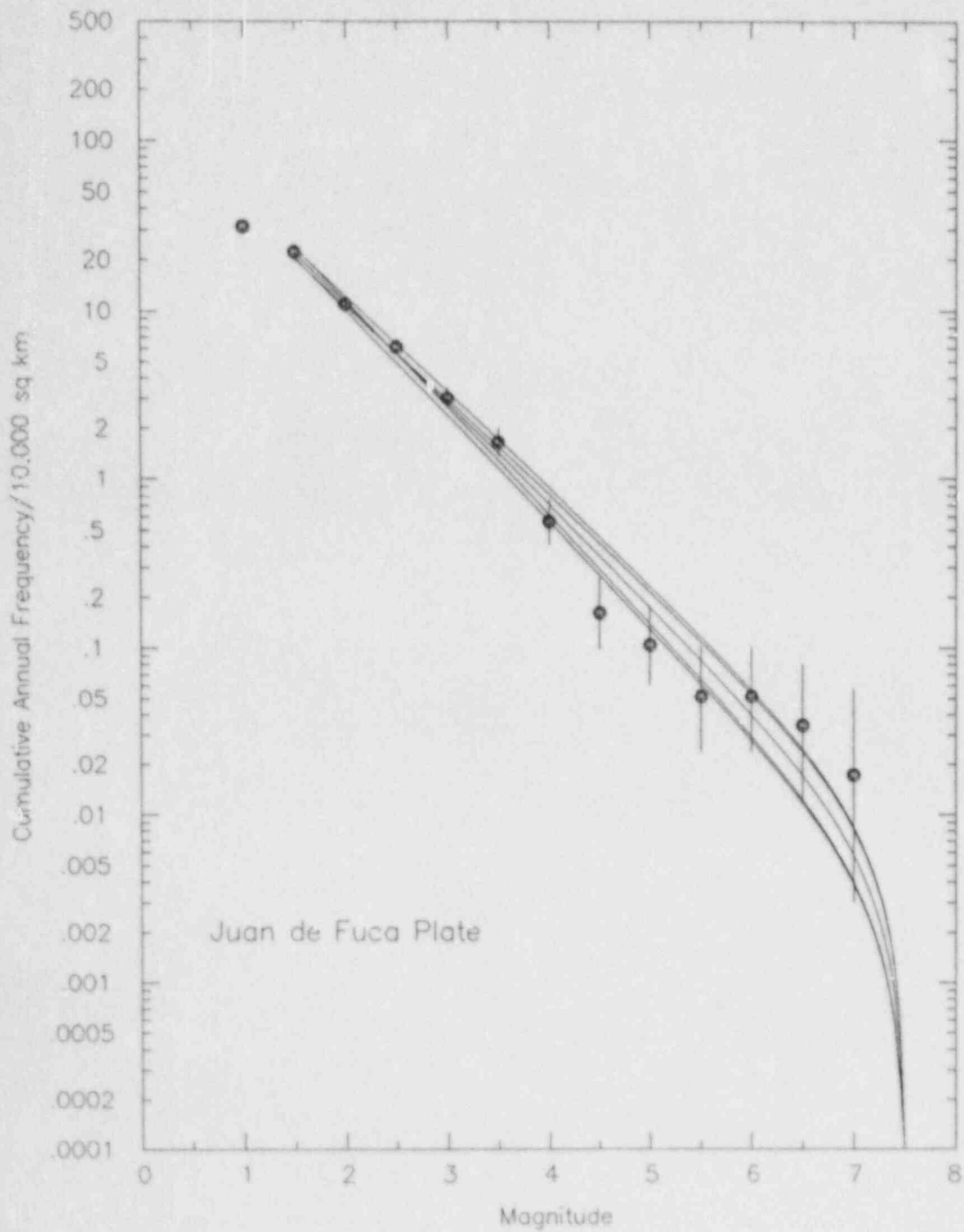


Figure C-25. Distribution of recurrence relationships for subducting Juan de Fuca plate used in hazard analysis.

## APPENDIX D

### ATTENUATION RELATIONSHIPS FOR SUBDUCTION ZONE SOURCES

Several empirically-based attenuation relationships have been published for ground motions from subduction zone earthquakes (Iwasaki and others, 1978; Sadigh, 1979; NOAA, 1982; Mori and others, 1984; Vyas and others, 1984; Kawashima and others, 1984). These relationships were developed from data recorded primarily at distances of 80 to 300 km from the earthquake rupture, with the majority of recordings obtained on soil sites in Japan. The findings of these studies typically indicate that at distances greater than 50 km peak accelerations from subduction zone earthquakes (both interplate and intraslab events) are substantially larger than those from shallow crustal earthquakes.

The applicability of the available attenuation relationships for estimating ground motions in the near field (distance to rupture  $\leq 50$  km) of large ( $M_w \geq 8$ ) interplate earthquakes has been hampered by the lack of near field recordings. Consequently, several studies have been conducted to provide estimates of near field motions on the basis of theoretical and numerical modeling techniques. Two studies, Heaton and Hartzell (1986) and S-Cubed (1988), are focused directly on estimating ground motions from potential large magnitude earthquakes on the Cascadia subduction zone.

The occurrence of the March 3, 1985  $M_w$  8 earthquake in Chile and the September 19, 1985  $M_w$  8 earthquake and its  $M_w$  7.6 aftershock in Mexico has greatly improved the data base for evaluating ground motions at close distances. Figure D-1 shows the distribution of available strong motion recordings on rock or rock-like material (shear wave velocity  $\geq 750$  m/sec) and on soil sites. As can be seen from Figure D-1, the recordings obtained in 1985 have significantly expanded the data base for large magnitude, near field strong motion recordings on rock sites. As many of these recordings were obtained in the same relative location with respect to earthquake rupture as is the postulated situation at the WNP-3 site (i.e., directly or nearly directly above the zone of rupture), the data set shown in Figure D-1 is more appropriate for evaluating ground motions at the WNP-3 site than the data bases used in previously developed attenuation relationships. The attenuation relationships used in the hazard computation were developed from analysis of the soil and rock site data set shown in Figure D-1.

Constraints on the extrapolation of these relationships to events of  $M_w > 8$  were developed from the results of ground motion simulations performed by S-Cubed (1988) and from the theoretical source spectra proposed by Joyner (1984).

#### D.1 Strong Motion Data

The data set collected for this study is listed in Table D-1. The primary sources of the data are: for Alaska, Beavan and Jacob (1984); for Chile and Peru, Saragoni and others (1982, 1985); for Japan, Mori and Crouse (1981); for Mexico, Bufaliza (1984), Anderson and others (1986, 1987a, 1987b); and for the Solomons, Crouse and others (1980). The data were characterized in terms of moment magnitude, as defined by Hanks and Kanamori (1979), and

closest distance to the rupture surface. If no seismic moment has been reported for an event, then the surface wave magnitude was used provided it fell in the appropriate range of  $M_s$  5 to 7.5, consistent with the definition of the moment magnitude scale. If only body wave magnitude was reported, then  $m_b$  values in the range of 5 to 6 were converted to  $M_s$  using the relationship  $M_s = 1.8 \cdot m_b - 4.3$  proposed by Wyss and Habermann (1982) and the resulting value taken to be equal to moment magnitude. This magnitude conversion approach was used by Beavan and Jacob (1984) in developing their catalog of strong motion data from Alaska. If no rupture area has been published for an event, then hypocentral distance was used.

The distinction between soil and rock site conditions was made primarily on the basis of the site conditions listed in the various data sources. The recording station at the Geophysical Institute in Lima, Peru was classified as a rock-like site on the basis of the reported subsurface shear wave velocities and evaluations of site response and damage distributions during past earthquakes (Repetto and others, 1980). The recording station at the School of Engineering in Santiago, Chile was also classified as a rock-like site as it is located on deposits similar in nature to those underlying the Lima site. It should be noted that several of the recording stations for the 1985 Chile earthquake listed as located on rock in Wyllie and others (1986) are actually located on soil deposits, notably the stations at Llolleo (Algermissen, 1985) and Melipilla (Algermissen, personal communication). The recordings obtained on the very soft lake deposits such as those in the Mexico City area were not included in the analysis as they may represent soil sites with special amplification characteristics.

The ground motion parameters (peak acceleration, spectral velocity) were characterized in terms of the geometric average of the two horizontal components of motion. This approach was used to remove the effect of component-to-component correlations that affect the validity of using statistical test assuming individual components of motion represent independent measurements of ground motion (Campbell, 1987). The results of the regression analyses indicate no significant difference between the estimates of variance about the median relationships obtained using the average of two components and the values obtained using both components as independent data points.

The complete data set consists of the following groups of data.

Subduction Zone	Number of Recordings		Magnitude Range	Distance Range
	On Rock	On Soil		
Alaska	18	3	5.2 - 8.0	27 - 231 km
Cascadia	0	5	6.7 - 7.1	55 - 80 km
Chile	20	25	5.3 - 8.0	39 - 175 km
Japan	0	59	5.2 - 7.6	42 - 390 km
Mexico	45	72	5.0 - 8.0	15 - 456 km
Peru	13	1	5.3 - 8.1	68 - 260 km
Solomons	9	35	5.0 - 8.1	38 - 418 km

## D.2 Attenuation Relationships for Peak Horizontal Acceleration on Rock

Figure D-2 shows the peak horizontal acceleration data for magnitude 5.5 to 8 earthquakes recorded on rock and soil sites. As can be seen, the soil recordings have on average greater peak motions than rock site recordings. Although exhibiting a large degree of scatter, the data show a trend toward near field saturation of ground motion levels for large magnitude events that is well established for ground motions from shallow crustal earthquakes. Consequently, the general form of attenuation model used for shallow crustal ground motions was employed in the analysis of the data. The specific form of relationship is:

$$\ln(a_{max}) = C_1 + C_2 M_w - C_3 \ln[R + C_4 \exp(C_5 M_w)] - \tau R + \epsilon \quad (D-1)$$

where R is closest distance to the zone of rupture in kilometers,  $\tau$  represents an anelastic attenuation coefficient,  $C_i$  are coefficients determined from the data and  $\epsilon$  represents a normally distributed random error with zero mean.

The parameters of equation D-1 were obtained from the data sets shown in Figure D-2 using nonlinear multiple regression techniques. The residuals obtained from fitting the data with  $\tau$  constrained to be  $\geq 0$  are plotted against magnitude and distance in Figure D-3. Inspection of the residuals indicated no trend with distance and a reduction in variance with increasing magnitude. Similar dependence of the variance in ground motion on earthquake magnitude have been reported by Sadigh (1983), and Abrahamson (1987). Both Sadigh (1983) and Abrahamson (1987) suggest that the variability in the variance for peak ground motions can be modeled by a linear relationship between magnitude and standard deviation. The coefficients of such a relationship can be obtained by minimizing the expression (Gallant, 1987):

$$\sum_{i=1}^N (|e_i| - \sqrt{\pi} \sigma^* / \sqrt{2})^2 \quad (D-2)$$

where  $e_i$  is the unnormalized residual for the  $i^{\text{th}}$  data point and  $\sigma^*$  represents the functional form for the standard deviation, assumed in this analysis to be:

$$\sigma^* = a + b M_w \quad (D-3)$$

As the differences in the variance estimates for the soil and rock data sets were not statistically significant, the residuals from two data sets were combined to estimate the parameters of  $\sigma^*$ . The resulting relationship for standard deviation of peak ground acceleration is

$$\sigma^* = 1.55 - 0.125 M_w \quad (D-4)$$

In all subsequent analyses, a weighted least squares approach (Draper and Smith, 1981; Gallant, 1987) was used with weights inversely proportional to the variance as defined by Equation D-4.

The results of unweighted and weighted regressions gave a value of zero for the anelastic attenuation coefficient,  $\tau$ , for both the rock site and soil site data sets. Accordingly, the term  $\tau R$  was dropped from the attenuation relationship.

Subduction zone earthquakes can be grouped into two basic types of events, low angle thrust earthquakes occurring on plate interfaces and high angle, predominantly normal faulting earthquakes occurring within the downgoing slab. As it has been suggested that the type of fault rupture may have an effect on median ground motion levels (e.g., McGarr 1984; Campbell, 1987) possible differences between ground motions from interface and intraslab events were investigated. The differentiation between interface and intraslab events was done on the basis of mechanisms, when reported, or on the basis of focal depth, with events below a depth of 50 km considered to be intraslab events. While it is unlikely that interface events would occur at depths greater than 50 km, intraslab events do occur at depths less than 50 km, and it is possible that some intraslab events have been misclassified as interface events.

The residuals for interface and intraslab events are differentiated in Figure D-3. As can be seen, the mean residual for intraslab events is greater than zero for both data sets, although the trend is not as obvious for the soil data as it is for the rock data. Application of the likelihood ratio test for nonlinear regression models suggested by Gallant (1975a, b) indicates that the hypothesis that the coefficients of Equation D-1 are the same for intraslab and interface events can be rejected at the 0.05 percentile level for both the rock and soil data sets.

As the intraslab events tend to be both deeper and to produce higher ground motions, the possibility of including a term proportional to depth of rupture in equation D-1 was explored. The results indicate that no significant reduction in the standard error is achieved beyond separation of the data into the two subsets.

The residuals were also examined for evidence of systematic differences between different subduction zones. Systematic differences in source characteristics have been reported previously from examination of teleseismic records. Hartzell and Heaton (1985) found that earthquakes from a particular subduction zone tended to have similar characteristics in terms of their source time functions of energy release and that these average characteristics varied among different subduction zones. However, they were unable to identify an obvious relationship between the physical parameters of an individual subduction zone and the characteristics of the rupture process for events occurring in the zone. Houston and Kanamori (1986) indicate that the source spectra for large earthquakes on the Mexican subduction zone tend to show lower levels of high frequency ground motion than an "average" large event source spectrum.

Preliminary analysis of the initial data set developed for this study (reported by Youngs and others, 1987) suggested that systematic differences may also exist in strong ground motion from different subduction zones.

However, subsequent addition of data and reclassification of site conditions at some of the recording stations has yielded a data set that does not exhibit statistically significant difference in the peak accelerations among the different subduction zones.

To test the significance of the observed differences in the residuals shown in Figure D-3, equation D-1 was modified to include a set of "dummy" variables (Draper and Smith, 1981) to identify data from interface and intraslab events, yielding the relationship:

$$\ln(a_{max}) = C_1 + C_2 \cdot M_w + C_3 \cdot \ln[R + C_4 \cdot \exp(C_5 \cdot M_w)] + \epsilon B Z_t + \epsilon \quad (D-5)$$

where  $Z_t$  is zero for interface events and one for intraslab events. The coefficient B measures the average difference between the ground motions from interface and intraslab events. Equation D-5 was fit to the data (using weighting based on the difference in variance shown in Figure D-2), resulting in an average value of  $B = 0.54$  for the soil and rock data sets. Application of the likelihood ratio test indicates that the hypothesis that  $B = 0$  can be rejected at the 0.05 percentile level for both rock and soil data sets. Further extensions of the model to include a modifying effect of rupture type on the other parameters of Equation D-1 produced no further decrease in the estimated variance and were rejected.

The validity of the systematic difference between ground motions from interface and intraslab events was further investigated using the data from sites with multiple recordings of both types of earthquakes. Equation D-5 was modified to include a set of dummy variables, one for each site to remove the differences between the median ground motions at a site and the overall median over all sites - in essence removing the effects of systematic site amplification. Coefficients  $C_1$  through  $C_5$  were held fixed at the values obtained from regression on the full data set and a linear regression was performed to obtain the individual site terms and B, the rupture type term. The resulting value of 0.55 agrees very well with the value obtained from the unconstrained regression using the full data set.

The resulting median attenuation equations are:

$$\ln(a_{max}) = 19.16 + 1.045M_w - 4.738\ln[R+205.5\exp(0.0968M_w)] + 0.54Z_t \quad (D-6)$$

for rock sites and

$$\ln(a_{max}) = 18.75 + 1.045M_w - 4.565\ln[R+162.5\exp(0.1309M_w)] + 0.54Z_t \quad (D-7)$$

for soil sites. In the analysis, parameter  $C_2$ , which represents the far field magnitude scaling term, and parameter B, the faulting type term were assumed to be the same for both soil and rock data. These relationships are compared with the recorded data in Figures D-4 and D-5 for rock and soil data, respectively. Figure D-6 presents plots of the normalized residuals about Equations D-6 and D-7 and indicate that a homogeneous variance has been obtained.

### D.3 Attenuation Relationships for Spectral Velocity

Attenuation relationships for spectral velocity ( $S_v$ ) were developed using the procedures employed by Sadigh (1983, 1984). This involves developing relationships for the ratio  $S_v/a_{max}$  as a function of magnitude and distance and then applying these relationships to attenuation relationships for peak acceleration. The advantages of this approach are that there is a much larger data base of peak acceleration data than spectral response data for establishing magnitude and distance scaling of absolute levels of ground motion and the use of spectral shapes results in attenuation relationships for various periods that are consistent over the full range of magnitudes and distances to which the relationships apply.

The procedure involves three steps: first, developing a spectral shape for a reference size event for which there is abundant data; second, developing relationships to scale the shape to other magnitudes; and third, computing the standard error of the absolute spectral values about the attenuation relationship. For this analysis, a reference magnitude of  $M_w$  8 was used as the largest number of available rock site response spectra are from recordings of  $M_w \sim 8$  events.

Figure D-7 presents median (mean of  $\ln[S_v/a_{max}]$ ) spectral shapes for 5 percent damping developed from magnitude  $M_w$  7.8 to 8.1 ground motion data. The top plot shows the computed spectral shapes for the data from distances less than 150 km and greater than 150 km. As can be seen, there is a significant difference in spectral shape for the two distances ranges. Because the interest in the hazard analysis is on near field ground motions, the spectral shape for the  $< 150$  km distance data was used to develop the spectral velocity attenuation relationships.

The bottom plot of Figure D-7 shows the smoothed spectral shape in terms of spectral acceleration. The maximum spectral acceleration amplification is 2.25 at a period of 0.15 seconds.

The second step is the specification of the variation in spectral shape with earthquake magnitude. Figure D-8 presents plots of the ratio  $[S_v/a_{max}(M_w)]/[S_v/a_{max}(M_w=8)]$  derived from the available response spectra data for recordings on rock sites for periods of vibration of 0.2 and 2.0 seconds. The ratios were obtained by dividing the spectral amplifications for individual events by the smoothed spectral shape for a magnitude  $M_w$  event shown in Figure D-7. The three curves shown represent relative spectral amplification for shallow crustal events derived on the basis of empirical attenuation relationships (Joyner and Boore, 1982; Sadigh and others, 1986) and on the basis of numerical models employing theoretical source spectra and random vibration theory to estimate ground motions (Hanks and McGuire, 1981; Boore, 1983, 1986). As can be seen, the data for subduction zone earthquakes follows the general trend defined by the relationships for shallow crustal earthquakes. Accordingly, the form of the relationship for spectral amplification employed by Sadigh (1983) was used. Specifically:

$$\ln(S_v/a_{max}) = C_6 + C_7(C_8 - M_w)^{C_9} \quad (D-8)$$

Equation D-8 was fit to the data for periods between 0.1 and 3 seconds. In conducting the regression  $C_8$  was fixed at 10 to provide for complete saturation at this magnitude level and  $C_9$  was fixed at 3 representing an average of the values obtained at longer periods which exhibit significant magnitude effect on spectral shape. Applying these constraints, parameter  $C_7$  could be fit by the relationship:

$$C_7 = -0.0145 - 0.0063 \ln(T) \quad (D-9)$$

where T is period of vibration. Parameter  $C_6$  was then constrained so that equation D-8 results in the spectral amplifications specified for magnitude 8 events by the spectral shapes shown in Figure D-7. The resulting relationships are compared with the empirical data and the relationships for shallow crustal earthquakes in Figure D-8.

Attenuation relationships were developed for three periods for use in the hazard analysis. The selected periods are 0.15, 0.8, and 2.0 seconds. The first two periods correspond to the periods of maximum amplification of spectral acceleration and spectral velocity, respectively, for a  $M_w$  8 earthquake. The spectral amplifications at these periods are given by the relationships:

$$\begin{aligned} T = 0.15 \text{ sec} & \quad \ln(S_v/a_{max}) = 3.985 - 0.0026(10 - M_w)^3 \\ T = 0.8 \text{ sec} & \quad \ln(S_v/a_{max}) = 5.164 - 0.0131(10 - M_w)^3 \\ T = 2.0 \text{ sec} & \quad \ln(S_v/a_{max}) = 4.960 - 0.0189(10 - M_w)^3 \end{aligned} \quad (D-10)$$

The units of Equations D-11 are cm/sec/g.

The third step is specification of the standard error in  $\ln(S_v)$ . The standard error was estimated by computing the residuals of the response spectral values about the median relationships for spectral velocity. The resulting values were less than or equal to the standard deviation for peak acceleration defined by Equation D-4 at all periods. Accordingly, Equation D-4 was used in the hazard analysis to define the standard deviation of ground motion about the median curves.

#### D.4 Ground Motions for Earthquakes of Magnitude Greater than 8

The attenuation relationships defined above are considered applicable for estimating ground motions in the magnitude range  $M_w$  5 to 8 and for distances of 20 to 500 km. However, the hazard analysis requires estimates of the ground motion from earthquakes potentially as large as  $M_w$  9.5. Extrapolation of the above attenuation relationships to larger magnitude events than have been recorded requires specification of the appropriate near field magnitude scaling law for ground motions. Past applications of the general form of the attenuation relationship defined by Equation D-1 have typically followed two limiting cases. One approach has been to assume that the scaling of ground motions with magnitude is independent of distance, implying parameter  $C_5 = 0$ . Examples of this approach are the attenuation relationships developed by Joyner and Boore (1981, 1982) for western U.S. strong motion data. Attenuation relationships based on self-similar scaling of earthquake source



spectra and random vibration theory (Hanks and McGuire, 1981; Boore, 1983, 1986) also imply distance independent magnitude scaling, except for the modifying effect of anelastic attenuation at large distances. The second approach has been to assume ground motions are independent of magnitude at zero distance, implying parameter  $C_5 = -C_2/C_3$ . Examples of this approach are the attenuation relationships developed by Campbell (1981, 1987).

It is likely that the true form of near field magnitude scaling law is intermediate between the above limiting cases. The attenuation relationships developed by Seed and Schnabel (1980), Sadigh (1983, 1984) and Sadigh and others (1986) are examples of intermediate magnitude scaling laws developed from empirical data. These relationships have nearly distance independent magnitude scaling for events below about magnitude 6.5 and nearly magnitude independent peak accelerations at zero distance for events of magnitude greater than about 6.5. Joyner (1984) has proposed that there is a critical earthquake above which the self-similar scaling of earthquake source spectra no longer applies. He suggests that the high frequency corner of the source spectrum becomes fixed for events that rupture the entire width of the seismogenic zone, resulting in a reduction by a factor of about 2 in the increase in ground motion amplitude per unit increase in magnitude for events above the critical size. Joyner estimates the critical magnitude to be approximately 6.5 for crustal events in the western U.S. These arguments suggest that the nearly distance independent magnitude scaling represented by Equations D-6 and D-7 may overestimate the near field magnitude scaling of ground motions from very large ( $M_w > 8$ ) earthquakes.

The characteristics of near field ground motions for events larger than those that have been recorded can be inferred from the results of ground motion simulations. An extensive set of simulations of ground motions from potential large interface earthquakes has been conducted for the WNP-3 site by S-Cubed (1988). Ground motions from large subduction zone thrust earthquakes were simulated by the superposition of the motions from a large number of subevents propagated to the recording site using ray theory (Day and Stevens, 1987). The radiation from each subregion was obtained numerically from a dynamic simulation of faulting based on three-dimensional finite difference solutions to propagating crack problems (Day, 1982a, b.; Stevens and Day, 1985). The ability of the model to generate near field ground motions from large subduction zone thrust earthquakes was tested by simulating the near field recordings from the  $M_w$  8.0 September 19, 1985 Michoacan, Mexico and March 3, 1985 Valparaiso, Chile earthquakes (Day and Stevens, 1987; S-Cubed, 1988). Figure D-9 compares the response spectra for simulated and recorded motions from these events.

The appropriate form of the near field magnitude scaling relationships were evaluated by examining the response spectra for a series of simulated ground motions at the WNP-3 site at distances of 30 to 40 km above the rupture surface of events in the magnitude range of  $M_w$  7.7 to 8.9. Figure D-10 compares the relative amplitudes of spectral velocity for various magnitude events obtained from the simulations with the near field magnitude scaling relationships derived from the empirical attenuation relationships defined by Equations D-6 and D-9. Also shown in Figure D-10 are the scaling

relationships obtained by imposing the two limiting conditions of distance independent magnitude scaling ( $C_5 = 0$ ) and magnitude independence at zero distance ( $C_5 = -C_2/C_3$ ) on the empirical data. There is considerable scatter in the simulation results but a linear fit to the data (dotted line) suggests that the magnitude scaling relationships for events above magnitude  $M_w 8$  should have a flatter slope than indicated by the empirical data from earthquakes of magnitude less than  $M_w 8$ .

#### D.5 Derived Attenuation Relationships for $M_w > 8$ Earthquakes

The magnitude scaling relationships developed from the S-Cubed (1988) simulation results and from use of the Joyner (1984) source model were used to develop attenuation relationships for peak acceleration applicable to earthquakes larger than  $M_w 8$ . The "S-Cubed Model" was developed by constraining parameter  $C_5$  in Equation D-1 such that the resulting near field magnitude scaling relationship approximated that indicated by the results of the simulations shown in Figure D-10 for events of  $M_w > 8$  and matches the median values given by Equation D-6 for  $M_w = 8$ . The resulting relationship is:

$$\ln(a_{max}) = 19.16 + 1.045M_w - 4.738\ln[R+154.7\exp(0.1323M_w)] \quad (D-11)$$

The "Joyner Model" was developed by setting parameter  $C_5$  in Equation D-1 equal to zero, consistent with distance independent magnitude scaling implied by the random vibration approach to developing attenuation relationships, and adjusting coefficients  $C_1$ ,  $C_2$ , and  $C_4$  in Equation D-1 such that the resulting magnitude scaling relationship equals that obtained using random vibration theory and the Joyner (1984) source model with the critical magnitude set equal to  $M_w 8$  (corresponding to a square rupture with a width of the seismogenic zone of about 100 km) and matches the median values given by Equation D-6 for the critical magnitude. The resulting relationship is:

$$\ln(a_{max}) = 24.64 + 0.36M_w - 4.738\ln(R+445.8) \quad (D-12)$$

The near field magnitude scaling relationships based on Equations D-11 and D-12 are shown in Figure D-11. The "Joyner" model results in a somewhat lower rate of increase in ground motions with magnitude than implied by the "S-Cubed" model. Equations D-11 and D-12 are considered applicable to interface earthquakes with magnitudes above the critical magnitude of  $M_w 8$ . The dispersion about the median relationships defined by Equations D-11 and D-12 was assumed to be 0.55, equal to the value obtained from the empirical data for  $M_w 8$  events.

#### D.5 Comparison with other Numerical Modelling Results

Heaton and Hartzell (1986) have used an empirical Green's function technique to estimate the motions that would result from a postulated large earthquake on the interface between the Juan de Fuca and North American plates at a depth of approximately 30 km beneath a site in the coast ranges of Washington state. They used empirical Green's functions developed from strong motion recordings of events in the magnitude range of  $M_w 7$  to 7.5 to simulate the ground motions above the rupture surface of earthquakes in the magnitude

range of  $M_w$  7.25 to 9.5. Figure D-12 compares their estimated spectra (Heaton and Hartzell, 1986, Figure 17) with the response spectra predicted by the attenuation models developed in this study. The comparisons show very good agreement except for motions at periods greater than about 0.8 seconds. The differences at longer periods are likely due to Heaton and Hartzell's use of soil site recordings from Japan as Green's functions. Empirical observations of shallow crustal earthquakes show that long period motions on soil sites are typically a factor of 2 greater than those on rock sites.

## REFERENCES

- Abrahamson, N.A. 1987, Some statistical properties of peak ground accelerations: Bulletin of the Seismological Society of America (in press).
- Algermissen, S.T. (ed.), 1985, Preliminary report of investigations of the central Chile earthquake of March 3, 1985: U.S. Geological Survey Open File Report 85-542.
- Anderson, J.G., Brune, J.N., Prince, J., Mena, E., Bodin, P., Onate, P., Quaas, R., and S.K. Singh, 1986, Aspects of strong motion from the Michoacan, Mexico earthquake of September 19, 1985: Proceedings of the 18th Joint Meeting on Wind and Seismic Effects, Washington D.C., May 12-16.
- Anderson, J., R. Quaas, D. Almora M., J.M. Velasco, E. Guevara O., L.E. de Pavia G., A. Gattierrez R., and R. Vazquez L., 1987a, Guerrero, Mexico accelerogram array - Summary of data collected in the year 1985: report prepared jointly by the Instituto de Ingenieria-UNAM and the Institute of Geophysics and Planetary Physics-UCSD (in press).
- Anderson, J., R. Quaas, D. Almora M., J.M. Velasco, E. Guevara O., L.E. de Pavia G., A. Gattierrez R., and R. Vazquez L., 1987b, Guerrero, Mexico accelerogram array - Summary of data collected in the year 1986: report prepared jointly by the Instituto de Ingenieria-UNAM and the Institute of Geophysics and Planetary Physics-UCSD (in press).
- Beavan, J., and K.H. Jacob, 1984, Processed strong-motion data from subduction zones: Alaska: Report prepared by Lamont-Doherty Geological Observatory of Columbia University, 250 p.
- Boore, D.M., 1983, Stochastic simulation of high-frequency ground motions based on seismological models of the radiated spectra: Bulletin of the Seismological Society of America, v. 73, no. 6A, p. 1865-1894.
- Boore, D.M., 1986, Short period P- and S-wave radiation from large earthquakes: Implications for spectral scaling relations: Bulletin of the Seismological Society of America, v. 76, no. 1, p. 43-64.

- Bufaliza, M.A., 1984, Atenuacion de intensidades sismicas con la distancia en sismos Mexicanos: Tesis, Maestro en Ingenieria (Estructuras), UNAM, facultad De Ingenieria, 94 p.
- Campbell, K.W., 1981, Near-source attenuation of peak horizontal acceleration: Bulletin of the Seismological Society of America, v. 71, no. 6.
- Campbell, K.W., 1987, Strong motion attenuation in Utah, in evaluation of urban and regional earthquake hazards and risk in in Utah: U.S. Geological Society Professional Paper (in press).
- Crouse, C.B, Hileman, J.A., Turner, B.E., and G.R. Martin, 1980, Compilation, assessment and Expansion of the strong motion data base: U.S. Nuclear Regulatory Commission NUREG/CR-1660, 125 p.
- Day, S.M., 1982a, Three-dimensional simulation of fault dynamics: rectangular faults with fixed rupture velocity: Bulletin of the Seismological Society of America, v. 72, no. 3, p. 705-728.
- Day, S.M., 1982b, Three-dimensional simulation of spontaneous rupture propagation: Bulletin of the Seismological Society of America, v. 72, no. 6, p. 1881-1902.
- Day, S.M., and J.L. Stevens, 1987, Simulation of ground motion from the 1985 Michoacan, Mexico earthquake (abs.): Eos, v. 68, no. 44, p. 1354.
- Draper, N., and H. Smith, 1981, Applied Regression Analysis, Second Edition, John Wiley and Sons, New York, 709 p.
- Gallant, A.R., 1975a, Nonlinear regression: The American Statistician, v. 29, no. 2, p. 73-81.
- Gallant, A.R., 1975b, Testing a subset of the parameters of a nonlinear regression model: Journal of the American Statistical Association, v. 70, no. 352, p. 927-932.
- Gallant, A.R., 1987, Nonlinear Statistical Models, John Wiley and Sons, New York, 610 p.
- Hanks, T.C., and Kanamori, H., 1979, A moment-magnitude scale: Journal of Geophysical Research, v. 84, p. 2348-2350.
- Hanks, T.C., and R.K. McGuire, 1981, The character of high frequency strong ground motion: Bulletin of the Seismological Society of America, v. 71, no. 6, p. 2071-2095.
- Hartzell, S.H., and Heaton, T.H., 1985, Strong ground motion for large subduction zone earthquakes: Earthquake Notes, Eastern Section, Seismological Society of America, v. 55, no. 1, January-March.

- Heaton, T.H., and Hartzell, S.H., 1986, Estimation of strong ground motions from hypothetical earthquakes on the Cascadia subduction zone, Pacific Northwest: U.S. Geological Survey Open-File Report 86-328, 69 p.
- Houston, H., and Kanamori, H., 1986, Source characteristics of the 1985 Michoacan, Mexico earthquake at periods of 1 to 30 seconds: Geophysical Research Letters, v. 13, no. 6, p. 596-600.
- Iwasaki, T., Katayama, T., Kawashima, K., and M. Saeki, 1978, Statistical analysis of strong-motion acceleration records obtained in Japan: Proceedings of the Second International Conference on Microzonation for Safer Construction, Research and Application, November-December.
- Joyner, W.B., 1984, A scaling law for the spectra of large earthquakes: Bulletin of the Seismological Society of America, v. 74, no. 4, p. 1167-1188.
- Joyner, W.B., and D.M. Boore, 1981, Peak horizontal acceleration and velocity from strong-motion records including records from the 1979 Imperial Valley, California earthquake: Bulletin of the Seismological Society of America, v. 71, no. 6, p. 2011-2038.
- Joyner, W.B., and D.M. Boore, 1982, Prediction of earthquake response spectra: U.S. Geological Survey Open File Report 82-977.
- Kawashima, K., Aizawa, K., and K. Takahashi, 1984, Attenuation of peak ground motion and absolute acceleration response spectra: in Proceedings of the Eighth World Conference on Earthquake Engineering, San Francisco, v. II, p. 257-264.
- McGarr, A., 1984, Scaling of ground motion parameters, state of stress, and focal depth: Journal of Geophysical Research, v. 89, no. B8, p. 6969-6979.
- Mori, A.W., and C.B. Crouse, 1981, Strong motion data from Japanese earthquakes: World Data Center A for Solid Earth Geophysics, Report SE-29, U.S. Department of Commerce, National Oceanic and Atmospheric Administration, Boulder Colorado.
- Mori, J., Jacob, K.H., and J. Beavan, 1984, Characteristics of strong ground motions from subduction zone earthquakes in Alaska and Japan: presented at the 1984 Annual Meeting of the Seismological Society of America.
- NOAA, 1982, Development and initial application of software for seismic exposure evaluation, report by Woodward-Clyde Consultants, prepared for National Oceanic and Atmospheric Administration, Two volumes, May.

- Repetto, P., Arango, I., and H.B. Seed, 1980, Influence of site characteristics on building damage during the October 3, 1974 Lima earthquake: University of California, Berkeley Earthquake Engineering Research Center Report EERC-80/41, 63 p.
- Sadigh, K., 1979, Ground motion characteristics for earthquakes originating in subduction zones and in the western United States: Sixth Pan-American Conference, Lima, Peru.
- Sadigh, K., 1983, Considerations in the development of site-specific spectra, Proceedings of Conference XXIII, Site-Specific Effects of Soil and Rock on Ground Motion and the Implications for Earthquake Resistant Design, U.S. Geological Survey Open-File Report 83-845.
- Sadigh, K., 1984, Characteristics of strong motion records and their implications for earthquake-resistant design, EERI Seminar No. 12, Stanford, California, July 19, 1984, EERI Publication No. 84-06.
- Sadigh, K., Egan, J.A., and R.R. Youngs, 1986, Specification of ground motion for seismic design of long period structures (abs.): Earthquake Notes, v. 57, no. 1, p. 13.
- Saragoni, R., Crempien, J., and R. Araya, 1982, Características experimentales de los movimientos sísmicos Sudamericanos: Universidad de Chile, Revista Del Idiém, v. 21, no. 2, p. 67-88.
- Saragoni, R., Fresard, M., and P. Gonzalez, 1985, Analisis de los acelerogramas del terremoto del 3 de Marzo de 1985: Universidad de Chile, Departamento de Ingeniería Civil, Publicación SES 1 4/1985(199).
- S-Cubed, 1988, Ground motion simulations for thrust earthquakes beneath western Washington: Final report submittal to Washington Public Power Supply System, February.
- Seed, H.B., and P. Schnabel, 1980, presented in Ground Motions and Soil Liquefaction During Earthquakes: Volume 5 in a series titled Engineering Monographs on Earthquake Criteria, Standard Design and Strong Motion Records, by Seed, H.B., and I.M. Idriss (1982): Earthquake Engineering Research Institute.
- Stevens, J.L., and S.M. Day, 1985, The physical basis of  $m_b$ ,  $M_s$  and variable frequency magnitude methods for earthquake/explosions discrimination: Journal of Geophysical Research, v. 90, no. B4, p. 3009-3020.
- Vyas, Y.K., Crouse, C.B., and Schell, B.A., 1984, Ground motion attenuation equations for Benioff Zone earthquakes offshore Alaska: Earthquake Notes, v. 55, no. 1, p. 17.

Wyllie, L.A., B. Bolt, M.E. Durkin, J.H. Gates, D. McCormick, P.D. Smith, N. Abrahamson, G. Castro, L. Escalante, R. Luft, R.S. Olsen, and J. Vallenias, 1986, The Chile earthquake of March 3, 1985: Earthquake Spectra, v. 2, no. 2, p. 249-512.

Wyss, M. and R.E. Habermann, 1982, Conversion of  $m_b$  to  $M_s$  for estimating the recurrence time of large earthquakes: Bulletin of the Seismological Society of America, v. 72, no. 5, p. 1651-1662.

Youngs, R.R., C.-Y., Chang, J.A. Egan, 1987, Empirical estimates of near field ground motions for large subduction zone earthquakes (abs.): Seismological Research Letters, v. 58, no. 1, p. 22.

Table D-1  
 STRONG MOTION DATA BASE

Date	Earthquake	Lat	Long	FD	RT	mb	Ms	Mw	Station	C	HD	RD	Comp	Amax
ALASKA														
1964.06.05	Alaska	60.35	-145.87	16	th?			5.2	Cordova	R	27		N286	0.0306
													N196	0.0349
1968.12.17	Alaska	60.15	-152.82	82	ss			6.3	Seward	R	205		N090	0.0224
													N000	0.0380
									Seldovia	R	130		N090	0.0269
													N000	0.0413
1971.05.02	Adak	51.42	-177.21	38	th?			6.8	Adak	R	77		N180	0.1168
													N090	0.2076
1974.04.06	Shumagin Is	54.87	-160.29	37	th	5.8		5.6	Sand Pt	R	65	65	N120	0.0768
													N030	0.0911
1974.04.06	Shumagin Is	54.90	-160.29	40	th	6.0		5.8	Sand Pt	R	64	64	N120	0.1002
													N030	0.1201
1974.08.13	Adak	51.49	-178.11	47	th?			6.1	Adak	R	123		N180	0.0223
													N090	0.0298
1974.11.11	Adak	51.59	-178.08	69	th?			6.1	Adak	R	128		N180	0.0310
													N090	0.0466
1975.07.25	Alaska	55.04	-160.41	38	n	5.8		5.6	Sand Pt	R	51		N120	0.0098
													N030	0.0130
1976.02.22	Aleutians	51.57	-176.81	61	n?			4.7	Adak	R	72		N180	0.0282
													N090	0.0670
1979.01.27	Alaska	54.79	-160.64	53	th			6.2	Sand Pt	R	82		N197	0.0077
													N107	0.0094
1979.02.13	Alaska	55.17	-156.94	47	th	5.8		6.5	Sand Pt	R	231		N197	0.0228
													N107	0.0422
1979.02.28	St Elias	60.64	-141.59	13	th		7.2	7.5	Yakutat	S	167	101	N009	0.0829
													N279	0.0620
									Icy Bay	S	76	43	N180	0.1747
													N090	0.0982
									Munday Creek	R	73	50	NS	0.0640
													EW	0.0416
1981.12.28	Alaska	54.67	-160.41	33	th?			3.8	Sand Pt	R	82		N070	0.0188
													N340	0.0246
1983.02.14	Alaska	54.74	-158.88	25	th			6.3	Sand Pt	R	125		N250	0.0077
													N160	0.0068
									Simeonof	RL	41		N070	0.0305
													N340	0.0567
									Chernabura	R	52		N070	0.0478
													N340	0.0413
									Pirate Shake	RL	87		N072	0.0121
													N342	0.0250
1983.02.14	alaska	54.85	-158.84	25	th			6.0	Sand Pt	R	121		N250	0.0058
													N160	0.0040
									Simeonof	RL	38		N070	0.0284
													N340	0.0413
									Chernabura	R	54		N070	0.0170
													N340	0.0206
									Pirate Shake	RL	81		N072	0.0151
													N342	0.0139
1986.05.07	Andreanof Is	51.41	-174.83	16	th	6.8	7.7	8.0	Adak Wanger	S	151	60	Long	0.2500
													Tran	0.2000



Table D-1 (cont'd)  
STRONG MOTION DATA BASE



Date	Earthquake	Lat	Long	FD	RT	mb	Ms	Mw	Station	C	HD	RD	Comp	Amax
CASCADIA														
1949.04.13	Puget Sound	47.10	-122.75	54	n		7.1		Olympia	S	56		N176	0.1743
													N266	0.3272
									Seattle	S	80		N182	0.0601
													N272	0.0765
1965.04.29	Seattle	47.40	-122.40	57	n		6.5	6.7	Olympia	S	80		N176	0.1641
													N266	0.2008
									Seattle SEF	S	61		N238	0.0836
													N148	0.0591
									Tacoma	S	60		N090	0.0754
													N180	0.0459
CHILE														
1945.09.13	central Chile			100	n?		7.1		Santiago E de I	RL	106		Long	0.1310
													Tran	0.0670
1952.04.29	central Chile			10	th?		6.0		Santiago E de I	RL	172		Long	0.0070
													Tran	0.0060
1953.09.04	central Chile			50	n?		6.4		Santiago E de I	RL	146		Long	0.0150
													Tran	0.0170
1958.09.04	central Chile			15	th?		6.8		Santiago E de I	RL	96		Long	0.0300
													Tran	0.0520
1965.03.28	La Ligua			61	n?	6.4	7.2	7.4	Santiago E de I	RL	146		Long	0.1870
													Tran	0.1710
1967.09.26	central Chile			84	n?		5.6		Santiago E de I	RL	87		Long	0.0280
													Tran	0.0250
1971.07.08	Valparaiso			40	th	6.6	7.7	7.8	Santiago E de I	RL	175	101	Long	0.1340
													Tran	0.1650
1973.10.05	central Chile			33	th?		6.7		Santiago E de I	RL	130		Long	0.0110
													Tran	0.0100
1974.11.12	central Chile			90	n?		6.2		Santiago E de I	RL	95		Long	0.0330
													Tran	0.0440
									Cerro St Lucia	R	94		Long	0.0310
1978.12.21	central Chile			46	n?		5.3		Chillan	SA	66		Long	0.0510
													Tran	0.0500
									Talca	SA	106		Long	0.0260
													Tran	0.0310
1979.07.05	central Chile			56	n?		5.8		La Ligua	A	63		Long	0.2020
									Papudo	R	68		Long	0.2000
									Vina del Mar	A	112		Long	0.0340
													Tran	0.0250
									Valparaiso	UTFSM	R	117	Long	0.0110
1981.11.07	central Chile	-32.20	-71.34	65	n?		6.8		Papudo	R	75		N50E	0.3790
													S40E	0.6050
									La Ligua	A	76		N70W	0.3660
													S20W	0.4720
									Llolleo	A	178		N10E	0.0730
													S80E	0.1970
									San Felipe	A	106		S20E	0.3760
													N70E	0.3710
									Peldehue	A	137		EW	0.2900

Table D-1 (cont'd)  
STRONG MOTION DATA BASE



Date	Earthquake	Lat	Long	FD RT	mb	Ms	Mw	Station	C	HD	RD	Comp	Amx	
								Santiago E de I	RL	166		NS	0.0770	
												EW	0.0600	
1985.03.03	San Antonio	-33.24	-71.85	33	th	6.9	7.8	8.0	Illapel	SA	194	142	N20W	0.1200
												S70W	0.1000	
								Los Vilos	R	157	107	NS	0.0300	
												EW	0.0400	
								La Ligua	A	114	67	N70W	0.1900	
												S20W	0.1300	
								Papudo	R	98	54	N50E	0.1300	
												S40E	0.4700	
								Zepallar	R	94	51	NS	0.3200	
												EW	0.3300	
								San Felipe	A	127	94	S10E	0.3500	
												N80E	0.4300	
								Llayllay	SA	103	73	N80W	0.3400	
												S10W	0.4900	
								Vina del Mar	A	53	42	N70W	0.2280	
												S20W	0.3560	
								Valparaiso E.A.	A	46	39	N50E	0.2930	
												S40E	0.1630	
								ValparaisoUTFSM	R	46	39	S20E	0.1640	
												N70E	0.1790	
								Peldehue	A	123	99	EW	0.6400	
								Quintay	A	39	37	NS	0.2000	
												EW	0.1800	
								Santiago E de I	RL	125	102	NS	0.1100	
												EW	0.1100	
								Llolleo	A	58	42	S80E	0.4260	
												N10E	0.6690	
								Melipilla	S	88	58	EW	0.6000	
												NS	0.6700	
								Papel	A	97	42	NS	0.3100	
												EW	0.1400	
								Pichilemu	R	145	42	NS	0.2700	
												EW	0.1800	
								San Fernando	A	168	102	NS	0.2300	
												EW	0.3400	
								Iloca	A	188	70	NS	0.2200	
												EW	0.2800	
								Hualane	A	188	77	NS	0.1700	
												EW	0.1400	
								Constitucion	R	239	119	NS	0.1400	
												EW	0.0800	
								Talca	SA	274	122	N80W	0.1600	
												N10E	0.1700	
								Cauquenes	A	308	181	NS	0.0900	
												EW	0.1200	
								Chillan Viejo	A	371	246	N80E	0.0600	
												N10W	0.0700	



Table D-1 (cont'd)  
STRONG MOTION DATA BASE

Date	Earthquake	Lat	Long	FD	RT	mb	Ms	Mw	Station	C	HD	RD	Comp	Amax
JAPAN														
1956.02.14	Chiba Pref	35.70	139.90	45	n		6.0		tk024	A	50		NS	0.0771
													EW	0.0589
1962.04.23	Japan	42.23	143.92	60	n		7.0		hk005	A	96		NS	0.2870
													EW	0.5275
1962.04.30	Miyagi Pref	38.73	141.13	35	ss		6.5		th001	A	69	54	NS	0.0731
													EW	0.0527
1963.05.08	Ibaragi	36.40	141.18	40	th?		6.1		kt001	A	63		NS	0.0301
													EW	0.0314
									kt003	A	63		NS	0.0620
													EW	0.0662
1963.08.04	Chiba	35.43	140.35	39	th?		5.1		kt001	A	52		NS	0.0944
													EW	0.0807
1964.02.05	Ibaragi	36.40	141.07	54	th	5.6	6.0		kt001	A	65		NS	0.0574
													EW	0.0405
													NS	0.2068
													EW	0.1393
													NS	0.0422
													EW	0.0323
1964.06.16	Niigata	38.35	139.18	40	r	6.1	7.4	7.6	1	SA	71	57	NS	0.1314
													EW	0.1742
1964.11.14	Ibaraki	36.47	140.63	69	n	4.9	5.1		kt001	A	69		NS	0.2655
													EW	0.2429
1965.04.20	Shizuoka	34.88	138.30	40	ss	5.6	6.1		cb002	SA	45		NS	0.1220
													EW	0.0674
									cb005	SA	50		NS	0.1107
													EW	0.1558
1965.10.26	Kunashiri Is	43.73	145.52	159	n	6.2	7.1		hk004	A	227		NS	0.1076
													EW	0.0681
1967.11.19	Ibaragi	36.43	141.22	48	th?	5.6	6.0		kt001	A	69		NS	0.4733
													EW	0.3570
1968.04.01	Hyuganada	32.28	132.53	37	th	6.2	7.6	7.5	kk014	SA	322	287	NS	0.1381
													EW	0.1695
									ks002	A	75	50	NS	0.2941
													EW	0.3581
									ks003	A	135	114	NS	0.0335
													EW	0.0330
									sk005	SA	167	127	NS	0.0720
													EW	0.1093
									sk006	A	88	59	NS	0.1967
													EW	0.2282
1968.04.01	Hyuganada AS	32.24	132.21	40	th	5.8	6.3		sk006	A	110		Long	0.0560
													Tran	0.0640
1968.05.16	Tokachi-Oki	40.73	143.58	20	th	6.0	8.2	8.2	hk003	A	291	120	NS	0.2258
													EW	0.1583
									hk009	SA	320	157	NS	0.1855
													EW	0.1972
									hk013	A	160	50	NS	0.1276
													EW	0.0772
									th014	A	188	81	NS	0.1681
													EW	0.1607

Table D-1 (cont'd)  
 STRONG MOTION DATA BASE

Date	Earthquake	Lat	Long	FD	RT	mb	Ms	Mw	Station	C	HD	RD	Comp	Amx
	Tokachi-Oki (cont'd)								th020	A	244	124	NS	0.2317
													EW	0.2003
									th029	A	188	84	NS	0.3177
													EW	0.2102
1968.05.16	Tokachi-Oki AS	41.42	142.58	26	n	6.3	7.3		hk003	A	237		NS	0.1160
													EW	0.0924
									hk013	A	79	43	NS	0.1091
													EW	0.1159
									th014	A	227	138	NS	0.1578
													EW	0.1268
1968.05.18	Tokachi-Oki AS	40.33	143.40	20	th	4.9	5.1		th005	A	203		NS	0.0870
													EW	0.0194
1968.05.23	Tokachi-Oki AS	40.25	142.57	30	th	5.4	6.3		th014	A	92		NS	0.1333
													EW	0.1179
1968.07.01	Saitama	35.98	139.43	68	n?	5.9	5.6	6.1	tk056	A	91		S03E	0.0819
													N87E	0.1299
1968.07.05	Miyagi	38.43	142.22	44	th	6.0	6.4		th005	A	76		S35E	0.0421
													N55E	0.0690
1968.08.06	W. Shikoku	33.30	132.38	48	n	6.3	6.5	6.8	cg005	SA	126		NS	0.0840
													EW	0.0683
1968.08.07	Hokkaido	42.97	144.97	68	n	5.6	5.7		hk004	A	75	63	NS	0.0499
													EW	0.0877
1968.10.08	Chiba	35.52	140.15	73	th	5.2	5.3		kt004	A	82		S33W	0.0743
													S57E	0.0341
1968.11.14	Iwate	40.15	142.78	40	th?	5.5	6.0		th014	A	92		NS	0.1114
													EW	0.0780
1969.04.21	Hyuganada	32.15	132.12	39	th	5.1	6.5		ks002	A	66		S30W	0.0874
													S60E	0.1225
1970.01.21	Hokkaido	42.38	143.13	25	th?	6.3	6.7		hk013	A	51		Long	0.1519
													Tran	0.2192
1970.04.01	Iwate	39.75	142.05	75	n	5.8	6.0		th014	A	77		NS	0.1934
													EW	0.1649
1970.07.26	Hyuganada	32.07	132.03	47	th	6.1	7.0	7.0	ks002	A	51		S30W	0.1393
													S60E	0.1424
									ks003	A	84	55	Long	0.0366
													Tran	0.0351
1970.07.26	Hyuganada As	32.12	132.10	47	th	6.1	6.0		ks002	A	51		S30W	0.0682
													S60E	0.0720
1971.01.05	Aichi	34.43	137.17	44	n	5.6	5.7		kk026	A	78		NS	0.0950
													EW	0.1062
1971.06.13	Ibaraki	36.23	140.97	55	th	5.5	5.3		kt001	A	65		NS	0.2529
													EW	0.1638
1971.08.02	Erimomisaki	41.23	143.70	45	n	6.6	7.3		hk004	A	201	159	S15W	0.0914
													S75E	0.0776
1971.10.11	Chiba	35.90	140.55	40	th	5.2	5.2		kt050	A	42		S29W	0.0485
													S61E	0.1726
1972.02.29	Hachijojima	33.18	141.27	50	th	6.5	7.2		kt004	A	260		S33W	0.0813
													S57E	0.0595
1972.05.11	Kushiro	42.60	144.93	63	n?	5.5	5.8		hk004	A	71		S15W	0.1456
													S75E	0.0817
1973.06.17	Nemuro-Oki	42.97	145.95	41	th	6.5	7.7	7.8	hk004	A	134		S15W	0.2048
													S75E	0.1293

Table D-1 (cont'd)  
STRONG MOTION DATA BASE



Date	Earthquake	Lat	Long	FD	RT	mb	Ms	Mw	Station	C	HD	RD	Comp	Amax
1973.11.19	Miyagi	38.88	142.15	56	th	6.1	6.5		th033	A	121		NS	0.0538
													EW	0.0648
1974.03.03	Chiba	35.57	140.88	56	th	5.6	6.1		kt036	A	63		NS	0.0384
													EW	0.1138
1974.07.08	Ibaragi	36.42	141.20	45	th	6.0	6.1		kt036	A	87		NS	0.0698
													EW	0.0527
1974.09.04	Iwate	40.18	141.93	52	ss	5.3	5.6		th029	A	67		NS	0.0890
													EW	0.0860
1974.11.09	Tomskomai	42.48	141.78	125	n?	6.0	6.5		hk016	SA	126		S08E	0.0899
													N92E	0.0854
1974.11.16	Chiba	35.75	141.25	44	th	5.8	5.6		kt036	A	58		NS	0.0704
													EW	0.0932
1978.06.12	Miyagi-Ken-Oki	38.15	142.17	40	th	6.8	7.5	7.6	th033	A	108	66	NS	0.3204
													EW	0.2938
									kt014	A	442	390	NS	0.0326
													EW	0.0442
									th028	A	108	66	NS	0.3252
													EW	0.3415
									th014	A	168	120	NS	0.1896
													EW	0.1468
									th029	A	275	229	NS	0.0908
													EW	0.0513
									th020	A	321	279	NS	0.0397
													EW	0.0397
									th013	A	179	156	NS	0.0710
													EW	0.0734
MEXICO														
1962.05.11	Mexico	17.25	-99.53	40	th?		7.0		Alameda Cen DF	SA	249		N11W	0.0480
													N79E	0.0420
1962.05.19	Mexico	17.12	-99.57	33	th?		6.7		Alameda Cen DF	SA	262		N11W	0.0390
													N71E	0.0310
1962.11.30	Mexico	17.30	-99.43	57	n?		5.8		Alameda Cen DF	SA	245		N11W	0.0070
													N71E	0.0050
1964.07.06	Mexico	18.03	-100.77	100	n?		7.4		Ciudad Univ	R	245		NS	0.0200
													EW	0.0150
									Nonoalco HS DF	S	256		EW	0.0480
									Nonoalco AS DF	S	256		NS	0.0310
													EW	0.0200
									Nonoalco MGS DF	S	256		NS	0.0310
													EW	0.0310
									Nonoalco HP DF	S	256		NS	0.0390
													EW	0.0450
1965.06.24	Mexico	17.00	-99.60	51	n?	4.6			Acapulco Pel	R	64		NS	0.0870
													EW	0.0980
1965.08.23	Mexico	16.30	-95.80	16	th		7.6	7.4	Ciudad Univ	R	499	447	NS	0.0042
													EW	0.0029
									Nonoalco AS DF	S	505	456	NS	0.0210
													EW	0.0095
1965.11.01	Mexico	17.00	-99.70	58	n?	4.4			Acapulco Pel	R	65		NS	0.0800
													EW	0.0570

Table D-1 (cont'd)  
STRONG MOTION DATA BASE



Date	Earthquake	Lat	Long	FD	RT	mb	Ms	Mw	Station	C	HD	RD	Comp	Amax
1965.12.09	Mexico	17.30	-100.00	57	n?	6.0	6.3		Acapulco Pel	R	77		NS	0.2350
												EW	0.1330	
									Nonoalco AS DF	S	262		NS	0.0071
												EW	0.0097	
1966.04.11	Mexico	17.98	-102.75	30	th?		5.5		Infiernillo Por	R	102		S68W	0.0230
												N22W	0.0230	
1966.09.25	Mexico	18.30	-100.80	79	n?	5.5	5.7		Infiernillo P	R	143		S68W	0.0170
												N22W	0.0260	
1967.04.20	Mexico	16.85	-99.50	76	n?	4.3			Acapulco Pel	R	88		NS	0.0480
												EW	0.0540	
1967.06.07	Mexico	17.10	-99.90	47	th?	4.4			Acapulco Pel	R	55		NS	0.0650
												EW	0.0490	
1968.02.03	Mexico	16.70	-99.40	9	th?	5.7	5.7		Acapulco Pel	R	59		NS	0.0210
												EW	0.0320	
1968.07.02	Mexico	17.64	-100.27	41	th?	5.9	6.5		Acapulco Pel	R	105		NS	0.0900
												EW	0.0570	
									Nonoalco AS DF	S	238		NS	0.0130
												EW	0.0160	
1968.08.02	Mexico	16.59	-97.70	16	th	6.3	7.1	7.2	Acapulco Pel	R	247	184	NS	0.0084
												EW	0.0120	
									Ciudad Univ	R	345	330	NS	0.0150
												EW	0.0120	
									Nonoalco AS DF	S	355	341	NS	0.0260
												EW	0.0420	
									Nonoalco HP DF	S	355	341	NS	0.0320
												EW	0.0470	
1971.09.05	Mexico	17.09	-99.81	50	n?	5.2	5.0		Acapulco SOP	S	57		N00E	0.1700
												N90W	0.2350	
1973.08.28	Mexico	18.27	-96.60	84	n?	6.8	7.1		Oaxaca F de Med	S	156		N00E	0.2030
												N90W	0.1670	
									Minatitlan	S	241		N00E	0.0170
												N90W	0.0180	
									Pajaritos	S	255		N00E	0.0600
												N90W	0.0570	
									Palacio dl Dep	S	302		N00E	0.0180
												N90W	0.0170	
1974.11.17	Mexico	17.00	-100.10	33	th?	4.7			Acapulco SOP	S	43		NS	0.1300
													EW	0.1160
1975.03.14	Mexico	16.60	-93.40	155	n?	5.5			Tuxtla, Gutier.	S	159		NS	0.0860
													EW	0.0840
1975.12.04	Mexico	16.59	-99.50	89	n?	5.0			Oaxaca F de Med	S	264		N00E	0.0270
													N90E	0.0170
1976.04.27	Mexico	16.43	-99.68	33	th?	4.9			Acapulco SOP	S	62		N00E	0.0420
													N90W	0.0470
1976.06.07	Mexico	17.40	-100.64	45	th?	6.1	6.4		Acapulco SOP	S	111		N00E	0.0560
													N90W	0.0500
1978.03.19	Mexico	17.03	-99.74	36	th?	6.4	6.4		Acapulco SOP	S	44		N00E	0.3910
													N90W	0.8500

Table D-1 (cont'd)  
STRONG MOTION DATA BASE



Date	Earthquake	Lat	Long	FD RT	mb	Ms	Mw	Station	C	HD	RD	Comp	Amax									
1978.11.29	Oaxaca	15.77	-96.80	18 th	6.8	7.8	7.6	Oaxaca F de Med	S	122	121	N00E	0.2200									
														N90W	0.1460							
								Minatitlan	S	322	296	N00E	0.0230									
														N90W	0.0310							
								Pajaritos	S	344	317	N00E	0.0160									
														N90W	0.0120							
								Puebla	S	376	348	N00E	0.0130									
														N90W	0.0200							
								Ciudad Univ	R	458	415	N00E	0.0180									
														N90W	0.0180							
								Hospital ABC	S	466	423	N00E	0.0051									
												N90W	0.0031									
								Nonoalco HP DF	S	466	424	N00E	0.0190									
												N90W	0.0260									
1978.11.29	Oaxaca 1st AS	16.16	-96.75	33 th	5.3			Oaxaca F de Med	S	108		N00E	0.0580									
														N90W	0.0390							
								Puebla	S	358		N00E	0.0020									
												N90E	0.0020									
								Ciudad Univ	R	441		N00E	0.0020									
												N90W	0.0020									
1978.11.29	Oaxaca 2nd AS	16.18	-96.63	22 th	5.7			Oaxaca F de Med	S	102		N00E	0.1000									
														N90E	0.0910							
								Puebla	S	361		N00E	0.0040									
												N90E	0.0040									
								Ciudad Univ	R	446		N00E	0.0051									
												N90W	0.0041									
1979.03.14	Guerrero	17.46	-101.46	20 th	6.5	7.6	7.5	Sicartsa CM	S	97	71	N00E	0.2600									
														N90E	0.2990							
																				N00E	0.2690	
																				N90W	0.3130	
																Infiernillo CM	R	103	73	N00E	0.1220	
																				N90W	0.1070	
																Ciudad Altemita	S	133	116	N00E	0.1610	
																				N90E	0.1230	
																Acapulco Pel	R	183	142	N00E	0.0280	
																				N90W	0.0350	
																Acapulco SOP	S	184	143	N00E	0.0430	
																				N90W	0.0420	
																Apatzingan	S	205	174	N00E	0.0510	
																				N90W	0.0630	
																Ciudad Univ	R	323	295	N00E	0.0170	
																				N90W	0.0140	
																Alberca Olimp.	S	326	299	N00E	0.0310	
																				N90W	0.0380	
																SAHOP	S	330		N00E	0.0340	
												N90W	0.0310									
								Loteria Nal Sot	S	332	305	N00E	0.0390									
												N90W	0.0330									
								Nonoalco AS DF	S	334	308	N00E	0.0420									
												N90W	0.0340									
								Ixcoco Chimal.	S	349	320	N00E	0.0330									
												N90W	0.0230									

Table D-1 (cont'd)  
STRONG MOTION DATA BASE



Date	Earthquake	Lat	Long	FD	RT	mb	Ms	Mw	Station	C	HD	RD	Comp	Amex
	Guerrero (cont'd)								Texcoco Cen. La	S	349	321	N00E	0.0420
													N90W	0.0490
									Texcoco Sosa	S	354	327	N00E	0.0560
													N90W	0.0530
									Puebla	S	394	356	N00E	0.0150
													N90W	0.0130
1981.09.17	Mexico	16.16	-99.83	17	th?	5.4			San Marcos	S	25		N00E	0.3600
													N90W	0.1550
									Acapulco SOP	S	58		N00E	0.2100
													N90W	0.1610
1981.10.25	Playa Azul	17.75	-102.25	20	th	6.2	7.3	7.3	Sicartsa CM	S	29	20	NS	0.2540
													EW	0.2380
									Sicartsa CT	S	29	20	NS	0.2120
													EW	0.2490
									Infiernillo Por R	R	72	43	S68W	0.1330
									Ciudad Altami.	S	187	154	NS	0.0450
													EW	0.0400
									Acapulco Pel	R	275	258	NS	0.0090
									Chilpancingo	S	301	274	N35W	0.0270
													N55E	0.0310
									Ciudad Univ	R	376	338	N00E	0.0120
													N90W	0.0140
									Hospital ABC	S	378	340	N00E	0.0049
													N90W	0.0084
									Viveros	S	379	341	N00E	0.0160
													N90W	0.0160
									Alberca Olimp.	S	380	342	NS	0.0270
													EW	0.0270
									Loteria Nat Sot	S	385	347	NS	0.0220
													EW	0.0170
									Palacio Deporte	S	397	359	NS	0.0180
													EW	0.0220
									Texcoco Chimal.	S	404	365	NS	0.0160
													EW	0.0100
									Texcoco Cen Lag	S	402	364	NS	0.0160
													EW	0.0220
									Texcoco Sosa	S	405	367	NS	0.0310
													EW	0.0290
									Puebla	S	461	422	N00E	0.0100
													N90W	0.0067
									Apatzingan	S	149	127	NS	0.0680
													EW	0.0760
									Nonoalco AS DF	S	386	348	NS	0.0130
													EW	0.0140
1985.09.19	Michoacan	18.18	-102.57	16	th	7.0	8.1	8.0	Caleta de Campo	R	28	15	N00E	0.1410
													N90E	0.1410
									La Villita	R	46	19	NS	0.1230
													EW	0.1230
									La Union	R	86	23	NS	0.1690
													EW	0.1500
									Zihuatenejo	R	136	28	NS	0.1050
													EW	0.1640



Table D-1 (cont'd)  
STRONG MOTION DATA BASE



Date	Earthquake	Lat	Long	FD	RT	mb	Ms	Mw	Station	C	HD	RD	Comp	Amx	
	Michoacan (cont'd)								Papanao	R	189	79	NS	0.1650	
													EW	0.1190	
									El Suchil	R	231	126	NS	0.1040	
														EW	0.0830
									Atoyac	R	252	148	NS	0.0540	
														EW	0.0601
									El Cayaco	S	275	166	NS	0.0418	
														EW	0.0489
									Coyuca	R	294	187	NS	0.0428	
														EW	0.0357
									La Venta	R	324	216	NS	0.0183	
														EW	0.0214
									Cerro de Piedra	R	349	241	NS	0.0275	
														EW	0.0153
									Las Mesas	R	355	246	NS	0.0224	
														EW	0.0183
									Xaltianguis	R	325	217	NS	0.0255	
														EW	0.0183
									El Ocotito	R	340	232	NS	0.0499	
														EW	0.0550
									Teacalco	R	333	251	NS	0.0499	
														EW	0.0245
									Ciudad Univ	R	379	290	NS	0.0285	
														EW	0.0347
									Ide l Patio	R	379	290	NS	0.0326	
														EW	0.0357
									Mesa Vibradora	R	379	290	NS	0.0377	
														EW	0.0398
									Sismex Puebla	S	469	380	NS	0.0306	
														EW	0.0336
									Tacubaya	S	380	291	NS	0.0347	
														EW	0.0336
								Sismex Viveros	S	381	292	NS	0.0449		
													EW	0.0428	
								C de Aba. Frig. SA	SA	389	300	NS	0.0826		
													EW	0.0968	
								C de Aba. Ofici SA	SA	389	300	NS	0.0703		
													EW	0.0815	
								S. de Com y Tra SA	SA	385	296	NS	0.0999		
													EW	0.1710	
								Tlahuac Bombas	SA	394	305	NS	0.1390		
													EW	0.1090	
								Tlahuac Deport. SA	SA	392	303	NS	0.1200		
													EW	0.1140	
								Zacatula	RL	122	20	S00E	0.2764		
												N90W	0.1859		
								Apatzingan	S	104	103	S00E	0.0693		
												N90W	0.0826		

Table D-1 (cont'd)  
 STRONG MOTION DATA BASE

Date	Earthquake	Lat	Long	FD RT	mb	Ms	Mw	Station	C	HD	RD	Comp	Am:ax
1985.09.21	Michoacan AS	17.62	-101.81	20	th	7.5	7.6	Zihuatenejo	R	39	25	S00E	0.1650
											N90W	0.1430	
								Papanao	R	85	34	S00E	0.2570
											N90W	0.2260	
								El Suchil	R	135	77	S00E	0.0887
											N90W	0.6744	
								Coyuca	R	199	138	S00E	0.0428
											N90W	0.0479	
								Cerro de Piedra	R	250	190	S00E	0.0133
											N90W	0.0102	
								Teacalco	R	278	246	N00E	0.0312
											N90E	0.0226	
								La Union	R	40	40	S00E	0.0497
											N90W	0.0781	
								La Villita	R	77	59	S00E	0.0341
											N90W	0.0410	
								Zacatula	RL	77	57	S00E	0.0741
			N90W	0.0732									
Atoyac	R	144	98	N90W	0.0761								
			S00E	0.0809									
El Cayaco	S	169	114	N90W	0.0439								
			S00E	0.0615									
Coyuca	R	199	138	N90W	0.0488								
			S00E	0.0429									
Xaltianguis	R	214	173	N90W	0.0166								
			S00E	0.0175									
La Venta	R	216	168	N90W	0.0195								
			S00E	0.0137									
1985.10.29	Michoacan AS	17.58	-102.64	20	th	5.6	5.4	5.9	Caleta de Campo	R	59	N90W	0.0390
												S00E	0.0303
1986.01.24	Michoacan AS	17.24	-101.44	20	th	4.5			Papanao	R	25	N90W	0.0166
												S00E	0.0214
									La Llave	R	43	N90W	0.0283
												S00E	0.0147
1986.02.01	Guerrero	16.95	-100.14	36		4.1			Ocotillio	R	47	N90W	0.0147
												S00E	0.0088
									Xaltianguis	R	60	N90W	0.0117
												S00E	0.0166
									El Ocotito	R	83	N90W	0.0107
												S00E	0.0147
1986.02.07	Michoacan AS	17.65	-101.45	20	th	4.9			Zihuatenejo	R	20	N90W	0.0137
												S00E	0.0058
									Papanao	R	60	N90W	0.0088
												S00E	0.0107
1986.04.30	Michoacan	18.02	-103.06	20	th	6.2	7.0	6.9	Caleta de Campo	R	38	N90W	0.0995
												S00E	0.0790
									Arteaga	R	90	N90W	0.0224
												S00E	0.0283
									Filo de Caballo	R	343	N90W	0.0039
												S00E	0.0039
									Xaltianguis	R	369	N90W	0.0019
												S00E	0.0010

Table D-1 (cont'd)  
STRONG MOTION DATA BASE



Date	Earthquake	Lat	Long	FD	RT	mb	Ms	Mw	Station	C	HD	RD	Comp	Amax
1986.05.05	Michoacan AS	17.77	-102.80	20		5.6	5.5	5.9	Caleta de Campo	R	40		N90W	0.0341
													S00E	0.0517
1986.05.29	Guerrero	16.85	-98.93	36		5.2	4.2	5.2	Las Vigas	R	49		N90W	0.0664
													S00E	0.0809
									Las Mesas	R	68		N90W	0.0449
													S00E	0.0322
									Cerro de Piedra	R	83		N90W	0.0147
													S00E	0.0117
									El Ocotito	R	84		N90W	0.0273
													S00E	0.0497
									Xaltianguis	R	95		N90W	0.0088
													S00E	0.0098
1986.06.11	Guerrero	17.86	-100.34	50		5.1			La Comunidad	R	61		N90W	0.0498
													S00E	0.0517
									La Llave	R	89		N90W	0.0244
													S00E	0.0205
1986.06.16	Guerrero	17.08	-99.62	34		4.5			Xaltianguis	R	36		N90W	0.0595
													S00E	0.1688
									Las Mesas	R	39		N90W	0.0702
													S00E	0.0341
									Cerro de Piedra	R	48		N90W	0.0205
													S00E	0.0195
									Coyuca	R	61		N90W	0.0117
													S00E	0.0088
									Las Vigas	R	64		N90W	0.0126
													S00E	0.0126
1986.11.04	Michoacan	17.79	-102.02	15		4.8			La Union	R	35		N90W	0.0312
													S00E	0.0263
									Zihuatenejo	R	65		N90W	0.0126
													S00E	0.0058
PERU														
1947.11.01	Peru			30	th?	7.3	7.7		Lima I G	RL	260		Long	0.0063
													Tran	0.0061
1951.01.31	Peru			50	n?	6.0			Lima I G	RL	116		Long	0.0620
													Tran	0.0810
1952.08.03	peru			50	n?	5.3			Lima I G	RL	125		Long	0.0270
													Tran	0.0270
1957.01.24	peru			50	n?	6.2			Lima I G	RL	120		Long	0.0100
													Tran	0.0090
1957.02.18	Peru			100	n	6.5			Lima I G	RL	152		Long	0.0400
													Tran	0.0340
1966.10.17	Peru	-10.92	-78.79	24	th	6.3	7.8	8.1	Lima I G	RL	206	167	Long	0.4040
													Tran	0.2740
1970.05.31	Peru	-9.36	-78.87	56	n	6.6	7.7	7.9	Lima I G	RL	374	255	Long	0.1290
													Tran	0.1320
1971.11.29	Peru			54	n	5.3			Lima I G	RL	138		Long	0.0600
													Tran	0.0900
1974.01.05	Peru	-12.40	-76.31	98	n	6.6			Lima I G	RL	123		Long	0.0900
													Tran	0.1100
									Zarate	RL	122		Long	0.1570
													Tran	0.1720

Table D-1 (cont'd)  
STRONG MOTION DATA BASE



Date	Earthquake	Lat	Long	RT	mb	Ms	Mw	Station	C	HD	RD	Comp	Amax
1974.10.03	Peru	-12.39	-77.66	27	th	6.6	7.8	8.1	Lima I G	RL	87	70 Long	0.2330
												Tran	0.2100
1974.11.09	Peru	-12.44	-77.46	30	th		7.2	Lima I G	RL	68		Long	0.0500
												Tran	0.6730
								La Molina	SA	103		Long	0.1200
												Tran	0.1000
SOLOMONS													
1967.11.14	Long Island	-5.46	147.05	194	n?	5.8		Yonki U Ramu	SA	243		Long	0.0473
												Tran	0.0471
1968.04.29	Long Is	-5.39	146.14	31	th?	5.6		Yonki U Ramu	SA	101		Long	0.0217
												Tran	0.0268
1968.06.03	Long Is	-5.46	146.91	182	n?	5.5		Yonki U Ramu	SA	226		Long	0.0266
												Tran	0.0337
1968.06.17	N. Huon	-6.25	146.56	106	n?	5.3		Yonki U Ramu	SA	124		Long	0.0306
												Tran	0.0389
1968.09.16	New Britain	-6.08	148.77	49	n?	5.9		Yonki U Ramu	SA	313		Long	0.0071
												Tran	0.0060
1969.01.07	Arona	-6.20	146.44	111	n?	5.2		Yonki U Ramu	SA	122		Long	0.0125
												Tran	0.0124
1968.03.10	Umboi Is	-5.60	147.29	194	n?	5.7		Lae Base	A	232		Long	0.0270
												Tran	0.0207
								Yonki U Ramu	SA	253		Long	0.0396
												Tran	0.0309
1969.06.24	Umboi Is	-5.85	146.79	111	n?	5.3		Lae Base	A	153		Long	0.0197
												Tran	0.0224
								Yonki U Ramu	SA	154		Long	0.0222
												Tran	0.0251
1969.08.02	Lee	-6.52	146.92	33	th?	5.2		Lae Base	A	40		Long	0.0264
												Tran	0.0312
1969.08.03	Danfu	-4.25	153.06	59	n?	5.4		Rabaul	A	113		Long	0.0290
												Tran	0.0192
1969.08.22	Solomon Is	-7.60	156.00	80	n?	5.1		Lae Base	A	999		Long	0.0074
												Tran	0.0126
1969.09.07	Taki	-6.61	155.74	174	n?	5.2		Panguna	R?	179		Long	0.0594
												Tran	0.0435
1970.03.28	Bougainville Is	-6.26	154.63	63	n?	5.9		Panguna	R?	114		Long	0.0828
												Tran	0.1221
1970.05.13	Umboi Is	-5.90	146.79	116	n?	5.0		Yonki U Ramu	SA	152		Long	0.0260
												Tran	0.0309
1970.10.31	Ulingan	-4.93	145.47	42	th	6.0	7.0	Yonki U Ramu	SA	162		Long	0.0864
												Tran	0.0934
1971.02.12	Wasu	-6.28	146.50	123	n?	5.6		Lae Base	A	109		Long	0.0406
												Tran	0.0340
								Yonki U Ramu	SA	136		Long	0.1604
												Tran	0.1659
1971.02.13	Wasu	-6.06	146.25	114	n?	5.4		Lae Base	A	158		Long	0.0103
												Tran	0.0090
								Yonki U Ramu	SA	120		Long	0.0797
												Tran	0.0474

Table D-1 (cont'd)  
STRONG MOTION DATA BASE



Date	Earthquake	Lat	Long	FD	RT	mb	Ms	Mw	Station	C	HD	RD	Comp	Amax
1971.03.13	Madang	-5.75	145.39	114	n?	6.2			Yonki U Ramu	SA	142		Long	0.0165
													Tran	0.0134
1971.07.14	New Britain Is	-5.52	153.86	43	th	6.0	7.8	8.0	Panguna	R?	205	153	Long	0.0875
													Tran	0.1245
1971.07.19	Annanberg	-4.90	144.52	75	n?	5.6			Yonki U Ramu	SA	232		Long	0.0176
													Tran	0.0150
1971.07.26	New Ireland Is	-4.93	153.26	43	th	6.6	7.9	8.1	Panguna	R?	301	251	Long	0.0370
													Tran	0.0596
1971.08.07	New Ireland Is	-3.87	152.04	24	th?	5.1			Rabaul	A	49		Long	0.0534
													Tran	0.0356
1971.09.14	New Britain Is	-6.46	151.55	22	th?	6.1	6.3		Rabaul	A	259		Long	0.0135
													Tran	0.0114
1971.09.25	Lee	-6.54	146.64	111	n?	6.3	7.0		Lae Base	A	119		Long	0.1323
													Tran	0.1144
1971.10.14	Kokopo	-4.38	152.40	25	th?	5.5			Rabaul	A	38		Long	0.0126
													Tran	0.0111
1971.10.28	Buka Is	-5.57	153.99	107	n?	5.8	6.5		Rabaul	A	271		Long	0.0624
													Tran	0.0695
1972.11.05	Long Is	-5.40	146.70	229	n?	5.4			Lae Com DW	A	274		Long	0.0229
													Tran	0.0227
1973.03.22	Wasu	-6.16	146.93	102	n?	5.1			Lae Civil Aviat	A	120		Long	0.0408
													Tran	0.0297
1973.08.13	Marienberg	-4.50	144.10	109	n?	5.9			Yonki U Ramu	SA	304		Long	0.0263
													Tran	0.0275
									Lae Civil Aviat	A	410		Long	0.0259
													Tran	0.0209
1973.11.25	Madang	-5.89	145.53	101	n?	5.0			Yonki U Ramu	SA	119		Long	0.0070
													Tran	0.0081
1974.03.04	Umboi Is	-5.88	147.11	67	n?	4.9			Yonki U Ramu	SA	148		Long	0.0158
													Tran	0.0127
1974.03.25	Saidor	-6.03	146.08	110	n?	5.4			Yonki U Ramu	SA	113		Long	0.0633
													Tran	0.0463
1974.09.20	Saidor	-6.20	146.10	105	n?	5.8			Intake U Ramu	R	106		Long	0.0155
													Tran	0.0323
									Yonki U Ramu	SA	106		Long	0.1554
													Tran	0.2299
1981.12.13	Solomon Is	-6.39	154.93	50	n?	5.9	6.0		460 B Panguna M R	R	80		Long	0.0745
													Tran	0.0972
1981.12.13	Solomon Is	-6.34	154.92	48	n?	5.5	5.7		460 B Panguna M R	R	80		Long	0.0262
													Tran	0.0636
1983.03.18	Solomon Is	-4.83	153.58	89	n?		7.9		Arawa Town	R	281		Long	0.0221
													Tran	0.0263
									Bato Bridge	R	285		Long	0.0346
													Tran	0.0329
									BVE 80 Panguna	S	285		Long	0.2890
													Tran	0.2750

Table D-1 (cont'd)  
STRONG MOTION DATA BASE

LEGEND

FD = focal depth (km)

RT = rupture type: th - shallow thrust  
n - normal  
r - reverse  
ss - strike slip

C = site classification: R - rock  
RL - rocklike  
A - alluvium  
S - soil  
SA - soft alluvium

HD = hypocentral distance (km)

RD = distance to rupture surface (km)

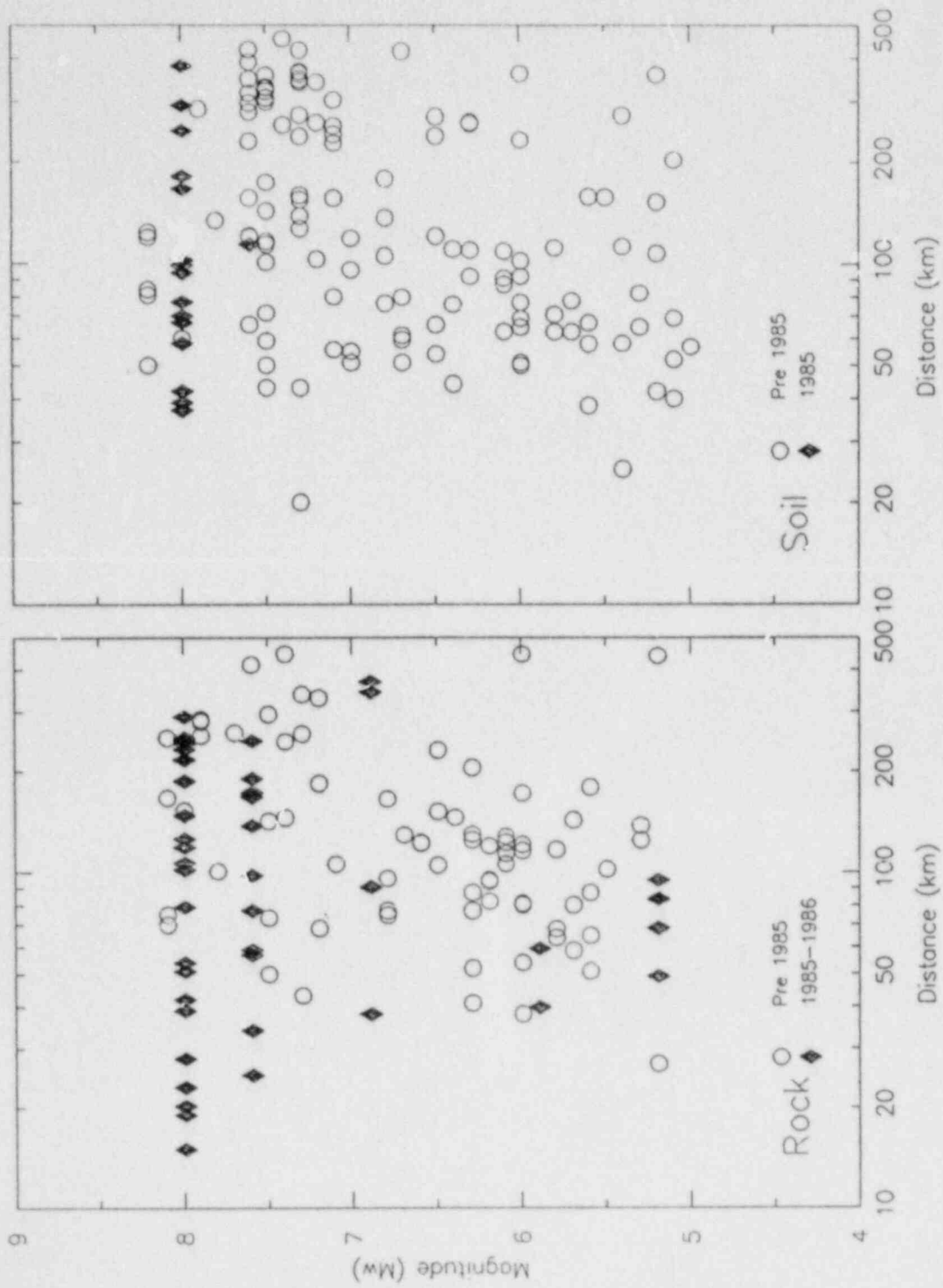


Figure D-1. Distribution of strong motion data used in analysis.

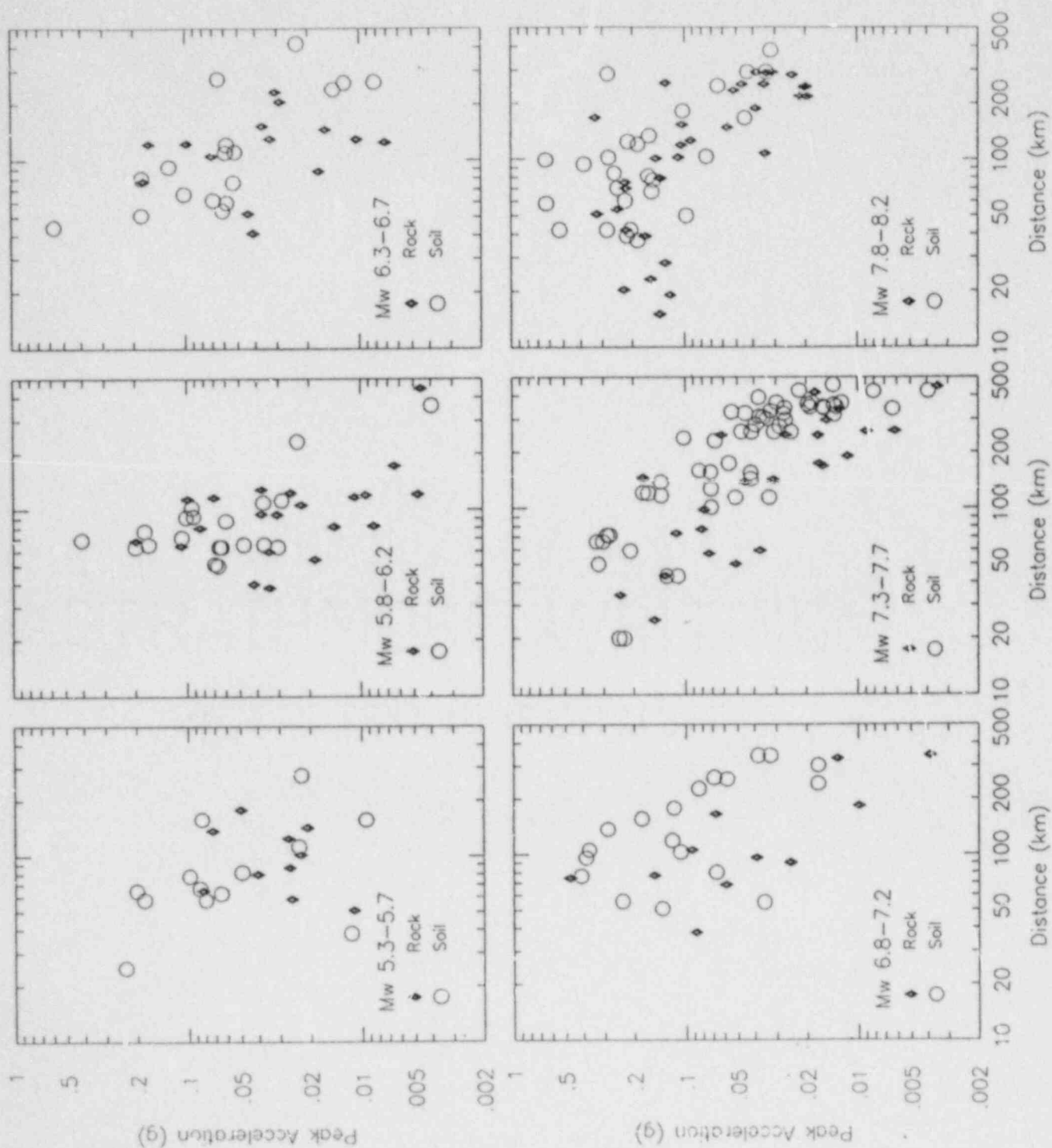


Figure D-2. Peak horizontal accelerations on rock and soil sites for magnitude 5.5 to 8 earthquakes. Shown is the geometric mean of the horizontal components.



Figure D-3. Normalized residuals for rock and soil data plotted against magnitude and distance. Residuals are based on fit of Equation D-1 to the data.

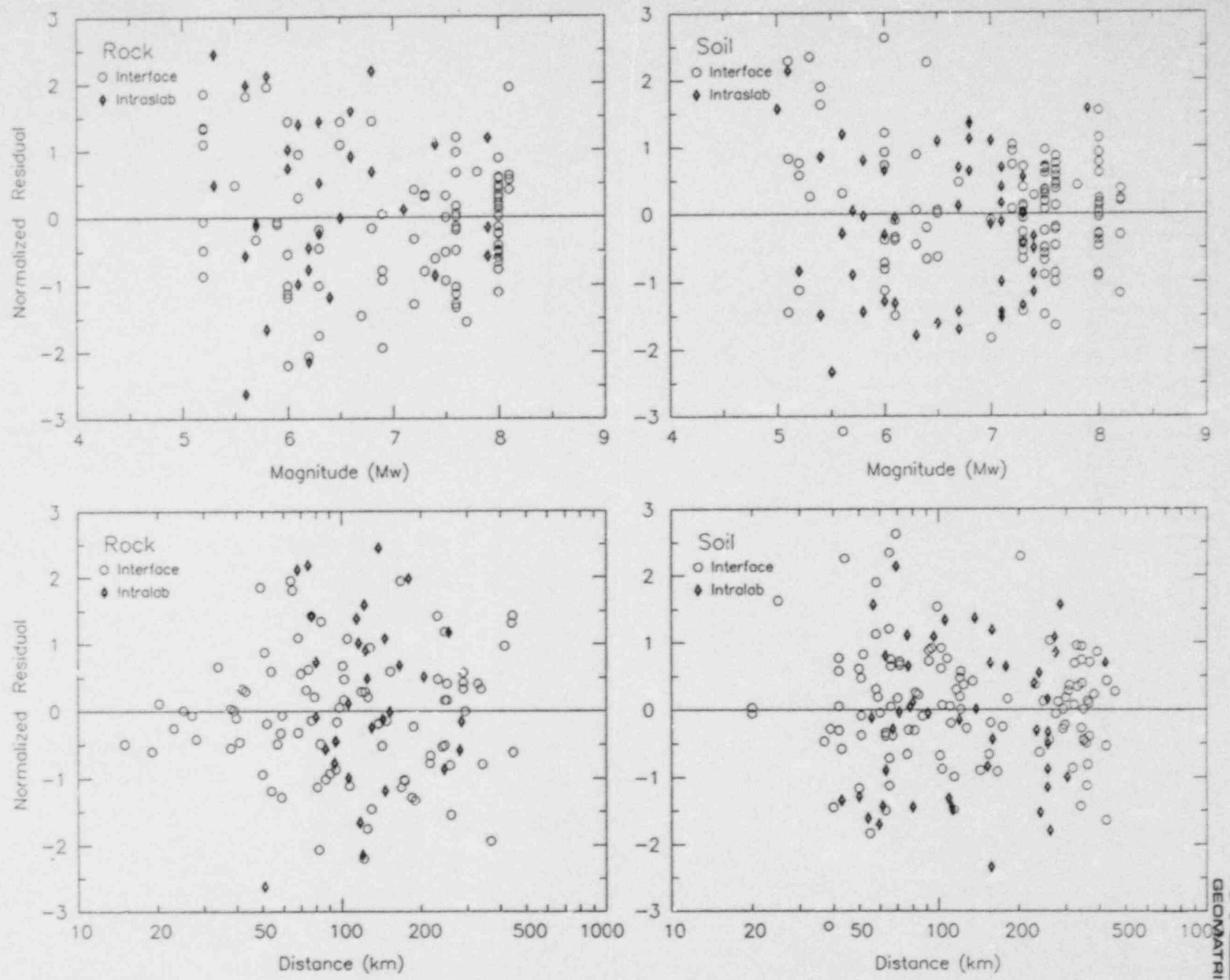


Figure D-4. Median attenuation relationships for rock sites based on Equation D-6.

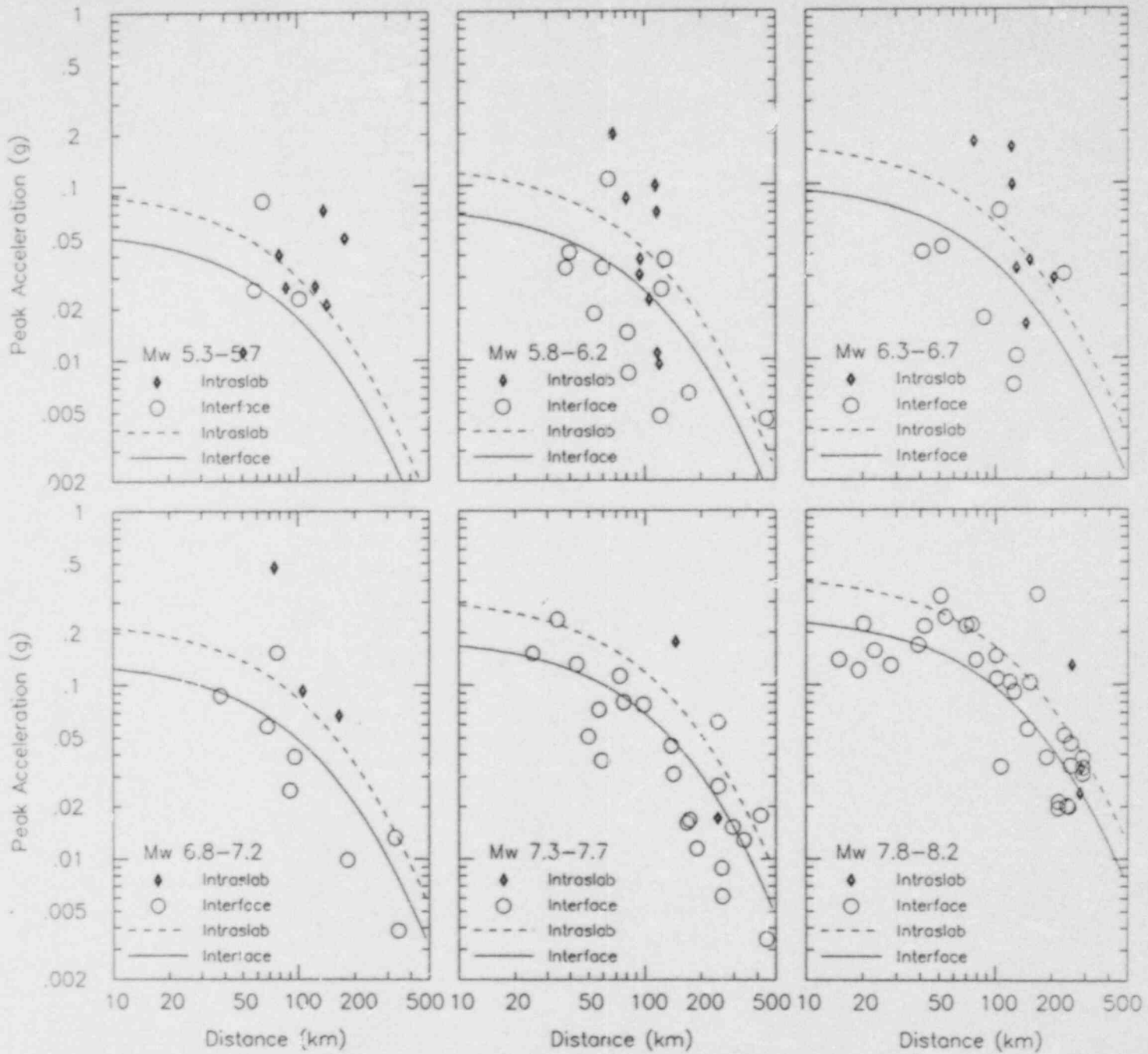


Figure D-5. Median attenuation relationships for soil sites based on Equation D-7.

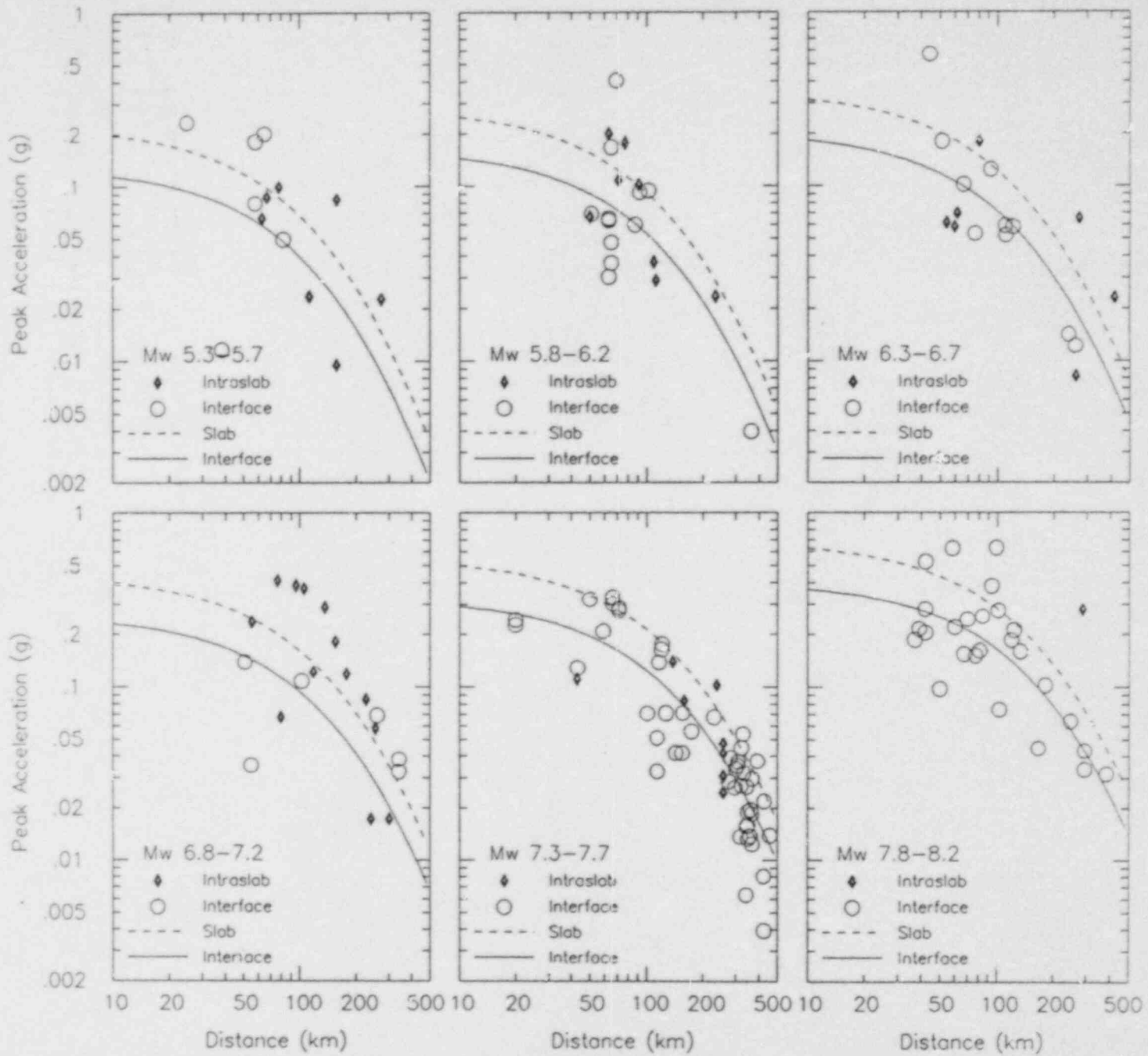
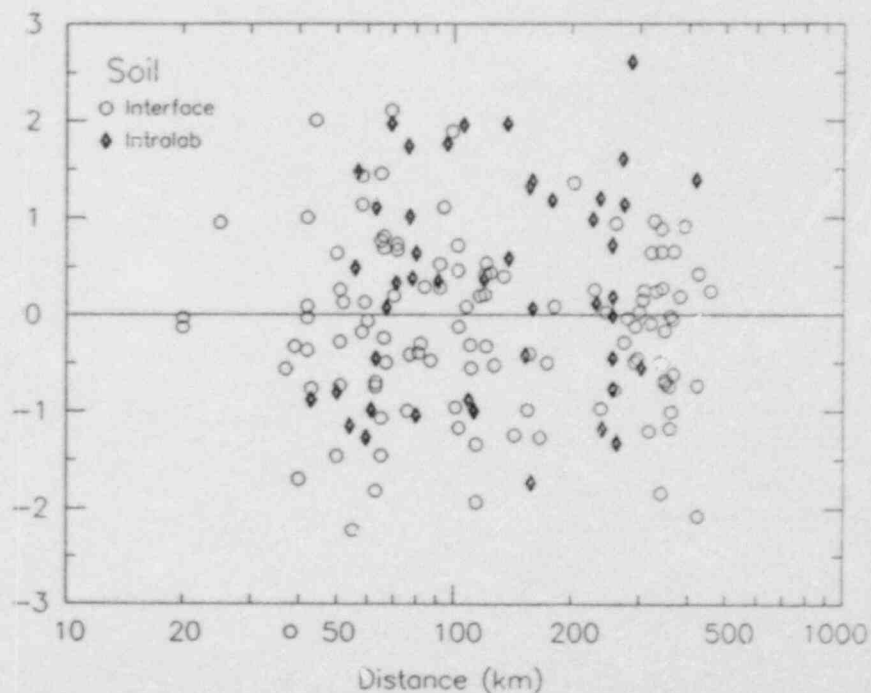
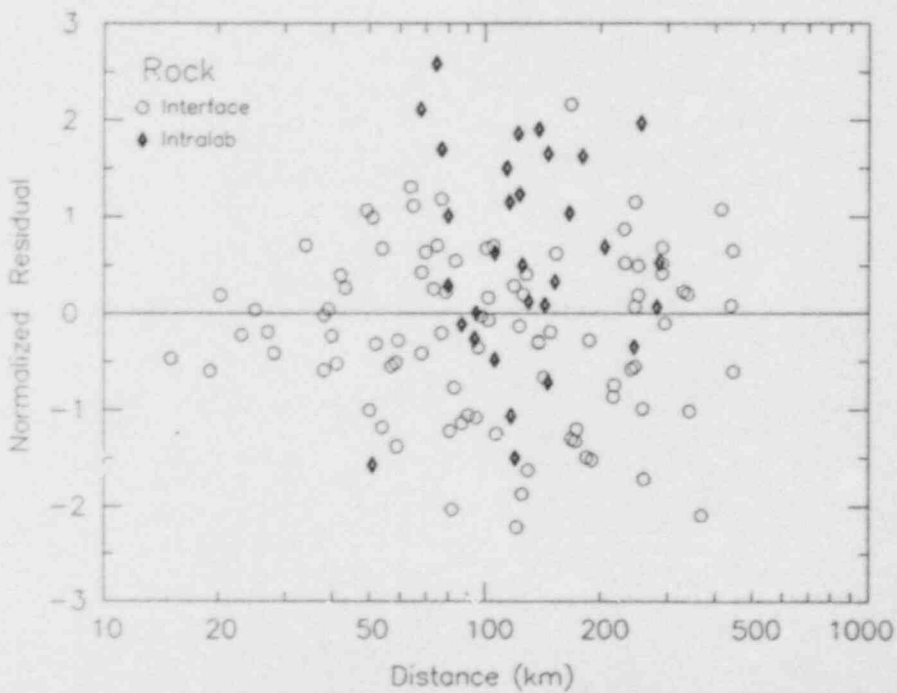
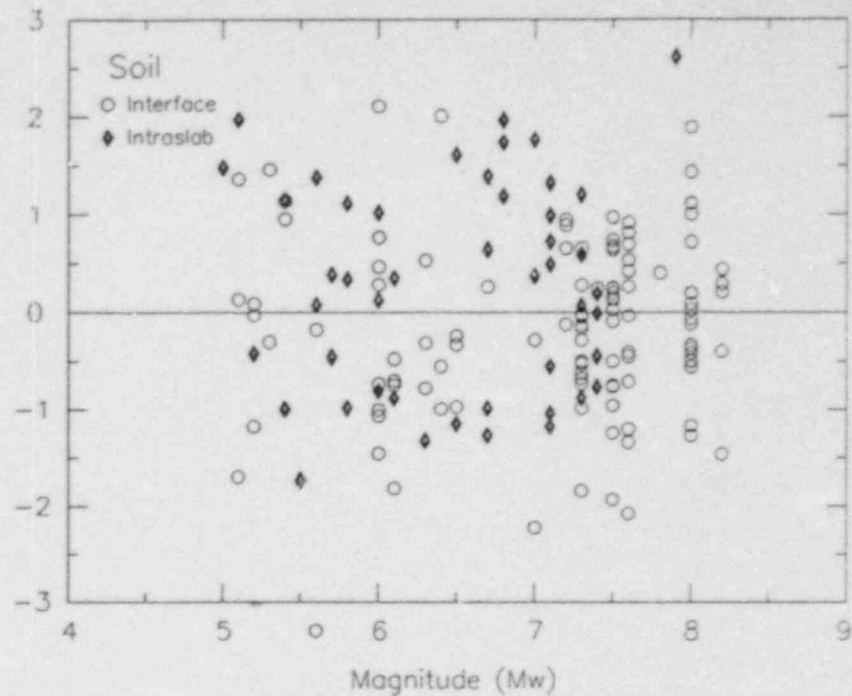
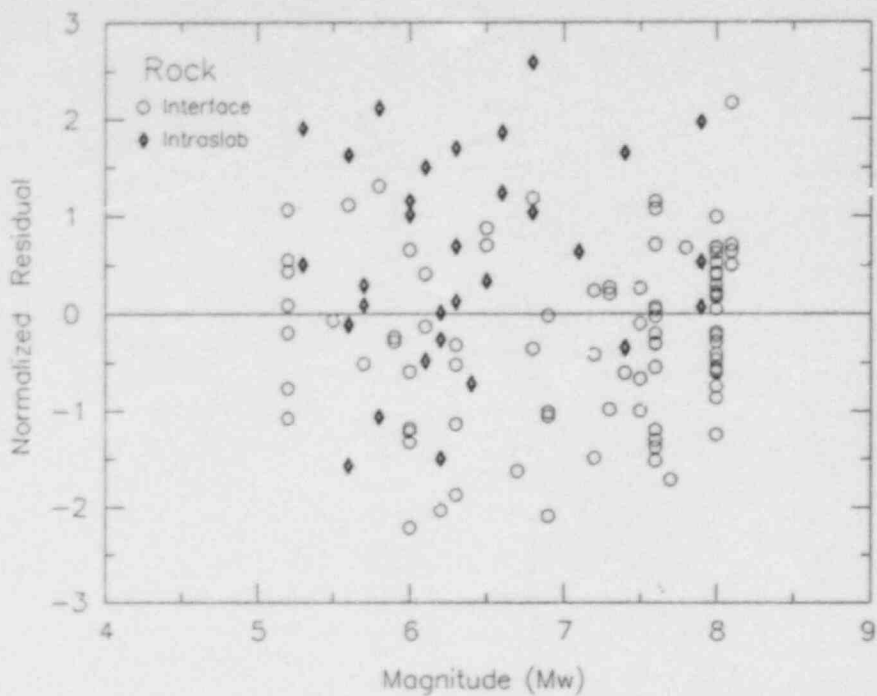


Figure D-6. Weighted normalized residuals for rock and soil data plotted against magnitude and distance. Residuals are based on fit of Equations D-6 and D-7.



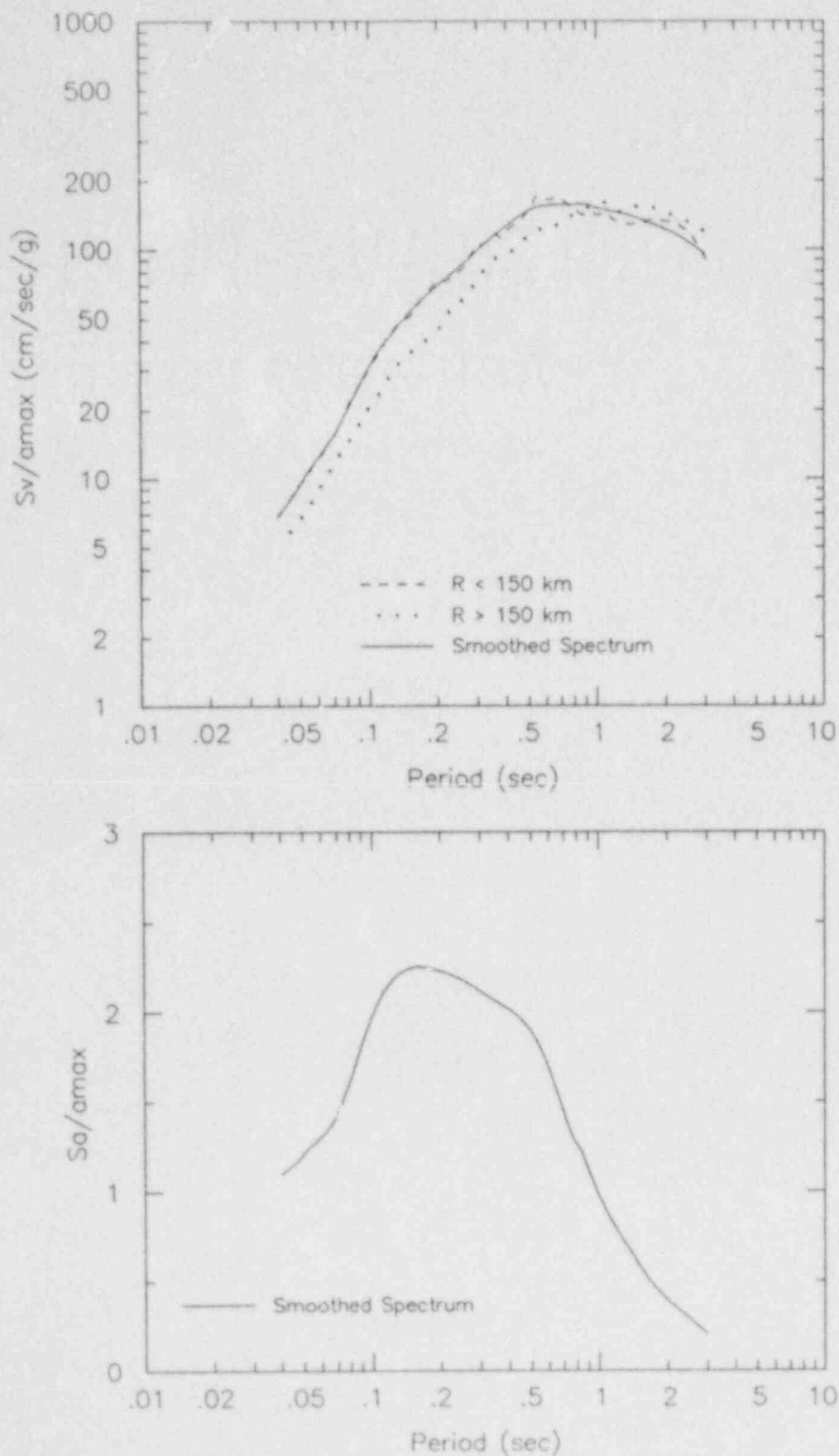


Figure D-7. Median spectral shapes (5% damping) for  $M_w$  8 subduction zone earthquake. Top plot shows median shapes for distance < 150 km and distance > 150 km and smoothed spectral shape. Bottom plot shows smoothed spectrum in terms of spectral acceleration amplification.

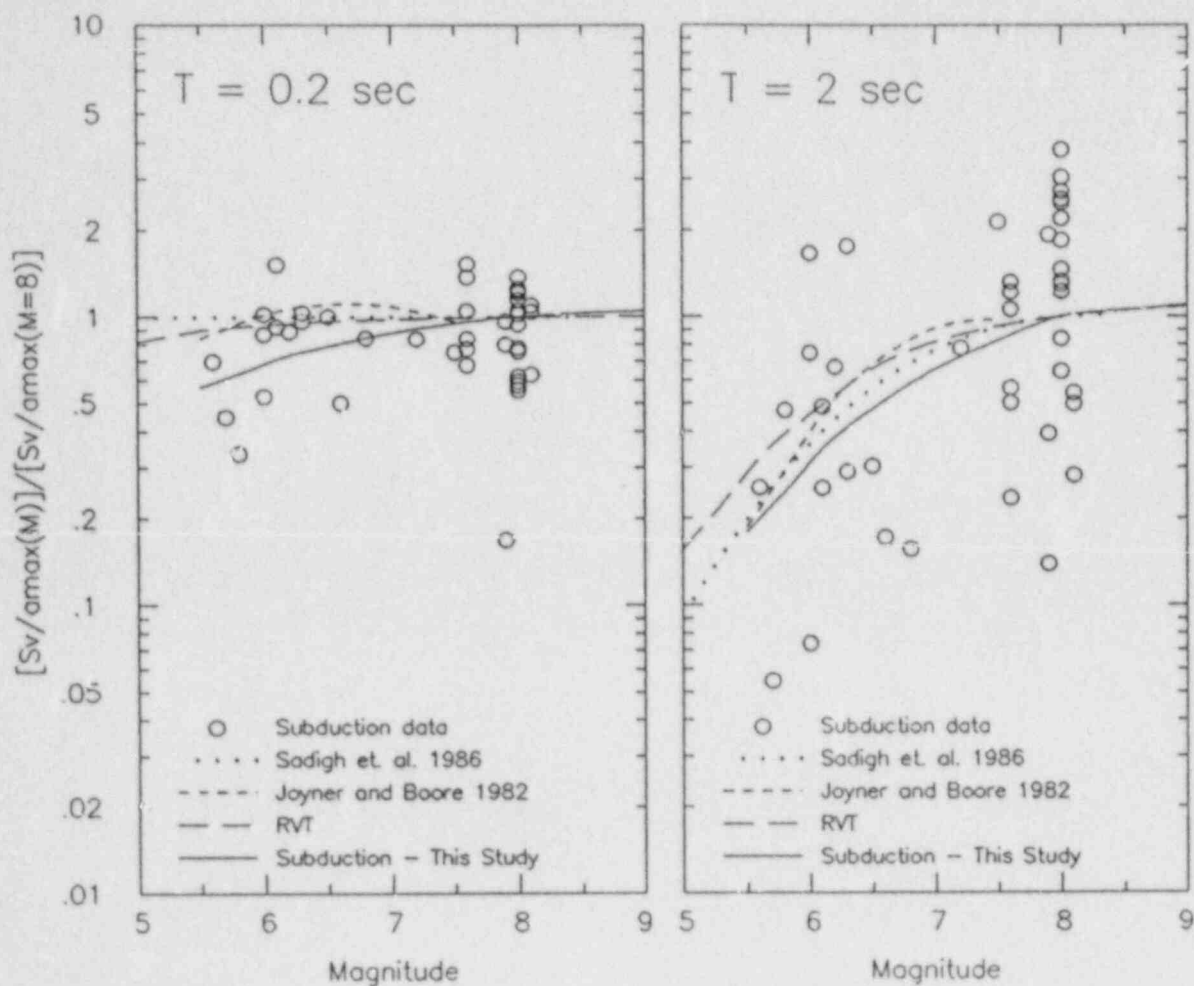


Figure D-8. Relative spectral amplification (5% damping) as a function of magnitude. The data points represent relative response spectral ordinates compared to the spectral shape for a  $M_w$  8 event shown in Figure D-7. The curves present relationship developed previously for crustal events and the relationship developed in this study for subduction zone earthquakes.

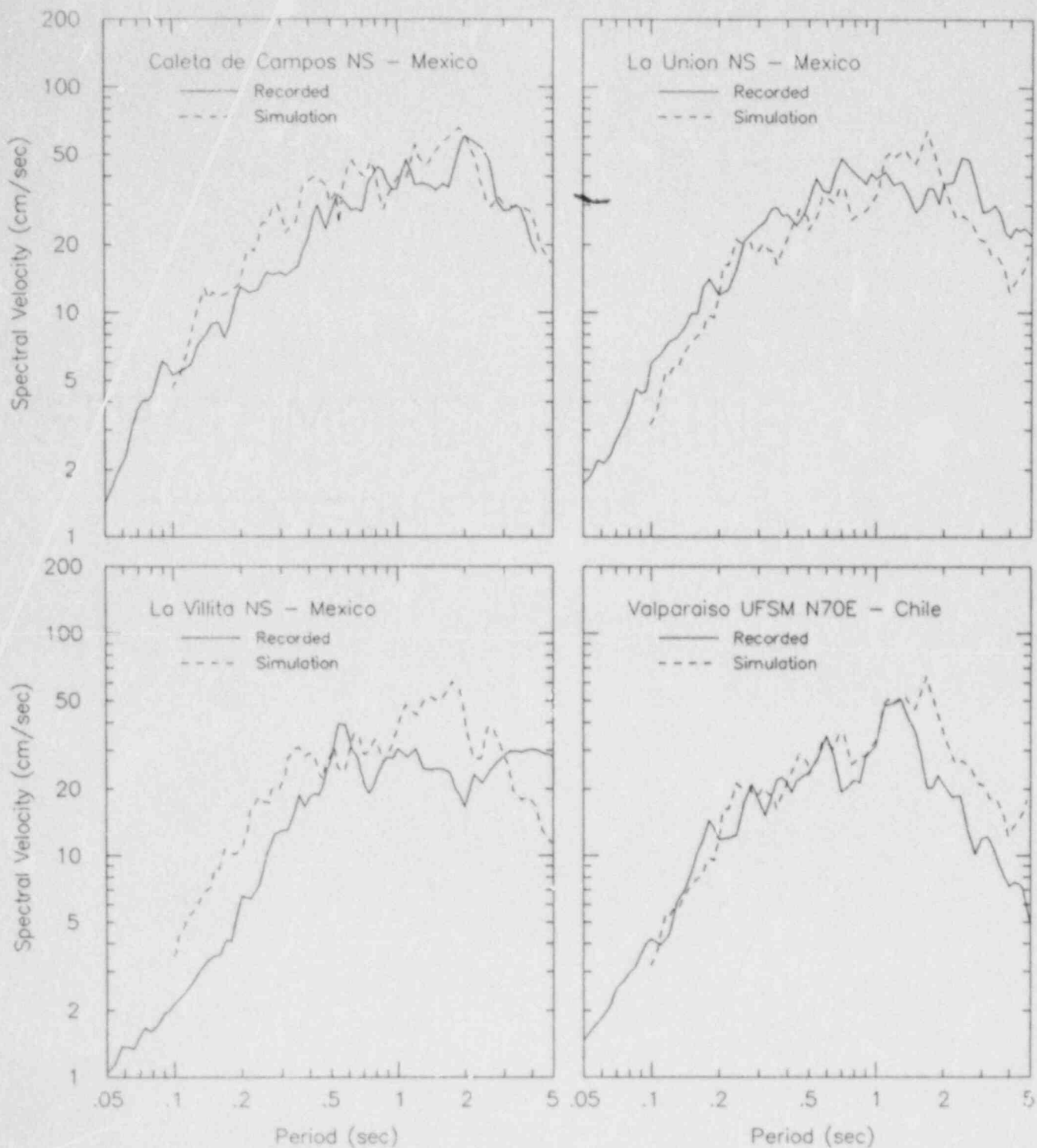


Figure D-9. Comparison of response spectra (5% damping) for simulated motions and recorded motion for the 1985  $M_w$  8 Mexico and Chile earthquakes.

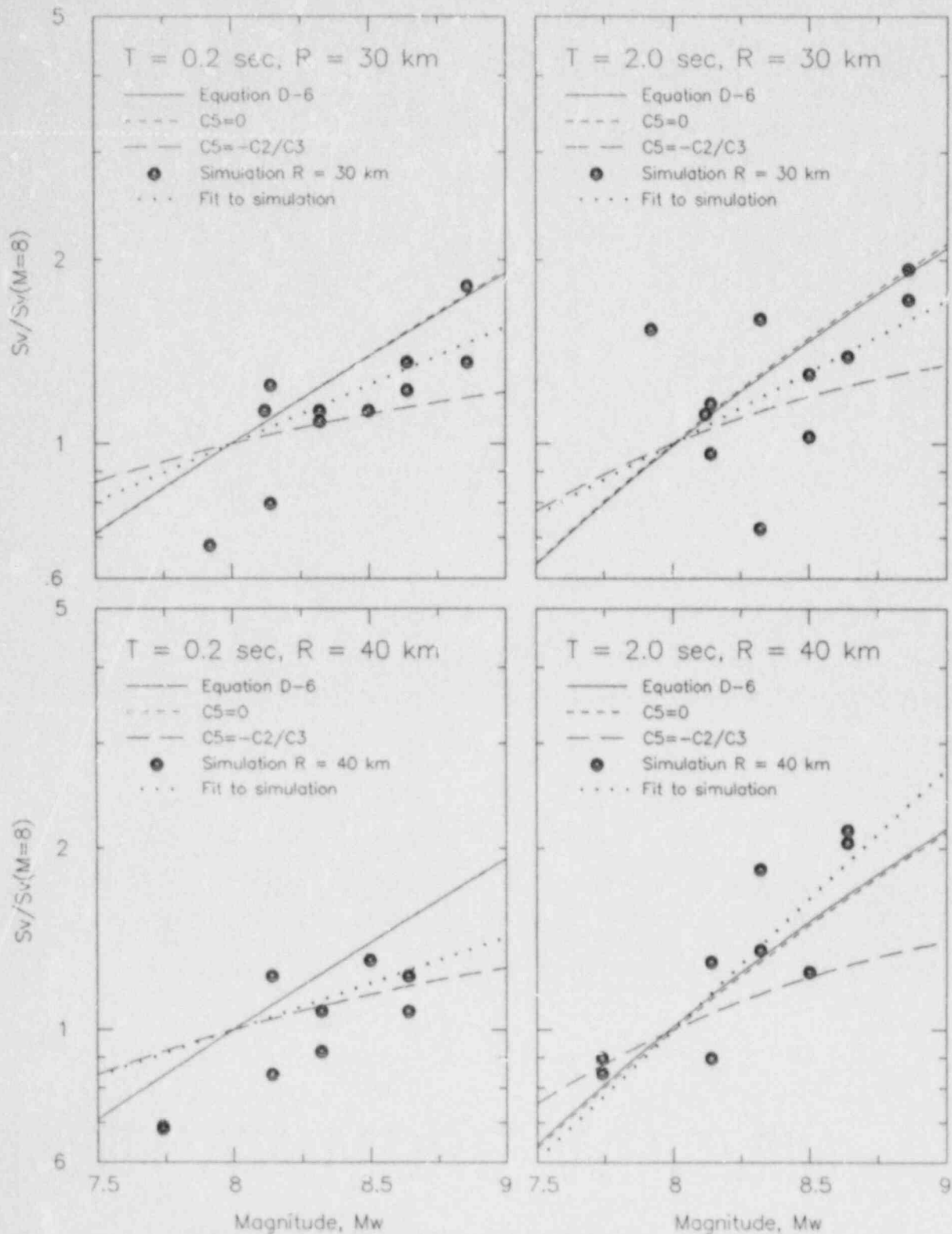


Figure D-10. Comparison of near field magnitude scaling relationships based on simulated motions with magnitude scaling based on empirical attenuation relationships. Solid curve is empirical attenuation relationship developed from data for  $M_w \leq 8$ . Short and long dashed curves are limiting constraints on parameter  $C_5$ . Dotted line is linear fit to simulated data constrained to pass through 1.0 at  $M_w = 8$ .



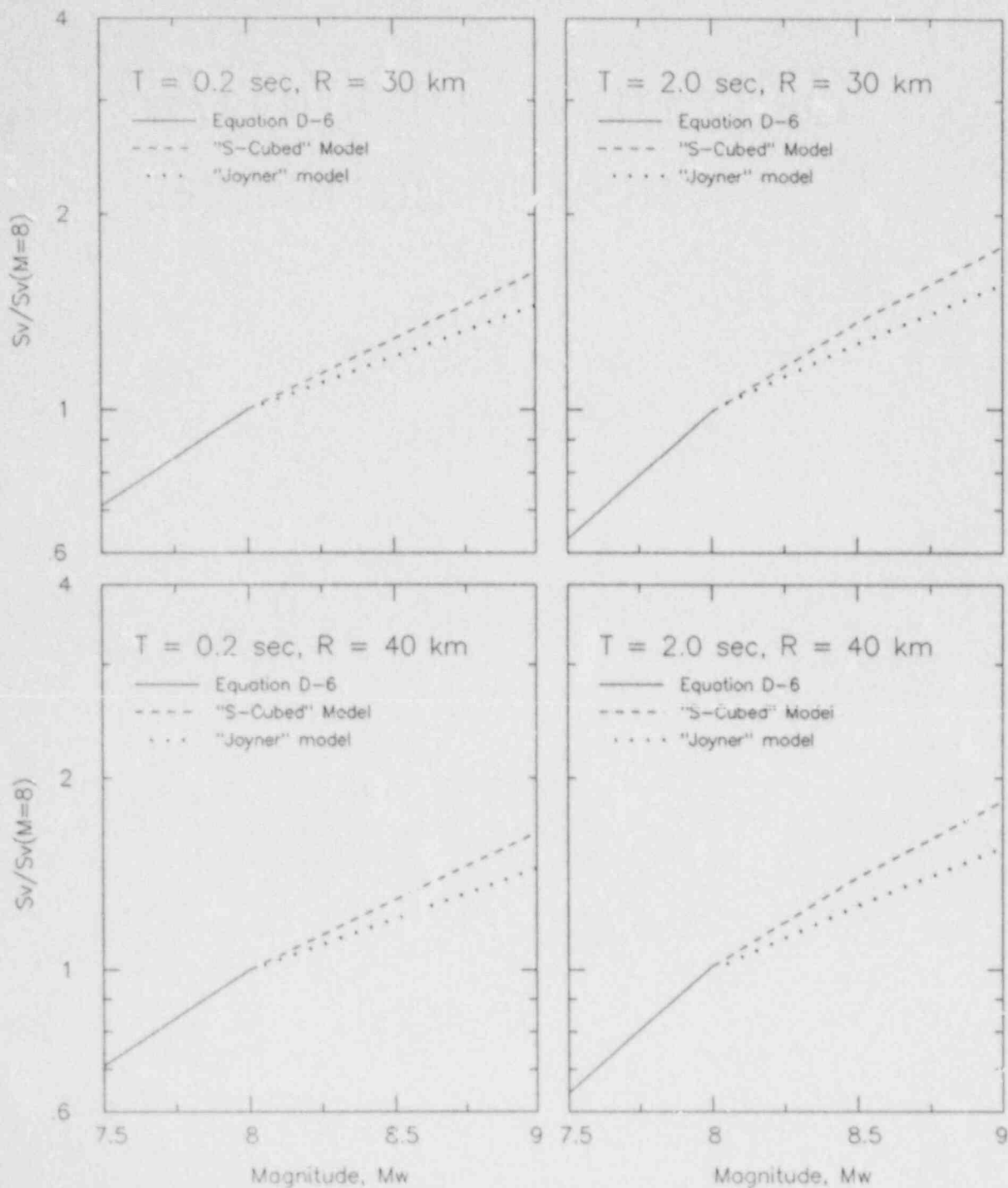


Figure D-11. Near field magnitude scaling for attenuation relationships developed in this study.

Figure D-12. Comparison of median response spectra (5% damping) predicted by relationship developed in this study with response spectra developed by Heaton and Hartzell (1986).

